

Final Report

Fountain Creek Watershed Rainfall Characterization Study



Contract C005501

January 28, 2011

Prepared for:
City of Colorado Springs
30 South Nevada Avenue
Suite 201
Mail Code 210
Colorado Springs, CO 80901

Table of Contents

EXECUTIVE SUMMARY.....	VII
1.0 INTRODUCTION	1.1
2.0 BACKGROUND	2.1
2.1 <i>Climate and Meteorology of Colorado Springs.....</i>	<i>2.1</i>
2.2 <i>Study Area.....</i>	<i>2.10</i>
3.0 DEPTH-DURATION-FREQUENCY CURVES.....	3.1
3.1 <i>Overview.....</i>	<i>3.1</i>
3.2 <i>Approach.....</i>	<i>3.2</i>
3.3 <i>Results.....</i>	<i>3.6</i>
3.4 <i>Key Findings</i>	<i>3.6</i>
4.0 STORM EVENT ANALYSIS AND SUMMARY	4.1
4.1 <i>Overview.....</i>	<i>4.1</i>
4.2 <i>Approach.....</i>	<i>4.1</i>
4.3 <i>Results.....</i>	<i>4.1</i>
4.4 <i>Key Findings</i>	<i>4.2</i>
5.0 ANTECEDENT RAINFALL CONDITIONS	5.1
5.1 <i>Objective.....</i>	<i>5.1</i>
5.2 <i>Approach.....</i>	<i>5.1</i>
5.3 <i>Results.....</i>	<i>5.3</i>
5.4 <i>Key Findings</i>	<i>5.6</i>
6.0 RADAR RAINFALL ANALYSIS.....	6.1
6.1 <i>Objective.....</i>	<i>6.1</i>
6.2 <i>Approach.....</i>	<i>6.1</i>
6.3 <i>Radar Rainfall Verification</i>	<i>6.7</i>
6.3.1 <i>Overview</i>	<i>6.7</i>
6.3.2 <i>Selection of Verification Gages.....</i>	<i>6.7</i>
6.3.3 <i>Verification Process and Results</i>	<i>6.10</i>
6.4 <i>Key Findings</i>	<i>6.12</i>
7.0 DETERMINE STORM PROPERTIES	7.1
7.1 <i>Background.....</i>	<i>7.1</i>
7.2 <i>Typical Storm Patterns.....</i>	<i>7.4</i>
7.3 <i>Depth Area Reduction Factors</i>	<i>7.31</i>
7.4 <i>Development of Radar-Based DARFs for Colorado Springs</i>	<i>7.34</i>
7.5 <i>DARF Refinement for the Fountain Creek Watershed.....</i>	<i>7.44</i>
7.6 <i>Temporal Analysis.....</i>	<i>7.49</i>
7.7 <i>Key Findings</i>	<i>7.53</i>
8.0 DESIGN STORM PROCESSOR	8.1
8.1 <i>Background.....</i>	<i>8.1</i>
8.2 <i>Static Design Storm Processor</i>	<i>8.1</i>
8.3 <i>Dynamic Design Storm Processor</i>	<i>8.3</i>
8.3.1 <i>Comparison of Moving Design Storm to June 17, 1965 Jimmy Camp Creek Flood Cloudburst</i>	<i>8.3</i>
8.3.2 <i>Comparison of Moving Design Storm to June 27, 2004 Cloudburst Near Colorado Springs Airport</i>	<i>8.5</i>
9.0 RECOMMENDATIONS FOR FUTURE RESEARCH.....	9.1
10.0 BIBLIOGRAPHY	10.2
11.0 APPENDIX A: GAGE-ADJUSTED RADAR RAINFALL ANALYSIS.....	A.1
12.0 APPENDIX B: TITAN GARR VERIFICATION GAGE LISTS AND ACCUMULATION PLOTS	B.1
13.0 APPENDIX C: APRIL 1999 STORM ANALYSIS	C.1

13.1	<i>Radar-Rainfall Images</i>	C.1
13.2	<i>Storm Characteristics</i>	C.4
13.3	<i>Storm Frequency</i>	C.7
14.0	<i>APPENDIX D: RESUMES</i>	D.1
14.1	<i>Principal Investigators</i>	D.2
14.2	<i>Project Sponsors</i>	D.34
14.3	<i>Peer Review / Technical Support</i>	D.35
15.0	<i>APPENDIX E: RESPONSE TO REVIEWER COMMENTS</i>	E.1
15.1	<i>Response to Detailed Comments From Peer Review of DRAFT Report dated August 21, 2009, Carlton Engineering Inc.</i>	E.1
15.2	<i>Review Comments of FINAL Report dated September, 2010, Carlton Engineering Inc.</i>	E.33
16.0	<i>APPENDIX F: ADDITIONAL TITAN ANALYSIS</i>	F.1

List of Figures

Figure 2-1: Average Annual Rainfall for Eastern Colorado.	2.2
Figure 2-2: Northern portion of the Fountain Creek Watershed.	2.3
Figure 2-3: Average Annual Rainfall for El Paso County and the Fountain Creek Watershed.	2.4
Figure 2-4: Average April Rainfall for El Paso County and the Fountain Creek Watershed.	2.4
Figure 2-5: Average May Rainfall for El Paso County and the Fountain Creek Watershed.	2.5
Figure 2-6: Average June Rainfall for El Paso County and the Fountain Creek Watershed.	2.5
Figure 2-7: Average July Rainfall for El Paso County and the Fountain Creek Watershed.	2.6
Figure 2-8: Average August Rainfall for El Paso County and the Fountain Creek Watershed.	2.6
Figure 2-9: Average September Rainfall for El Paso County and the Fountain Creek Watershed.	2.7
Figure 2-10: Average October Rainfall for El Paso County and the Fountain Creek Watershed.	2.7
Figure 2-11: Colorado Statewide Precipitation 1998-2009.	2.8
Figure 2-12: Colorado Statewide Precipitation 1895-2009.	2.9
Figure 2-13: Colorado Statewide Palmer Hydrological Drought Index -1900-2009.	2.9
Figure 2-14: Approximate Study Area (Shaded area denotes Fountain Creek Watershed.)	2.10
Figure 3-1: Hourly and Daily Rain Gage Locations.	3.2
Figure 3-2: Colorado Springs Airport DDFs.	3.5
Figure 3-3: 1-Hour DDF Comparison.	3.6
Figure 4-1: Colorado Springs Airport Storm Frequency.	4.2
Figure 4-2: Colorado Springs Airport Storm Duration.	4.3
Figure 4-3: Colorado Springs Airport Storm Intensity.	4.3
Figure 4-4: Greenland 6NE Storm Frequency.	4.4
Figure 4-5: Greenland 6NE Storm Duration.	4.4
Figure 4-6: Greenland 6NE Storm Intensity.	4.5
Figure 4-7: Greenland 9SE Storm Frequency.	4.5
Figure 4-8: Greenland 9SE Storm Duration.	4.6
Figure 4-9: Greenland 9SE Storm Intensity.	4.6
Figure 4-10: Manitou Springs Storm Frequency.	4.7
Figure 4-11: Manitou Springs Storm Duration.	4.7
Figure 4-12: Manitou Springs Storm Intensity.	4.8
Figure 4-13: Storm Frequency Summary - All Stations.	4.8
Figure 4-14: Storm Duration Summary - All Stations.	4.9
Figure 4-15: Storm Intensity Summary - All Stations.	4.9
Figure 5-1: Cloudburst vs. Five Day Antecedent Rainfall.	5.3
Figure 5-2: Cloudburst vs. HSPF Soil Moisture.	5.4
Figure 5-3: Maximum Annual 2-Hr Rainfall vs 5-Day Antecedent Rainfall.	5.6
Figure 5-4: Five-Day Antecedent Rainfall (%Annual) vs. Maximum Annual 2-Hr Rainfall.	5.7
Figure 5-5: Number of Antecedent Rain Days vs. 2-Hr Rainfall.	5.7
Figure 6-1: Jimmy Camp Creek Stream Gage at Fountain, CO (http://wdr.water.usgs.gov/nwisgmap/)	6.2
Figure 6-2: USGS Gage 07105900 Peak Runoff Event, 1999.	6.2
Figure 6-3: USGS Gage 07105900 Peak Runoff Event 2003.	6.3
Figure 6-4: Frequency Distribution of Selected Radar Data Months.	6.4
Figure 6-5: Rain Gage Network 1994-95.	6.5
Figure 6-6: Rain Gage Network 1999.	6.5
Figure 6-7: Rain Gage Network 2001.	6.6
Figure 6-8: Rain Gage Network 2002-2008.	6.6
Figure 6-9: Verification gages for pre-1999 study periods.	6.9
Figure 6-10: Verification gages for 1999-2002 study periods.	6.9
Figure 6-11: Verification gages for post-2002 study periods.	6.10
Figure 6-12: Average accumulation plot for verification gages and co-located radar pixels for July 2006 dataset.	6.11
Figure 6-13: Event totals for verification gages and co-located radar pixels for July 2006 dataset.	6.11
Figure 6-14: Monthly rainfall scatter-plot of verification gages and co-located radar pixels.	6.12
Figure 7-1: Example Radar Image with Storm Cells Enclosed by Fitted Ellipses.	7.3
Figure 7-2: Idealized Storm Cell Derived from TITAN Statistics.	7.3
Figure 7-3: 15-Minute Cell Count - Eastern Colorado (Fountain Creek watersheds are shown in outline.)	7.7
Figure 7-4: Median 15-Minute Cell Area.	7.7
Figure 7-5: 15-Minute Cell Count El Paso County.	7.8
Figure 7-6: Median 15-Minute Cell Area - El Paso County.	7.8
Figure 7-7: 15-Minute Cell Count - Eastern Colorado (35 dBz Threshold, 0.22 iph)	7.9
Figure 7-8: Median 15-Minute Cell Area - Eastern Colorado (35 dBz Threshold, 0.22 iph)	7.9
Figure 7-9: 15-Minute Cell Count - El Paso County (35 dBz Threshold, 0.22 iph)	7.10
Figure 7-10: Median 15-Minute Cell Area - Eastern Colorado (35 dBz Threshold, 0.22 iph)	7.10

Figure 7-11: 1-Hour Cell Count - Eastern Colorado (29 dBz Threshold, 0.09 iph)	7.11
Figure 7-12: Median 1-Hour Cell Area - Eastern Colorado (29 dBz Threshold, 0.09 iph)	7.11
Figure 7-13: 1-Hour Cell Count – El Paso County (29 dBz Threshold, 0.09 iph)	7.12
Figure 7-14: Median 1-Hour Cell Area - El Paso County (29 dBz Threshold, 0.09 iph).....	7.12
Figure 7-15: 3-Hour Cell Count - Eastern Colorado (25 dBz Threshold, 0.05 iph)	7.13
Figure 7-16: Median 3-Hour Cell Area - Eastern Colorado (25 dBz Threshold, 0.05 iph)	7.13
Figure 7-17: 3-Hour Cell Count - El Paso County (25 dBz Threshold, 0.05 iph)	7.14
Figure 7-18: Median 3-Hour Cell Area - El Paso County (25 dBz Threshold, 0.05 iph).....	7.14
Figure 7-19: Distribution of 15-Minute Cell Sizes – Eastern Colorado (35 dBz Threshold, 0.22 iph)	7.15
Figure 7-20: 15-Minute Cell Count Distribution (35 dBz Threshold, 0.22 iph)	7.15
Figure 7-21: 15-Minute Cell Size vs. Peak Intensity (35 dBz Threshold, 0.22 iph).....	7.16
Figure 7-22: Distribution of 1-Hour Cell Sizes - Eastern Colorado (29 dBz Threshold, 0.09 iph)	7.16
Figure 7-23: Distribution of Peak 1-Hour Rainfall (29 dBz Threshold, 0.09 iph).....	7.17
Figure 7-24: 1-Hour Cell Size vs. Peak Intensity (29 dBz Threshold, 0.09 iph).....	7.17
Figure 7-25: Distribution of 3-Hour Cell Sizes (25 dBz Threshold, 0.05 iph)	7.18
Figure 7-26: Distribution of Peak 3-Hour Rainfall (25 dBz Threshold, 0.05 iph).....	7.18
Figure 7-27: 3-Hour Cell Size vs. Peak Intensity (25 dBz Threshold, 0.05 iph).....	7.19
Figure 7-28: Fountain Creek Watershed Cloudburst Areas vs. Recurrence	7.20
Figure 7-29: Fountain Creek Watershed Maximum 15-Minute Cloudburst Area	7.20
Figure 7-30: Areal Coverage for June 2, 1994 Storm (2.3 hr) over Jimmy Camp Creek Watershed.....	7.21
Figure 7-31: Areal Coverage for June 2, 1995 Storm (1.0 hr) over Jimmy Camp Creek Watershed.....	7.21
Figure 7-32: Areal Coverage for June 4, 1996 (1.3 hr) Storm over Jimmy Camp Creek Watershed.....	7.22
Figure 7-33: Areal Coverage for July 31, 1999 Storm (2.3 hr) over Jimmy Camp Creek Watershed	7.22
Figure 7-34: Areal Coverage for August 4, 1999 Storm (2.0 hr) over Jimmy Camp Creek Watershed	7.23
Figure 7-35: Areal Coverage for July 13, 2001 Storm (1.0 hr) over Jimmy Camp Creek Watershed	7.23
Figure 7-36: Areal Coverage for June 19, 2003 Storm (1.2 hr) over Jimmy Camp Creek Watershed.....	7.24
Figure 7-37: Areal Coverage for August 11, 2003 Storm (0.8 hr) over Jimmy Camp Creek Watershed	7.24
Figure 7-38: Areal Coverage for June 15, 2004 Storm (1.5 hr) over Jimmy Camp Creek Watershed.....	7.25
Figure 7-39: Areal Coverage for June 27, 2004 Storm near Jimmy Camp Creek Watershed	7.25
Figure 7-40: Areal Coverage for July 16, 2004 (1.3 hr) Storm over Jimmy Camp Creek Watershed	7.26
Figure 7-41: Areal Coverage for August 5, 2004 Storm (0.8 hr) over Jimmy Camp Creek Watershed	7.26
Figure 7-42: Areal Coverage for July 14, 2005 Storm (1.5 hr) over Jimmy Camp Creek Watershed	7.27
Figure 7-43: Areal Coverage for July 15, 2005 (0.8 hr) Storm over Jimmy Camp Creek Watershed	7.27
Figure 7-44: Areal Coverage for August 11, 2005 Storm (1.0 hr) over Jimmy Camp Creek Watershed	7.28
Figure 7-45: Areal Coverage for July 3, 2007 Storm (1.0 hr) over Jimmy Camp Creek Watershed	7.28
Figure 7-46: Areal Coverage for August 22, 2007 Storm (1.0 hr) over Jimmy Camp Creek Watershed	7.29
Figure 7-47: Areal Coverage for August 15, 2008 Storm (1.0 hr) over Jimmy Camp Creek Watershed	7.29
Figure 7-48: Areal Coverage for August 16, 2008 Storm (1.3 hr) over Jimmy Camp Creek Watershed	7.30
Figure 7-49: Areal Coverage for September 16, 2008 Storm (2.5 hr) over Jimmy Camp Creek Watershed.....	7.30
Figure 7-50: Depth Area Reduction Factors (From NWS TP29 as shown in NWS TP40, 1961)	7.32
Figure 7-51: One-Hour Radar Based DARFs in the Denver Area (After Geronimo, 2004)	7.33
Figure 7-52: Radar Based DARFs in the Denver Area (After Geronimo, 2004)	7.34
Figure 7-53: Area Normalized 15-Minute Cell Size	7.36
Figure 7-54: Area Normalized Cells for >2-Year Recurrence.....	7.37
Figure 7-55: Normalized 15-Minute DARF (19 dBz Threshold, 0.022 iph).....	7.38
Figure 7-56: 15-Minute DARF (19 dBz Threshold, 0.022 iph).....	7.38
Figure 7-57: 15-Minute DARF for El Paso County (19 dBz Threshold, 0.022 iph)	7.39
Figure 7-58: Normalized 15-Minute DARF (35 dBz Threshold, 0.22 iph)	7.39
Figure 7-59: 15-Minute DARF (35 dBz Threshold, 0.22 iph)	7.40
Figure 7-60: 15-Minute DARF (35 dBz Threshold, 0.22 iph) - El Paso County	7.40
Figure 7-61: Normalized 1-Hour DARF (29 dBz Threshold, 0.09 iph).....	7.41
Figure 7-62: One-Hour DARF(29 dBz Threshold, 0.09 iph)	7.41
Figure 7-63: One-Hour DARF - El Paso County (29 dBz Threshold, 0.09 iph)	7.42
Figure 7-64: Normalized 3-Hour DARF (25 dBz Threshold, 0.05 iph)	7.42
Figure 7-65: Three-Hour DARF (25 dBz Threshold, 0.05 iph).....	7.43
Figure 7-66: Three-Hour DARF - El Paso County (25 dBz Threshold, 0.05 iph).....	7.43
Figure 7-67: One-Hour DARF - El Paso County with DARF Data Points from Geronimo, 2004	7.44
Figure 7-68: Two-Year DARF.....	7.45
Figure 7-69: Five-Year DARF.....	7.46
Figure 7-70: Ten-Year DARF	7.46
Figure 7-71: Twenty-Five-Year DARF.....	7.47
Figure 7-72: Fifty-Year DARF.....	7.47

Figure 7-73: One Hundred-Year DARF	7.48
Figure 7-74: Temporal Distributions of Study Storms.....	7.50
Figure 7-75: Average and Median Storm Distributions.....	7.50
Figure 7-76: Distribution of Storm Durations	7.51
Figure 7-77: Distribution of Times of Peak Rainfall	7.51
Figure 7-78: Storm Quartiles of Times of Peak Rainfall	7.52
Figure 7-79: Non-Dimensional Rainfall Distribution.....	7.52
Figure 8-1: 10-Year Stationary Design Storm	8.2
Figure 8-2: June 17, 1965 Cloudburst (Rainfall, inches)	8.4
Figure 8-3: June 17, 1965 Cloudburst (Rainfall, inches)	8.4
Figure 8-4: Jimmy Camp Creek, June 16, 1965, Depth Area Comparison	8.5
Figure 8-5: June 27, 2004 Cloudburst (Rainfall, inches)	8.6
Figure 8-6: Dynamic Processor Fit for June 27, 2004 Event (Rainfall, inches)	8.6
Figure 8-7: Jimmy Camp Creek, June 27, 2004, Depth Area Comparison	8.7
Figure 13-1: Storm Total Gage-Adjusted Radar Rainfall.....	E.1
Figure 13-2: Gage-Adjusted Radar Rainfall: April 27, 1999	E.2
Figure 13-3: Gage-Adjusted Radar Rainfall: April 28, 1999	E.2
Figure 13-4: Gage-Adjusted Radar Rainfall: April 29, 1999	E.3
Figure 13-5: Gage-Adjusted Radar Rainfall: April 30, 1999	E.3
Figure 13-6: Storm Sequence Near Colorado Springs.....	E.4
Figure 13-7: Storm Sequence near Air Force Academy Football Stadium.....	E.5
Figure 13-8: Maximum 4-Day Rainfall in Fountain Creek Watershed	E.5
Figure 13-9: 15-Minute Storm Cell Size Distribution	E.6
Figure 13-10: Cumulative 15-Minute Cell Size Distribution	E.6
Figure 16-1: TITAN Cell Topology Comparison	F.1

List of Tables

Table E2.1-1: Data Months Selected for Storm Properties Analysis	viii
Table 2.1-1: Colorado Springs Precipitation Summary (1948-2010).....	2.1
Table 2.1-2: Colorado Springs Snowfall Summary (1948-2010).....	2.1
Table 3.1-1: Average Cloudburst Season Precipitation.....	3.1
Table 3.2-1: Parameters for Colorado Springs Airport DDF Equations	3.3
Table 3.2-2: Depth Duration Frequency Tables	3.4
Table 3.3-1: 1-Hour DDF Comparison	3.6
Table 5.2-1: Antecedent Moisture Conditions for Maximum Annual Cloudbursts	5.2
Table 5.3-1: Colorado Springs Airport ranked antecedent rainfall.....	5.5
Table 5.3-2: One Day Antecedent Moisture Probability	5.5
Table 5.3-3: Five Day Antecedent Moisture Probability	5.5
Table 6.2-1: Rain Events for the Jimmy Camp Creek Analysis	6.1
Table 6.2-2: Data Months Selected for Storm Properties Analysis.....	6.3
Table 6.3-1: Verification Gages for the Pre-1999 Period.....	6.8
Table 7.1-1: dBz Values with Equivalent Rainfall Intensities, iph.	7.2
Table 7.2-1: Fountain Creek Watershed Cloudburst Storms.....	7.19
Table 7.5-1: Depth Area Reduction Factor Curve Parameters.....	7.45
Table 7.6-1: Storms Evaluated in Temporal Analysis.....	7.49
Table 13.3-1: Peak Observed Depth Duration Storm Frequencies	C.7

Executive Summary

Carlton Engineering conducted a Fountain Creek Watershed Rainfall Characterization Study for the City of Colorado Springs, CO, and the Colorado Water Conservation Board, to determine typical rainfall patterns and design storms that could be applied in the planning and design of storm water facilities.

The key study findings and results include:

1. Depth Area Reduction Factors (DARFs) in the Colorado Springs area are significantly different than published National Weather Service DARFs,
2. DARFs were found to vary with recurrence interval and location, and
3. A proof of concept Design Storm Processor was created that produces realistic spatially and temporally variable design storms.

The climate and meteorology in the Fountain Creek Watershed and Colorado Springs were reviewed for the study. On average, rainfall generally tracks the terrain patterns in the area with annual precipitation ranging from 12-14 inches at the lower elevation downstream portions of the Fountain Creek Watershed to 32-34 inches in the highest elevation portions on the western ridge.

Depth duration frequency (DDF) curves were developed from available rain gage data in and near Colorado Springs. Analysis showed that the DDFs for Greenland and Manitou Springs were in reasonable agreement with NOAA Atlas 2. However, DDF values at the Colorado Springs Airport gage were significantly higher. (Note: Records at the Colorado Springs record began in 1976 and were not included in NOAA Atlas 2.)

Frequencies of occurrence of storm totals, median storm duration by storm total, and average storm intensity by storm total were computed for five gages: Colorado Springs Airport, Greenland 6 NE, Greenland 9 SE, and Manitou Springs. Again, statistics for the Colorado Springs Airport gage stood out from the rest suggesting that the Colorado Springs Airport experiences higher frequency, longer duration and higher intensities for large cloudburst events.

The expected impact of antecedent moisture conditions on hydrologic response in the Fountain Creek Watershed was investigated. No obvious correlation between summertime storm depths, stream response and antecedent moisture conditions was observed. In general, antecedent soil moisture conditions can be assumed as very dry for design conditions. Since most floods in the Fountain Creek Watershed result from summertime cloudburst events, runoff is more likely governed by limitations of infiltration rates rather than antecedent soil moisture conditions.

Gage-adjusted radar rainfall (GARR) estimates were provided for six events on Jimmy Camp Creek in May 1995, August, 1996, July/August 1999, August 2004, July 2005, and August 2006 to support hydrologic modeling efforts. The data were provided in ArcView GIS format.

Gage-adjusted radar-rainfall estimates were developed for 24 months with significant rainfall from 1994 to 2008 to evaluate the geometric properties of storm cells in the region. (See Table E2.1-1 below¹.) The specific objective was to develop insights and recommendations for improving design storm standards in the Fountain Creek Watershed.

A software tool known as TITAN (Thunderstorm Identification, Tracking, Analysis and Nowcasting) was used to identify and evaluate more than 340,000 15-minute storm cells, more than 45,000 1-hour storm

¹ Note: Just prior to completing this final report, it was discovered that three months of GARR (June 1995, April 1999, and June 2003.) were inadvertently omitted from the TITAN Analysis. These three months were subsequently processed through TITAN to ascertain any impacts on the results and conclusions of this report. As shown in Figure 16-1, the additional data presented no significant differences in median cell sizes over the full range of peak cell intensities observed in the study and, therefore, no changes to the results and conclusions of this report were warranted.

cells, and approximately 20,000 3-hour cells. Storm cell properties were analyzed over all of eastern Colorado, El Paso County, and the Fountain Creek Watershed.

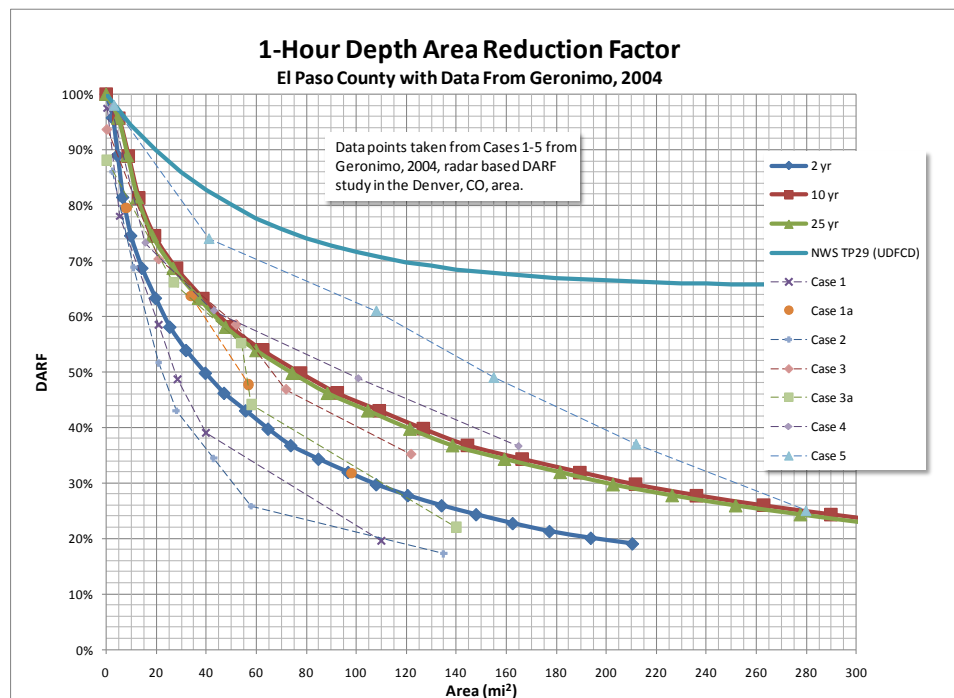
Storm centered Depth Area Reduction Factors (DARFs) were computed and compared to DARFs published by the National Weather Service (NWS) that are widely used in hydrologic design. The results

Table E2.1-1: Data Months Selected for Storm Properties Analysis

June-95	July-03	June-05	October-06
April-99	August-03	July-05	July-07
July-99	April-04	August-05	August-07
August-99	June-04	July-06	August-08
July-01	July-04	August-06	September-08

show significant departures from the standard NWS curves. The radar-based storm centered DARFs developed in this study decay much more sharply than the standard curves published by the NWS in Technical Paper 29.

The DARFs developed in this study are consistent with the results found by Geronimo (2004) during a similar evaluation of radar-based storm centered DARFs in the Denver area. One-hour DARFs for the 2-yr, 10-yr, and 25-yr events in El Paso County are shown in the figure below with the Geronimo results for seven individual storm events (Case 1-5) for Denver and the standard NWS TP29 DARF.



DARF variability with recurrence interval is another significant departure from the NWS TP29 DARF. The Fountain Creek Study showed that for a given peak intensity, a population of storm cell sizes exists and that the median storm cell size varies significantly with peak intensity. Thus, the resulting DARFs, which are area dependent, vary with recurrence interval. Note that low frequency events (i.e. > 50 year return frequency) were not well represented in the available months of rainfall data used in this study.

DARFs were further refined for application to the Fountain Creek Watershed. A proof of concept Design Storm Processor was developed that produces very realistic spatially and temporally variable design storms.

The DARFs found in this study suggest sharply lower design rainfall volumes for stormwater design and planning projects.

1.0 Introduction

Carlton Engineering was authorized by the City of Colorado Springs, on January 12, 2009 to analyze available rain gage and radar rainfall data to determine typical rainfall patterns and design storms for Fountain Creek within El Paso County for planning and design of storm water facilities under Contract C005501, Fountain Creek Watershed Rainfall Characterization Study. The study was funded by the City of Colorado Springs and the Colorado Water Conservation Board.

The Fountain Creek Watershed Rainfall Characterization Study team was led by Carlton Engineering with OneRain, Inc., and HydMet, Inc. as the principal subcontractors. The project



- ✓ Provided radar and rain gage data processing based on national database of radar rainfall estimates and an extensive database of local rain gage observations,
- ✓ Executed specialized software to identify the geometric properties of storms, and
- ✓ Provided gage adjusted radar rainfall estimates for selected storms over the Jimmy Camp Creek drainage.
- ✓ Identified typical storm patterns,
- ✓ Assessed the applicability of uniformity assumptions related to design rain,
- ✓ Assessed Depth Area Reduction Factors,
- ✓ Related local rainfall characteristics to published data,
- ✓ Assessed the suitability of design storm characteristics that may vary with return period,
- ✓ Compared identified storm patterns with other design storms currently used in the region,
- ✓ Assessed the spatial distribution of storm characteristics within the Fountain Creek Watershed and surrounding areas,
- ✓ Evaluated intensity-frequency relationships for short duration events
- ✓ Quantified the distribution of rainfall amounts as a percentage of rainfall events over time, and
- ✓ Identified antecedent runoff conditions for various design storms.

In addition, as proof of concept, a Design Storm Processor was developed to produce realistic static and/or dynamic design storms that represent conditions local to the Fountain Creek Watershed.

2.0 Background

2.1 Climate and Meteorology of Colorado Springs

El Paso County lies in east central Colorado and has an area of 2,158 square miles. Elevations range from 5,095 feet on the southeast border to 14,410 feet at the summit of Pike’s Peak, near the western boundary. The City of Colorado Springs is located in Fountain Creek valley and the adjacent uplands between the plains and the foothills of the Rocky Mountains in eastern central Colorado and in northwest El Paso County. It has an area of 186 square miles and an elevation of 6,035 ft. To the east of the city are rolling prairie grasslands with forested areas to the west in the Rocky Mountain foothills and north in the Palmer Divide.

A main climatic division in Colorado occurs between the Rocky Mountains to the west and plains to the east. The foothills form a transitional zone between the two. At elevations between 5000 and 6000 feet the plains give way abruptly to foothills with elevations of 7000 to 9000 feet and significantly higher annual precipitation and snowfall. To the west of the foothills are the Rocky Mountains with higher peaks over 14,000 feet.

The climate of the plains is semi-arid continental, with low humidity and moderately low precipitation, from 12 -18 inches per year, with higher amounts in the foothills. About 75% of the precipitation falls within the growing season, from April to September. Most of this precipitation comes in the form of thunderstorms, which when severe are called cloudbursts, concentrated in the months of June, July and August. (See Table 2.1-1: Colorado Springs Precipitation Summary) Average annual snowfall at Colorado Springs is 44.6 inches, occurring from mid-October to mid-April. (See Table 2.1-2: Colorado Springs Snowfall Summary) Significant snowmelt runoff flooding has not occurred in the Fountain Creek watershed.

Table 2.1-1: Colorado Springs Precipitation Summary (1948-2010)

Source: National Weather Service, www.crh.noaa.gov/pub/?n=/climate/cli/coloradosprings.php

Jan	Feb	Mar	Apr	May	Jun	Jul	Aug	Sep	Oct	Nov	Dec	Annual
0.28	0.35	1.06	1.62	2.39	2.34	2.85	3.48	1.23	0.86	0.52	0.42	17.40

Table 2.1-2: Colorado Springs Snowfall Summary (1948-2010)

Source: : National Weather Service, www.crh.noaa.gov/pub/?n=/climate/cli/coloradosprings.php

Jan	Feb	Mar	Apr	May	Jun	Jul	Aug	Sep	Oct	Nov	Dec	Annual
5.40	5.10	9.40	6.30	1.30	T	0.00	0.00	0.50	3.70	6.20	6.70	44.60

The climate is influenced by differences in elevation, and to a lesser degree by the orientation of foothills and valleys with respect to general air mass movements from the south, west and north. Major sources of moisture are the Pacific Ocean and the Gulf of Mexico. Storms moving from the west and north generally carry little moisture. Occasional winter interaction of polar outbreaks from the north with moist air from the south results in blizzard conditions.

Warm, moist air from the south arrives intermittently by late spring through summer and generates convective precipitation. The resulting intermittent showers and thundershowers predominate in the June, July and August months. These often become quite severe cloudbursts with strong winds, hail damage and flash flooding. Moist air masses coming from the south are channeled and uplifted by the rising topography of the Fountain Creek watershed east of Colorado Springs. This has created a maximum frequency of cloudbursts in the vicinity of Colorado Springs Airport and north to the Monument Divide.

Figure 2-1 and Figure 2-3 through Figure 2-9 show annual and monthly precipitation maps for the region. Figure 2-2 shows the topographic relief in the immediate vicinity of Colorado Springs in the Fountain Creek Watershed. As noted in Figure 2-3, Fountain Creek annual precipitation varies from 12-14 inches

in the southern tip of the watershed to 32-34 inches in the highest elevation portions along the western watershed boundary.

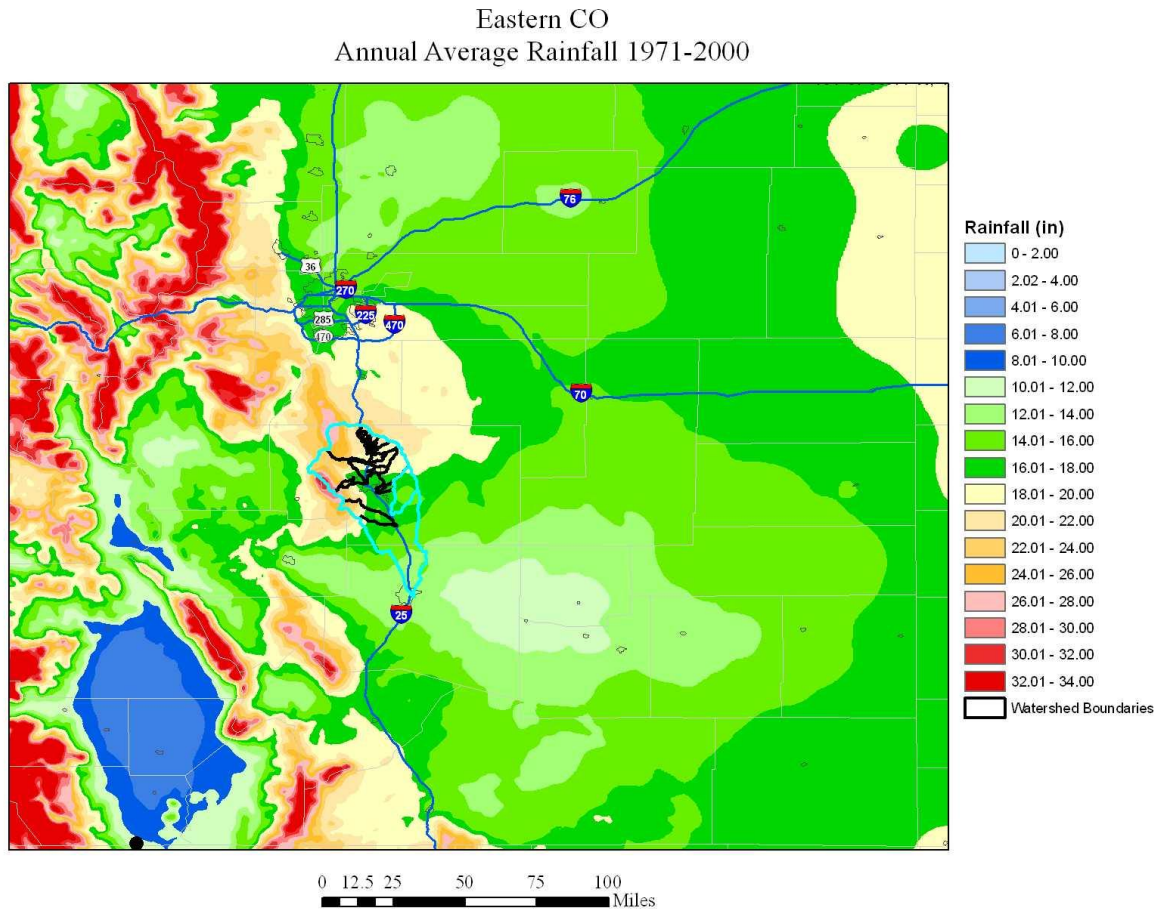


Figure 2-1: Average Annual Rainfall for Eastern Colorado.
(Source: Oregon State University, www.prismclimate.org. Created 28 August, 2006)

The effect of elevation on the distribution of monthly average rainfall in the Fountain Creek Watershed is also clearly seen in Figure 2-3 through Figure 2-9. Higher average monthly rainfall amounts track the higher elevations along the northern periphery of the Fountain Creek Watershed.

Note that there are differences between monthly precipitation totals shown in Table 2.1-1 and Figures 2.1-3 through 2.1-9 in Colorado Springs due to differences in the period of record used in each case.



Figure 2-2: Northern portion of the Fountain Creek Watershed.

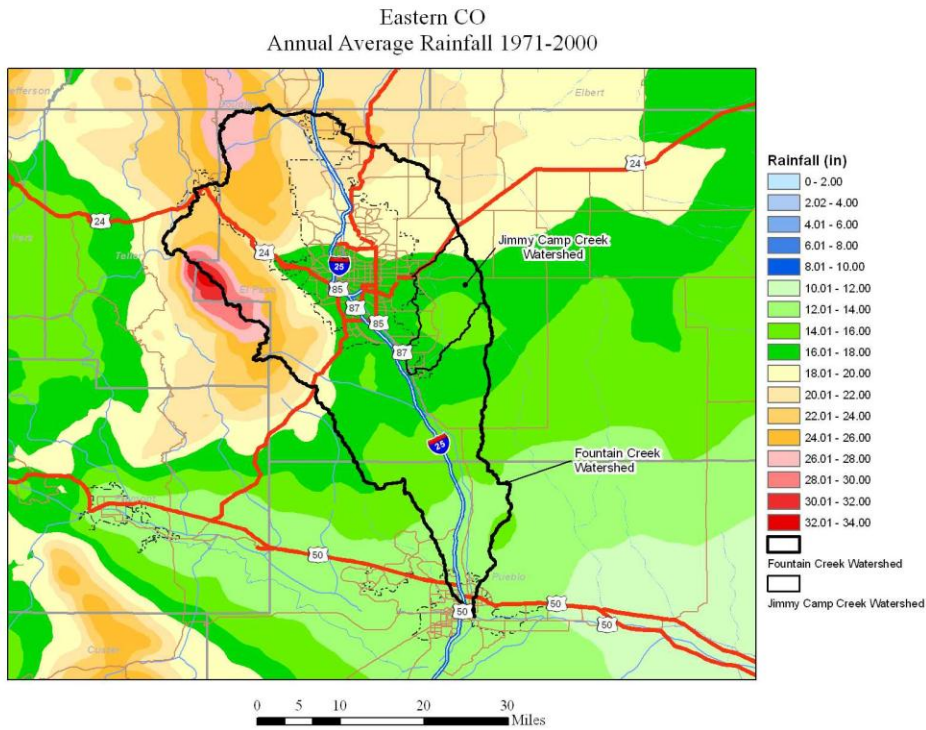


Figure 2-3: Average Annual Rainfall for El Paso County and the Fountain Creek Watershed.
(Source: Oregon State University, www.prismclimate.org. Created 28 August, 2006)

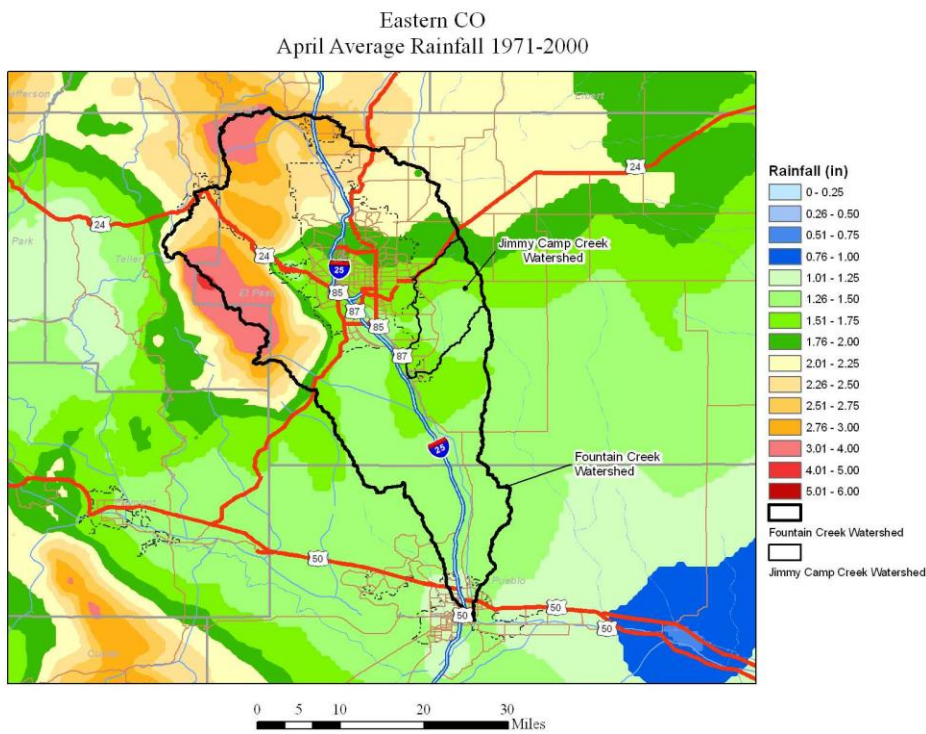
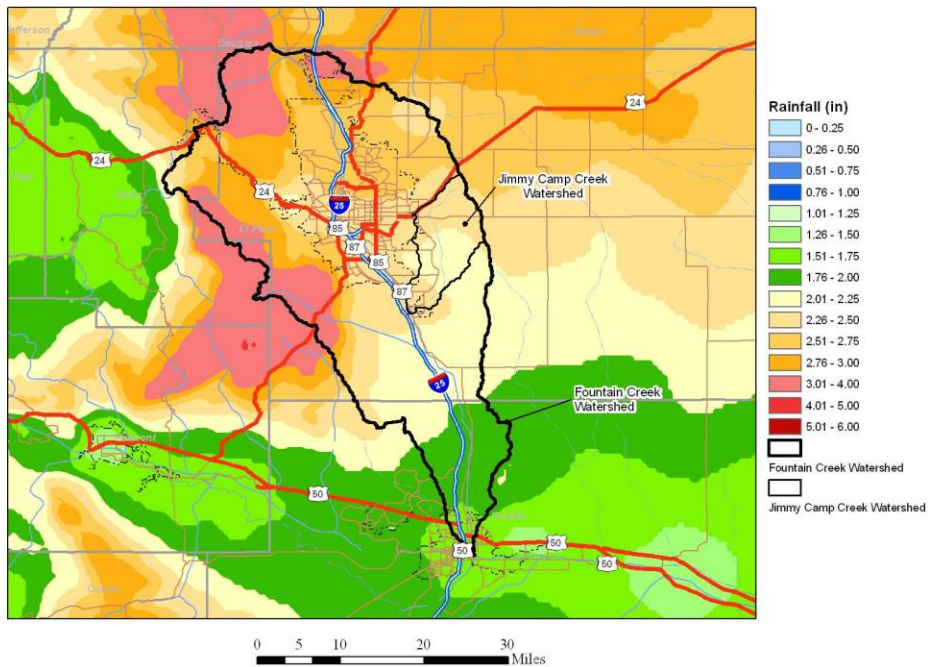


Figure 2-4: Average April Rainfall for El Paso County and the Fountain Creek Watershed
(Source: Oregon State University, www.prismclimate.org. Created 28 August, 2006)

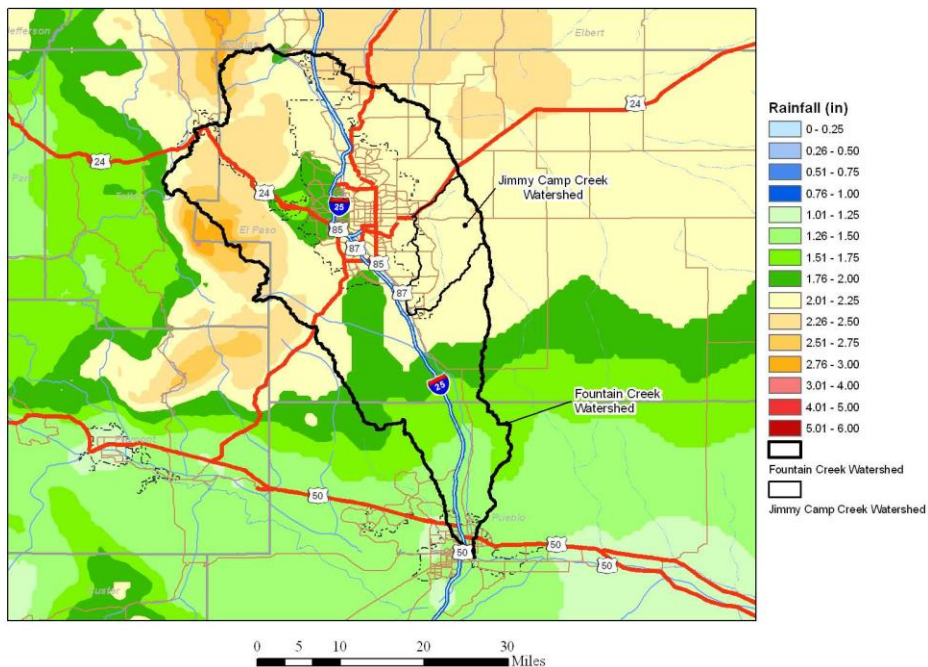
Eastern CO
May Average Rainfall 1971-2000



PRISM Group, Oregon State University, <http://www.prismclimate.org>, created 28 August 2008.

Figure 2-5: Average May Rainfall for El Paso County and the Fountain Creek Watershed (Source: Oregon State University, www.prismclimate.org. Created 28 August, 2006)

Eastern CO
June Average Rainfall 1971-2000



PRISM Group, Oregon State University, <http://www.prismclimate.org>, created 28 August 2008.

Figure 2-6: Average June Rainfall for El Paso County and the Fountain Creek Watershed (Source: Oregon State University, www.prismclimate.org. Created 28 August, 2006)

Eastern CO
July Average Rainfall 1971-2000

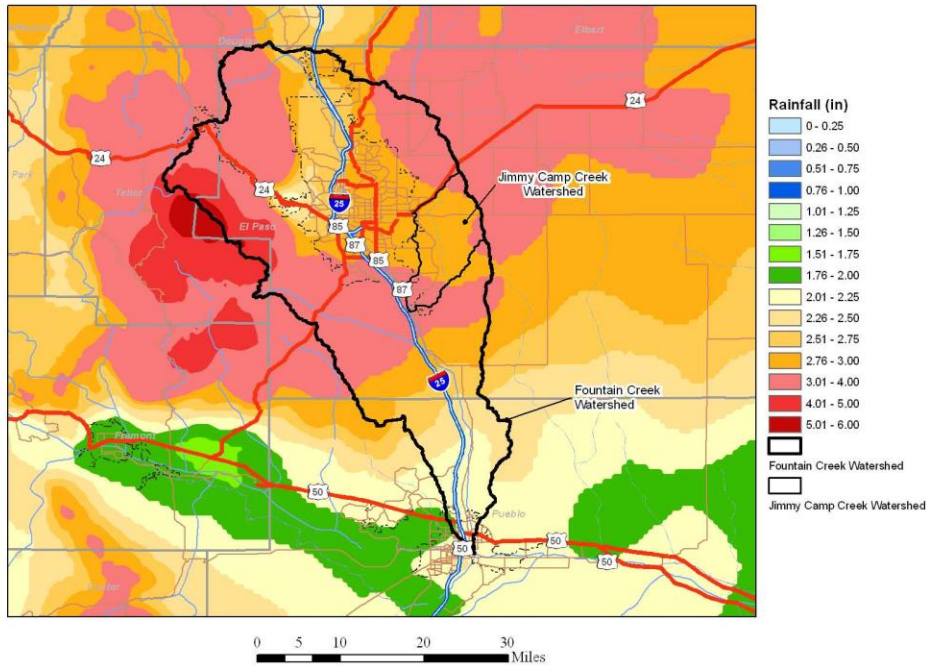


Figure 2-7: Average July Rainfall for El Paso County and the Fountain Creek Watershed (Source: Oregon State University, www.prismclimate.org. Created 28 August, 2006)

Eastern CO
August Average Rainfall 1971-2000

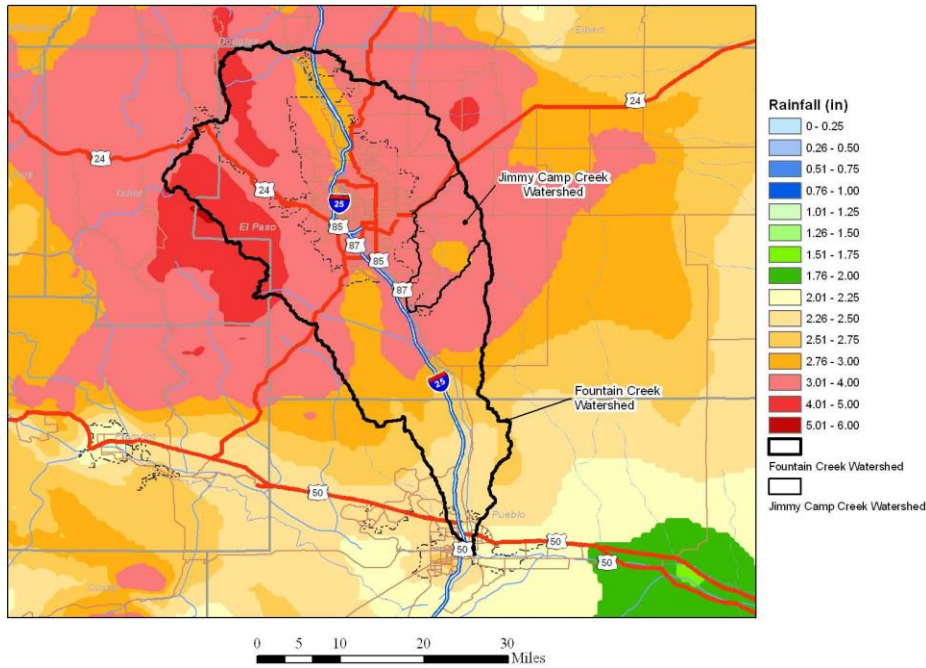


Figure 2-8: Average August Rainfall for El Paso County and the Fountain Creek Watershed (Source: Oregon State University, www.prismclimate.org. Created 28 August, 2006)

Eastern CO
September Average Rainfall 1971-2000

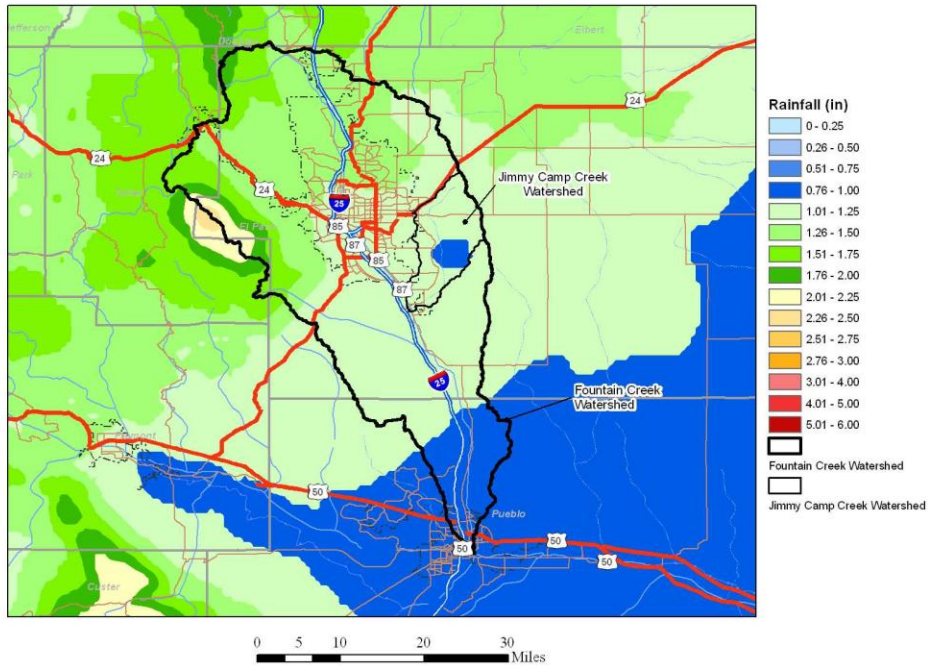


Figure 2-9: Average September Rainfall for El Paso County and the Fountain Creek Watershed (Source: Oregon State University, www.prismclimate.org. Created 28 August, 2006)

Eastern CO
October Average Rainfall 1971-2000

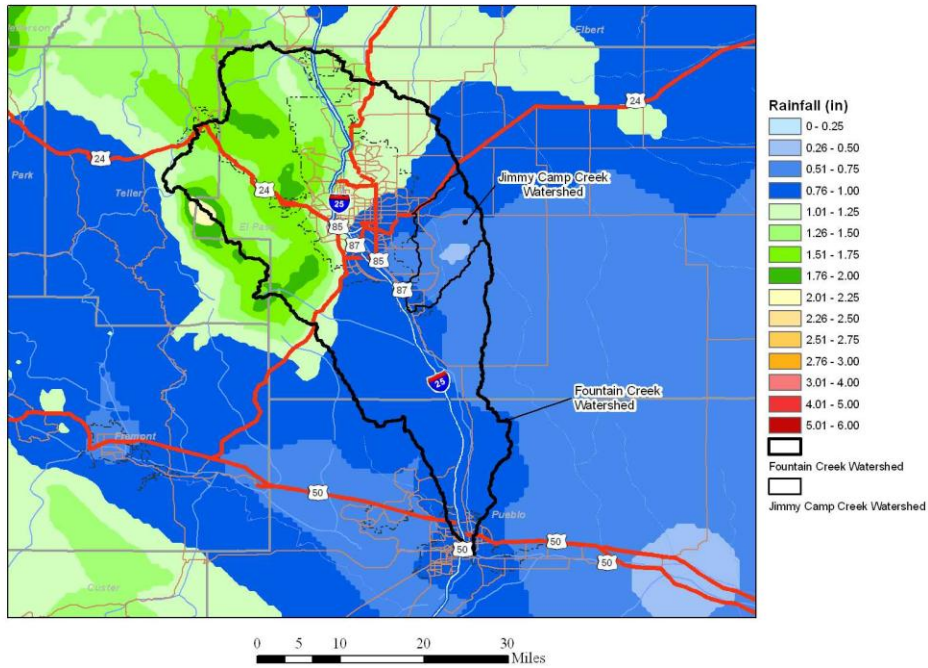
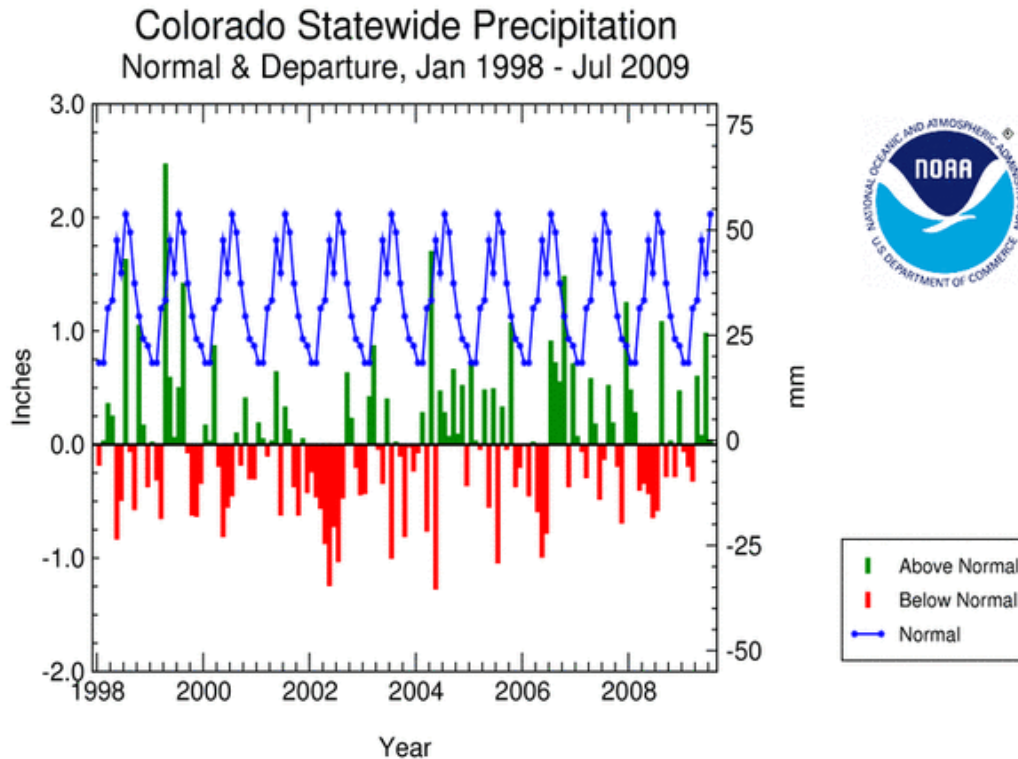


Figure 2-10: Average October Rainfall for El Paso County and the Fountain Creek Watershed (Source: Oregon State University, www.prismclimate.org. Created 28 August, 2006)

In recent years, the western US and Colorado, in particular, have experienced drought conditions more often than not. Figure 2-11 shows Colorado statewide precipitation departures from normal for the period Jan 1998 – July 2009 with a bias toward negative departures.

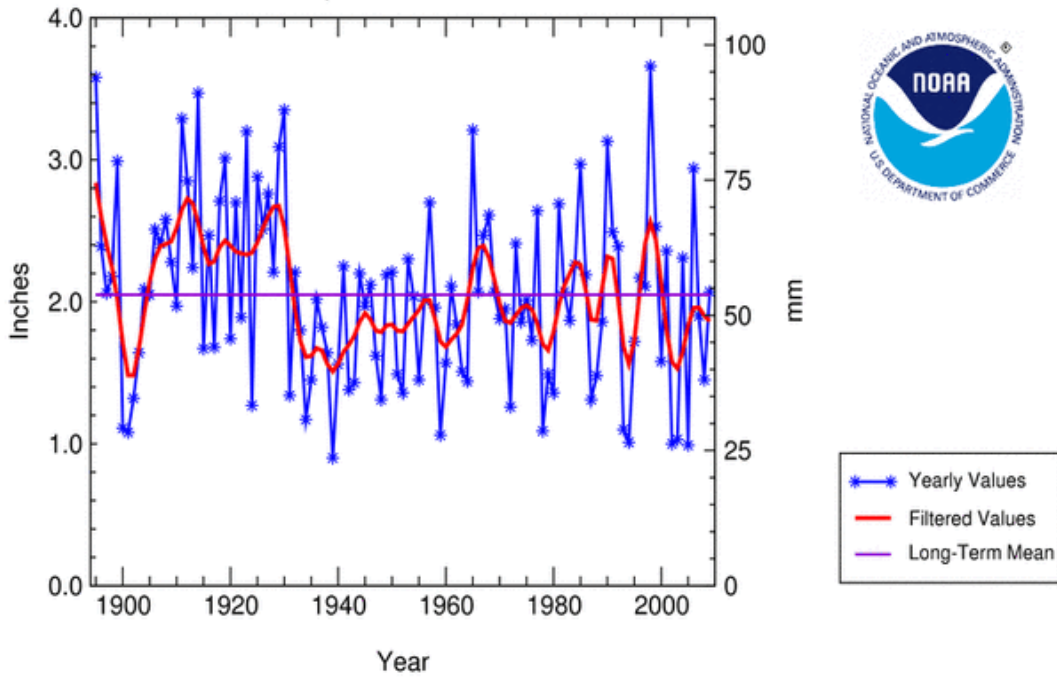


National Climatic Data Center / NESDIS / NOAA

Figure 2-11: Colorado Statewide Precipitation 1998-2009

Figure 2-12 shows 1895-2009 July statewide Colorado precipitation with a strong bias toward drought conditions over the past 75 years relative to the 114 year average. Figure 2-13 presents the Colorado Statewide Palmer Hydrologic Drought Index (PHDI) for the past 109 years. (Note: PDHI measures hydrological impacts of drought (e.g., reservoir levels, groundwater levels, etc.) which take longer to develop and longer to recover from. See <http://www.ncdc.noaa.gov/oa/climate/research/drought/palmer-maps/index.php>) The PDHI shows the strength and dominance of drought conditions in Colorado over the last decade.

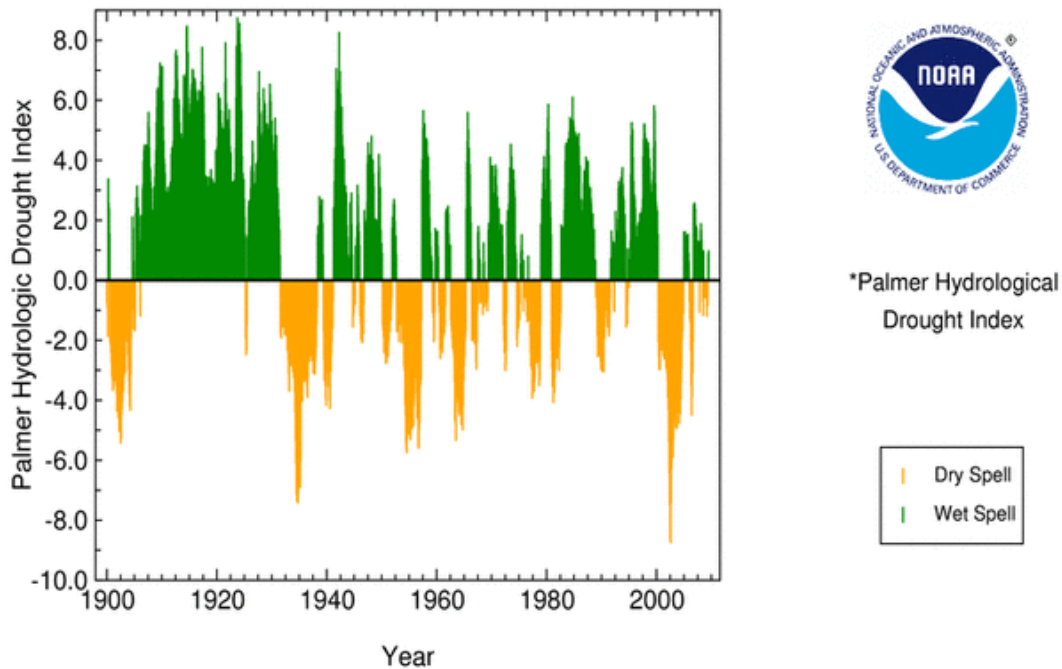
Colorado Statewide Precipitation July, 1895 - 2009



National Climatic Data Center / NESDIS / NOAA

Figure 2-12: Colorado Statewide Precipitation 1895-2009

Colorado Statewide PHDI* January 1900 - July 2009



National Climatic Data Center / NESDIS / NOAA

Figure 2-13: Colorado Statewide Palmer Hydrological Drought Index -1900-2009

2.2 Study Area

Figure 2-14 shows the approximate study area covering approximately 79,000 square miles of eastern Colorado and the Fountain Creek Watershed covering about 929 square miles. The Fountain Creek Watershed and one of its major subwatersheds, Jimmy Camp Creek, are the primary areas of interest in this study. The larger study area is required to accommodate the expected size of some rain cells, to observe as large a sample of storm cells as possible within study time constraints, and to see the spatial variability of storm properties over the region.

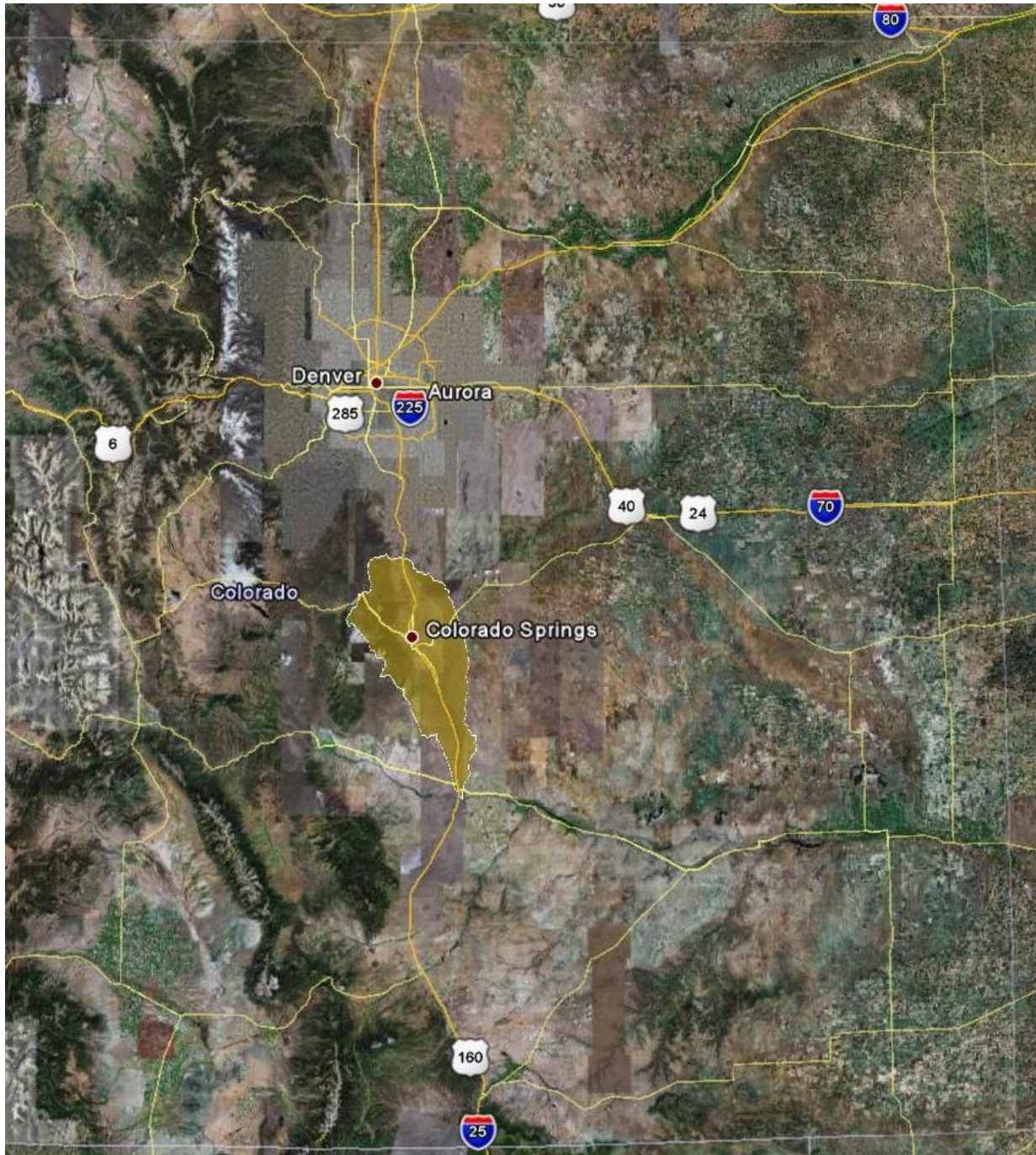


Figure 2-14: Approximate Study Area (Shaded area denotes Fountain Creek Watershed.)

3.0 Depth-Duration-Frequency Curves

3.1 Overview

Compared to synoptic scale storms (for example, fronts and lows), the characteristics of cloudburst storms are severe thunderstorms of limited area, a short duration, and a high intensity precipitation core. Most cloudburst events occur in the June-July-August period with a much lower frequency of occurrence in April-May and September-October. Of the 36 annual flood peaks observed at Jimmy Camp Creek stream gage (USGS 07105900), 34 occurred in the June-August period and two in April and May.

Table 3.1-1 includes rain gages examined to determine average cloudburst season rainfall as well as the average rainfall at these stations during the months included in the TITAN study period. Observed average June-July-August precipitation is provided for comparison with the radar record. The radar record was deliberately biased toward months with more frequent storm events, in order to provide more data for analyses. Higher averages for the radar data were expected.

Figure 3-2 shows the map of these gage locations.

Table 3.1-1: Average Cloudburst Season Precipitation

El Paso County Precipitation Stations									
Station Name	Start	End	Type	Years	Latitude	Longitude	Elevation	Jun-Aug Avg (in)	Radar Avg (in)
Big Springs Ranch	1948	1967	Daily	20	38.8667	104.3167	6043	2.27	3.11
Colorado Springs WSO	1976	2008	Hourly	32	38.8119	104.7111	6140	2.86	3.95
Eastonville 2 NNW	1971	2000	Daily	30	39.1167	104.6000	7210	2.84	3.55
Fountain	1953	1997	Hourly	45	38.6778	104.7014	5560	2.34	3.37
Greenland 6 NE	1948	2008	Hourly	60	39.2167	104.7383	6900	2.36	3.42
Greenland 9 SE	1948	2008	Hourly	60	39.1044	104.7286	7480	2.5	3.73
Manitou Springs	1948	2006	Hourly	53	38.8547	104.9339	6630	2.63	3.49
Monument 2 WSW	1948	1965	Hourly	18	39.0833	104.9167	7346	2.04	3.12
Palmer Lake	1965	1986	Hourly	22	39.1167	104.9167	7220	2.12	3.46
Rush 1N	1971	2000	Daily	30	38.8667	104.1000	6054	2.41	3.46
Simla	1948	2000	Hourly	53	39.1414	104.0844	5980	2.4	3.82
Yoder 2 WNW	1976	2008	Hourly	33	38.8575	104.2561	6180	2.44	3.32
							Averages	2.43	3.48

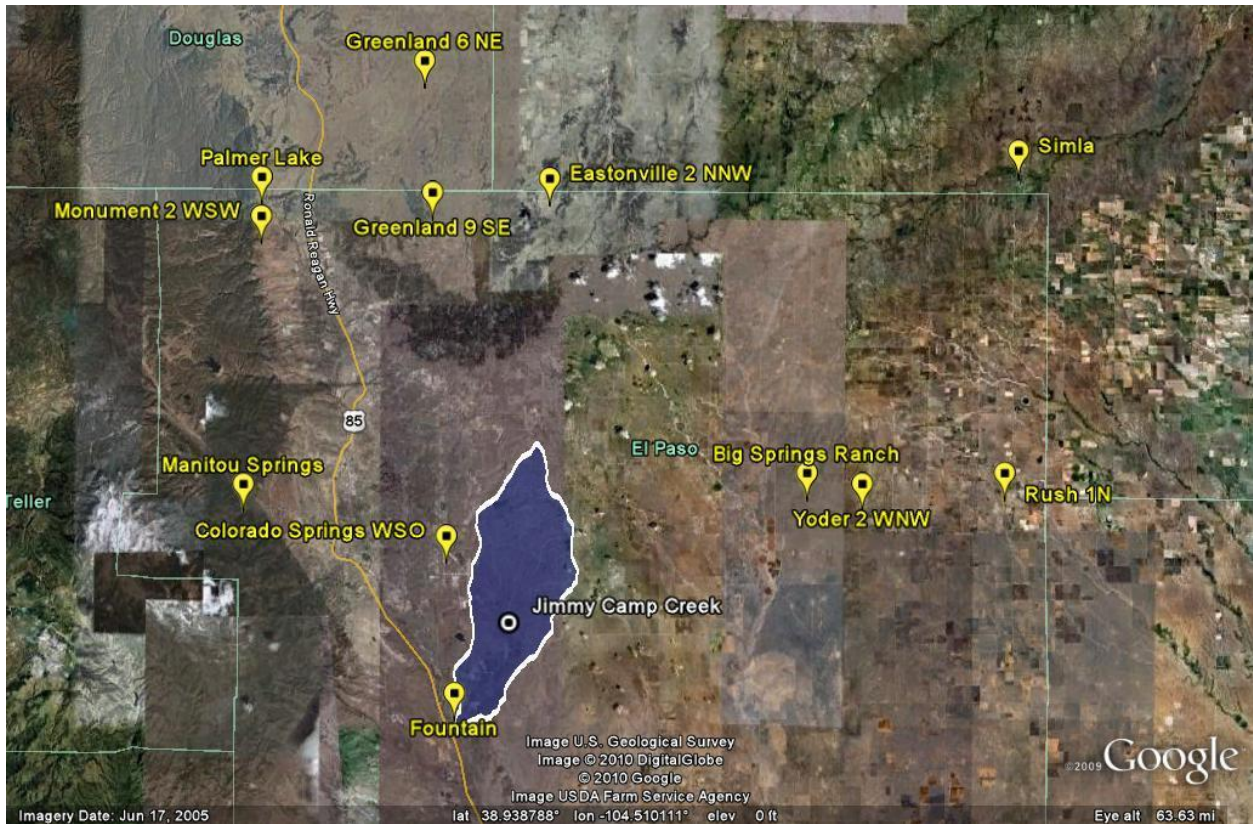


Figure 3-1: Hourly and Daily Rain Gage Locations

3.2 Approach

Short duration precipitation frequency analyses (Depth-Duration-Frequency, DDF, or Intensity-Depth-Frequency, IDF) are used to construct design storms for drainage projects. Existing DDFs for the Fountain Creek watershed were last provided by NOAA National Weather Service in NOAA Atlas 2 Colorado, 1972. NOAA Atlas 2 provided maps and nomographs for determining 1-, 2-, 3-, 6-, 12- and 24-hr precipitation of 2-yr, 5-yr, 10-yr, 25-yr, 50-yr and 100-yr recurrence. A report published by Arkell & Richards (1986) provided a methodology for estimating 15 and 30 minute precipitation from 1-hr values. All records of 5-, 10-, 15-minute data from other sources including NCDC, MesoWest and WeatherUnderground were examined. None of these records were long enough or had reasonable quality for performing DDF analyses.

At the publication date of NOAA Atlas 2 Colorado Springs Airport hourly precipitation data were not available. Other stations, with reasonably long records, in the vicinity of western El Paso County included Manitou Springs, Greenland 9 SE, Greenland 6 NE and Fountain. As part of this study, an analysis was made of hourly DDF for Colorado Springs Airport, Manitou Springs and Greenland 9 SE. The hourly record at Fountain was not used because it was much shorter, poor quality and discontinued in 1980. Greenland 6 NE was outside of El Paso County and outside of Fountain Creek watershed, on the north side of the Palmer Divide. Data from this gage was used to fill in missing events at the Greenland 9 SE gage. The DDF analyses were made using maximum 1-hr through 6-hr values observed in May through September. This period was selected to limit the data sample to cloudburst events. Inclusion of the few significant synoptic scale events exceeding three hours would not have any influence on the design cloudburst parameters. Given the size of Fountain Creek sub-basins, times of concentrations are typically

under three hours. Storm durations longer than three hours of hydrologic significance in the Fountain Creek Watershed are rare and typically comprised of multiple storm cell complexes with single cells of shorter durations.

The data were analyzed using log-normal probability curve fitting with adjustments for the partial duration series and clock hour, as described in NOAA Atlas 2. DDF curves were developed using equations of the form shown in Equation 3.2-1 and 3.2-2.

For durations, $t = 5$ to 30 minutes, and recurrence intervals, T , the rainfall total, $P_{t,T}$, in inches is

$$P_{t,T} = a_1 t^{b_1} \tag{3.2-1}$$

where a_1 and b_1 are parameters. For durations, $t = 30$ to 360 minutes, and recurrence intervals, T , the rainfall total, $P_{t,T}$, in inches is

$$P_{t,T} = a_2 t^{b_2} \tag{3.2-2}$$

where a_2 and b_2 are parameters.

Numerous studies performed by the principle investigators and numerous literature citations have found that DDF and IDF data often fit simple power equations, (i.e. straight-line relationships on log-log plots ($I=At^B$)). Curved or kinked relationships were found to be the result of mixed populations (such as air mass cloudbursts and tropical storms) or mixed records (short length for short durations, long length for long durations). In many cases, the short duration data, 15-minute and shorter, have many more missing annual events than 60-minute or longer data, which frequently introduces a pronounced (steeper slope) curve below 30-60 minutes.

The fitted parameters for Equation 3.2-1 and 3.2-2 are presented in Table 3.2-1. Calculated DDFs for the Colorado Springs Airport are shown in Table 3.2-2 and in Figure 3-2.

Table 3.2-1: Parameters for Colorado Springs Airport DDF Equations

5-min to 30-min			30-min to 360-min		
$P_{t,T} = a_1 t^{b_1}$			$P_{t,T} = a_2 t^{b_2}$		
Recurrence	a_1	b_1	Recurrence	a_2	b_2
1-Year	0.134	0.510	1-Year	0.336	0.240
2-Year	0.184	0.510	2-Year	0.460	0.240
5-Year	0.281	0.510	5-Year	0.703	0.240
10-Year	0.332	0.510	10-Year	0.831	0.240
25-Year	0.406	0.510	25-Year	1.017	0.240
50-Year	0.476	0.510	50-Year	1.194	0.240
100-Year	0.538	0.510	100-Year	1.348	0.240
500-Year	0.706	0.510	500-Year	1.768	0.240
1000-Year	0.847	0.510	1000-Year	2.122	0.240

Table 3.2-2: Depth Duration Frequency Tables

Equations														
5 to 30 minute		$P_{t,T} = a_1 t^{b_1}$												
30 to 360 minute		$P_{t,T} = a_2 t^{b_2}$												
Colorado Springs Airport														
Recurrence	a_1	b_1	a_2	b_2		5	15	30	60	120	180	240	300	360
1-Year	0.134	0.510	0.336	0.240	1-Year	0.30	0.53	0.76	0.90	1.06	1.17	1.25	1.32	1.38
2-Year	0.184	0.510	0.460	0.240	2-Year	0.42	0.73	1.04	1.23	1.45	1.60	1.71	1.81	1.89
5-Year	0.281	0.510	0.703	0.240	5-Year	0.64	1.12	1.59	1.88	2.22	2.44	2.62	2.76	2.89
10-Year	0.332	0.510	0.831	0.240	10-Year	0.75	1.32	1.88	2.22	2.62	2.89	3.10	3.27	3.41
25-Year	0.406	0.510	1.017	0.240	25-Year	0.92	1.62	2.30	2.72	3.21	3.54	3.79	4.00	4.18
50-Year	0.476	0.510	1.194	0.240	50-Year	1.08	1.90	2.70	3.19	3.77	4.15	4.45	4.69	4.90
100-Year	0.538	0.510	1.348	0.240	100-Year	1.22	2.14	3.05	3.60	4.25	4.69	5.02	5.30	5.54
500-Year	0.706	0.510	1.768	0.240	500-Year	1.60	2.81	4.00	4.72	5.58	6.15	6.59	6.95	7.26
1000-Year	0.847	0.510	2.122	0.240	1000-Year	1.92	3.37	4.80	5.67	6.69	7.38	7.91	8.34	8.71
Manitou Springs														
Recurrence	a_1	b_1	a_2	b_2		5	15	30	60	120	180	240	300	360
1-Year	0.193	0.334	0.200	0.330	1-Year	0.33	0.48	0.60	0.77	0.97	1.11	1.22	1.31	1.40
2-Year	0.243	0.345	0.249	0.339	2-Year	0.42	0.62	0.79	1.00	1.26	1.45	1.59	1.72	1.83
5-Year	0.311	0.357	0.333	0.339	5-Year	0.55	0.82	1.05	1.34	1.69	1.94	2.14	2.31	2.46
10-Year	0.365	0.362	0.392	0.345	10-Year	0.65	0.97	1.25	1.61	2.04	2.35	2.59	2.80	2.98
25-Year	0.438	0.368	0.422	0.378	25-Year	0.79	1.19	1.53	1.98	2.58	3.00	3.35	3.64	3.90
50-Year	0.493	0.375	0.527	0.358	50-Year	0.90	1.36	1.76	2.29	2.93	3.39	3.76	4.07	4.35
100-Year	0.552	0.381	0.588	0.365	100-Year	1.02	1.55	2.01	2.62	3.38	3.92	4.35	4.72	5.04
500-Year	0.727	0.387	0.820	0.357	500-Year	1.35	2.07	2.71	3.54	4.54	5.24	5.81	6.29	6.72
1000-Year	0.790	0.392	0.919	0.360	1000-Year	1.48	2.28	3.00	4.01	5.15	5.96	6.61	7.16	7.65
Greenland 9 SE														
Recurrence	a_1	b_1	a_2	b_2		5	15	30	60	120	180	240	300	360
1-Year	0.180	0.334	0.187	0.330	1-Year	0.31	0.44	0.56	0.72	0.91	1.04	1.14	1.23	1.30
2-Year	0.228	0.345	0.234	0.339	2-Year	0.40	0.58	0.74	0.94	1.18	1.36	1.50	1.62	1.72
5-Year	0.290	0.357	0.311	0.339	5-Year	0.51	0.76	0.98	1.25	1.58	1.81	2.00	2.16	2.29
10-Year	0.331	0.362	0.355	0.345	10-Year	0.59	0.88	1.14	1.46	1.85	2.13	2.35	2.54	2.70
25-Year	0.398	0.368	0.383	0.378	25-Year	0.72	1.08	1.39	1.80	2.34	2.73	3.04	3.31	3.54
50-Year	0.442	0.375	0.473	0.358	50-Year	0.81	1.22	1.58	2.05	2.63	3.04	3.37	3.65	3.90
100-Year	0.486	0.381	0.518	0.365	100-Year	0.90	1.36	1.77	2.31	2.97	3.45	3.83	4.16	4.44
500-Year	0.640	0.387	1.204	0.357	500-Year	1.19	1.82	2.38	3.20	4.16	4.86	5.43	5.92	6.36
1000-Year	0.707	0.392	0.823	0.360	1000-Year	1.33	2.04	2.68	3.59	4.61	5.34	5.92	6.41	6.85

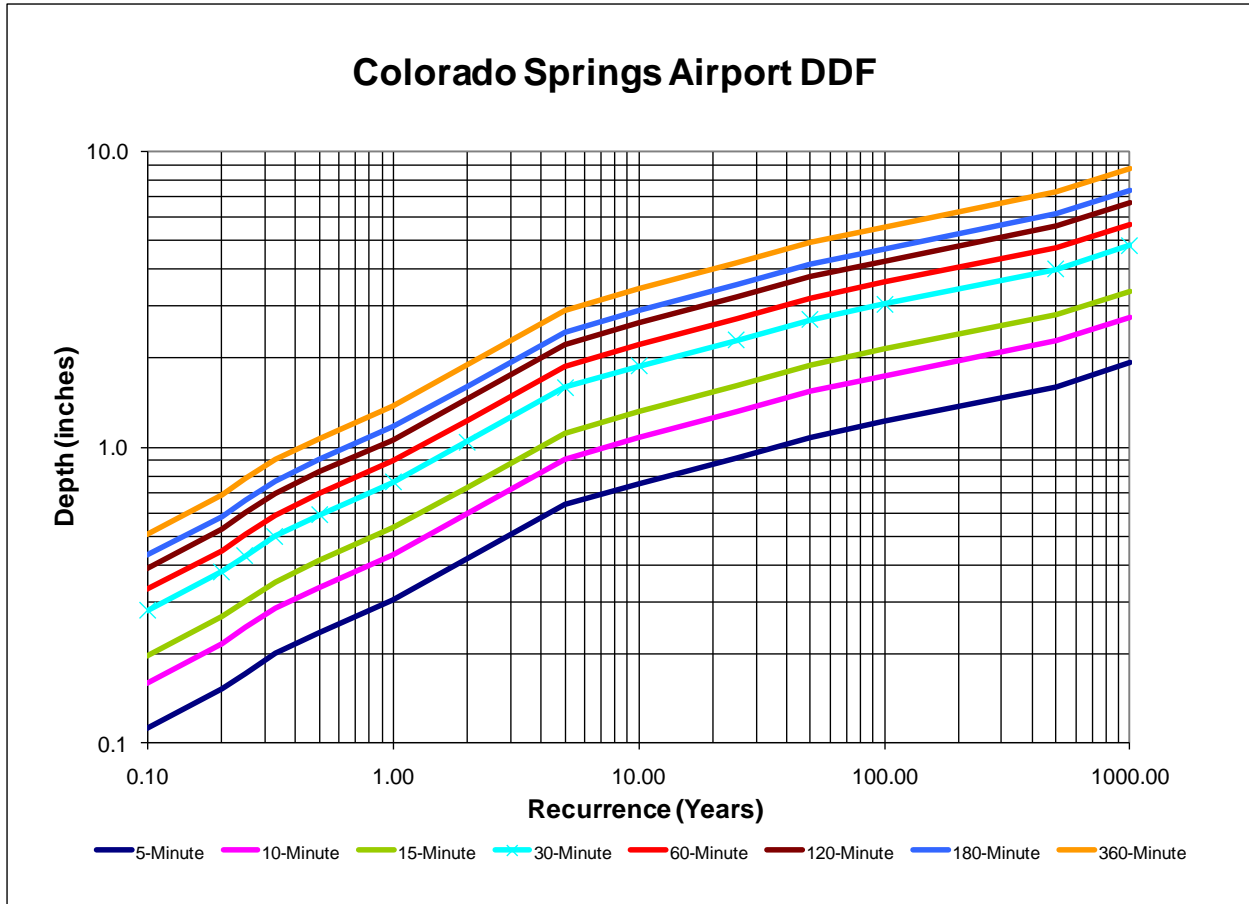


Figure 3-2: Colorado Springs Airport DDFs

3.3 Results

Table 3.3-1 shows the 1-hour distributions compared to NOAA Atlas 2. This table shows that Greenland and Manitou Springs gages have reasonable agreement with the NOAA Atlas, as would be expected since these stations were used by NOAA for their analyses. However, Colorado Springs Airport shows significantly greater values not reflected on the NOAA Atlas 2 maps. Colorado Springs Airport data was not available for Atlas 2.

Table 3.3-1: 1-Hour DDF Comparison

Station	1-Yr	2-Yr	5-Yr	10-Yr	25-Yr	50-Yr	100-Yr
Greenland 9SE	0.72	0.94	1.25	1.46	1.80	2.05	2.31
Manitou Springs	0.77	1.00	1.34	1.61	1.98	2.29	2.62
Colorado Springs Airport	0.90	1.23	1.88	2.22	2.72	3.19	3.60
NOAA Atlas 2		1.17	1.55	1.79	2.00	2.35	2.57

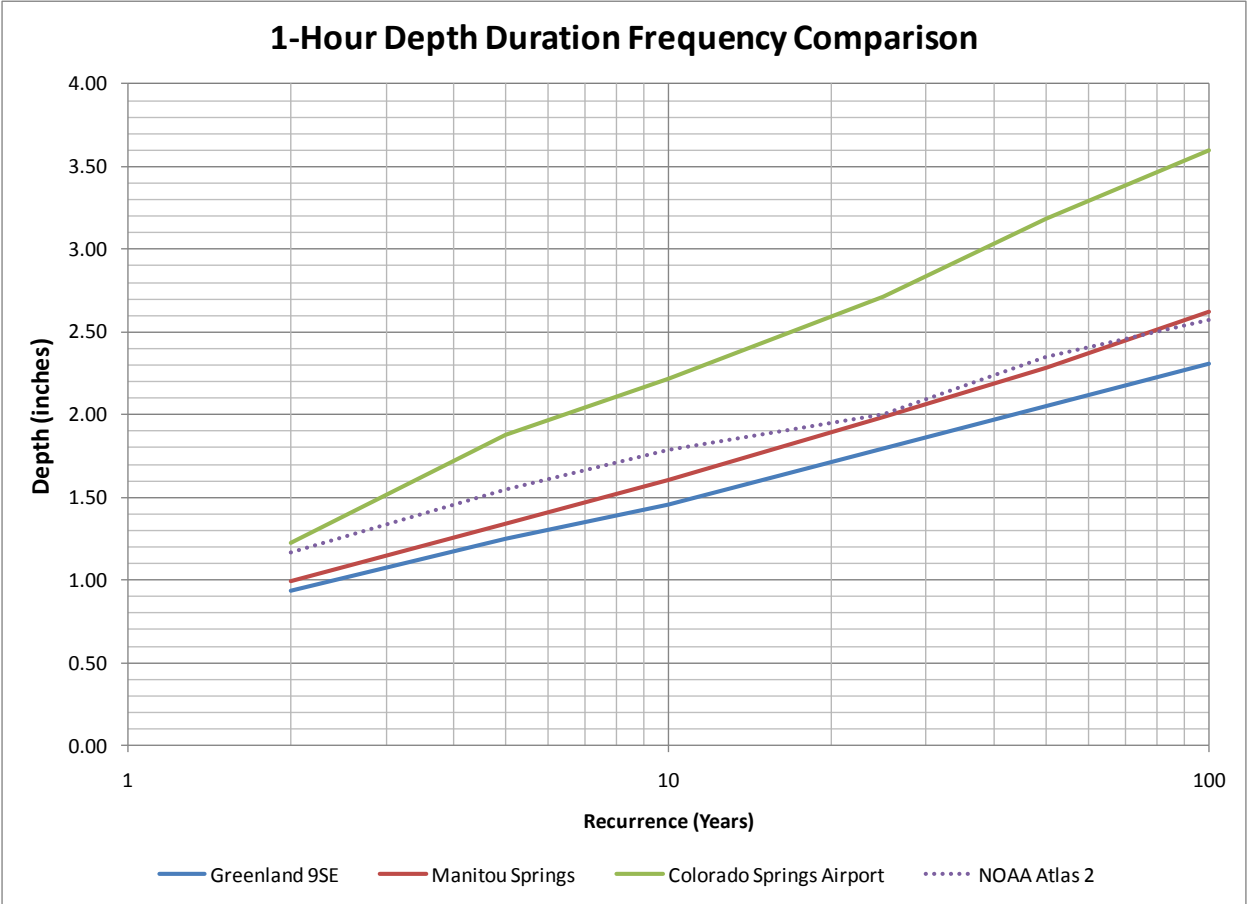


Figure 3-3: 1-Hour DDF Comparison

3.4 Key Findings

- Colorado Springs Airport shows significantly greater values not reflected on the NOAA Atlas 2 maps.

4.0 Storm Event Analysis and Summary

4.1 Overview

The distributions of historical rainfall amounts as defined by available long-term rain gage records were reviewed. It is intended that these distributions will be used to evaluate the effectiveness of water quality and runoff reduction

4.2 Approach

Five long-term hourly stations were available for this analysis in the Fountain Creek watershed or vicinity including:

- Colorado Springs Airport (1974-2008),
- Manitou Springs (1948-2006),
- Fountain (1953-1997),
- Greenland 9SE (1949-2008), and
- Greenland 6NE (1949-2008).

The months of November through March were not used since nearly all events were snowfall.

The Fountain record had many missing months of data and was not used. Although Greenland 6 NE is just north of the El Paso County line, it had a fairly complete record and was used for comparison to Greenland 9 SE.

The Colorado Springs Airport record had only a few minor events with missing distributions and was by far the most accurate. The other three stations had problems of various types. When entire months were missing data, records were substituted from the nearest of the four stations. When the length and accumulated depth of the missing event were shown, rainfall was distributed equally over the hours missing. In most cases, the station was shown as missing data for several days, with an accumulated total at the end. In these cases, events from surrounding stations were adjusted by an accumulated depth ratio and substituted. For events during the radar data months, some distributions were determined from the radar data. It was found that nearly all significant missing events were one or two hour duration cloudbursts.

Since the recommended design storms from this study will depend on the Colorado Springs Airport data and the radar data, the procedures for filling in rainfall data had no influence on the results. As expected, the DDF analyses for Manitou Springs and Greenland 9 SE essentially agreed with NOAA Atlas 2. Approximately 10% of the annual maximum 2-hour data for these gages were estimated. The data filling procedure was not likely to influence the results for these gages.

The number of rainfall events of a given total depth and duration was accumulated and summarized. A storm event was defined as measured rainfall equal to and greater than 0.1 inches occurring 6 hours or more from another event greater than 0.1 inches. Storm events were grouped by 0.1 inch intervals up to a storm total of 5.0 inches.

4.3 Results

Three types of graphs were prepared: storm frequency, storm duration and storm intensity. Figure 4-1 through Figure 4-12 show results for Colorado Springs Airport, Greenland 6 NE, Greenland 9 SE, and Manitou Springs. Several events were shown with long durations. These were all multiple cloudburst events (i.e. High intensity segments separated by several hours of no or very low intensity rainfall or

preceded/followed by hydrologically insignificant low intensity rainfall) or continuous relatively low intensity rainfall associated with slow moving fronts or synoptic lows.

The most significant finding is that Colorado Springs Airport has quite different statistics compared to the other three gages. For storm frequency, all gage records show a maximum for the lowest interval (0.1-0.2 in.). At the 1 event per year frequency, the gages agree with storm depth in the interval of 0.5 to 0.6 in. The maximum observed storm depth was 4.5 in. at Colorado Springs Airport, with 3.0 in. at the other stations. However, for storm duration, Colorado Springs Airport has three events over three inches, with the other gages one event over three inches.

For storm intensity, the differences are greater, with Colorado Springs Airport six events over 2.5 inches per hour, Greenland 6 NE one event, Manitou Springs one event and Greenland 9 SE two events. It is also noteworthy that Colorado Springs Airport has a much shorter record. This suggests that Colorado Springs Airport has significantly higher frequency, longer duration and higher intensity for the largest cloudburst events.

Figure 4-13 through Figure 4-15 summarizes the results of Figure 4-1 through Figure 4-12 for each category: storm frequency (i.e. average number of events/year), median storm duration, and average storm intensity.

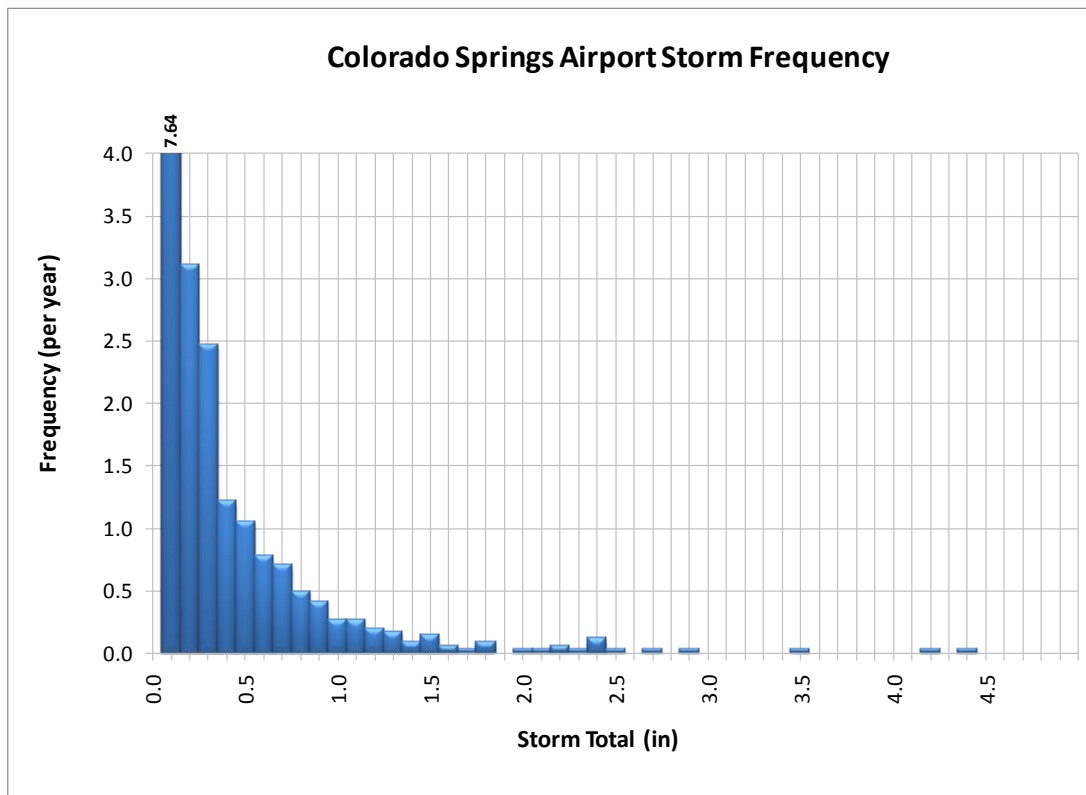


Figure 4-1: Colorado Springs Airport Storm Frequency

4.4 Key Findings

- Colorado Springs Airport has quite different statistics compared to the Greenland 6NE, Greenland 9E, and Manitou Springs gages.

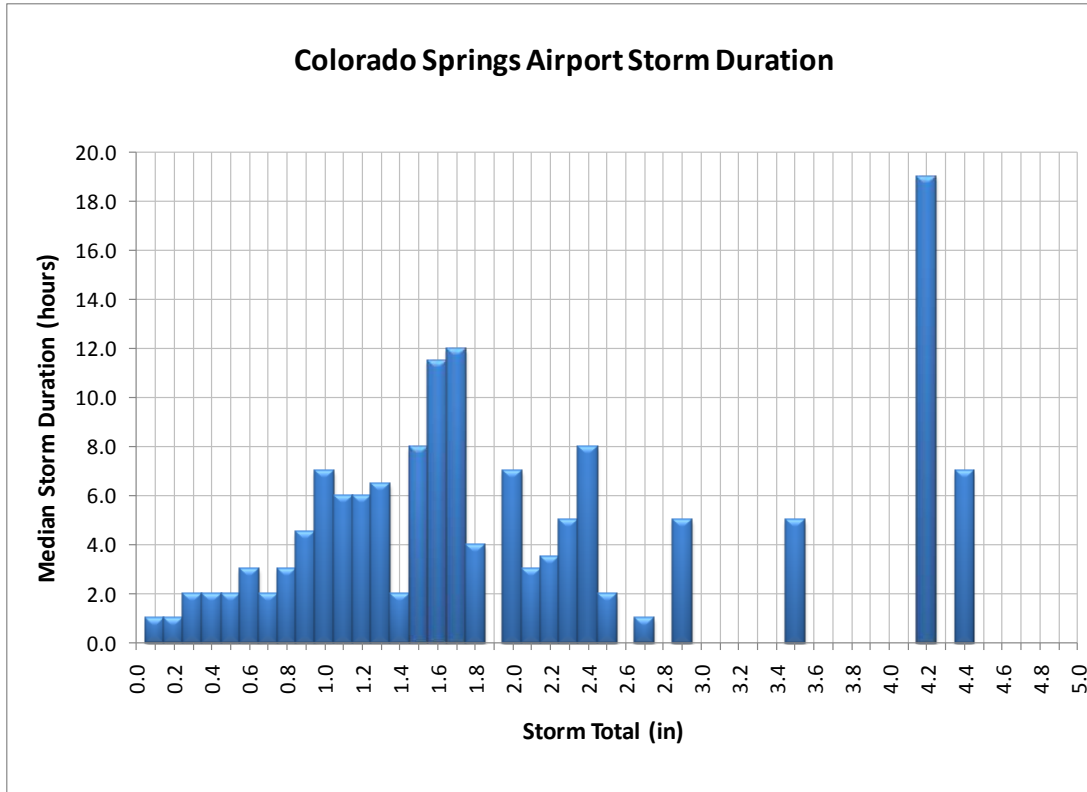


Figure 4-2: Colorado Springs Airport Storm Duration

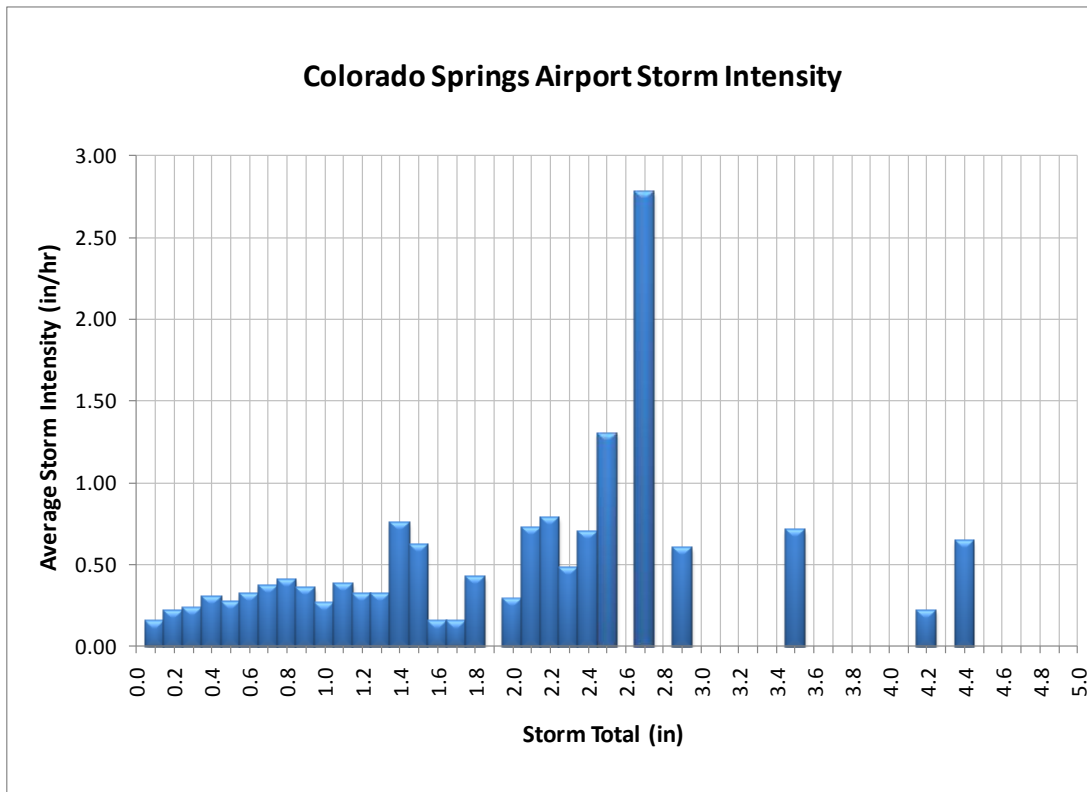


Figure 4-3: Colorado Springs Airport Storm Intensity

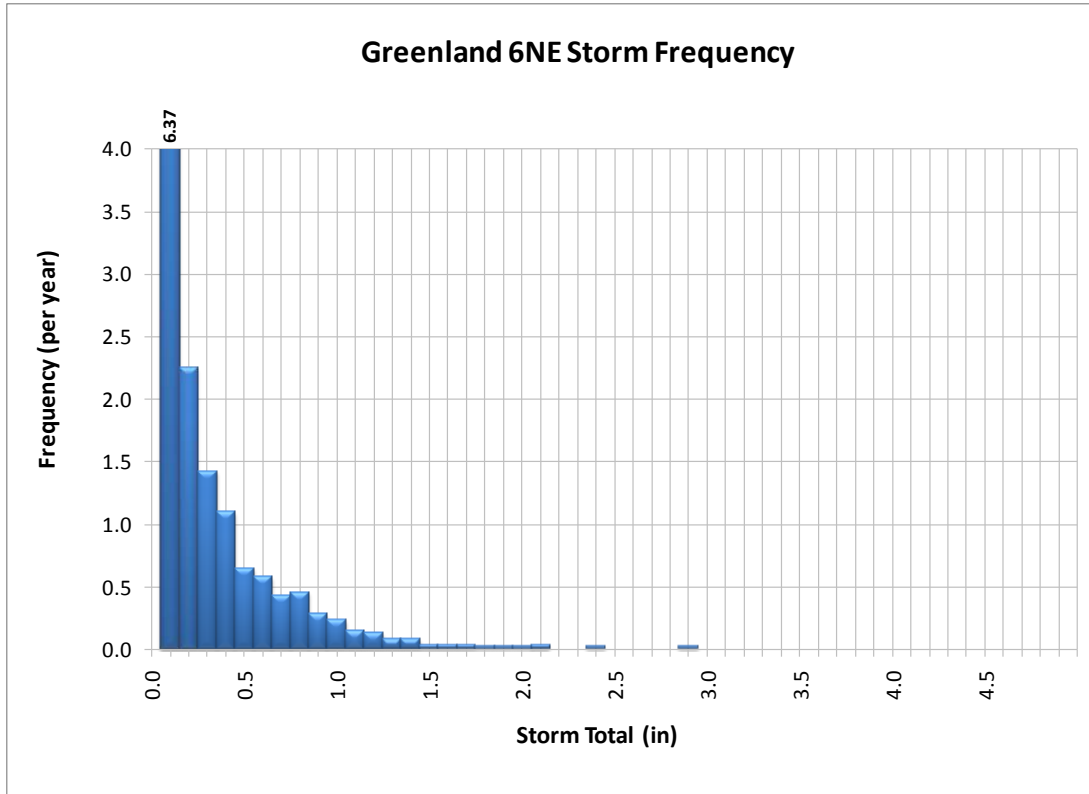


Figure 4-4: Greenland 6NE Storm Frequency

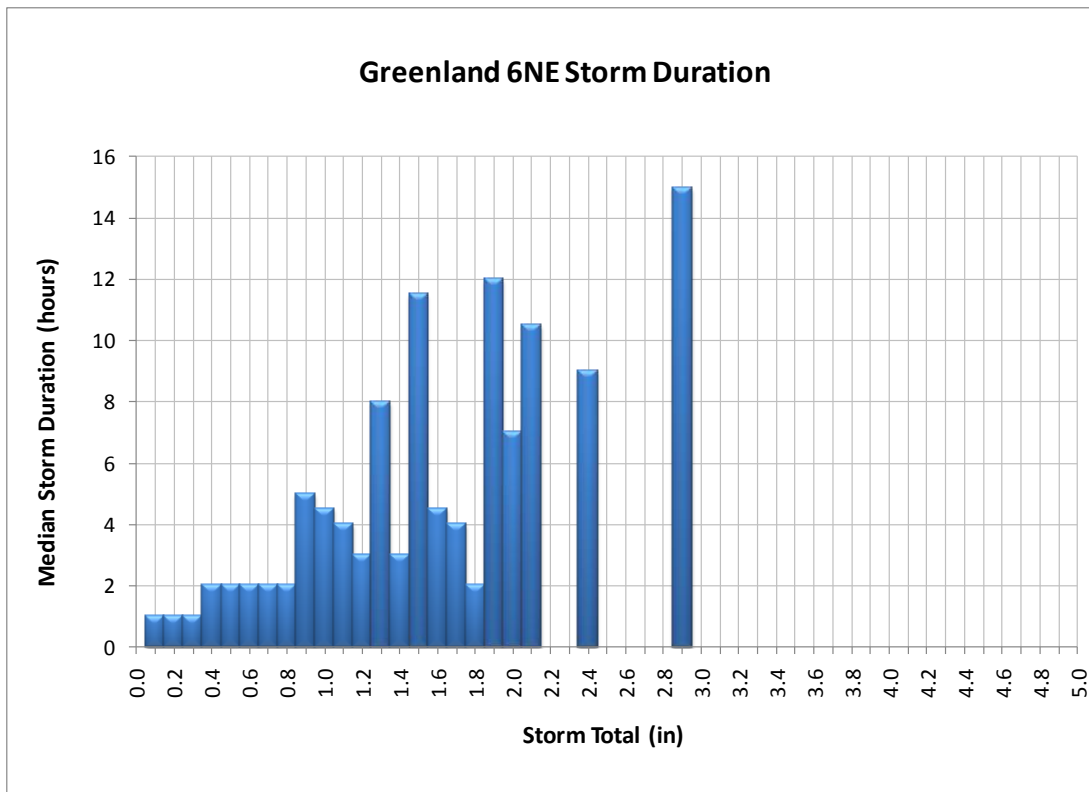


Figure 4-5: Greenland 6NE Storm Duration

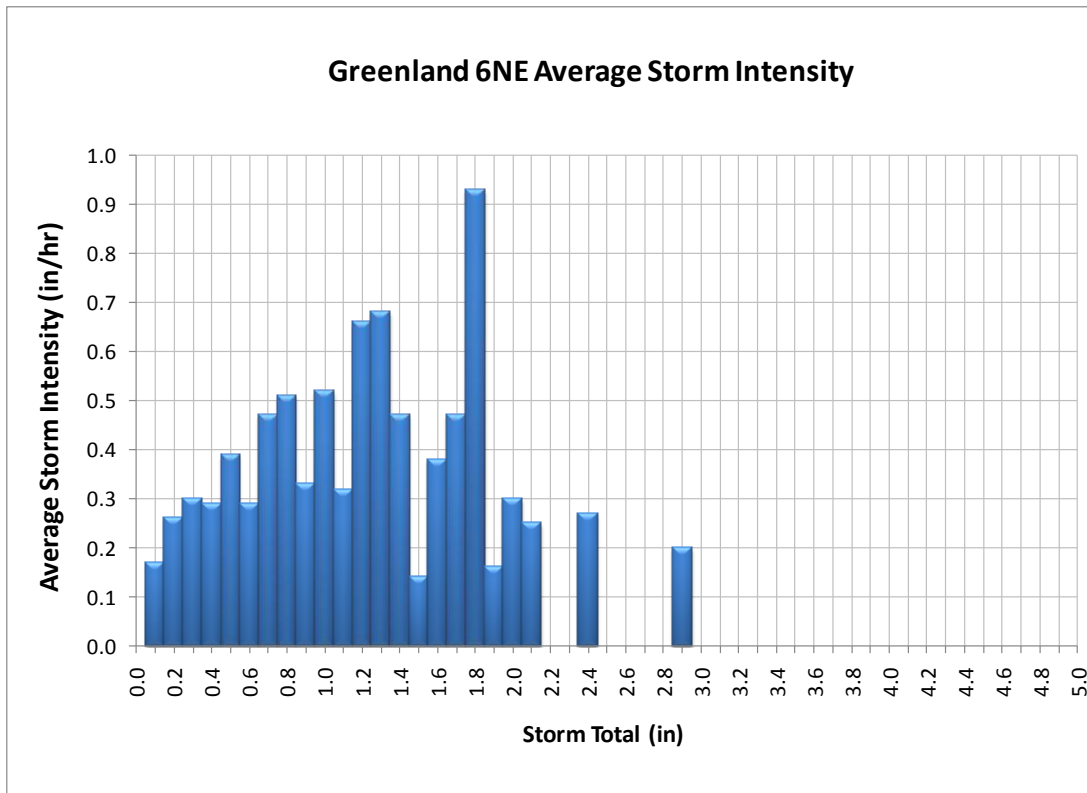


Figure 4-6: Greenland 6NE Storm Intensity

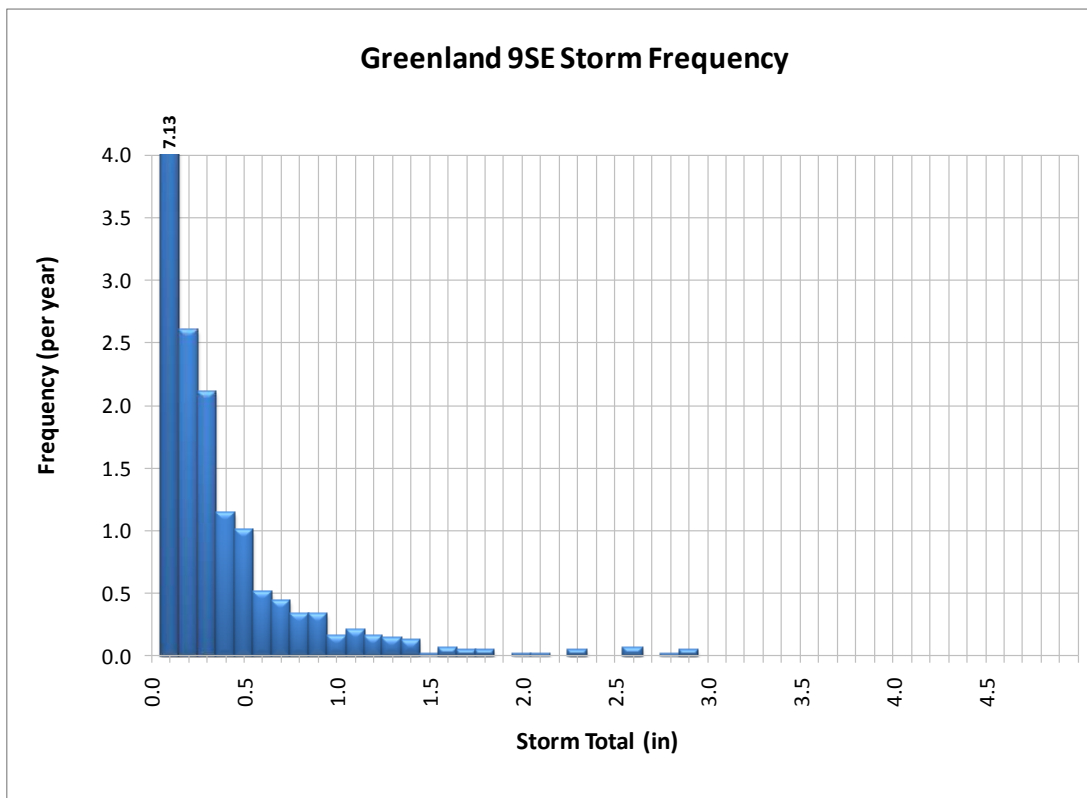


Figure 4-7: Greenland 9SE Storm Frequency

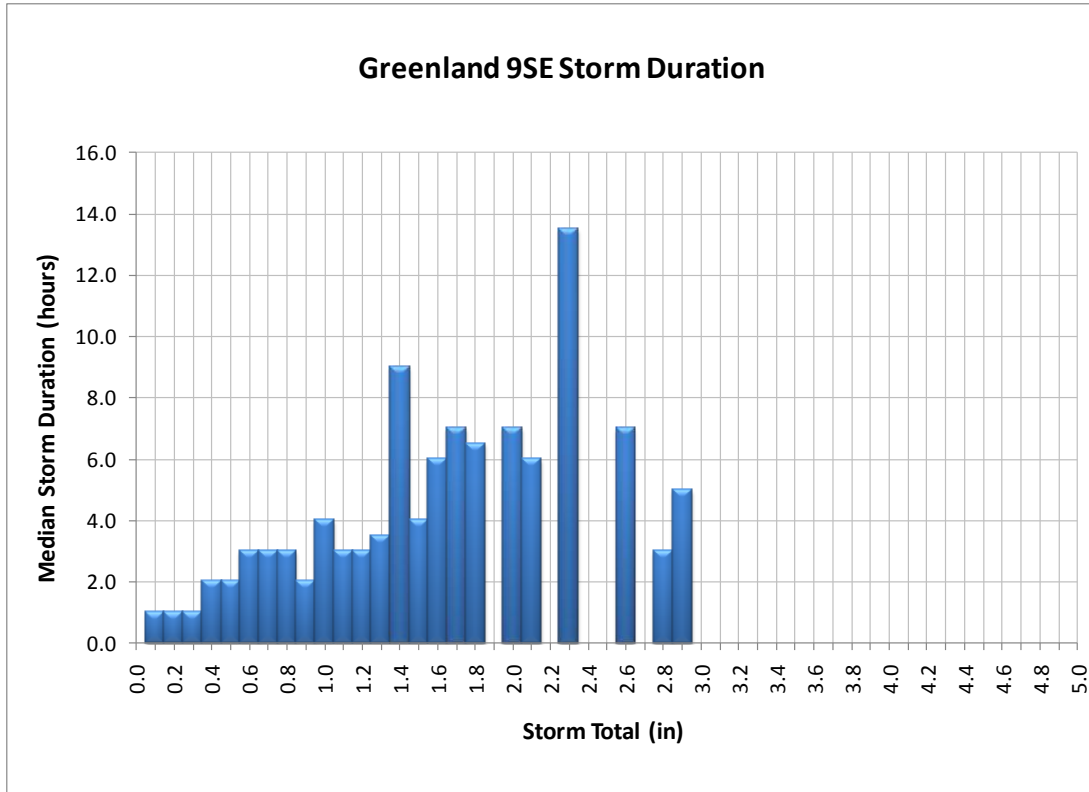


Figure 4-8: Greenland 9SE Storm Duration

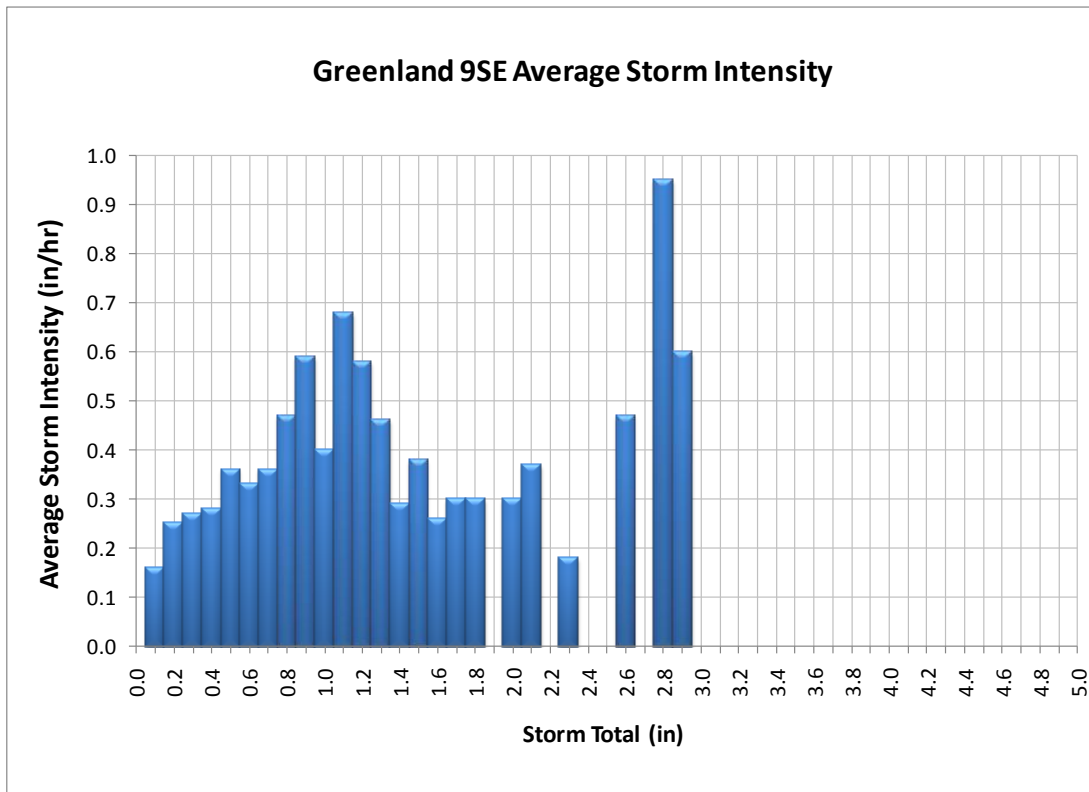


Figure 4-9: Greenland 9SE Storm Intensity

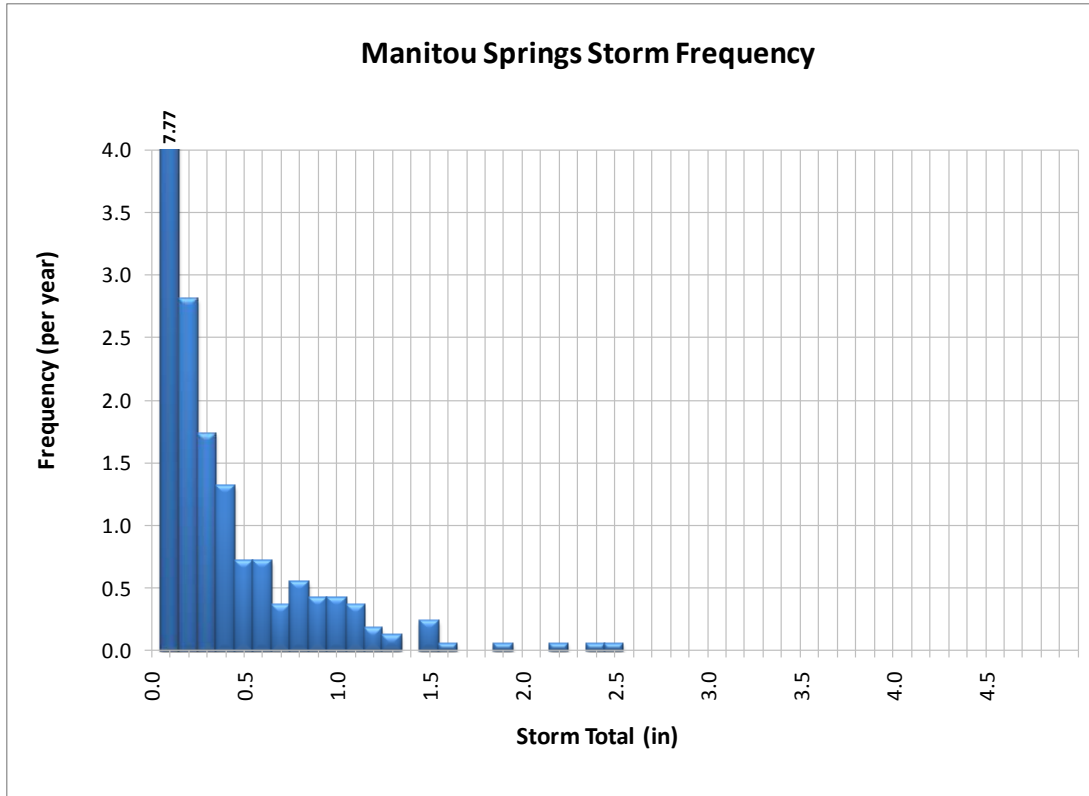


Figure 4-10: Manitou Springs Storm Frequency

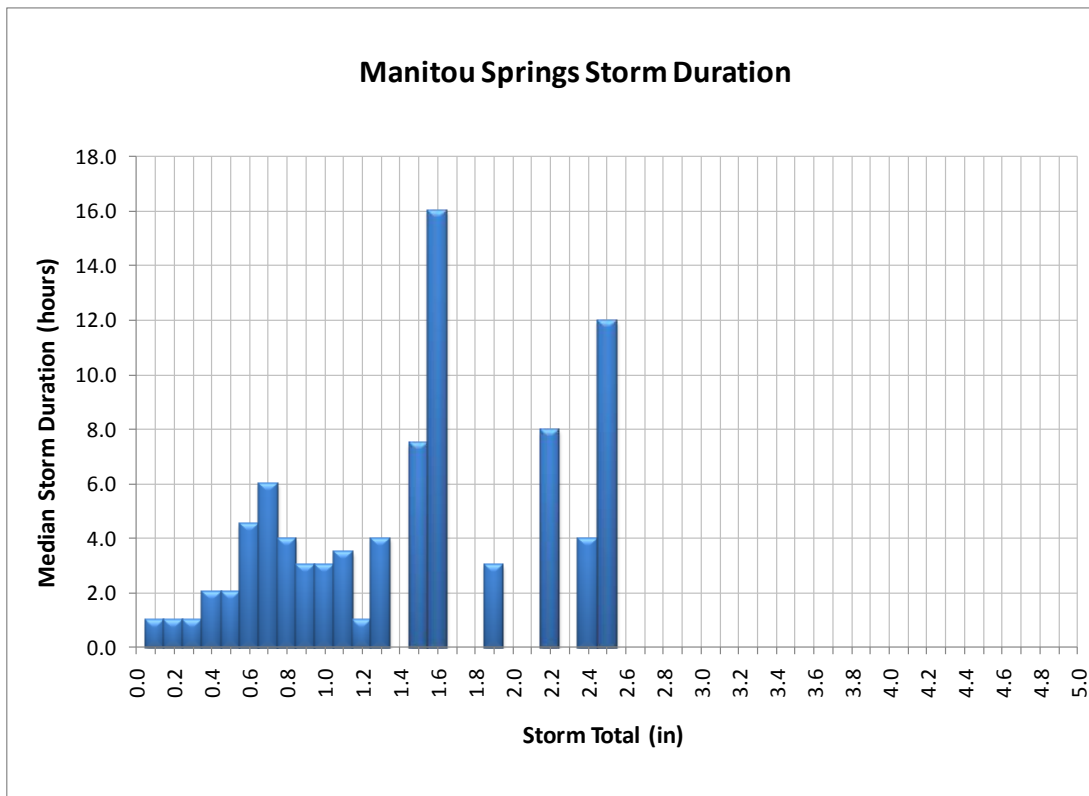


Figure 4-11: Manitou Springs Storm Duration

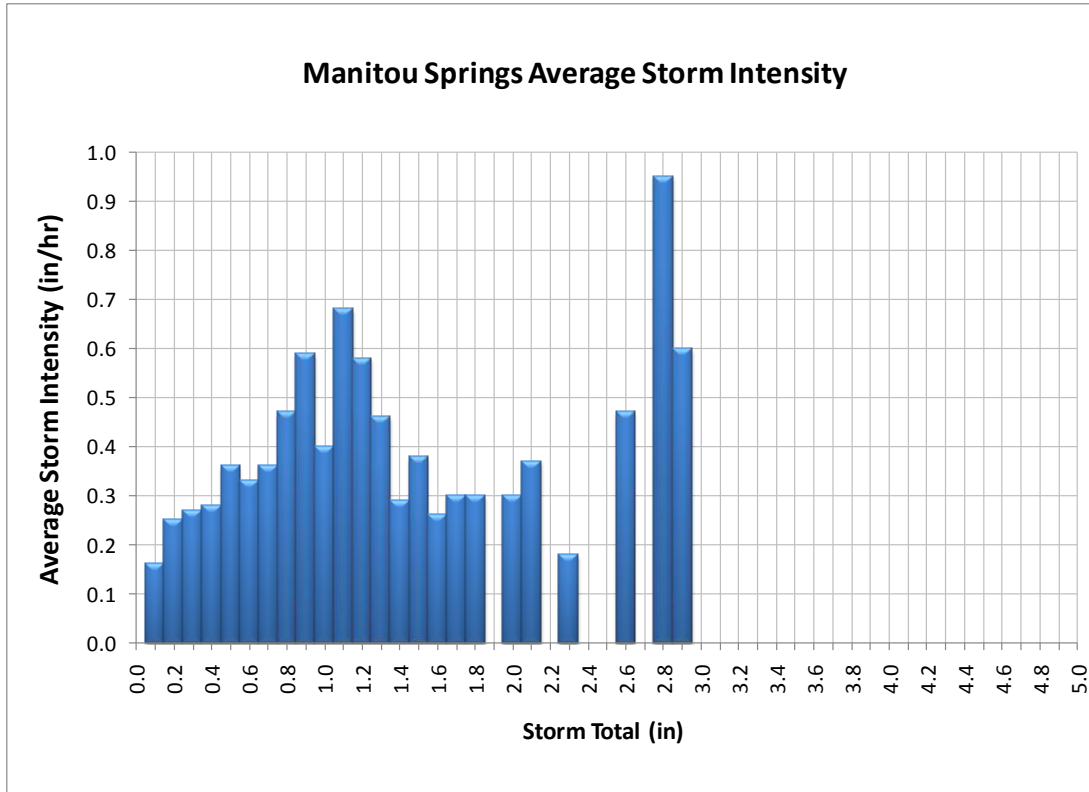


Figure 4-12: Manitou Springs Storm Intensity

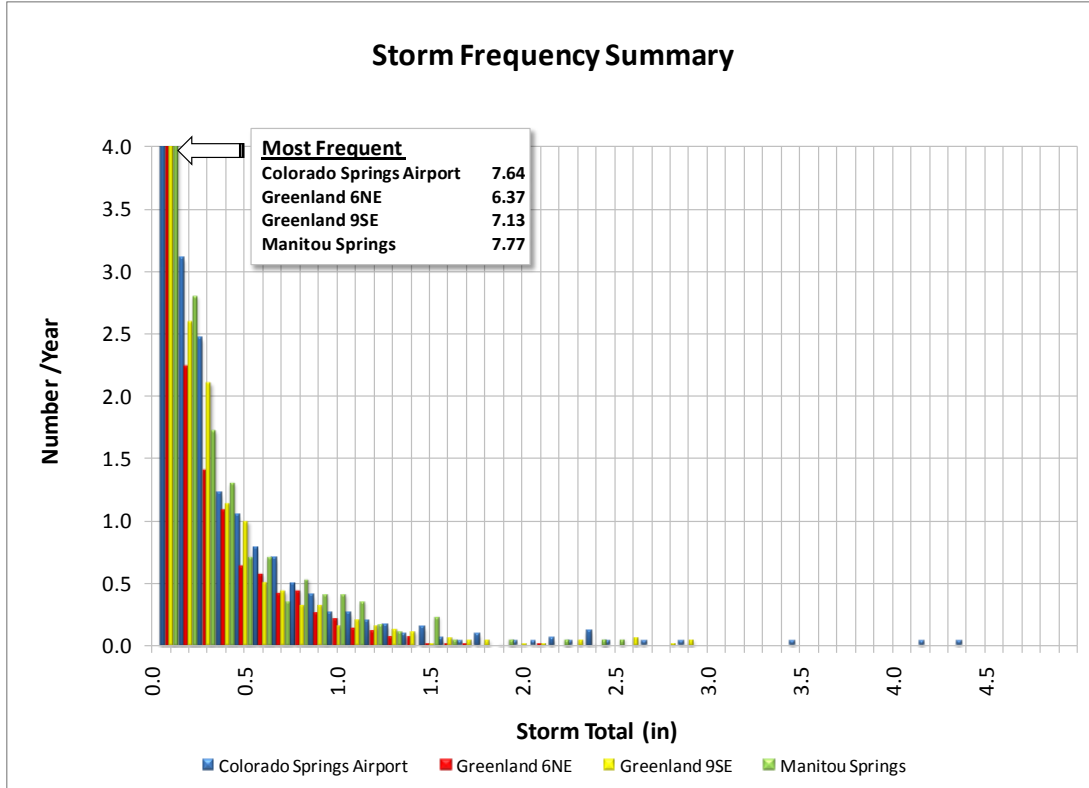


Figure 4-13: Storm Frequency Summary - All Stations

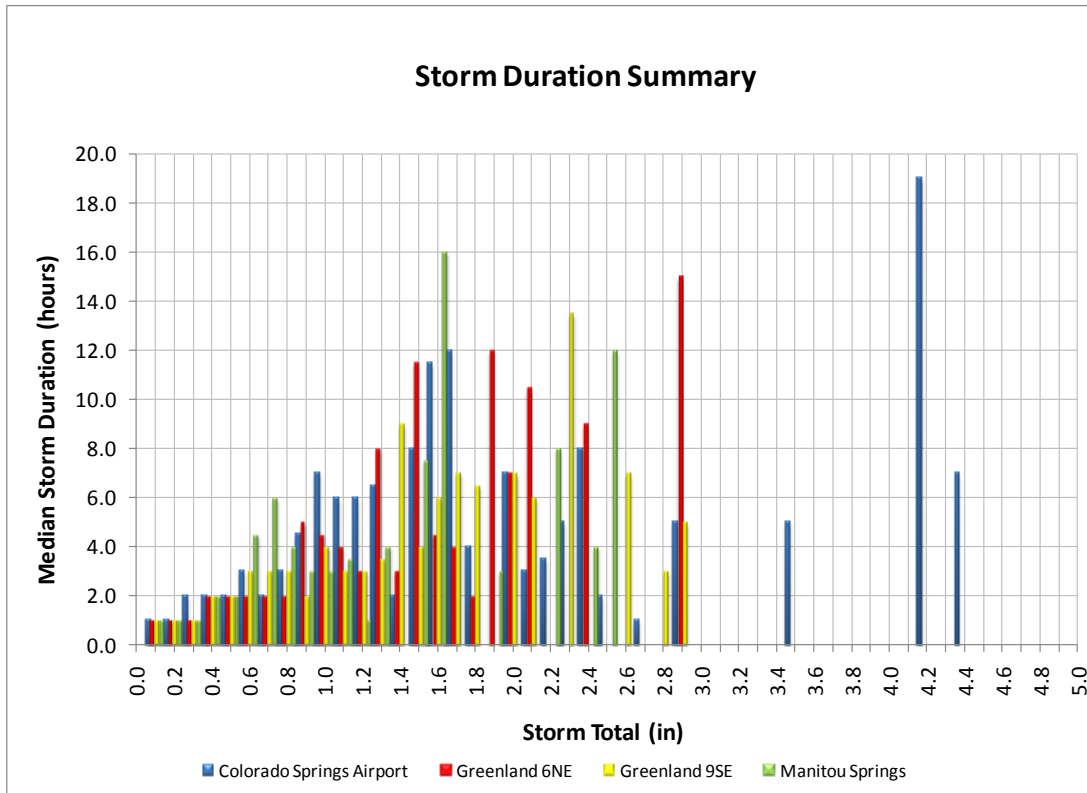


Figure 4-14: Storm Duration Summary - All Stations

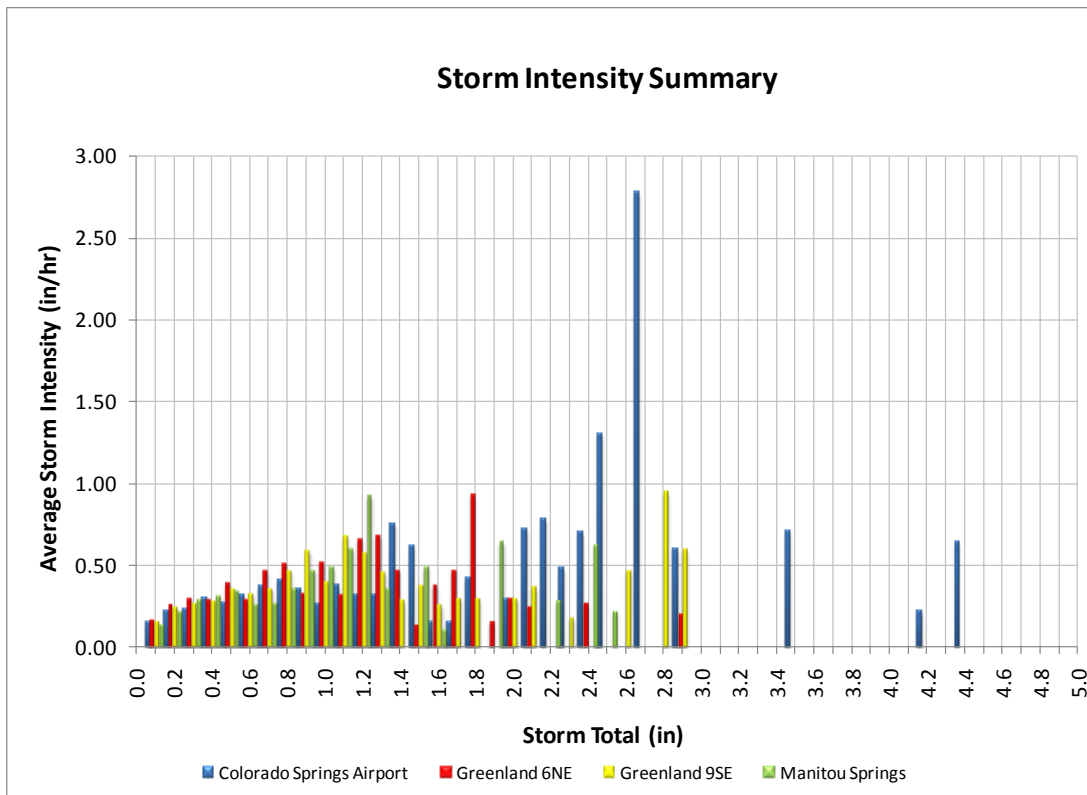


Figure 4-15: Storm Intensity Summary - All Stations

5.0 Antecedent Rainfall Conditions

5.1 Objective

The purpose of this study is to evaluate antecedent moisture conditions which can be important for estimating hydrologic model rainfall loss and infiltration coefficients.

5.2 Approach

Rainfall for the period of five days before a storm event has been used to define antecedent moisture conditions. The hourly precipitation record at Colorado Springs Airport was used to compile the list of maximum annual cloudburst events shown in Table 5.2-1. These cloudburst events were defined by 2-hour rainfall values. The annual recurrence interval for the 2-hour events was estimated from depth-duration-frequency analyses. Significant peak flows at Jimmy Camp Creek are also listed along with additional events observed in Fountain Creek watershed in the radar record. Rainfall data for the five days preceding the events were listed in the table.

The U.S. Environmental Protection Agency Hydrologic Simulation Program (HSPF) was set up to determine antecedent soil moisture. HSPF is a comprehensive model of watershed hydrology that allows integrated simulation of land, soil and channel runoff processes. It produces a time history of runoff flow rate and soil moisture conditions. HSPF was set up with Colorado Springs Airport hourly precipitation record and monthly pan evaporation at Pueblo. Land surface hydrologic parameters were a NRCS Hydrologic Soil type C, six inches of nominal soil moisture capacity, and a grassland vegetation cover.

HSPF parameters were based on typical values for semi-arid watershed simulations in Utah and California. Type C hydrologic classification soil was the most widespread in the Jimmy Camp Creek watershed. Decreased monthly pan evaporation for the cooler temperatures in Jimmy Camp Creek watershed compared to Pueblo would have no significant influence on the results, since evaporation greatly exceeds mean monthly precipitation. Table 5.2-1 lists the HSPF lower zone soil water content and the percent of soil moisture storage capacity immediately prior to each cloudburst. (Note: HSPF Lower Zone Soil Moisture (LZSN) is a nominal capacity where the model algorithms allow greater values than 100%.)

Table 5.2-1: Antecedent Moisture Conditions for Maximum Annual Cloudbursts at Colorado Springs Airport and Jimmy Camp Creek Watershed

Year	Month	Day	Hr	CS Airport Max 2-hr	Jimmy Camp Cr Peak (cfs)	Return Period (Years)	N th Day Antecedent Rainfall (in)						HSPF Soil Moist	HSPF % LZ Soil Moist
							-1	-2	-3	-4	-5	Total		
1974	Aug	28	18	0.75			0.00	0.00	0.00	0.00	0.00	0.00	0.2	4
1975	July	23	14	0.94			0.02	0.00	0.18	0.00	0.00	0.20	1.1	22
1976	Aug	1	18	2.50	1930	7	0.22	0.00	0.00	0.00	0.00	0.22	1.3	26
1977	July	20	21	0.46	334		0.17	0.00	0.00	0.00	0.00	0.17	1.9	38
1977	Aug	14	18	2.78		10	0.00	0.00	0.00	0.09	0.07	0.16	1.4	28
1978	July	9	16	1.06	318		0.00	0.00	0.00	0.00	0.00	0.00	0.5	10
1978	Aug	28	22	1.25		1.5	0.01	0.00	0.00	0.00	0.00	0.01	0.4	8
1979	July	17	17	0.83			0.00	0.04	0.00	0.00	0.00	0.04	1.1	22
1979	Aug	25	17	0.11	242		0.68	0.00	0.00	0.00	0.00	0.68	2.0	40
1980	Aug	14	17	2.71	1240	9	0.36	0.00	0.01	0.00	0.00	0.37	1.5	30
1981	July	24	15	0.78			0.02	0.02	0.00	0.00	0.00	0.04	1.4	28
1981	Aug	5	20	0.54	1100		0.00	0.06	0.20	0.00	0.00	0.26	1.8	36
1982	Aug	20	18	1.83		4	0.62	0.00	0.00	0.00	0.44	1.06	3.8	76
1983	Aug	19	18	0.53			0.00	0.00	0.28	0.00	0.07	0.35	1.1	22
1984	July	28	20	1.58		3	0.00	0.30	0.00	0.00	0.00	0.30	1.3	26
1984	Aug	1	21	0.34	590		0.01	0.02	0.00	0.00	1.58	1.61	2.7	54
1985	July	19	22	1.90		4	0.39	0.00	0.00	0.00	0.00	0.39	1.7	34
1985	July	28	15	0.90	3600		0.00	0.02	0.10	0.11	0.01	0.24	3.0	60
1986	Aug	2	1	1.77		3	0.27	0.18	0.00	0.00	0.00	0.45	1.0	20
1986	Aug	22	21	0.57	1970		0.19	0.00	0.00	0.00	0.00	0.19	2.6	52
1987	Aug	26	18	0.74			0.12	0.01	0.01	0.57	0.19	0.90	1.0	20
1988	July	9	12	1.15		1	0.76	0.66	0.12	0.00	0.00	1.54	0.8	16
1989	July	13	20	1.10		1	0.46	0.07	0.00	0.00	0.00	0.53	1.5	30
1989	Aug	27	22	0.37	668		0.00	0.00	0.00	0.03	0.01	0.04	1.8	36
1990	July	6	18	1.21		1.5	0.70	0.00	0.00	0.00	0.00	0.70	3.4	68
1990	July	19	22	0.22	354		0.00	0.00	0.00	0.00	0.25	0.25	3.1	62
1991	July	20	18	1.03			0.13	0.09	0.00	0.00	0.00	0.22	1.0	20
1992	June	28	18	0.89			0.22	0.52	0.55	0.14	0.08	1.51	2.8	56
1993	July	11	18	1.00			0.00	0.00	0.00	0.00	0.00	0.00	0.7	14
1994	June	2	21	2.23	4810	5	0.46	0.00	0.00	0.00	0.07	0.53	4.3	86
1995	June	2	20	0.66	4530		0.36	0.00	0.06	0.14	0.62	1.18	6.1	122
1995	June	4	16	2.15		5	0.06	2.17	0.06	1.07	0.00	3.36	6.3	126
1996	Aug	23	15	0.97			0.04	0.00	0.00	0.00	0.00	0.04	0.7	14
1997	June	13	21	2.50	1740	7	0.28	0.00	0.41	0.53	0.18	1.40	3.1	62
1997	July	29	18	3.19		15	0.12	0.12	0.00	0.00	0.05	0.29	1.4	28
1998	July	30	15	1.44		2	0.05	0.41	0.02	0.07	0.12	0.67	2.0	40
1998	Aug	11	16	0.27	1610		0.00	0.52	0.00	0.00	0.00	0.52	2.7	54
1999	April	30	15	2.64		9	1.78	0.35	0.00	0.30	0.00	2.43	4.4	88
1999	July	31	15	1.58	1710	3	0.07	0.00	0.51	0.00	0.00	0.58	2.4	48
1999	Aug	4	21	1.98		4	2.22	2.11	0.19	1.58	0.07	6.17	5.5	110
2000	Aug	28	18	1.89		3	0.00	0.27	0.49	0.16	0.00	0.92	1.5	30
2001	July	13	19	0.95			0.95	0.10	0.02	0.44	0.00	1.51	2.0	40
2002	June	14	14	0.70			0.00	0.01	0.32	0.00	0.00	0.33	0.5	10
2003	June	14	15	1.58		3	0.00	0.15	0.00	0.00	0.08	0.23	1.8	36
2003	June	19	18	1.39	233	2	0.04	0.24	0.06	1.58	0.00	1.92	4.0	80
2003	July	28	17	0.60			0.00	0.40	0.60	0.10	0.00	1.10	1.4	28
2003	Aug	30	24	0.70			0.20	0.20	0.10	0.00	0.00	0.50	0.9	18
2004	April	23	18	0.60			0.07	0.36	0.09	0.00	0.00	0.52	2.0	40
2004	June	15	14	0.89			0.47	0.00	0.00	0.00	0.00	0.47	0.7	14
2004	June	27	15	2.10		4	0.10	0.09	0.18	0.00	0.00	0.37	2.5	50
2004	July	16	7	0.70			0.48	0.16	0.00	0.01	0.00	0.65	2.6	52
2004	Aug	5	18	0.78	1440		0.26	0.00	0.00	0.00	0.02	0.28	3.0	60
2005	June	3	15	0.71			0.32	0.00	0.00	0.13	0.04	0.49	1.5	30
2005	July	14	20	0.42	869		0.00	0.00	0.00	0.00	0.00	0.00	0.7	14
2005	Aug	20	15	0.83			0.01	0.16	0.02	0.06	0.37	0.62	1.7	34
2006	July	9	16	0.88			0.67	0.18	0.05	0.03	0.45	1.38	3.2	64
2006	Aug	11	n/a	0.00	698		0.00	0.02	0.12	0.35	0.00	0.49	2.3	46
2006	Sept	21	6	0.33			0.20	0.00	0.08	0.00	0.00	0.28	1.5	30
2006	Oct	8	15	0.16			0.20	0.00	0.00	0.10	0.10	0.40	1.7	34
2007	July	3	19	0.77			0.00	0.00	0.08	0.00	0.00	0.08	1.1	22
2007	Aug	22	18	0.09	242		0.00	0.00	0.00	0.08	0.30	0.38	1.5	30
2008	Aug	15	15	1.42		2	0.53	0.00	0.02	0.00	0.00	0.55	1.0	20
2008	Aug	16	15	0.48	124		1.42	0.57	0.53	0.00	0.02	2.54	2.8	56
2008	Sept	11	14	3.36		20	0.93	0.00	0.00	0.00	0.00	0.93	3.7	74

5.3 Results

There were no obvious relationships between storm depths, Jimmy Camp Creek flood peaks, and antecedent moisture as shown in Figure 5-1 and Figure 5-2. Statistically, the squared correlation coefficient, R^2 , was 0.05 or less than in both cases. There was a tendency for larger storms to have lower antecedent rainfall. In general, antecedent moisture could be characterized as very dry, with average five-day antecedent rainfall of less than one inch and average soil moisture of 2 inches (40% of capacity).

Figure 5-1 shows the relationship between storm depth and antecedent HSPF hydrologic model soil moisture content. The soil moisture content shown by the HSPF model reflects precipitation and evapotranspiration for several preceding months. The data shows that some flood events on Jimmy Camp Creek may have been influenced by higher than normal soil moisture, particularly June 2, 1995, June 4, 1995 and August 4, 1999. This provides limited justification for using soil moisture values near capacity when simulating spring (April-early June) cloudbursts, although conservatively high runoff should be expected.

HSPF parameters were based on typical values for semi-arid watershed simulations in Utah and California. Type C hydrologic classification soil was the most widespread in the Jimmy Camp Creek watershed. Decreased monthly pan evaporation for the cooler temperatures in Jimmy Camp Creek watershed compared to Pueblo would have no significant influence on the results, since evaporation greatly exceeds mean monthly precipitation. A future project could set up HSPF in much greater subbasin detail using radar rainfall.

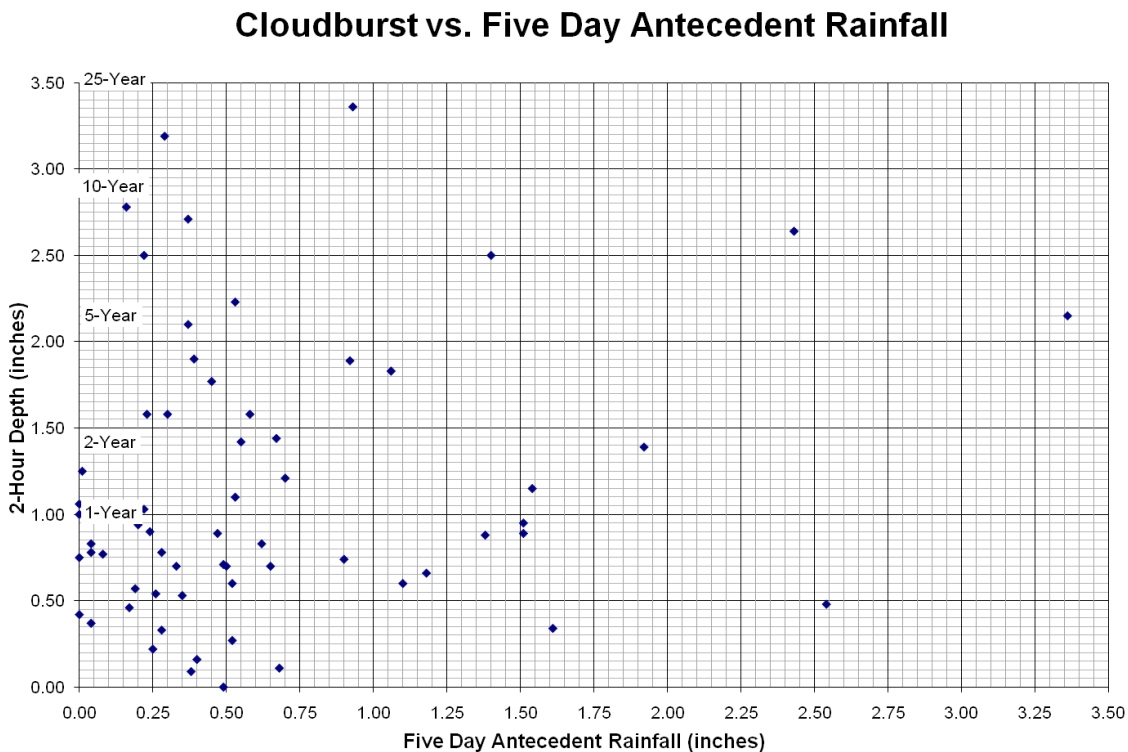


Figure 5-1: Cloudburst vs. Five Day Antecedent Rainfall

Cloudburst vs. HSPF Antecedent Condition

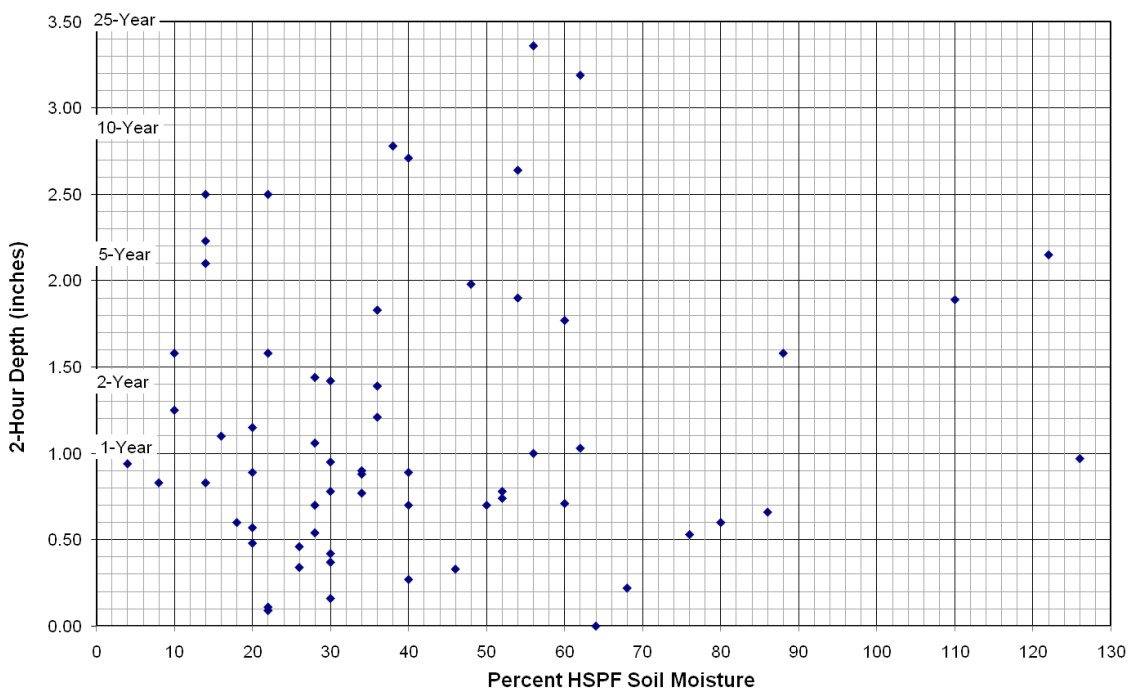


Figure 5-2: Cloudburst vs. HSPF Soil Moisture

An extended analysis was done for all events exceeding 0.10 inch, and spaced by six hours or more for the four hourly station records (described in Section 3.0). There were 675 events defined for Colorado Springs Airport, 301 events for Manitou Springs, 723 events for Greenland 9SE and 866 events for Greenland 6NE. The events were compiled in spreadsheets, ranked, and assigned frequency values. Example results from these analyses are shown in Table 5.3-1 through Table 5.3-3.

The analysis of all events as recorded at the four stations confirmed the conclusions of the first analysis using maximum cloudbursts only. It was apparent from the precipitation and radar data that cloudburst events in Fountain Creek watershed were typically independent events from day to day. In other words, the occurrence of a cloudburst day or a dry day does not influence the probability of the previous days or following days from having a cloudburst or a dry day.

This means that antecedent moisture assigned to a modeled design storm should be the most likely value, that is, 50% probability or zero for one day and 0.28 in. for five days. Using a less likely value, for example, 10% probability 1.39 in., for five days antecedent at Colorado Springs Airport, would be equivalent to reducing the probability (or increasing the recurrence interval) of the hydrologic event (by increasing runoff). The magnitude of the effect would depend on the relative importance of antecedent moisture to other factors influencing runoff coefficients.

However, flood events on Jimmy Camp Creek appeared to be caused by high intensity rain exceeding the infiltration capacity of the soil/vegetation surface and have little relationship to a soil moisture index. Soil moisture is also not important to hydrologic modeling of urban areas, which generally have high impervious area percentages and low infiltration capacity soils.

Table 5.3-1: Colorado Springs Airport ranked antecedent rainfall.

Year	Month	Hour	Airport	Jimmy Camp Cr	Recurr. Interval	Antecedent Rainfall									
						1-day	%	2-day	%	3-day	%	4-day	%	5-day	Total
2008	Sept	14	3.36		20-year	0.93	100	0.00	100	0.00	100	0.00	100	0.00	0.93
1997	July	18	3.19			0.12	41	0.12	83	0.00	83	0.00	83	0.05	0.29
2009	August	18	2.78		10-year	0.00	0	0.00	0	0.00	0	0.09	56	0.07	0.16
1998	August	17	2.71	1240		0.36	97	0.00	97	0.01	100	0.00	100	0.00	0.37
1999	April	15	2.64			1.78	73	0.35	88	0.00	88	0.30	100	0.00	2.43
2000	August	18	2.50	1930		0.22	100	0.00	100	0.00	100	0.00	100	0.00	0.22
1997	June	21	2.50	1740		0.28	20	0.00	20	0.41	49	0.53	87	0.18	1.40
1994	June	21	2.23	4810	5-year	0.46	87	0.00	87	0.00	87	0.00	87	0.07	0.53
1995	June	16	2.15			0.06	2	2.17	66	0.06	68	1.07	100	0.00	3.36
2004	June	15	2.10			0.10	27	0.09	51	0.18	100	0.00	100	0.00	0.37
1999	August	21	1.98			2.22	36	2.11	70	0.19	73	1.58	99	0.07	6.17
2005	July	22	1.90			0.39	100	0.00	100	0.00	100	0.00	100	0.00	0.39
2000	August	18	1.89			0.00	0	0.27	29	0.49	83	0.16	100	0.00	0.92
2006	August	18	1.83			0.62	58	0.00	58	0.00	58	0.00	58	0.44	1.06
2001	August	1	1.77			0.27	60	0.18	100	0.00	100	0.00	100	0.00	0.45
2002	July	20	1.58			0.00	0	0.30	100	0.00	100	0.00	100	0.00	0.30
1999	July	15	1.58	1710		0.07	12	0.00	12	0.51	100	0.00	100	0.00	0.58
2003	June	15	1.58			0.00	0	0.15	65	0.00	65	0.00	65	0.08	0.23
1998	July	15	1.44		2-year	0.05	7	0.41	69	0.02	72	0.07	82	0.12	0.67
2008	August	15	1.42			0.53	96	0.00	96	0.02	100	0.00	100	0.00	0.55
2003	June	18	1.39	233		0.04	2	0.24	15	0.06	18	1.58	100	0.00	1.92
2009	August	22	1.25			0.01	100	0.00	100	0.00	100	0.00	100	0.00	0.01
2004	July	18	1.21			0.70	100	0.00	100	0.00	100	0.00	100	0.00	0.70
2005	July	12	1.15			0.76	49	0.66	92	0.12	100	0.00	100	0.00	1.54
2006	July	20	1.10		1-year	0.46	87	0.07	100	0.00	100	0.00	100	0.00	0.53
					Averages	0.42	50	0.28	72	0.08	82	0.22	93	0.04	1.04

Table 5.3-2: One Day Antecedent Moisture Probability

One Day (inches)							
	100%	50%	20%	10%	4%	2%	1%
	1-year	2-year	5-year	10-year	25-year	50-year	100-year
Colorado Springs	0.00	0.00	0.20	0.40	0.74	1.11	1.49
Manitou Springs	0.00	0.00	0.17	0.33	0.80	1.12	1.25
Greenland 9SE	0.00	0.00	0.10	0.30	0.65	0.96	1.00
Greenland 6NE	0.00	0.00	0.20	0.40	0.80	1.00	1.20

Note: Column headings indicated the probability of antecedent rainfall; not storm event probability.

Table 5.3-3: Five Day Antecedent Moisture Probability

Five Days (inches)							
	100%	50%	20%	10%	4%	2%	1%
	1-year	2-year	5-year	10-year	25-year	50-year	100-year
Colorado Springs	0.02	0.28	0.79	1.39	2.24	2.81	3.43
Manitou Springs	0.01	0.27	0.74	1.12	1.71	2.14	2.69
Greenland 9SE	0.00	0.10	0.52	0.89	1.50	1.96	2.77
Greenland 6NE	0.01	0.22	0.77	1.27	1.90	2.24	2.80

There was a correspondence between rainfall depths and rainfall occurring in the preceding days. However, Table 5.3-1 through Table 5.3-3 show that this correspondence is low. For example, in Table 5.3-3: Five Day Antecedent Moisture Probability, there is a 50% chance that a 2-year event will have 0.28 in. of antecedent rainfall and a 1% chance it will be 3.4 in. Using the most likely antecedent moisture condition is unlikely to affect the probability of a resulting hydrologic event. However, using a less likely value would significantly affect the probability of the hydrologic event in an unpredictable way (although

definitely producing a much higher and unrealistic recurrence interval), depending on hydrologic characteristics of the watershed.

Figure 5-3 through Figure 5-5 illustrate the results shown in Tables 5.2-1 and Table 5.3-3. Figure 5-3 shows a graph of events versus 5-day antecedent rainfall. There was clearly no statistical relationship ($R^2 \sim 0.05$) with most likely 5-day antecedent rainfall 0.3” as shown in Table 5.2-4. Figure 5-4 shows the 5-day antecedent as a percent of annual rainfall. The most likely 5-day antecedent rainfall was approximately 2% of annual rainfall. Figure 5-5 shows the number of days with antecedent rainfall versus event magnitude. There is no statistical relationship. ($R^2 \sim 0.002$)

Antecedent rainfall for a watershed is not the same as antecedent rainfall derived for a gage. As watershed area increases there is an increasing probability that antecedent rainfall would occur somewhere in the watershed. However, there is also an increasing probability that a design event would occur somewhere in the watershed. The degree of overlap or coincidence of the areal coverage of antecedent events with the areal coverage of the design event is hydrologically significant. This cannot be modeled using single gage statistics and requires long-term radar precipitation over the watershed of interest.

5.4 Key Findings

- There were no obvious relationships between storm depths, Jimmy Camp Creek flood peaks, and antecedent moisture.
- In general, antecedent moisture could be characterized as very dry, with average five-day antecedent rainfall of less than one inch and average soil moisture of 2 inches (40% of capacity).
- There is limited justification for using soil moisture values near capacity when simulating spring (April-early June) cloudbursts

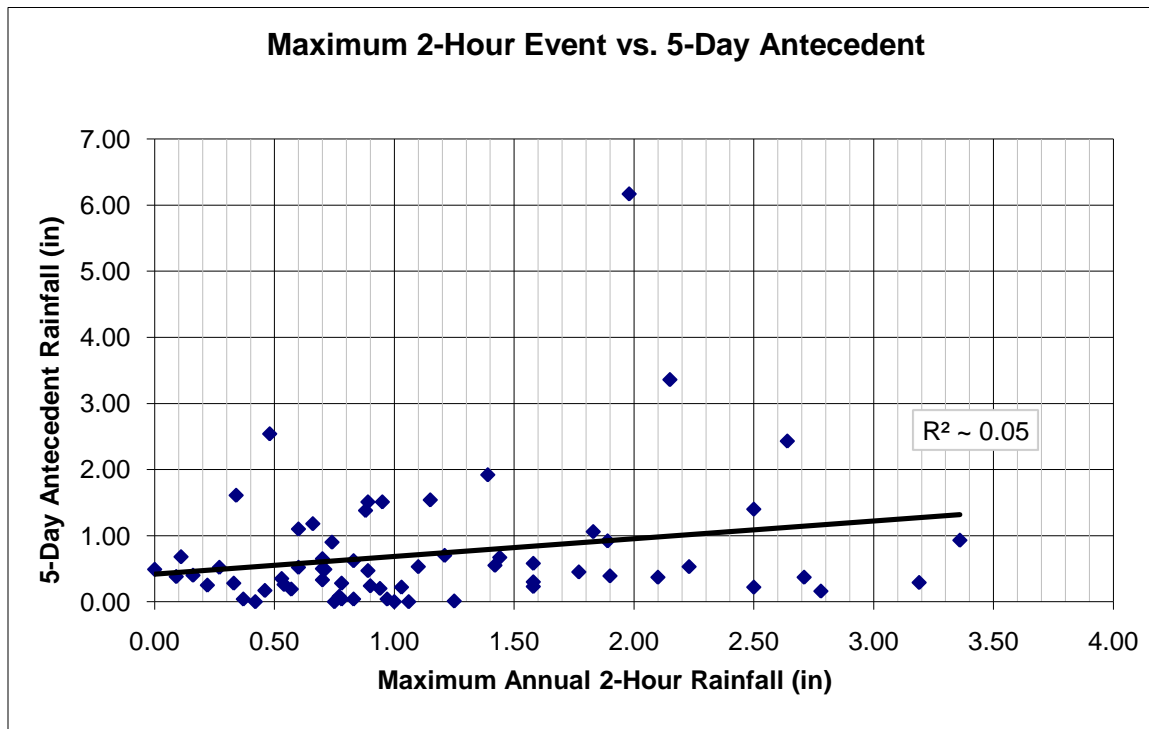


Figure 5-3: Maximum Annual 2-Hr Rainfall vs 5-Day Antecedent Rainfall

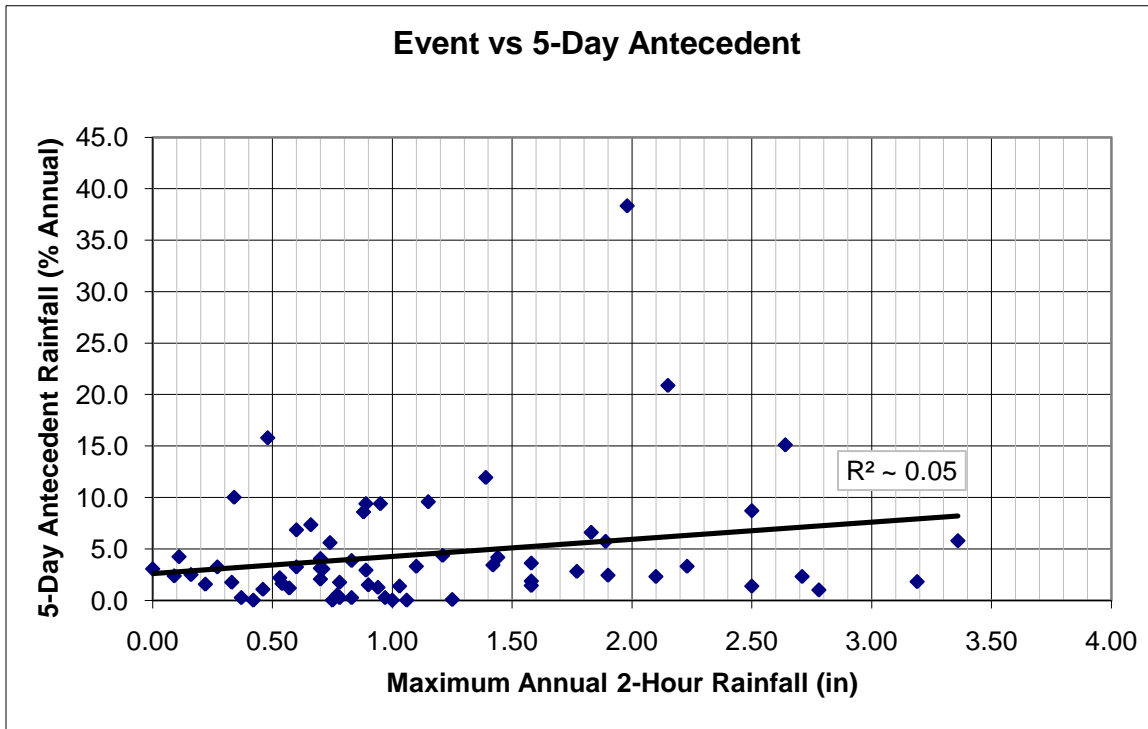


Figure 5-4: Five-Day Antecedent Rainfall (%Annual) vs. Maximum Annual 2-Hr Rainfall

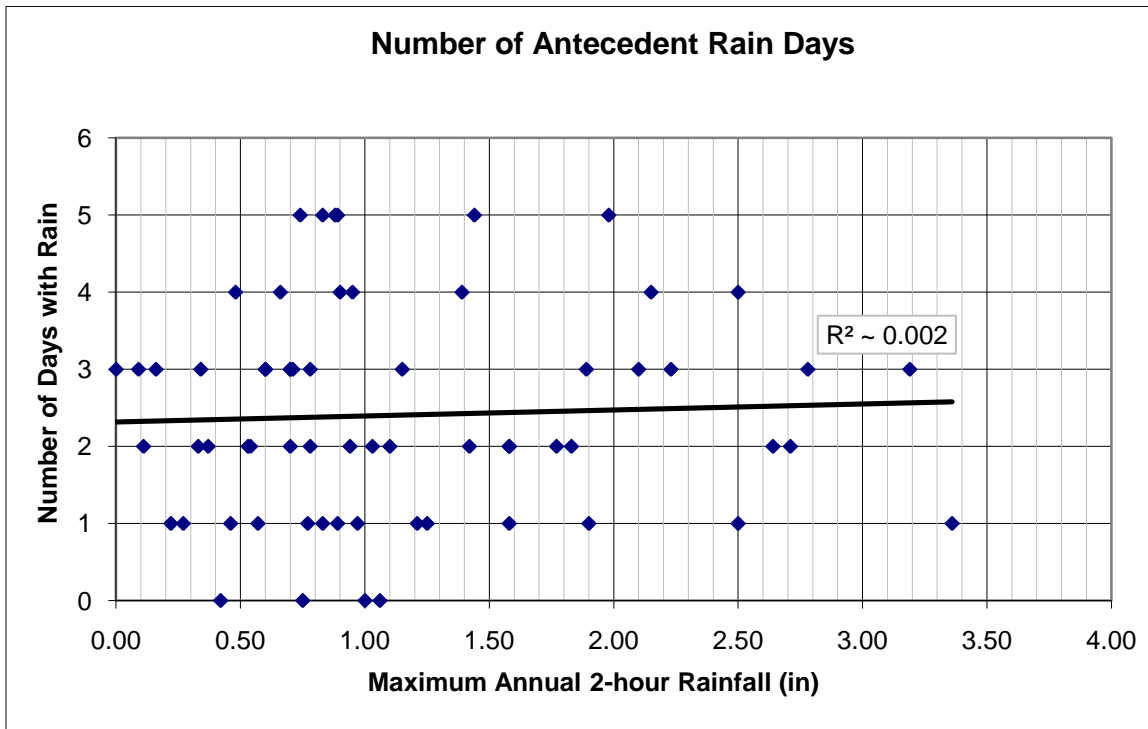


Figure 5-5: Number of Antecedent Rain Days vs. 2-Hr Rainfall

6.0 Radar Rainfall Analysis

6.1 Objective

Two different radar rainfall analyses were completed during this project:

1. Develop gage-adjusted radar-rainfall for the Jimmy Camp Creek Watershed, and
2. Develop gage-adjusted radar rainfall data for eastern Colorado to assess the geospatial characteristics of storm cells.

The data developed for Jimmy Camp Creek was intended for use in hydrologic modeling efforts. Data developed for eastern Colorado was intended for evaluating the spatial structure of storms to provide insights on potential design storm improvements in the Fountain Creek Watershed and Colorado Springs.

6.2 Approach

The Jimmy Camp Creek data covered six individual rain events of interest as shown in Table 6.2-1. The events were selected based on a review of rain gage and stream gage records where significant runoff occurred during the periods of radar rainfall data availability. The Jimmy Camp Creek stream gage (USGS 07105900) at Fountain, CO, was used to aid event selection. (See stream gage location in Figure 6-1.) Figure 6-2 and Figure 6-3 show example peak runoff events considered in data selection.

The start times for each study period were selected in order to include any rainfall in the 24-48 hours preceding the specific time of interest. The end times were selected in order to provide at least four hours of no rainfall and no other significant rain events in the subsequent 12 hours.

Table 6.2-1: Rain Events for the Jimmy Camp Creek Analysis

Event	Year	Start	End	Time step (min)	Resolution (km)
1	1995	05/16 00:00	05/19 06:00	15	2x2
2	1996	08/13 03:00	08/17 00:00	15	2x2
3	1999	07/30 03:00	08/06 06:00	15	2x2
4	2004	08/04 09:00	08/07 19:00	5	1x1
5	2005	07/14 12:00	07/16 06:00	5	1x1
6	2006	08/24 07:00	08/27 04:00	5	1x1

Events prior to the year 2000 were analyzed using 15-minute radar data with a 2x2 km pixel resolution. For events occurring after 2000, 5-minute radar data with a 1x1 km pixel resolution was used. Gage-adjusted radar rainfall data were provided in ArcView shapefile format. A complete description of the Jimmy Camp Creek radar rainfall analysis appears as a separate document and is included in Appendix A of this report.

Gage-adjusted radar rainfall data for the eastern Colorado study area (See Figure 2.2-1) was developed using 15-minute, 2 km x 2 km data for 24-months. As with Jimmy Camp Creek, rain gage records and stream gage records were reviewed to select the months of interest.

Monthly rainfall records for the Colorado Springs area from 1994-2008 were reviewed and months with the most rainfall activity were considered for selection. Table 6.2-1 shows the final list of data months used in the storm properties analysis. Figure 6-4 shows the distribution of radar data months.

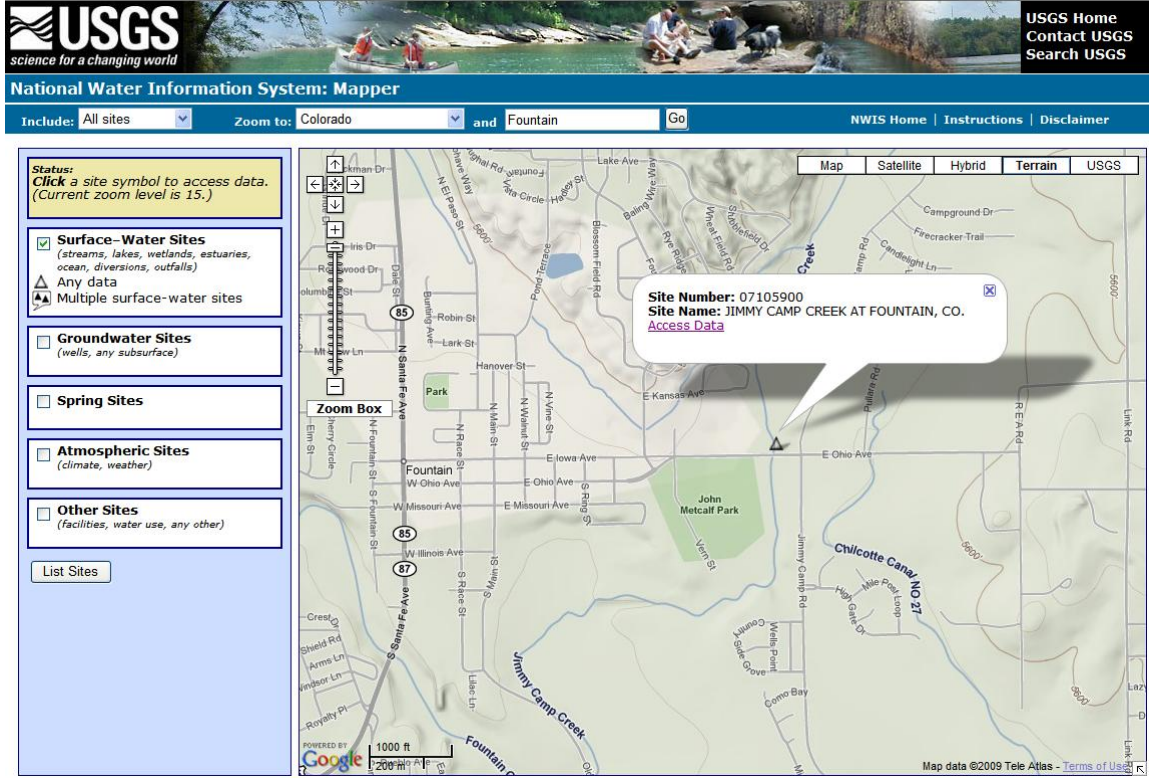


Figure 6-1: Jimmy Camp Creek Stream Gage at Fountain, CO (<http://wdr.water.usgs.gov/nwisgmap/>)

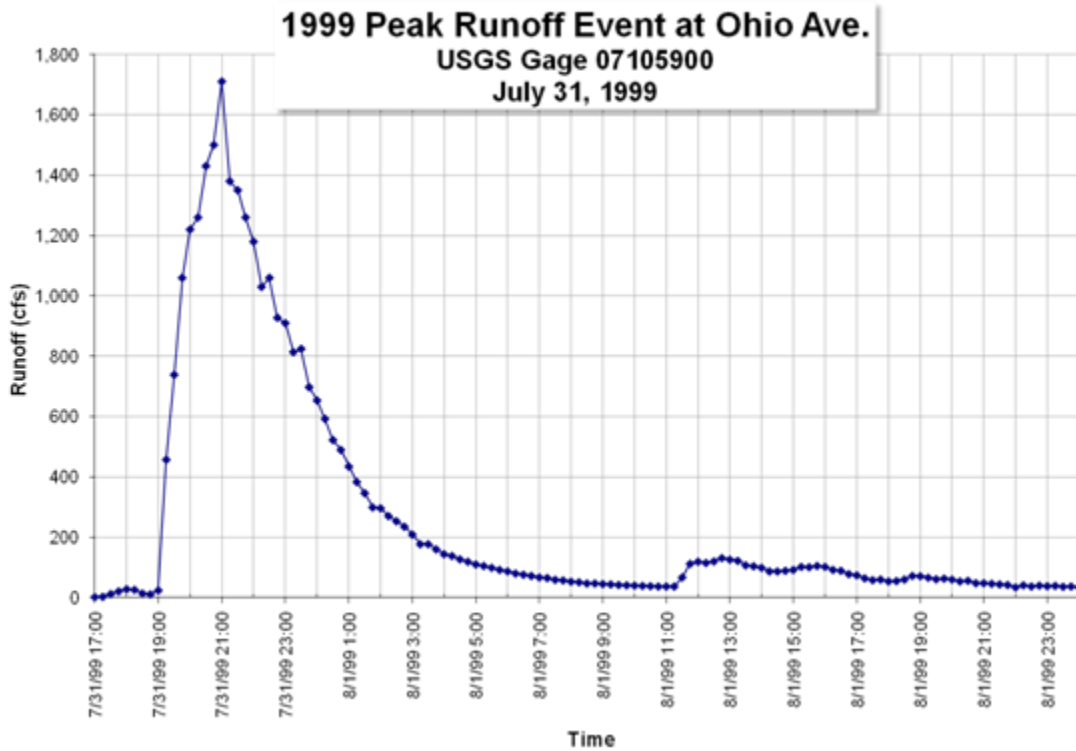


Figure 6-2: USGS Gage 07105900 Peak Runoff Event, 1999

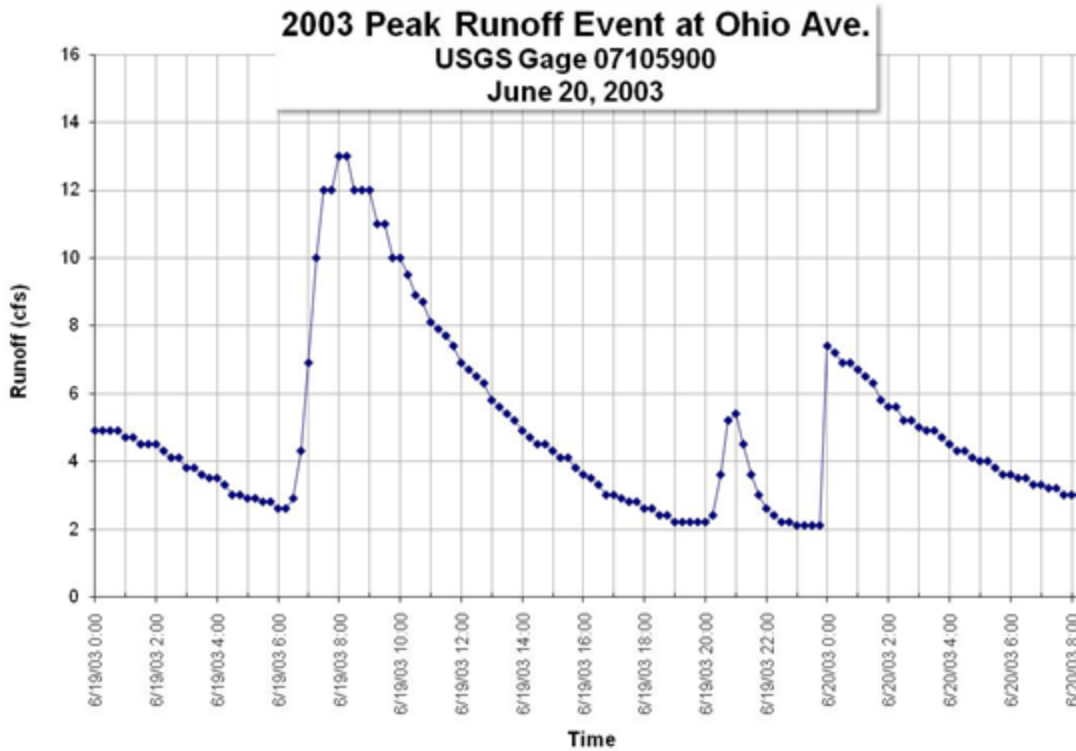


Figure 6-3: USGS Gage 07105900 Peak Runoff Event 2003.

Table 6.2-2: Data Months Selected for Storm Properties Analysis

June-94	June-03	August-04	September-06
June-95	July-03	June-05	October-06
April-99	August-03	July-05	July-07
July-99	April-04	August-05	August-07
August-99	June-04	July-06	August-08
July-01	July-04	August-06	September-08

The number and location of rain gages available for calibrating radar rainfall estimates varied widely from 1994 to 2008. The number of automated rain gages in eastern Colorado expanded dramatically during this period ranging from about 50 gages in 1994 to more than 250 gages in 2008. Figure 6-5 through Figure 6-7 show the rain gage network growth during the period.

The approach used to develop the gage adjusted radar rainfall data for the eastern Colorado study area was exactly the same as those used to develop the Jimmy Camp Creek data set as described in Appendix A.

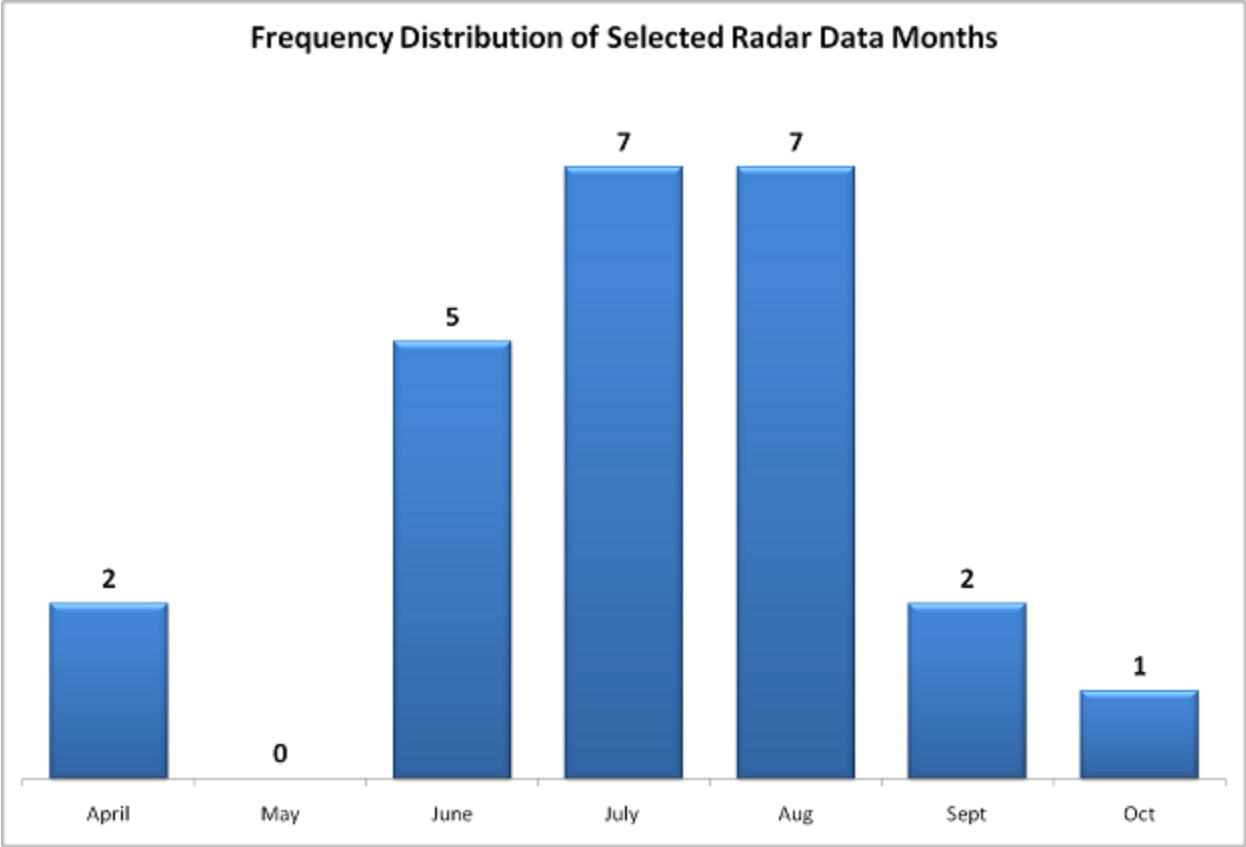


Figure 6-4: Frequency Distribution of Selected Radar Data Months

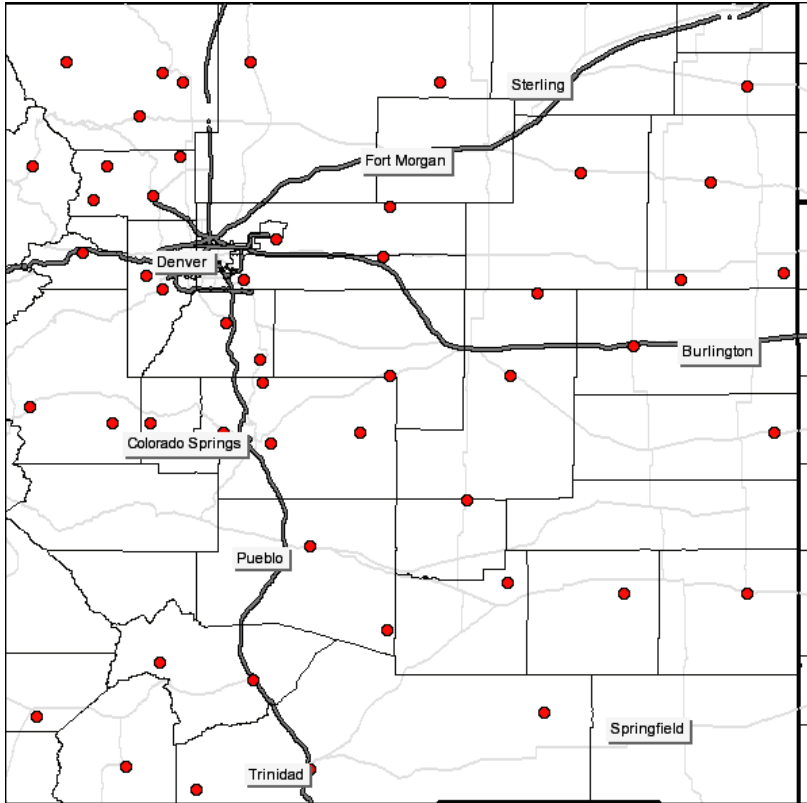


Figure 6-5: Rain Gage Network 1994-95

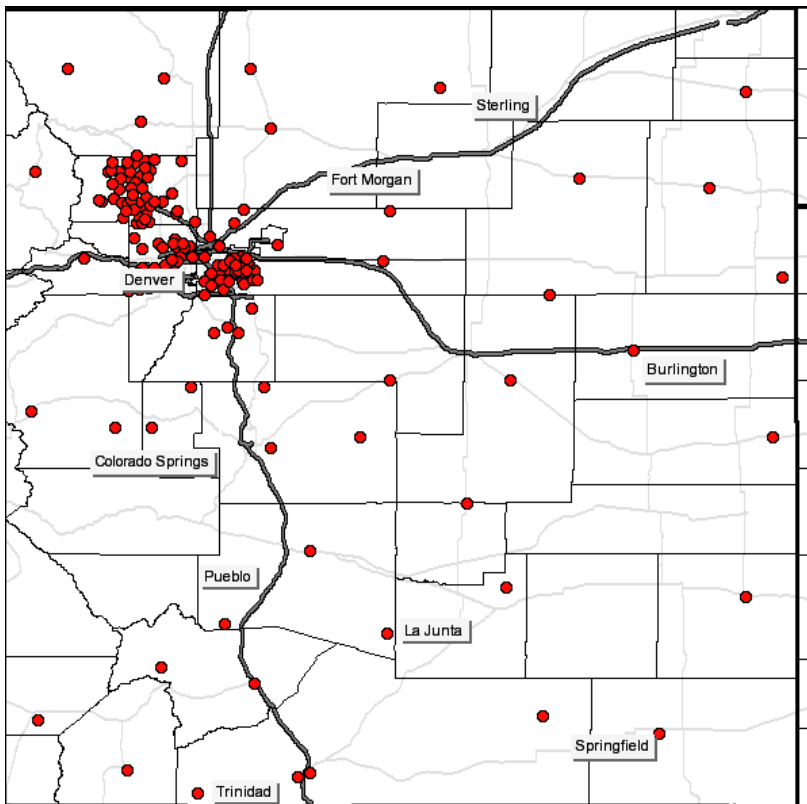


Figure 6-6: Rain Gage Network 1999

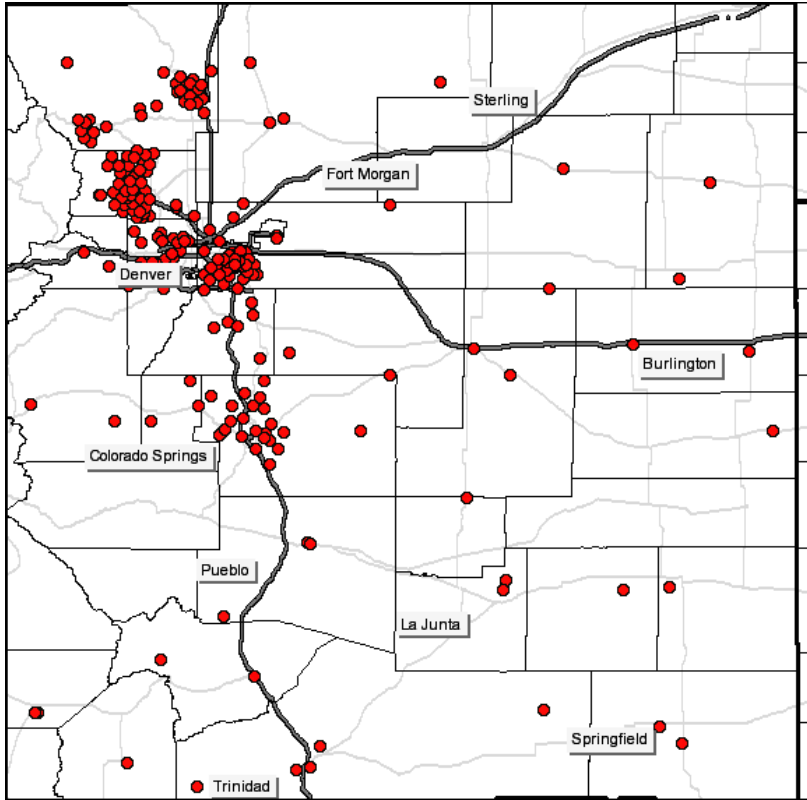


Figure 6-7: Rain Gage Network 2001

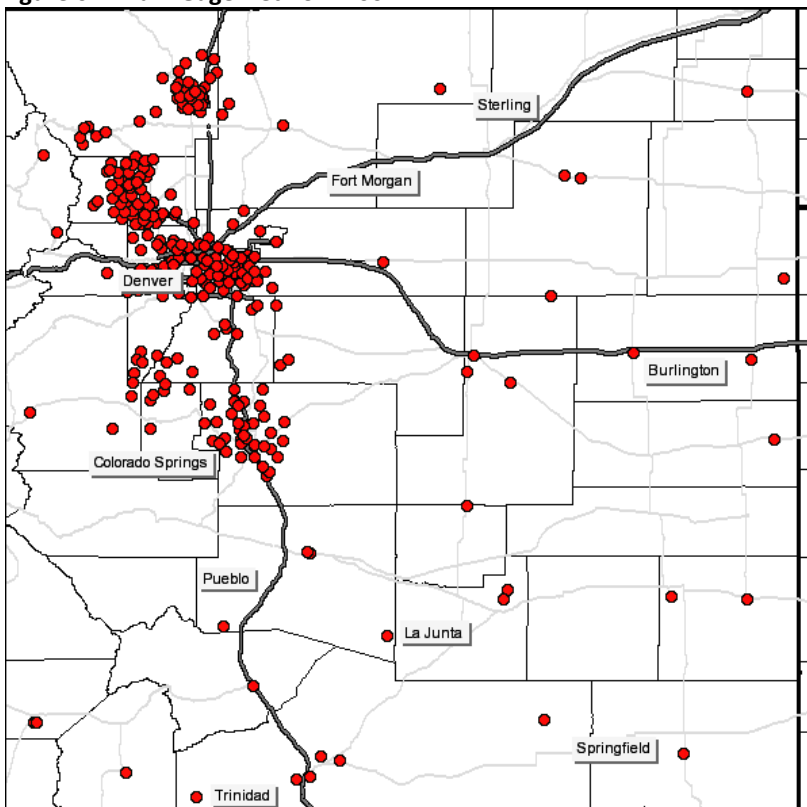


Figure 6-8: Rain Gage Network 2002-2008

6.3 Radar Rainfall Verification

6.3.1 Overview

The accuracy of the twenty-four monthly gage-adjusted radar rainfall (GARR) datasets was assessed by a process called gage verification. This verification process involved comparing GARR estimates with rain gages not used in the production of the adjusted radar data. The goal was to achieve a maximum monthly difference of 5% between the withheld verification gages and the GARR co-located pixels.

The rain gages were divided into two groups, one referred to as the calibration gages, and the other verification gages. The verification gages acted as an independent data source with which to assess the accuracy of the radar rainfall estimates. Approximately 10% of the available gages were selected to be verification gages.

After presenting an overview of the verification gage selection process and maps showing the verification gage locations for three distinct periods of the 1994-2008 analysis, the details of the verification process are presented for a sample month, July 2006.

6.3.2 Selection of Verification Gages

The verification gages selection process was somewhat subjective in nature. Several criteria were considered when developing the list of verification gages:

- Spatial Distribution. Preference was given to gages in areas of higher gage densities. Given rainfall spatial variability, isolated gages, such the majority in the eastern two-thirds of the study area, often more than thirty miles apart, were poor candidates for verification gages.
- Gage Maintenance. Preference was also placed on ALERT gages in the Colorado Springs and Denver areas. OneRain has been involved in the maintenance of these gages since the late 1990's and has increased confidence in their performance.
- Gage Performance. A test run creating GARR datasets were generated using all gages. The gage-radar performance was reviewed and gages that were the better performing were considered for selection.

Performance was based on the percentage of the time the gages were left in the analysis. The process of removing suspect gages from the GARR analysis is referred to as “masking out” gages. (See Appendix A for more information on “masking gages.”) The goal was to select gages left in the analysis for a minimum of 66% of the monthly study periods. This corresponds to a maximum masking percentage of 33%.

However, another goal was not to eliminate the very best performing gages from the calibration process. If a gage was removed from the original analysis for less than 10% of the study period, there was a bias to include the gage in the calibration gage set and not select it as a verification gage. (Removing all of the best performing gages for verification purposes biases the results to poorer performing gages and degrades GARR quality.)

From 1994 to 2008 the number of rain gages in the study area rose from about 50 to over 250. For simplicity, the period of analysis was divided into three “network era.”

1. Pre-1999: 50 NCDC and METAR (airport) gages.
2. 1999-2002: A combination of 55 NCDC and METAR and 120 ALERT gages.
3. Post-2002: A combination of 91 NCDC and METAR and >250 ALERT gages.

For the pre-1999 period, only NCDC and METAR gages were available. Five gages were selected as verification gages. Table 6.3-1 presents the fifty pre-1999 gages and the masking percentages in the

original TITAN GARR analysis. The gages highlighted in green were selected as verification gages based on the criteria outlined above. Appendix B includes gage verification tables for the 1999-2002 and post-2002 periods.

Table 6.3-1: Verification Gages for the Pre-1999 Period. (Green highlights indicate verification gages.)

Gage ID	Mask %						
ncdc_9285	38	ncdc_1179	18	ncdc_7557	10	ncdc_6326	3
ncdc_7519	28	ncdc_3386	18	ncdc_2965	9	ncdc_183	3
ncdc_1539	27	ncdc_3584	15	ncdc_8220	9	ncdc_3553	3
ncdc_4877	26	ncdc_3500	13	ncdc_2790	7	ncdc_7572	3
ncdc_4155	25	ncdc_4380	13	ncdc_109	7	ncdc_7866	3
ncdc_5352	23	ncdc_3063	12	ncdc_3579	7	ncdc_4082	2
ncdc_7320	23	ncdc_2535	12	ncdc_1401	5	ncdc_3477	0
ncdc_843	22	ncdc_4538	12	ncdc_1778	5	ncdc_130	0
ncdc_9210	22	ncdc_5121	12	ncdc_3007	5	ncdc_304	0
ncdc_4172	20	ncdc_3005	11	ncdc_263	5	ncdc_4742	0
ncdc_834	19	ncdc_1547	11	ncdc_6023	5	ncdc_8436	0
ncdc_4388	19	ncdc_5922	11	ncdc_6136	5	ncdc_8781	0
		ncdc_7664	11	ncdc_6740	5		

For the 1999-2008 period, ALERT gages were available and verification gages were selected from that pool. Analyses from the 1999-2002 were surveyed and a consistent set of 17 gages from the 174 ALERT gages available were selected. This was done for the post-2002 analyses to select a consistent set of 25 gages from the 254 available ALERT gages. Figure 6-9 through Figure 6-11 present the gages used for verification during these periods.

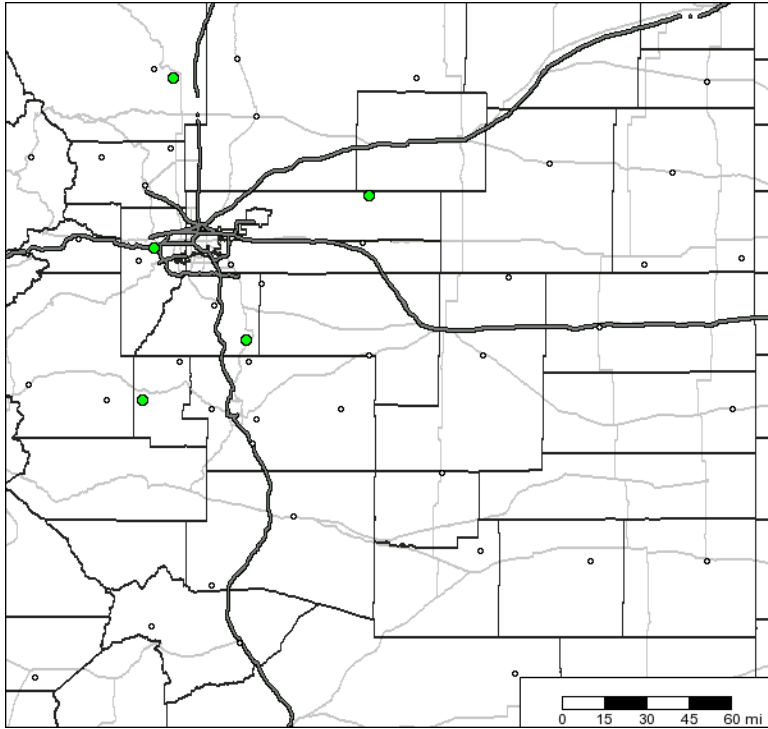


Figure 6-9: Verification gages for pre-1999 study periods.
 (Note: Larger green dots indicate verification gages.)

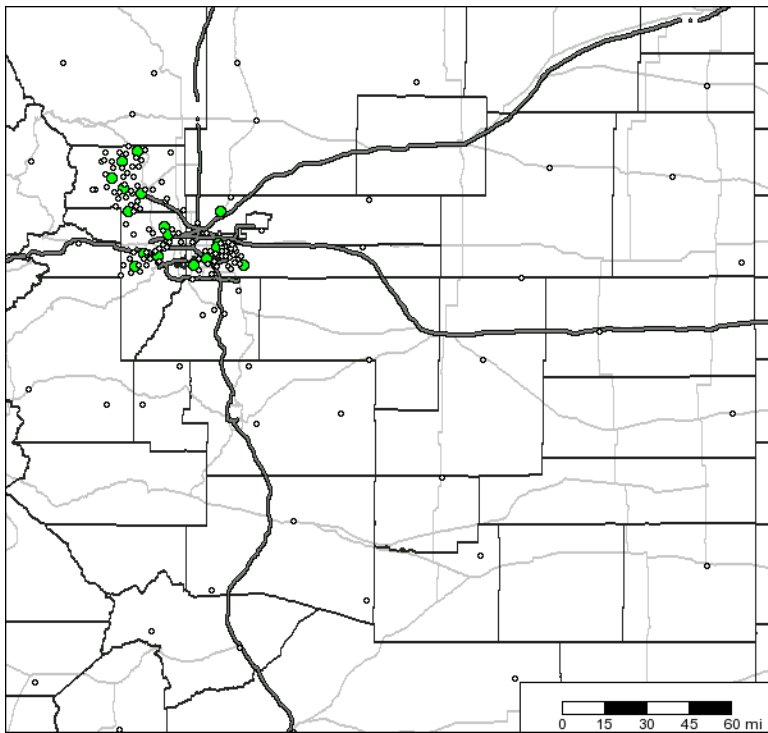


Figure 6-10: Verification gages for 1999-2002 study periods.
 (Note: Larger green dots indicate verification gages.)

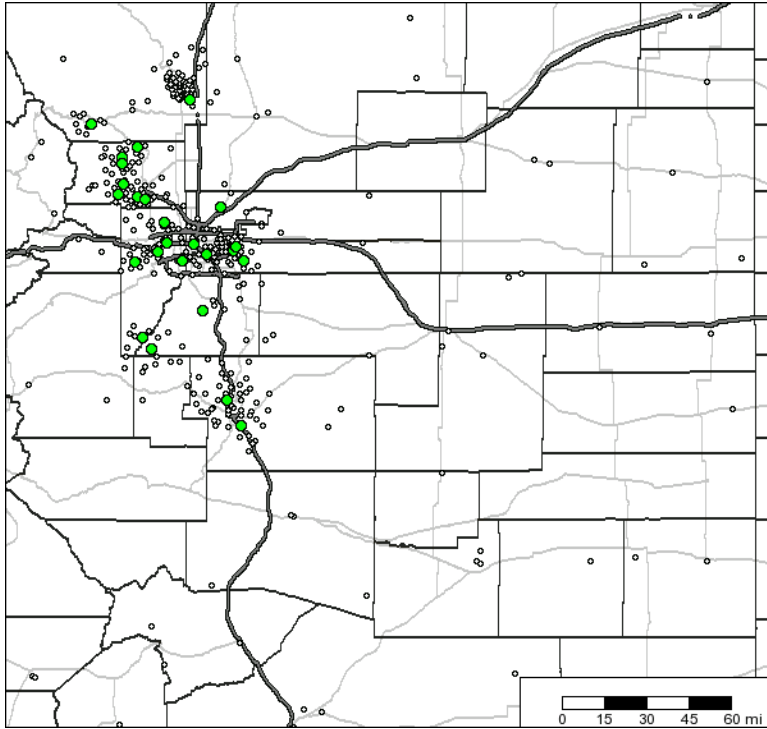


Figure 6-11: Verification gages for post-2002 study periods.
(Note: Larger green dots indicate verification gages.)

6.3.3 Verification Process and Results

To illustrate in detail how the verification process was performed, verification of the July 2006 dataset is described in detail. The following steps were taken:

1. A calibration gage dataset, including 289 non-verification gages, was assembled.
2. A verification gage dataset, consisting of the 25 gages, was assembled.
3. The GARR dataset was generated using only the calibration gages.
4. Radar pixels co-located with the verification gages were extracted from the GARR dataset.
5. The co-located rain gage and GARR results were compared.

Figure 6-12 presents the average accumulation plot for the verification gages and their co-located radar pixels. The average accumulation of the verification gages was 3.31 inches. The average accumulation of the adjusted radar pixels was 3.45 inches, 4.5% higher than the verification gages. Figure 6-12 presents the event totals from the July 2006 dataset. For the most significant event of July 9, 2006, the difference between the gages and radar was 3.1%.

Appendix B presents the average accumulation plots for the 24 GARR datasets.

The results of the verification process for the 24 GARR datasets are summarized in Figure 6-14. Overall, the average percentage difference in monthly rainfall amount was 4.8 % or 0.12 inches.

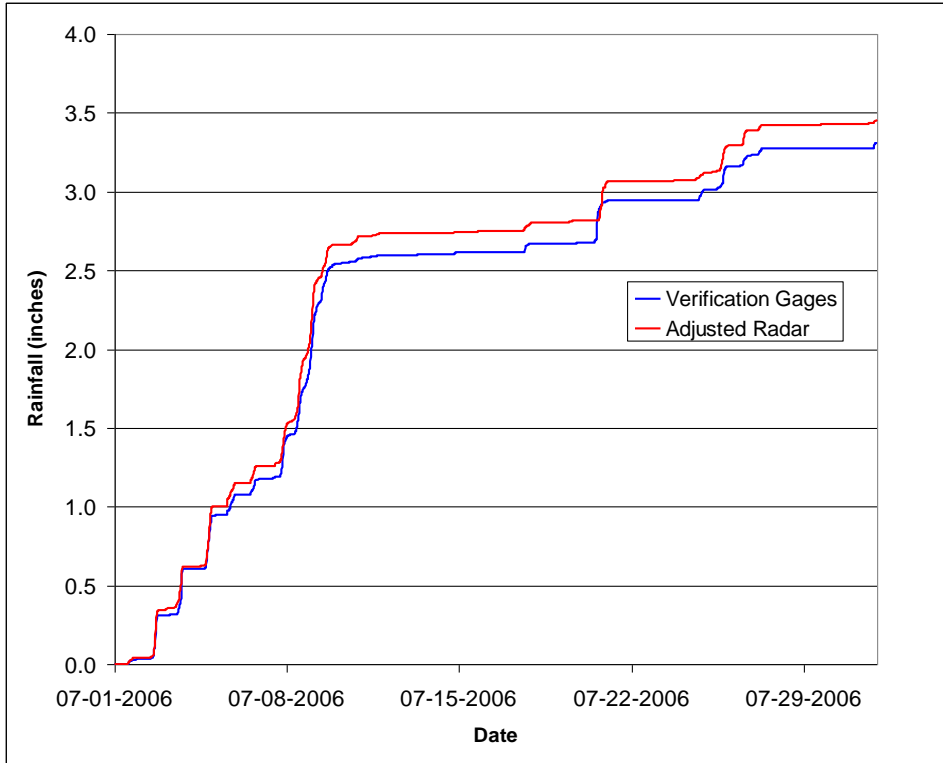


Figure 6-12: Average accumulation plot for verification gages and co-located radar pixels for July 2006 dataset.

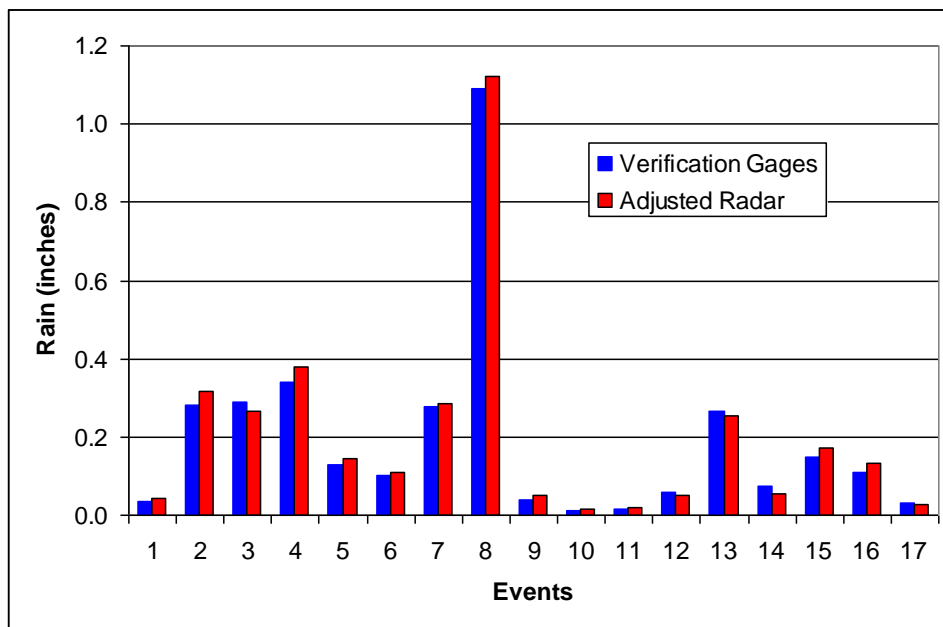


Figure 6-13: Event totals for verification gages and co-located radar pixels for July 2006 dataset.

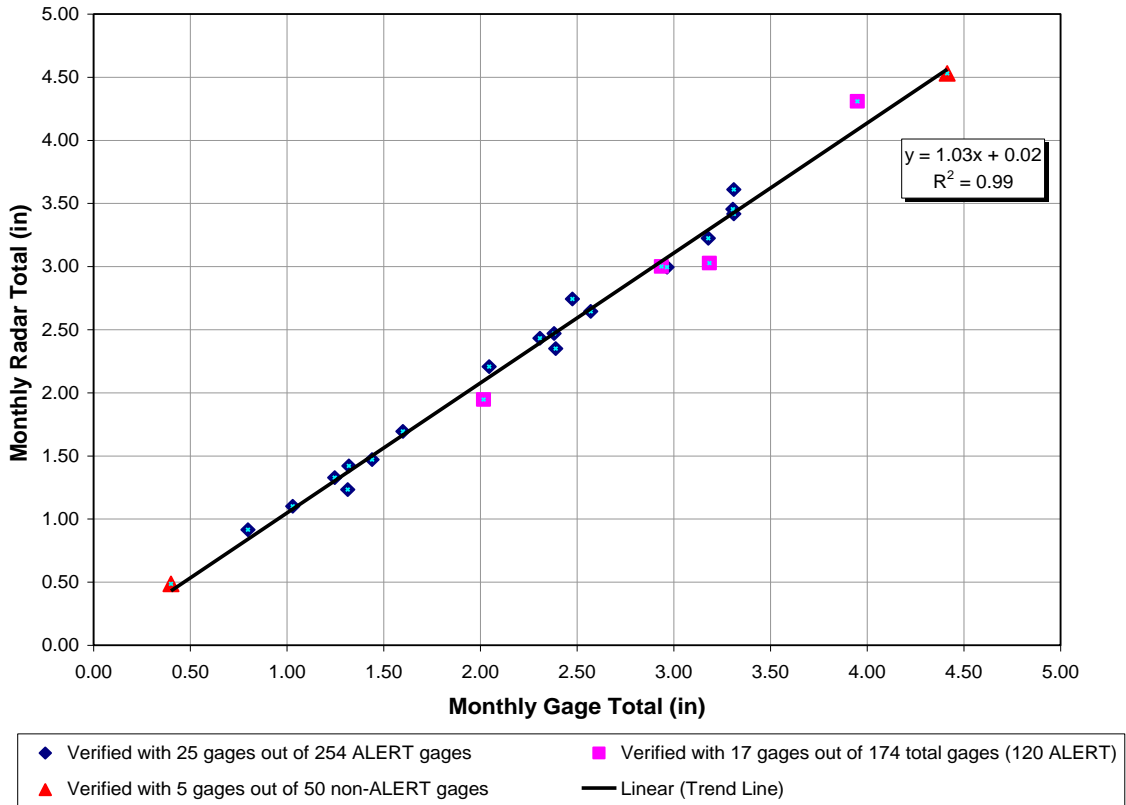


Figure 6-14: Monthly rainfall scatter-plot of verification gages and co-located radar pixels for the 24 months of GARR datasets.

6.4 Key Findings

- The results of the radar rainfall calibration verification process for the 24 GARR datasets showed that the average difference in monthly rainfall between observed gages and gage-adjusted radar rainfall was 4.8 % or 0.12 inches.

7.0 Determine Storm Properties

7.1 Background

The key to analyzing very large high resolution data sets are the tools needed to manage large geospatial data sets. In this study, a software tool known as TITAN (Thunderstorm Identification, Tracking, Analysis and Nowcasting, Dixon, 2005) was the primary tool used to identify and evaluate storm cells. TITAN evolved from efforts in South Africa during the 1980's to monitor and evaluate cloud seeding efforts. TITAN's theoretical background was formally presented by Dixon and Wiener, 1993.

Recently, Choi, et. al. (2009) published a new methodology for storm identification and tracking for modeling rainfall fields. The approach looks promising and warrants consideration for future work.

The principle investigators in this study have successfully used TITAN for similar analyses for the past decade (e.g. Hoblit, et. al, 2004, Curtis, 2007, Arsenault and Humphrey, 2007) and elected to use TITAN for this study as well.

In principle, TITAN analyzes gridded rainfall estimates at each time step. Areas of contiguous rainfall above a user-selected threshold are identified as storm cells. An ellipse is fit to each identified storm cell as shown in Figure 7-1.

From each elliptical area at each time step, a variety of geospatial properties are identified including cell area, location of cell centroid, peak average intensity within the cell, the area covered by each rainfall band, major and minor cell axes, and cell orientation as indicated by the declination of the cell major axis from North. Cell tracking information is also provided that includes cell speed and direction at each time step.

The collection of geospatial properties such as peak intensity, median cell area and shape, and average rainfall distribution with cells represent idealized storm cells as depicted in Figure 7-2. Note in Figure 7-1 that within each cell, the radar image shows an irregular rainfall surface with multiple peaks and valleys. Each surface is just one possible realization of a given combination of rainfall distributions within the cell. In theory, the idealized cell shown in Figure 7-2 is one of those infinite possibilities. The idealized storm cell concept forms the basis of understanding for radar-based DARFs and for tools to create realistic design rainfall input for hydrologic analyses.

TITAN processing requires data expressing in decibels, dBz, which were related to rainfall intensity by the following equation:

$$R = \frac{\left(\frac{10 \left(\frac{dBz}{10} \right)^{\frac{1}{1.6}}}{200} \right)}{25.4} \quad 7.1-1$$

where R is average rainfall intensity in in/hr and dBz is decibels. The gage-adjusted radar rainfall data set for all 24 months in the study period were converted to dBz for processing by TITAN. For analysis of 1-hour and 3-hour time steps, the 15-minute data were summed to the appropriate interval before converting to average rainfall rates in dBz. TITAN processed the rainfall data and summarized results in 1 dBz increments or bins as shown in Table 7.1-1.

Table 7.1-1: dBz Values with Equivalent Rainfall Intensities, iph.

dBz	Average Intensity (iph)						
19	0.022	29	0.093	39	0.393	49	1.658
20	0.026	30	0.108	40	0.454	50	1.914
21	0.029	31	0.124	41	0.524	51	2.211
22	0.034	32	0.144	42	0.605	52	2.553
23	0.039	33	0.166	43	0.699	53	2.948
24	0.045	34	0.191	44	0.807	54	3.404
25	0.052	35	0.221	45	0.932	55	3.931
26	0.061	36	0.255	46	1.077	56	4.540
27	0.070	37	0.295	47	1.243	57	5.242
28	0.081	38	0.340	48	1.436	58	6.054

Equation 7.1.1 was only used to convert the previously calibrated radar rainfall data (GARR) in inches/hour to dBz for TITAN processing. Appendix A contains the details of the radar rainfall calibration process. The non-linear conversion from already calibrated radar rainfall to dBz is a direct explicit one-to-one relationship. It has no significant effect on our interpretation of the results. TITAN analyzes the areal coverages to determine individual storm cell sizes and the area covered by each rainfall intensity.

TITAN results were summarized in 1 dBz increments of maximum cell intensity to determine cell counts and cell areas. Since equal bin size increments of 1 dBz were used in dBz “space”, the non-linear conversion does create unequal bin size increments in “rainfall space.” This resulted in smaller bin sizes for the more frequently occurring light rainfall intensities and larger bin sizes for the less frequently occurring heavy rainfall intensities.

The remainder of the TITAN processing for DARF estimation is summarized as follows:

1. TITAN detects all cells in the study area,
2. Geospatial statistics are reported by TITAN for each cell,
3. Geostatistics are plotted using ArcView GIS,
4. Cell statistics are imported into an Excel spreadsheet to
 - a. Sort all cells by peak intensity (1 dBz increments)
 - b. Compute median cell size for each peak intensity (1 dBz increments)
 - c. Compute average rainfall distribution for cells of each peak intensity which defines the average shape of the idealized cell at each peak intensity,
 - d. Compute DARFs.
5. Use computed DARF information for parameters to a prototype design storm processor.

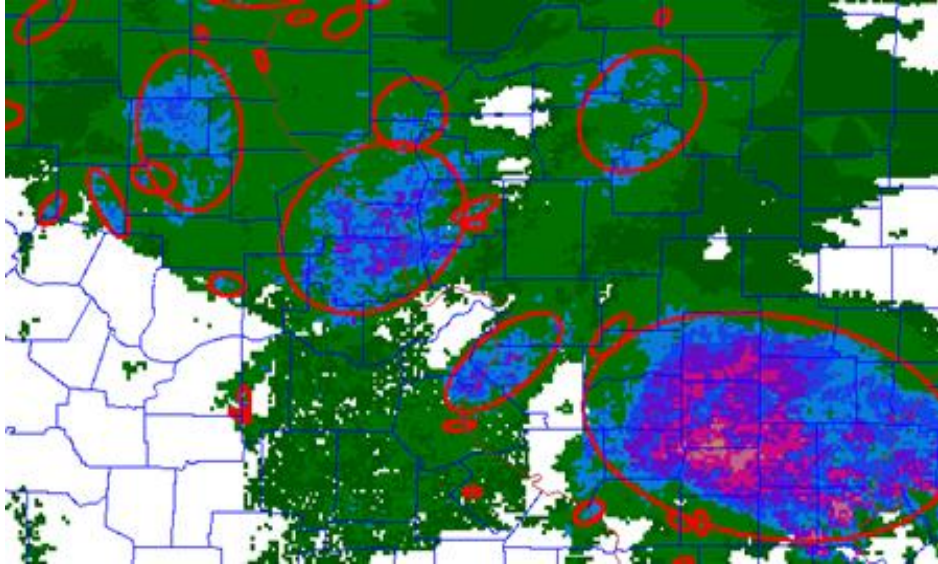


Figure 7-1: Example Radar Image with Storm Cells Enclosed by Fitted Ellipses.

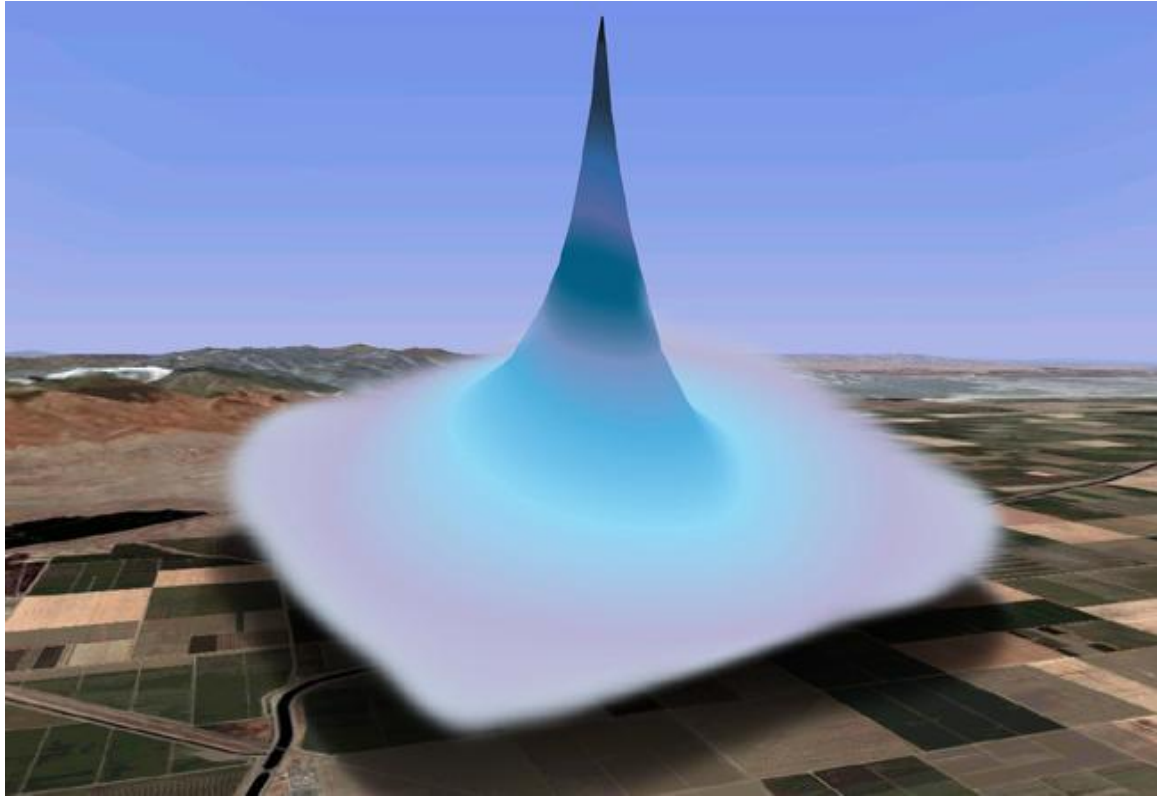


Figure 7-2: Idealized Storm Cell Derived from TITAN Statistics

7.2 Typical Storm Patterns

The TITAN analyses provided statistics, location of cloudburst centers, direction of cloudburst center movement, speed of cloudburst center, and relationships, for selected durations, between maximum pixel depth and areal averages of rainfall depths within the cloudburst.

TITAN results and analyses of rain gage data were used to determine general storm patterns in eastern Colorado as well as in and near the Fountain Creek and Jimmy Camp Creek Watersheds for specific storms. Figure 7-3 through Figure 7-18 show the spatial variability of cell count and median cell size for 15-minute, 1-hour, and 3-hour cells. Analyses for the full eastern Colorado study area and for El Paso County are included.

The time steps of 15 minute, 1 hour, and 3 hours were chosen to enable direct comparison to publish NWS DARFs. The 15-minute time step was the smallest time increment possible since the GARR data for this portion of the study were in 15-minute increments.

The maximum time step of 3-hours was used for several different reasons. The first has to do with TITAN processing. TITAN was originally design to process instantaneous radar rainfall rates. In this application, rainfall totals for a given time step are converted to average intensity in inches/hour over the selected time step. As time steps increase, light rain is averaged over ever larger time steps; creating some uncertainty at the edges of storm cells as average rainfall rates fall to “noise” levels. This affects the estimates of cell area. Investigators tried to mitigate this problem by changing the cell edge definition in dBz for each time step to be approximately the equivalent of 0.1 inches/hour. (This is an area for further scrutiny in future work.) Secondly, events of 3-hours were quite infrequent as the longer storms were typically composed of multiple smaller duration events. A third consideration was budget. This was a big effort but, unfortunately, unlimited resources were not available.

Figure 7-3 shows the spatial distribution of 15-minute cell count where cell count is the number of occurrences that the centroid of a cell was observed in a given 4 mi. x 4 mi. grid. Figure 7-4 shows the median cell area for cells whose centroids were observed in a given 4 mi. x 4 mi. grid. *(Note: The 1 km and 2 km grids were associated with the raw and calibrated radar rainfall data. The 4 mi x 4 mi grid was established to summarize the TITAN results for storm counts and storm cell areas by location. A larger grid size was needed to gain sufficient numbers of cells in each grid to yield sufficiently stable statistical results. From observation, a minimum of 20 counts per grid seemed to produce reasonable results.)* The general finding drawn from these two figures suggest that more 15-minute storm cells were observed over the Front Range than over the plains of eastern Colorado. At the same time, 15-minute storm cells were generally larger over the plains than along the Front Range. The differences are likely orographic in origin as the more variable terrain fosters more small cells where as cells tend to form larger complexes over the flatter terrain with fewer uplift triggers.

Figure 7-5 and Figure 7-6 show cell count and median storm sizes for El Paso County and the Fountain Creek Watersheds. Even over this smaller area, the same pattern holds: more small storms to the west, fewer but larger storms to the east. The high elevation terrain along the western boundary of the Fountain Creek Watershed generates cells at twice the rate (or more) than the lower elevation areas to the east and southeast. Conversely, cells in the eastern portions of the watershed do appear slightly larger but the difference is not as pronounced.

Figure 7-7 through Figure 7-10 also show results for 15-minute cells but with a higher detection threshold (35 dBz or 0.22 iph compared to 19 dBz or 0.022 iph). The higher detection threshold reduces the amount of very light rainfall from the analysis. The same general findings are present in the 35 dBz case – more small cells to the west, fewer but larger cells to the east.

Figure 7-11 through Figure 7-18 present similar results for 1-hour and 3-hour storm cells. More cells occur along the Front Range but cells in the eastern planes tend to larger sizes. However, the differences

tend to decrease somewhat as the time period increases. As time step increases, individual storm cells tend to decay and/or merge with other cells leaving larger overall footprints throughout the region.

Figure 7-19 presents the frequency distribution of 15-minute cells as a function of cell area and peak intensity. As expected, the vast majority of the more than 100,000 15-minute cells have low peak intensity and small cell sizes.

Figure 7-20 shows the frequency distribution of 15-minute cells as a function of peak intensity for Eastern Colorado and for El Paso County. Again, as expected, most observed cells have low rainfall rates. Approximately 93% of all 15-minute cells have peak rainfall rates less than one inch per hour. El Paso County cells follow a similar pattern.

Figure 7-21 charts median 15-minute cell areas versus peak cell intensity (iph) for the eastern Colorado and El Paso County study areas. (Note: Peak rainfall intensities were grouped by intensity ranges and median size sizes were computed for each intensity range.) The key finding from Figure 7-21 is the strong relationship between peak cell intensity and cell area. As peak intensity increases, cell sizes tend to increase, up to a point. Then cell sizes decrease as intensities increase.

In previous studies by the principal investigators, similar behaviors have been observed in a variety of locations and climates around the US, including eastern Missouri, central Texas, Florida, and southern Nevada. For 15-minute cells, the maximum cell area occurs at intensities in the 2-5 year recurrence range. The 2-5 year recurrence range at the Colorado Springs Airport is 2.80 – 4.28 iph for 15-minutes. Figure 7-21 shows that the maximum median cell area occurs at about 4.2-4.4 iph for 15-minutes which is consistent with earlier experience of the principal investigators.

In this study, the data set was relatively limited and too few high intensity events were observed to stabilize the statistical median. From observation in this study, the statistical median cell size wasn't stable when the number of observations in an intensity range was less than about 20-30 cells. Beyond a general observation that cell size appears to continue to decrease at higher intensities, the statistics in this study weren't stable enough to estimate median cell sizes above about the 20-25 year event.

The finding that cell size varies with intensity is important from a design perspective. It potentially means that the cell size for a 100-year design storm should be substantially different than the cell size for a 5-year design storm. The 100-year design storm could be 40-50% smaller than the 5-year design storm.

Figure 7-21 also compares 15-minute cell size versus peak intensity for the eastern Colorado and El Paso County. In general, cell sizes are smaller for El Paso County than for eastern Colorado as a whole. El Paso County results reflect its Front Range location increased influence by the highly variable terrain.

Figure 7-22 through Figure 7-27 provide similar results for 1-hour and 3-hour cells. The general results are consistent with the 15-minute cell results. Note that the differences in the cell size versus peak intensity relationship decreases with increased time increments. By the 3-hour time step, these differences virtually disappear.

Specific cloudburst events, generally thunderstorms with durations less than 3 hours, were analyzed for the Jimmy Camp Creek watershed area using available gage-adjusted radar rainfall data to define areal coverage. Detailed rain gage and bucket survey information for a major event over Jimmy Camp Creek Watershed from June 17, 1965 (Snipes, 1974) were also included. Table 7.2-1 shows the dates and times of the individual events. Storm totals, durations, areas were determined and presented Table 7.2-1 and also in Figure 7-28. A recurrence interval was assigned to each storm total using the Colorado Springs Airport recurrence statistics for the appropriate storm duration. Maximum 15-minute intensities for each event and cell area at the 15-minute maximum were determined and shown in Table 7.2-1. A recurrence interval was assigned to each 15-minute peak intensity using the Colorado Springs Airport recurrence statistics then presented in graphical form (Figure 7-29). Areas for each storm event where radar data were available were determined from images presented in Figure 7-30 through Figure 7-49.

The curves shown in Figure 7-28 relate median cell areas from the TITAN analysis to recurrence interval by storm duration. The individual observed storm events noted in Table 7.2-1 are plotted on Figure 7-28 showing storm date and duration of each event. There is very good agreement between the individual event observations and the general curves shown in Figure 7-28. Similar agreement is noted in Figure 7-29 for cell areas at the 15-maximum peak intensity.

Figure 7-28 indicates that a maximum storm cell size, for 1-, 2- and 3-hour events, occurs between the 5-year and 25-year recurrence. These relationships are consistent with cloudburst analyses conducted by the principal investigators in the greater St. Louis area, Florida, and Texas. The Fountain Creek data actually had very few observed events exceeding the 5-year recurrence and the curves shown cannot be justified for those few events. Much greater reliability can be assigned to the envelope curve shown in Figure 7.2-27, which shows that maximum 15-minute cloudburst area for recurrences up to 100-years is 200-250 square miles. The importance of area for describing a cloudburst design storm for watersheds would indicate that the database of observed radar events in the Fountain Creek watershed should be increased.

15 Minute Cell Count
Eastern Colorado
19 dBz Threshold

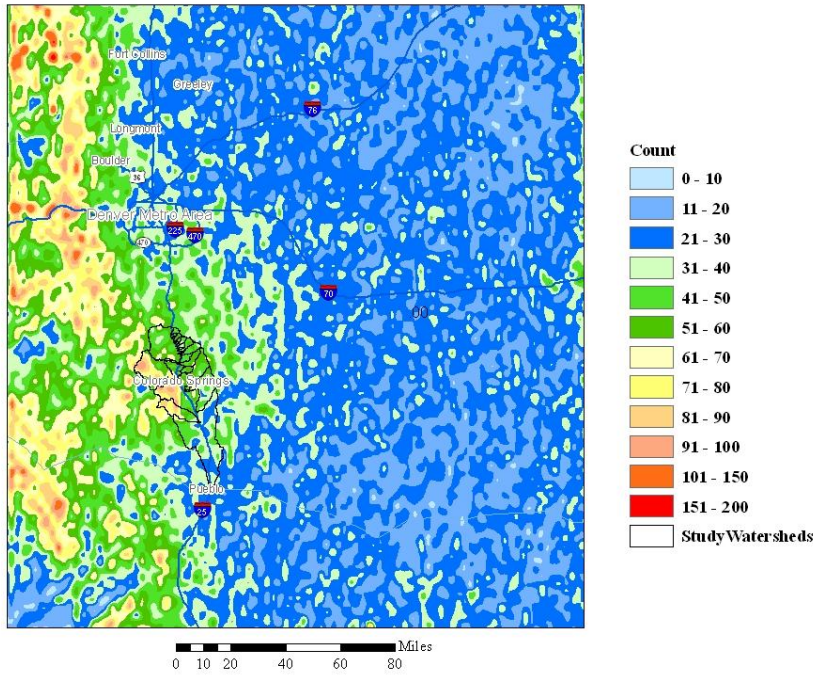


Figure 7-3: 15-Minute Cell Count - Eastern Colorado (Fountain Creek watersheds are shown in outline.)

Median 15 Minute Cell Area
Eastern Colorado
19 dBz Threshold

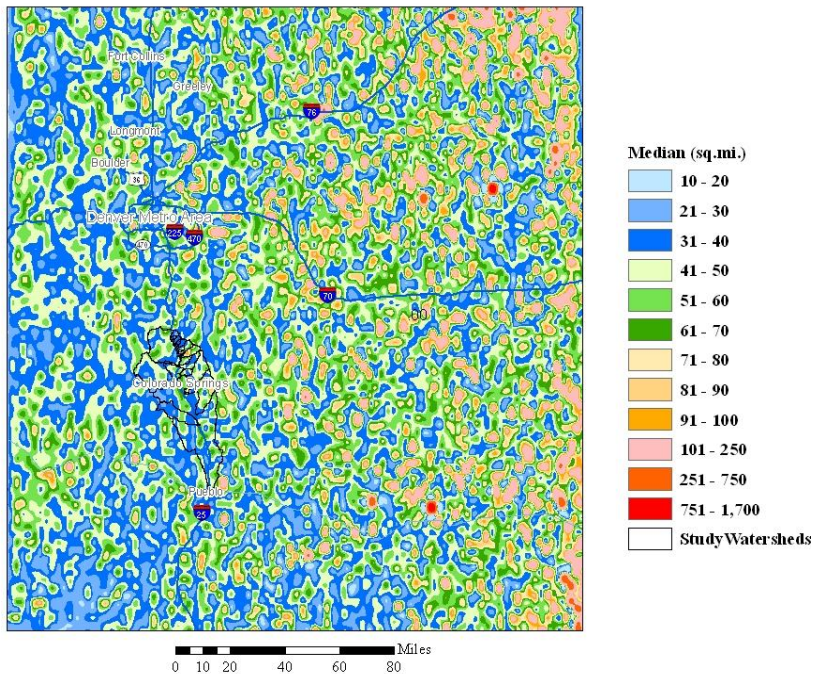


Figure 7-4: Median 15-Minute Cell Area

15 Minute Cell Count
Eastern Colorado
19 dBz Threshold

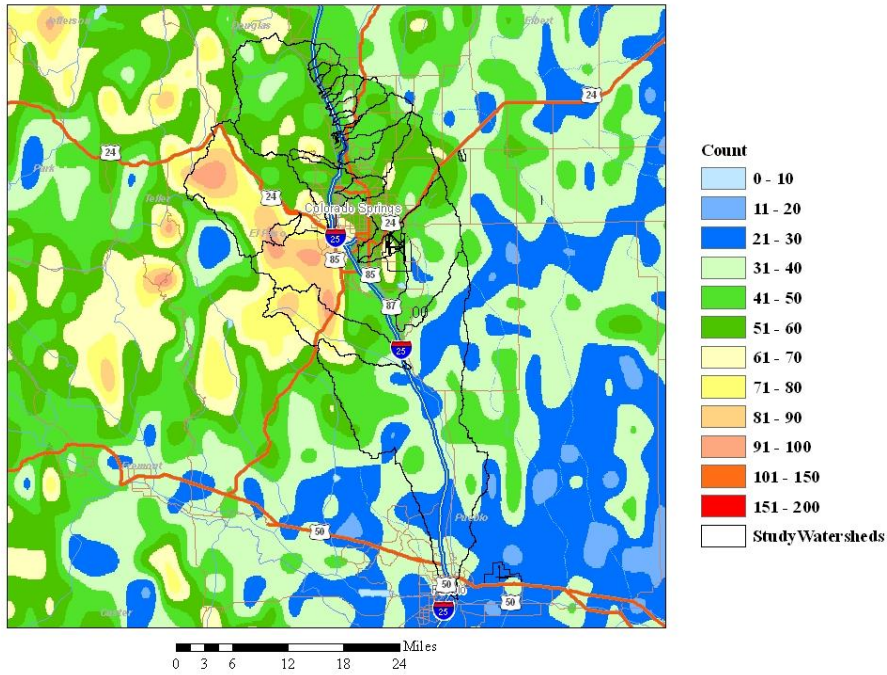


Figure 7-5: 15-Minute Cell Count El Paso County

Median 15 Minute Cell Area
Eastern Colorado
19 dBz Threshold

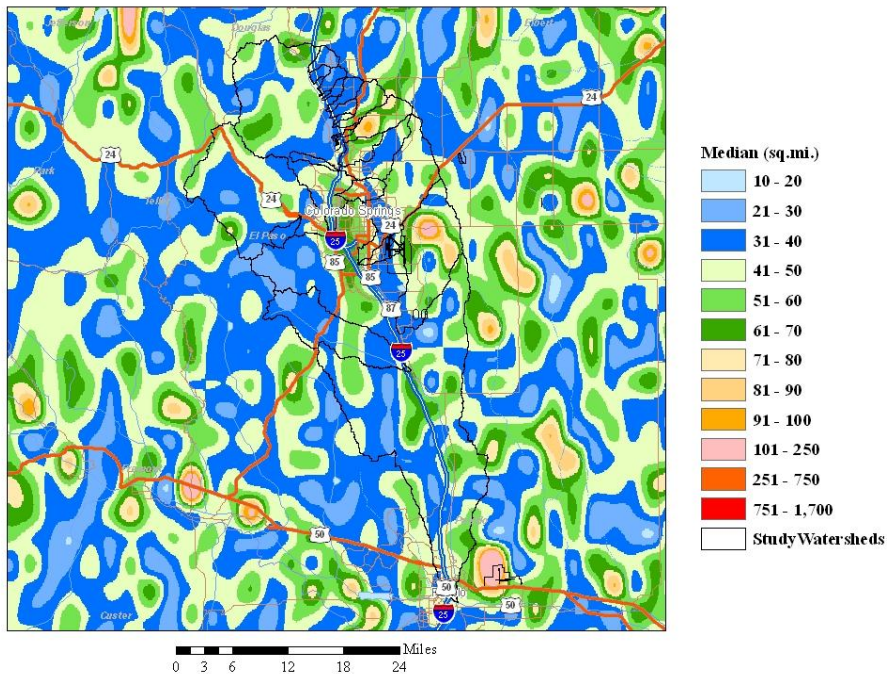


Figure 7-6: Median 15-Minute Cell Area - El Paso County

15 Minute Cell Count
Eastern Colorado
35 dBz Threshold

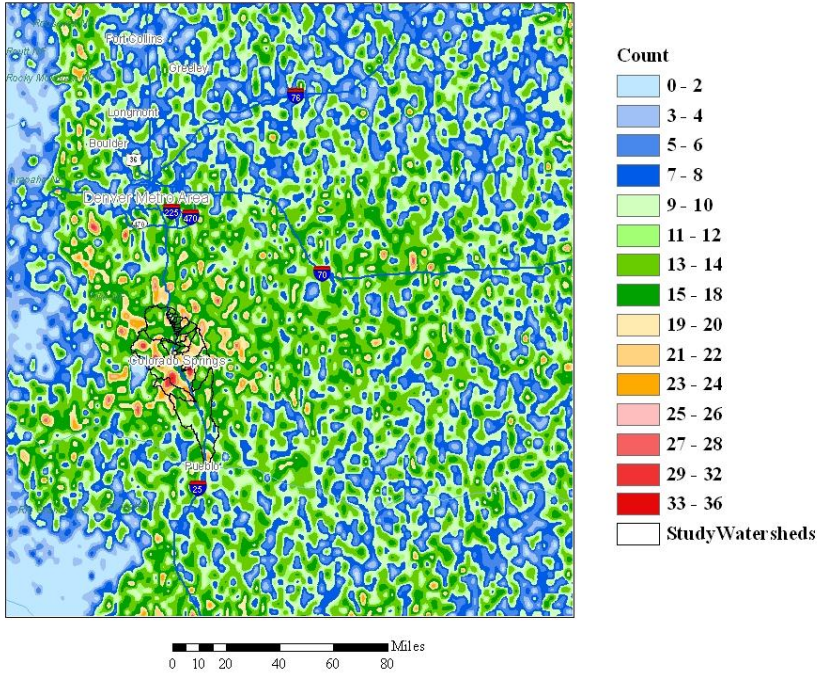


Figure 7-7: 15-Minute Cell Count - Eastern Colorado (35 dBz Threshold, 0.22 iph)

Median 15 Minute Cell Area
Eastern Colorado
35 dBz Threshold

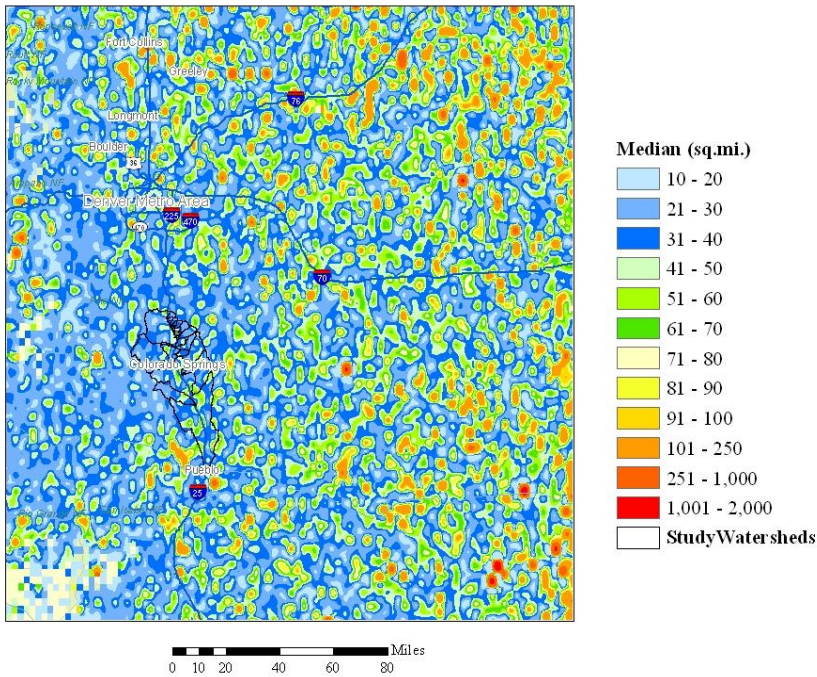


Figure 7-8: Median 15-Minute Cell Area - Eastern Colorado (35 dBz Threshold, 0.22 iph)

15 Minute Cell Count
Eastern Colorado
35 dBz Threshold

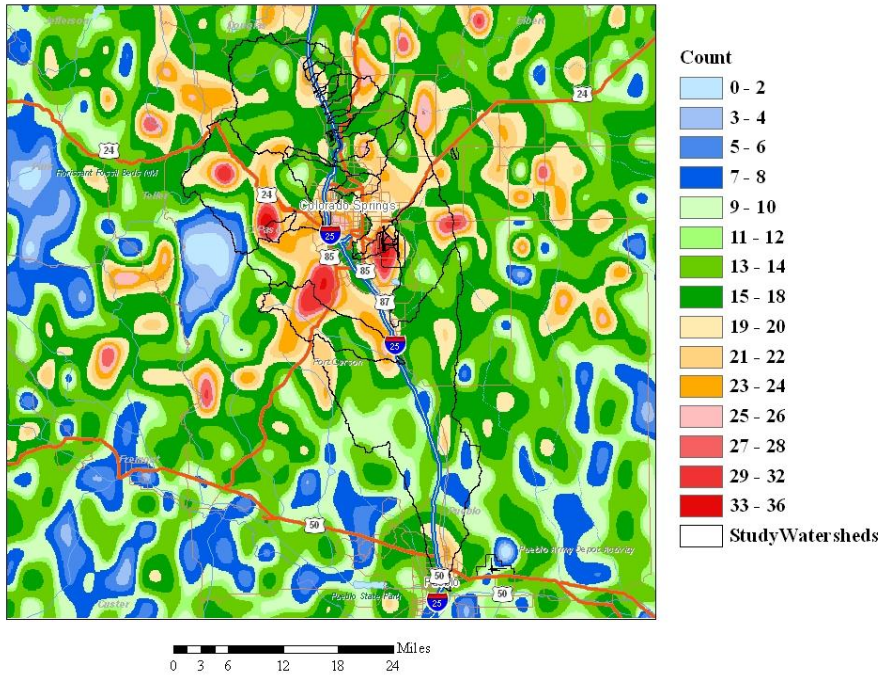


Figure 7-9: 5-Minute Cell Count - El Paso County (35 dBz Threshold, 0.22 iph)

Median 15 Minute Cell Area
Eastern Colorado
35 dBz Threshold

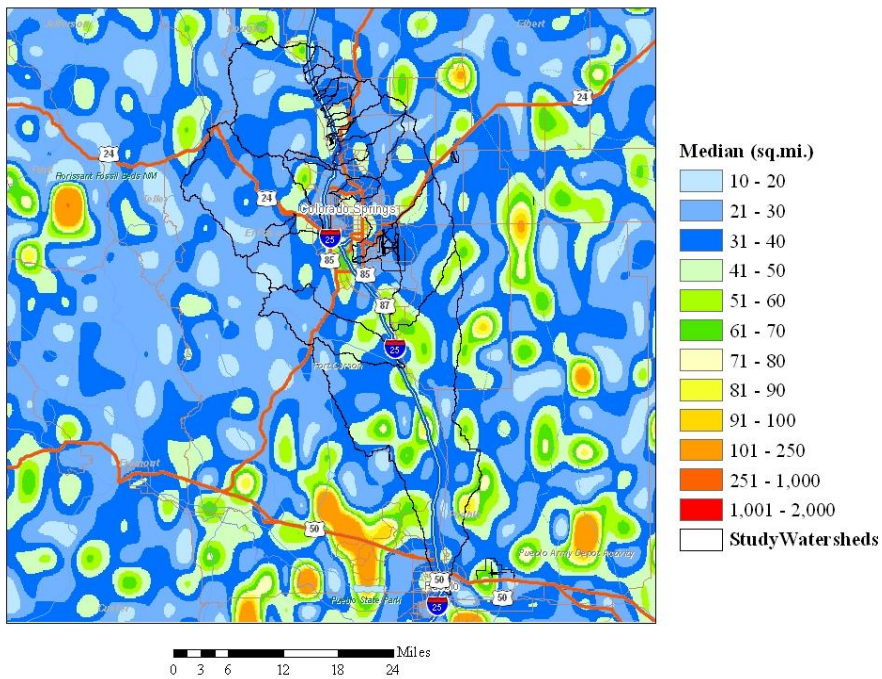


Figure 7-10: Median 15-Minute Cell Area - Eastern Colorado (35 dBz Threshold, 0.22 iph)

**1-Hour Cell Count
Eastern Colorado**

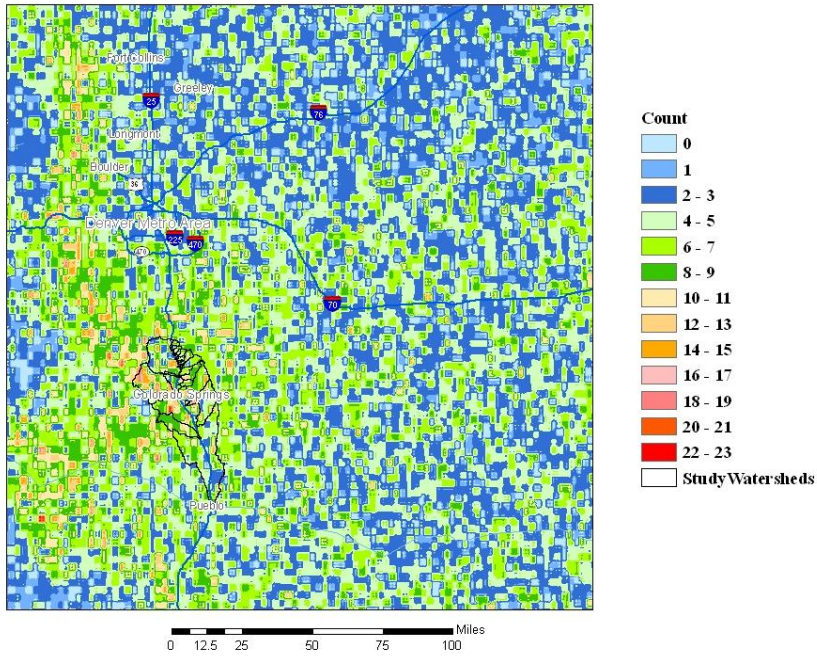


Figure 7-11: 1-Hour Cell Count - Eastern Colorado (29 dBz Threshold, 0.09 iph)

**Median 1-Hour Cell Area
Eastern Colorado**

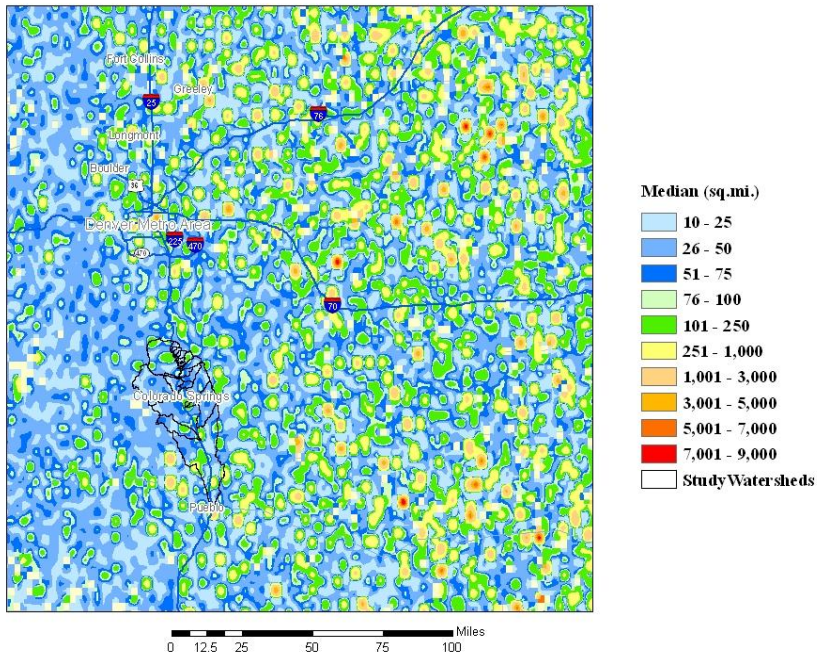


Figure 7-12: Median 1-Hour Cell Area - Eastern Colorado (29 dBz Threshold, 0.09 iph)

**1-Hour Cell Count
Eastern Colorado**

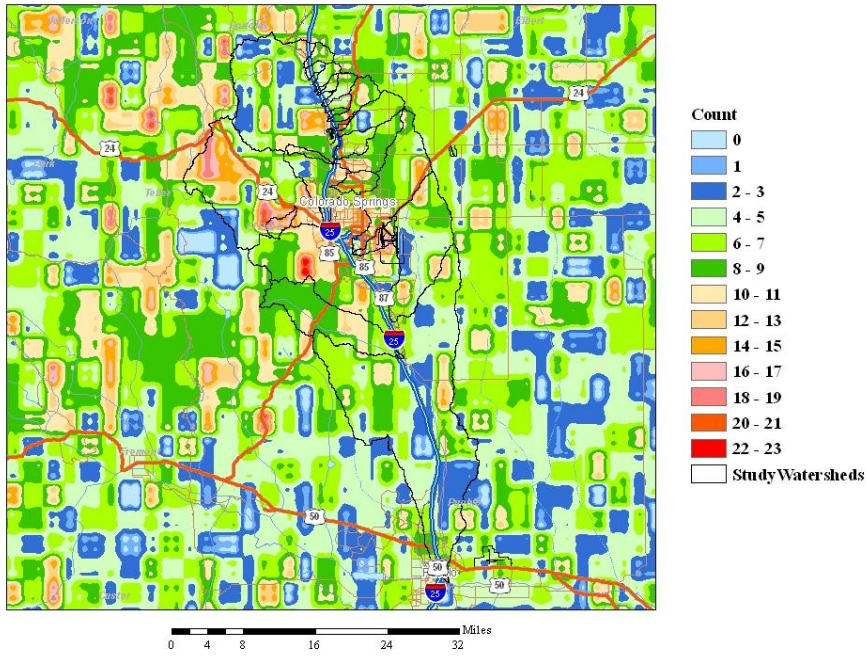


Figure 7-13: 1-Hour Cell Count – El Paso County (29 dBz Threshold, 0.09 iph)

**Median 1-Hour Cell Area
Eastern Colorado**

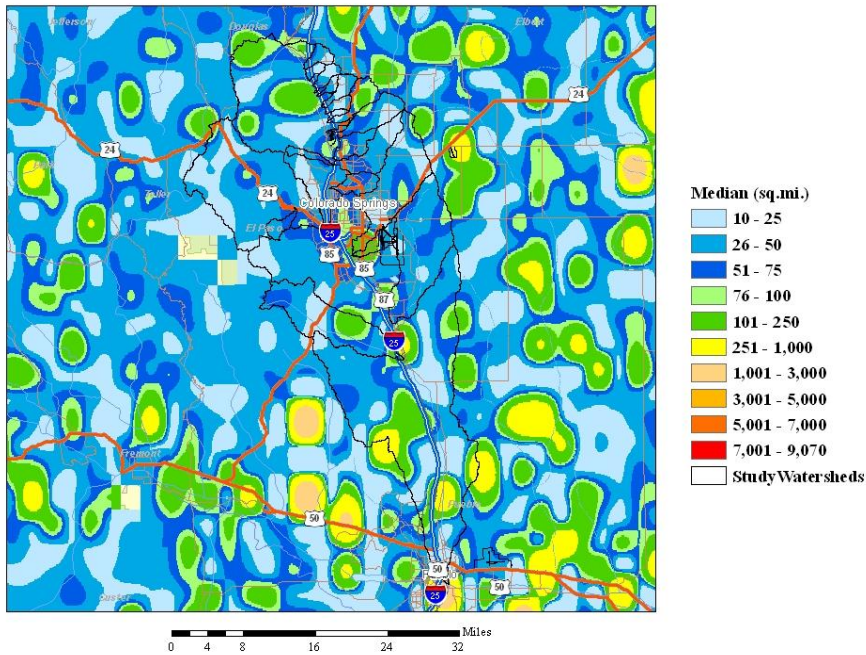


Figure 7-14: Median 1-Hour Cell Area - El Paso County (29 dBz Threshold, 0.09 iph)

3-Hour Cell Count
Eastern Colorado

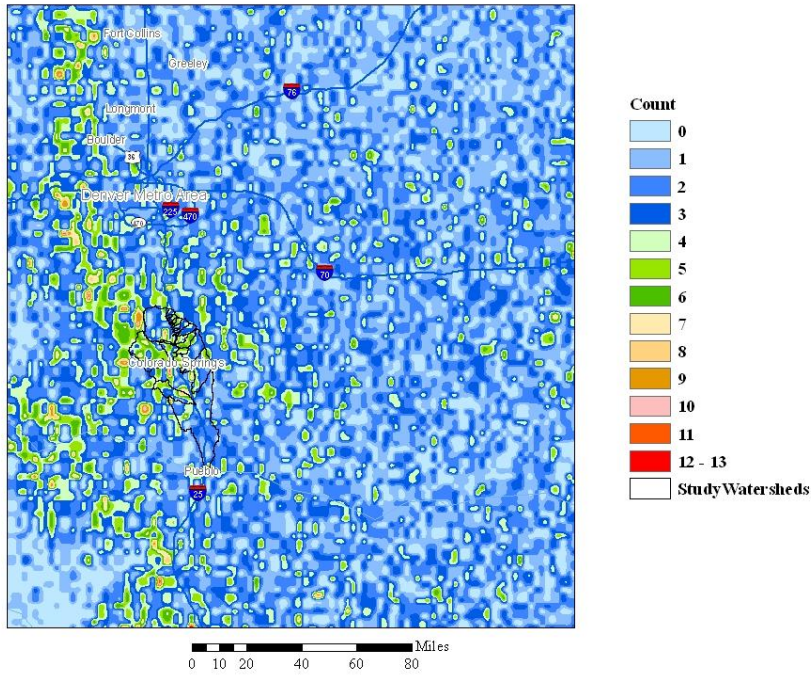


Figure 7-15: 3-Hour Cell Count - Eastern Colorado (25 dBz Threshold, 0.05 iph)

Median 3-Hour Cell Area
Eastern Colorado

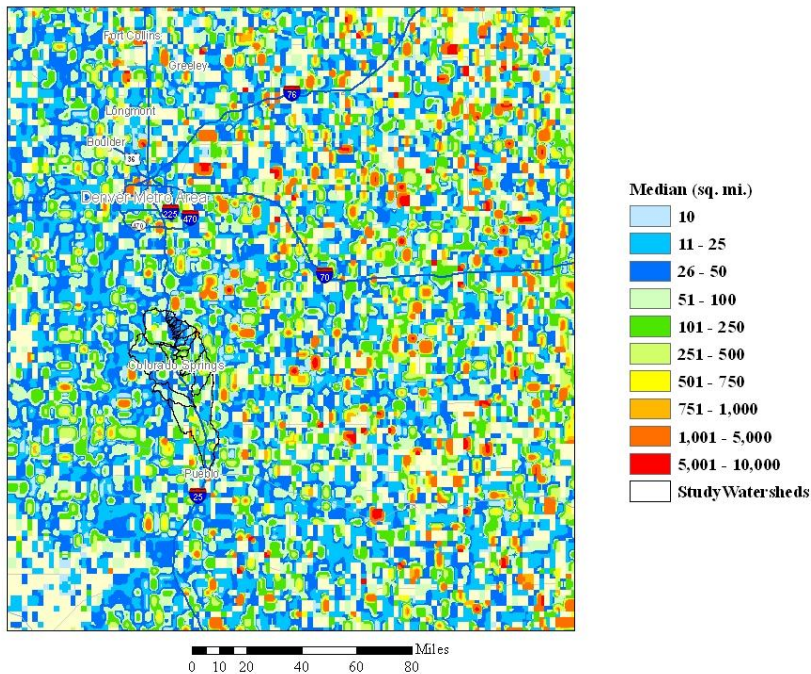


Figure 7-16: Median 3-Hour Cell Area - Eastern Colorado (25 dBz Threshold, 0.05 iph)

3-Hour Cell Count
Eastern Colorado

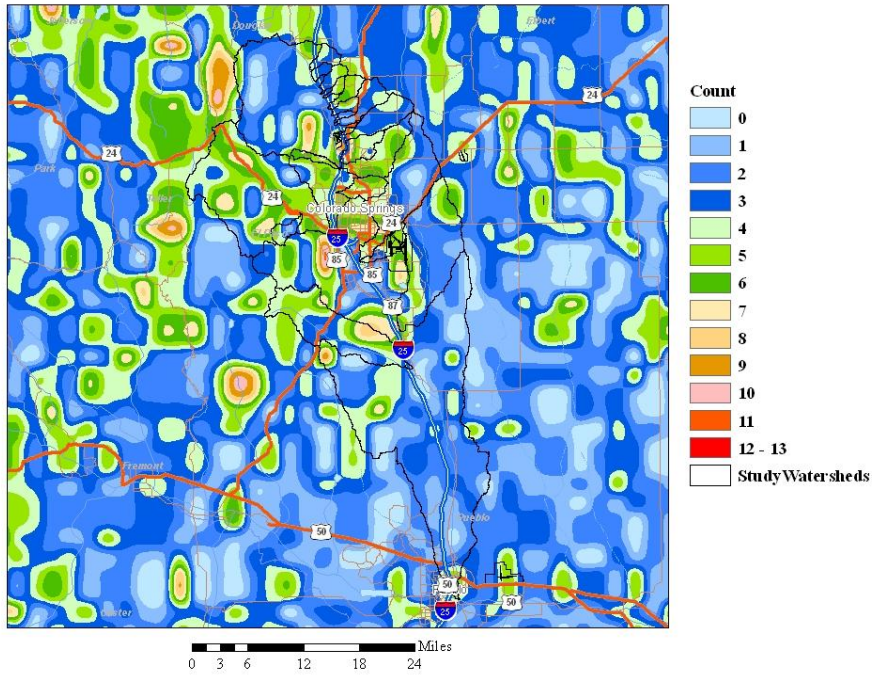


Figure 7-17: 3-Hour Cell Count - El Paso County (25 dBz Threshold, 0.05 iph)

Median 3-Hour Cell Area
Eastern Colorado

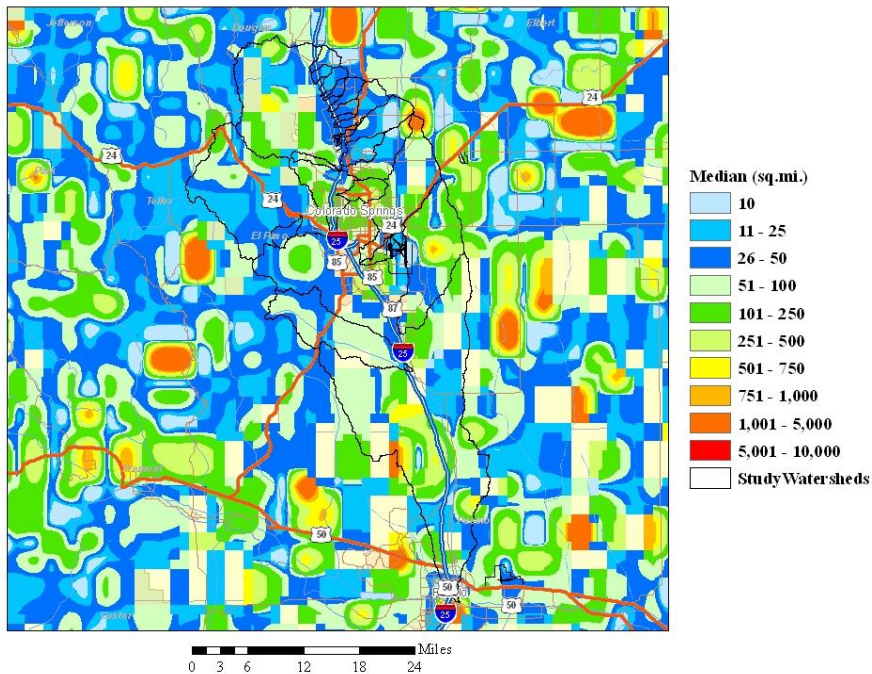


Figure 7-18: Median 3-Hour Cell Area - El Paso County (25 dBz Threshold, 0.05 iph)

Distribution of 15-Minute Cell Sizes
19 dBz Threshold (0.02 iph)

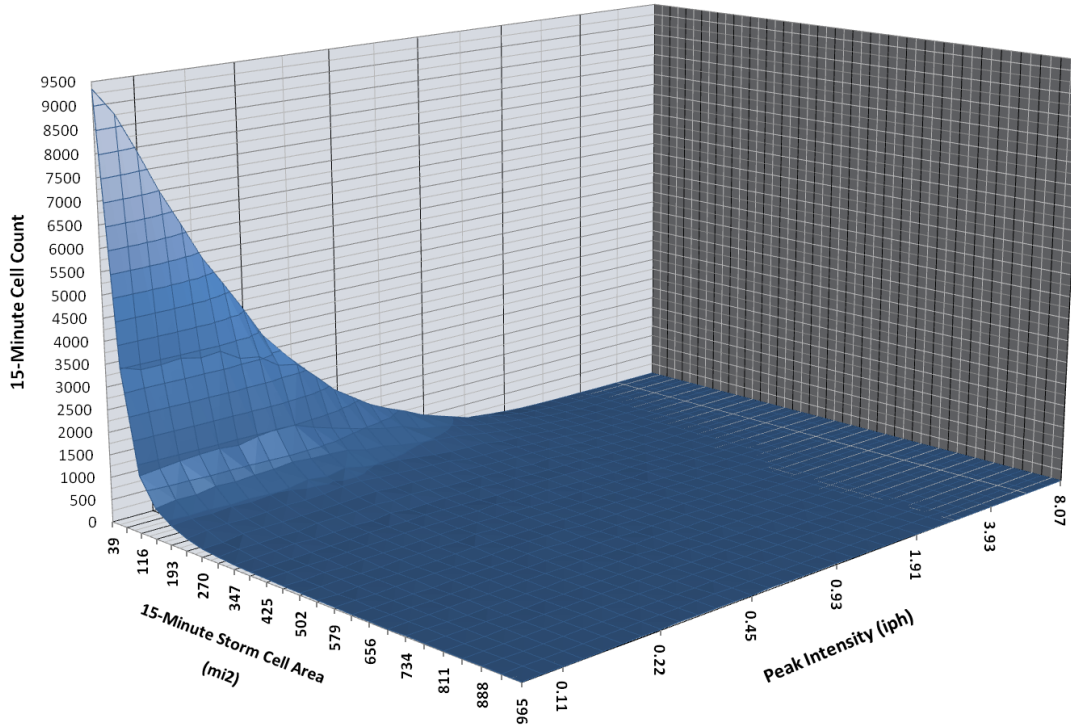


Figure 7-19: Distribution of 15-Minute Cell Sizes – Eastern Colorado (35 dBz Threshold, 0.22 iph)

15-Minute Storm Cell Count

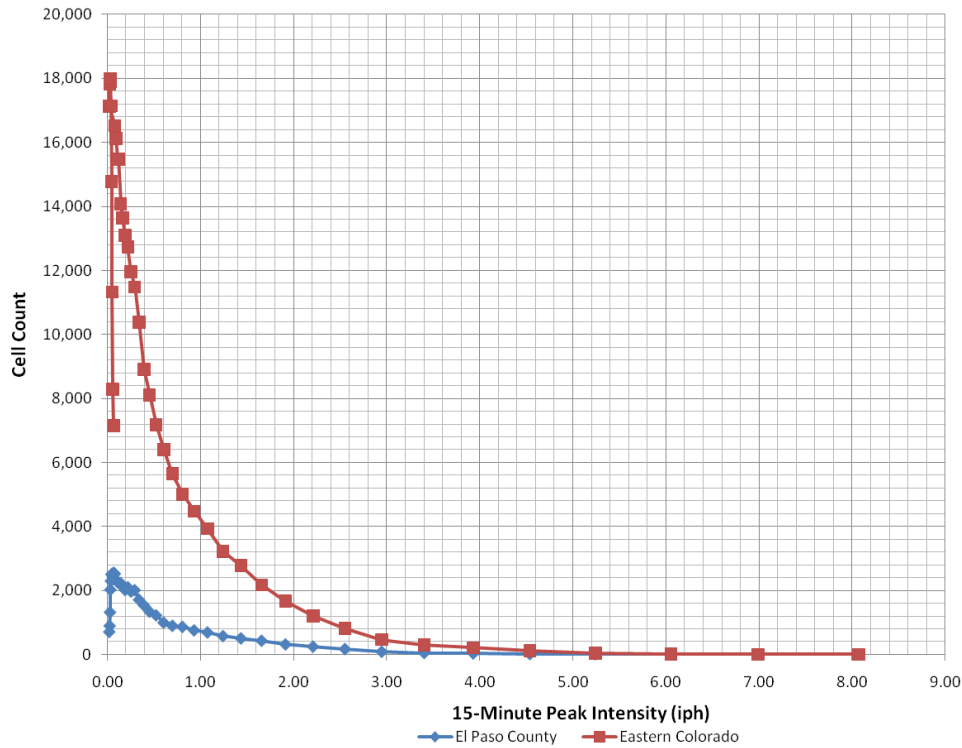


Figure 7-20: 15-Minute Cell Count Distribution (35 dBz Threshold, 0.22 iph)

15-Minute Cell Size vs. Peak Intensity

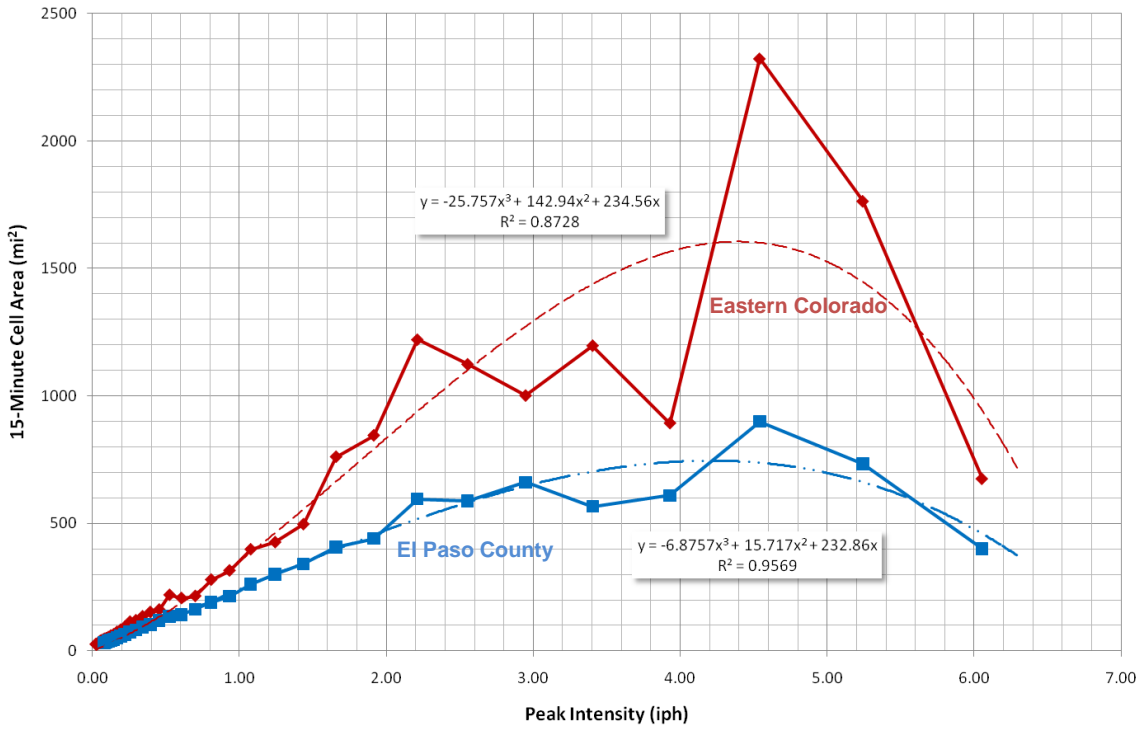


Figure 7-21: 15-Minute Cell Size vs. Peak Intensity (35 dBz Threshold, 0.22 iph)

Distribution of 1-Hour Cell Sizes

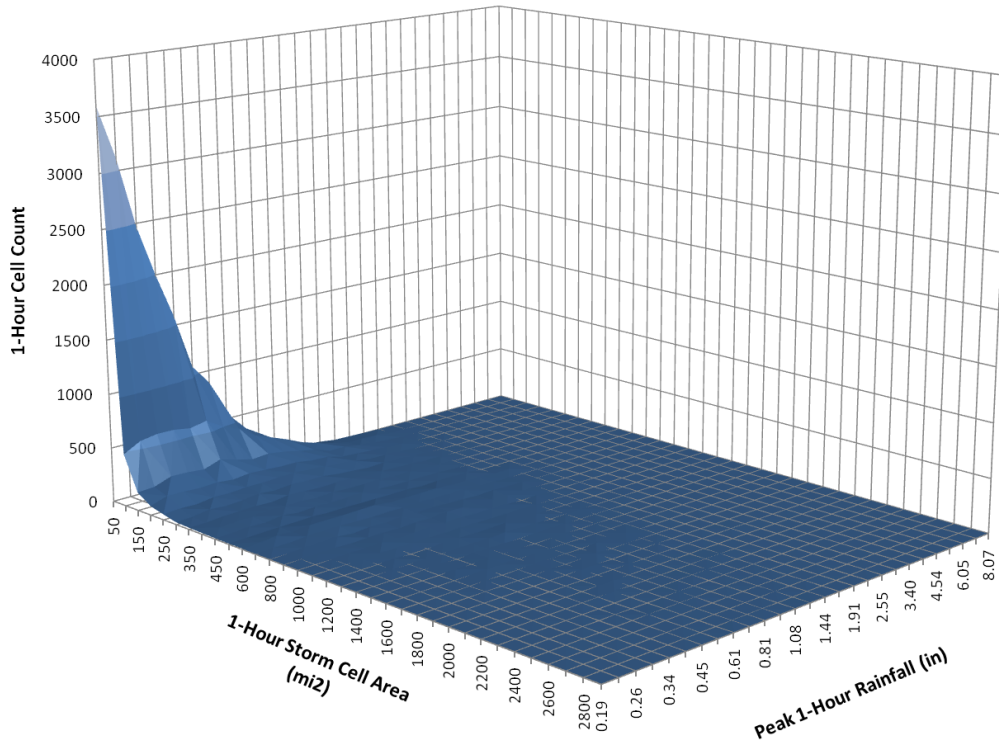


Figure 7-22: Distribution of 1-Hour Cell Sizes - Eastern Colorado (29 dBz Threshold, 0.09 iph)

Distribution of Peak 1-Hour Rainfall

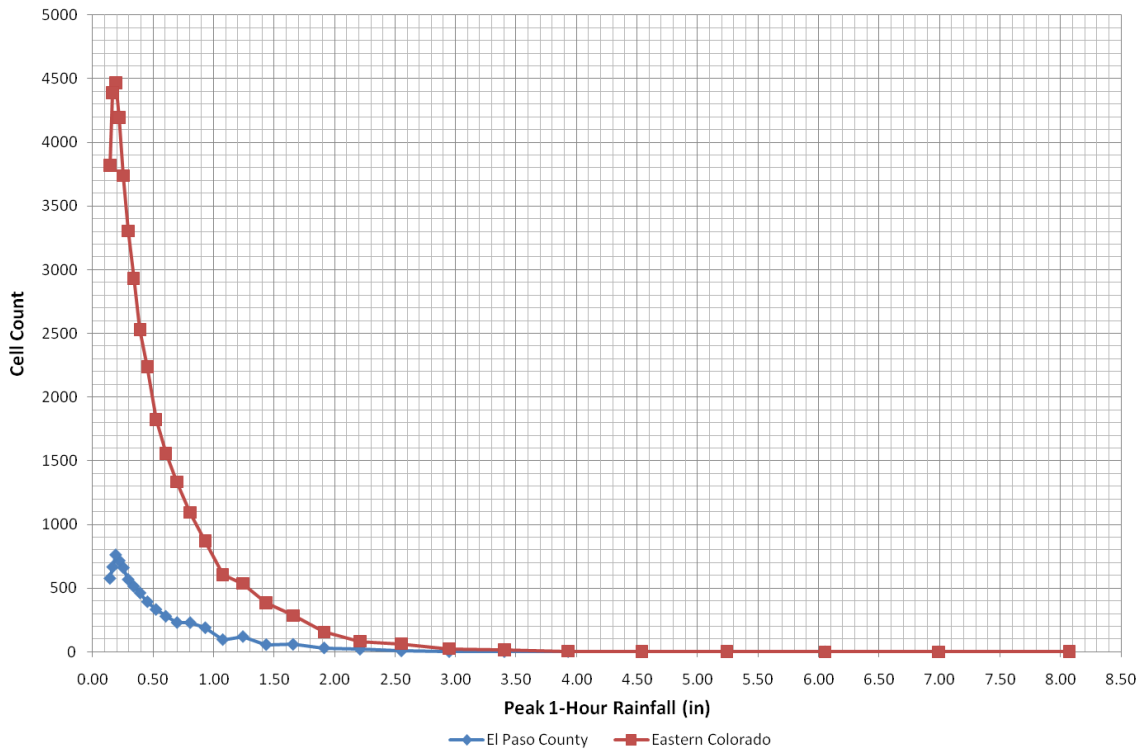


Figure 7-23: Distribution of Peak 1-Hour Rainfall (29 dBz Threshold, 0.09 iph)

1-Hour Cell Size vs. Peak Intensity

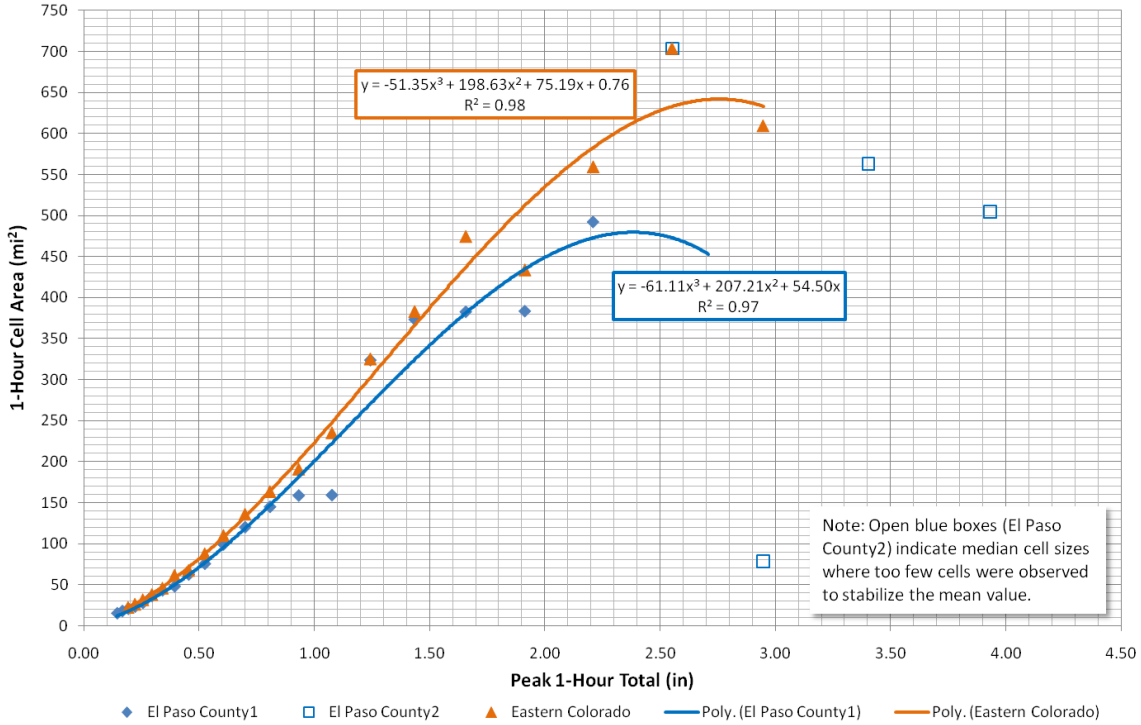


Figure 7-24: 1-Hour Cell Size vs. Peak Intensity (29 dBz Threshold, 0.09 iph)

Distribution of 3-Hour Cell Sizes

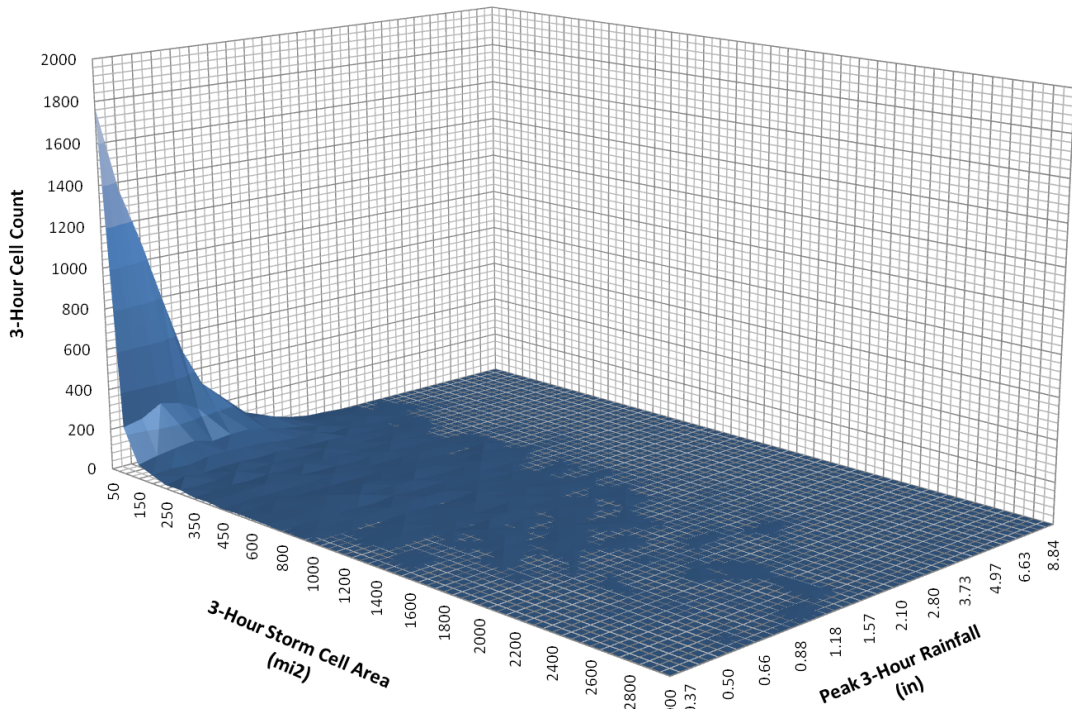


Figure 7-25: Distribution of 3-Hour Cell Sizes (25 dBz Threshold, 0.05 iph)

3-Hour Storm Cell Count

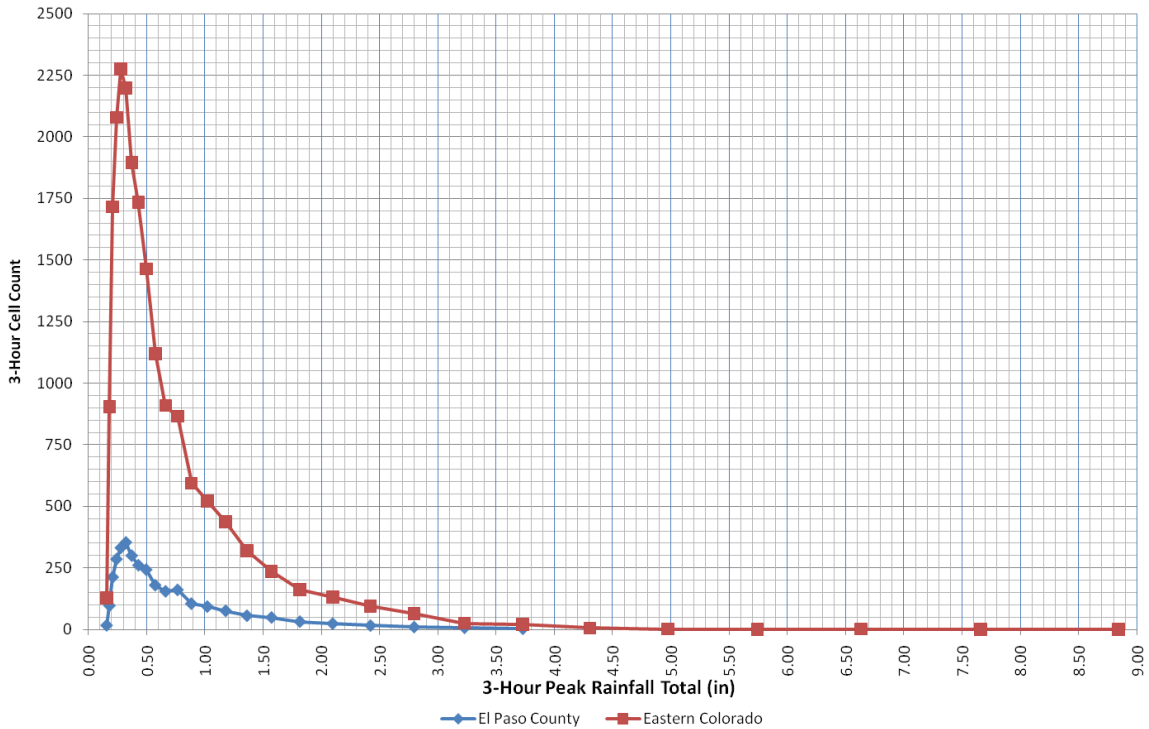


Figure 7-26: Distribution of Peak 3-Hour Rainfall (25 dBz Threshold, 0.05 iph)

3-Hour Cell Size vs. Peak Intensity

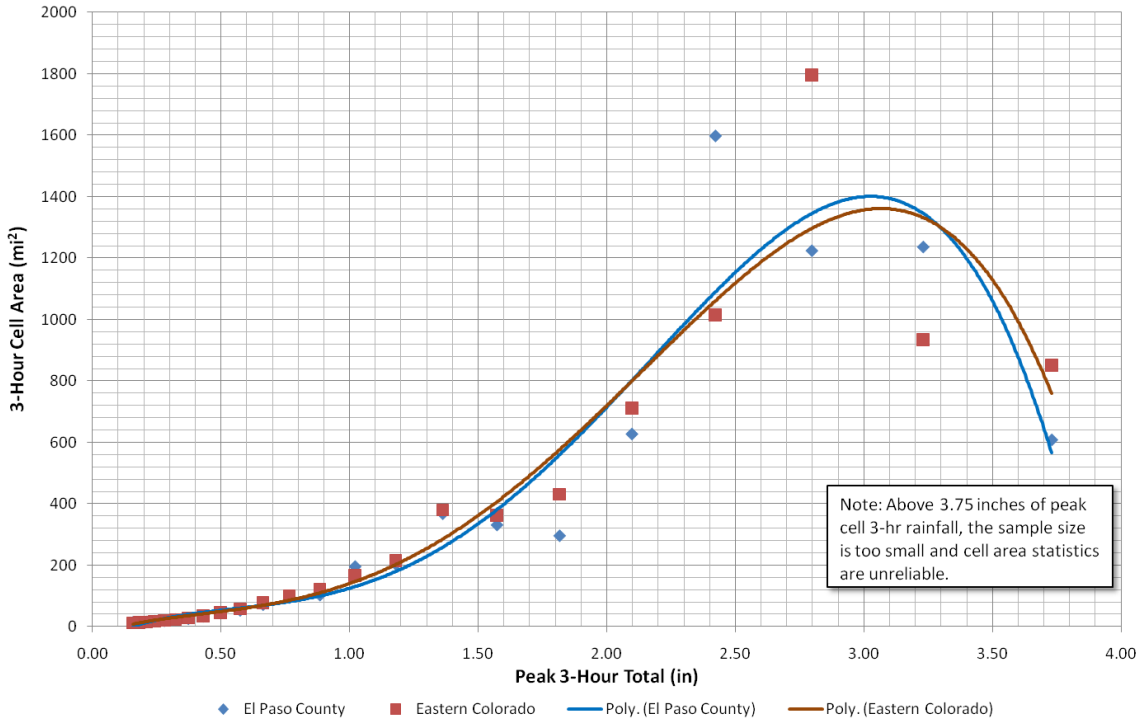


Figure 7-27: 3-Hour Cell Size vs. Peak Intensity (25 dBz Threshold, 0.05 iph)

Table 7.2-1: Fountain Creek Watershed Cloudburst Storms

Date	Start MDT	End MDT	Duration (hr)	Maximum 15 min. intensity (in/hr)	Area (sq mi)	Recur. (yr)	Maximum Depth (in)	Area (sq mi)	Recur. (yr)
17-Jun-65	1300	1530	2.5	10.00	200	100	12.00	300	100
2-Jun-94	2045	2300	2.3	1.04	150	5	1.54	300	2
2-Jun-95	2030	2130	1.0	1.60	180	25	1.69	180	4
4-Jun-96	1530	1645	1.3	1.80	110	35	1.65	170	4
31-Jul-99	1445	1700	2.3	1.20	160	8	1.43	400	2
4-Aug-99	2115	2315	2.0	1.90	250	40	2.34	500	4
13-Jul-01	1915	2015	1.0	1.64	150	25	1.02	200	1
19-Jun-03	1800	1915	1.2	1.80	210	35	1.44	250	1
11-Aug-03	2115	2200	0.8	0.80	120	3	0.37	150	1
15-Jun-04	1415	1600	1.5	1.20	120	7	1.40	450	1
27-Jun-04	1400	1615	2.0	0.70	130	2	1.00	200	2
16-Jul-04	1315	1445	1.3	1.48	180	15	2.82	320	25
5-Aug-04	1845	1930	0.8	0.68	100	2	2.42	250	10
14-Jul-05	1900	2030	1.5	1.00	120	4	1.68	250	3
15-Jul-05	1630	1715	0.8	1.40	110	12	1.21	200	4
11-Aug-05	1700	1800	1.0	0.50	80	1	0.27	140	1
3-Jul-07	1730	1830	1.0	0.56	100	1	1.04	210	1
22-Aug-07	1730	1830	1.0	0.70	80	2	1.66	150	4
15-Aug-08	1530	1630	1.0	0.60	100	1.5	1.25	170	3
15-Aug-08	1415	1530	1.3	1.28	180	10	1.46	300	3
11-Sep-08	2045	2315	2.5	2.00	250	50	3.83	400	10

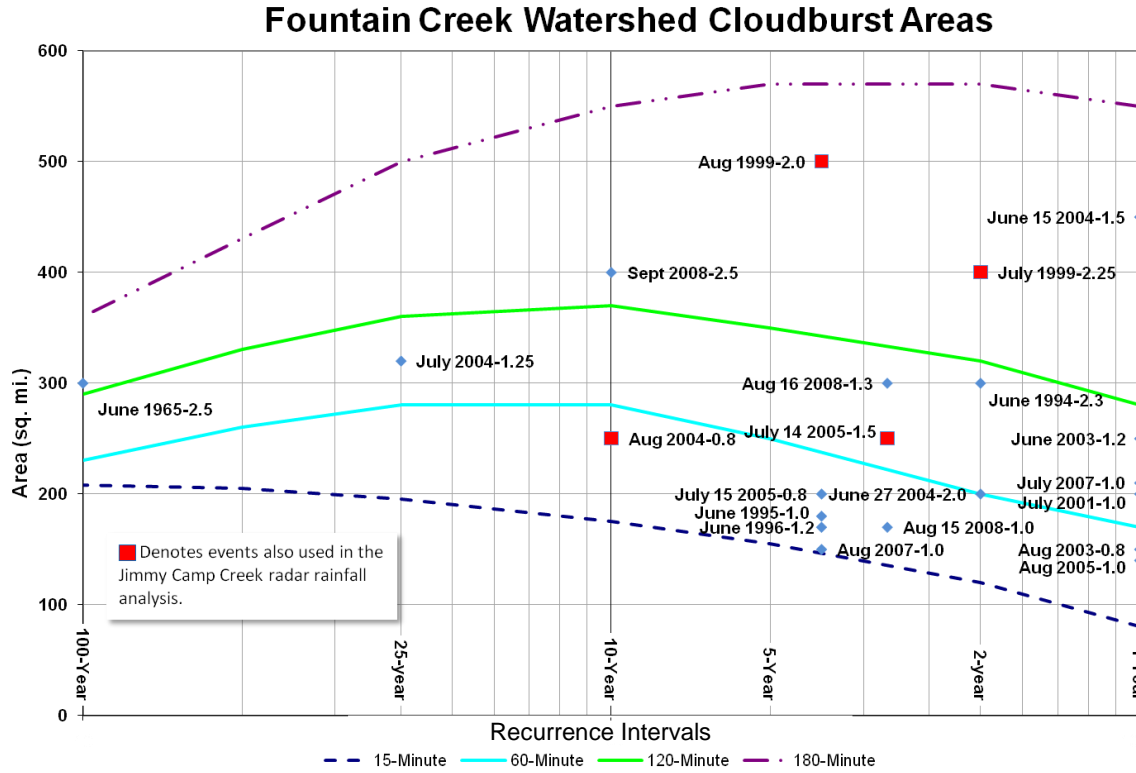


Figure 7-28: Fountain Creek Watershed Cloudburst Areas vs. Recurrence (Note: Events from Table 7.2-1 are plotted and identified by date and duration in hours.)

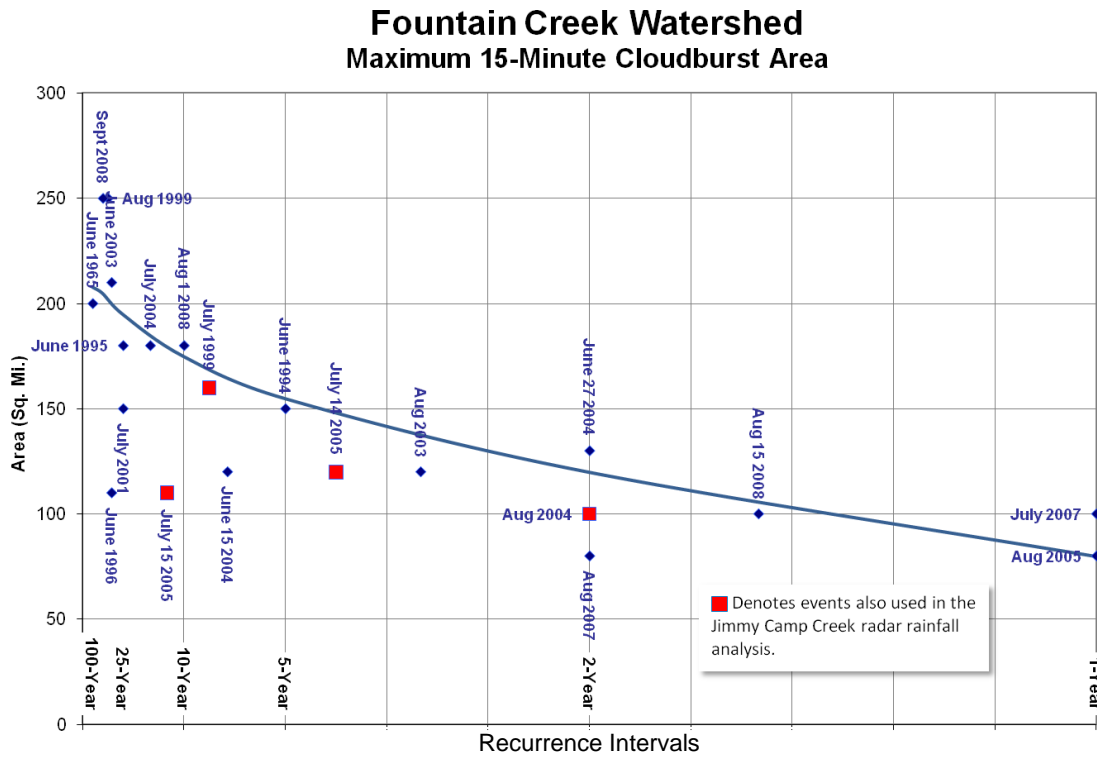


Figure 7-29: Fountain Creek Watershed Maximum 15-Minute Cloudburst Area (Note: Events from Table 7.2-1 are plotted and identified by date.)

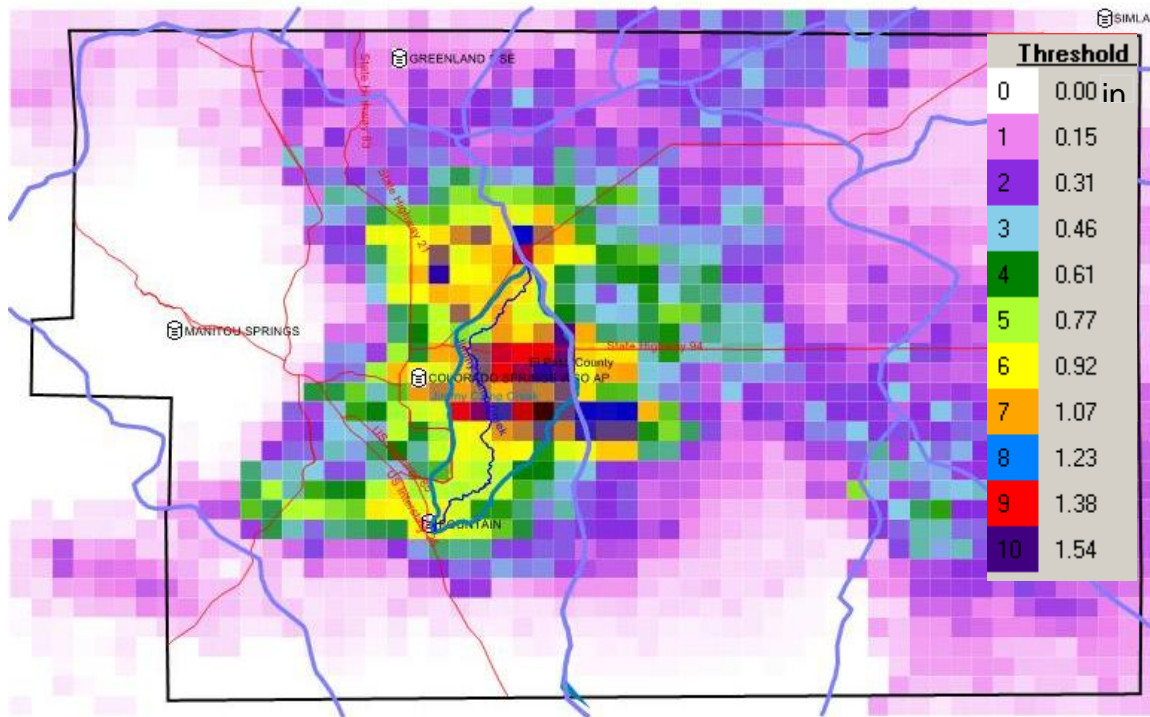


Figure 7-30: Areal Coverage for June 2, 1994 Storm (2.3 hr) over Jimmy Camp Creek Watershed

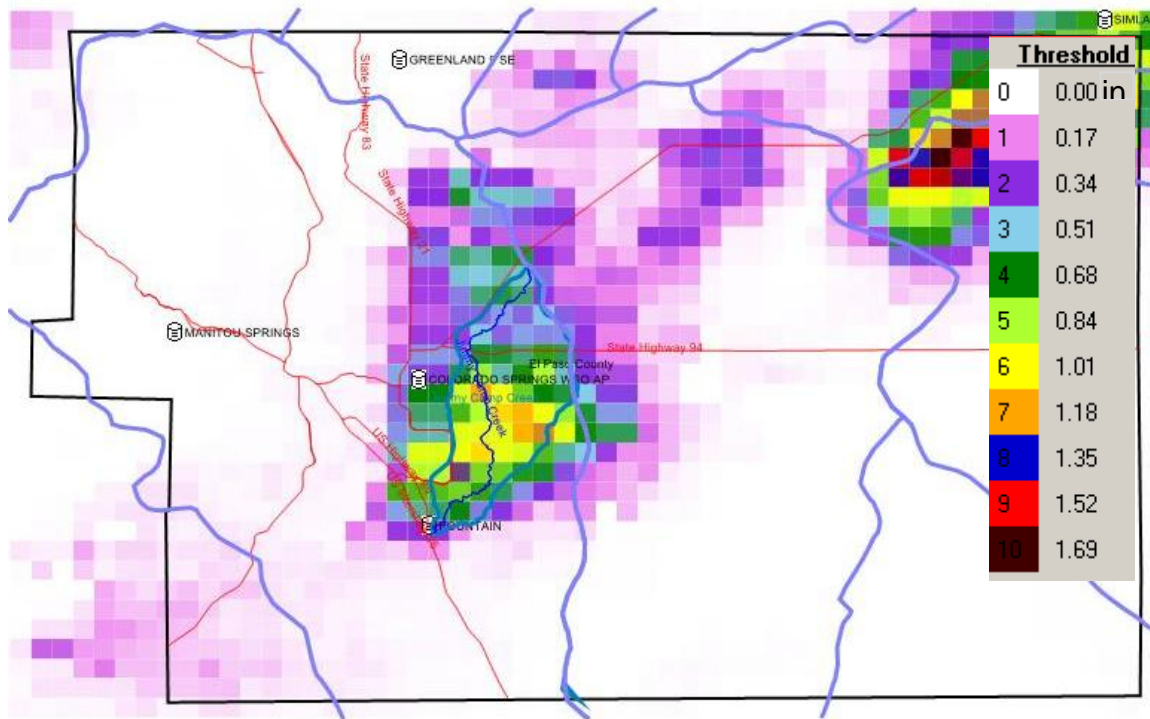


Figure 7-31: Areal Coverage for June 2, 1995 Storm (1.0 hr) over Jimmy Camp Creek Watershed

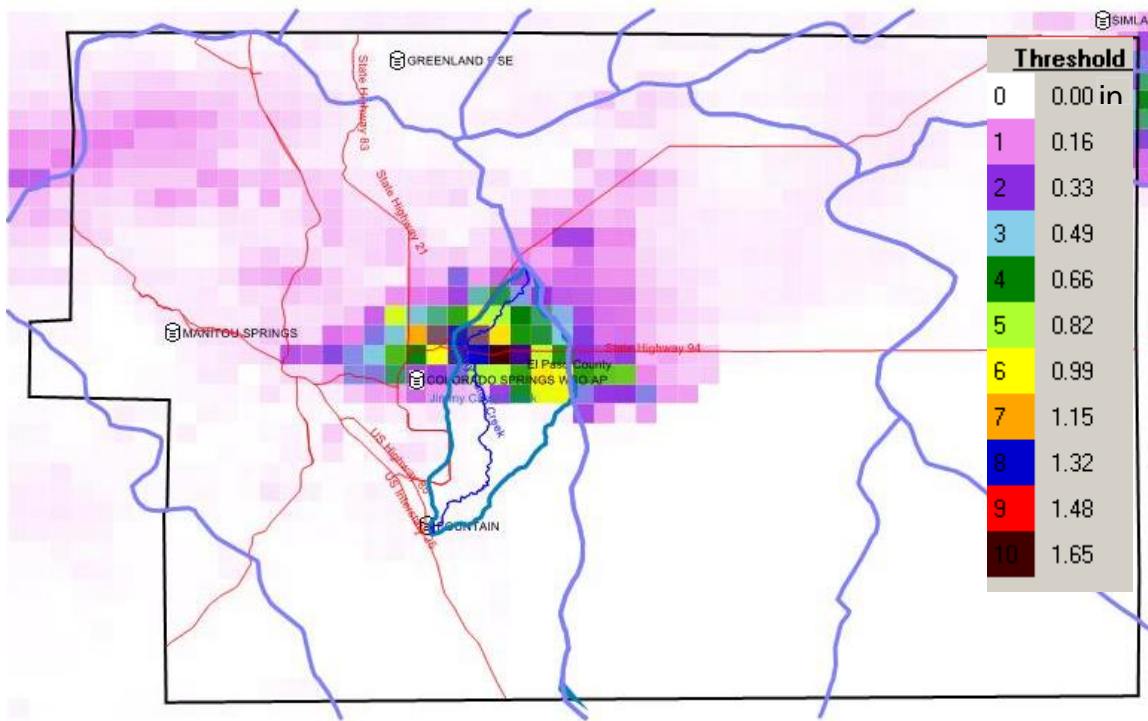


Figure 7-32: Areal Coverage for June 4, 1996 (1.3 hr) Storm over Jimmy Camp Creek Watershed

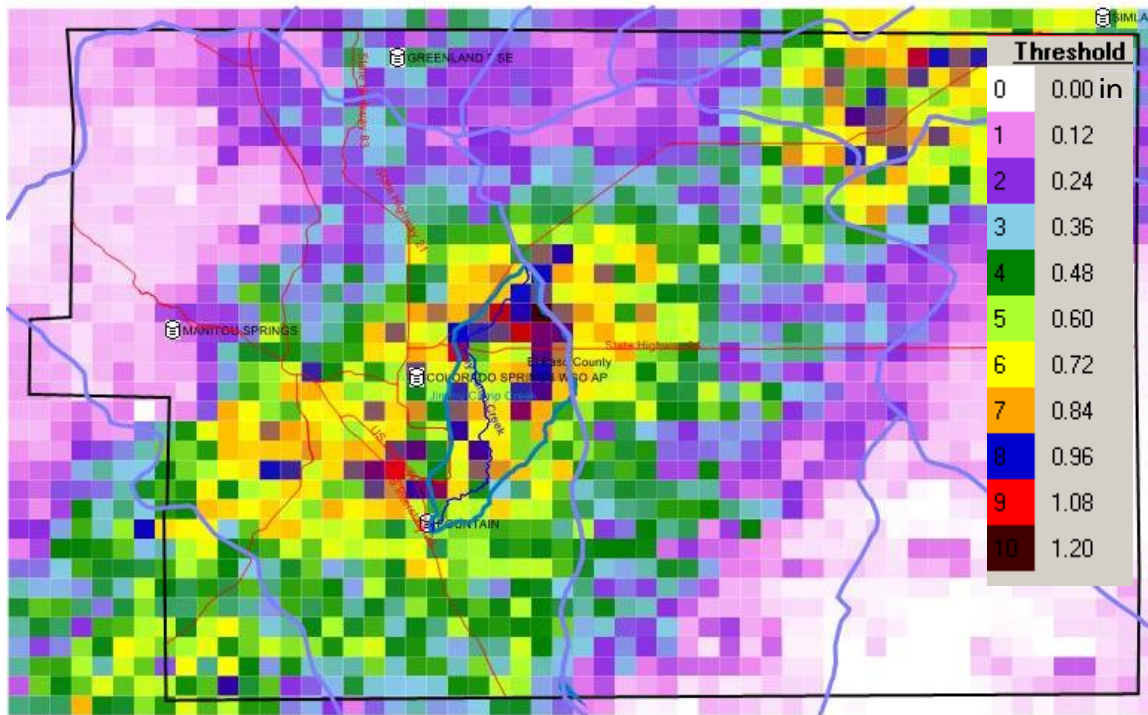


Figure 7-33: Areal Coverage for July 31, 1999 Storm (2.3 hr) over Jimmy Camp Creek Watershed

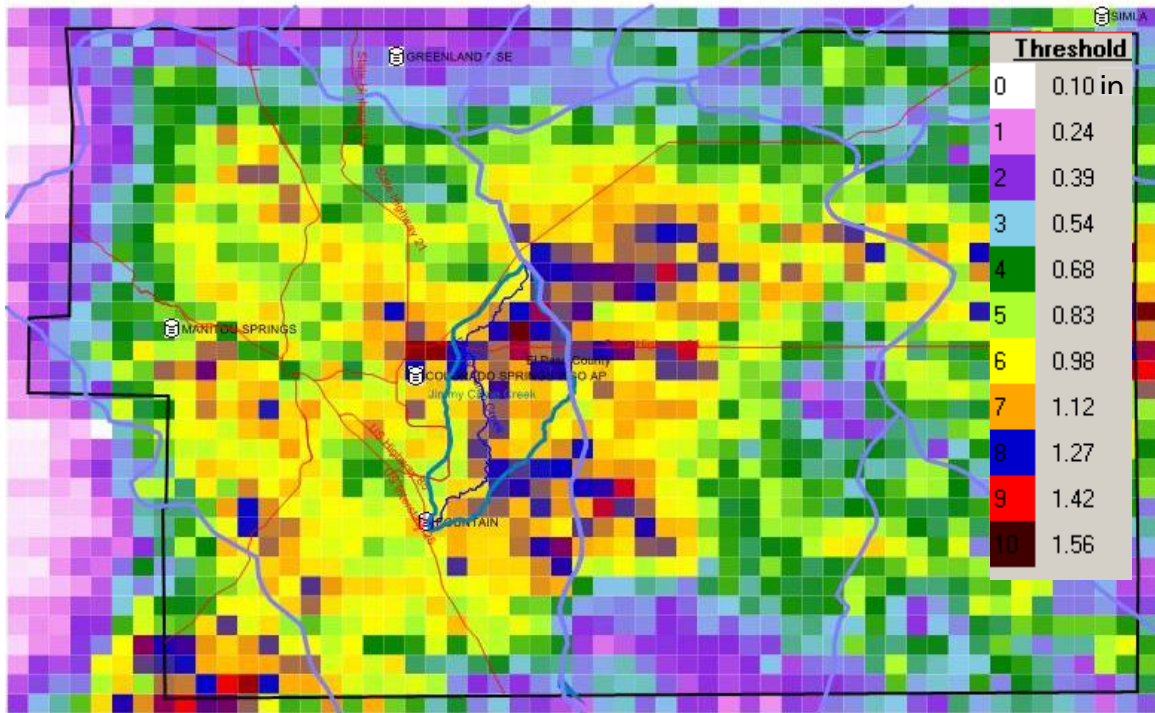


Figure 7-34: Areal Coverage for August 4, 1999 Storm (2.0 hr) over Jimmy Camp Creek Watershed

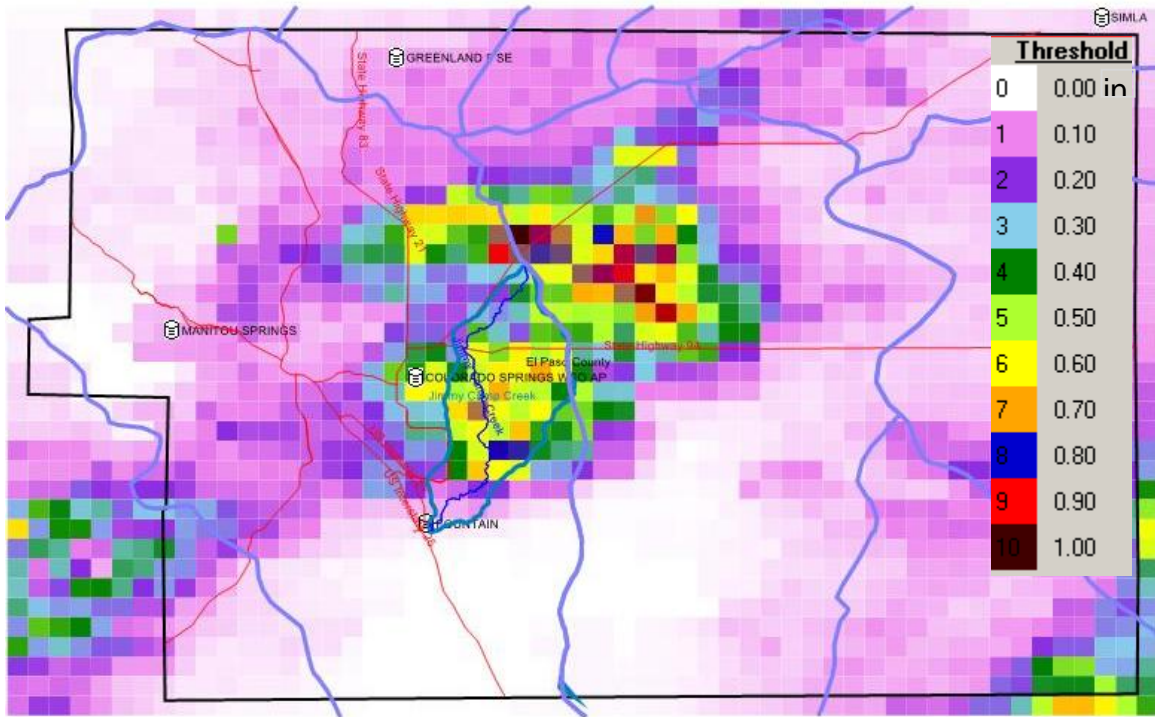


Figure 7-35: Areal Coverage for July 13, 2001 Storm (1.0 hr) over Jimmy Camp Creek Watershed

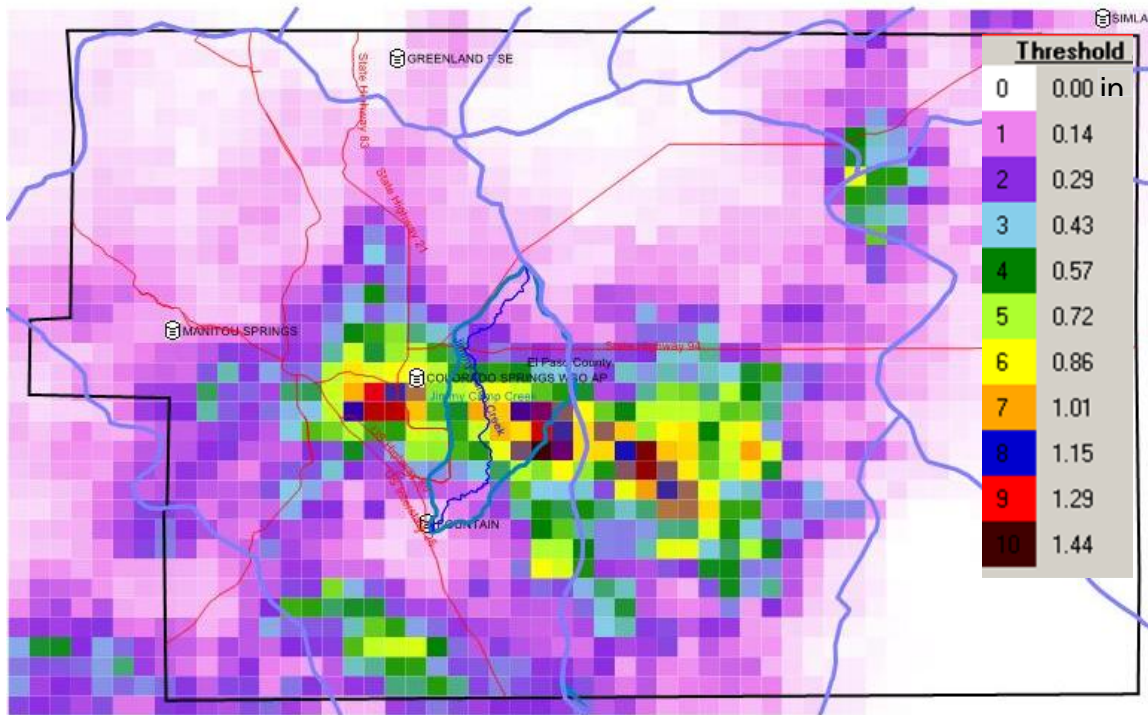


Figure 7-36: Areal Coverage for June 19, 2003 Storm (1.2 hr) over Jimmy Camp Creek Watershed

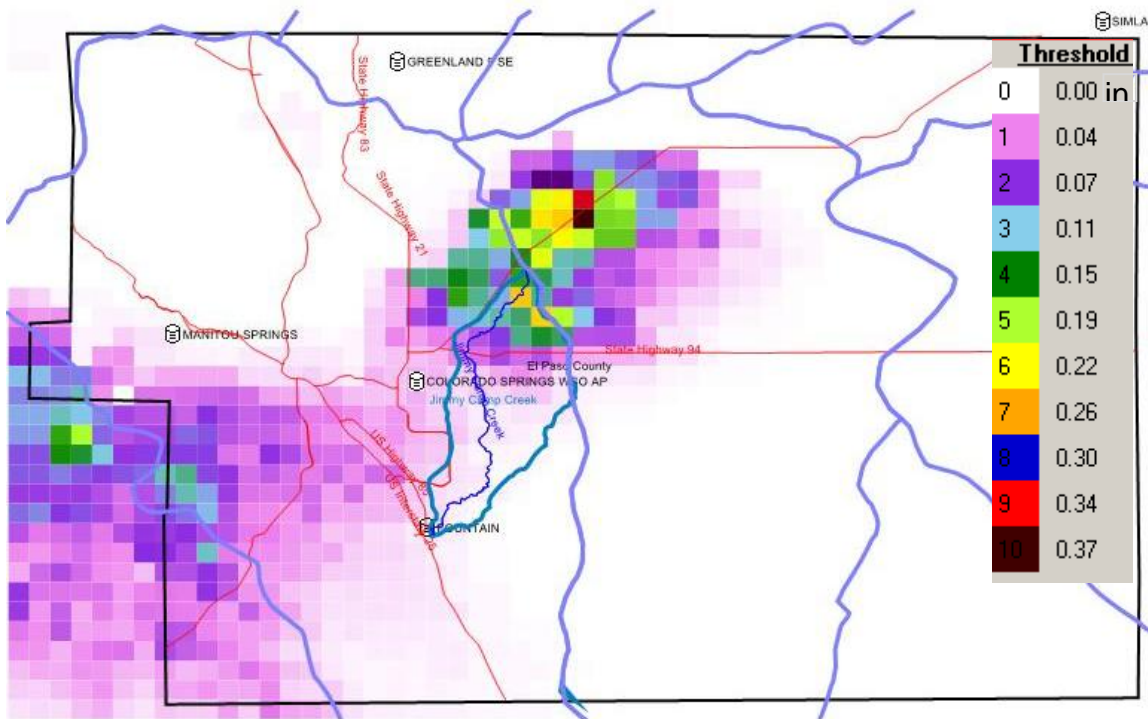


Figure 7-37: Areal Coverage for August 11, 2003 Storm (0.8 hr) over Jimmy Camp Creek Watershed

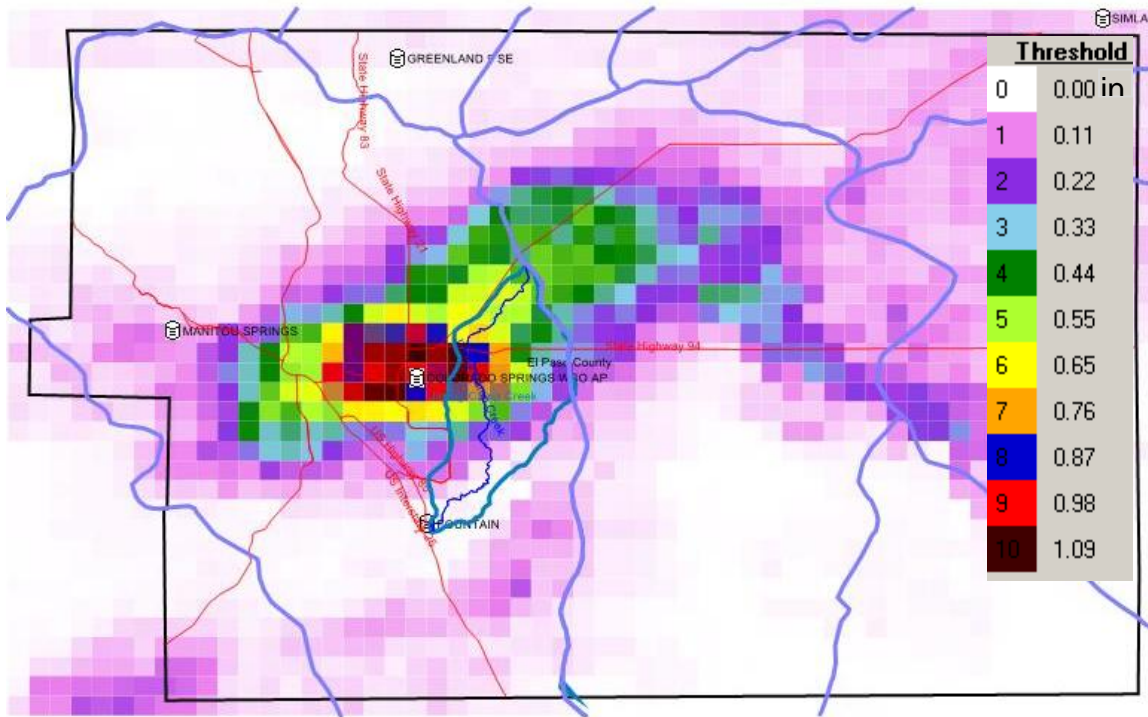


Figure 7-38: Areal Coverage for June 15, 2004 Storm (1.5 hr) over Jimmy Camp Creek Watershed

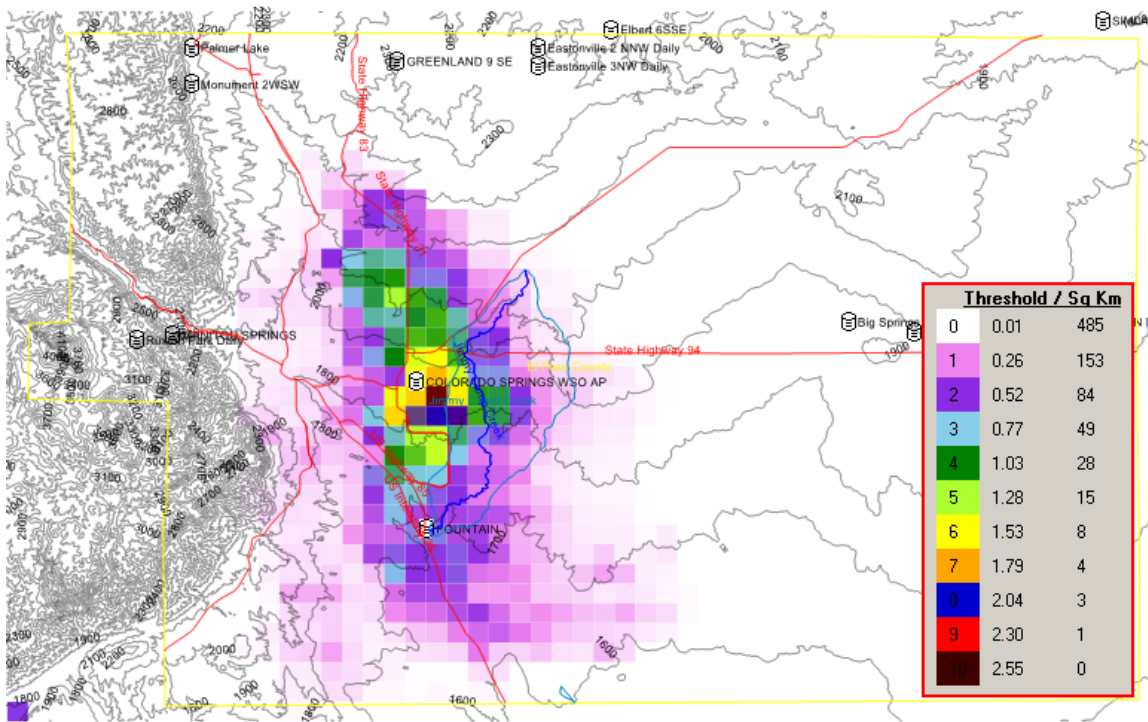


Figure 7-39: Areal Coverage for June 27, 2004 Storm near Jimmy Camp Creek Watershed

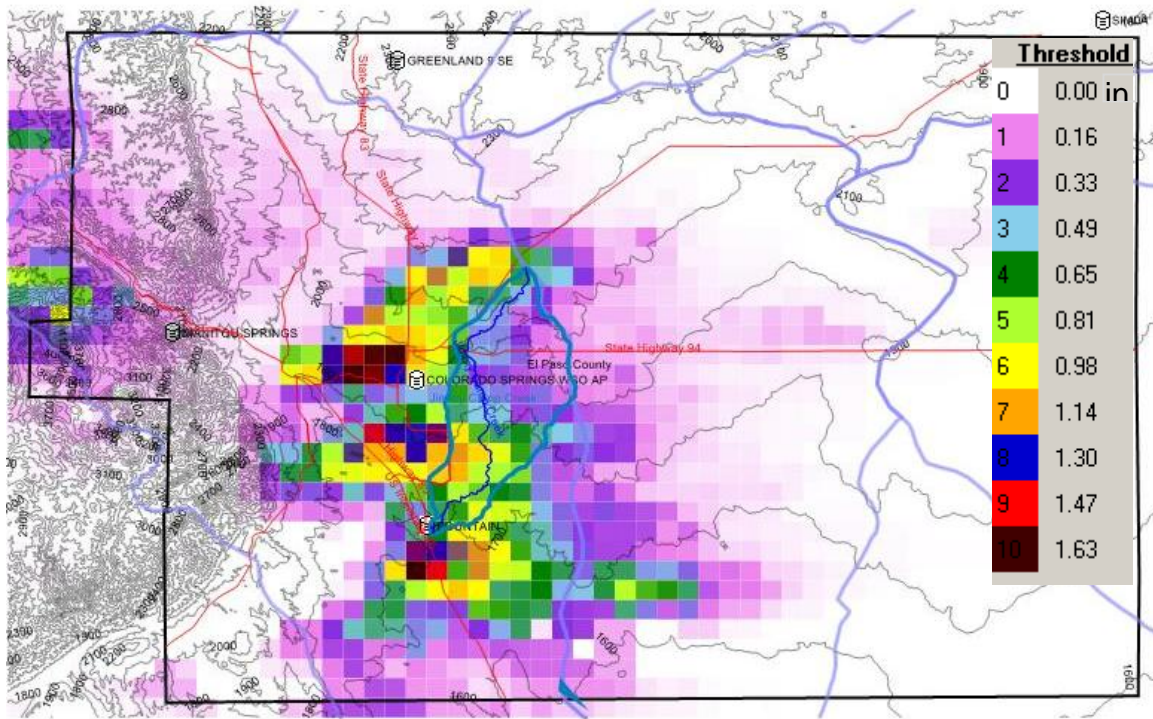


Figure 7-40: Areal Coverage for July 16, 2004 (1.3 hr) Storm over Jimmy Camp Creek Watershed

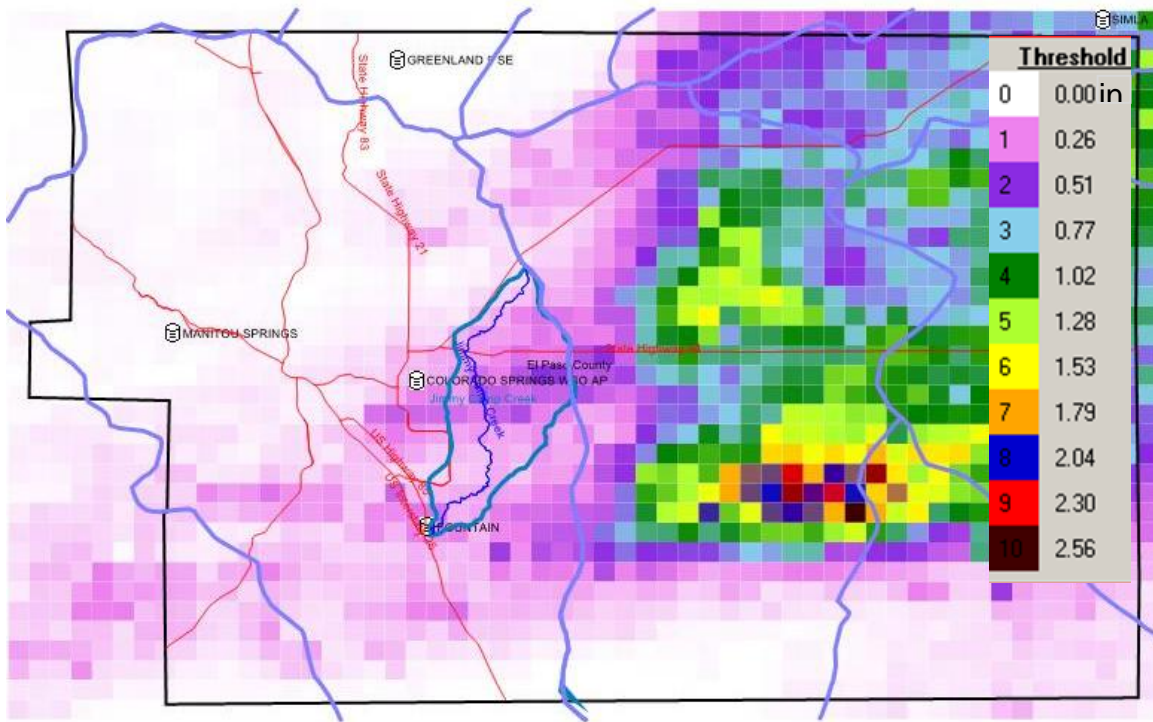


Figure 7-41: Areal Coverage for August 5, 2004 Storm (0.8 hr) over Jimmy Camp Creek Watershed

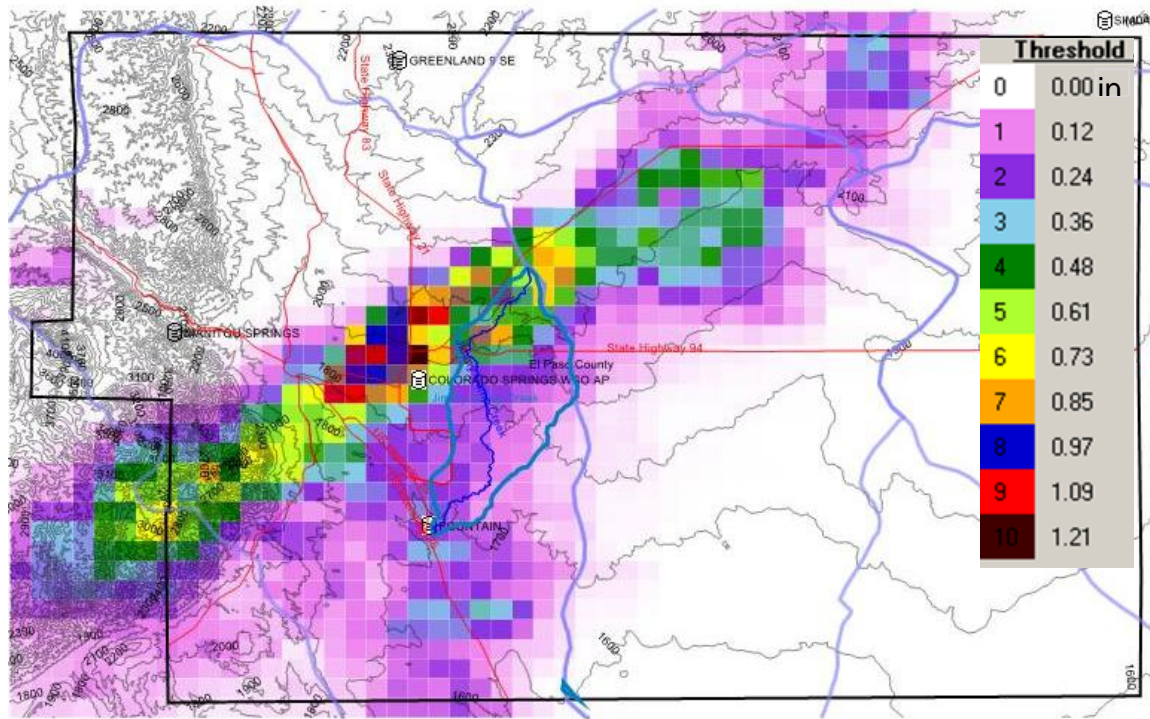


Figure 7-42: Areal Coverage for July 14, 2005 Storm (1.5 hr) over Jimmy Camp Creek Watershed

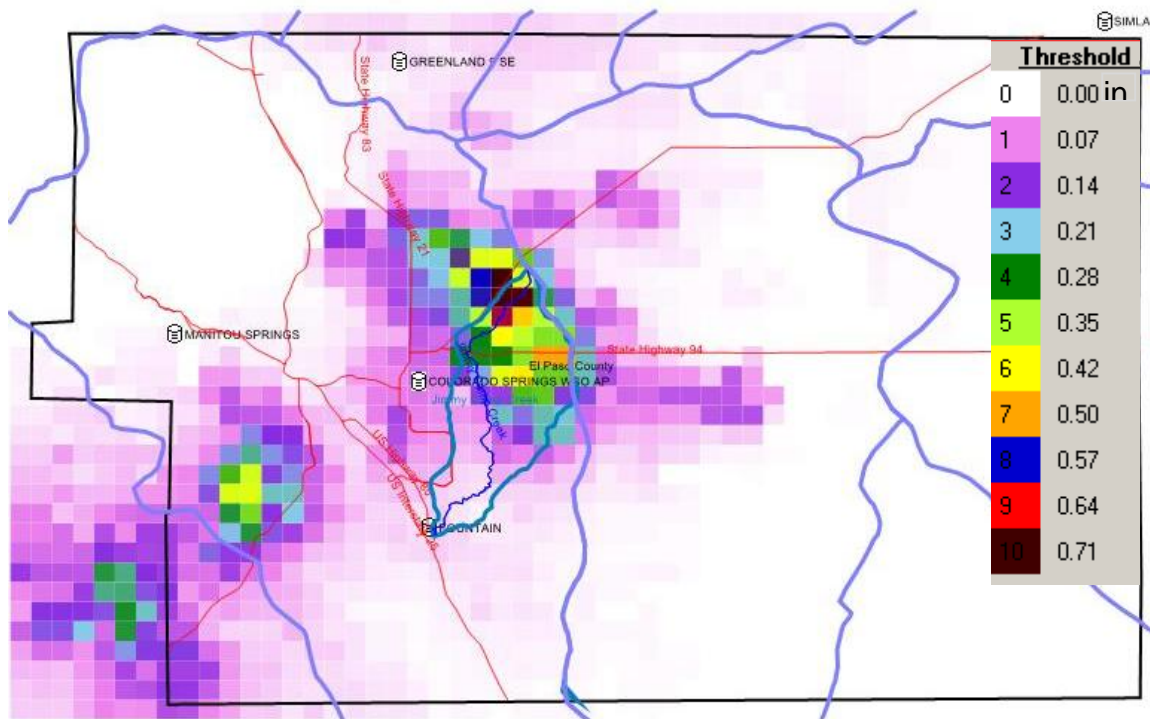


Figure 7-43: Areal Coverage for July 15, 2005 (0.8 hr) Storm over Jimmy Camp Creek Watershed

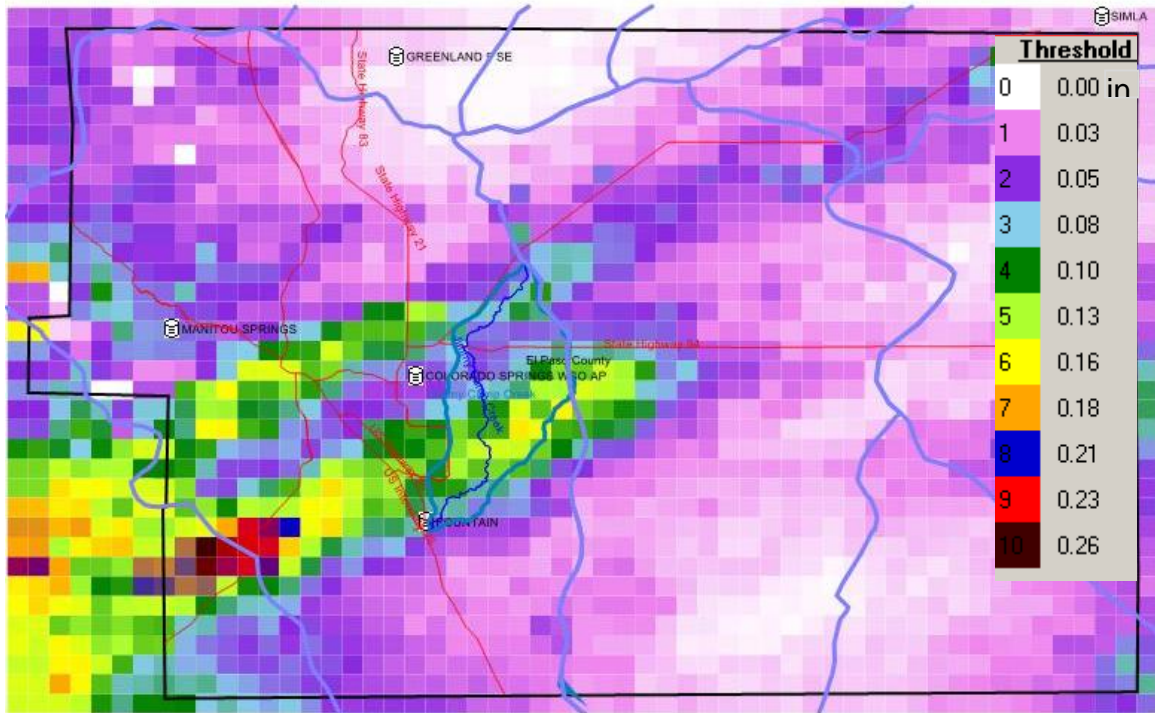


Figure 7-44: Areal Coverage for August 11, 2005 Storm (1.0 hr) over Jimmy Camp Creek Watershed

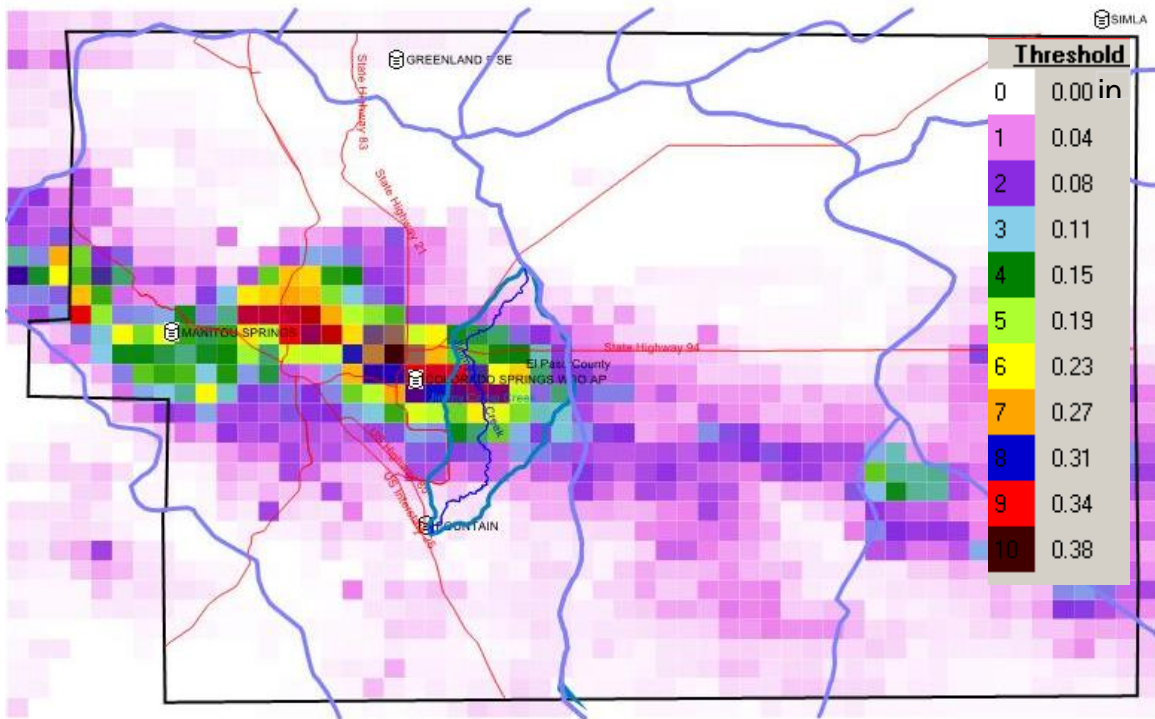


Figure 7-45: Areal Coverage for July 3, 2007 Storm (1.0 hr) over Jimmy Camp Creek Watershed

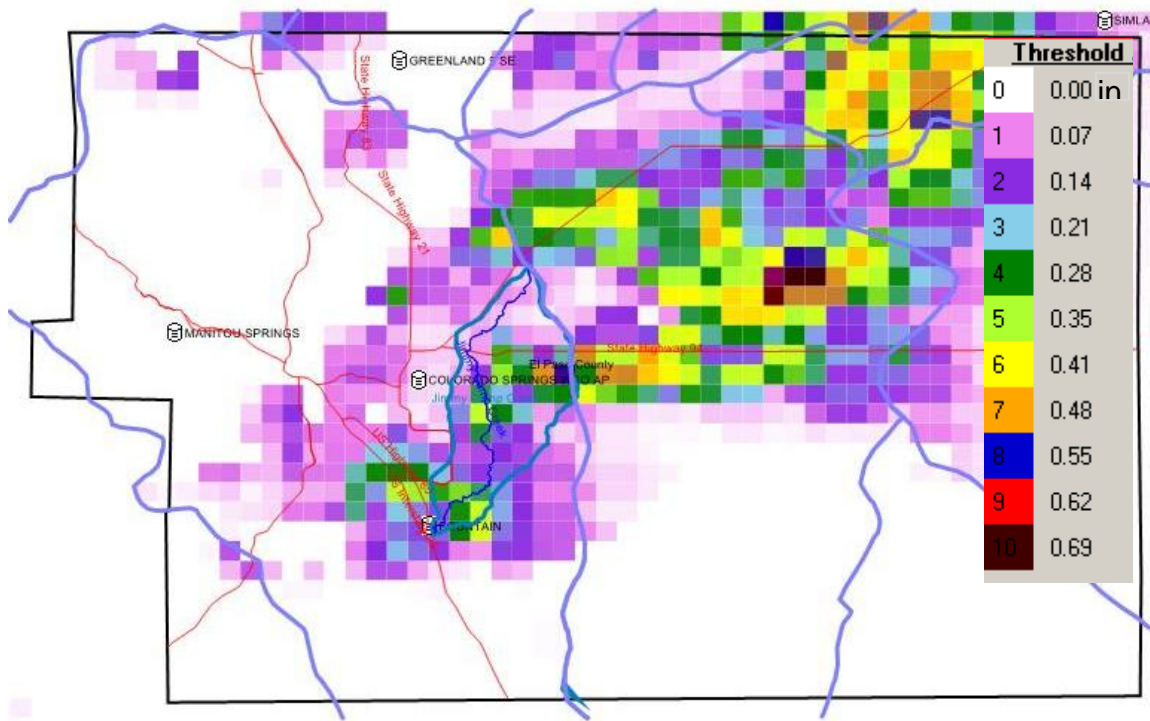


Figure 7-46: Areal Coverage for August 22, 2007 Storm (1.0 hr) over Jimmy Camp Creek Watershed

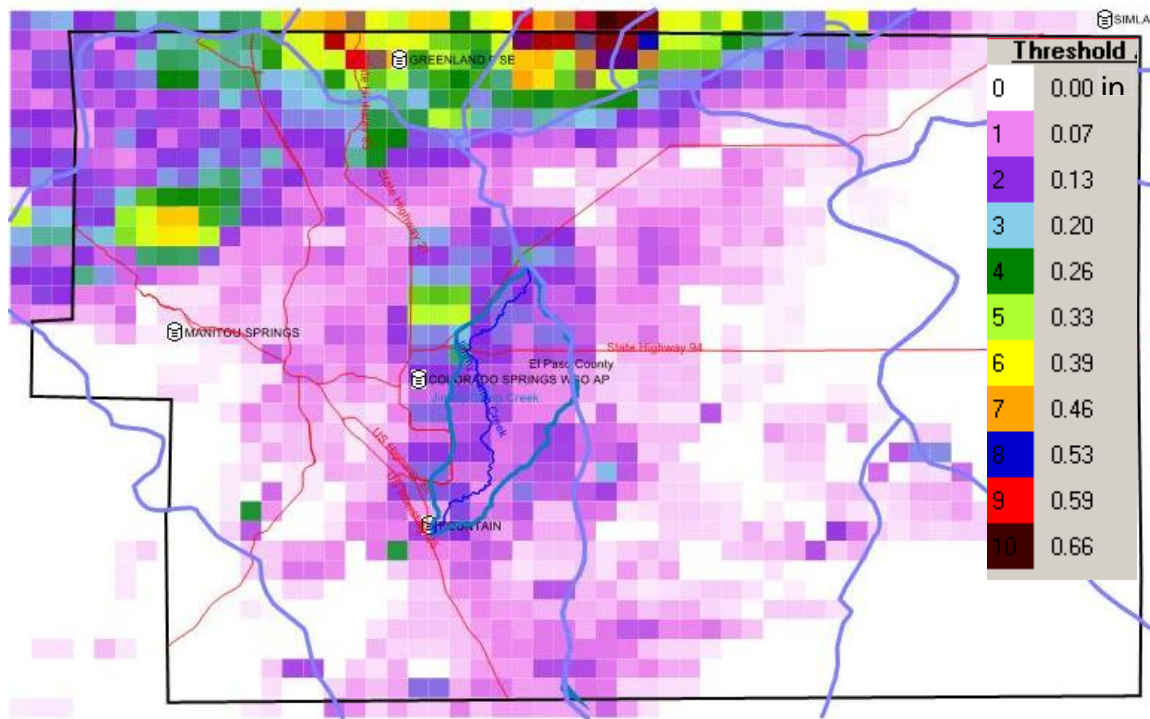


Figure 7-47: Areal Coverage for August 15, 2008 Storm (1.0 hr) over Jimmy Camp Creek Watershed

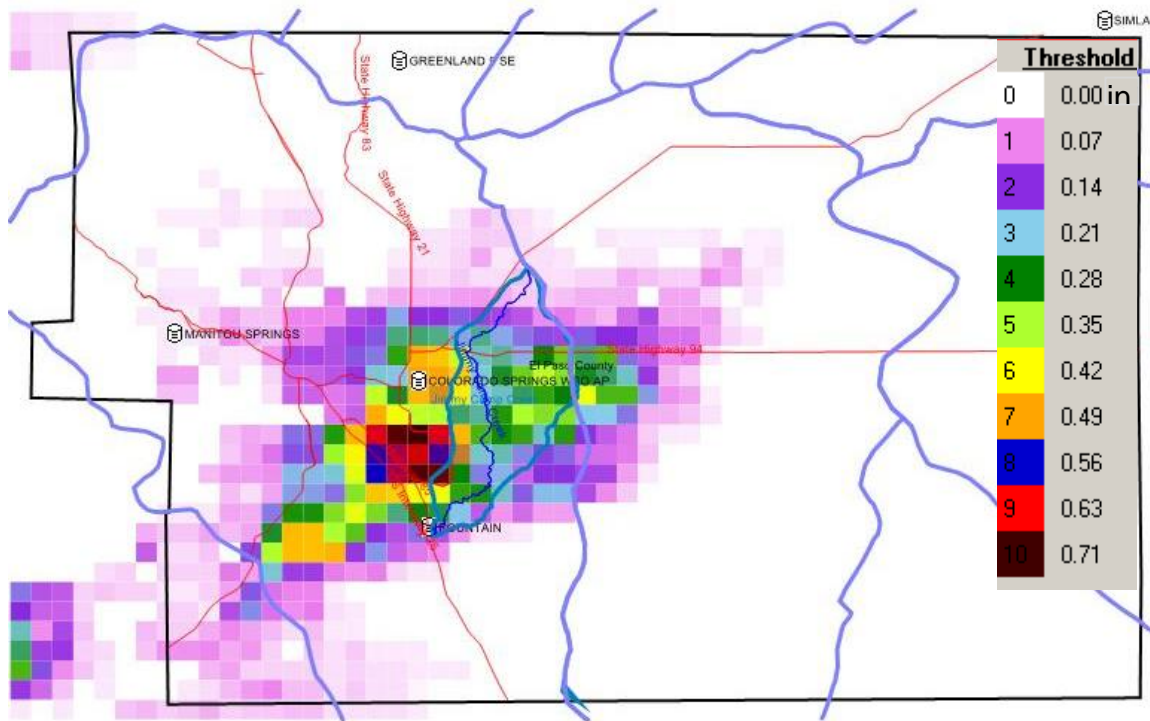


Figure 7-48: Areal Coverage for August 16, 2008 Storm (1.3 hr) over Jimmy Camp Creek Watershed

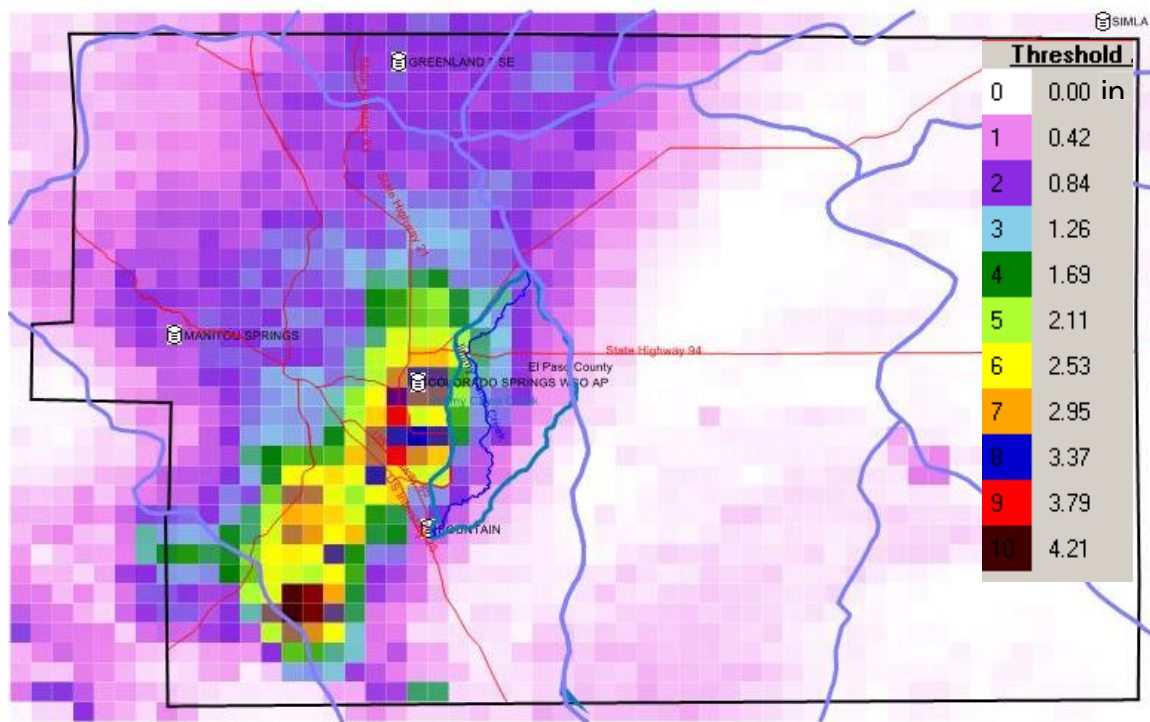


Figure 7-49: Areal Coverage for September 16, 2008 Storm (2.5 hr) over Jimmy Camp Creek Watershed

7.3 Depth Area Reduction Factors

Ordinarily in hydrologic design applications, design rainfall values are selected from point depth duration frequency curves. However, these point values are often applied to watershed areas and, for a given rainfall frequency, area average rainfall is lower than point rainfall. Depth Area Reduction Factors (DARF) are used to convert point precipitation values of a given recurrence interval to an area average precipitation value of the same recurrence. DARFs, which vary from 0.0 – 1.0, are applied to reduce point values to representative area average precipitation values.

Several methodologies have been developed to derive DARFs and were summarized by Srikanthan (1995). The two most popular categories of DARF methodologies are “geographically fixed” and “storm centered” approaches.

Geographically fixed DARFs relate rainfall at a given point to rainfall in a given area that includes that point. (Olivera and Gill, 2004) The storm center has an arbitrary location relative to the measurement array. (Eagleson, 1970) (i.e. Sometimes the measurement array captures the storm center, sometimes the array captures the edge of the storm.)

Storm centered DARFs refer to observed events where the spatial variability of the storm relates to the storm center. The isohyetal peak in a storm centered analysis lies within the measurement array.

Geographically fixed versus storm centered DARFs is a key consideration which could warrant a major study on the appropriateness of either approach. The investigators feel that both are fundamentally flawed as they infer storm geometries from event totals. The investigators contend that the watershed response is driven by the storm geometry at each time step and that the total storm geometry can differ significantly from individual time step geometries. In Section 8.3, the investigators present a new type of design storm methodology in the form of the Dynamic Design Storm Processor. The Dynamic Design Storm Processor provides realistic design storm totals derived from the appropriately defined geometries at each time step.

Geographically fixed DARFs are computed as

$$DARF_{GF} = \frac{R_{GF}}{P_{GF}} \quad 7.3-1$$

where $DARF_{GF}$ is the geographically fixed depth areal reduction factor, R_{GF} is the mean of the annual maximum rainfall values, and P_{GF} is the weighted mean of annual maximum point rainfall values in the area under consideration. (Olivera and Gill, 2004)

The National Weather Service Technical Paper 29 (TP29) is the source of perhaps the most common geographically fixed DARF methodology (Allen and DeGaetano, 2005) and is defined by

$$DARF_{TP29} = \frac{\frac{1}{n} \sum_{j=1}^n \hat{R}_j}{\frac{1}{k} \sum_{i=1}^k \left(\frac{1}{n} \sum_{j=1}^n R_{ij} \right)} \quad 7.3-2$$

where \hat{R}_j is the annual maximum areal rainfall for year j, R_{ij} is the annual maximum point rainfall for the year j at station i, k is the number of stations in the area, and n is the number of years.

Figure 7-50 shows the NWS TP29 DARFs and presented in National Weather Service Technical Paper 40 (1961). Leclerc and Shaake (1972) proposed a function with the following form to express the DARF curves of NWS TP29 shown in Figure 7-50.

$$DARF_{TP29} = 1 - e^{-at^b} + e^{(-at^b - cA)} \quad 7.3-3$$

where t is the event duration (hr), and A is the area (mi²). The coefficients a and c as well as the exponent b are empirically fit. Olivera and Gill (2004) report coefficients of a = -1.1, b = 0.25, and c = 0.01.

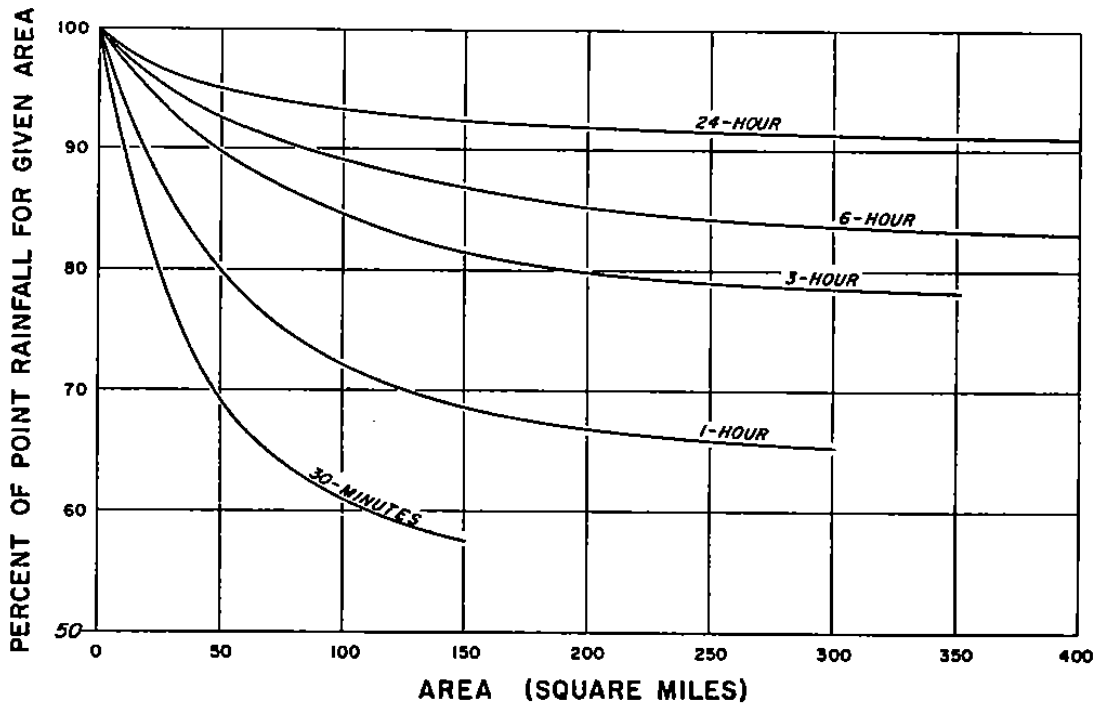


Figure 7-50: Depth Area Reduction Factors (From NWS TP29 as shown in NWS TP40, 1961)

As noted by Geronimo (2004) the curves NWS TP29 DARFs were derived based on 20 dense rain gage networks scattered across the eastern United States. None were in the mountain west region. NWS TP29 DARFs were developed for 1-hour and 24-hour durations with the remaining curves determined by interpolation. The 30-minute curve was based on only one network in Muskingum, Ohio. Despite the relatively small and scattered source data sets, NWS TP29 DARFs were judged applicable over large regions and have been used by agencies throughout the US, including Colorado.

Storm centered depth area reduction factors are computed as

$$DARF_{SC} = \frac{R_{SC}}{P_{SC}} \quad 7.3-4$$

where R_{SC} is the areal storm rainfall enclosed by a selected isohyets and within which the rainfall is everywhere equal to or greater than the value for the isohyets and P_{SC} is the maximum point rainfall at storm center. (Olivera and Gill, 2004) The storm centered approach to compute DARFs is difficult to implement on multi-centered storms and historically has been preferred for individual storms.

Geographically fixed and storm centered methods of computed DARFs produce different results. Geographically fixed DARFs generally decrease less rapidly with increasing area than storm centered DARFs.

Historically, DARF methodologies have been defined by rain gage observations (See Allen and DeGaetano, 2004) or from statistical theory. (see Veneziano and Langousis, 2005) Rain gage networks rarely have the necessary resolution over large areas to adequately resolve the spatial variability. Radar rainfall estimates provide high resolution observations in both space and time to resolve detailed structures within rain events. More than three decades ago, Frederick, et. al. (1977) first tested the idea that radar observations could be used to develop DARFs. In the intervening years, only a handful of

radar-based DARF studies have been conducted due to the difficulties of creating and managing high quality gage-adjusted radar rainfall data sets.

Durrans, et. al., 2002 explored the development of radar-based DARFs by utilizing NWS 1-hour, 4 km x 4 km gage adjusted radar rainfall estimates for approximately 7.5 year during 1993-2000 for the Arkansas-Red River Basin region in the south central US. Durrans et. al. utilized a statistical approach that depended upon annual rainfall maxima. With such a short period of record, the results were promising but inconclusive.

Gill (2005) studied DARFs in Texas utilizing NWS 1-hour, 4 km x 4 km gage adjusted radar rainfall estimates for approximately 10 years from 1995-2004 in covering the state of Texas. Again, the relatively short record did not produce reliable statistical conclusions but the study did show the DARFs varied regionally within the state of Texas.

Geronimo (2004) conducted a study of high resolution radar data to estimate radar-based DARFs from gage-adjusted radar rainfall data in the Denver, CO, area. Data resolution was on the order of 5-minute, 0.25 square miles for seven convective storms from 1996 to 2002. The short record precluded reliable statistical determinations however storm centered DARFs were computed.

Figure 7-51 shows the storm centered DARFs estimated by Geronimo and compared to the Urban Drainage and Flood Control District of Denver (UDFCD) 1-Hour DARF (identical to NWS-TP29). As expected the convective storm centered DARFs decay at a faster rate than the geographically fixed DARFs used by UDFCD based on NWS TP29.

Figure 7-52 shows similar results for storm centered DARFs in the 1-3 hour range. The curves decay at a faster rate with increasing area than the NWS TP29 3-hour DARFs shown in Figure 7-50.

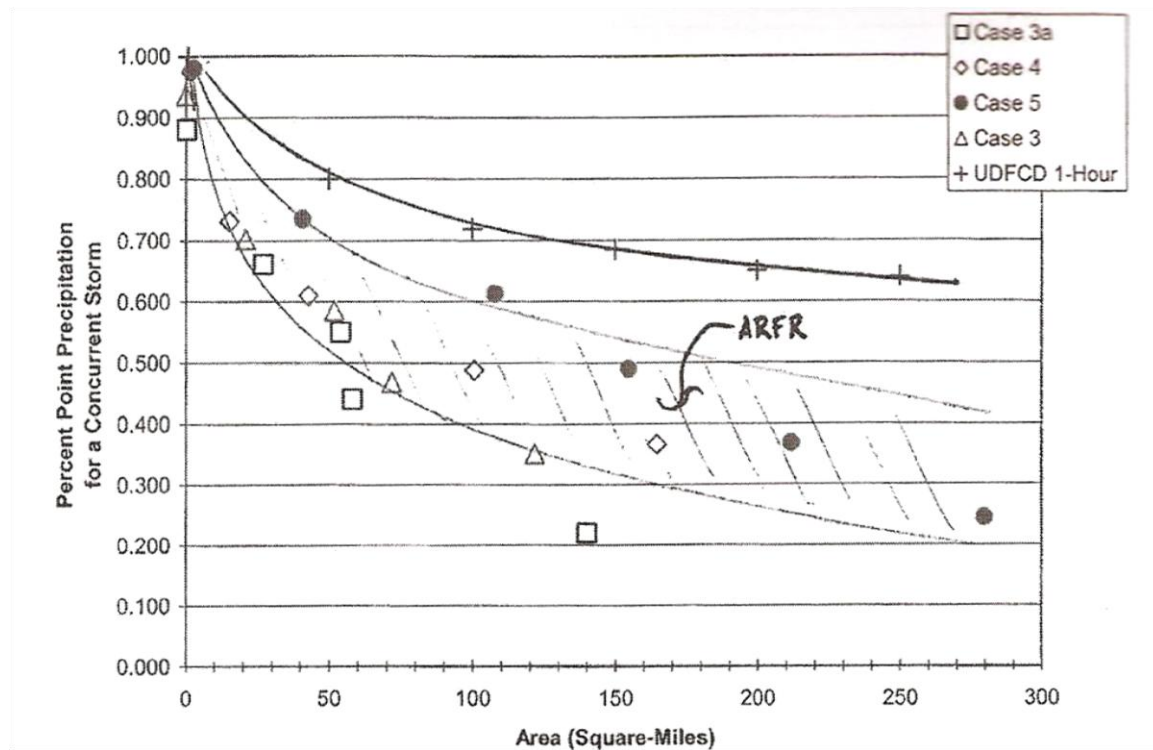


Figure 7-51: One-Hour Radar Based DARFs in the Denver Area (After Geronimo, 2004)

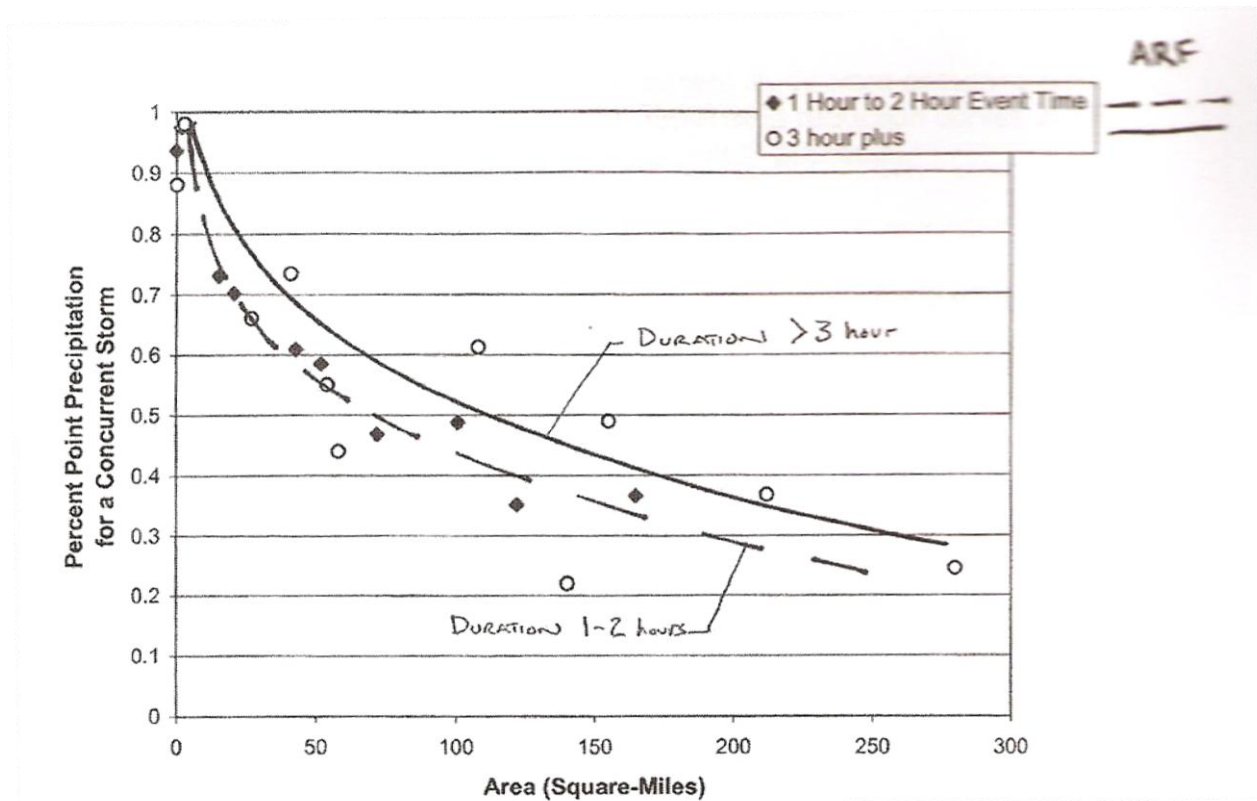


Figure 7-52: Radar Based DARFs in the Denver Area (After Geronimo, 2004)

7.4 Development of Radar-Based DARFs for Colorado Springs

Past studies that attempted to develop DARFs from radar data sets were hampered by the lack of long term records needed for statistical stability, by data resolution in both space and time, and/or by the lack of large scale data sets to assess regional variability.

The approach used in this study addresses these issues. First, this study relaxes the statistical requirement for “annual maxima” to select storms for evaluation. Second, a large study area encompassing all of eastern Colorado and the Front Range is included. And third, high resolution, 15-minute, 2 km x 2 km, gage-adjusted radar estimates were used in the analysis to provide more fidelity in identifying storm structures.

By avoiding the “annual maxima” constraint, the study can investigate a largely unanswered question “What are the geospatial properties of all storms in the region?” The study examines all storm cells in eastern Colorado from which a subset in the region near Colorado Springs were selected for comparison. By examining all cells, a much larger population of storm cells was available for assessing geospatial characteristics rather than a single realization associated with a cell containing the annual maximum. Multiple realizations of cells with a given peak rainfall, provide opportunities for evaluation of the distribution of cell sizes for each peak rainfall range.

Depth-Areal-Reduction Factors (DARF) were determined from cloudburst area versus peak intensity TITAN analyses for 15-min, 1-hr and 3-hr time steps. Cloudburst cell areas for 15-minutes were based on a threshold decibel cutoff of 19 dBz corresponding to precipitation rates of 0.022 iph, 35 dBz, or approximately 0.22 inches per hour (0.05 inches in 15-minutes). Cloudburst cell areas for 1-hr were based on a threshold decibel cutoff of 29 dBz, corresponding to precipitation rates of about 0.09 inches per hour. Cloudburst cell areas for 3 hours were based on a threshold decibel cutoff of 25 dBz, corresponding to precipitation rates of 0.05 inches per hour (0.15 inches for 3 hours).

Different cutoff or detection thresholds were used in each case because TITAN analyzes average rainfall rates over the time step analyzed. If the same threshold was used for all studies the 35 dBz rate would yield a storm edge of about 0.05 inches, which would require about a 16 dBz threshold at hourly time steps and about an 8 dBz threshold at three hours. These dBz values are very low and are at or below the minimum rainfall rates of the original data set. The practical result of low thresholds would be artificially high storm areas as too much “false positive” rain would be “detected.”

Threshold sensitivity can affect DARFs in at least two ways. First, a lower threshold increases median cell sizes as more area under very light rain is included in the determination of cell sizes. The net effect is larger cell sizes. Secondly, a lower threshold increases the probability of multiple peaks will be included in the same identified cell. Conversely, a higher threshold does a better job of isolating cell peaks and increases the number of cells identified.

DARFs were estimated from data covering the eastern Colorado study area. DARFs were also estimated from a subset of data that covered El Paso County which includes Colorado Springs and the Fountain Creek Watershed area. The El Paso County data sets were used to localize the analysis to the areas of most interest to Colorado Springs and to determine differences between localized DARFs and DARFs generated from data for the entire eastern Colorado region.

Normalized cell area curves were created from the eastern Colorado and El Paso County data sets. The normalized cell area curves represent the average distribution of rainfall over the cell as a percentage of cell area. These curves define the basic shape of an idealized cell.

Figure 7-53 presents the family of area normalized curves for a wide range of peak intensities. Curves for lowest peak intensities start in the upper right and transition to the highest intensity curves in the lower left. The curves represent average distributions and appear very smooth at lower peak intensities where the cell counts are highest and the averages are relatively stable. At higher peak intensities, cell counts are lower and averages are less stable which results in the more irregular shaped curves to the lower left.

Figure 7-54 includes only curves representing peak intensities of the 2-year event or greater. These curves show very little difference. This suggests that the characteristic shape of the idealized 15-minute cells are essentially the same for cells representing the 2-year event or greater. Because it has been shown earlier that median cell sizes vary with peak intensity and by extension recurrence interval, the same area normalized curve for cell sizes can be used to scale curves for specific return frequencies by the median cell size.

A limiting or characteristic area normalized cell size curve was selected for each time step. (i.e. 15-minute, 1-hour, and 3-hour.) DARFs were then estimated by scaling the area normalized curves by the appropriate median cell size then performing volumetric integration to compute area averaged rainfall as a percentage of peak intensity.

Computed DARFs were based on the on median cell sizes for the 2-year, 10-year, and 25-year events. Too few cells with peak intensities higher than the 25-year event were observed to provide reliable estimates of median cell size for these events.

Figure 7-55 presents area normalized DARFs for the 15-minute event using data from the 19 dBz (0.022iph) detection threshold case. Curves for eastern Colorado and for El Paso County are included. For comparison, the NWS TP29 DARF is also included. Figure 7-56 presents 15-minute DARFs scaled for the 2-year, 10-year, and 25-year events for eastern Colorado. The El Paso County 15-minute DARFs are presented in Figure 7-57. Figure 7-58 through Figure 7-60 present curves for the 35 dBz (0.22 iph) case.

The 15-minute radar-based DARFs decay at a rate slightly greater than or slightly lower rate than the 15-minute NWS TP29 DARF used by UDFCD depending on the return period. (i.e. median cell size)

Figure 7-61 through Figure 7-66 present DARFs for the 1-hour and 3-hour time steps. The NWS TP29 curves were also plotted for comparison. At the 1-hour and 3-hour time steps, the radar-based DARFs

deviate significantly from the widely used NWS TP29 DARFs. The radar-based DARFs decay at a much higher rate than the NWS curves. The NWS curves were developed from a broader range of storm types than the convectively dominated cells from eastern Colorado and the Front Range that were analyzed in this study.

DARFs for El Paso County decayed at a higher rate than the DARFs for eastern Colorado. This is consistent with earlier findings that the median cell sizes in eastern Colorado were larger than those found in El Paso County largely due to differences in terrain influences on local meteorology.

Figure 7-67 presents the 1-hour El Paso County DARFs with data points from the Geronimo, 2004, study of storm centered 1-hour DARFs in the Denver area. The El Paso County DARFs were derived from thousands of individual cells and the curves represent median cell sizes. The El Paso County results fall right in the middle of the Geronimo results which represent individual events. Note that the Geronimo data points were derived from gage-adjusted radar rainfall data supplied from a different vendor, processed differently, and representative of individual storms. Thus, the current results are very consistent with the Geronimo findings from the Denver area.

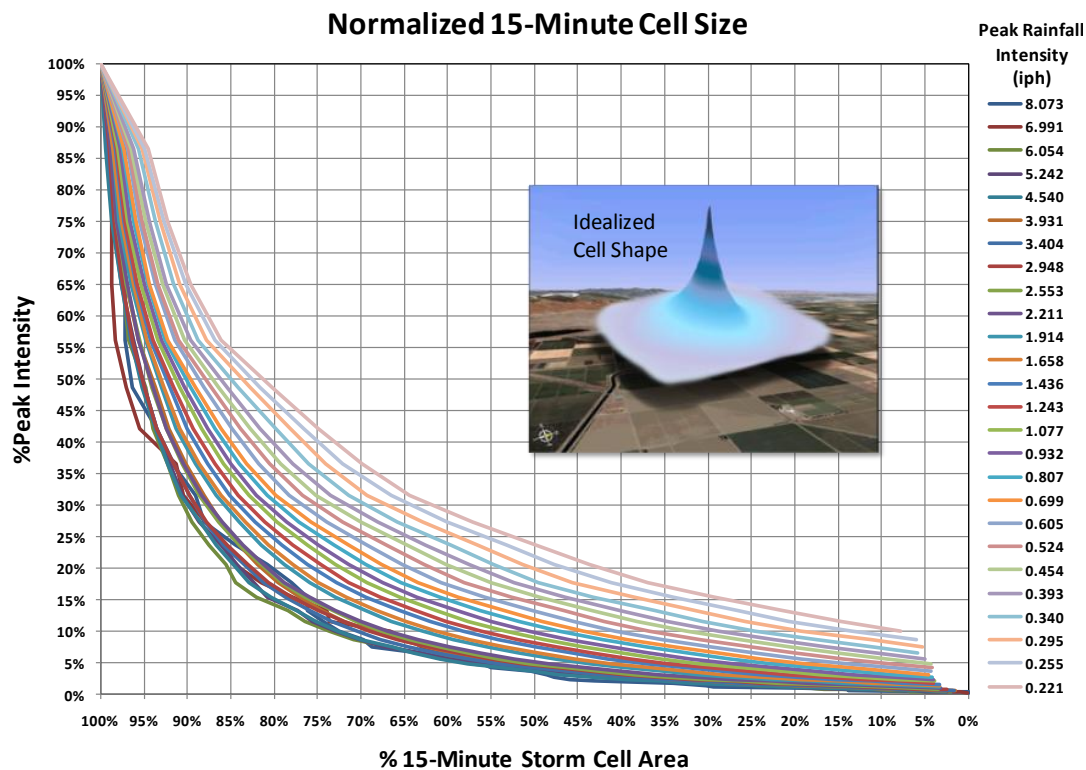


Figure 7-53: Area Normalized 15-Minute Cell Size

Normalized 15-Minute Cell Size

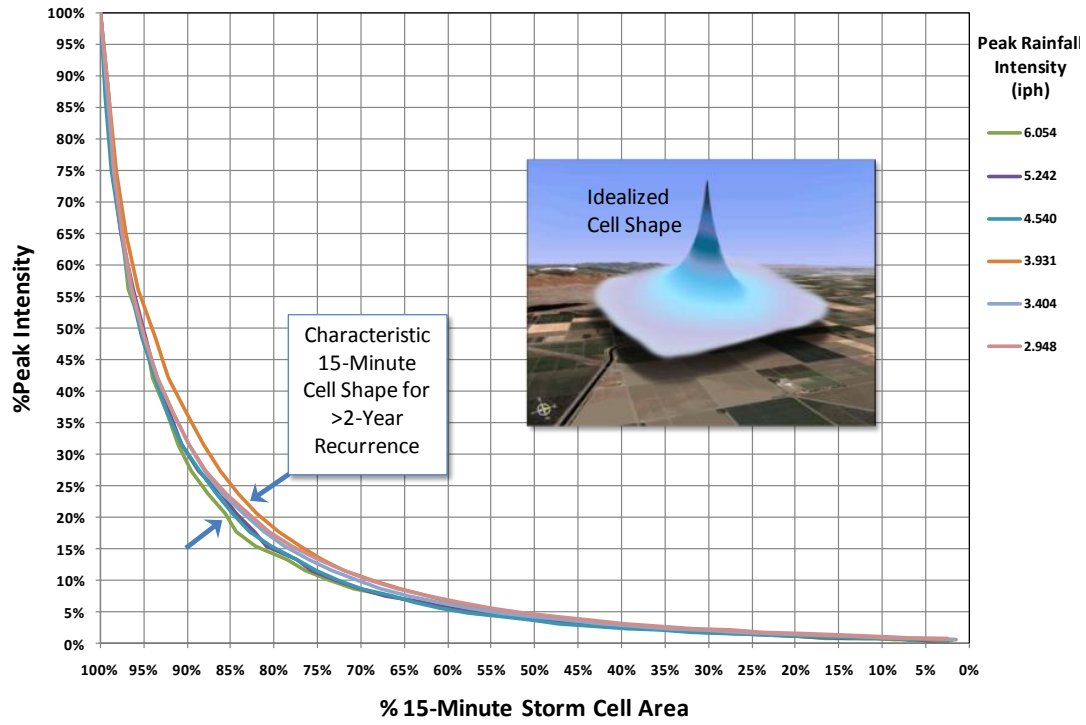


Figure 7-54: Area Normalized Cells for >2-Year Recurrence

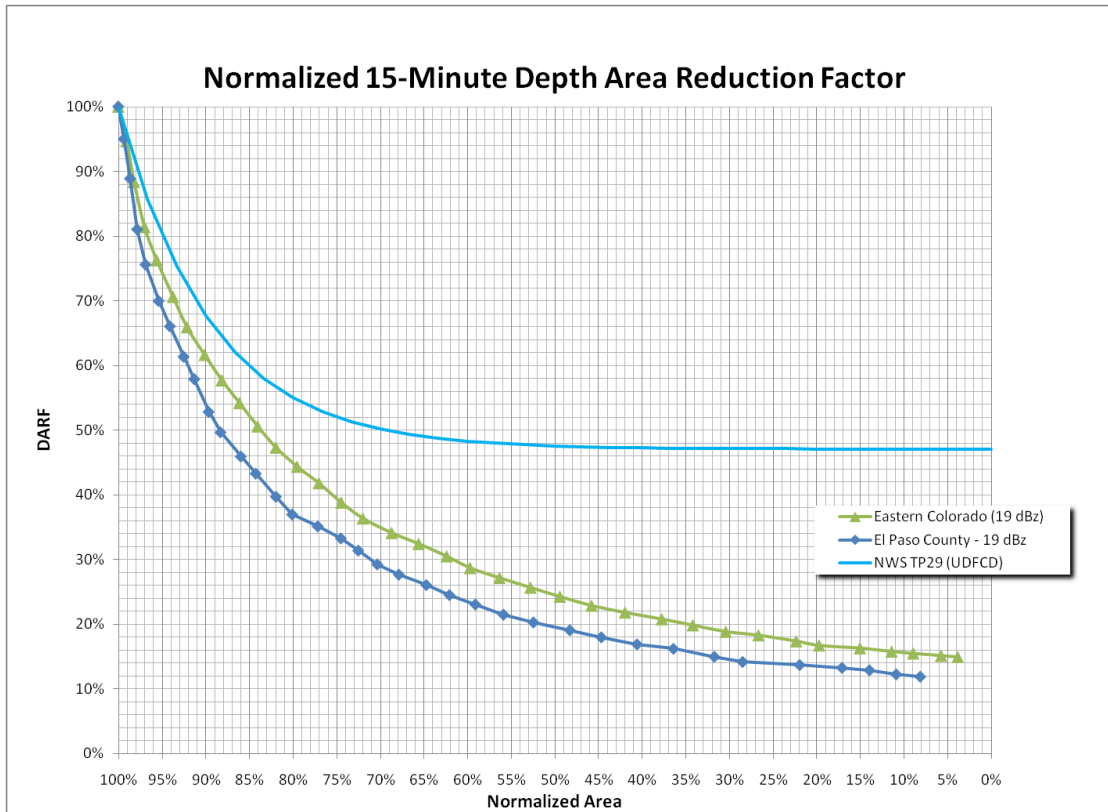


Figure 7-55: Normalized 15-Minute DARF (19 dBz Threshold, 0.022 iph)

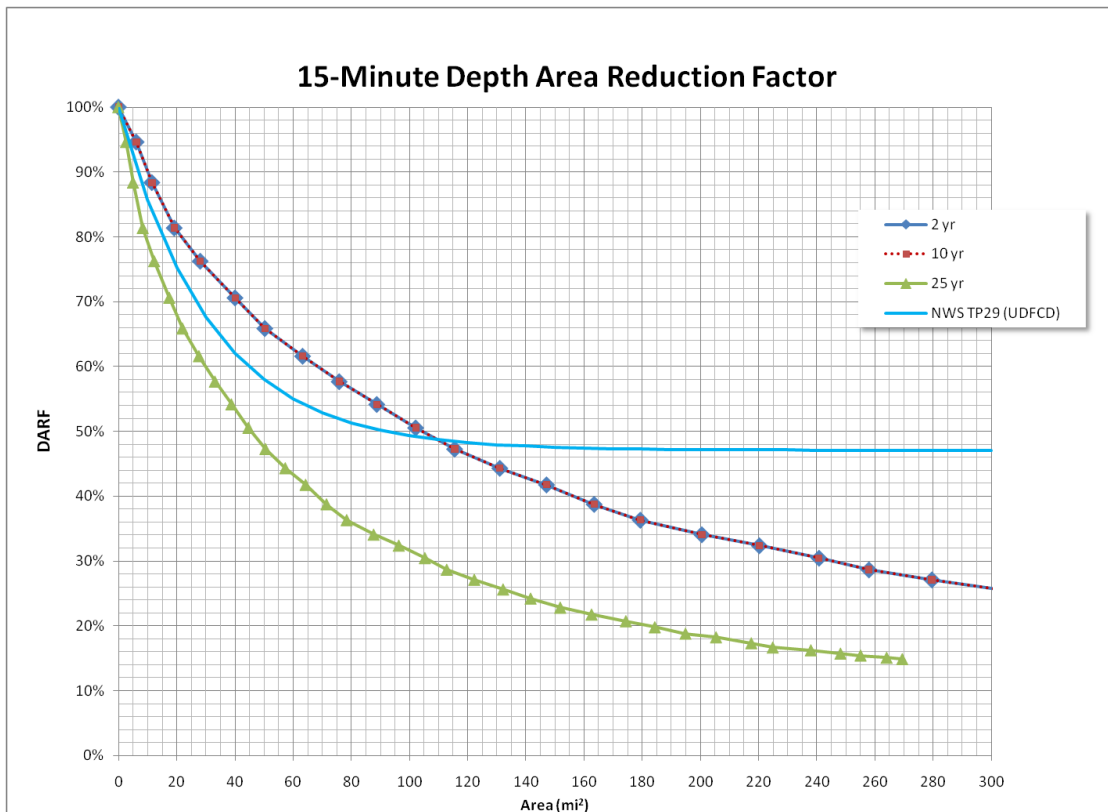


Figure 7-56: 15-Minute DARF (19 dBz Threshold, 0.022 iph)

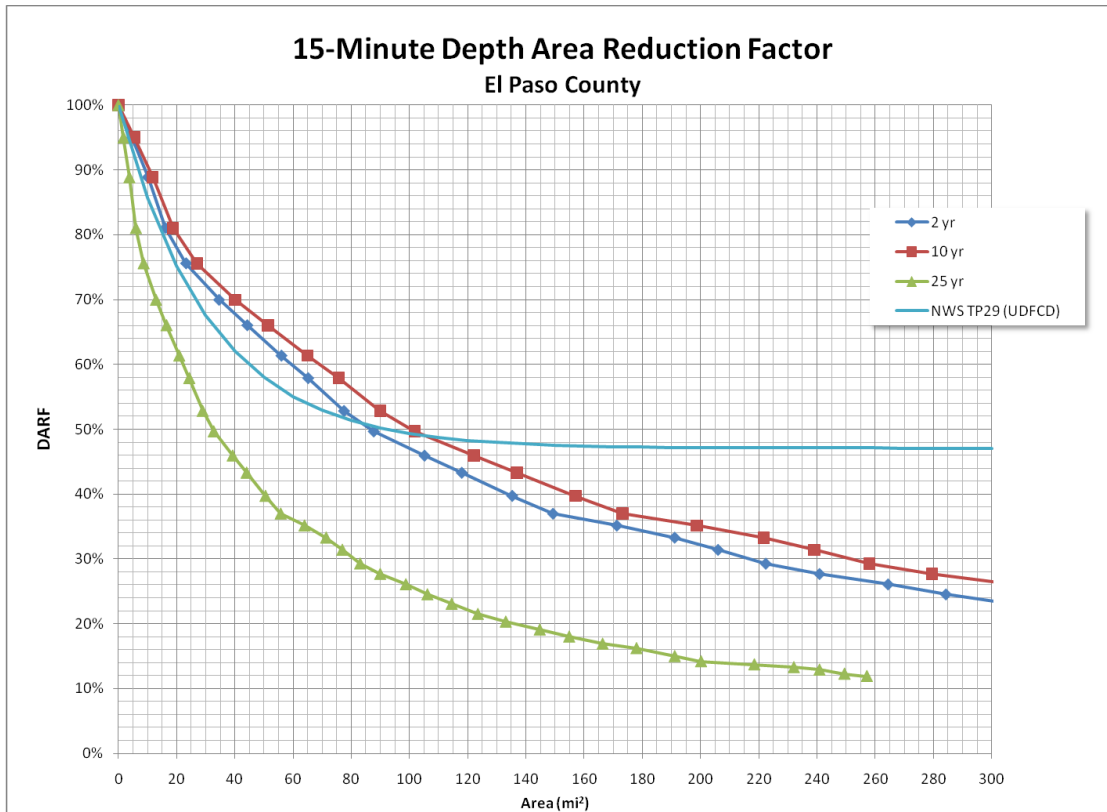


Figure 7-57: 15-Minute DARF for El Paso County (19 dBz Threshold, 0.022 iph)

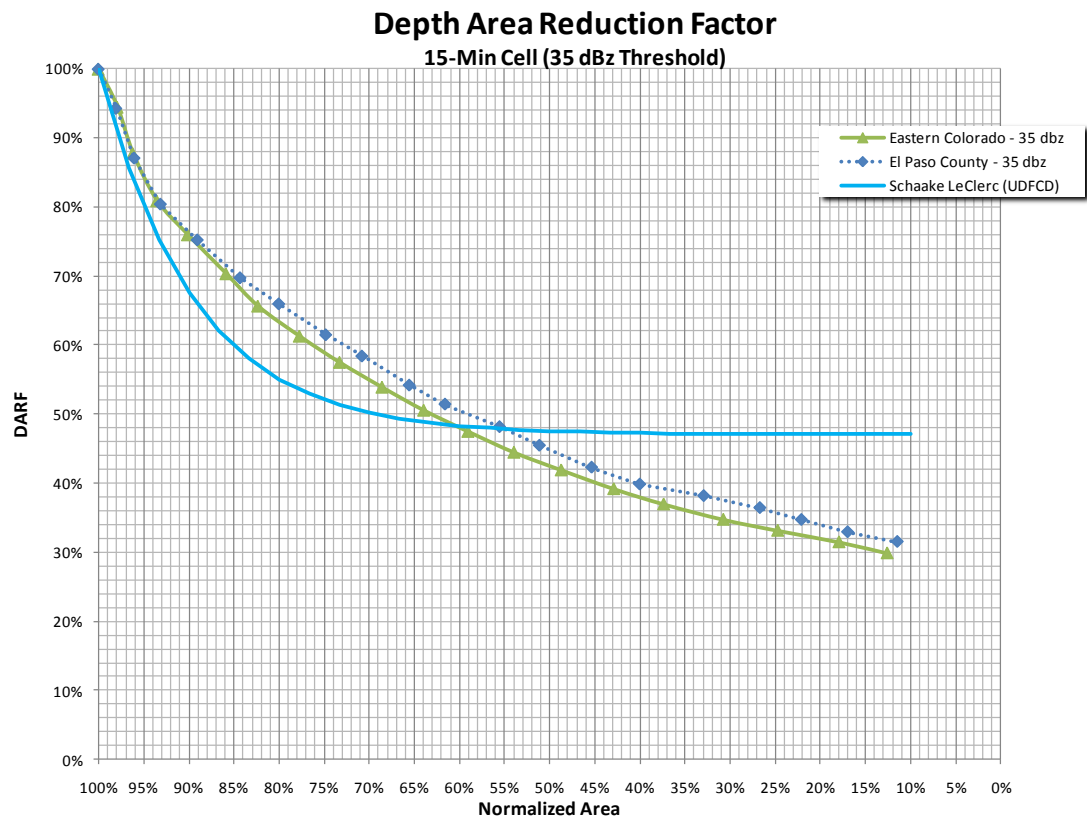


Figure 7-58: Normalized 15-Minute DARF (35 dBz Threshold, 0.22 iph)

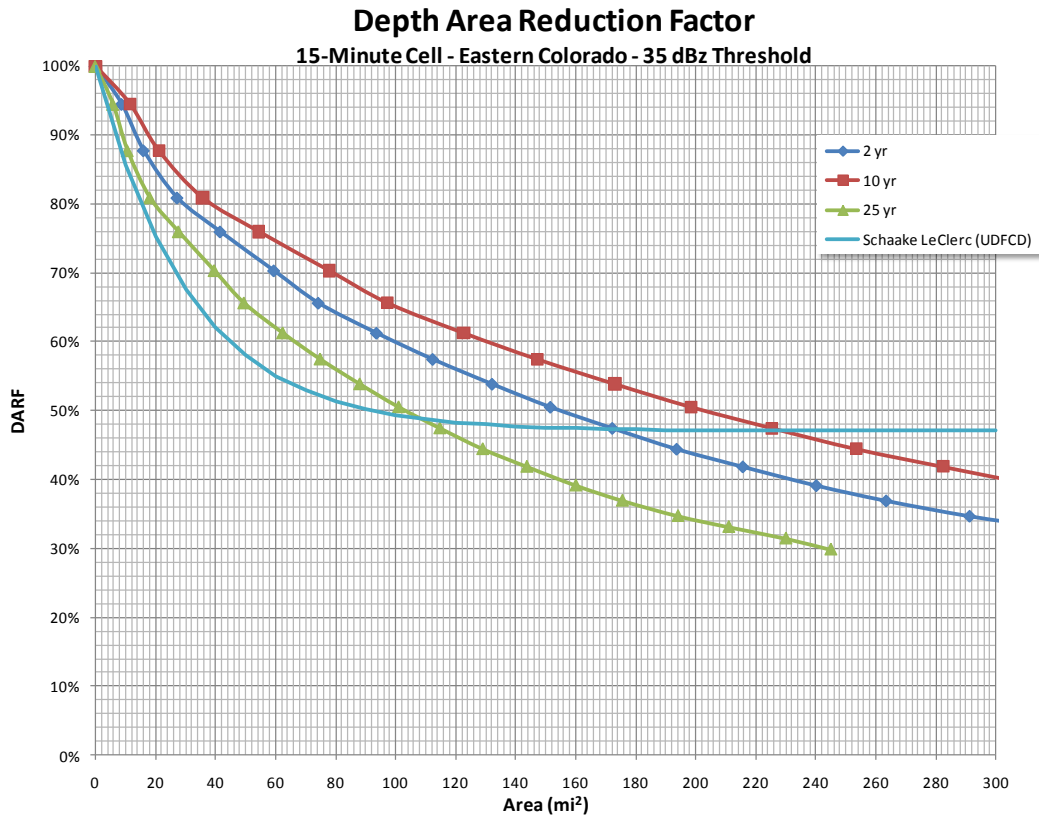


Figure 7-59: 15-Minute DARF (35 dBz Threshold, 0.22 iph)

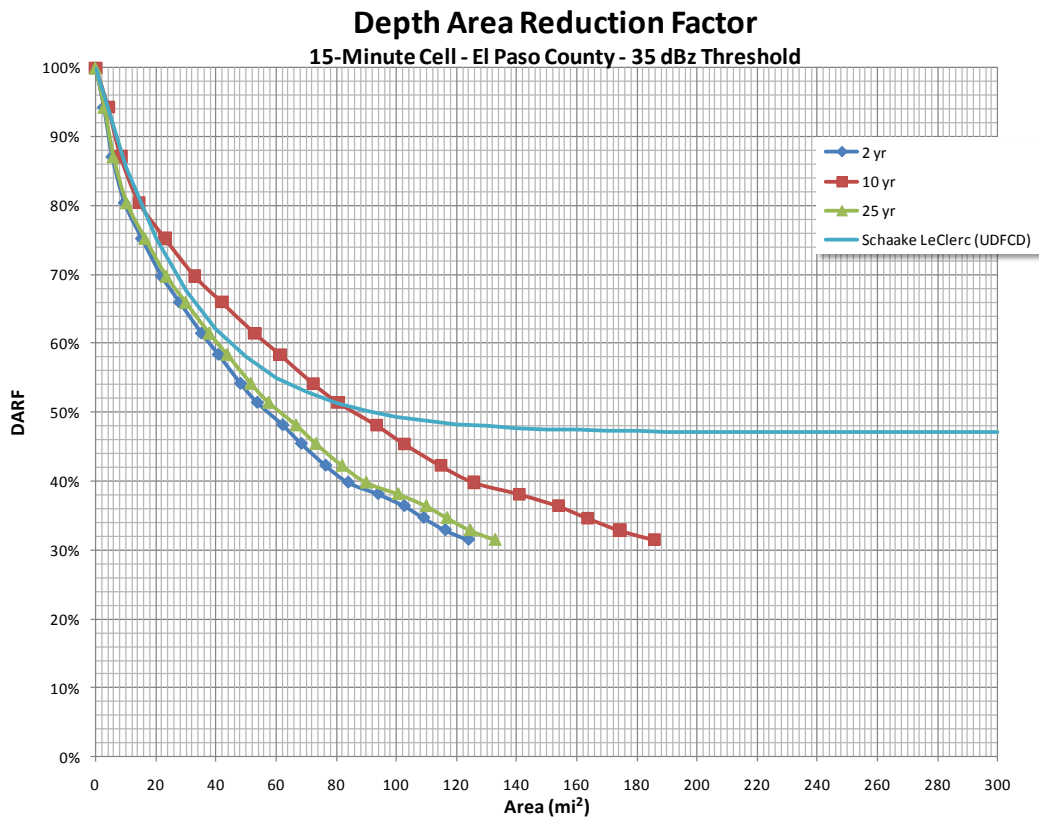


Figure 7-60: 15-Minute DARF (35 dBz Threshold, 0.22 iph) - El Paso County

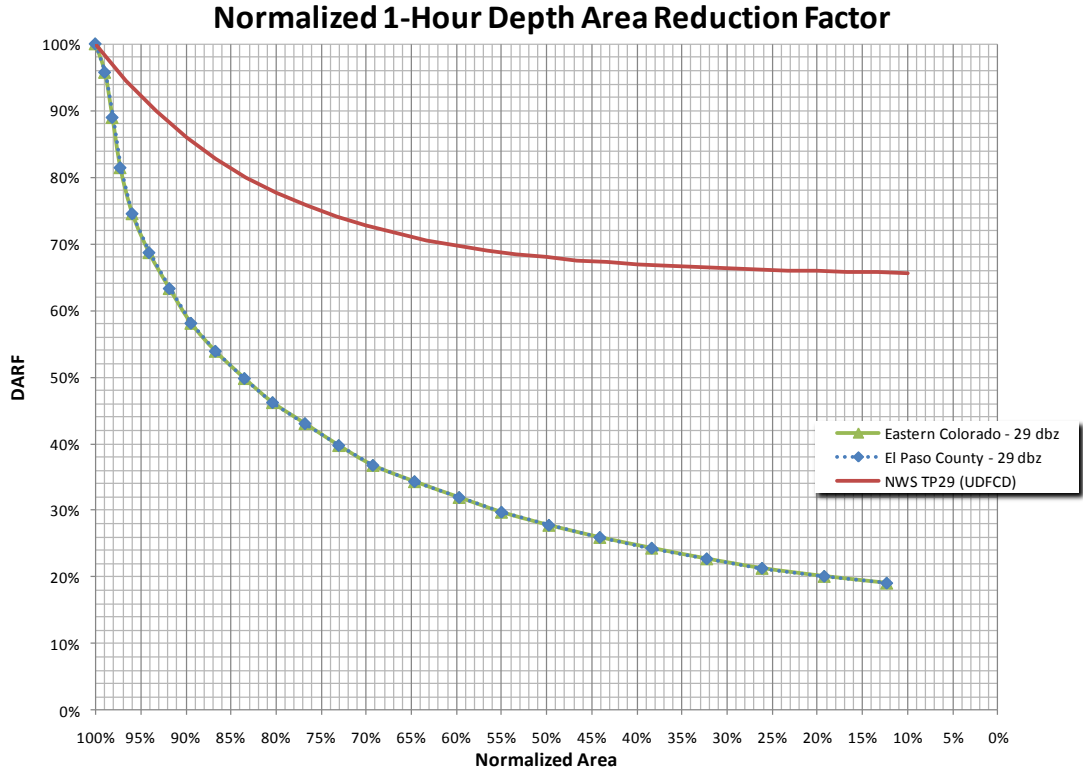


Figure 7-61: Normalized 1-Hour DARF (29 dBz Threshold, 0.09 iph)

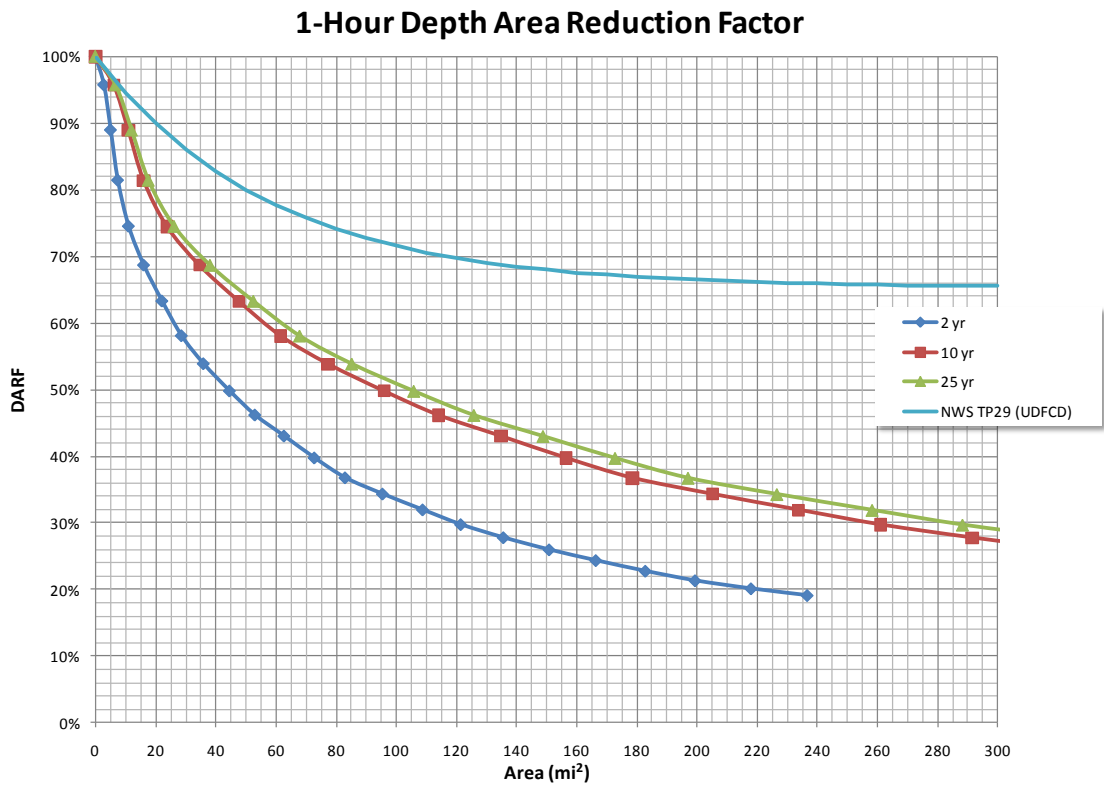


Figure 7-62: One-Hour DARF(29 dBz Threshold, 0.09 iph)

1-Hour Depth Area Reduction Factor

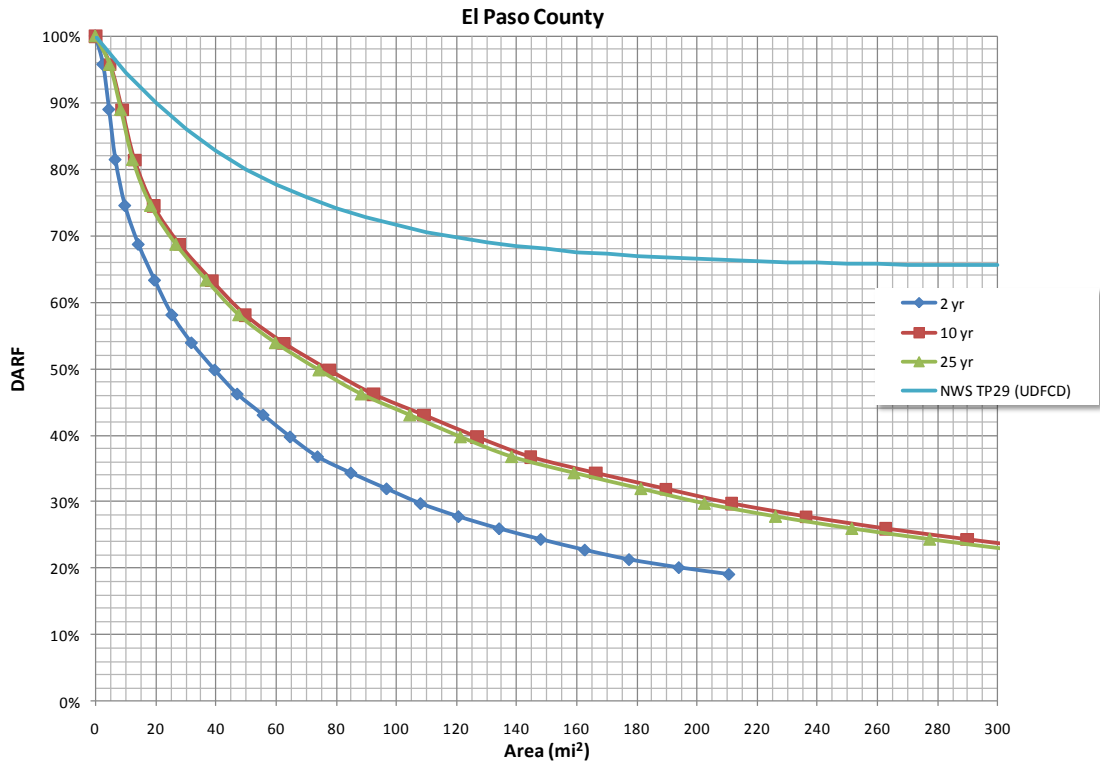


Figure 7-63: One-Hour DARF - El Paso County (29 dBz Threshold, 0.09 iph)

Normalized 3-Hour Depth Area Reduction Factor

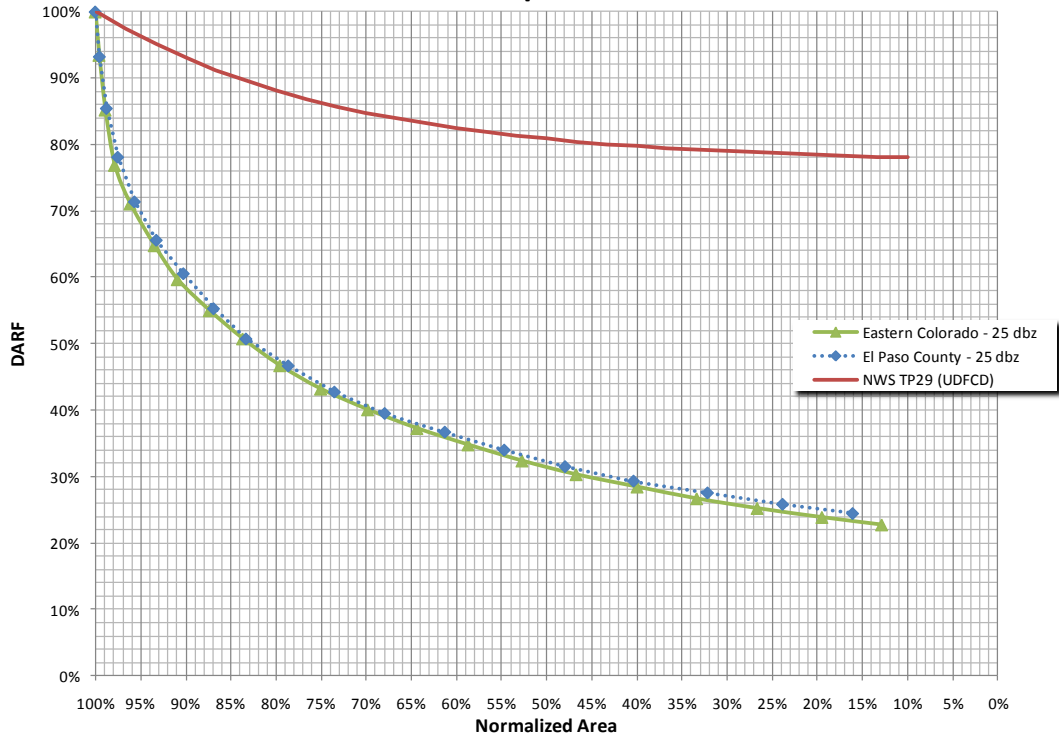


Figure 7-64: Normalized 3-Hour DARF (25 dBz Threshold, 0.05 iph)

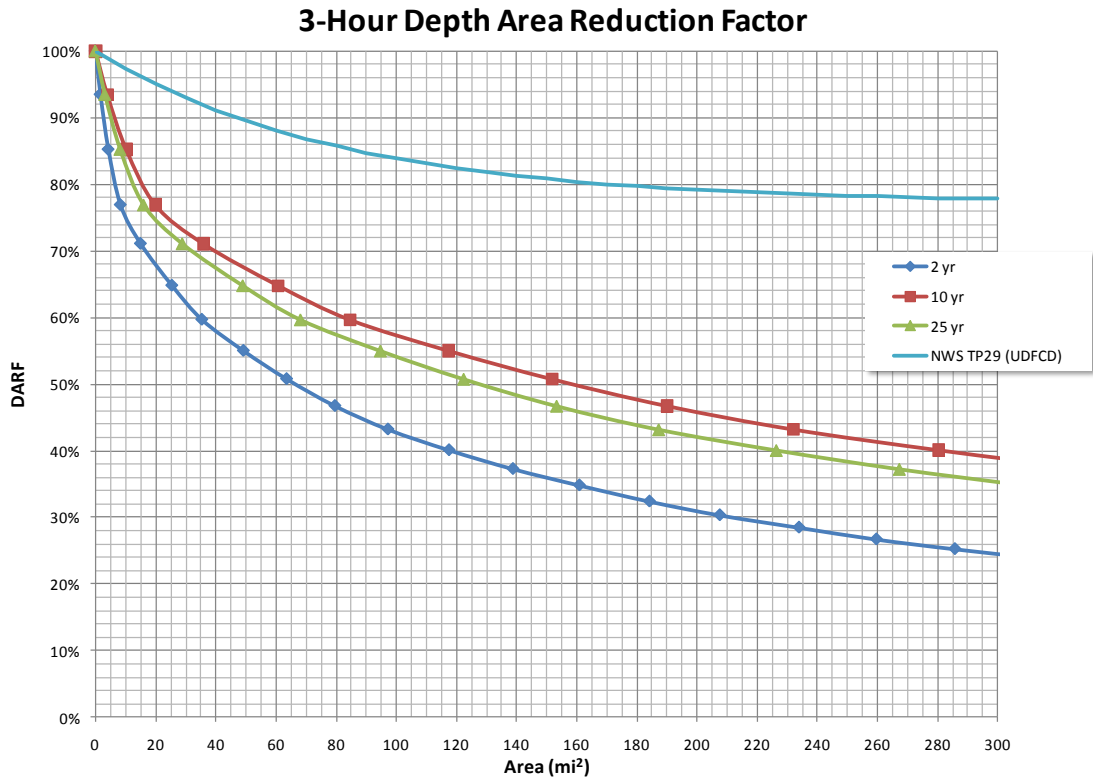


Figure 7-65: Three-Hour DARF (25 dBz Threshold, 0.05 iph)

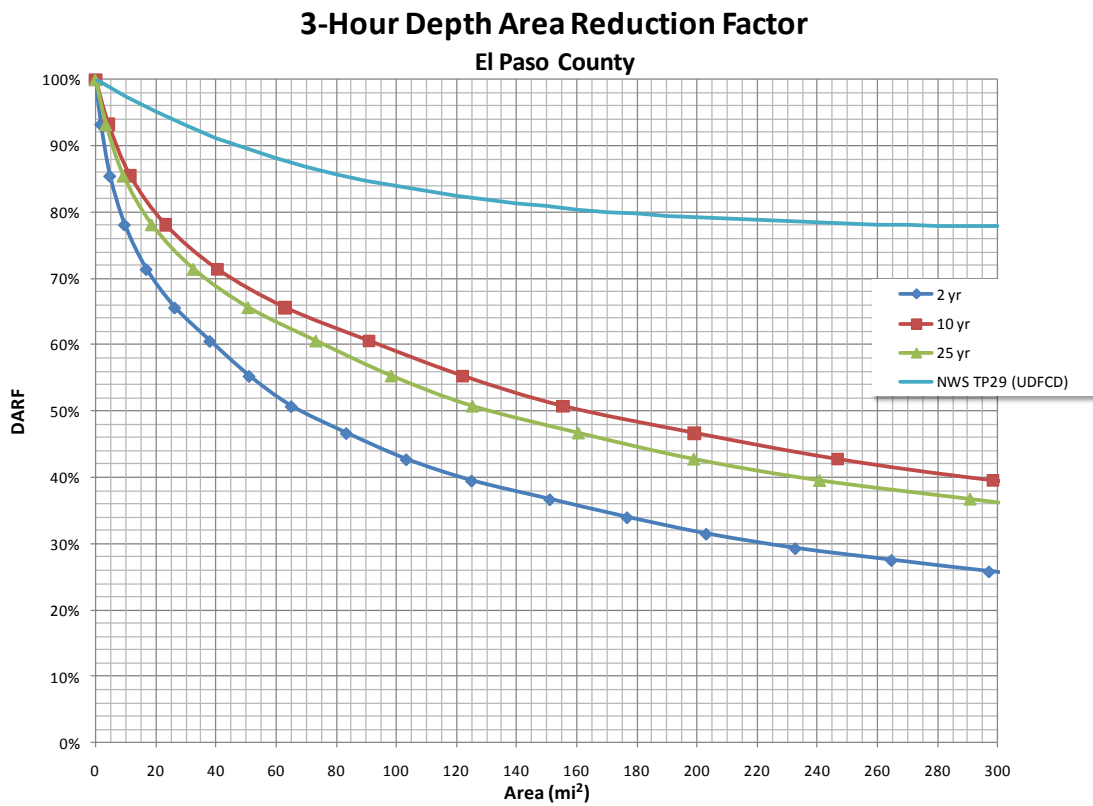


Figure 7-66: Three-Hour DARF - El Paso County (25 dBz Threshold, 0.05 iph)

1-Hour Depth Area Reduction Factor El Paso County with Data From Geronimo, 2004

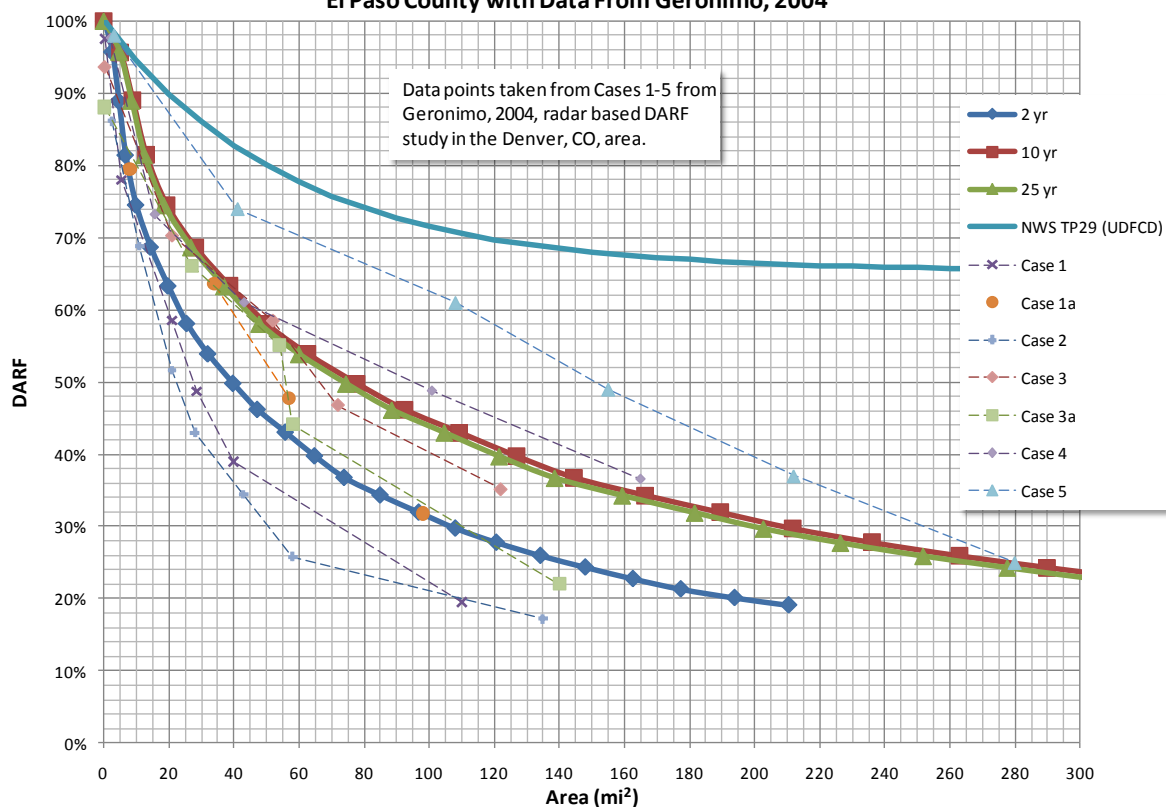


Figure 7-67: One-Hour DARF - El Paso County with DARF Data Points from Geronimo, 2004

7.5 DARF Refinement for the Fountain Creek Watershed

Storm centered DARFs are more appropriate for simulating design rainfall for point locations or sub-watersheds. However, the TITAN methodology integrates all the radar pixel depths in its selected elliptical areas. In most cases, the TITAN ellipses encompass more than one cloudburst cell in space or multiple events in time. This is nearly always the case for durations longer than one hour. These TITAN elliptical storm areas are generally much larger than the small urban watersheds or larger watershed sub-areas of interest for simulating design flows. The hydrologic response of these small watersheds is typically less than one hour.

It was observed in the Fountain Creek examples, Figure 7-30 through Figure 7-49, that a single cloudburst with a clearly defined center typically produced observed flood runoff. These cloudburst center high intensities are necessary in hydrologic models to limit significant runoff to small areas, with much lower contributions from the outer edges of the elliptical storms. Therefore the cloudburst areas shown in Figure 7-28 were used to determine DARFs for the Fountain Creek watershed.

A three component exponential equation, Equation 7.5-1 was fit to the observed DARFs for cloudburst durations 15-min, 1-hr and 3-hours. DARF coefficients P_1 - P_5 for 30-minutes and 3-hours were interpolated using a logarithmic relationship.

$$DARF = P_1 + P_2 e^{-(A-1)P_3} + P_4 e^{-(A-1)P_5} \quad 7.5-1$$

where parameters, P_1 - P_5 , are coefficients fit by trial and error. Coefficients for Fountain Creek DARFs are listed in Table 7.5-1. Figure 7-68 through Figure 7-73 show proposed DARFs for 2-year through 100-year design storm events for 15-minute, 30-minute, 1-hour, 2-hour, and 3-hour time intervals.

Table 7.5-1: Depth Area Reduction Factor Curve Parameters

2-Year	15-min	30-min	60-min	120-min	180-min	25-Year	15-min	30-min	60-min	120-min	180-min
	Median Area (mi ²)						Median Area (mi ²)				
	120	145	200	320	560		180	215	280	360	500
P1	0.0500	0.0800	0.1200	0.1700	0.2200	P1	0.0580	0.0800	0.1000	0.1600	0.2000
P2	0.5000	0.5400	0.5700	0.5900	0.6100	P2	0.5000	0.5200	0.5300	0.5400	0.5500
P3	0.0200	0.0150	0.0120	0.0090	0.0075	P3	0.0130	0.0110	0.0080	0.0077	0.0075
P4	0.4500	0.3800	0.3100	0.2400	0.1700	P4	0.4420	0.4000	0.3700	0.3000	0.2500
P5	0.1200	0.1200	0.1200	0.1200	0.1200	P5	0.1200	0.1200	0.1200	0.1200	0.1200
5-Year	15-min	30-min	60-min	120-min	180-min	50-Year	15-min	30-min	60-min	120-min	180-min
	Median Area (mi ²)						Median Area (mi ²)				
	155	180	230	350	570		200	220	270	330	430
P1	0.0500	0.0800	0.1200	0.1700	0.2200	P1	0.0580	0.0800	0.1000	0.1600	0.2000
P2	0.5000	0.5400	0.5700	0.5900	0.6000	P2	0.5000	0.5100	0.5200	0.5300	0.5400
P3	0.0180	0.0140	0.0100	0.0080	0.0075	P3	0.0110	0.0100	0.0080	0.0077	0.0075
P4	0.4500	0.3800	0.3100	0.2400	0.1800	P4	0.4420	0.4100	0.3800	0.3100	0.2600
P5	0.1200	0.1200	0.1200	0.1200	0.1200	P5	0.1200	0.1200	0.1200	0.1200	0.1200
10-Year	15-min	30-min	60-min	120-min	180-min	100-Year	15-min	30-min	60-min	120-min	180-min
	Median Area (mi ²)						Median Area (mi ²)				
	175	200	280	370	550		210	220	250	290	360
P1	0.0520	0.0800	0.1100	0.1700	0.2100	P1	0.0600	0.0800	0.1000	0.1300	0.1600
P2	0.5000	0.5300	0.5500	0.5700	0.5800	P2	0.5000	0.5100	0.5200	0.5300	0.5400
P3	0.0170	0.0130	0.0080	0.0078	0.0075	P3	0.0110	0.0090	0.0080	0.0077	0.0075
P4	0.4480	0.3900	0.3400	0.2600	0.2100	P4	0.4400	0.4100	0.3800	0.3400	0.3000
P5	0.1200	0.1200	0.1200	0.1200	0.1200	P5	0.1200	0.1200	0.1200	0.1200	0.1200

2-Year DARF

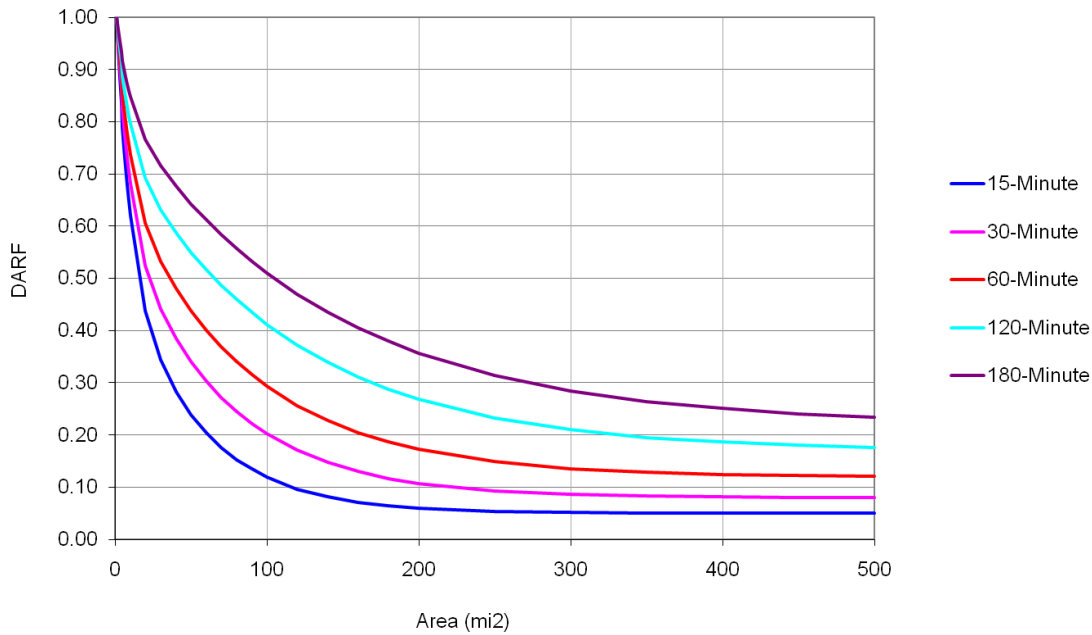


Figure 7-68: Two-Year DARF

5-Year DARF

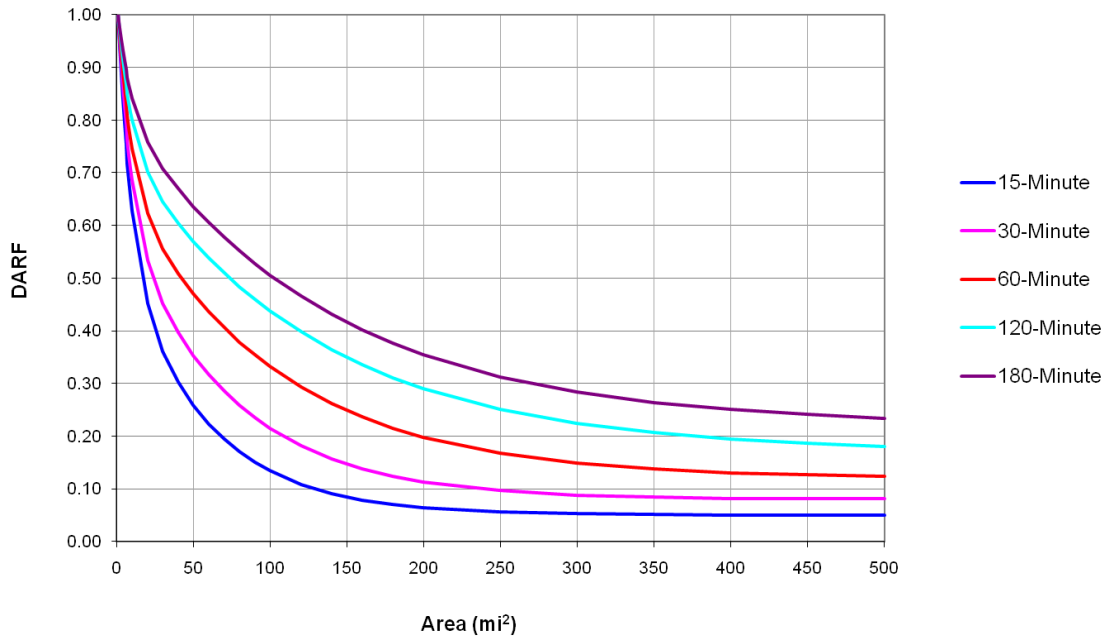


Figure 7-69: Five-Year DARF

10-Year DARF

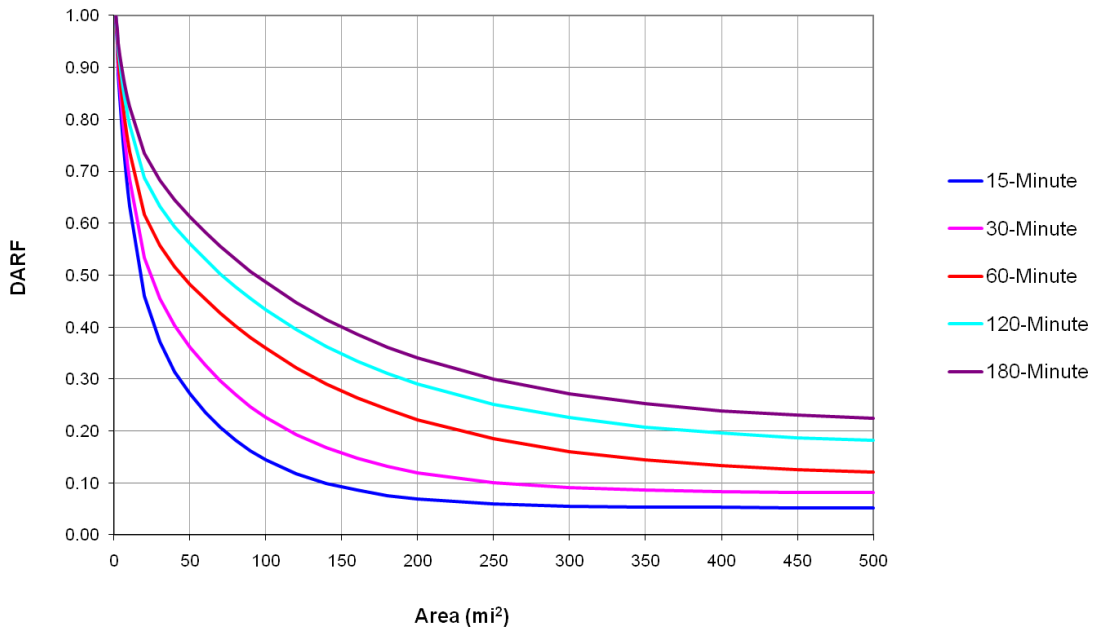


Figure 7-70: Ten-Year DARF

25-Year DARF

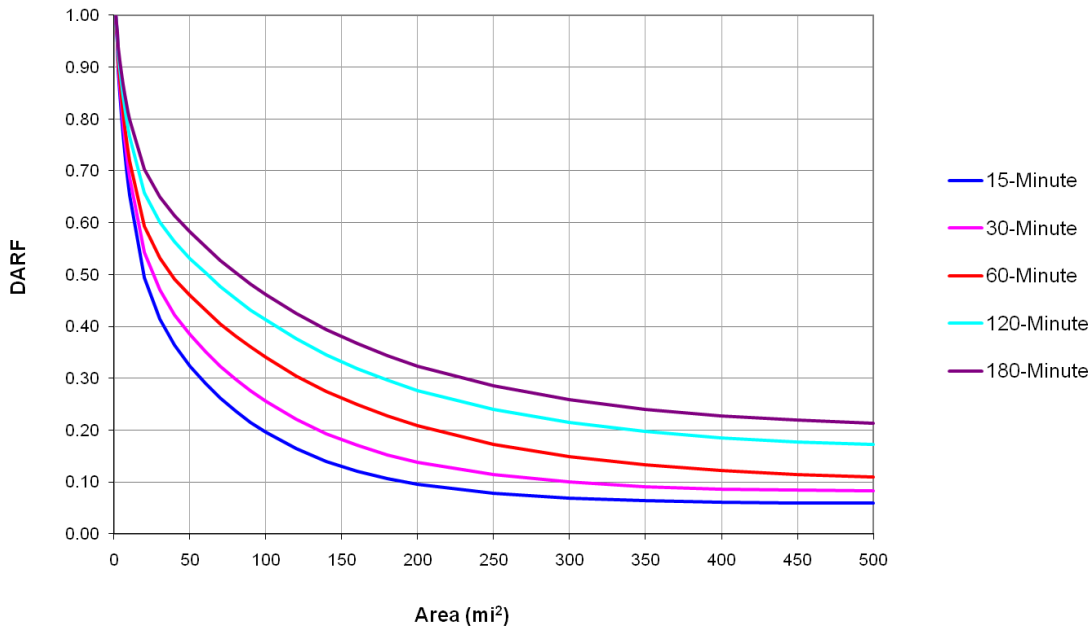


Figure 7-71: Twenty-Five-Year DARF

50-Year DARF

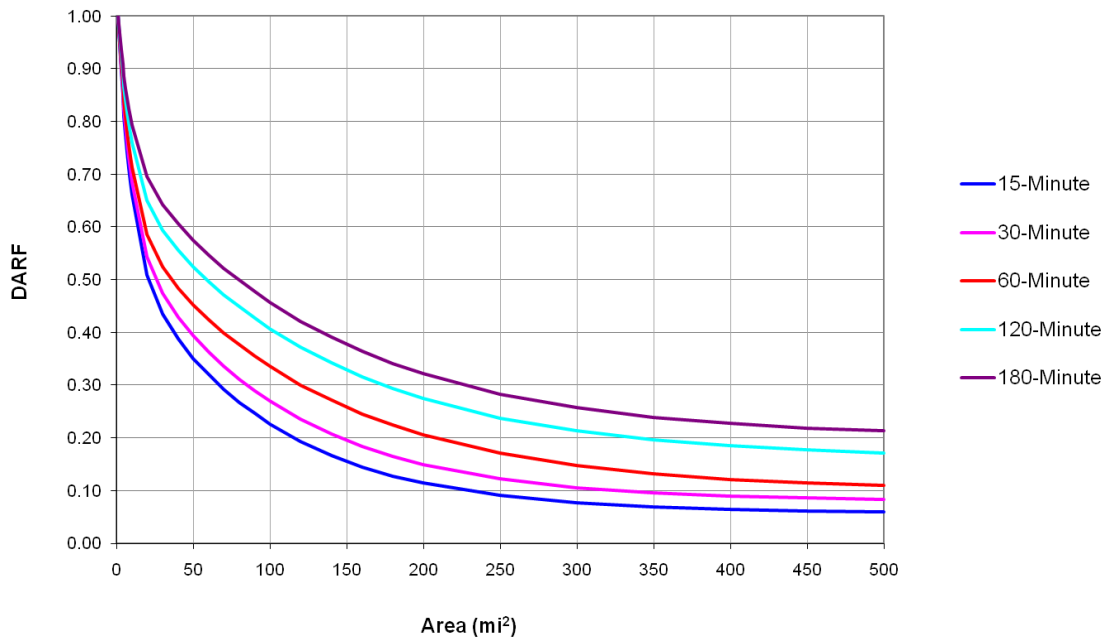


Figure 7-72: Fifty-Year DARF

100-Year DARF

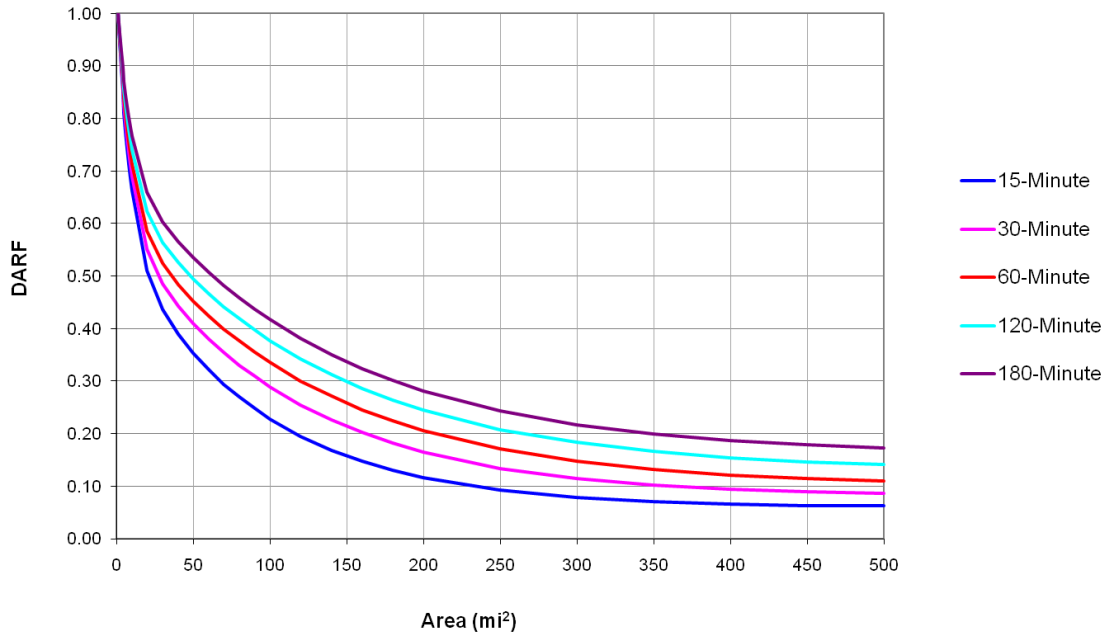


Figure 7-73: One Hundred-Year DARF

7.6 Temporal Analysis

The temporal distributions of 22 storms in the Fountain Creek Watershed were evaluated. (See Table 7.6-1) The remaining storms in the data set were considered too small for this analysis.

The maximum storm total location and storm area were identified for each event using a GIS analysis of the radar data. Once the location of each storm maximum rainfall was identified, the time series of rainfall associated with that location was extracted for the entire storm.

Table 7.6-1: Storms Evaluated in Temporal Analysis

Storm Date	Storm Duration (Minutes)	Storm Area (mi ²)	Storm Date	Storm Duration (Minutes)	Storm Area (mi ²)
6/2/1994	135	450	6/27/2004	180	100
5/17/1995	330	300	7/16/2004	90	350
6/2/1995	75	800	8/5/2004	135	400
6/4/1995	45	150	7/14/2005	105	450
5/15/1996	60	150	7/15/2005	60	250
7/31/1999	195	350	8/26/2006	45	150
8/4/1999	90	350	7/3/2007	90	250
7/13/2001	75	400	8/22/2007	75	80
6/19/2003	210	500	8/15/2008	60	500
8/11/2003	135	150	8/16/2008	75	300
6/15/2004	165	400	9/11/2008	135	250

Storm durations ranged from 45 minutes to 330 minutes. Storm areas ranged from 80 to 800 square miles, with a median of 300.

Figure 7-74 presents the normalized rainfall accumulations for each event along with the average and median accumulations. The shapes of the accumulation curves vary widely for the study storms. The median curve is a more stable representation of the typical accumulation. The average curve can significantly be affected by a small number of longer storm durations.

Figure 7-75 isolates the average and median storm accumulations and includes the distributions of incremental rainfall for each. The median storm duration was between 90-105 minutes and the median time of peak rainfall occurred at 45 minutes.

Figure 7-76 shows the distribution of storm durations. Durations ranged from 45 minutes to 330 minutes with a median of 90 minutes.

The distribution of the times of peak rainfall is presented in Figure 7-77. The median time of peak rainfall is 45 minutes with 30 minutes as the most frequent peak time.

The distribution of the times of peak rainfall by storm quartile is shown in Figure 7-78. Fifteen of the 22 storms evaluated (68%), had peak rainfall in the second and third quartiles suggesting that the majority of storms were approximately “center loaded” storms.

Figure 7-79 presents the non-dimensional rainfall distributions for all storms evaluated. Figure 7-79 also presents the median, average, and the 2-Hour, 10-Year, SCS Type II distribution from the Colorado Springs/El Paso County Drainage Criteria Manual (1994).

Figure 7-79 shows a wide variation of storm time distribution characteristics and suggests very little relationship between time distribution and event duration. There is, however, a very distinct variance between the median observed distribution and the SCS Type II distribution defined in the City’s drainage manual.

Guo (2009) notes, in a study of design rainfall distribution in the Denver area, that the SCS rainfall distributions are not intended to represent observed average or median time distributions. Rather, the SCS distributions are intended to represent a “worst case” distribution to form a severe storm for design purposes. The SCS Type II distribution in Figure 7-79 shows aggressive front end loading on the design storm near the upper bounds of rainfall intensities observed in this study.

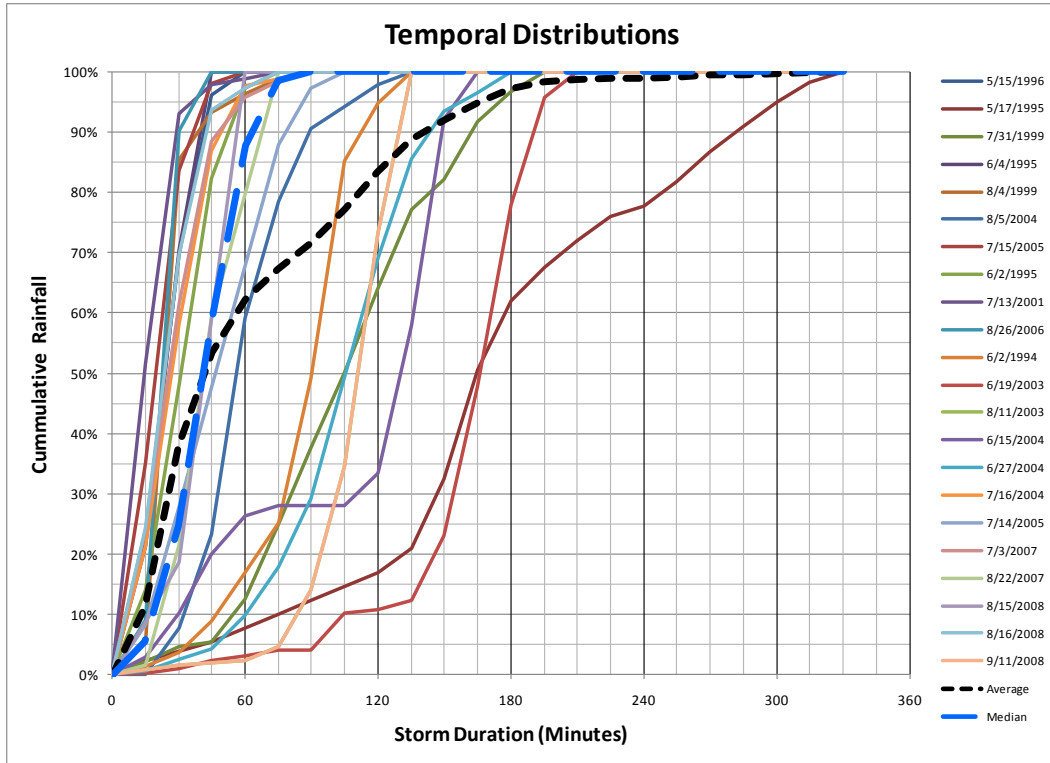


Figure 7-74: Temporal Distributions of Study Storms

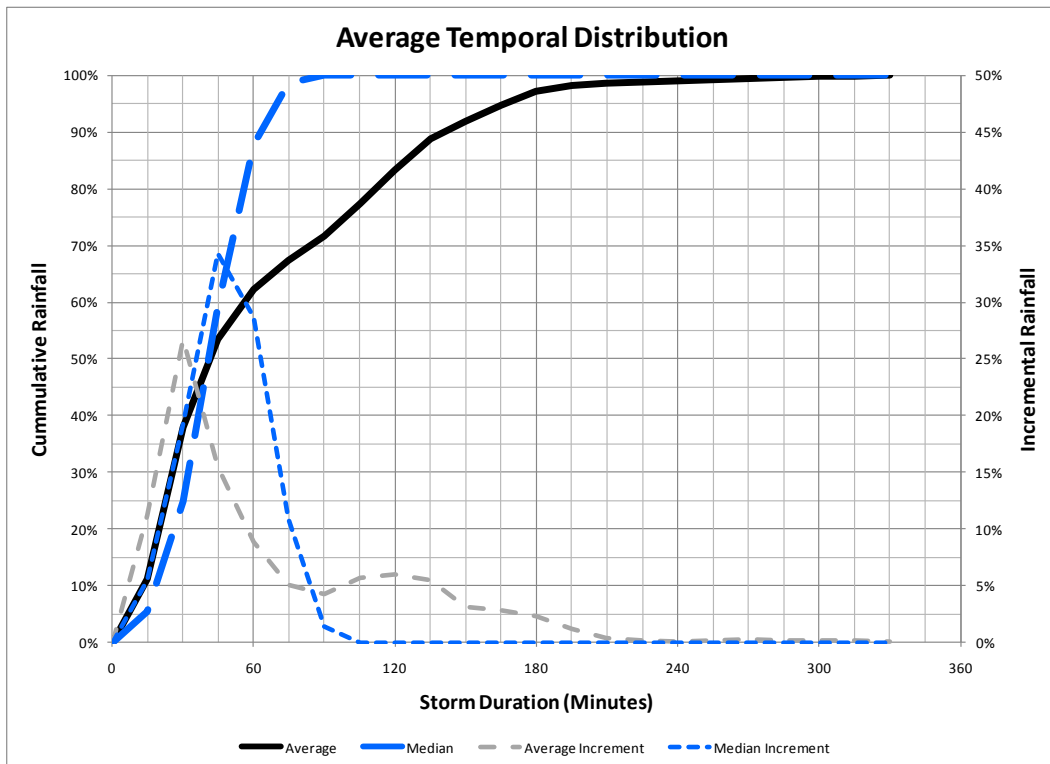


Figure 7-75: Average and Median Storm Distributions

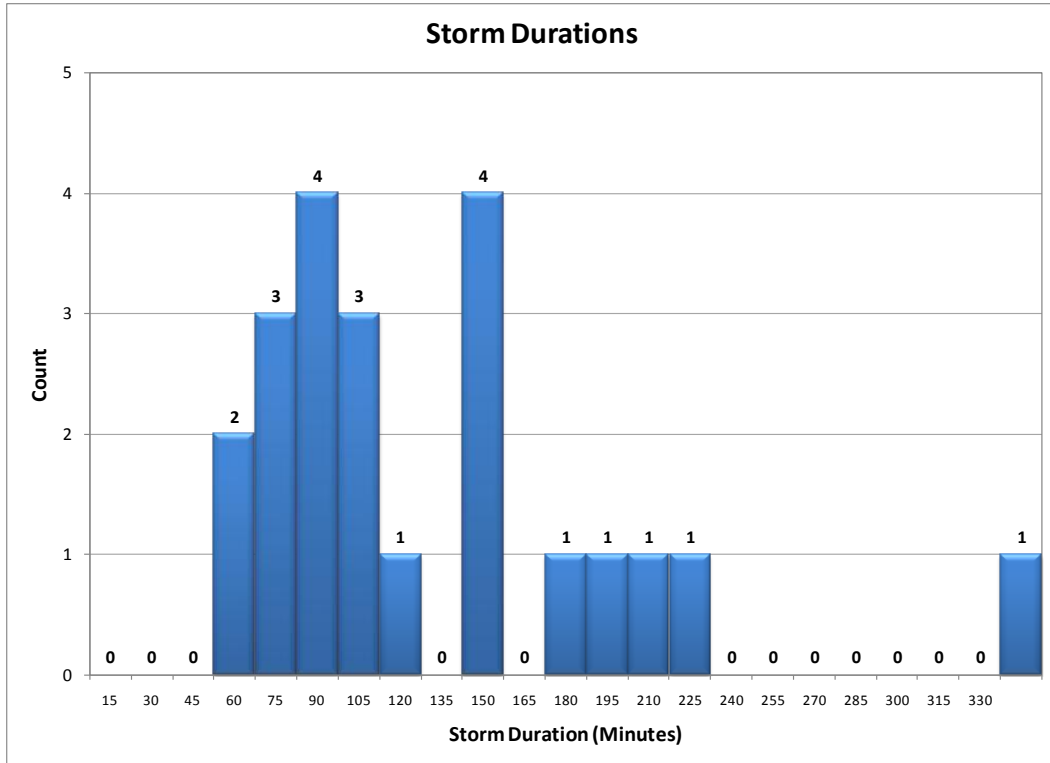


Figure 7-76: Distribution of Storm Durations

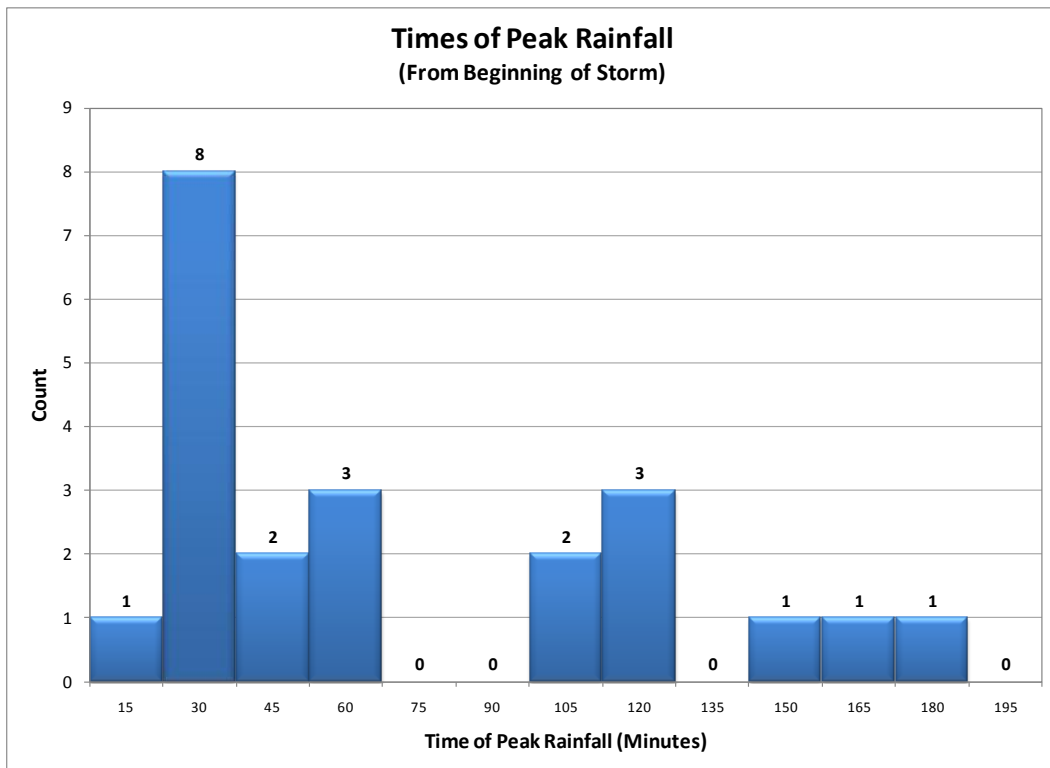


Figure 7-77: Distribution of Times of Peak Rainfall

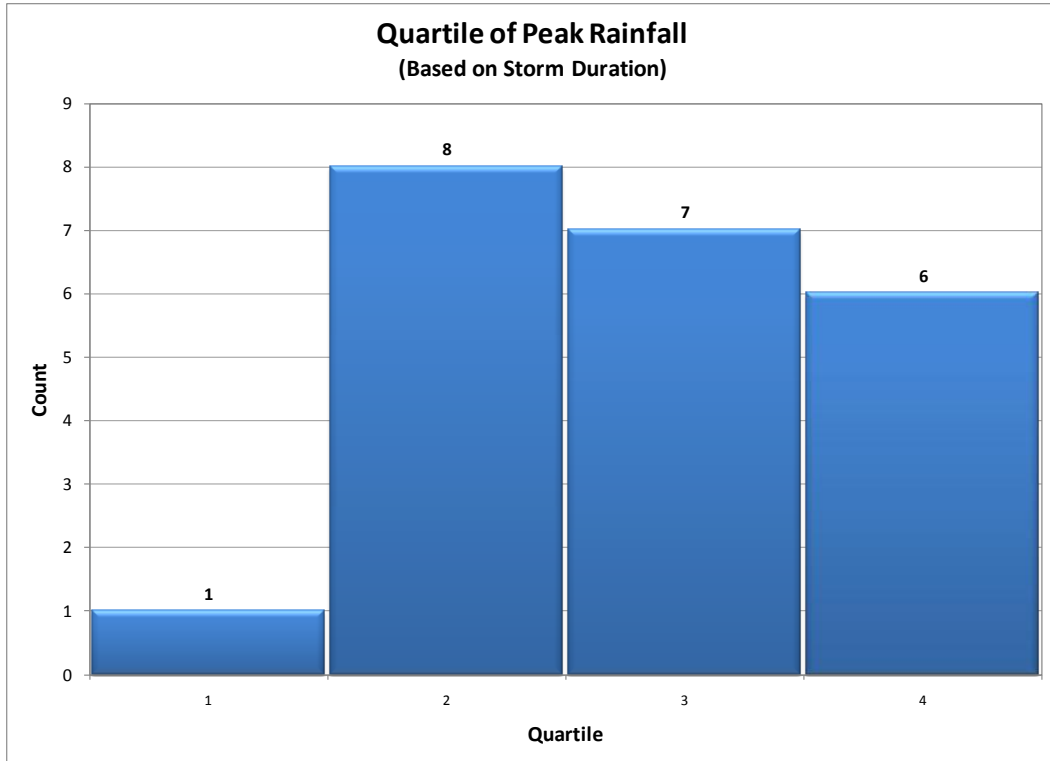


Figure 7-78: Storm Quartiles of Times of Peak Rainfall

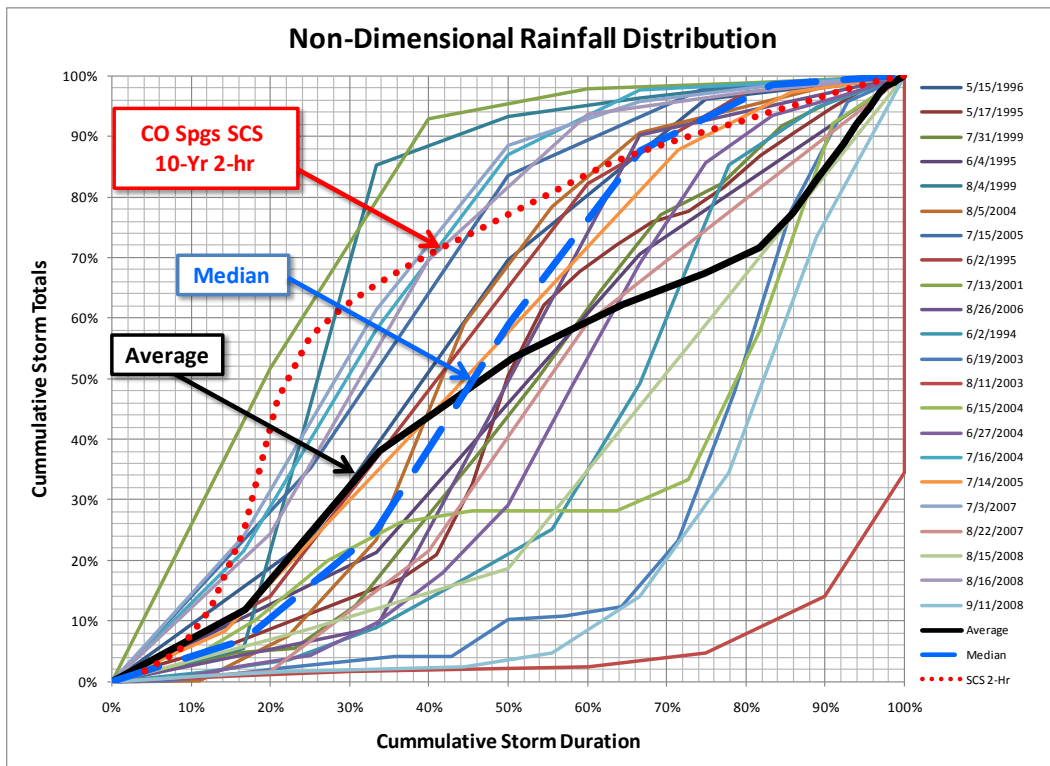


Figure 7-79: Non-Dimensional Rainfall Distribution

7.7 Key Findings

- Geometric properties of storm cells are variable across eastern Colorado and even within El Paso County.
- Mountainous areas tend to produce more but smaller identifiable cells whereas somewhat fewer but larger cells were found in the less variable terrain to the east.
- Typical cell sizes vary with peak intensity, reaching a size maximum in the 2-5 year frequency range.
- Storm cells from 2-100 year frequency range have approximately identical characteristic shapes.
- Depth Area Reduction Factors in the Colorado Springs area are significantly different than the published NWS Depth Area Reduction Factors.
- Depth Area Reduction Factors in the Colorado Springs area were shown to vary by location and return period.
- A wide variation of storm time distribution characteristics was observed and suggests very little relationship between time distribution and event duration.
- The SCS Type II distribution used in Colorado Springs' drainage criteria shows aggressive front end loading on the design storm near the upper bounds of rainfall intensities observed in this study.

8.0 Design Storm Processor

8.1 Background

Several other studies (Makson, 2008; Arsenault 2006) have determined that cloudbursts (severe short-duration, limited area thunderstorms), should have separate design storm parameters compared to synoptic scale, large area, long-duration storms. Depth Areal-Reduction-Factors (DARFs) should be applied to the short duration, limited-area, cloudburst storm. Design storms elsewhere (for example, St. Louis (MSD 2008), Las Vegas (Clark County 1999), Dallas (iSWM 2008), Maricopa County (Sabol 1995), Salt Lake County (2008) used DARF for 1, 2, 3 and 6 hours storm duration for the cloudburst type.

Cloudburst events, which have produced all significant flood events observed in the Fountain Creek watershed, were defined by center annual maximum depth-duration-frequency (DDF) data from Colorado Springs Airport and used area-reduction-factors (DARF) obtained from the OneRain TITAN studies. A prototype proof of concept cloudburst design storm processor was developed for the Fountain Creek watershed. This processor can be configured with storm duration, recurrence interval, storm area, time step and time loading (i.e. central, front end, or rear end loading) and produces Excel worksheet output files. The results are realistic design storms which can accurately model events for varying recurrence intervals and drainage basin areas. The processor can produce static or stationary design storms as well as dynamic or moving design storms.

8.2 Static Design Storm Processor

TITAN results were used to determine DARFs for time intervals 15-min, 30-min, 1-hr, 2-hr and 3-hour. These time intervals are used to determine 15-minute storm depths for all time steps within a 3-hour design storm. Time steps for a stationary storm are constructed using appropriate DDF and DARF for 15-min, 30-min, 45-min, 60-min, etc .before and after the central value. For example, one computes 15-minute DDF and 15-minute DARF, 30-minute DDF using 30-minute DARF and so on. The 12 steps in the 3-hr storm are then re-arranged with the center the maximum (time step 6) and alternating lower values before and after.

The static cloudburst processor includes options for DDF adjustment, basin area (0 to 1000 sq mi), storm duration (1, 2, 3 and 6 hours), storm loading (front, center, and back), recurrence interval (1, 2, 5, 10, 25, 50, 100, 500, 1000 years), time step 5, 10, 15, 30, 60 minutes and HEC-1 hyetograph or text file output.

DARF equations for the cloudburst design storm use the following equation:

$$DARF = P_1 + P_2 e^{-(A-1)P_3} + P_4 e^{-(A-1)P_5} \quad 8.2-1$$

where DARF is the Depth Area Reduction Factor for a given recurrence interval, A is watershed area in square miles and P_1 - P_2 - P_3 - P_4 - P_5 are constants dependent on time and recurrence interval. Parameter values for the DARF equation constants are listed in Section 7.0. Figure 8-1 shows an example of static design storm output.

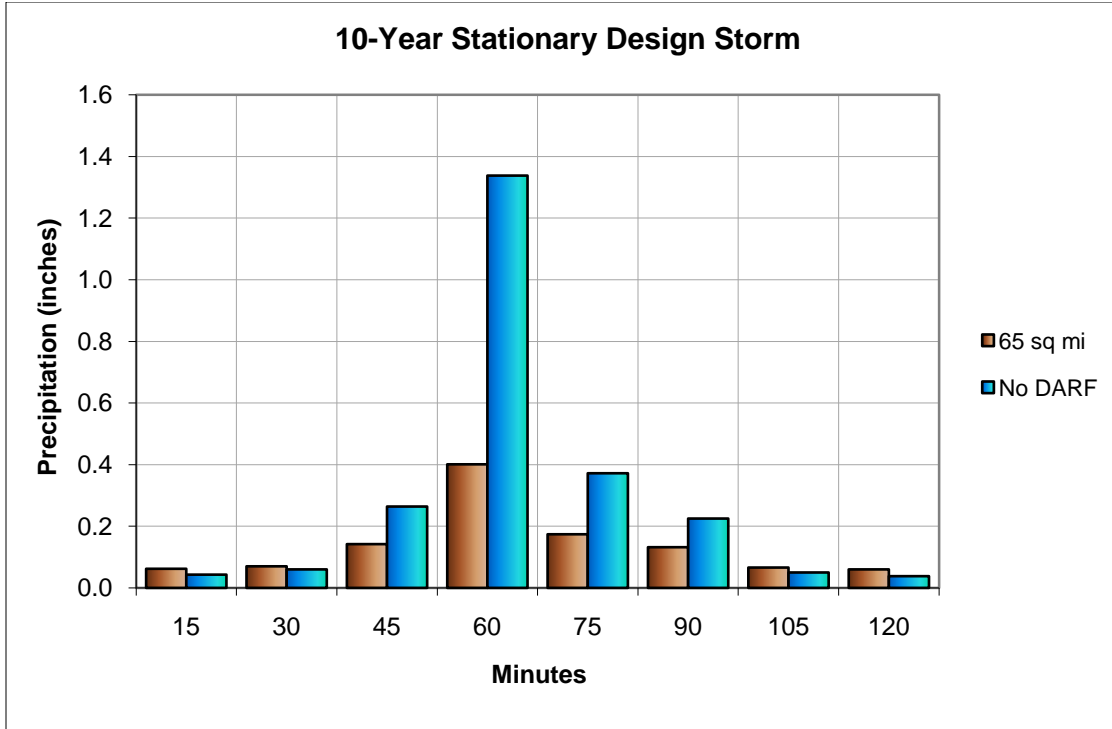


Figure 8-1: 10-Year Stationary Design Storm

8.3 Dynamic Design Storm Processor

A dynamic or moving storm more realistically simulates the behavior of cloudburst storms. Cloudburst design storms can be constructed using the Dynamic Cloudburst Storm Processor on the El Paso County pixel grid based on following:

- Elliptical shape with axis 2:1
- Area: (1-500 sq. mi.)
- Recurrence Interval: 1-, 2-, 5-, 10-, 25-, 50-, 100-, 500-, 1000-years.
- Central pixel in ellipse assigned 15-minute DDF for selected recurrence interval.
- Duration: 15 minutes to 3 hours. (default 90 minutes.)
- Time Step: 15, 30, 60 minutes (default 15 minutes)
- Orientation angle: 0 to 60 deg. (default 30 degrees clockwise of storm direction)
- Direction: 0 to 360 deg. (default 180 degrees (south to north))
- Speed: (5-30 km/hr) (default 10 km/hr.)
- DARF for the area, time step and recurrence
- DDF adjustment for locations other than Colorado Springs Airport
- Starting DDF multiplier for linear growth and decay

The following sections offer comparisons of dynamic design storm processor results with specific storm events. Note that design storms are abstractions based on statistical averages and are not likely to reproduce the exact characteristics of a specific observed event. Also, the dynamic storm processor is a simplification using the representation of a single cell moving across the area. Observed storm patterns often result from more complex realizations of multiple cells which can create additional spatial variability. The intent of the comparisons is to show general agreement and overall reasonableness of the dynamic design storm processor output.

8.3.1 Comparison of Moving Design Storm to June 17, 1965 Jimmy Camp Creek Flood Cloudburst

Figure 8-2 was based on the precipitation map in USGS Water Supply Paper 1850-D (USGS, 1974) for a major flood event on Jimmy Camp Creek, June 17, 1965. Hourly precipitation was partially recorded at stations Fountain and Eastonville 3 NW on June 17th between 1400 and 1900 (5 hours). Approximately 70% of the precipitation fell in a 2-hour period at Eastonville. The direction of movement was 200 deg. (south to north) at 15 km/hr. The area of precipitation was approximately 300 square miles. With three-hour accumulations over 12 inches, the central 1-hour intensity exceeded 6 inches per hour, a 1000-year event. Figure 8-3 shows a dynamic moving storm processor fit to this event. Figure 8-4 shows the depth area comparison for the actual storm of June 17, 1965 and the design storm processor output. The general shape of the depth area relationship is very similar but the observed storm appeared to cover a somewhat larger area.

Comparison to the June 17, 1965 event is challenging because no radar data were available for the event to provide an accurate picture of storm evolution. Only data from point rain gages and a post-event bucket survey were available. The rainfall distribution pattern shown in Figure 8-2 is derived from manually drawn isohyetal lines based on the original point data and subject to the spatial biases associated with such interpolation. Also, little to no storm movement information was available for the event so design storm speeds were estimated.

Figure 8-4 suggests that the observed event covered a larger area than the design storm processor output. While that is entirely possible that this individual storm was spread out more than the design storm, it is also a characteristic of traditional sparse point data interpolation to smooth and spread out storm distributions. It is part of the reason why the standard NWS DARFs decay much more slowly than the radar rainfall-based DARFs derived in this study.

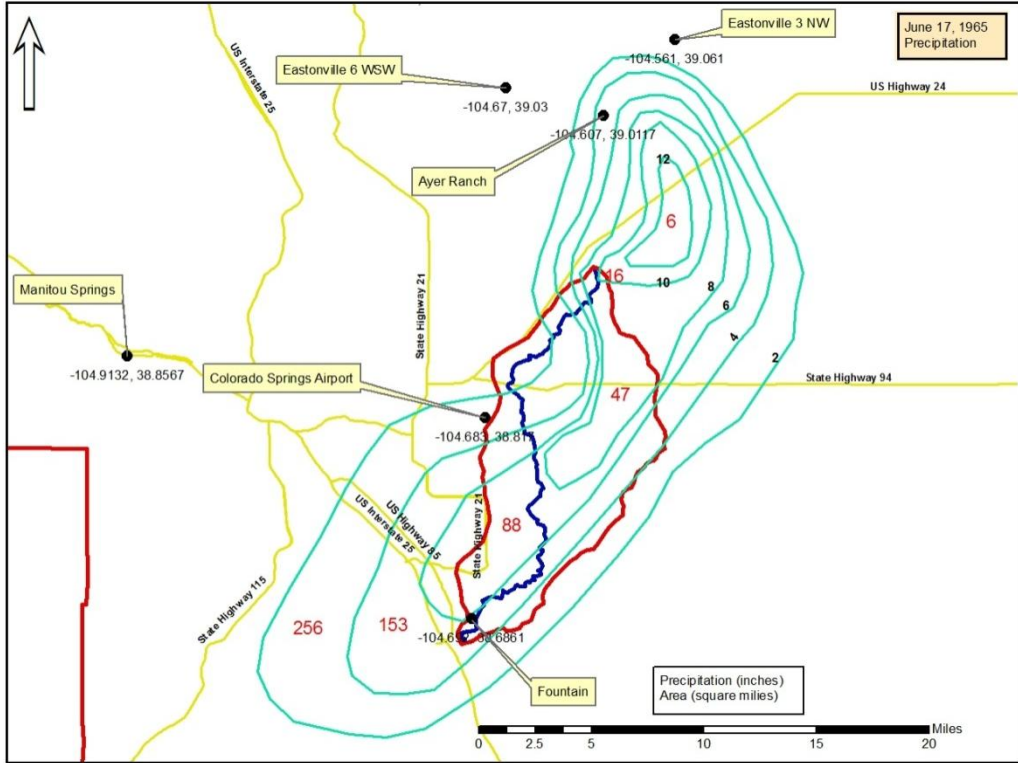


Figure 8-2: June 17, 1965 Cloudburst (Rainfall, inches)

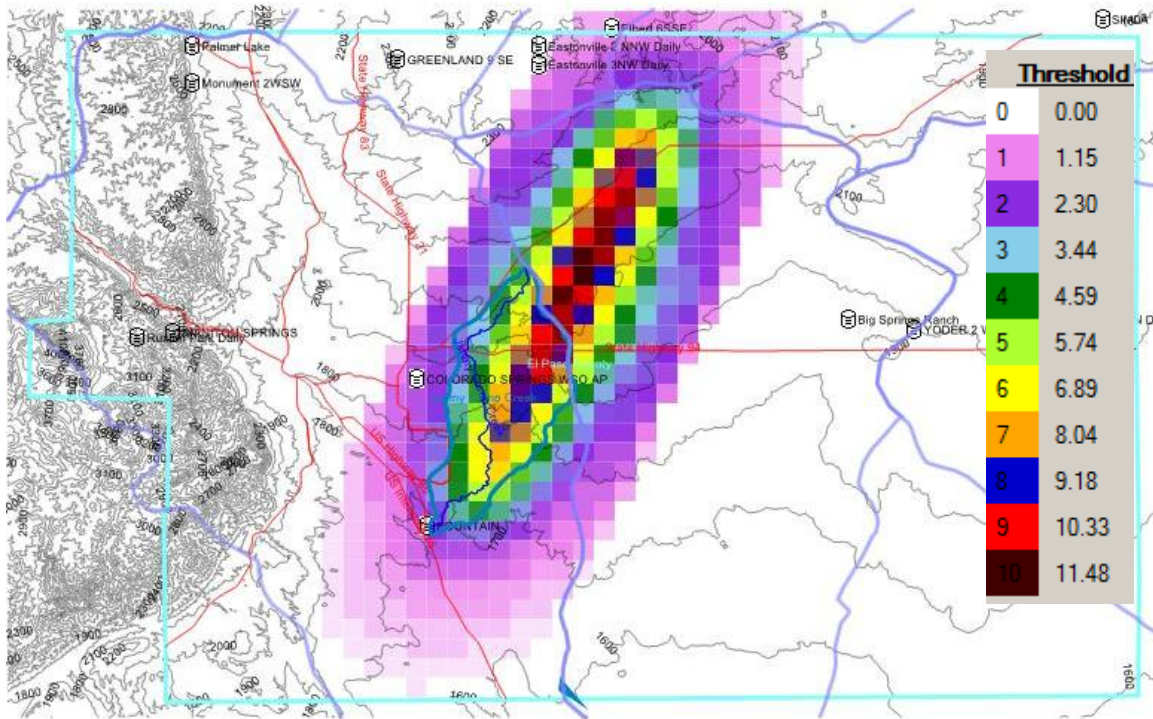


Figure 8-3: June 17, 1965 Cloudburst (Rainfall, inches)

Jimmy Camp Creek Cloudburst June 16, 1965

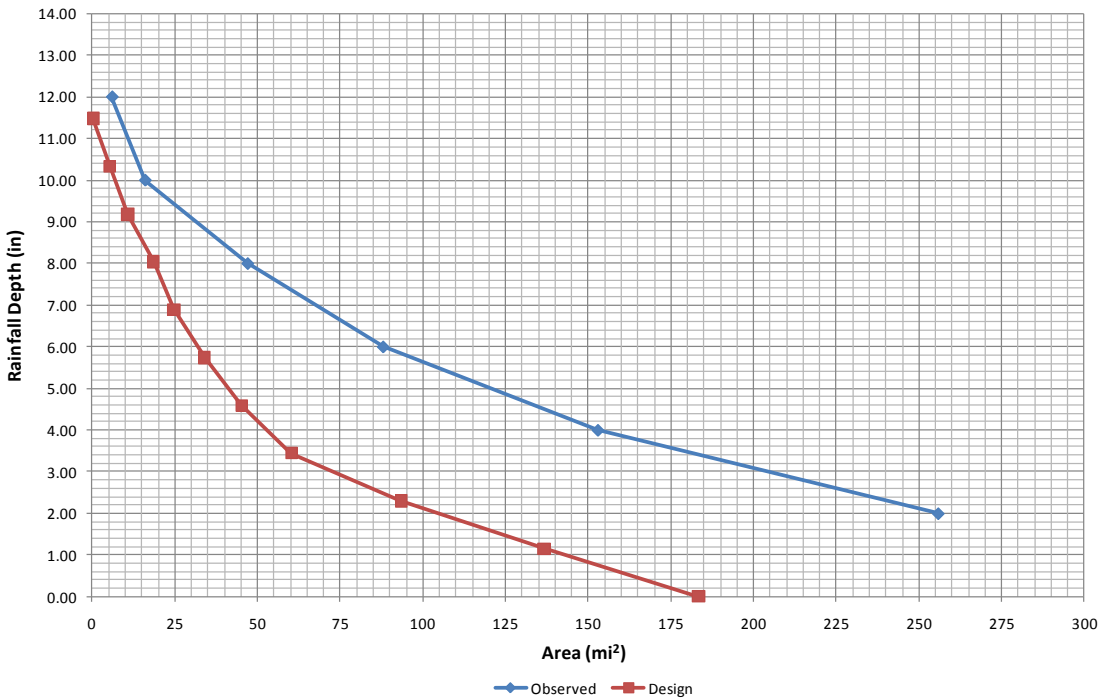


Figure 8-4: Jimmy Camp Creek, June 16, 1965, Depth Area Comparison

8.3.2 Comparison of Moving Design Storm to June 27, 2004 Cloudburst Near Colorado Springs Airport

The processor was used to construct a moving design storm fit to the June 27, 2004 cloudburst in Fountain Creek watershed. The center of this cloudburst passed one or two kilometers east of the Colorado Springs Airport recording precipitation gage. Figure 8-5 shows the composite storm with the 15-minute radar frames edited to remove precipitation not associated with the cloudburst. Figure 8-6 shows the best fit for the design storm. The best fit design storm has a direction from 180 degrees, orientation of 30 degrees, speed of 10 km/hr, area of 150 square miles, duration 135 minutes and central intensity of approximately 2.0 in/hr (2-year recurrence).

Isohyetal areas for the June 27, 2004 cloudburst and the event generated by the design storm processor are compared in Figure 8-7. The design storm processor results provide a very realistic comparison to the observed cloudburst event.

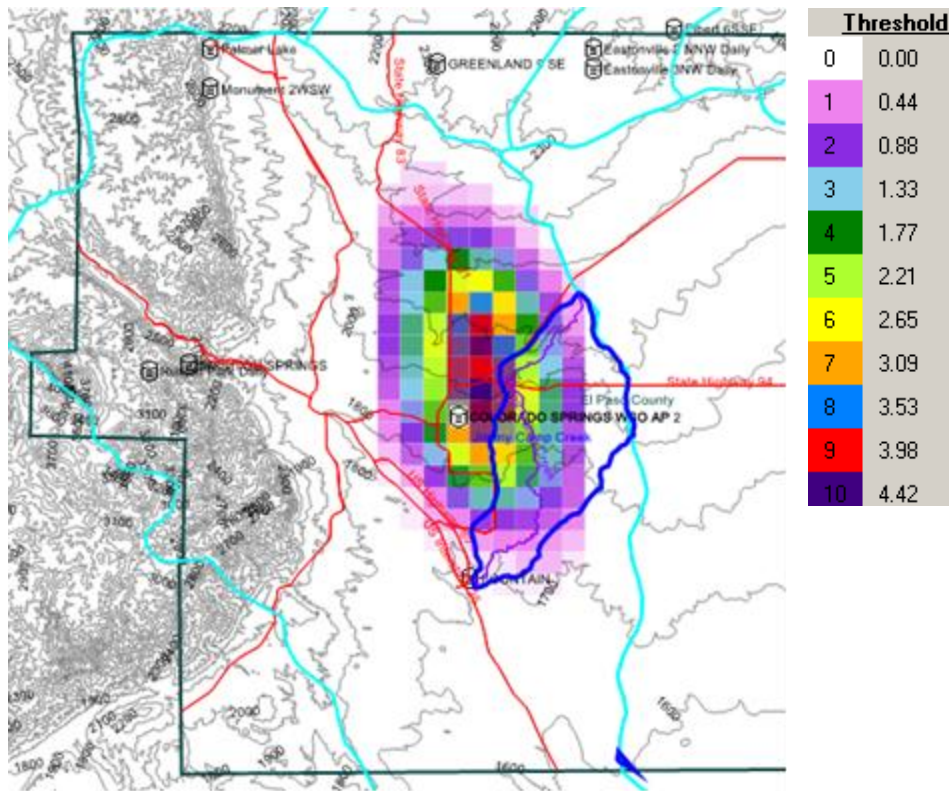


Figure 8-5: June 27, 2004 Cloudburst (Rainfall, inches)

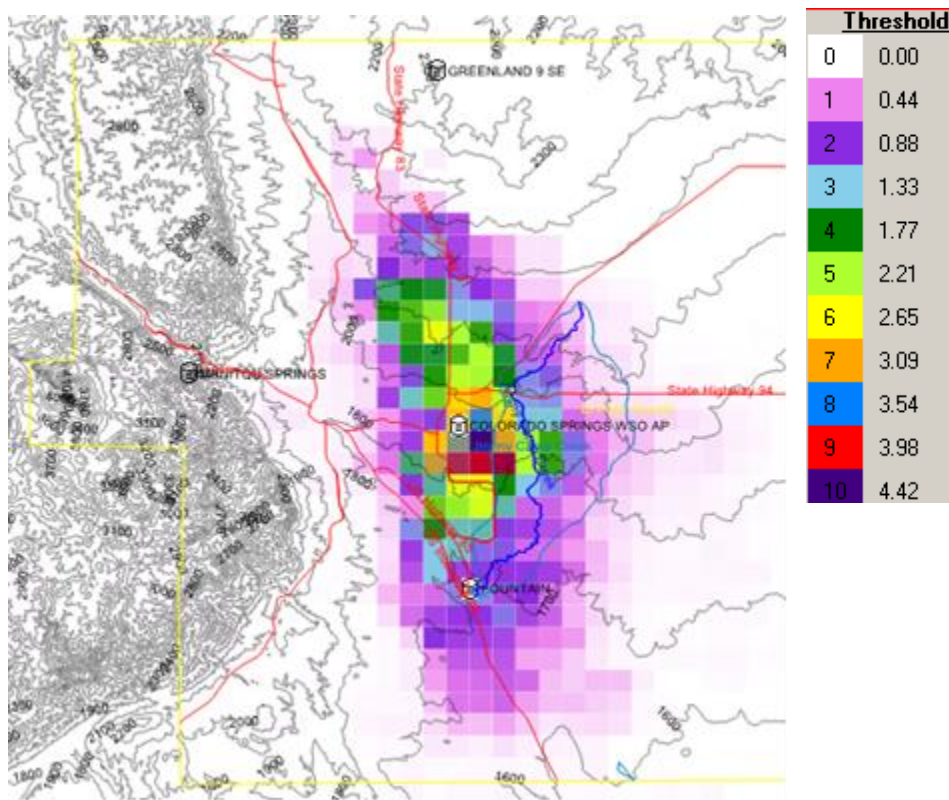


Figure 8-6: Dynamic Processor Fit for June 27, 2004 Event (Rainfall, inches)

Jimmy Camp Creek Cloudburst June 27, 2004

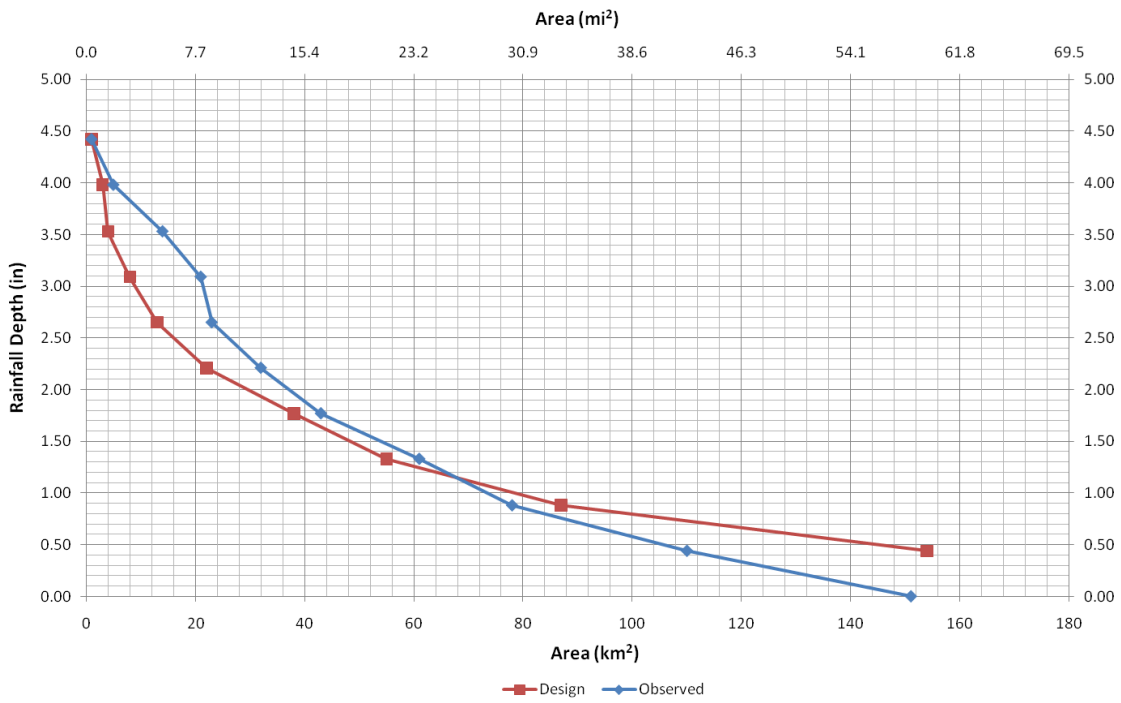


Figure 8-7: Jimmy Camp Creek, June 27, 2004, Depth Area Comparison

9.0 Recommendations for Future Research

Since large scale gage-adjusted radar rainfall data records are only available for about 15 years or so, very few studies of the type conducted herein have been attempted to date. However, the results reported in this report are intriguing and suggest major implications for hydrologic design standards. Based on these results, the following issues should receive consideration for future research.

1. Budget constraints limited the study to 24 months of data with the Fountain Creek watershed as the primary area of interest. These 24 months limited the number of viable storms for analysis which resulted in a very small number of events greater than the 25 year event. Two recommendations are suggested to reduce study uncertainties:
 - a. Use the existing gage-adjusted radar rainfall data set to a more in-depth investigation of storm cell properties throughout eastern Colorado,
 - b. Expand the data set to include a broader selection of data months not limited to storms producing runoff events within the Fountain Creek Watershed.
2. A fertile area of new research requires a new type of statistical analysis that merges information from short term highly resolved spatial data sets with longer term point data sets for frequency analyses. In this study, the data sets are too small for incorporating GARR into traditional frequency analysis. (i.e. analysis of annual maxima to determine frequency.) However, there may be information in the spatial data set that can extend the effective length of the relatively short radar rainfall datasets.
3. Storm cell identification within TITAN depends on the definition of the threshold dBz value delimiting the outer edges of cells. Further investigation should be conducted to better understand the sensitivity of the results to threshold detection values.
4. The TITAN process fits an ellipse to areas of contiguous rainfall above a user defined threshold. Further research is needed to assess how well the area contained within the ellipse (i.e. the assumed cell area) represents the true cell area.
5. A Design Storm Processor was introduced that shows promise as a tool to produce spatially and temporally variable design storms that produce the desired statistics at a point. While temporally and spatially variable design storms may be more accurate representations of natural processes, additional research should be conducted to investigate their impact on design standards. Assessing watershed response to Design Storm Processor output using detailed hydrologic models may be a fertile avenue of research.

10.0 Bibliography

1. Allen, Robert J., and Arthur T. DeGaetano. "Areal Reduction Factors for Two Eastern United States Regions with High Rain-Gauge Density." *Journal of Hydrologic Engineering*. July/August, 2005, 327-335.
2. Allen, Robert J., and Arthur T. DeGaetano. "Re-Evaluation of Extreme Rainfall Areal Reduction Factors." Northeast Regional Climate Center, Cornell University, Ithaca, NY. 2004
3. Arkell, Richard E., and Frank Richards. "Short Duration Rainfall Relations for the Western United States." Conference on Climate and Water Management—A Critical Era and Conference on the Human Consequences of the 1985's Climate, Asheville, NC. August, 1986.
4. Arsenault, P. and Humphrey, J., St. Louis Dynamic Design Storm Technical Report. Metropolitan St. Louis Sewer District. June 2006
5. Asquith, William H. "Areal-Reduction Factors for the Precipitation of the 1-Day Design Storm in Texas." U.S. Geological Survey: Water-Resources Investigations Report 99-4267. Austin, Texas. 1999.
6. Bacchi, Baldassare, and Roberto Ranzi. "On the Derivation of the Areal Reduction Factor of Storms." *Atmospheric Research* 42 (1996): 123-135.
7. Baigorria, G.A., J.W. Jones, and J.J. O'Brien. "Understanding Rainfall Spatial Variability in Southeast USA at Different Timescales." *International Journal of Climatology* 27: 749-760 (2007).
8. Basista, J, Esan, M. and Humphrey, J. Proceedings of the WEFTEC'08 Conference, San Diego, CA. "Risk Analysis for SSO Projects," Water Environment Federation, 2008.
9. Berne, A., G. Delrieu, and B. Boudevillain. "Variability of the Spatial Structure of Intense Mediterranean Precipitation." *Advances in Water Resources* 32 (2009) 1031-1042.
10. Berne, Alexis, Guy Delrieu, Jean-Dominique Creutin, and Charles Obled. "Temporal and Spatial Resolution of Rainfall Measurements Required for Urban Hydrology." *Journal of Hydrology* 299 (2004): 166-179.
11. Bonnin, Geoffry M., Bingzhang Lin, and Tye Parzybok. "Updating NOAA/NWS Rainfall Frequency Atlases." Office of Hydrologic Development, National Weather Service, NOAA. Silver Spring, MD.
12. Bonnin, Geoffry M. "Updating NOAA Rainfall Frequency Atlases." 2002 Conference on Water Resources Planning and Management, May 19-22, 2002, Roanoke, VA.
13. Choi, Janghwoan, Francisco Olivera, and Scott A. Socolofsky. "Storm Identification and Tracking Algorithm for Modeling of Rainfall Fields Using 1-h NEXRAD Rainfall Data in Texas." *Journal of Hydrologic Engineering*. July 2009: 721-730.
14. City of Colorado Springs, "City of Colorado Springs/El Paso County Drainage Criteria Manual", 1994

15. Clark County Regional Flood Control District, Hydrological Criteria and Drainage Manual Volume 2: Hydrology Standards, Sacramento, CA, 2002.
16. Curtis, David C.; "Evaluation of the Spatial Structure of Storms and the Development of Design Storms", Proceedings of the ASCE/EWRI World Environmental and Water Resources Congress 2007: Restoring Our Natural Habitat, May 15, 2007.
17. DeLannoy, Gabrielle J.M., Niko E.C. Verhoest, and Francois P. DeTroch. "Characteristics of Rainstorms over a Temperate Region Derived from Multiple Time Series of Weather Radar Images." *Journal of Hydrology* 307 (2005): 126-144.
18. Dixon, Michael and Gerry Wiener. "TITAN: Thunderstorm Identification, Tracking, Analysis, and Nowcasting—A Radar-based Methodology." *Journal of Atmospheric and Oceanic Technology*. Vol. 10, No. 6. December, 1993.
19. Dixon, Mike. "MDV Format: Interface Control Document (ICD)." Research Applications Laboratory, National Center for Atmospheric Research, Boulder, CO, November 2006.
20. Dixon, Mike. "TITAN Users Guide: Catalog of TITAN Applications." Research Applications Laboratory, National Center for Atmospheric Research, Boulder, CO, October 2005.
21. Dixon, Mike. "TITAN Users Guide: Data Flow Diagrams." Research Applications Laboratory, National Center for Atmospheric Research, Boulder, CO, October 2005.
22. Dixon, Mike. "TITAN Users Guide: Installing TITAN." Research Applications Laboratory, National Center for Atmospheric Research, Boulder, CO, October 2005.
23. Dixon, Mike. "TITAN Users Guide: Overview." Research Applications Laboratory, National Center for Atmospheric Research, Boulder, CO, October 2005.
24. Dixon, Mike. "TITAN Users Guide: Running TITAN." Research Applications Laboratory, National Center for Atmospheric Research, Boulder, CO, October 2005.
25. Dixon, Mike. "TITAN Users Guide: TITAN Data Systems." Research Applications Laboratory, National Center for Atmospheric Research, Boulder, CO, October 2005.
26. Dixon, Mike. "TITAN Users Guide: UNIX Basics." Research Applications Laboratory, National Center for Atmospheric Research, Boulder, CO, October 2005.
27. Durrans, S. Rocky, Lesley T. Julian, and Michael Yekta, "Estimation of Depth-Area Relationships Using Radar-Rainfall Data, *Journal of Hydrologic Engineering*, Vol. 7, No. 5, September 1, 2002
28. Eagleson, Peter S., "Dynamic Hydrology," McGraw-Hill Book Company, 1970
29. Farmer, Eugene E. and Joel E. Fletcher, "Some Intra-storm Characteristics of High-Intensity Rainfall Bursts", *Distribution of Precipitation in Mountainous Areas*, WMO/OMM NO. 326, Volume II, Unipub, New York, 1972.
30. Feral, L., F. Mesnard, H. Sauvageot, L. Castanet, and J. Lemorton. "Rain Cells Shape and Orientation Distribution in South-West of France." *Phys. Chem. Earth (B)*, Vol. 25, No. 10-12, pp. 1073-1078. 2000.

31. Flood Control District of Maricopa County. Drainage Design Manual Hydrology 2009, Phoenix, Arizona.
32. Frederick, R.H., V.A. Myers, and E.P. Auciello, "Storm Depth Area Relations from Digitized Radar Returns", *Water Resources Research* 13(3): 675-679, 1977.
33. Geronimo, Vincent, "Regional Approach to Estimate Depth-Area Reduction Curves Using Radar-Derived Rainfall Data For Front Range", Colorado, CE-5960-900 Master's Report, University of Colorado at Denver, April 2004
34. Gill, Tarun Deep. "Transformation of Point Rainfall to Areal Rainfall by Estimating Areal Reduction Factors, Using Radar Data, for Texas." Submitted to Texas A & M University. May, 2005.
35. Guevara, Edilberto. "Engineering Design Parameters of Storms In Venezuela." *Hydrology Days*. 2003, 80-91.
36. Guo, James C. Y., Kelly Hargadin, "Conservative Design Rainfall Distribution," *Journal of Hydrologic Engineering*, Vol. 14, No. 5, May 1, 2009.
37. Hershfield, David M. "Technical Paper No. 40: Rainfall Frequency Atlas of the United States for Durations from 30 Minutes to 24 Hours and Return Periods from 1 to 100 Years." Department of Commerce, Weather Bureau, Washington D.C. May, 1961.
38. Hoblit, Brian, Steve Zelinka, Cris Castello, and David Curtis. "Spatial Analysis of Storms Using GIS." Proceedings of the Twenty-Fourth Annual ESRI International User Conference, San Diego, California, 2004
39. Huff, F.A. Time Distributions of Heavy Rainstorms in Illinois. Illinois State Water Survey, Champaign, Illinois, 17 pp, 1990.
40. "Interface Control Document for Meterological Data Volume (MDV) XML Format." Research Applications Laboratory, National Center for Atmospheric Research, Boulder, CO, January 2008.
41. "Interface Control Document for TITAN Storms (TSTORMS) XML Format." Research Applications Laboratory, National Center for Atmospheric Research, Boulder, CO, October 2005.
42. Johnson, J.T., Chip Barrer, Michael Eilts, Nathan Kuhnert, Michael Mathis, and Duncan Axisa. "Weather Modification Operations with NEXRAD Level-II Data and Products." The 85th AMS Annual Meeting, 16th Conference on Planned and Inadvertent Weather Modification, San Diego, CA. January 12, 2005.
43. Leclerc, G., and J.C. Shaake, "Derivation of Hydrologic Frequency Curves," MIT Report 142, Cambridge, MA, 1972
44. Mandapaka, Pradeep V., Witold F. Karjewski, Grzegorz J, Ciach, Gabriele Villarini, and James A. Smith. "Estimation of Radar-Rainfall Error Spatial Correlation." *Advances in Water Resources* 32 (2009): 1020-1030.

45. Markus, Momcilo, James R. Angel, Lin Yang, and Mohamad I. Hejazi. "Changing Estimates of Design Precipitation in Northeastern Illinois: Comparison Between Different Sources and Sensitivity Analysis." *Journal of Hydrology*. (2007) 347, 211-222.
46. Marzen, Joseph and Henry E. Fuelberg. "Developing a High Resolution Precipitation Dataset for Florida Hydrologic Studies." Joint Session 9, GIS Applications Part III (Joint Session with Hydrology and active Information Processing Systems for Meteorology, Oceanography, and Hydrology), January 12, 2005.
47. Metropolitan Sewer District of St. Louis (MSD), "Determination of Moving Cloudburst Storm Parameters Using NEXRAD Radar," MSD, St. Louis, Missouri. 2009
48. Miller, J.F., R.H. Frederick, and R.J. Tracey. "Precipitation-Frequency Atlas of the Western United States." Volume III-Colorado. U.S. Department of Commerce National Oceanic and Atmospheric Administration. 1974.
49. Miller, John F. "Technical Paper No. 49: Two- to Ten-Day Precipitation for Return Periods of 2 to 100 Years in the Contiguous United States." Department of Commerce, Weather Bureau, Washington D.C. 1964.
50. Morin, Efrat, David C. Goodrich, Robert A. Maddox, Xiaogang Gao, Hoshin V. Gupta, and Soroosh Sorooshian. "Spatial Patterns in Thunderstorm Rainfall Events and their Coupling with Watershed Hydrological Response." *Advances in Water Resources* 29 (2006): 843-860.
51. Myers, V.A. and R.M. Zehr, "A Methodology for Point-to-Area Frequency Ratios." NOAA Tech. Rep. NWS 24, National Weather Service, Silver Spring, MD. February, 1980.
52. O'Brien, Jimmy S., and Bing Zhao. "Real Time Rainfall-Runoff Modeling on Alluvial Fans, Floodplains and Watersheds." pp. 1-9, (doi 10.1061/40737 (2004)17) www.pubs.asce.org/WWWdisplay.cgi?0410318.
53. Olivera, Francisco, and Tarun Gill. "GIS Static Storm Model Development: Literature Review and Progress Report." Texas Transportation Institute, College Station, TX. September 2004.
54. Olivera, Francisco, Dongkyun Kim, Janghwoan Choi, and Ming-Han Li. "Calculation of Areal Reduction Factors Using NEXRAD Precipitation Estimates." Texas Transportation Institute, College Station, TX. October, 2005.
55. Oklahoma Climatological Survey, Average Number of Thunderstorm Days per Year in the United States. 1999.
56. Omolayo, A.S. "On the Transposition of Areal Reduction Factors for Rainfall Frequency Estimation, *Journal of Hydrology* 145: 191-203, 1993.
57. Osborn, H.B. and L.J. Lane. "Depth-Area Relationships for Thunderstorm Rainfall in Southeastern Arizona". *Transactions of the ASAE*, Vol. 15, No. 4, pp. 670-680, 1972.
58. National Oceanic and Atmospheric Administration, National Weather Service (formerly U.S. Weather Bureau), "Rainfall Frequency Atlas of the United States for Durations of 30 Minutes to 24 Hours and Return Periods from 1 to 100 Years," Technical Paper No. 40, U.S. Department of Commerce, Washington, DC, 1961

59. National Oceanic and Atmospheric Administration, National Weather Service, NOAA Atlas-2: Precipitation-Frequency Atlas of the Western United States, Silver Springs, MD, 1973.
60. National Oceanic and Atmospheric Administration, National Weather Service. "Depth-Area Ratios in the Semi-Arid Southwest United States". Hydrometeorological Report HYDRO-40, Washington, D.C. 1984.
61. National Oceanic and Atmospheric Administration, National Weather Service Forecast Office, Pueblo, Colorado. Colorado Lightning Resource Page. 1996-2000 Lightning Flash Density Map for the United States. 2002.
62. National Oceanic and Atmospheric Administration, National Weather Service, Office of Hydrologic Development, Hydrometeorological Design Studies Center Quarterly Progress Report, 1 April 2009 to 30 June 2009 (NOAA Atlas-14), Silver Springs, Maryland, 2009
63. Nguyen, Van-Thanh-Van, Nelly Peyron and Gilles Rivard. "Rainfall Temporal Patterns for Urban Design in Southern Quebec", Urban Drainage 2002: Global Solutions for Urban Drainage, 9th International Conference on Urban Drainage, ASCE, 2002.
64. Reilly, Jill A., and Thomas C. Piechota. "Actual Storm Events Outperform Synthetic Design Storms: A Review of SCS Curve Number Applicability." [ASCE Conference Proceedings 173, 95 (2005)] link.aip.org/link/?ASCECP/173/95/1.
65. Ruiz-Columbir, Arquimedes, Orlando Nunez-Russis, and Dale Lee Bates. "Radar Uncertainties in Cell-based TITAN Analyses." _Sixth International Symposium on Hydrological Applications of Weather Radar. 2-4 February 2004.
66. Sacramento Department of Water Resources. Sacramento City/County Drainage Manual Volume 2: Hydrology Standards, Sacramento, CA, 2002.
67. Srikanthan, R. "A Review of the Methods for Estimating Areal Reduction Factors for Design Rainfalls." Cooperative Research Center for Catchment Hydrology. June, 1995.
68. "State Standard for Hydrologic Modeling Guidelines." Arizona Department of Water Resources Flood Mitigation Section. August, 2007.
69. Salt Lake City Department of Public Works. Salt Lake City Hydrology Manual 1993. Salt Lake City, Utah.
70. Snipes, R.J., "Floods of June 1965, in Arkansas River basin, Colorado, Kansas and New Mexico," U.S. Geological Survey, Water-supply Paper, no. 1850-D, 1974
71. Thompson, David B., Theodore Cleveland, and Xing Fang. "Application of Storm Statistics to TxDOT Construction and Stormwater Management Maintenance." Center for Multidisciplinary Research in Transportation, Texas Tech University, Lubbock, TX. August 2007.
72. Urban Drainage and Flood Control District. Urban Storm Drainage Criteria Manual, Volumes I-II-1999, Denver, Colorado.

73. Veneziano, Daniele and Andreas Langousis, The Rainfall Areal Reduction Factor: A Multifractal Analysis, European Geosciences Union 1st General Assembly, Nice, France, April 2004, Department of Civil and Environmental Engineering, M.I.T., Cambridge, Mass., 2004
74. Veneziano, D., and A. Langousis “The Areal Reduction Factor: A Multifractal Analysis, Water Resources Research (2005), 41, W07008, doi:10.1029/2004 WR003765.
75. Zehr, Raymond M. and Vance A. Myers. “Depth-Area Ratios in the Semi-Arid Southwest United States.” NOAA Technical Memorandum NWS HYDRO 40. NOAA, National Weather Service, Silver Spring, MD. August, 1984.

11.0 Appendix A: Gage-Adjusted Radar Rainfall Analysis

Jimmy Camp Creek, El Paso County, Colorado

Gage-Adjusted Radar Rainfall Analysis

Jimmy Camp Creek, El Paso County, Colorado

Events analyzed:

May 15, 1995
August 8, 1996
July 31, 1999
August 5, 2004
July 15, 2005
August 26, 2006

Prepared for

**City of Colorado Springs
and
Carlton Engineering**

Prepared by
OneRain, Inc.
1531 Skyway Drive
Unit D
Longmont, CO 80504

Tel: 303-774-2033
Fax: 303-774-2037
Email: info@onerain.com
Web: www.onerain.com

June 17, 2009



HEADQUARTERS

1531 Skyway Drive
Unit D
Longmont, CO 80504

800-758-RAIN
303-774-2033
Fax: 303-774-2037

NEW JERSEY

1640 Nixon Drive
Suite 292
Moorestown, NJ 08057

OFFICE: 856.778.8446
MOBILE: 303.709.2025
FAX: 856.234.8744

www.onerain.com
information@onerain.com

Gage-Adjusted Radar Rainfall Analysis

Jimmy Camp Creek, Colorado

Introduction

Accurate estimation of the spatial distribution of rainfall is critical to successfully model hydrologic processes. Rainfall distributions are typically estimated by assuming a spatial geometry tied to one or more rain gage observations at discrete points. These estimations are usually calculated using methods such as Thiessen polygons, inverse distance squared weighting, or statistical Kriging techniques. Unfortunately, the spatial distributions used by these approaches can have erroneous representations as to how the rain actually falls. From a modeling perspective, these techniques too often place the wrong rain at the wrong place at the wrong time.

Decades of research have made radar a viable tool to improve the estimation of rainfall between the gages. Radar provides a high resolution view of rain falling over broad regions. However, radar *by itself* is not an accurate estimator of the actual rainfall amounts.

The strength of a rain gage network is its ability to accurately estimate rain falling on a number of discrete points. Its weakness is the network's inability to observe rain falling between the gages. Conversely, radar's strength is its ability to see rainfall intensity over a broad region; but is less precise and accurate than gages at estimating the rainfall volume that actually reached the ground.

By merging data from a rain gage network and radar rainfall estimates, hydrologists can take advantage of the strengths of each measurement system while minimizing their respective weaknesses. Essentially, a radar image is used as a template for the spatial distribution of rainfall. The radar data are used to assess the rainfall spatial distribution and timing, while the rain gage data are used to assess the rainfall volume. The net result is a gage-adjusted radar rainfall data set that combines the spatial distribution characteristics of the radar image with the volumetric information from the gages.

Six rainfall events were selected by the City of Colorado Springs by surveying stream flow records at the USGS Site 071059500 in the Jimmy Camp Creek basin (67 square miles). The selected events were:

- May 17, 1995
- August 15, 1996
- July 31, 1999
- August 5, 2004
- July 15, 2005
- August 26, 2006

This report summarizes the results for the Gage-Adjusted Radar Rainfall (GARR) analysis done for the Jimmy Camp Creek study area.

Jimmy Camp Creek Study Area

GARR datasets were developed for the six selected rain events occurring between 1995 and 2006. Since the Jimmy Camp Creek basin has so few rain gages within its perimeter, OneRain used a technique where an analysis is done on a larger area that encompasses more rain gages (referred to as a “super-area”). After this analysis was completed, the original Jimmy Camp Creek “sub-area” is extracted from the super-area, and data products are derived from there. Figure 1 shows both the super-area that the GARR datasets were generated for and the Jimmy Camp Creek study area.

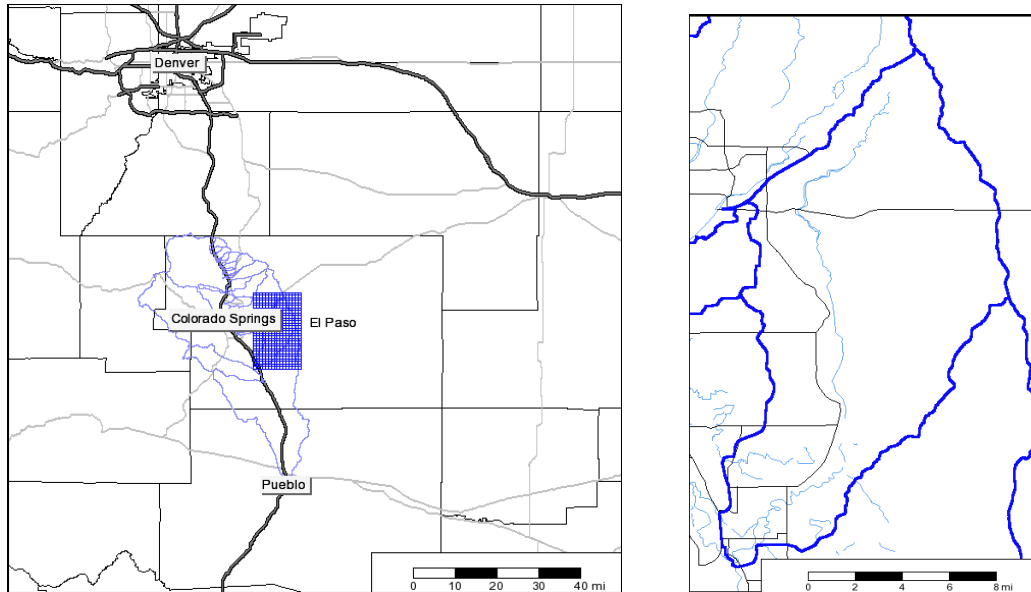


Figure 1 - Jimmy Camp Creek super-area (left) and sub-area (right) – Note, the sub-area is highlighted in the super-area as a blue rectangle near the center.

Table 1 presents the study periods selected for the six rain events of interest. For each event, a time of maximum area stream flows were provided. The rainfall just before and after were then examined. The start times for each study period were selected in order to include any rainfall in the 24-48 hours preceding the specific time of interest. The end times were selected in order to provide at least four hours of no rainfall and no other significant rain events in the subsequent 12 hours.

Event	Year	Start	End	Duration (hrs)
1	1995	05/16 00:00	05/19 06:00	78
2	1996	08/13 03:00	08/17 00:00	93
3	1999	07/30 03:00	08/06 06:00	171
4	2004	08/04 09:00	08/07 19:00	82
5	2005	07/14 12:00	07/16 06:00	42
6	2006	08/24 07:00	08/27 04:00	69

Table 1: Rain events covered in GARR analysis. All hours are listed in Standard Mountain Time Zone (UTC -7).

Rain Gage Data

Rain gage data for this GARR analysis was attained from three sources: airport rain gages (METAR), the National Climatic Data Center (NCDC), and the ALERT rain gage networks in the Colorado Springs and Denver areas.

The number of rain gages available for the radar adjustments increased significantly over the period between 1995 and 2006. The study area selection was based on the availability of gages in 1995 when much fewer gages were available. Figure 2 presents all the gages that were available at some point in the study in and around El Paso County. Table 2 lists the number of gages used for each year of the study. Figures 3-9 display the gages that were available for each event. Note that during the July 12, 2005 event a significant portion of the Denver-area gages were not available. Please consult Appendix A for a table that lists specific gages that were used for each study period.

Year	# of Gages
1995	20
1996	23
1999	97
2004	141
2005	97
2006	167

Table 2 - Listing of gages used for GARR adjustments.

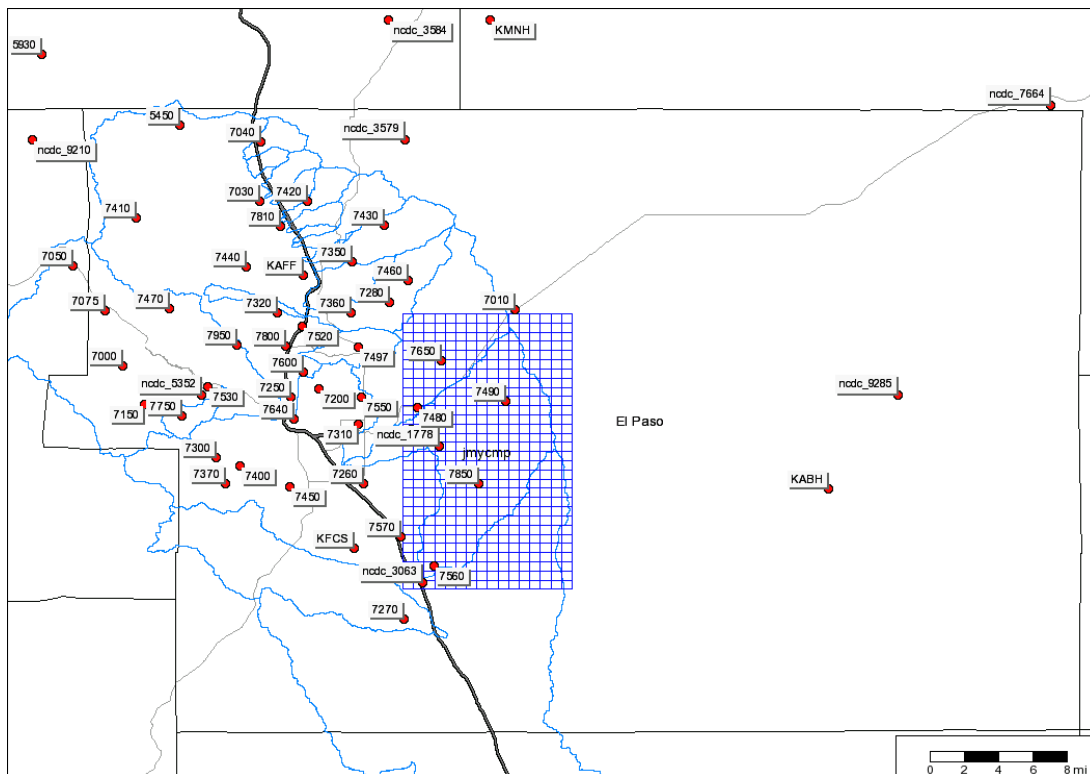


Figure 3 – Gages in and near El Paso County that were collected for use in the Jimmy Camp Creek analyses.

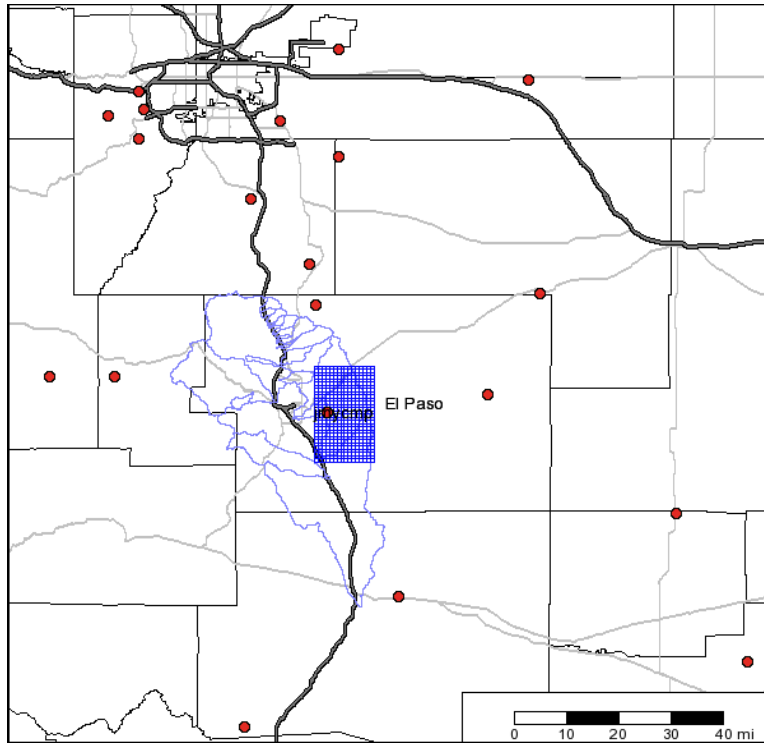


Figure 4 - Gages used for May 17, 1995 Jimmy Camp Creek adjustments.

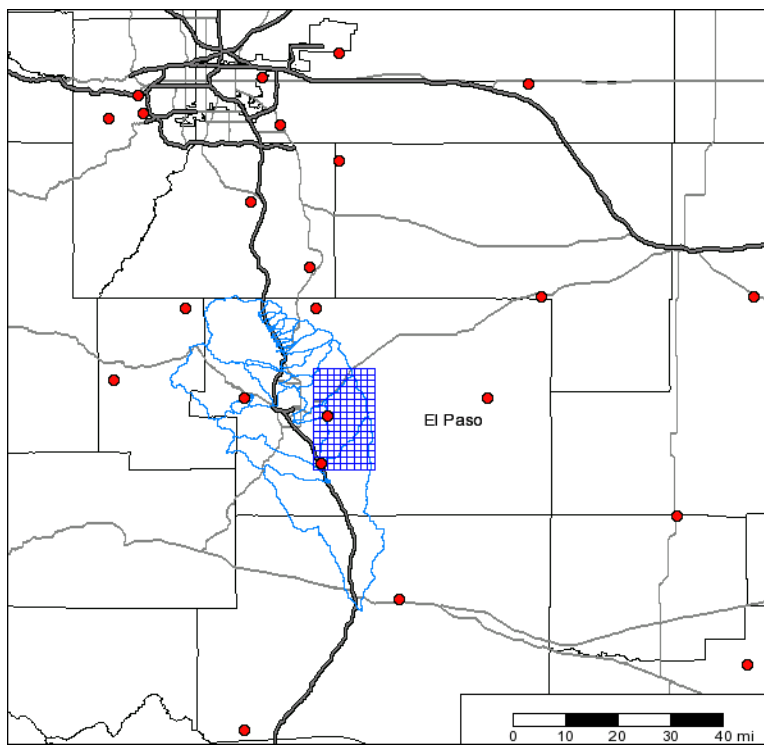


Figure 5 - Gages used for August 15, 1996 Jimmy Camp Creek adjustments.

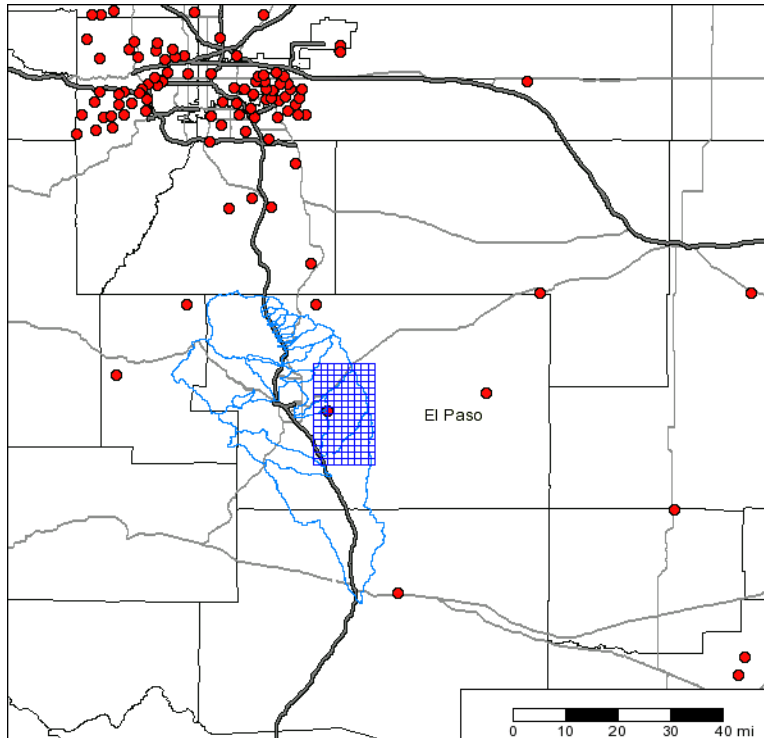


Figure 6 - Gages used for July 31, 1999 Jimmy Camp Creek adjustments.

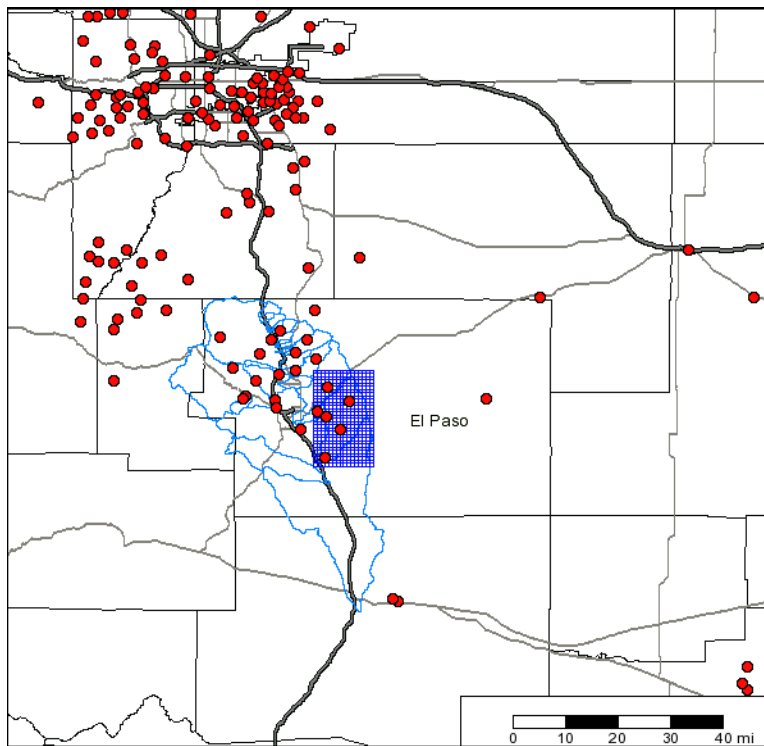


Figure 7 - Gages used for August 5, 2004 Jimmy Camp Creek adjustments.

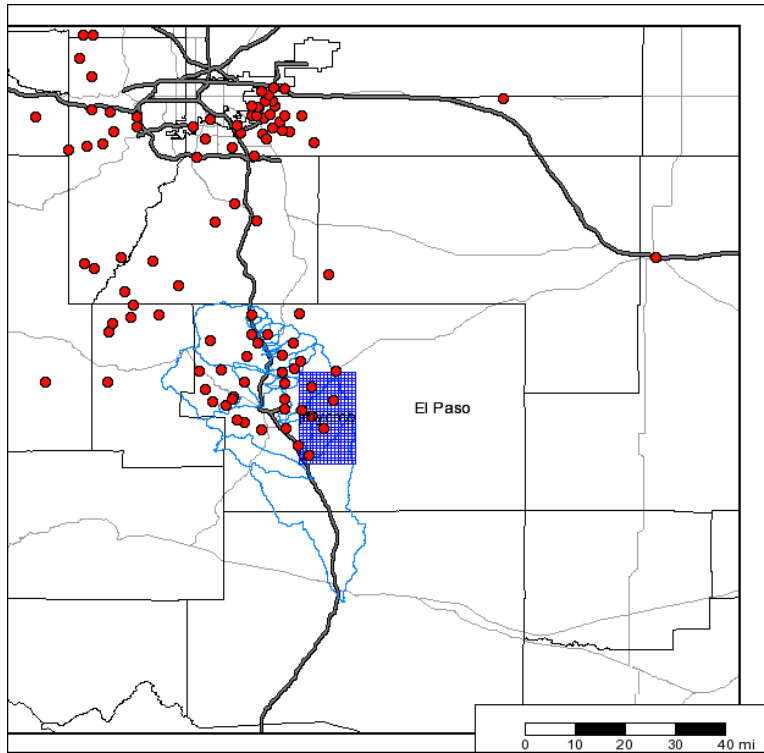


Figure 8 - Gages used for July 15, 2005 Jimmy Camp Creek adjustments.

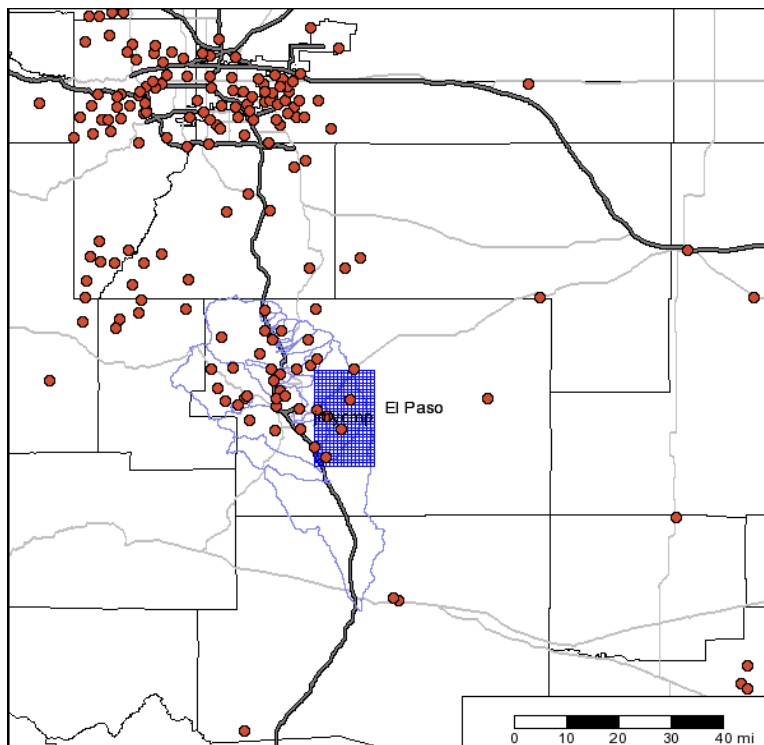


Figure 9 - Gages used for August 26, 2006 Jimmy Camp Creek adjustments.

Radar Data

Events prior to the year 2000 were analyzed using 15-minute radar data with a 2x2 km pixel resolution. For events occurring after 2000, 5-minute radar data with a 1x1 km pixel resolution was used. These radar details are summarized in Table 3.

Event	Year	Start	End	Time step (min)	Resolution (km)
1	1995	05/16 00:00	05/19 06:00	15	2x2
2	1996	08/13 03:00	08/17 00:00	15	2x2
3	1999	07/30 03:00	08/06 06:00	15	2x2
4	2004	08/04 09:00	08/07 19:00	5	1x1
5	2005	07/14 12:00	07/16 06:00	5	1x1
6	2006	08/24 07:00	08/27 04:00	5	1x1

Table 3 - Storm events covered in GARR analysis. All hours are listed in MTN time zone (UTC -7).

	1x1 Pixel Grid	2x2 Pixel Grid
Pixels in area	480	144
Rows	30	16
Columns	16	9
Min Latitude	38.659	38.646
Max Latitude	38.929	38.934
Min Longitude	-104.718	-104.722
Max Longitude	-104.553	-104.550

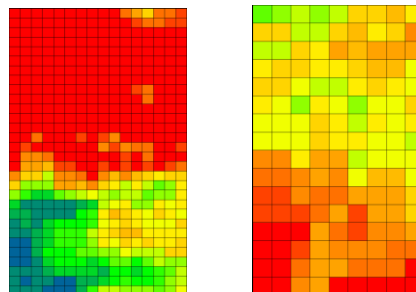


Figure 10 – Radar grid summaries.

The 2x2 km radar data were provided by WSI, Inc., and the 1x1 km radar data were provided by Barons Services, Inc. The two radar grids are described in Figure 10.

The following radars are all within range of the study area used: Pueblo - KPUX, Denver – KFTG, Cheyenne – KCYS, and Goodland - KGLD. Figure 11 shows the coverage of these radar for the Jimmy Camp Creek study area. The redlines represent the 230 KM radius from distance radars, which is considered the operational limit for the radars. The Denver and Pueblo radar are located in the study area. The horizontal red arc across the center of the study area is the Cheyene radar. The more vertical arc is the Goodland radar extent.

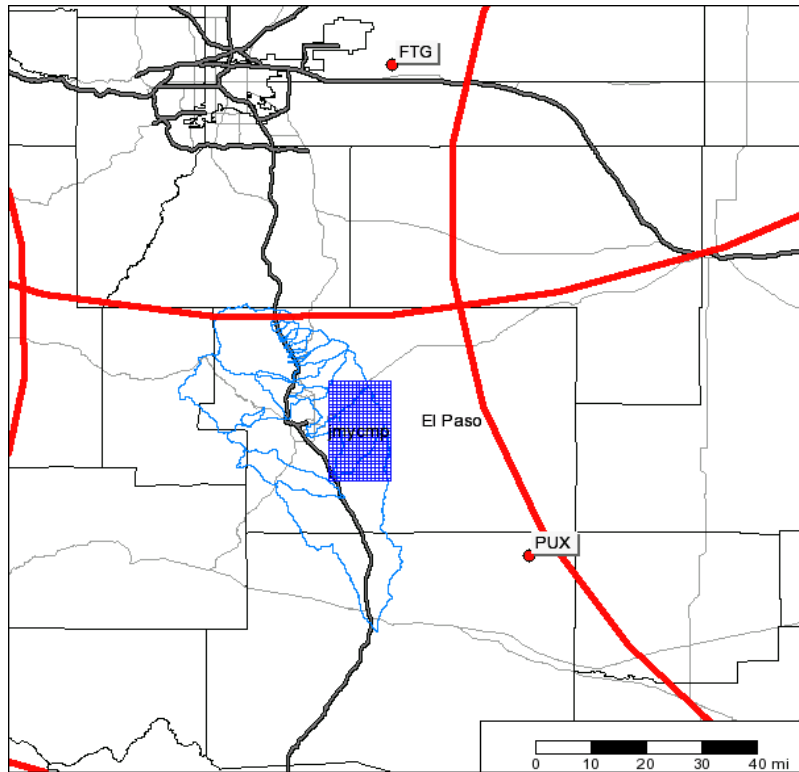


Figure 11 – Radar coverage for the Jimmy Camp Creek study area.

Radar Filtering

GARR analysis for the Jimmy Camp Creek analysis was based on ‘raw’ radar data obtained from the WSI, Inc and Barons Services, Inc. These radar vendors perform a level of data transformation and clean-up before delivering the data to OneRain. They assemble the gridded mosaic from the native polar data of the individual radar installations. During this process some radar artifacts such as ground-clutter are removed.

OneRain then applied a second round of clean-up including further removal of bad radar pixels due to noise, ground clutter, and other reasons. These types of artifacts, and those due to the assembly of the gridded radar mosaic, tend to stand out more with larger study areas and longer study periods (This was another reason to start with a larger study area.) Therefore, month-long radar datasets of the Jimmy Camp Creek super-area were extracted.

The monthly radar accumulations were used to identify pixels affected by ground cluster and to assess any mosaic artifacts. The radar data for the Jimmy Camp Creek study area did not show mosaic artifacts commonly seen in larger study areas and other areas of the county. This study area is equally covered and dominated by both the Denver and Pueblo radars, which 230 KM extents are well outside the study area.

Figure 12 shows the radar summation for July 1999 and highlights areas of suspected bad pixels. These artifacts are typically seen as stationary pixels that report reflectivity

data, but do not move as a storm cell would. They cause isolated anomalies at specific pixels resulting in high outlier values. These pixels are removed and replaced

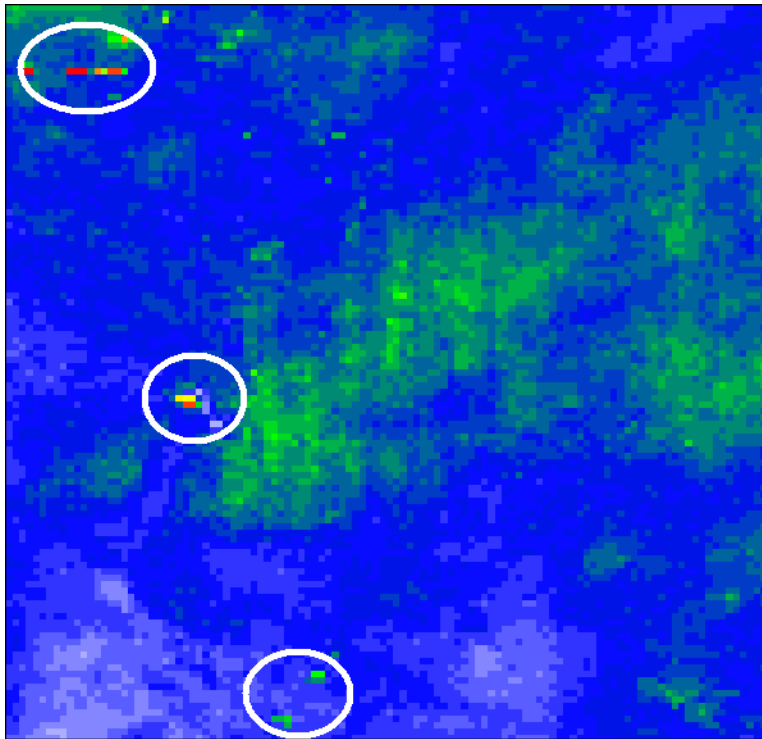


Figure 12 – Radar accumulations for July 1999. Areas with bad pixels are highlighted.

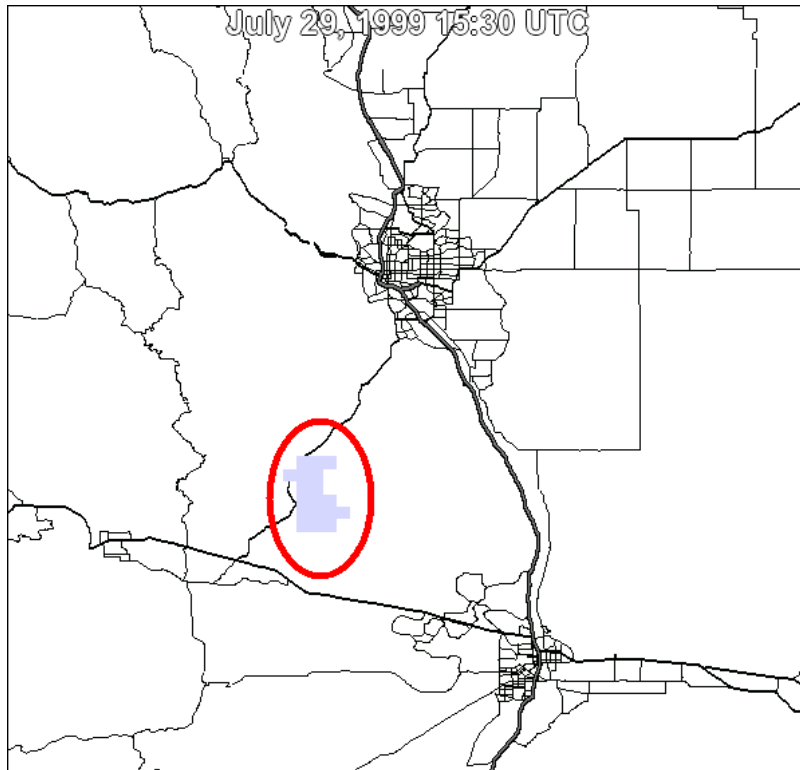


Figure 13 – Example of radar noise.

by linearly interpolating the surrounding pixel values at each time step. The Jimmy Camp Creek study area consisted of 12,995 pixels. For the six study periods, an average of less than 2% of these pixels were identified as bad pixels.

Radar noise was found in typical quantities for each of the six study periods. Figure 13 provides an example of a single radar frame with noise. This isolated cluster of pixels remained stationary for four frames, and occurred when no gages recorded rain. This noise is detected by both animating the radar data and with automated tools. The automated tools add up the radar rainfall for each frame and nominate frames that contain radar noise. The radar analyst then animates the radar and determines which frames contain rainfall and which contain noise. Noise in the raw radar appears as isolated and abrupt patterns that typically occur during times of no rainfall. The noise is eliminated by setting the single radar frame's pixel values to zero for either the entire study area or within specified pixel areas. On average, less than 7% of the raw radar time-steps showed signs of non-rainfall noise that was removed.

Rain Gage Data QA/QC Procedures

After the raw radar data has been filtered, comparisons and integration with the collected gage data begins. During this step, the radar data is used to help assess the quality of the gage data. When comparing event accumulations from a large number of gages with radar data, we expect to see that the gage/radar correlations approximate a linear relationship. Typically when the gage and radar accumulations from any given

rainfall event are graphed, there is a cluster of gage/radar pixel pairs, along with outliers due to gages with poor performance.

Rain gages require periodic calibration and site maintenance to perform at their best. Gages should be calibrated at least once a year. Ideally, the gage data should be reviewed on a continuous basis and suspect gages should be visited more frequently. Common rain gage problems include poor site selection due to vegetation or structures compromising the gages' 'catch', debris clogging the rain gage bucket, unlevel tipping buckets, and out of calibration gages. There are also significant timing differences between the radar and gage rainfall measurement systems. Rain gages typically have a 'bucket' size of 0.04 inches, although newer gages commonly have a size of 0.1 inches. Therefore the time between tips is the amount of time it took to collect this amount of rain. As the rainfall rate decreases, the time between tips increases. Furthermore, if the tipping bucket gets only partially filled during the trailing end of an event, that volume may get attributed to the subsequent event unless it completely evaporates between events. On the other hand, the radar data has a smaller resolution, scans the atmosphere on a 5-6 minute interval and thus better captures the rainfall timing.

During the analysis decisions are made about whether to leave a gage in the analysis. This process is referred to as gage 'masking', i.e. when a gage is removed from a period of the analysis it is said to be masked out. Much of this masking process is automated based on consistent rules. For example, if any gage did not record any data for the entire study period, it is completely removed from the analysis. Other gages may perform well during most of the study period, but not be in operation for a single event. Such gages are included during the periods of acceptable performance, but masked out of the analysis when it was not working. [emphasize wanting to avoid the bad effects of isolated bad gages)

After these automated maskings, a radar analyst reviews each rainfall event and determines additional gages that appear as outliers when compared to the rest of the gages.

For the Jimmy Camp Creek analyses, the radar and rain gage data were reviewed and checked for quality using several steps:

- Gages that failed to report rainfall for the entire study period were removed from the analysis.
 - $\sum G = 0$ removed
- The study period was divided into separate rainfall events and scatter-plots were generated to compare the gage volumes with their corresponding unadjusted radar pixel, for each of these rainfall events.
- When reviewing these scatter-plots, under- and over-reporting gages are removed from the group. When comparing unadjusted radar with gages, any radar pixel-gage pair with a multiplier of 30 or higher automatically has that gage removed from the analysis.
 - $G/R > 30$

- For individual events, gages are removed that report no data while their co-located radar pixel reports more than 0.1 inches of rainfall.
 - $G = 0, R > 0.1$ removed
- For individual events, gages are removed that report more than 0.1 inches while their co-located radar pixel reports no rainfall.
 - $R = 0, G > 0.1$ removed
- After these gage masking, initial gage-adjusted radar rainfall estimates are generated using a spatial adjustment.
- When comparing gages with adjusted radar, the removal criteria is set to a multiplier of 4.
 - $G/R_{adj} > 4$
- After these gage masking, the gage-adjusted radar rainfall estimates are generated again.
- The gage maskings are finalized by the analyst by reviewing the radar/gage correlations for each event. During this last step decisions are made about remaining gage/radar accumulations that appear to be outliers. Time-series plots of suspect gages and their co-located radar pixel are studied to help determine if the gage was performing normally during the rainfall event.

What follows is a graphical discussion of the gage quality assurance steps for the July 31, 1999 event. The steps outlined here were performed uniformly for each of the six Jimmy Camp Creek study periods selected by the City. Appendix C includes a complete record of how gages were masked for each of the six study periods.

Again, the first step is removing gages that reported no data during the entire study period. Figure 14 shows the average rainfall accumulation time-series plot for the 207 gages in the radar study area and their co-located radar pixels. *Note that these accumulation plots are a function of the gage maskings in effect at that time. For example, as non-reporting gages are removed from the analysis the average gage accumulation will increase. And depending on the radar data from the pixels co-located with these removed gages, the average radar accumulation will change too.*

Figure 15 shows the scatter-plot of gage and radar accumulations for the entire July 1999 study period. Non-reporting gages are plotted on the Y-axis. Figures 16 and 17 show the accumulation and scatter plots for the study period after the 110 non-reporting gages are removed from the analysis, leaving 97 gages that reported at least once during the study period.

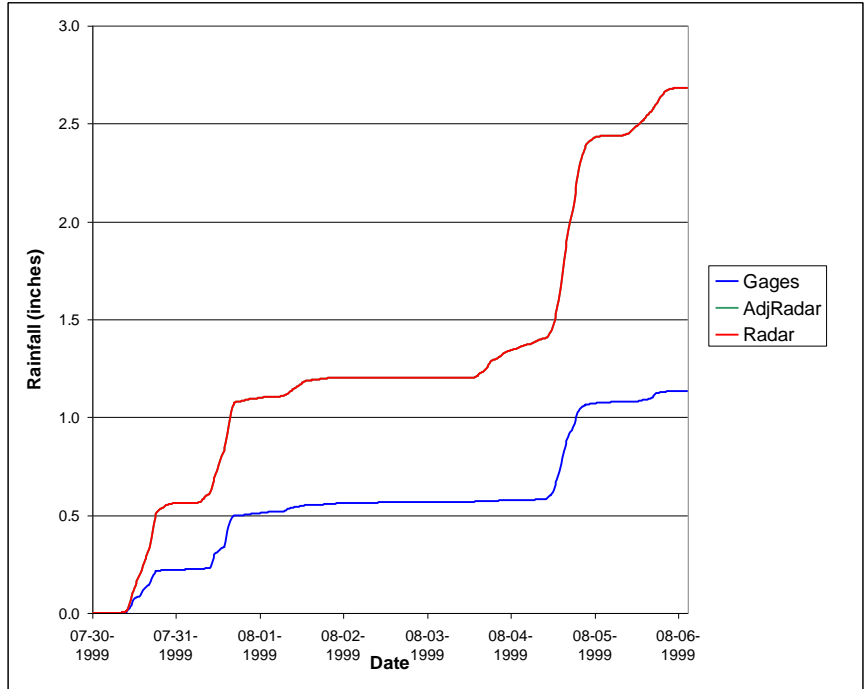


Figure 14 - Average rainfall accumulation time-series plot for the gages in the radar study area and their co-located radar pixels. This plot is based on no gage maskings.

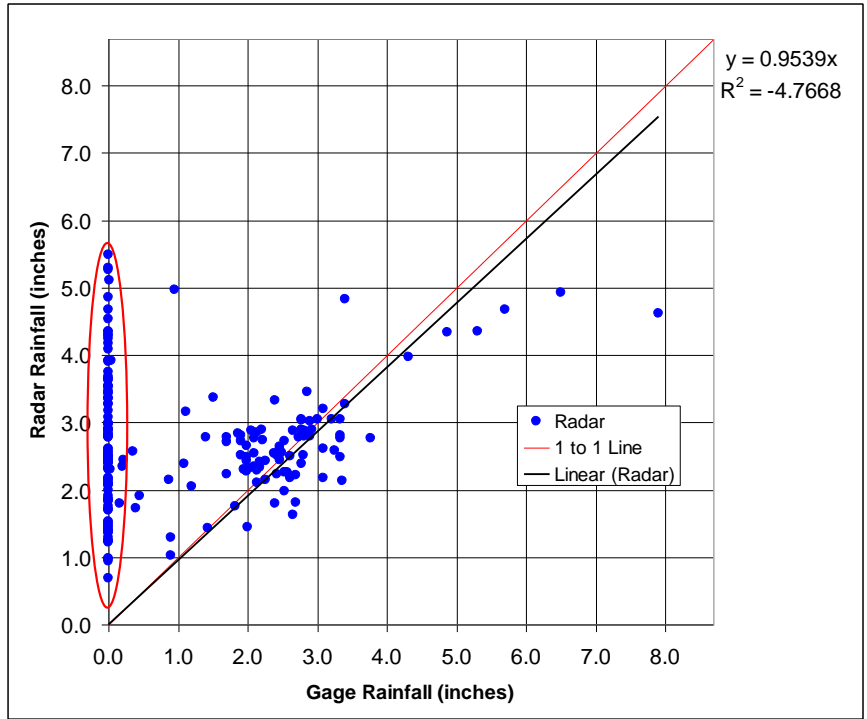


Figure 15 – Scatter-plot of gage and radar accumulation for the study period. Non-reporting gages are on the Y-axis.

The study period was then divided into separate rainfall events. The accumulation plot is used to delineate the events by splitting the study period with ‘breakpoints.’ Figure 18 presents how the July 31, 1999 study period was divided into separate rainfall events.

Breakpoints are also occasionally used to isolate periods when there are radar ‘events’ with no corresponding gage ‘event’ and vice versa. These situations can occur when there are periods when there is radar reflectivity detected when there are no gage data recorded on the ground. The opposite situation can occur when one of more rain gages are generating erroneous tips, including field maintenance calibration tips, during times of no rainfall.

Scatter-plots of individual rainfall events are then generated. These event scatter-plots are used to further assess gage performance during individual rainfall events. Figures 19 and 20 present the scatter-plots of events 2 & 6.

After the individual events have been isolated, the next level of automated gage maskings are applied. Non-reporting gages co-located with radar pixels with more than 0.1 inches of rainfall ($G = 0, R > 0.1$) and gages with more than 0.1 inches co-located with a pixel with no data ($R = 0, G > 0.1$) are removed. Also, any gage/radar pair that has a multiplier greater than 30 is removed. Figure 21 shows the scatter-plot of study period accumulations after these maskings.

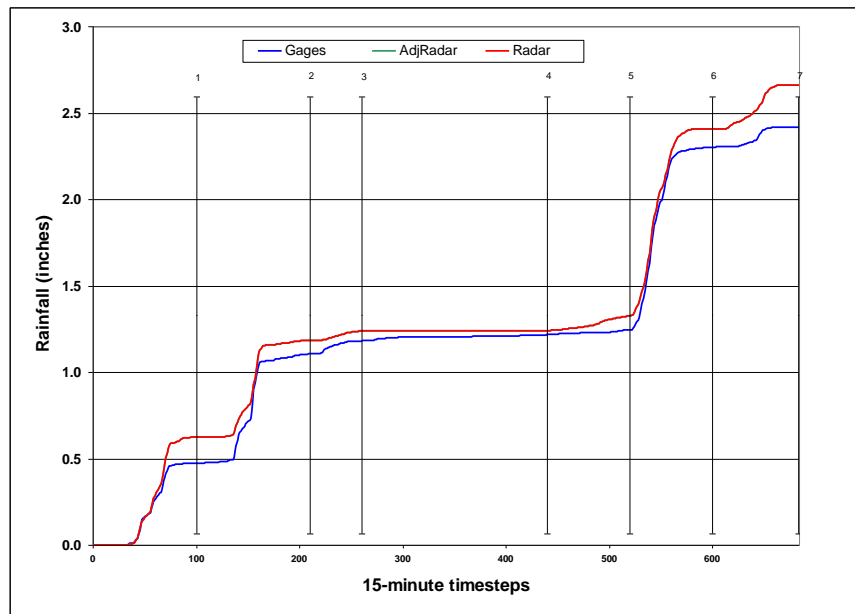


Figure 16 - Average rainfall accumulation time-series plot of gages and radar after removal of non-reporting gages.

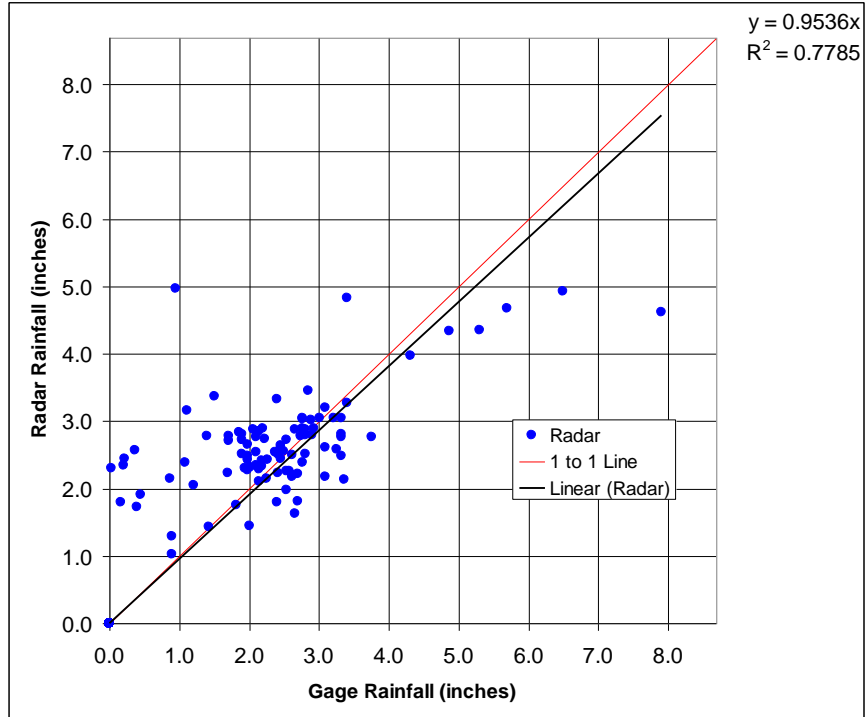


Figure 17 - Scatter-plot of gage and radar accumulations for the study period after removal of non-reporting gages.

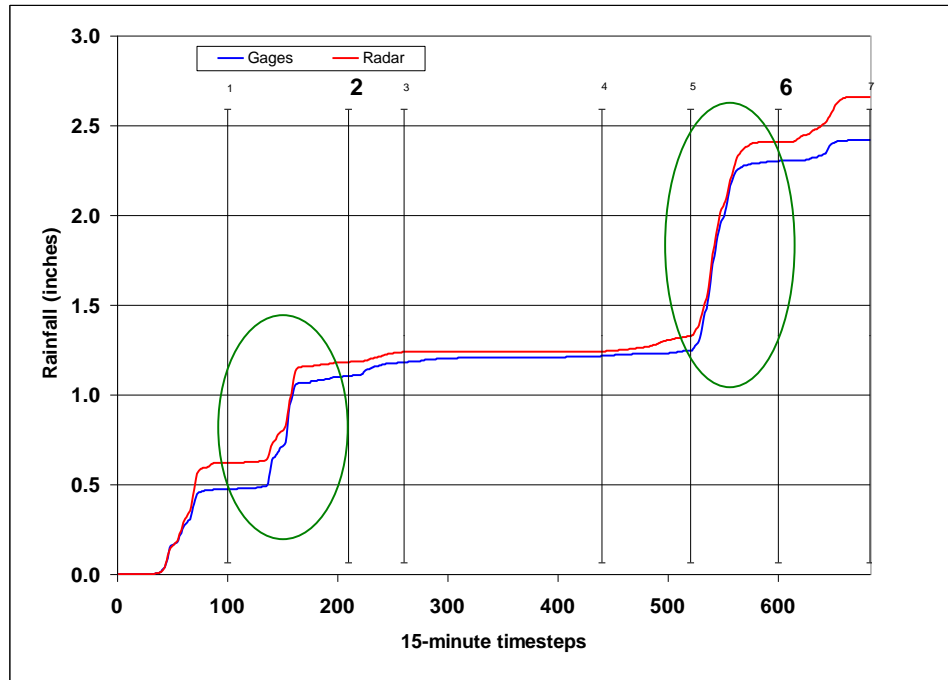


Figure 18 – Study period delineated into separate rainfall events.

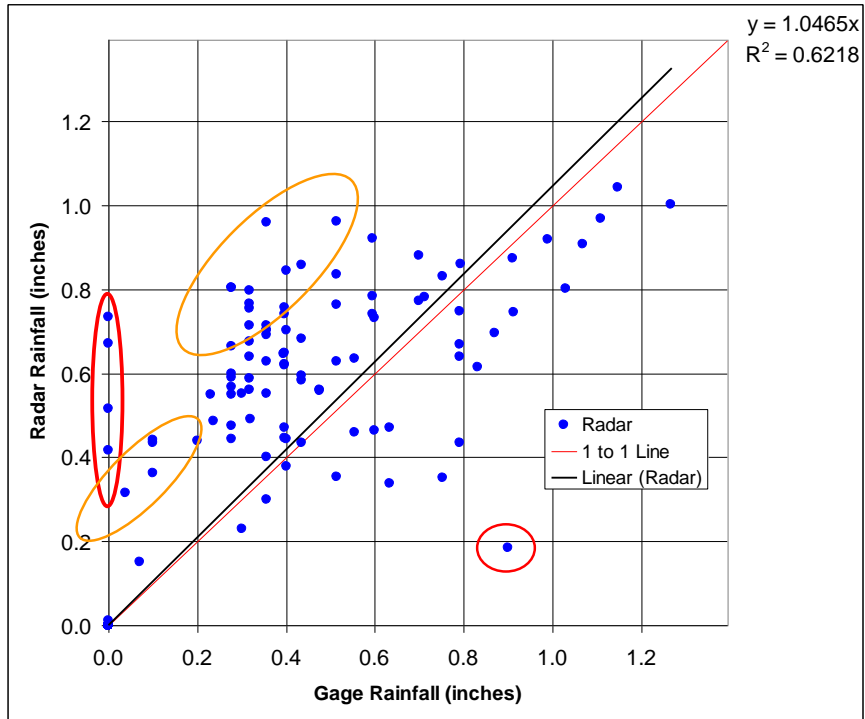


Figure 19 – Scatter-plot for event 2 of the study period. Non-reporting and suspect gages are highlighted in red. More border-line gages are highlighted in orange.

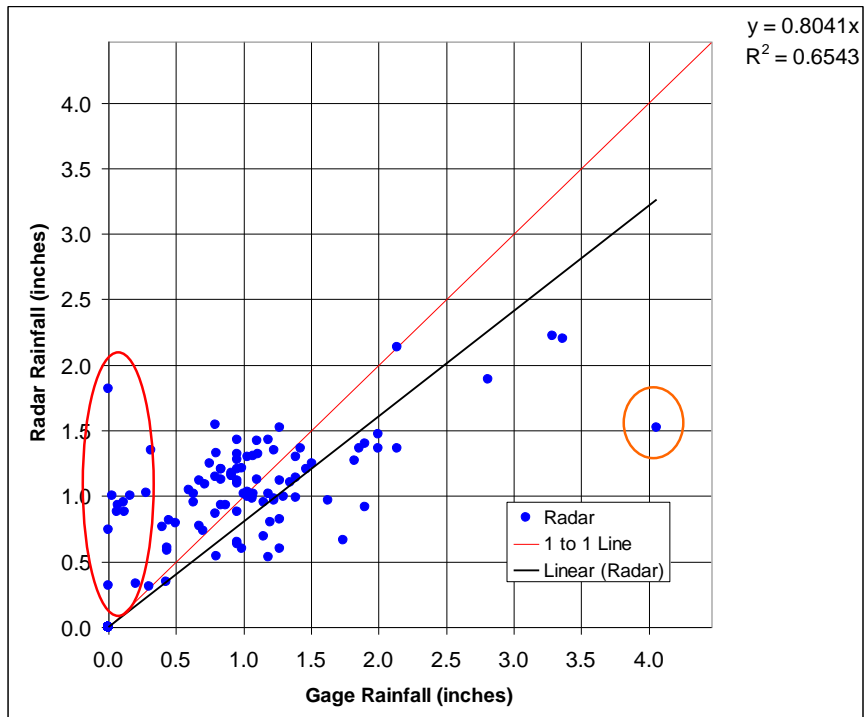


Figure 20 – Scatter-plot for event 6 of the study period. Non-reporting and suspect gages are highlighted in red. A more borderline gage is highlighted in orange.

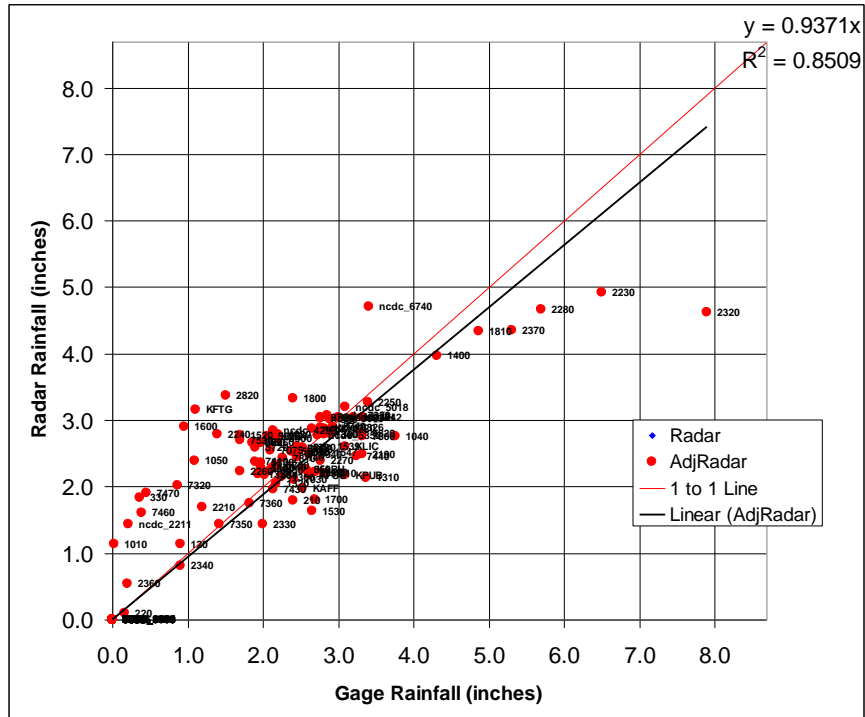


Figure 21- Scatter-plot of study period accumulations after event-based removal of $[G = 0, R > 0.1]$, $[R = 0, G > 0.1]$, and $G/R > 30$ gages.

At this point, initial gage-adjusted radar rainfall estimates were generated. The individual events were reviewed again and gages with a $G/R > 4$ were removed. Figure 22 displays these maskings for event 6.

After these automated gage maskings are applied, the spatial adjustments are generated again. At this point, the individual scatter-plots are reviewed by the radar analyst and additional gages are identified for further investigation and potential removal for the event time period. Figure 23 shows one such gage for event 6. Several steps can be taken to further assess such gages, including the following:

- Examining the time-series accumulation plot of the individual gage with its co-located radar pixel.
- Surveying the performance of the gage during other events.
- Animating the radar data to examine the event ‘topography’ over and around the gage during the period in question.

All of the above steps were taken for this example gage, and the radar animation showed no evidence of intense rainfall over and near the gage during the three hour time period in question.

In summary, 110 of the 207 gages in the Jimmy Camp Creek radar study area were removed because they were not operational during the July 31, 1999 study period. There remained 97 gages that reported at least once, and the study period was divided

into seven 'events.' Therefore, this study period had a potential of 679 gage maskings. The following gage maskings were made for the analysis:

G = 0, R > 0.1: 41 maskings

- R = 0, G > 0.1: 6 maskings
- G/R > 30: 0 maskings
- G/R > 4: 22 maskings
- Non-automated maskings: 25 maskings

13.8% of the potential maskings were made.

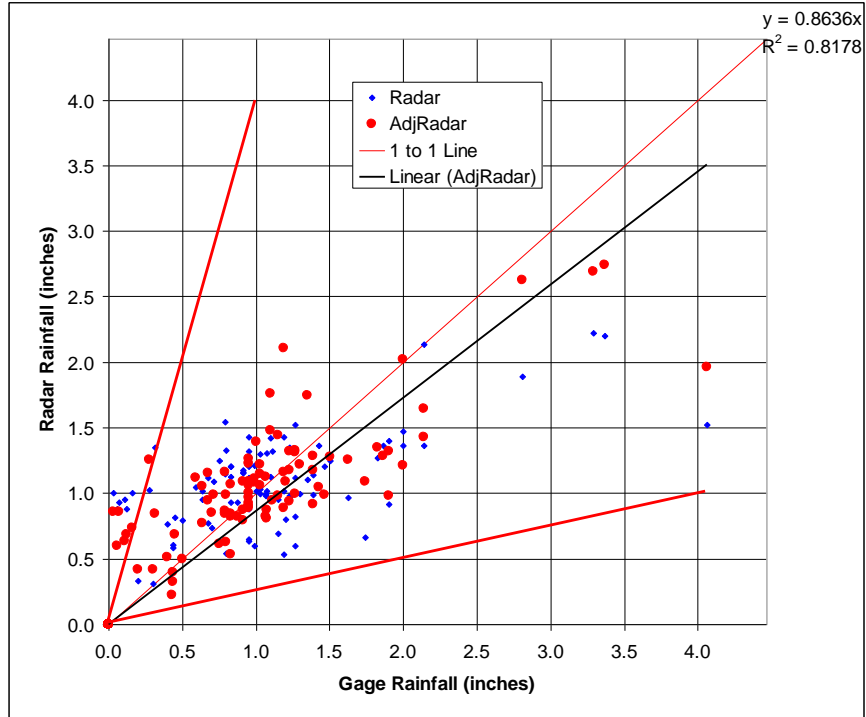


Figure 22 - Event 6 of the study period. Gages with a G/R > 4 are shown outside the red lines.

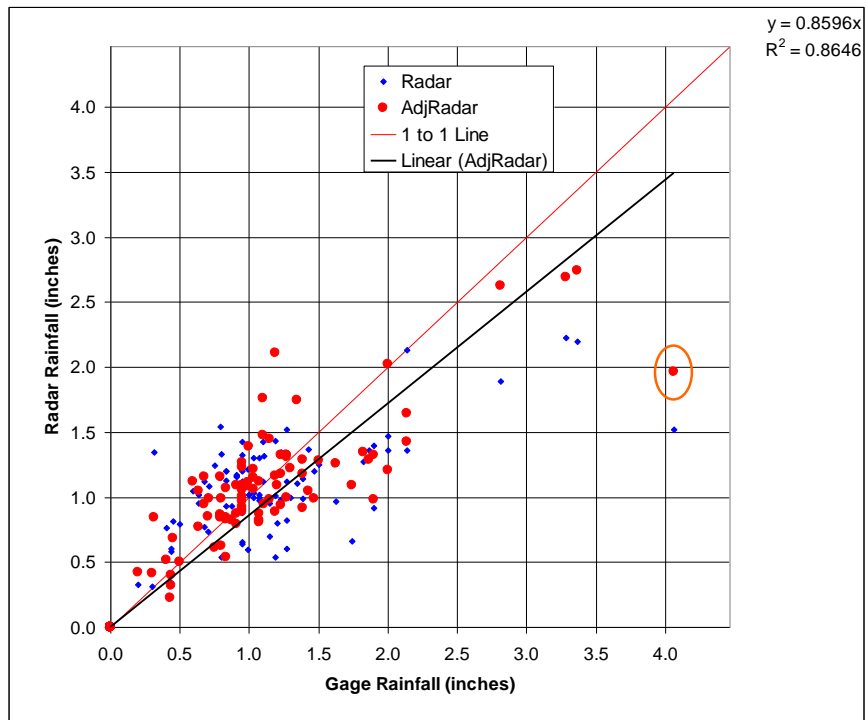


Figure 23 – Scatter-plot for Event 6 after automated gage maskings are applied. One gage is highlighted that is investigated further.

Radar Adjustment Procedure

GARR estimates are generated by multiplying the unadjusted radar values by a gage/radar ratio (G/R). The G/R ratios applied for this study were both temporally and spatially variable. Temporally, the G/R ratios for this study were computed based on event or event segment totals then applied at each time step during the event or event segment. (Note: event segments are often defined when there are rainfall gaps within the overall rain event.) At each pixel containing a gage location, a gage/radar (G/R) ratio was computed by dividing the gage's measurement by the radar's during each time step (time steps are chosen to match individual rainfall sub-events).

This approach of developing event-based G/R ratios has evolved over the past 15 years as a method to accommodate, among other things, the natural differences between when rain gages report rainfall and when radar observes rainfall. For example, ALERT gages typically have 1 mm or 0.04" tipping buckets and report when the bucket tips. Radar, on the other hand, reports whatever it sees in each time step. Let's say it is raining at a rate of 0.04 inches per hour. Table 4 presents a typical rainfall time series as measured by a rain gage and its co-located radar pixel, and the resulting G/R ratio. As you can see, both the gage and radar reported 0.04 inches for the hour, resulting in an effective G/R ratio of 1.0. However, if you compute the G/R at each time step, the radar rainfall would be "zeroed out" until the final period when a G/R of 4.0 would be necessary to compensated for the "lost" rainfall. This creates sudden and unnatural changes in the rainfall image sequence. Figure 24 shows this difference in timing by plotting an example rain increment time-series from rain gage and radar data. In general the radar pattern is smoother and tends to precede the rain gage. The jagged "tipping" nature of rain gage data is also apparent.

While it is well understood that the G/R ratio can vary between and within storms, this approach accounts for the variation from event to event and is flexible enough to accommodate intra-storm variation when segments are well defined. Overall, this approach has proven to produce reasonable results with realistic transitions from time step to time step.

These event-based ratios were then spatially distributed across the study area. A Kriging-based interpolation technique was used to determine the appropriate geometry and distance-weighted G/R ratio for every other pixel in the domain. Kriging is a method of interpolation which solves a set of linear equations while minimizing estimation variance (Seo, 1990). Kriging assumes the parameter being estimated (gage/radar ratio) may be modeled as a regionalized variable (intermediate between random and deterministic). A regionalized variable is characterized as one for which nearby points have a high degree of spatial correlation, while widely separated points are statistically independent. The variogram equation currently used by OneRain is a power function as follows:

Time	Rain Gage	Radar	G/R
1:15	0.00	0.01	0.00
1:30	0.00	0.01	0.00
1:45	0.00	0.01	0.00
2:00	0.04	0.01	4.00
Total	0.04	0.04	1.00

Table 4 – Example data records from radar and rain gage.

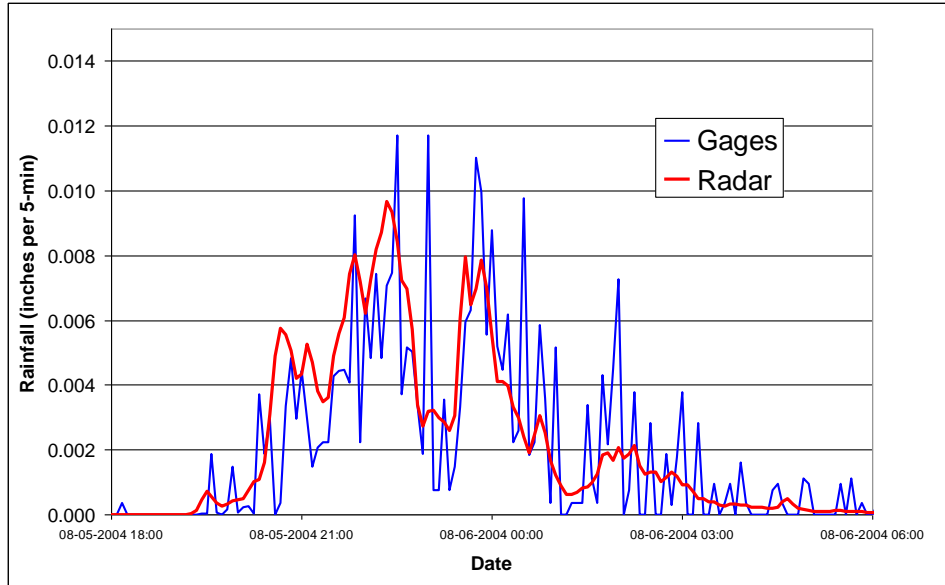


Figure 24 – Example rainfall increments as measured by radar and rain gages.

$$\lambda(x) = Ax^B,$$

where A is a constant equal to 1, x is the distance to the gage, and B is calculated using a least squares fit to the available data points. B is typically a small value (~0.2). Gage influence is limited to the five closest gages. The gage ratio adjustments determined by Kriging are also subject to minimum and maximum ratio constraints.

The Kriging method obtains gage ratio adjustments (gage/radar) for every nth row and column or the pixel grid. The default and normal operational value of n is 8 so that every 64th pixel is determined. The process also uses k nearest gages for the computation, where the default and normal operational value of k is 5. Gage-Radar ratios are then found at all intermediate points by performing bilinear interpolation.

The filtered radar dataset was then multiplied by the G/R ratios for each time period during the study to determine the gage-adjusted radar rainfall amounts. This process was repeated for each event during the study period. Figure 25 presents a block diagram description of the spatially variable gage-adjusted radar rainfall process. The result is a gage-adjusted radar rainfall dataset that matches the volume and timing of the rain gage network, but includes the spatial information from the radar.

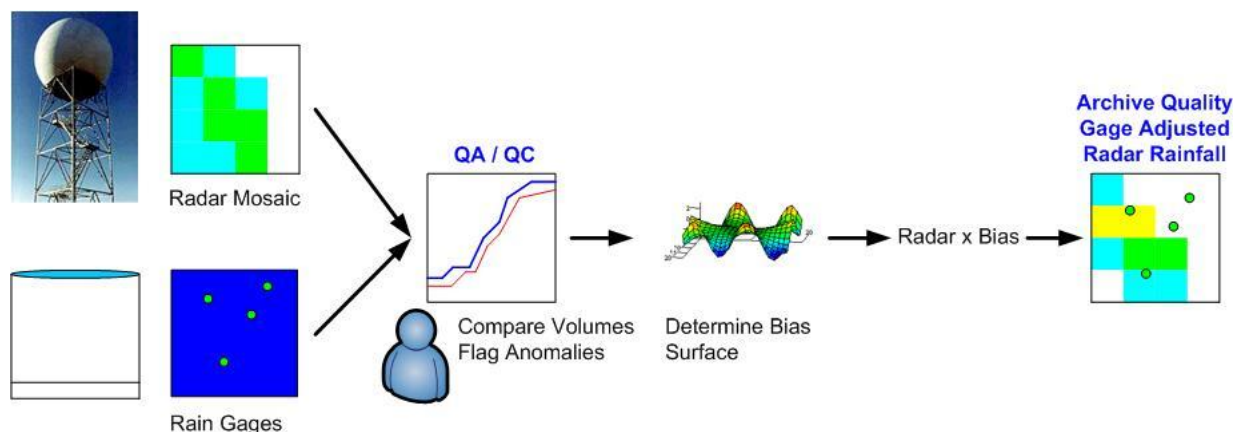


Figure 25 – Block diagram depicting spatially variable gage adjustment process.

Gage-Radar Analysis Results

Figures 26-37 present the accumulation and scatter-plots for the six rain events. These plots compare the gages, unadjusted radar, and adjusted radar for each of the study periods

In the accumulation plots, the *Gages* line shows the average accumulated rainfall for the gages with valid rainfall data. The *Radar* line shows the average accumulated rainfall from the unadjusted radar pixels that lie over the rain gages. The *AdjRadar* line shows the average GARR estimates for the pixels at the rain gages. Note that these accumulation plots reflected the gage maskings discussed above. Therefore, if a given gage was removed for a portion of the study period, its and the co-located pixel's accumulations removed from the average time-series.

The scatter-plots compare of gage measured rainfall with both unadjusted and adjusted radar. Each dot represents a gage and its co-located radar pixel. If the gage and GARR estimates were identical, all points would lie on the 45-degree best fit line. However, due to scaling issues, measuring errors, natural variability, and other uncertainties, these values usually will not match. Nevertheless, the GARR data is expected to cluster around the 45-degree line. As can be seen in the scatter-plot of gage/radar accumulations, the gage volumes correlate strongly with adjusted radar estimates. The coefficient of determination, R^2 , is an indicator of how well the gages and radar correlate after adjustments, and can be seen in the upper right hand corner of the scatter plots.

In a companion study to this Jimmy Camp Creek analysis, a Thunderstorm Identification Tracking Analysis and Nowcasting (TITAN) study was conducted based on twenty-four (24) months of GARR developed for a study area consisting of the eastern half of Colorado. Five of the Jimmy Camp Creek events coincided with the 24 months selected for TITAN analysis. Since that project covered a larger study area with more gages, the 24 months of TITAN GARR data were subjected to a verification process to confirm that the GARR rainfall estimates

matched within 5% of the verification gages withheld from the GARR analysis. For verification purposes, 10% of the rain gages were withheld from the analysis. Since the Jimmy Camp Creek study was based on a smaller study area with fewer gages (particularly for the 1995, 1996 and 1999 events), withholding gages and applying the verification process was not applied directly to this analysis. However, the GARR process and techniques for the two studies were identical. Furthermore, the Jimmy Camp Creek radar and gage data were a subset of the datasets used for the TITAN analysis.

For the 24 months of GARR data developed for the TITAN analysis, the verification process showed that there was an average difference of 4.8% between the withheld verification gages and their co-located radar pixels. Table 5 presents the average rain gage and radar accumulations for the six Jimmy Camp Creek events.

Event	Average Gage (in)	Average Radar (in)	Absolute Difference (in)	%
May 17, 1995	2.114	2.100	0.014	0.65%
August 8, 1996	0.200	0.204	0.003	1.62%
July 31, 1999	2.614	2.615	0.001	0.04%
August 8, 2005	0.704	0.700	0.004	0.51%
July 15, 2005	0.339	0.337	0.002	0.45%
August 26, 2006	0.599	0.594	0.005	0.81%

Table 5 – Average gage and radar accumulations for the six Jimmy Camp Creek analyses.

Figures 38-43 display the “event totals” for the six study periods. The rain scale for these plots was normalized to 4 inches. Since the 1996 and 1999 events had rain amounts outside of that range, these plots are also presented in Appendix C with event-specific rain scales, which better highlights the ‘topography’ of each event. Note that these totals reflect the entire period study selected to generate the GARR datasets (see Table 1 for start and end times).

Project Deliverables

For each of the six rain event analyzed, the following files were provided:

- Shape files that provide the geographic location of the radar pixels for the Jimmy Camp Creek study area, including rain totals for each event. These shape files assign a unique numeric ID to each radar pixel. This shape file is in the NAD 83 projection using decimal degrees.
 - Filename: sub_jcc_pixel_dd83_YYYY_MM_DD.zip
- Zip file containing text files that map pixel IDs to 5- or 15-minute rainfall estimates for the entire study period. **Timestamps are in Mountain Standard Time.**
 - Filename: pixelData_YYYY_MM_DD.zip
- Spreadsheet files that map pixel IDs to 5- or 15-minute rainfall estimates for the entire study period. **Timestamps are in Mountain Standard Time.**
 - JCC_YYYY_MM_DD.zip

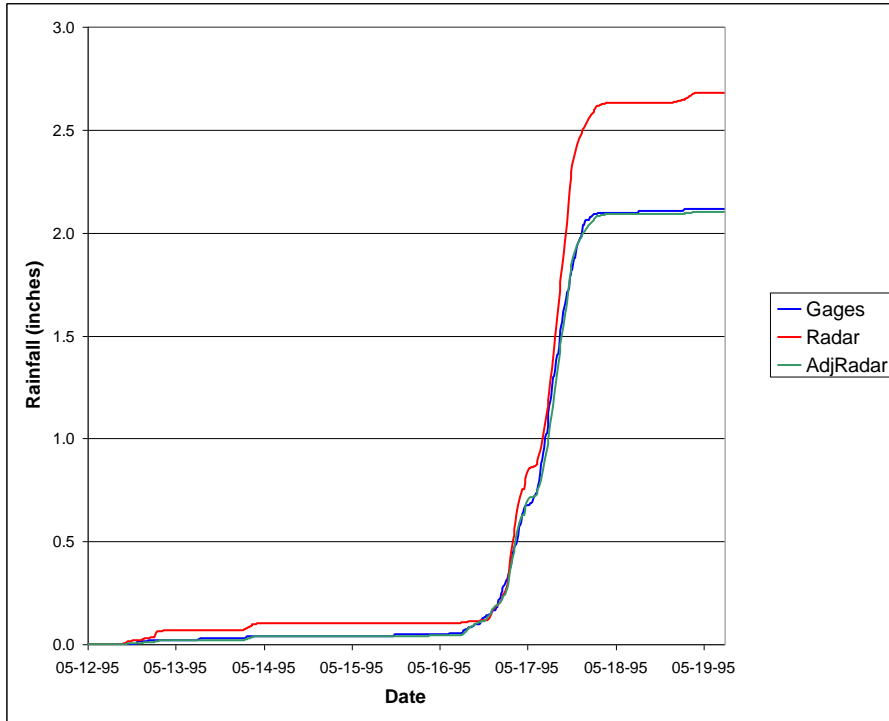


Figure 26 - Accumulation plot for Event 1 - May 17, 1995.

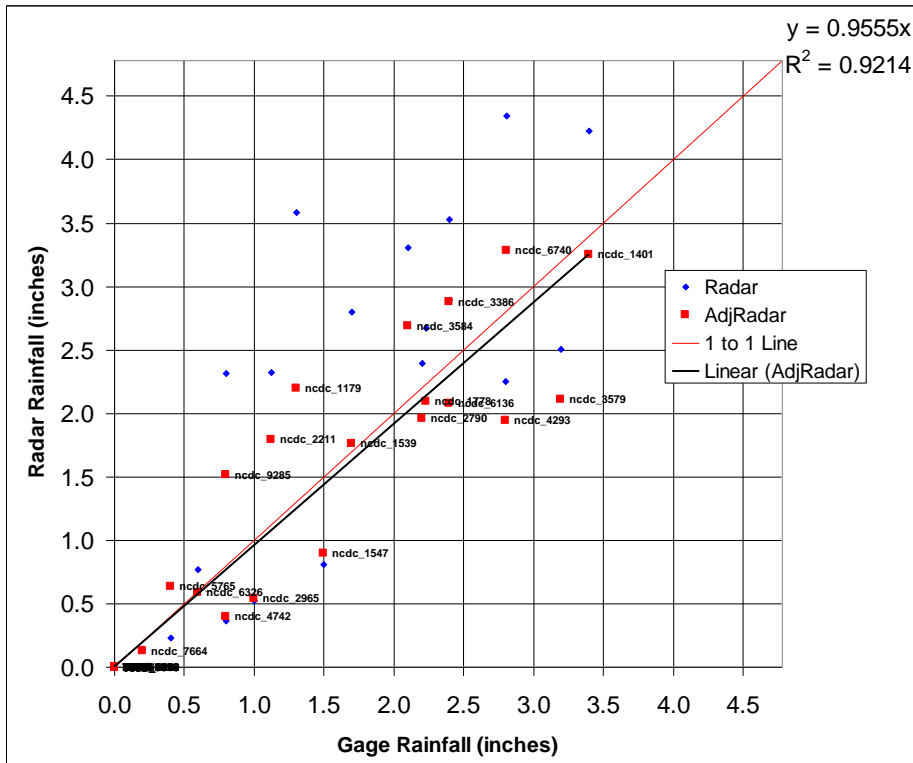


Figure 27 - Scatter-plot for Event 1 - May 17, 1995.

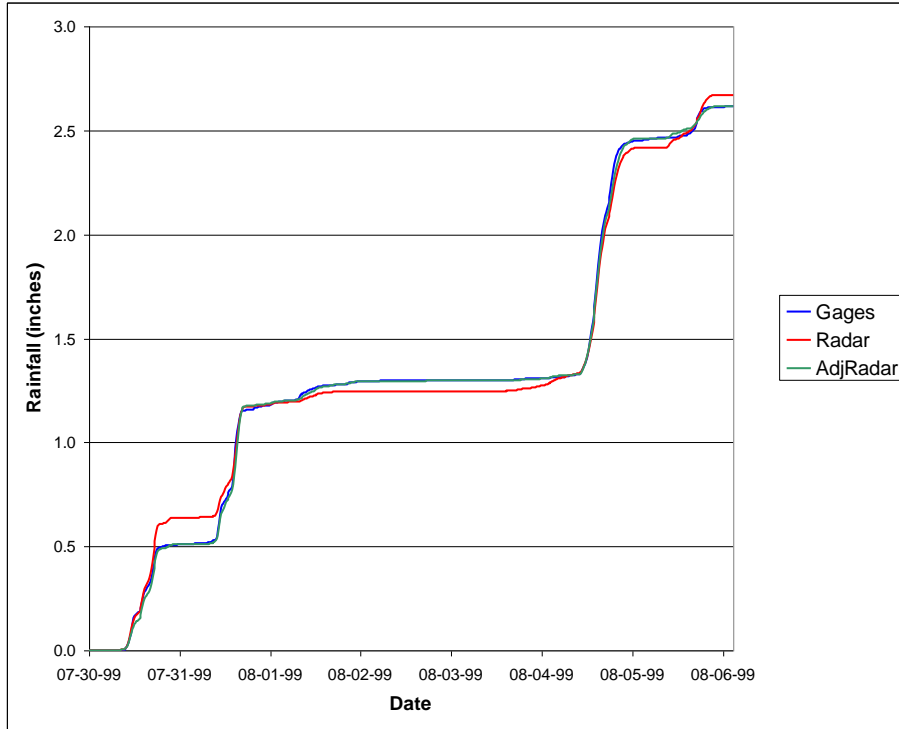


Figure 30 – Accumulation plot for Event 3 - July 31, 1999.

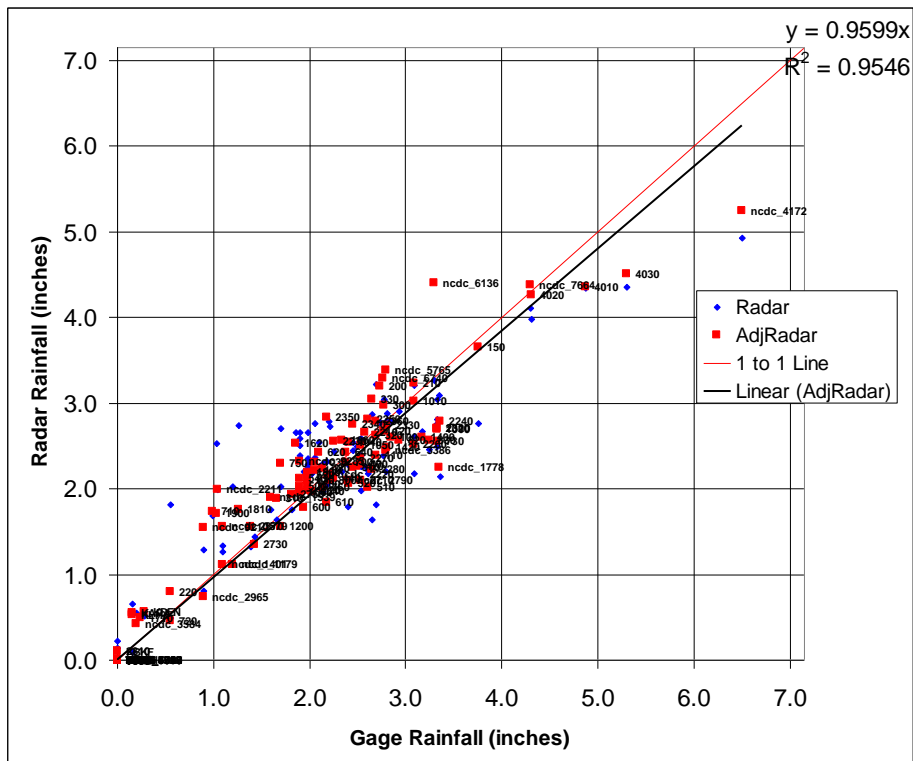


Figure 31 – Scatter-plot for Event 3 - July 31, 1999.

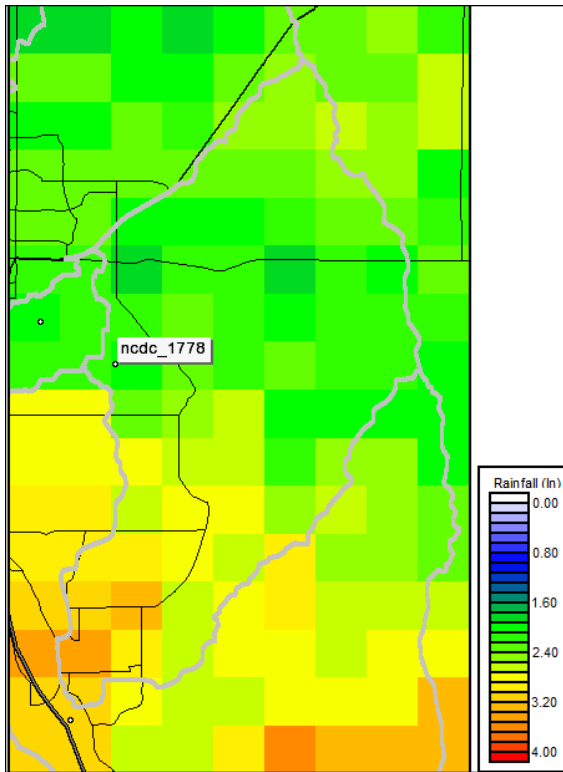


Figure 38 – May 17, 1995 event totals.

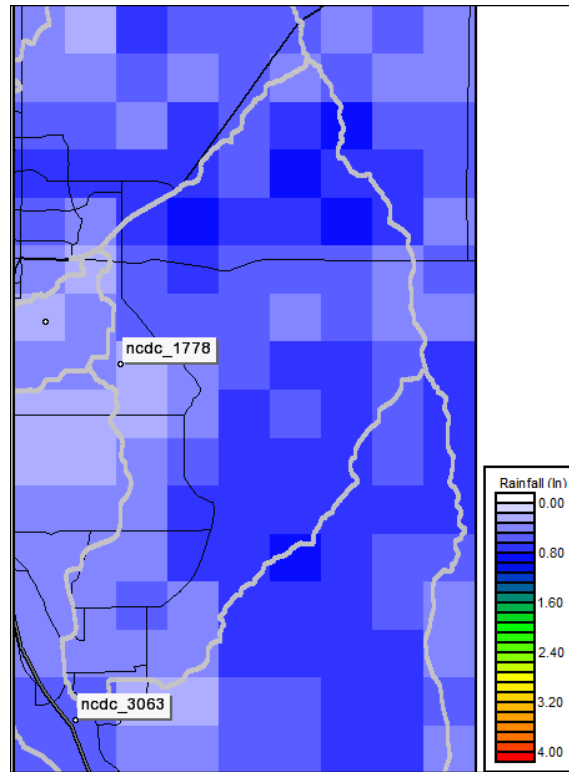


Figure 39 – August 15, 1996 event totals.

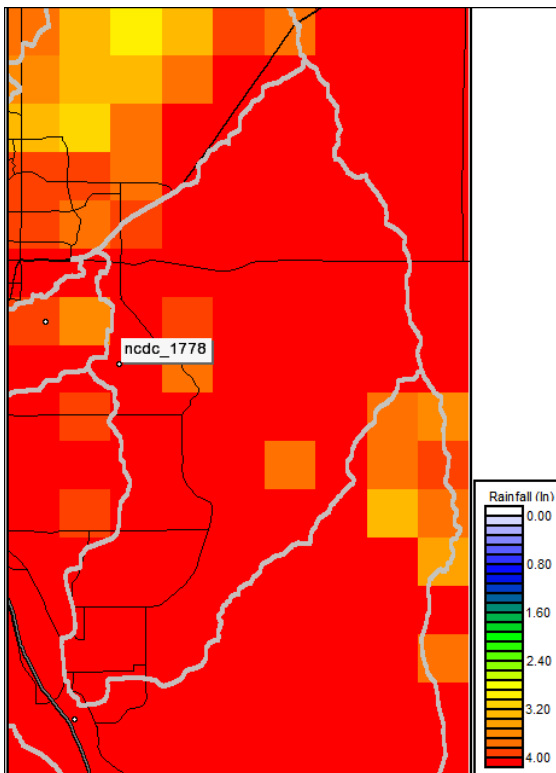


Figure 40 – July 31, 1999 event totals.

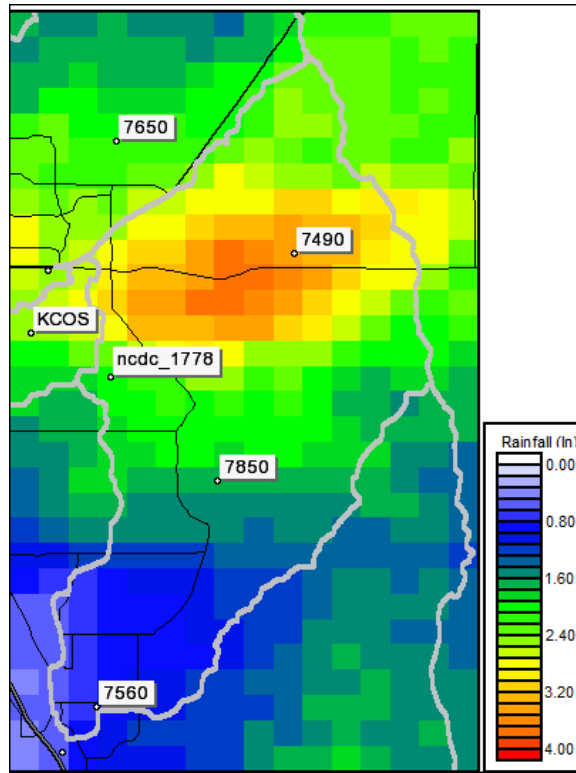


Figure 41 – August 4, 2004 event totals.

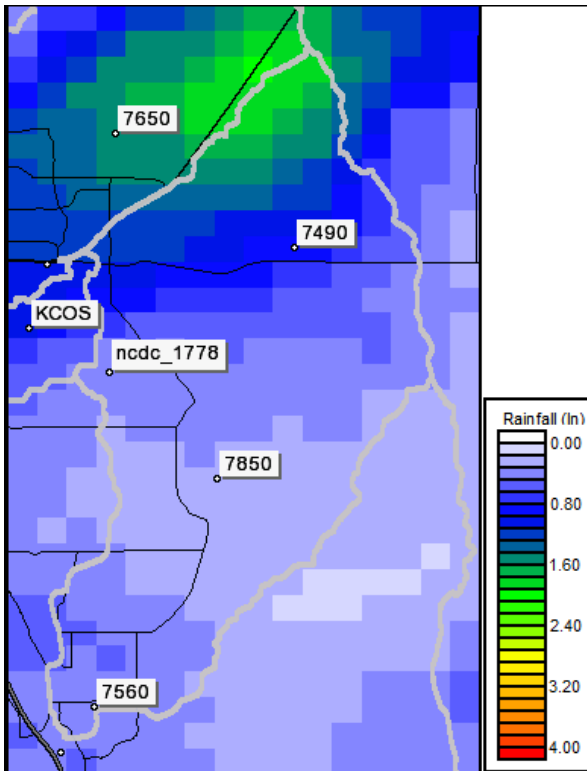


Figure 42 – July 15, 2005 event totals.

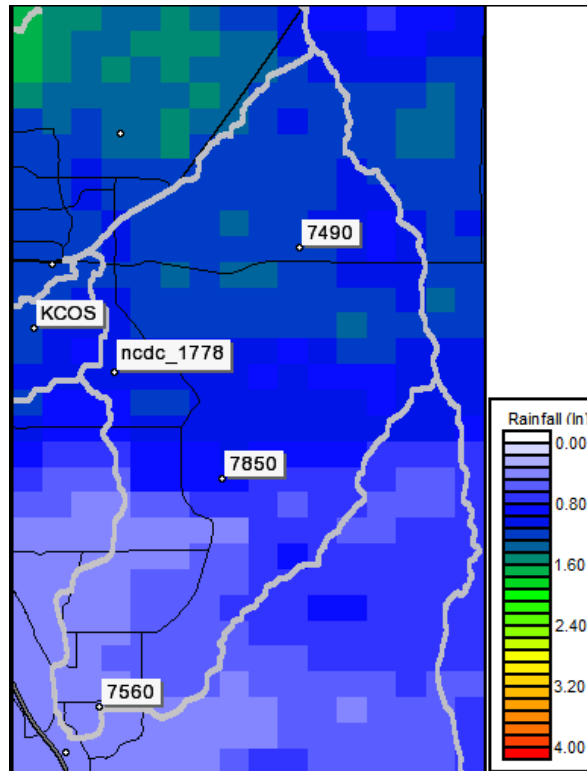


Figure 43 – August 26, 2006 event totals.

Conclusions

OneRain's gage-radar adjustment procedure was able to successfully merge the data from the rain gage networks and the Barons Services and WSI radar data. Ground clutter and noise filtering was required. The timing of the rain gage and radar measurement systems showed a high degree of correlation.

Good correlation was also found between the available rain gages and the filtered radar, as well as between accumulations with the adjusted radar product.

The result is six gage-adjusted radar rainfall datasets with individual rainfall estimates at each pixel. These adjustments have resulted in a distribution of rainfall that has the spatial resolution of radar, with better accuracy being insured by rain gage data.

Appendix A – Gages used in GARR process

Table A.1 catalogs what gages were used for the 1995, 1996, 1999 and 2004 study periods.

Table A.2 catalogs what gages were used for the 2005 and 2006 study periods.

Table A.3 presents the latitude and longitude for all the gages used in the study.

1995	1996	1999	2004			
ncdc_1179	ncdc_1179	100	1720	120	1500	5960
ncdc_1401	ncdc_1401	110	1800	150	1520	7250
ncdc_1539	ncdc_1539	120	1810	200	1530	7260
ncdc_1547	ncdc_1547	150	1900	220	1600	7350
ncdc_1778	ncdc_1778	200	2210	300	1640	7360
ncdc_2211	ncdc_2211	210	2230	310	1660	7410
ncdc_2790	ncdc_2220	220	2240	330	1710	7420
ncdc_2965	ncdc_2790	300	2250	400	1720	7430
ncdc_3386	ncdc_2965	310	2260	410	1800	7440
ncdc_3579	ncdc_3063	320	2270	420	2190	7460
ncdc_3584	ncdc_3386	330	2280	430	2210	7470
ncdc_4293	ncdc_3579	400	2310	440	2230	7490
ncdc_4742	ncdc_3584	410	2320	500	2240	7520
ncdc_5765	ncdc_4172	420	2330	510	2250	7530
ncdc_6136	ncdc_5352	430	2340	520	2260	7560
ncdc_6326	ncdc_5765	440	2350	530	2270	7640
ncdc_6740	ncdc_6136	500	2360	540	2280	7650
ncdc_7320	ncdc_6326	510	2370	600	2310	7810
ncdc_7664	ncdc_6740	520	2710	610	2320	7850
ncdc_9285	ncdc_7320	530	2730	620	2330	7950
	ncdc_7664	540	2750	630	2340	KAPA
	ncdc_9210	600	2810	640	2350	KCOS
	ncdc_9285	610	4010	700	2360	KDEN
		620	4020	710	2370	KLHX
		630	4030	720	2730	KLIC
		640	KAPA	730	2750	KPUB
		700	KBKF	750	2810	ncdc_1401
		710	KDEN	760	2820	ncdc_1539
		720	KLHX	800	2840	ncdc_1547
		730	ncdc_1179	810	2850	ncdc_1778
		750	ncdc_1401	820	4010	ncdc_2965
		760	ncdc_1539	830	4020	ncdc_3579
		800	ncdc_1778	840	4030	ncdc_3584
		810	ncdc_2211	850	4820	ncdc_4172
		820	ncdc_2220	870	5720	ncdc_4293
		830	ncdc_2790	900	5730	ncdc_4720
		1000	ncdc_2965	1000	5740	ncdc_5352
		1010	ncdc_3386	1040	5760	ncdc_5765
		1030	ncdc_3579	1050	5770	ncdc_6740
		1040	ncdc_3584	1060	5780	ncdc_7664
		1050	ncdc_4172	1200	5790	ncdc_9285
		1060	ncdc_5765	1310	5800	
		1200	ncdc_6136	1320	5810	
		1400	ncdc_6740	1340	5820	
		1420	ncdc_7664	1350	5830	
		1600	ncdc_9210	1370	5860	
		1620	ncdc_9285	1400	5880	
		1640		1420	5900	
		1660		1440	5930	
		1710		1480	5940	

Table A.1 – Gages used for 1995-2004 events.

2005		2006			
150	5860	100	1360	5820	ncdc_1778
310	5880	110	1370	5830	ncdc_2790
420	5930	120	1400	5860	ncdc_3386
430	5940	140	1420	5880	ncdc_3579
440	5960	150	1440	5900	ncdc_3584
510	7000	200	1480	5930	ncdc_4172
520	7010	210	1500	5940	ncdc_4293
600	7030	220	1520	5960	ncdc_4720
630	7040	300	1530	7000	ncdc_4742
640	7075	330	1600	7010	ncdc_5352
700	7150	400	1620	7030	ncdc_5765
710	7260	420	1640	7040	ncdc_6136
720	7280	430	1710	7075	ncdc_6740
730	7300	440	1720	7150	ncdc_7320
750	7310	500	1800	7200	ncdc_7664
760	7350	510	1810	7250	ncdc_9210
800	7360	520	1900	7260	ncdc_9285
810	7400	530	2190	7280	
820	7410	540	2210	7300	
830	7420	600	2230	7310	
840	7430	610	2240	7320	
850	7440	620	2250	7360	
870	7450	630	2260	7410	
900	7460	640	2270	7420	
1500	7470	650	2280	7430	
1530	7490	700	2310	7440	
1600	7497	710	2320	7450	
1710	7530	720	2330	7460	
1800	7550	730	2340	7470	
2190	7560	750	2350	7490	
2260	7570	760	2360	7520	
2270	7650	800	2370	7530	
2280	7750	810	2710	7560	
2320	7810	820	2730	7570	
2330	7850	830	2750	7600	
2340	7950	840	2810	7640	
2360	KAPA	860	2820	7750	
2370	KCOS	870	2840	7800	
2710	KLIC	900	4010	7810	
2750	KMNH	1000	4020	7850	
2810	ncdc_1179	1010	4030	KAPA	
2820	ncdc_1547	1030	4820	KCOS	
4010	ncdc_1778	1040	5720	KDEN	
4020	ncdc_2965	1050	5740	KLHX	
5720	ncdc_3579	1060	5760	KLIC	
5730	ncdc_4742	1300	5770	KMNH	
5740	ncdc_5352	1310	5780	KPUB	
5770		1320	5790	ncdc_1179	
5790		1340	5800	ncdc_1539	
5810		1350	5810	ncdc_1547	

Table A.2 – Gages used for 2005 & 2006 events.

Gage ID	Latitude	Longitude	Gage ID	Latitude	Longitude	Gage ID	Latitude	Longitude
100	39.805	-105.091	1530	39.653	-105.033	7310	38.821	-104.763
110	39.823	-105.246	1550	39.7276	-105.07	7320	38.93	-104.842
120	39.82	-105.173	1600	39.589	-104.918	7350	38.98	-104.769
140	39.87	-105.297	1620	39.608	-104.985	7360	38.93	-104.77
150	39.852	-105.366	1640	39.633	-105.014	7370	38.763	-104.893
200	39.84	-105.167	1660	39.922	-104.867	7400	38.781	-104.879
210	39.823	-105.123	1700	39.742	-104.999	7410	39.023	-104.981
220	39.844	-105.234	1710	39.631	-104.828	7420	39.04	-104.813
300	39.795	-105.146	1720	39.713	-104.949	7430	39.016	-104.737
310	39.797	-105.331	1800	39.757	-104.831	7440	38.975	-104.873
320	39.802	-105.117	1810	39.806	-104.941	7450	38.76	-104.83
330	39.802	-105.224	1900	39.857	-104.988	7460	38.962	-104.714
400	39.748	-104.879	2190	39.68	-105.494	7470	38.935	-104.948
410	39.733	-104.888	2210	39.672	-105.347	7480	38.838	-104.705
420	39.711	-104.859	2230	39.632	-105.321	7490	38.844	-104.618
430	39.685	-104.844	2240	39.666	-105.275	7497	38.897	-104.763
440	39.676	-104.823	2250	39.638	-105.381	7520	38.917	-104.818
500	39.733	-104.864	2260	39.582	-105.397	7530	38.858	-104.911
510	39.707	-104.839	2270	39.594	-105.343	7550	38.848	-104.76
520	39.682	-104.86	2280	39.601	-105.296	7560	38.683	-104.688
530	39.711	-104.92	2310	39.702	-105.264	7570	38.711	-104.721
540	39.696	-104.897	2320	39.696	-105.275	7600	38.872	-104.817
600	39.672	-104.982	2330	39.653	-105.195	7640	38.826	-104.826
610	39.669	-104.942	2340	39.702	-105.33	7650	38.884	-104.681
620	39.639	-104.936	2350	39.671	-105.241	7750	38.83	-104.936
630	39.632	-104.891	2360	39.637	-105.264	7800	38.898	-104.834
640	39.656	-104.902	2370	39.68	-105.197	7810	39.015	-104.839
650	39.674	-104.911	2710	39.562	-105.019	7850	38.763	-104.645
700	39.725	-104.818	2730	39.499	-104.776	7950	38.899	-104.882
710	39.687	-104.803	2750	39.376	-104.846	KABH	38.7578	-104.301
720	39.667	-104.777	2810	39.372	-104.966	KAFF	38.9667	-104.817
730	39.638	-104.748	2820	39.424	-104.908	KAPA	39.5667	-104.85
750	39.639	-104.769	2840	39.517	-104.746	KBJC	39.9167	-105.117
760	39.649	-104.796	2850	39.4356	-104.77	KBKF	39.71	-104.758
800	39.745	-104.808	4010	39.922	-105.354	KCOS	38.8158	-104.711
810	39.725	-104.797	4020	39.922	-105.327	KDEN	39.8333	-104.65
820	39.711	-104.79	4030	39.932	-105.292	KFCS	38.7	-104.767
830	39.684	-104.763	4820	39.932	-105.257	KFTG	39.7833	-104.55
840	39.762	-104.761	5450	39.1135	-104.938	KLHX	38.05	-103.517
850	39.766	-104.793	5720	39.167	-105.232	KLIC	39.2667	-103.667
860	39.7406	-104.781	5730	39.099	-105.133	KMNH	39.2167	-104.633
870	39.685	-104.71	5740	39.091	-105.215	KPUB	38.29	-104.498
900	39.606	-104.674	5760	39.23	-105.282	ncdc_1179	39.7333	-104.117
920	39.7122	-104.812	5770	39.267	-105.244	ncdc_1401	39.4	-104.9
940	39.5831	-104.709	5780	39.289	-105.325	ncdc_1539	38.1	-103.5
950	39.595	-104.744	5790	39.248	-105.351	ncdc_1547	39.6167	-104.817
970	39.7364	-104.669	5800	39.179	-105.362	ncdc_1778	38.8	-104.683
1000	39.756	-105.137	5810	39.127	-105.207	ncdc_2211	39.8167	-104.65
1010	39.732	-105.152	5820	39.132	-105.367	ncdc_2220	39.75	-104.867
1030	39.741	-105.176	5830	39.065	-105.374	ncdc_2790	39.6333	-105.3
1040	39.725	-105.193	5860	39.046	-105.281	ncdc_2965	38.9	-105.283
1050	39.721	-105.168	5880	39.073	-105.27	ncdc_3063	38.6667	-104.7
1060	39.71	-105.212	5900	39.231	-105.201	ncdc_3386	39.7	-105.217
1200	39.928	-105.064	5930	39.183	-105.074	ncdc_3579	39.1	-104.717
1300	39.818	-105.035	5940	39.254	-105.149	ncdc_3584	39.2167	-104.733
1310	39.813	-105.013	5960	39.234	-105.324	ncdc_4172	39.1333	-103.483
1320	39.722	-105.01	7000	38.878	-104.994	ncdc_4293	39.5667	-105.217
1330	39.797	-104.901	7010	38.933	-104.609	ncdc_4720	38.0333	-103.5
1340	39.684	-105.05	7030	39.04	-104.86	ncdc_4742	38.9	-105.467
1350	39.557	-105.078	7040	39.098	-104.859	ncdc_5018	39.1833	-103.7
1360	39.751	-104.954	7050	38.976	-105.043	ncdc_5352	38.85	-104.917
1370	39.581	-105.138	7075	38.932	-105.012	ncdc_5765	39.65	-105.2
1400	39.754	-105.079	7150	38.841	-104.973	ncdc_6136	38.5167	-103.7
1420	39.754	-105.016	7200	38.856	-104.802	ncdc_6326	39.5167	-104.65
1440	39.245	-104.589	7250	38.848	-104.829	ncdc_6740	38.2833	-104.483
1460	39.769	-104.867	7260	38.763	-104.758	ncdc_7320	37.9167	-104.917
1480	39.892	-104.732	7270	38.631	-104.718	ncdc_7664	39.1333	-104.083
1500	39.616	-104.997	7280	38.941	-104.732	ncdc_9210	39.1	-105.083
1520	39.638	-105.073	7300	38.789	-104.903	ncdc_9285	38.85	-104.233

Table A.3 - Gage IDs and locations for gages surveyed for study.

Appendix B – Gage Masking Details

Presented below are complete gage maskings for each of the six study periods. For each study period an accumulation plot is presented that shows how the study period was divided into separate rainfall ‘events.’ The vertical lines on these plots, what we refer to as ‘breakpoints’, indicate the time steps of the study period that bracket individual events.

The gage maskings cataloged below indicate the range of time steps the gage was removed from the analysis with ‘begin’ and ‘end’ columns. Each masking also includes a comment indicating the reason for the masking. Maskings labeled with “HGR” indicate a gage removed because it appeared as an over-reporting gage. Maskings labeled with “LGR” indicate a gage removed because it appeared as an under-reporting gage. The other comments are self-explanatory and correspond to the types of maskings discussed in the ‘Rain Gage Data QA/QC Procedures’ section.

The maskings highlighted in the blue sections correspond to the gage maskings made for the most significant ‘events’ during the study period.

Gage Maskings for May 17, 1995

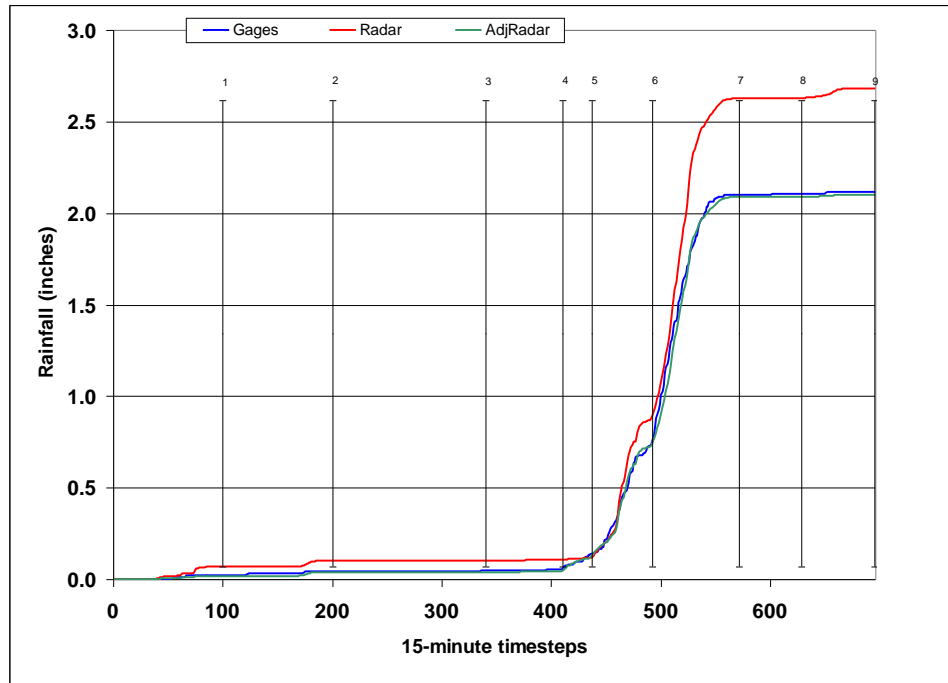


Figure B.1 – Study period breakpoints.

Gage	Begin	End	Reason
ncdc_1547	1	100	No Gage Data with radar data > 0.1
ncdc_2211	1	100	No Gage Data with radar data > 0.1
ncdc_6326	1	100	No Gage Data with radar data > 0.1
ncdc_7320	1	100	HGR
ncdc_1547	101	200	No Gage Data with radar data > 0.1
ncdc_7664	101	200	HGR
4010	201	340	HGR
ncdc_2790	201	340	HGR
ncdc_6326	201	340	HGR
ncdc_1179	341	410	No Gage Data with radar data > 0.1
ncdc_1539	341	410	No Gage Data with radar data > 0.1
ncdc_1547	341	410	HGR
ncdc_5765	341	410	HGR
ncdc_6136	341	410	No Gage Data with radar data > 0.1
ncdc_1401	411	437	No Gage Data with radar data > 0.1
ncdc_2790	411	437	No Gage Data with radar data > 0.1
ncdc_3386	411	437	No Gage Data with radar data > 0.1
ncdc_4293	411	437	No Gage Data with radar data > 0.1
ncdc_4742	411	437	No Gage Data with radar data > 0.1
ncdc_6326	411	437	No Gage Data with radar data > 0.1
ncdc_5765	438	492	No Gage Data with radar data > 0.1
ncdc_7320	438	492	HGR
ncdc_7664	438	492	No Gage Data with radar data > 0.1
KMNH	493	571	LGR
ncdc_1547	493	571	LGR
ncdc_4720	493	571	LGR
ncdc_5765	493	571	LGR
ncdc_6326	493	571	LGR
ncdc_7320	493	571	HGR
ncdc_7664	493	571	No Gage Data with radar data > 0.1
ncdc_1401	572	628	HGR
ncdc_2790	572	628	HGR
ncdc_3386	572	628	HGR
ncdc_5765	572	628	No Gage Data with radar data > 0.1
ncdc_1401	629	695	No Gage Data with radar data > 0.1
ncdc_2211	629	695	HGR
ncdc_3579	629	695	No Gage Data with radar data > 0.1
ncdc_7664	629	695	No Gage Data with radar data > 0.1

Table B.1 – Study period gage maskings.

Gage Maskings for August 15, 1996

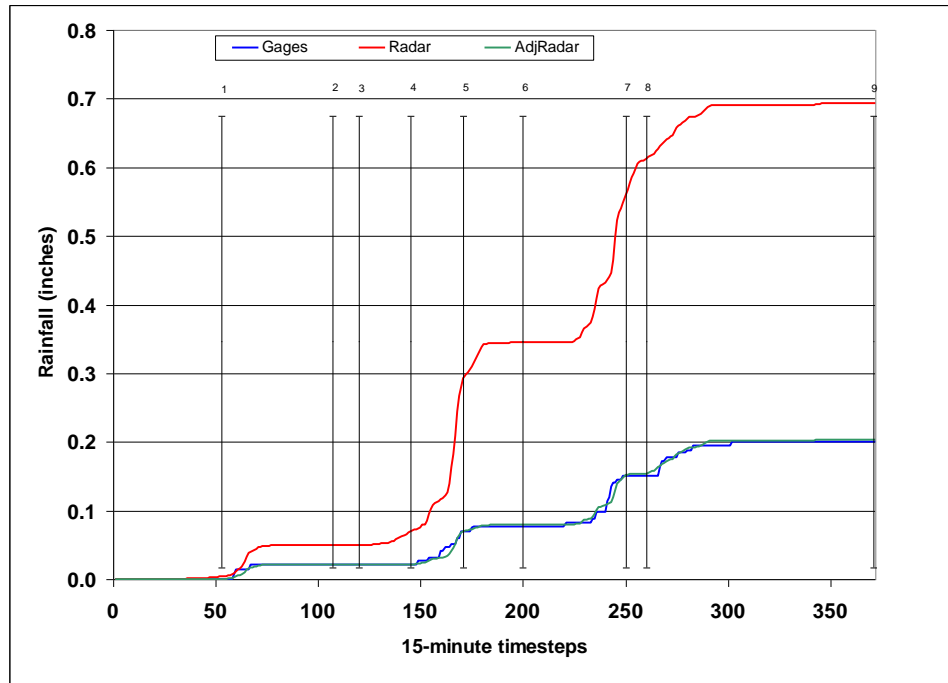


Figure B.2 – Study period breakpoints.

Gage	Begin	End	Reason
920	1	53	HGR
ncdc_1539	1	53	HGR
ncdc_1539	54	107	No Gage Data with radar data > 0.1
ncdc_2220	54	107	No Gage Data with radar data > 0.1
ncdc_3386	54	107	No Gage Data with radar data > 0.1
ncdc_3579	54	107	No Gage Data with radar data > 0.1
ncdc_3584	54	107	No Gage Data with radar data > 0.1
ncdc_6136	54	107	No Gage Data with radar data > 0.1
ncdc_6326	54	107	No Gage Data with radar data > 0.1
ncdc_7664	54	107	No Gage Data with radar data > 0.1
ncdc_9285	54	107	No Gage Data with radar data > 0.1
ncdc_3584	108	120	HGR: Gage more than 8.3 times higher than radar
KDEN	146	171	HGR
ncdc_1401	146	171	No Gage Data with radar data > 0.1
ncdc_3063	146	171	HGR: Gage more than 26.9 times higher than radar
ncdc_4172	146	171	HGR: Gage more than 6. times higher than radar
ncdc_1778	172	200	No Gage Data with radar data > 0.1
ncdc_3063	172	200	No Gage Data with radar data > 0.1
ncdc_3386	172	200	HGR
ncdc_4172	172	200	No Gage Data with radar data > 0.1
ncdc_6136	172	200	No Gage Data with radar data > 0.1
KBJC	201	250	HGR
ncdc_1547	201	250	No Gage Data with radar data > 0.1
ncdc_2220	201	250	No Gage Data with radar data > 0.1
ncdc_2965	201	250	HGR: Gage more than 11.1 times higher than radar
ncdc_5352	201	250	HGR
ncdc_1179	261	371	No Gage Data with radar data > 0.1
ncdc_1401	261	371	No Gage Data with radar data > 0.1
ncdc_2790	261	371	HGR: Gage more than 16.7 times higher than radar
ncdc_3063	261	371	LGR
ncdc_3386	261	371	HGR: Gage more than 4.5 times higher than radar
ncdc_3579	261	371	No Gage Data with radar data > 0.1
ncdc_9285	261	371	No Gage Data with radar data > 0.1

Table B.2 – Study period gage maskings.

Gage Maskings for July 31, 1999 Event

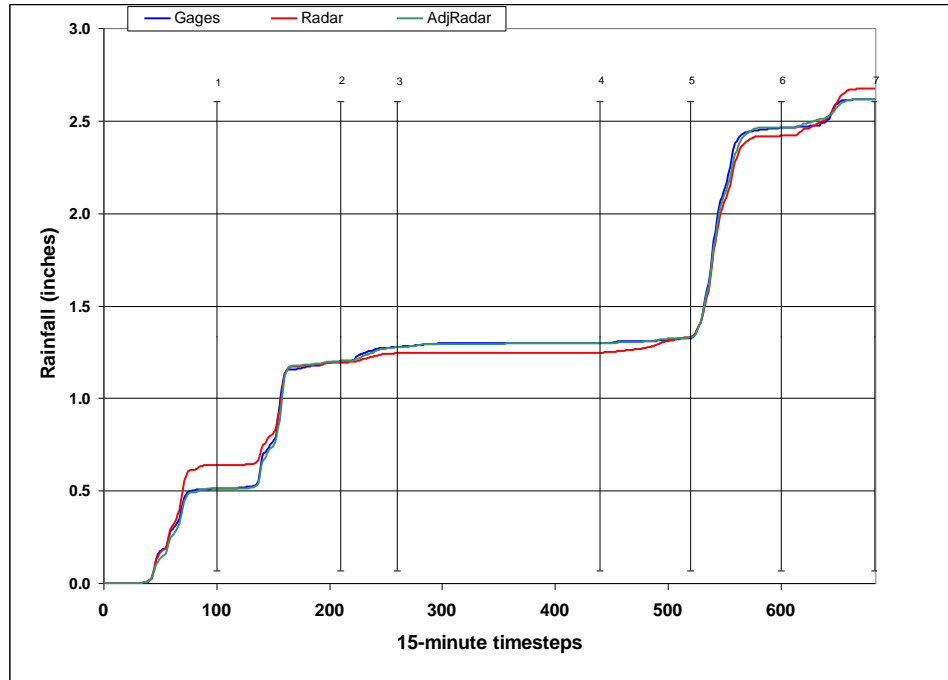


Figure B.3 – Study period breakpoints.

Gage	Begin	End	Reason
1200	1	100	LGR
1710	1	100	LGR: Radar more than 5.3 times higher than gage
2810	1	100	LGR: Radar more than 8.5 times higher than gage
KAPA	1	100	No Gage Data with radar data > 0.1
KBKF	1	100	No Gage Data with radar data > 0.1
KDEN	1	100	No Gage Data with radar data > 0.1
KLHX	1	100	No Gage Data with radar data > 0.1
ncdc_1179	1	100	LGR
ncdc_1401	1	100	HGR
ncdc_3579	1	100	LGR
110	101	210	LGR
1810	101	210	LGR
1900	101	210	LGR: Radar more than 10.9 times higher than gage
220	101	210	LGR
2810	101	210	LGR: Radar more than 4.6 times higher than gage
710	101	210	HGR
720	101	210	LGR
KBKF	101	210	No Gage Data with radar data > 0.1
KLHX	101	210	No Gage Data with radar data > 0.1
ncdc_1179	101	210	LGR
ncdc_1539	101	210	LGR: Radar more than 5.4 times higher than gage
ncdc_2965	101	210	No Gage Data with radar data > 0.1
ncdc_3584	101	210	No Gage Data with radar data > 0.1
ncdc_9285	101	210	LGR
KLHX	211	260	No Radar Data with gage data > 0.1
110	261	440	HGR
120	261	440	No Radar Data with gage data > 0.1
2810	261	440	HGR
420	261	440	No Radar Data with gage data > 0.1
630	261	440	No Radar Data with gage data > 0.1
640	261	440	No Radar Data with gage data > 0.1
ncdc_1778	261	440	HGR
ncdc_5765	261	440	No Radar Data with gage data > 0.1
ncdc_7664	261	440	HGR

Table B.3 – Study period gage maskings.

Gage	Begin	End	Reason
1710	521	600	LGR: Radar more than 5.4 times higher than gage
220	521	600	No Gage Data with radar data > 0.1
2370	521	600	LGR: Radar more than 4.4 times higher than gage
2810	521	600	LGR: Radar more than 5.6 times higher than gage
310	521	600	LGR
720	521	600	LGR: Radar more than 4.5 times higher than gage
KAPA	521	600	LGR: Radar more than 9.5 times higher than gage
KBKF	521	600	LGR: Radar more than 27.7 times higher than gage
KDEN	521	600	LGR: Radar more than 11.5 times higher than gage
KLHX	521	600	No Gage Data with radar data > 0.1
ncdc_1778	521	600	HGR
ncdc_3584	521	600	No Gage Data with radar data > 0.1
100	601	683	LGR: Radar more than 4.4 times higher than gage
1030	601	683	LGR
1040	601	683	LGR: Radar more than 8.3 times higher than gage
1050	601	683	LGR
1060	601	683	LGR
110	601	683	LGR
1400	601	683	LGR: Radar more than 6.3 times higher than gage
1620	601	683	No Gage Data with radar data > 0.1
1640	601	683	No Gage Data with radar data > 0.1
1660	601	683	No Gage Data with radar data > 0.1
1720	601	683	No Gage Data with radar data > 0.1
2350	601	683	No Gage Data with radar data > 0.1
2370	601	683	LGR: Radar more than 8. times higher than gage
310	601	683	No Gage Data with radar data > 0.1
320	601	683	LGR
400	601	683	No Gage Data with radar data > 0.1
410	601	683	No Gage Data with radar data > 0.1
500	601	683	No Gage Data with radar data > 0.1
520	601	683	No Gage Data with radar data > 0.1
530	601	683	No Gage Data with radar data > 0.1
540	601	683	No Gage Data with radar data > 0.1
600	601	683	No Gage Data with radar data > 0.1
610	601	683	No Gage Data with radar data > 0.1
630	601	683	No Gage Data with radar data > 0.1
720	601	683	No Gage Data with radar data > 0.1
760	601	683	No Gage Data with radar data > 0.1
810	601	683	No Gage Data with radar data > 0.1
830	601	683	No Gage Data with radar data > 0.1
KAPA	601	683	No Gage Data with radar data > 0.1
KDEN	601	683	LGR: Radar more than 12.1 times higher than gage
ncdc_2211	601	683	LGR
ncdc_2220	601	683	No Gage Data with radar data > 0.1
ncdc_3386	601	683	No Gage Data with radar data > 0.1
ncdc_3579	601	683	No Gage Data with radar data > 0.1
ncdc_3584	601	683	No Gage Data with radar data > 0.1
ncdc_6136	601	683	HGR
ncdc_7664	601	683	HGR

Table B.3 – Study period gage maskings (continued).

Gage Maskings for August 5, 2004 Event

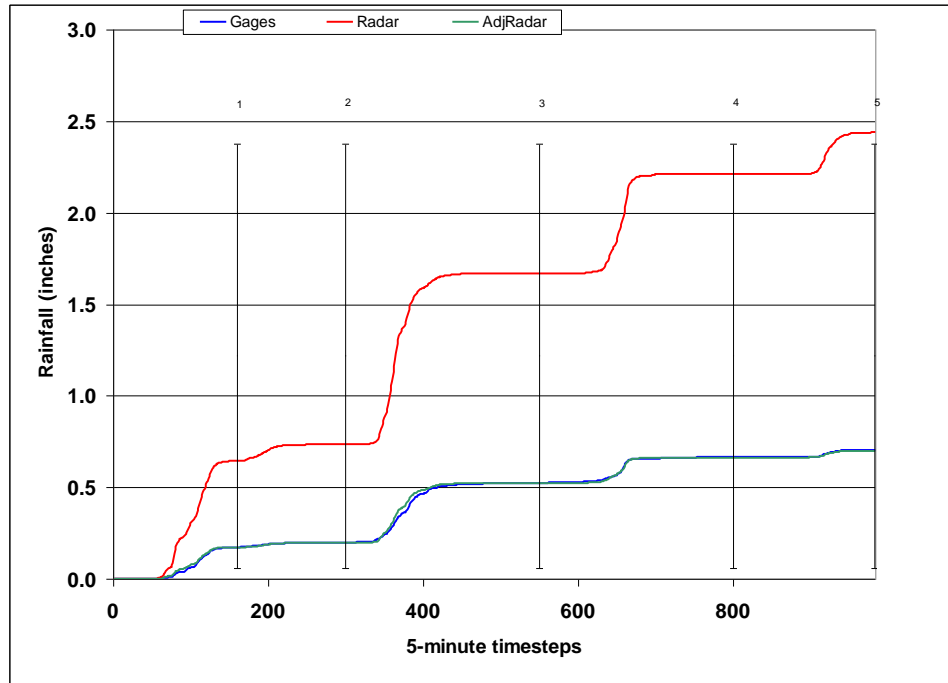


Figure B.4 - Study period breakpoints.

Gage	Begin	End	Reason
1600	1	160	No Gage Data with radar data > 0.1
2190	1	160	No Gage Data with radar data > 0.1
2750	1	160	LGR: Radar more than 4.1 times higher than gage
5730	1	160	LGR: Radar more than 5.6 times higher than gage
5740	1	160	LGR: Radar more than 5.2 times higher than gage
5760	1	160	HGR: Gage more than 6.6 times higher than radar
5790	1	160	HGR: Gage more than 9.8 times higher than radar
5810	1	160	No Gage Data with radar data > 0.1
5830	1	160	HGR: Gage more than 4.6 times higher than radar
5900	1	160	HGR: Gage more than 14.8 times higher than radar
5930	1	160	HGR: Gage more than 9.9 times higher than radar
5940	1	160	HGR: Gage more than 4.2 times higher than radar
5960	1	160	HGR: Gage more than 7.5 times higher than radar
720	1	160	No Gage Data with radar data > 0.1
7360	1	160	LGR: Radar more than 9.4 times higher than gage
7420	1	160	LGR: Radar more than 12.2 times higher than gage
7530	1	160	LGR
760	1	160	No Gage Data with radar data > 0.1
7810	1	160	LGR: Radar more than 4.5 times higher than gage
870	1	160	No Gage Data with radar data > 0.1
KLIC	1	160	No Gage Data with radar data > 0.1
ncdc_1401	1	160	No Gage Data with radar data > 0.1
ncdc_3584	1	160	No Gage Data with radar data > 0.1
ncdc_5352	1	160	No Gage Data with radar data > 0.1
1350	161	300	No Gage Data with radar data > 0.1
2250	161	300	No Gage Data with radar data > 0.1
2260	161	300	No Gage Data with radar data > 0.1
2270	161	300	No Gage Data with radar data > 0.1
2280	161	300	No Gage Data with radar data > 0.1
2750	161	300	No Gage Data with radar data > 0.1
2810	161	300	No Gage Data with radar data > 0.1
2820	161	300	No Gage Data with radar data > 0.1
2850	161	300	No Gage Data with radar data > 0.1
5770	161	300	No Gage Data with radar data > 0.1
5790	161	300	LGR
7260	161	300	No Gage Data with radar data > 0.1
7350	161	300	No Gage Data with radar data > 0.1
7360	161	300	No Gage Data with radar data > 0.1
7560	161	300	No Gage Data with radar data > 0.1
7640	161	300	No Gage Data with radar data > 0.1
7950	161	300	HGR: Gage more than 5.9 times higher than radar
ncdc_1401	161	300	No Gage Data with radar data > 0.1
ncdc_3579	161	300	No Gage Data with radar data > 0.1
ncdc_4293	161	300	HGR: Gage more than 4.9 times higher than radar
1060	301	550	No Gage Data with radar data > 0.1
1200	301	550	No Gage Data with radar data > 0.1
1500	301	550	HGR: Gage more than 9. times higher than radar
1520	301	550	No Gage Data with radar data > 0.1
1600	301	550	LGR: Radar more than 17.4 times higher than gage

Table B.4 – Study period gage maskings (continued).

Gage	Begin	End	Reason
2210	301	550	LGR
2230	301	550	No Gage Data with radar data > 0.1
2340	301	550	LGR: Radar more than 4.3 times higher than gage
2350	301	550	No Gage Data with radar data > 0.1
2370	301	550	No Gage Data with radar data > 0.1
4030	301	550	LGR: Radar more than 4.1 times higher than gage
420	301	550	HGR: Gage more than 4.2 times higher than radar
430	301	550	No Gage Data with radar data > 0.1
440	301	550	No Gage Data with radar data > 0.1
4820	301	550	No Gage Data with radar data > 0.1
520	301	550	No Gage Data with radar data > 0.1
5830	301	550	HGR
5960	301	550	LGR: Radar more than 5.8 times higher than gage
620	301	550	No Gage Data with radar data > 0.1
630	301	550	LGR: Radar more than 7.8 times higher than gage
700	301	550	No Gage Data with radar data > 0.1
710	301	550	No Gage Data with radar data > 0.1
720	301	550	LGR: Radar more than 7.7 times higher than gage
7360	301	550	No Gage Data with radar data > 0.1
7430	301	550	No Gage Data with radar data > 0.1
7520	301	550	No Gage Data with radar data > 0.1
7810	301	550	No Gage Data with radar data > 0.1
800	301	550	No Gage Data with radar data > 0.1
810	301	550	No Gage Data with radar data > 0.1
820	301	550	No Gage Data with radar data > 0.1
830	301	550	LGR: Radar more than 5.7 times higher than gage
840	301	550	No Gage Data with radar data > 0.1
850	301	550	No Gage Data with radar data > 0.1
KDEN	301	550	No Gage Data with radar data > 0.1
ncdc_4293	301	550	No Gage Data with radar data > 0.1
200	551	800	No Gage Data with radar data > 0.1
2190	551	800	LGR: Radar more than 4.2 times higher than gage
2210	551	800	LGR
2260	551	800	No Gage Data with radar data > 0.1
2330	551	800	LGR: Radar more than 8.1 times higher than gage
2340	551	800	LGR
300	551	800	LGR
530	551	800	LGR: Radar more than 4.1 times higher than gage
5780	551	800	No Gage Data with radar data > 0.1
5860	551	800	No Gage Data with radar data > 0.1
7530	551	800	No Gage Data with radar data > 0.1
830	551	800	No Gage Data with radar data > 0.1
KCOS	551	800	LGR
KDEN	551	800	LGR: Radar more than 6.2 times higher than gage
ncdc_1401	551	800	No Gage Data with radar data > 0.1
ncdc_4172	551	800	No Gage Data with radar data > 0.1
ncdc_4293	551	800	No Gage Data with radar data > 0.1
ncdc_7664	551	800	LGR
ncdc_9285	551	800	HGR: Gage more than 4.1 times higher than radar

Table B.3 – Study period gage maskings (continued).

Gage	Begin	End	Reason
1050	801	983	No Gage Data with radar data > 0.1
1370	801	983	No Gage Data with radar data > 0.1
1420	801	983	No Gage Data with radar data > 0.1
150	801	983	LGR
1710	801	983	No Gage Data with radar data > 0.1
220	801	983	No Gage Data with radar data > 0.1
2250	801	983	No Gage Data with radar data > 0.1
2320	801	983	No Gage Data with radar data > 0.1
2330	801	983	No Gage Data with radar data > 0.1
2340	801	983	No Gage Data with radar data > 0.1
2350	801	983	No Gage Data with radar data > 0.1
2370	801	983	No Gage Data with radar data > 0.1
330	801	983	No Gage Data with radar data > 0.1
400	801	983	No Gage Data with radar data > 0.1
4020	801	983	No Gage Data with radar data > 0.1
410	801	983	No Gage Data with radar data > 0.1
420	801	983	No Gage Data with radar data > 0.1
430	801	983	No Gage Data with radar data > 0.1
440	801	983	No Gage Data with radar data > 0.1
4820	801	983	No Gage Data with radar data > 0.1
500	801	983	No Gage Data with radar data > 0.1
510	801	983	No Gage Data with radar data > 0.1
520	801	983	No Gage Data with radar data > 0.1
540	801	983	No Gage Data with radar data > 0.1
5740	801	983	HGR: Gage more than 11.3 times higher than radar
5760	801	983	No Gage Data with radar data > 0.1
5790	801	983	No Gage Data with radar data > 0.1
5830	801	983	No Gage Data with radar data > 0.1
5930	801	983	HGR: Gage more than 4.9 times higher than radar
5960	801	983	No Gage Data with radar data > 0.1
600	801	983	No Gage Data with radar data > 0.1
610	801	983	No Gage Data with radar data > 0.1
640	801	983	No Gage Data with radar data > 0.1
710	801	983	No Gage Data with radar data > 0.1
720	801	983	No Gage Data with radar data > 0.1
7250	801	983	No Gage Data with radar data > 0.1
7260	801	983	HGR: Gage more than 4.9 times higher than radar
7350	801	983	No Gage Data with radar data > 0.1
7360	801	983	No Gage Data with radar data > 0.1
7410	801	983	No Gage Data with radar data > 0.1
7530	801	983	LGR
7810	801	983	No Gage Data with radar data > 0.1
7950	801	983	No Gage Data with radar data > 0.1
820	801	983	No Gage Data with radar data > 0.1
830	801	983	No Gage Data with radar data > 0.1
KCOS	801	983	LGR
ncdc_4720	801	983	No Gage Data with radar data > 0.1
ncdc_5765	801	983	No Gage Data with radar data > 0.1

Table B.4 – Study period gage maskings (continued).

Gage Maskings for July 15, 2005

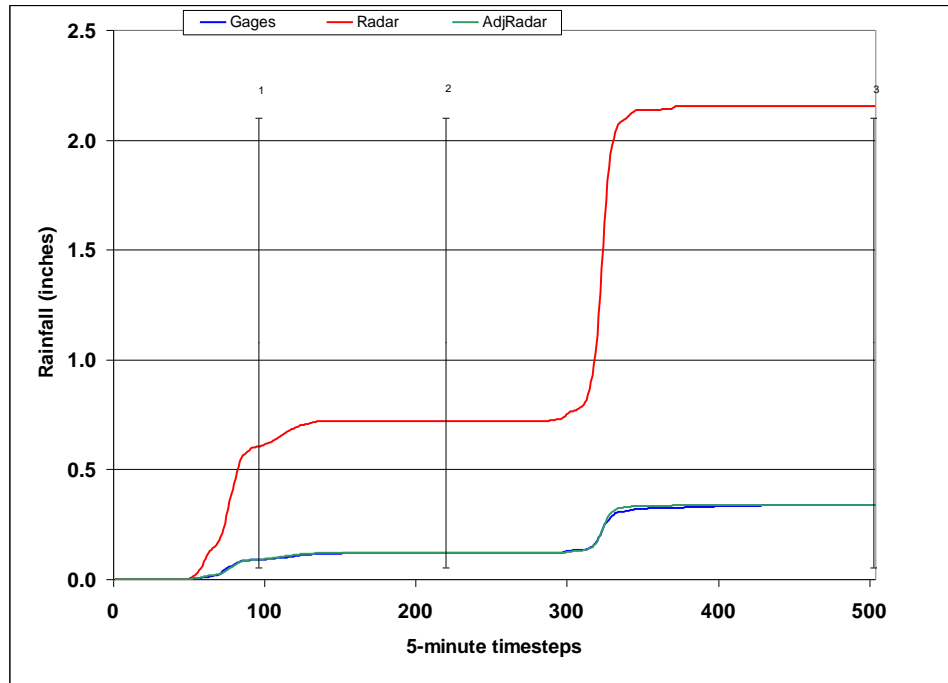


Figure B.5– Study period breakpoints.

Gage	Begin	End	Reason
7000	1	96	No Gage Data with radar data > 0.1
7010	1	96	LGR
7030	1	96	No Gage Data with radar data > 0.1
7075	1	96	No Gage Data with radar data > 0.1
7300	1	96	LGR
7400	1	96	LGR: Radar more than 4.4 times higher than gage
7470	1	96	No Gage Data with radar data > 0.1
7550	1	96	LGR: Radar more than 11.5 times higher than gage
7950	1	96	No Gage Data with radar data > 0.1
ncdc_2965	1	96	HGR
1500	97	220	HGR: Gage more than 5.2 times higher than radar
2810	97	220	LGR
420	97	220	HGR
5790	97	220	No Gage Data with radar data > 0.1
5960	97	220	No Gage Data with radar data > 0.1
600	97	220	HGR: Gage more than 4.9 times higher than radar
7030	97	220	No Gage Data with radar data > 0.1
7040	97	220	No Gage Data with radar data > 0.1
7260	97	220	No Gage Data with radar data > 0.1
7310	97	220	No Gage Data with radar data > 0.1
7400	97	220	No Gage Data with radar data > 0.1
7420	97	220	No Gage Data with radar data > 0.1
7440	97	220	No Gage Data with radar data > 0.1
7560	97	220	HGR
830	97	220	HGR
ncdc_1778	97	220	No Gage Data with radar data > 0.1
ncdc_2965	97	220	No Gage Data with radar data > 0.1
1500	221	503	No Gage Data with radar data > 0.1
1600	221	503	LGR
2280	221	503	No Gage Data with radar data > 0.1
2330	221	503	No Gage Data with radar data > 0.1
2360	221	503	No Gage Data with radar data > 0.1
420	221	503	No Gage Data with radar data > 0.1
430	221	503	LGR
510	221	503	LGR
520	221	503	LGR: Radar more than 9.4 times higher than gage
5720	221	503	No Gage Data with radar data > 0.1
5730	221	503	No Gage Data with radar data > 0.1
5740	221	503	No Gage Data with radar data > 0.1
5810	221	503	No Gage Data with radar data > 0.1
7150	221	503	No Gage Data with radar data > 0.1
7260	221	503	No Gage Data with radar data > 0.1
7310	221	503	No Gage Data with radar data > 0.1
7470	221	503	No Gage Data with radar data > 0.1
7550	221	503	No Gage Data with radar data > 0.1
7570	221	503	No Gage Data with radar data > 0.1
7850	221	503	No Gage Data with radar data > 0.1
850	221	503	LGR
KMNH	221	503	LGR: Radar more than 5.4 times higher than gage
ncdc_3579	221	503	No Gage Data with radar data > 0.1
ncdc_5352	221	503	No Gage Data with radar data > 0.1

Table B.5 – Study period gage maskings.

Gage Maskings for August 26, 2006

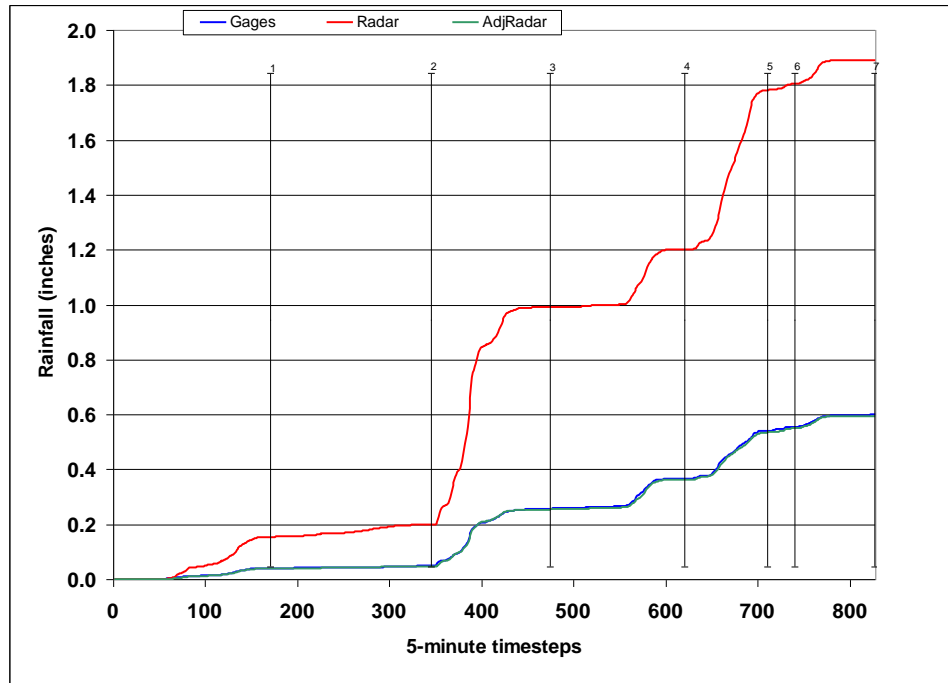


Figure B.6– Study period breakpoints.

Gage	Begin	End	Reason
1000	1	170	No Gage Data with radar data > 0.1
1010	1	170	No Gage Data with radar data > 0.1
1030	1	170	No Gage Data with radar data > 0.1
1040	1	170	No Gage Data with radar data > 0.1
1050	1	170	No Gage Data with radar data > 0.1
1060	1	170	No Gage Data with radar data > 0.1
1320	1	170	No Gage Data with radar data > 0.1
1340	1	170	No Gage Data with radar data > 0.1
1350	1	170	No Gage Data with radar data > 0.1
1360	1	170	No Gage Data with radar data > 0.1
1370	1	170	No Gage Data with radar data > 0.1
1420	1	170	No Gage Data with radar data > 0.1
1440	1	170	No Gage Data with radar data > 0.1
1480	1	170	HGR: Gage more than 6. times higher than radar
1500	1	170	No Gage Data with radar data > 0.1
1600	1	170	No Gage Data with radar data > 0.1
1620	1	170	No Gage Data with radar data > 0.1
1640	1	170	No Gage Data with radar data > 0.1
1710	1	170	No Gage Data with radar data > 0.1
1720	1	170	No Gage Data with radar data > 0.1
220	1	170	No Gage Data with radar data > 0.1
2230	1	170	No Gage Data with radar data > 0.1
2240	1	170	No Gage Data with radar data > 0.1
2250	1	170	No Gage Data with radar data > 0.1
2270	1	170	No Gage Data with radar data > 0.1
2310	1	170	No Gage Data with radar data > 0.1
2320	1	170	No Gage Data with radar data > 0.1
2330	1	170	No Gage Data with radar data > 0.1
2350	1	170	No Gage Data with radar data > 0.1
2360	1	170	No Gage Data with radar data > 0.1
2370	1	170	No Gage Data with radar data > 0.1
2710	1	170	No Gage Data with radar data > 0.1
2730	1	170	No Gage Data with radar data > 0.1
300	1	170	No Gage Data with radar data > 0.1
430	1	170	No Gage Data with radar data > 0.1
440	1	170	No Gage Data with radar data > 0.1
520	1	170	No Gage Data with radar data > 0.1
530	1	170	No Gage Data with radar data > 0.1
5770	1	170	No Gage Data with radar data > 0.1
600	1	170	No Gage Data with radar data > 0.1
610	1	170	No Gage Data with radar data > 0.1
620	1	170	No Gage Data with radar data > 0.1
630	1	170	No Gage Data with radar data > 0.1
640	1	170	No Gage Data with radar data > 0.1
650	1	170	No Gage Data with radar data > 0.1
7030	1	170	No Gage Data with radar data > 0.1
7040	1	170	No Gage Data with radar data > 0.1
720	1	170	No Gage Data with radar data > 0.1
7260	1	170	No Gage Data with radar data > 0.1
7320	1	170	No Gage Data with radar data > 0.1
7420	1	170	No Gage Data with radar data > 0.1
7440	1	170	No Gage Data with radar data > 0.1

Table B.6 – Study period gage maskings.

Gage	Begin	End	Reason
750	1	170	No Gage Data with radar data > 0.1
7530	1	170	No Gage Data with radar data > 0.1
760	1	170	No Gage Data with radar data > 0.1
7600	1	170	No Gage Data with radar data > 0.1
7810	1	170	No Gage Data with radar data > 0.1
830	1	170	No Gage Data with radar data > 0.1
870	1	170	No Gage Data with radar data > 0.1
KPUB	1	170	No Gage Data with radar data > 0.1
ncdc_1547	1	170	No Gage Data with radar data > 0.1
ncdc_3386	1	170	No Gage Data with radar data > 0.1
ncdc_3584	1	170	No Gage Data with radar data > 0.1
ncdc_4293	1	170	No Gage Data with radar data > 0.1
ncdc_5352	1	170	No Gage Data with radar data > 0.1
ncdc_5765	1	170	No Gage Data with radar data > 0.1
ncdc_6740	1	170	No Gage Data with radar data > 0.1
ncdc_9285	1	170	No Gage Data with radar data > 0.1
1440	171	345	No Gage Data with radar data > 0.1
1500	171	345	HGR: Gage more than 31.2 times higher than radar
2260	171	345	No Gage Data with radar data > 0.1
2270	171	345	HGR: Gage more than 4.9 times higher than radar
5810	171	345	HGR: Gage more than 29.5 times higher than radar
5940	171	345	HGR: Gage more than 5.6 times higher than radar
ncdc_1179	171	345	No Gage Data with radar data > 0.1
ncdc_1539	171	345	No Gage Data with radar data > 0.1
ncdc_6136	171	345	No Gage Data with radar data > 0.1
ncdc_7320	171	345	No Gage Data with radar data > 0.1
1350	346	474	No Gage Data with radar data > 0.1
1360	346	474	No Gage Data with radar data > 0.1
150	346	474	LGR: Radar more than 5.1 times higher than gage
1500	346	474	No Gage Data with radar data > 0.1
1520	346	474	No Gage Data with radar data > 0.1
1530	346	474	No Gage Data with radar data > 0.1
1600	346	474	No Gage Data with radar data > 0.1
1620	346	474	No Gage Data with radar data > 0.1
1640	346	474	No Gage Data with radar data > 0.1
1720	346	474	No Gage Data with radar data > 0.1
1800	346	474	No Gage Data with radar data > 0.1
2350	346	474	No Gage Data with radar data > 0.1
2710	346	474	No Gage Data with radar data > 0.1
2810	346	474	No Gage Data with radar data > 0.1
2840	346	474	No Gage Data with radar data > 0.1
330	346	474	No Gage Data with radar data > 0.1
400	346	474	No Gage Data with radar data > 0.1
430	346	474	No Gage Data with radar data > 0.1
440	346	474	No Gage Data with radar data > 0.1
500	346	474	No Gage Data with radar data > 0.1
520	346	474	No Gage Data with radar data > 0.1
530	346	474	No Gage Data with radar data > 0.1
540	346	474	No Gage Data with radar data > 0.1
5790	346	474	No Gage Data with radar data > 0.1
5800	346	474	No Gage Data with radar data > 0.1
5810	346	474	LGR: Radar more than 33.2 times higher than gage

Table B.6 – Study period gage maskings (continued).

Gage	Begin	End	Reason
5880	346	474	LGR: Radar more than 5.3 times higher than gage
600	346	474	No Gage Data with radar data > 0.1
610	346	474	No Gage Data with radar data > 0.1
620	346	474	No Gage Data with radar data > 0.1
650	346	474	No Gage Data with radar data > 0.1
700	346	474	No Gage Data with radar data > 0.1
710	346	474	No Gage Data with radar data > 0.1
800	346	474	No Gage Data with radar data > 0.1
810	346	474	No Gage Data with radar data > 0.1
820	346	474	No Gage Data with radar data > 0.1
840	346	474	No Gage Data with radar data > 0.1
860	346	474	No Gage Data with radar data > 0.1
870	346	474	No Gage Data with radar data > 0.1
900	346	474	No Gage Data with radar data > 0.1
KCOS	346	474	HGR
ncdc_1179	346	474	No Gage Data with radar data > 0.1
ncdc_3386	346	474	No Gage Data with radar data > 0.1
ncdc_4172	346	474	HGR: Gage more than 100. times higher than radar
ncdc_4742	346	474	No Gage Data with radar data > 0.1
ncdc_5352	346	474	LGR: Radar more than 5.4 times higher than gage
ncdc_5765	346	474	No Gage Data with radar data > 0.1
1320	475	620	No Gage Data with radar data > 0.1
1420	475	620	No Gage Data with radar data > 0.1
1800	475	620	No Gage Data with radar data > 0.1
430	475	620	HGR
520	475	620	No Gage Data with radar data > 0.1
7570	475	620	HGR: Gage more than 7.8 times higher than radar
7640	475	620	LGR
800	475	620	No Gage Data with radar data > 0.1
840	475	620	No Gage Data with radar data > 0.1
ncdc_4742	475	620	HGR
1440	621	710	LGR
5760	621	710	LGR
5800	621	710	LGR: Radar more than 4.4 times higher than gage
5820	621	710	LGR
7640	621	710	LGR
KLIC	621	710	HGR
ncdc_3579	621	710	LGR
ncdc_7320	621	710	LGR: Radar more than 4.5 times higher than gage
ncdc_7320	621	710	HGR
ncdc_7320	621	710	HGR
ncdc_1539	711	740	LGR
ncdc_4172	711	740	No Data
2240	741	827	HGR
5760	741	827	No Data
5830	741	827	HGR
7040	741	827	LGR
7530	741	827	No Data
ncdc_1547	741	827	HGR
ncdc_4172	741	827	HGR
ncdc_4742	741	827	HGR

Table B.6 – Study period gage maskings (continued).

Appendix C – Other supporting graphics

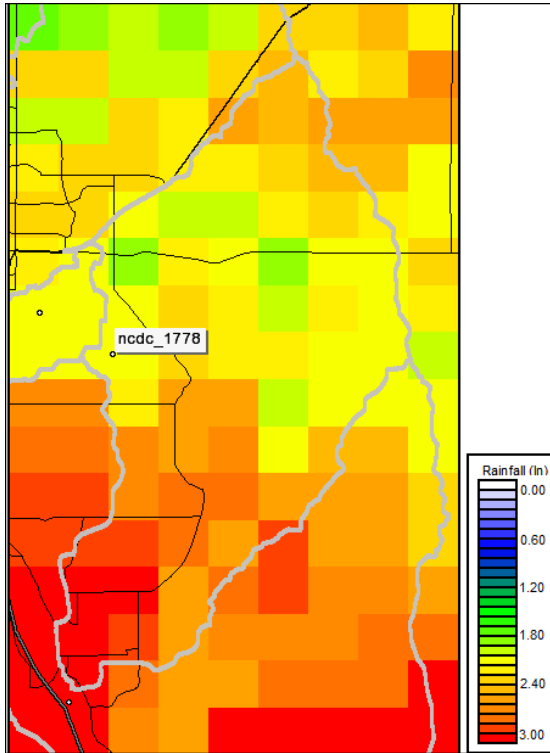


Figure C1 – May 17, 1995 event totals.

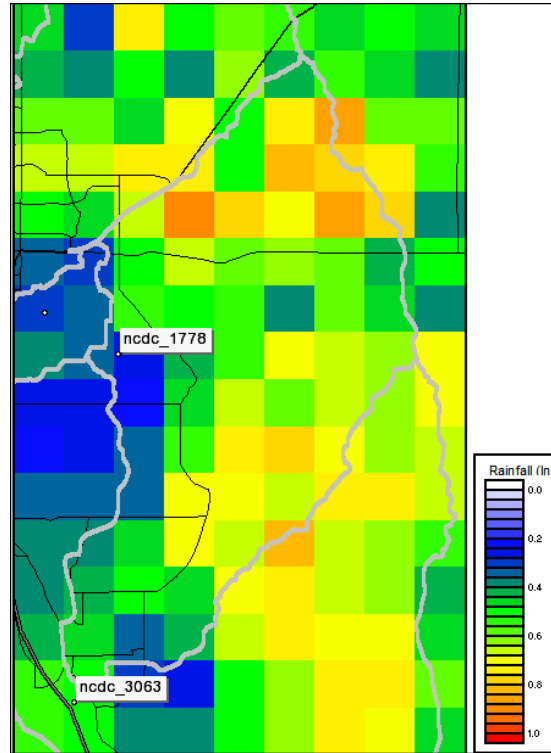


Figure C2 – August 15, 1996 event totals.

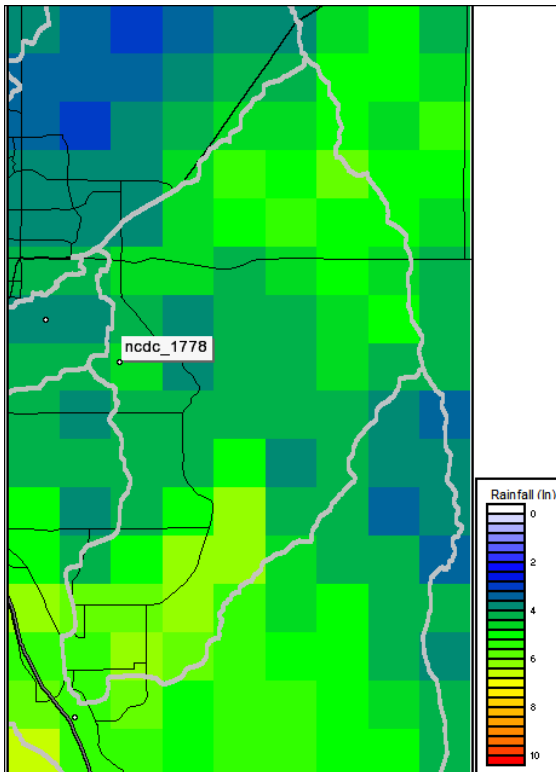


Figure C3 – July 31, 1999 event totals.

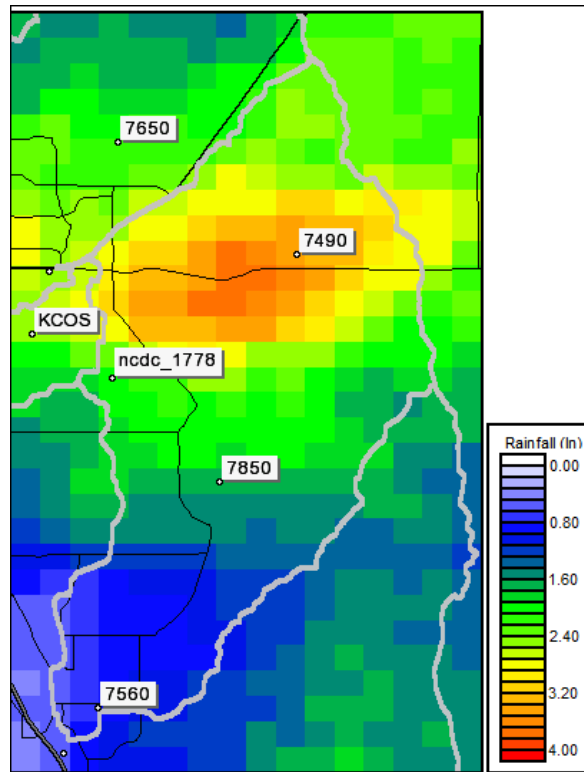


Figure C4 – August 4, 2004 event totals.

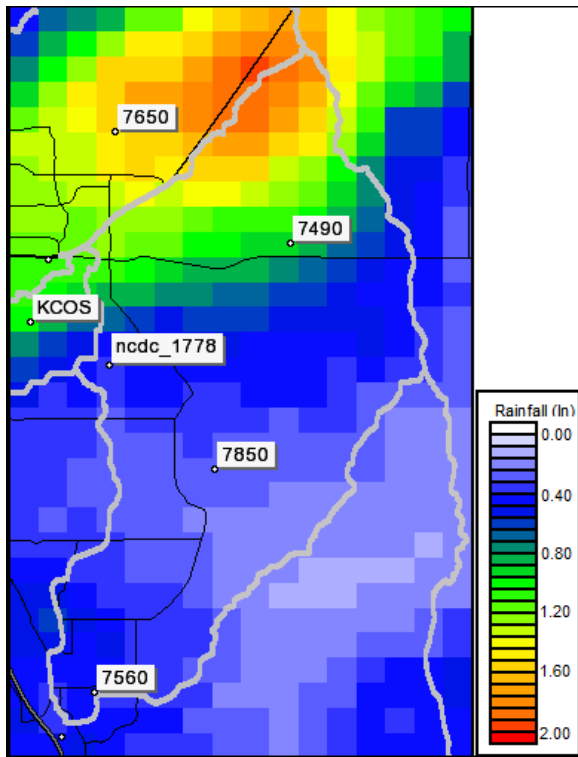


Figure C5 – July 15, 2005 event totals.

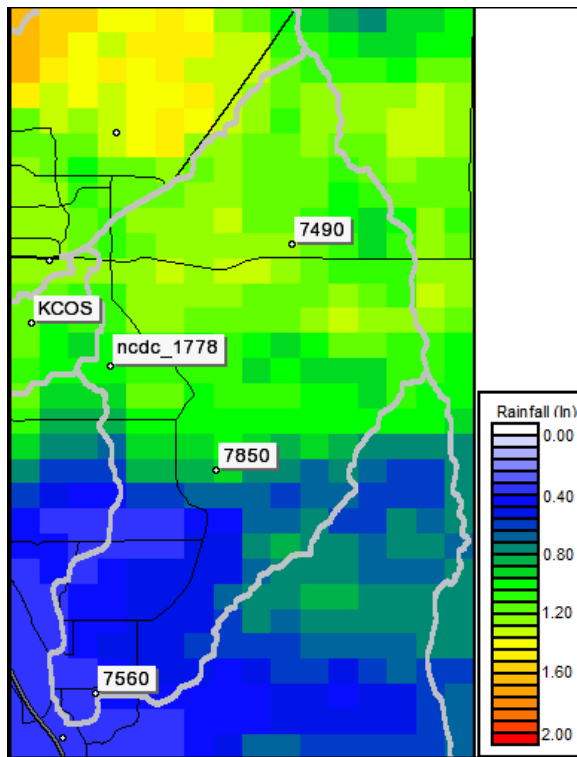


Figure C6 – August 26, 2006 event totals.

References

Seo, D.J., Krajewski, W.F and Bowles, D.S., 1990. Stochastic Interpolation of Rainfall Data From Rain Gages and Radar Using CoKriging 1. Design of Experiments, *Water Resources Research*, 26, NO. 3, 469-477.



Experts at measuring rainfall and its consequences.

12.0 Appendix B: TITAN GARR Verification Gage Lists and Accumulation Plots

Green highlights indicate verification gages

Gage ID	Mask %						
KCOS	79	4100	49	4270	38	4340	24
KLIC	76	1110	49	4510	38	ncdc_843	24
ncdc_7428	74	4060	49	2710	37	ncdc_4742	24
2750	72	ncdc_1179	49	ncdc_2790	37	610	24
1400	71	4260	48	ncdc_2354	36	530	24
ncdc_5881	71	KLHX	48	ncdc_3386	36	410	24
4190	69	1420	47	440	35	400	24
ncdc_9285	67	4080	47	510	35	1660	24
ncdc_1547	66	ncdc_5352	47	4530	35	1920	24
4470	65	1710	46	ncdc_3579	33	1620	24
ncdc_4877	65	760	46	540	31	1640	24
KPUB	62	820	46	1810	31	ncdc_183	23
2810	61	700	46	2370	31	ncdc_5121	23
4220	61	420	46	2320	31	ncdc_6023	23
4310	61	500	46	1000	31	ncdc_7664	23
4300	59	1800	46	100	31	ncdc_4538	22
4250	58	2850	45	300	31	4490	21
ncdc_3007	58	630	45	1030	31	640	21
2360	56	620	45	120	31	2330	21
1010	56	310	45	200	31	2230	21
330	56	4020	45	220	31	4180	21
110	56	ncdc_3553	45	4050	31	2250	21
1900	56	ncdc_7296	45	4550	31	1100	21
4070	56	2260	44	4360	31	ncdc_109	20
4090	56	4030	44	4010	31	ncdc_1778	19
4150	56	ncdc_2211	41	4570	31	ncdc_263	17
4230	56	ncdc_7866	41	4110	31	ncdc_7572	16
4330	56	4790	40	4140	31	1200	14
210	54	ncdc_2220	40	4130	31	ncdc_4388	14
2730	53	ncdc_130	40	4160	31	ncdc_2965	13
750	53	ncdc_6136	40	4290	31	ncdc_8781	11
710	53	ncdc_8429	40	ncdc_4172	31	ncdc_1539	10
520	53	1600	38	4170	30	ncdc_1401	10
430	53	600	38	4350	30	ncdc_3584	10
4040	53	2350	38	730	29	ncdc_3477	8
ncdc_5922	53	2240	38	830	29	ncdc_2535	7
ncdc_8220	53	2310	38	810	29	ncdc_6740	7
2280	52	320	38	800	29	ncdc_8436	7
150	52	2270	38	ncdc_5765	29	ncdc_9210	7
4200	51	2210	38	2340	28	ncdc_7560	6
1720	49	4240	38	4730	28	ncdc_304	0
1050	49	4710	38	KALS	28	ncdc_4380	0
1040	49	4520	38	ncdc_3500	28	ncdc_7519	0
1060	49						

*Table A1 – Verification gages selected for 1999-2002 study periods.
Masking percentages are from April 1999.*

Gage ID	Mask %								
7640	62	4360	25	4170	18	4140	11	7450	5
ncdc_7560	58	4100	25	2340	17	4230	11	7250	5
ncdc_834	55	KDEN	25	300	17	4220	11	7600	5
ncdc_4293	55	ncdc_3005	25	330	17	ncdc_5934	11	7800	5
ncdc_7519	54	ncdc_8429	25	4470	17	7150	10	830	5
ncdc_1401	53	1310	24	4520	17	7420	10	1340	5
7370	50	ncdc_3477	24	4260	17	7410	10	2330	5
ncdc_3386	49	ncdc_843	24	6330	17	1920	10	4730	5
KAPA	47	630	23	6200	17	6550	10	4710	5
KITR	47	600	23	KCOS	17	2250	10	7300	4
5450	45	1400	23	KLIC	17	1200	10	7350	4
1810	45	200	23	ncdc_4380	17	1100	10	7320	4
ncdc_109	45	310	23	650	16	4200	10	5730	4
1360	44	1900	23	610	16	4150	10	5940	4
1030	44	4770	23	530	16	4160	10	5760	4
ncdc_304	44	4350	23	2190	16	6610	10	750	4
ncdc_7428	40	820	22	4010	16	6440	10	1800	4
1500	38	2710	22	3339	16	6070	10	1530	4
1040	38	2280	22	6620	16	KFNL	10	120	4
2320	37	2350	22	6190	16	KLHX	10	2270	4
7560	36	2360	22	6010	16	ncdc_6740	10	1110	4
1420	36	4040	22	2730	15	ncdc_7572	10	4190	4
KGXY	36	4810	22	710	15	KPUB	10	3439	4
2310	35	4250	22	430	15	4090	9	3119	4
4490	35	ncdc_2535	22	840	15	ncdc_5881	9	3219	4
ncdc_2220	35	5930	21	700	15	7260	8	6350	4
2840	34	2750	21	4020	15	730	8	6480	4
4550	34	2810	21	4130	15	870	8	6290	4
ncdc_4155	34	900	21	4240	15	4750	8	6090	4
7570	33	1600	21	KLAA	15	4330	8	6180	4
110	32	4050	21	ncdc_3007	15	4290	8	6230	4
ncdc_5121	32	6430	21	7360	14	4340	8	6340	4
ncdc_5765	32	ncdc_1547	21	1520	14	ncdc_3500	8	6100	4
7750	31	ncdc_4082	21	3239	14	7010	7	510	3
7040	31	7400	20	6060	14	7850	7	7490	0
1330	31	7470	20	ncdc_7320	14	7530	7	7430	0
1320	31	7000	20	7950	13	1440	7	5860	0
ncdc_7296	31	7110	20	500	13	7810	7	5880	0
ncdc_7664	31	6510	20	7100	13	5740	7	5720	0
7460	30	KALS	20	6630	13	440	7	5900	0
2370	30	KAKO	20	1370	13	520	7	5960	0
4310	30	ncdc_2354	20	320	13	100	7	5830	0
5780	29	ncdc_6023	20	210	13	4530	7	5790	0
1620	29	7650	19	2260	13	4270	7	1710	0
1000	29	5820	19	4060	13	3319	7	760	0
ncdc_2790	29	5800	19	4180	13	6250	7	640	0
ncdc_8781	29	620	19	3379	13	6380	7	420	0
7520	28	410	19	6280	13	6040	7	1300	0
540	28	1720	19	6470	13	6490	7	150	0
4820	28	400	19	6030	13	6530	7	4570	0
7497	27	1480	19	6600	13	6130	7	4850	0
7075	27	1660	19	6460	13	6210	7	4860	0
4790	27	1010	19	4830	12	6320	7	4300	0
5770	26	ncdc_183	19	4110	12	6270	7	3359	0
4510	26	ncdc_3553	19	7550	11	6370	7	6020	0
3419	26	ncdc_4172	19	7200	11	ncdc_130	7	6420	0
KSPD	26	7280	18	7440	11	ncdc_5352	7	6160	0
5810	25	2820	18	7030	11	ncdc_8436	7	KMNH	0
850	25	810	18	720	11	ncdc_9210	7	ncdc_1539	0
2240	25	800	18	1350	11	KTAD	7	ncdc_1778	0
2230	25	2210	18	1050	11	6640	6	ncdc_4720	0
1060	25	4030	18	220	11	7310	5	ncdc_8997	0
4840	25	4070	18	4080	11				

*Table A2 – Verification gages selected for post-2002 study periods.
Masking percentages are from August 2005.*

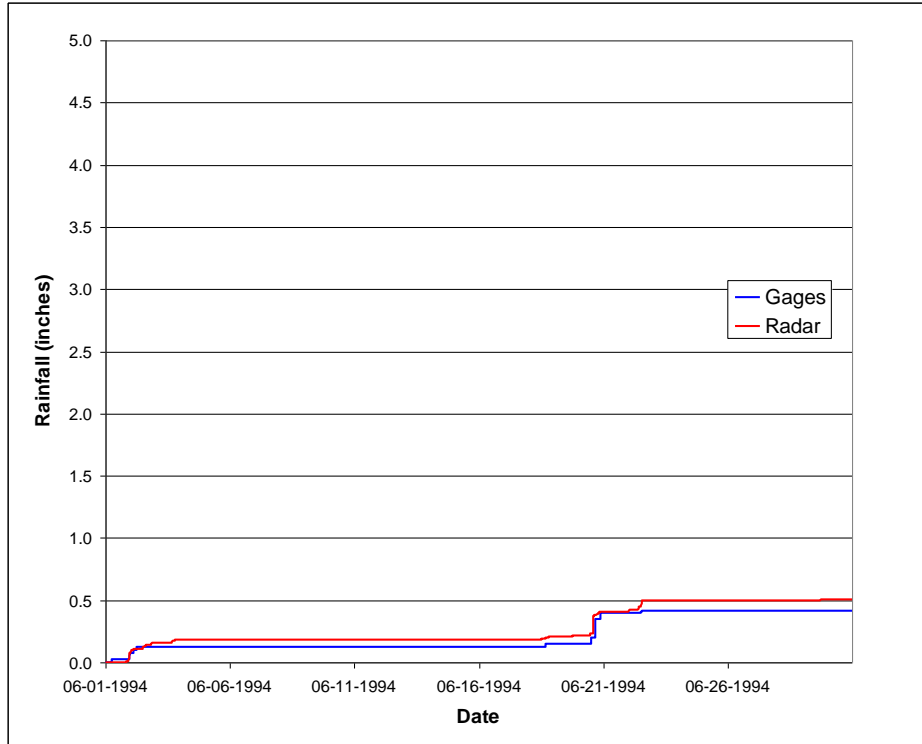


Figure A1 - Average accumulation plot for verification gages and co-located radar pixels.

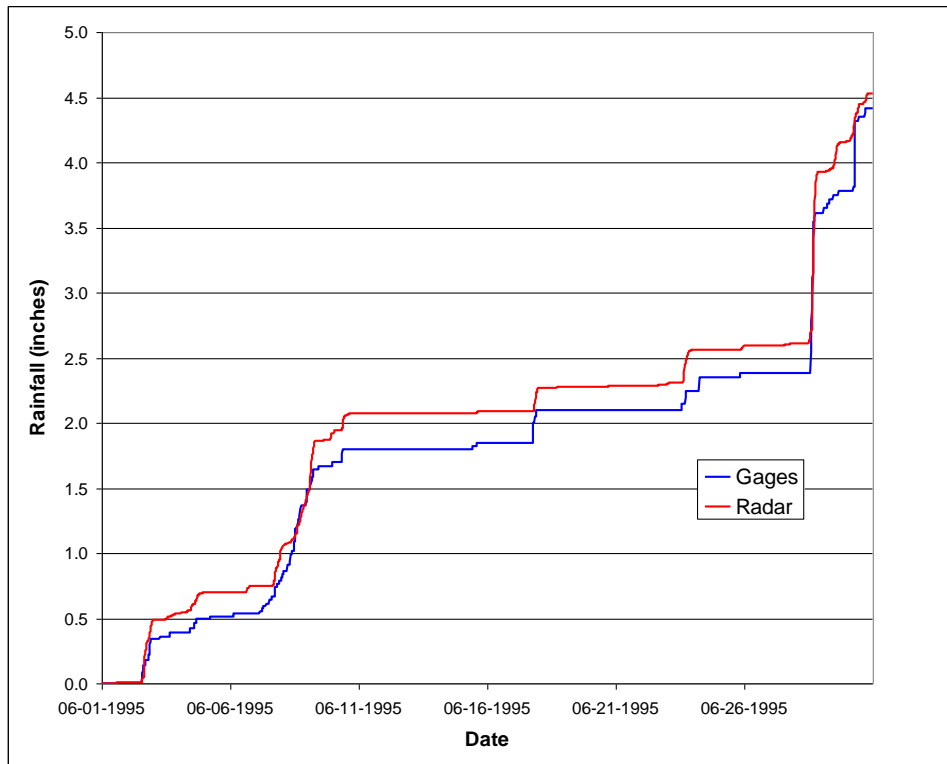


Figure A2 - Average accumulation plot for verification gages and co-located radar pixels.

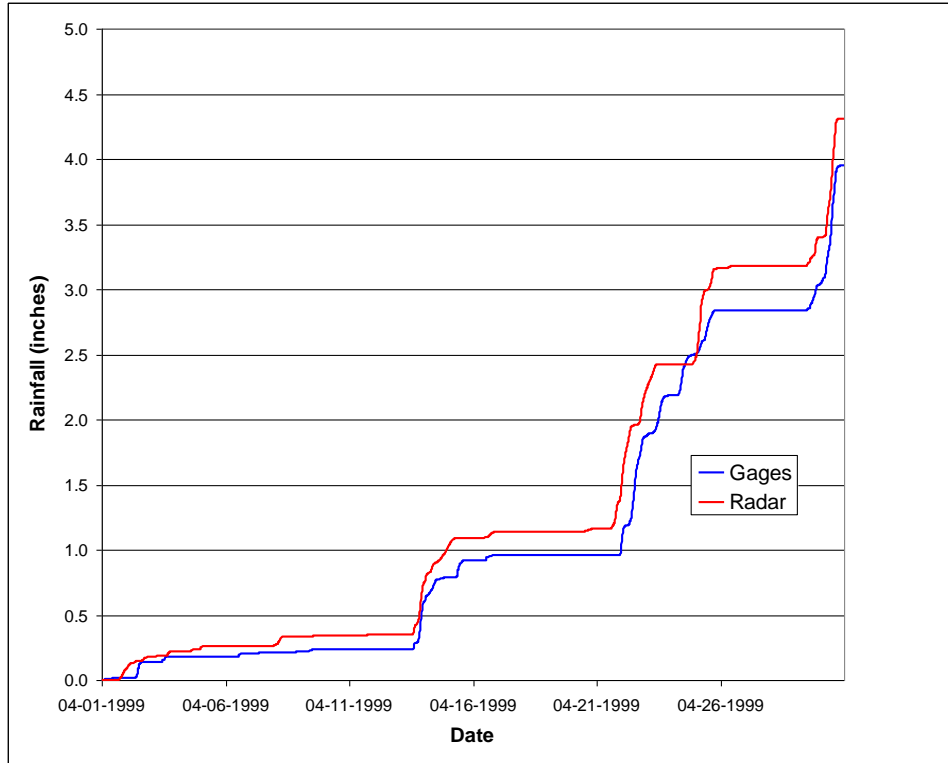


Figure A3 - Average accumulation plot for verification gages and co-located radar pixels.

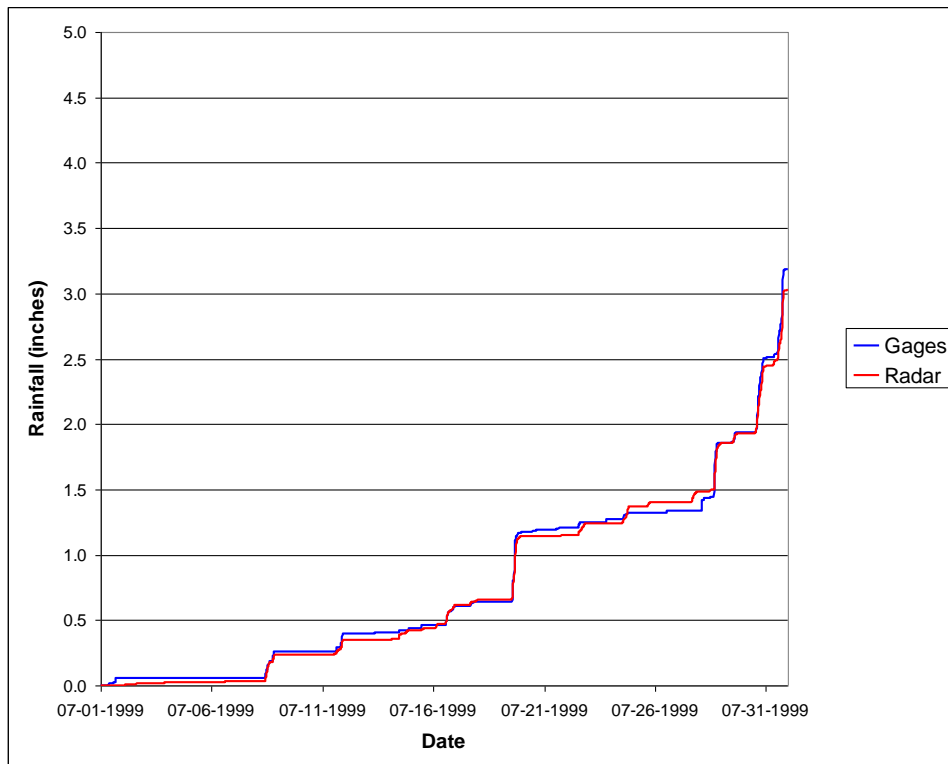


Figure A4 - Average accumulation plot for verification gages and co-located radar pixels.

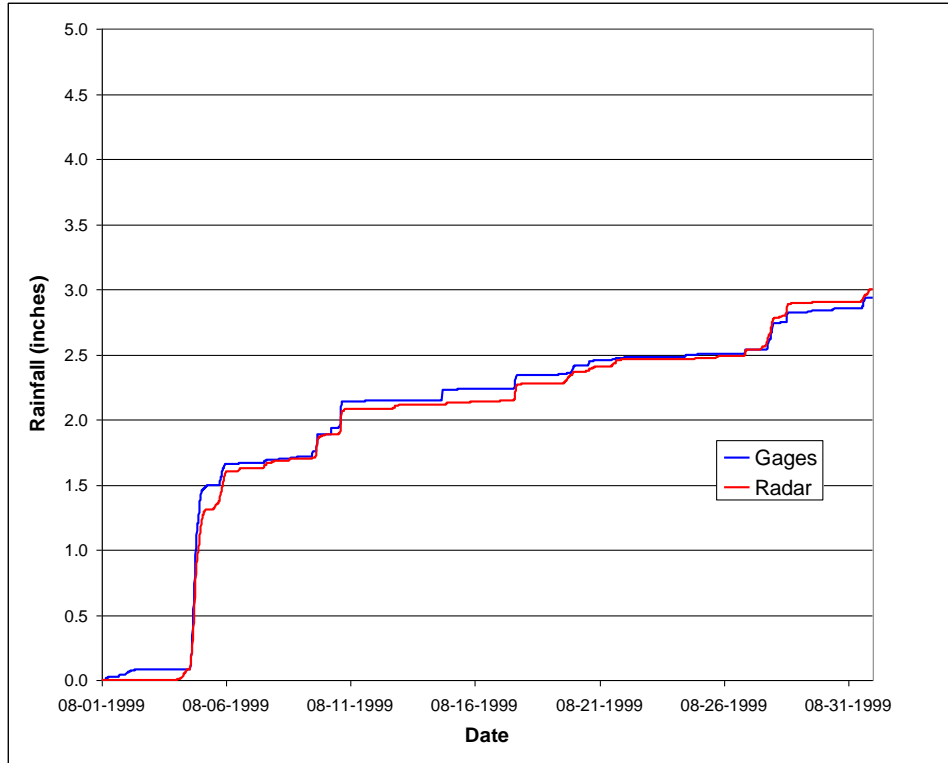


Figure A5 - Average accumulation plot for verification gages and co-located radar pixels.

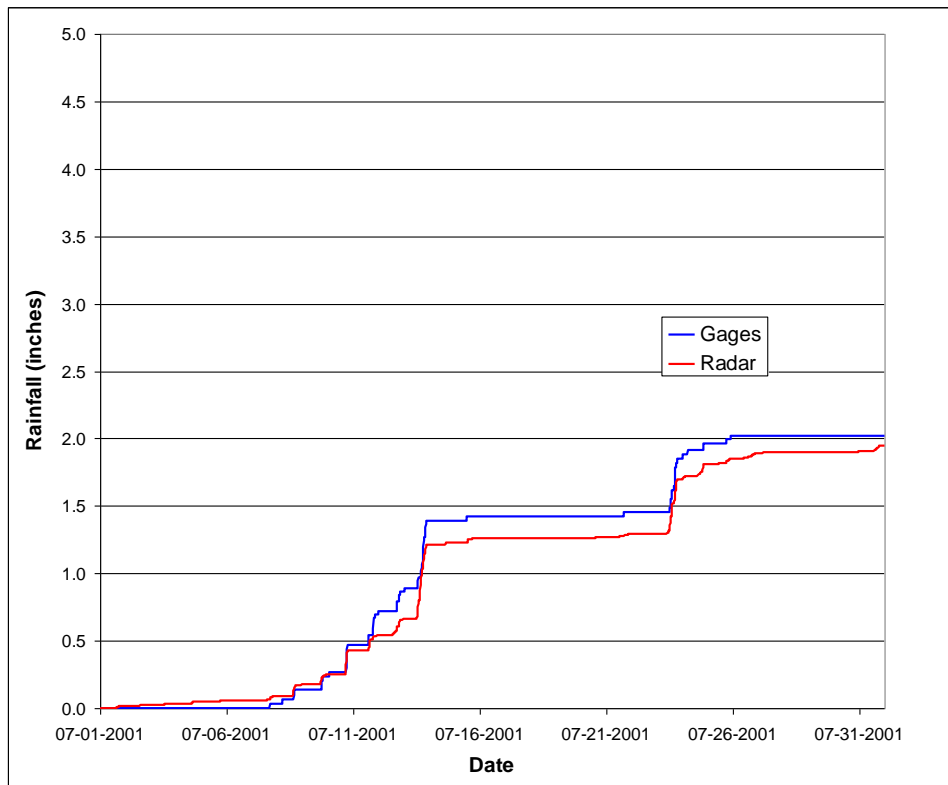


Figure A6 - Average accumulation plot for verification gages and co-located radar pixels.

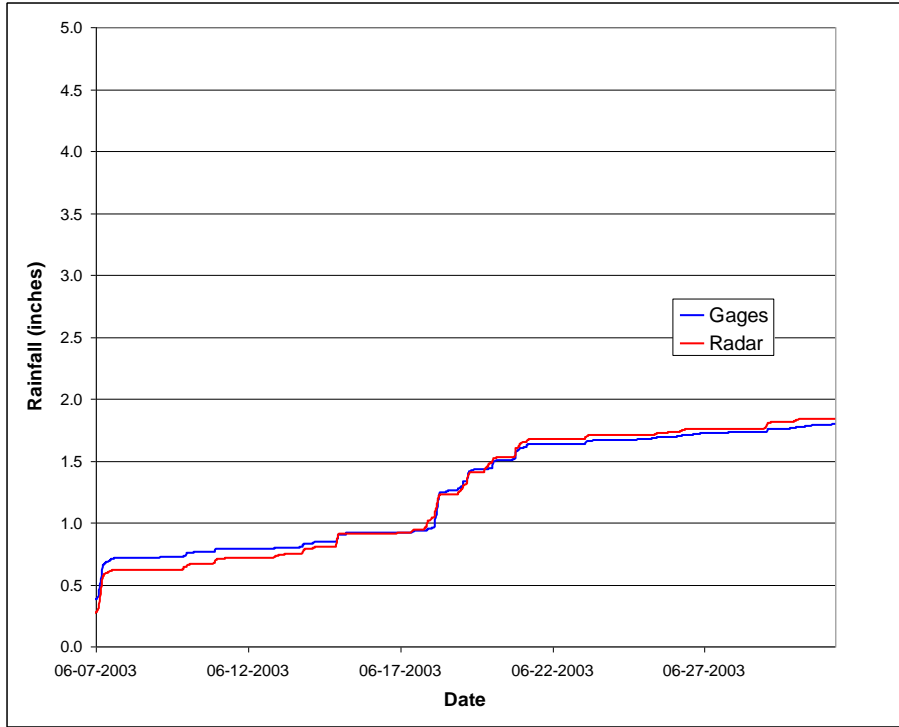


Figure A7 - Average accumulation plot for verification gages and co-located radar pixels.

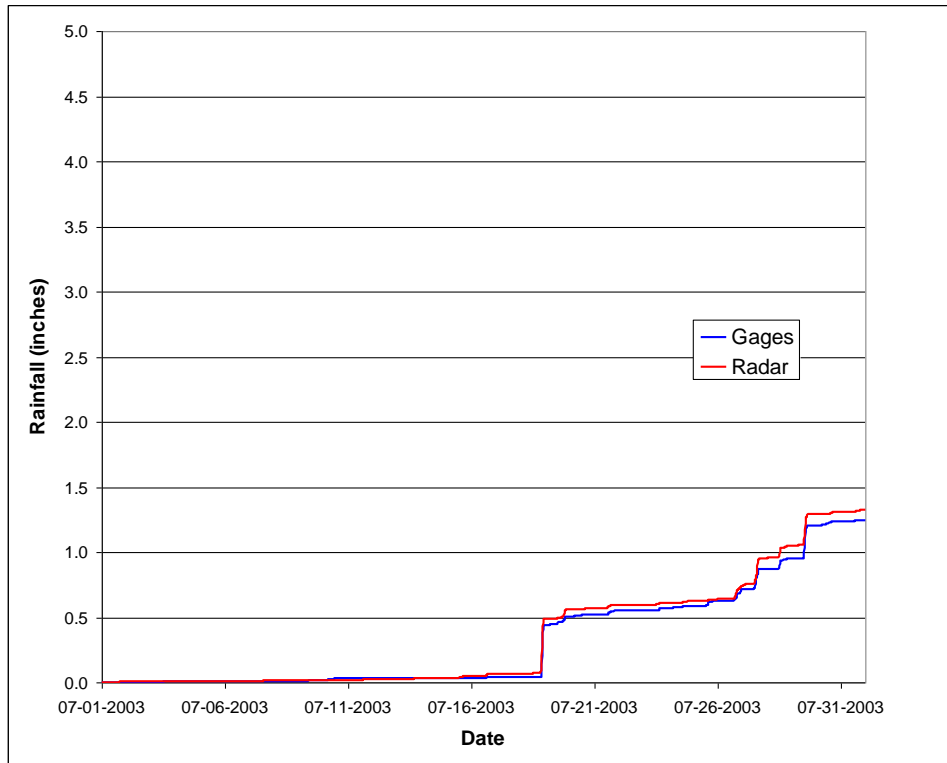


Figure A8 - Average accumulation plot for verification gages and co-located radar pixels.

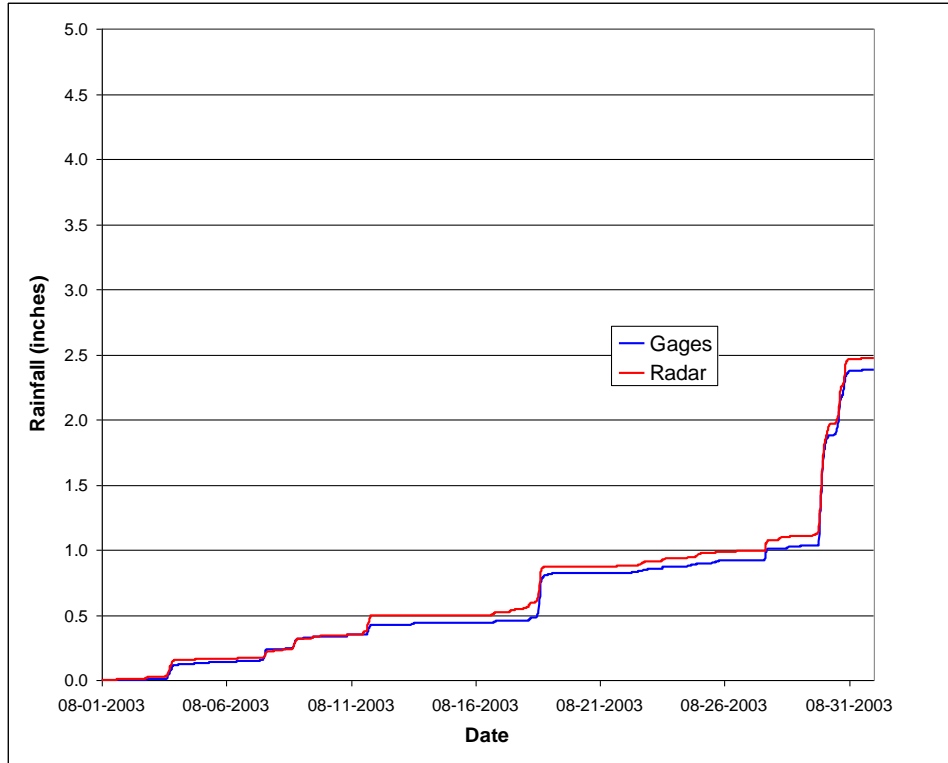


Figure A9 - Average accumulation plot for verification gages and co-located radar pixels.

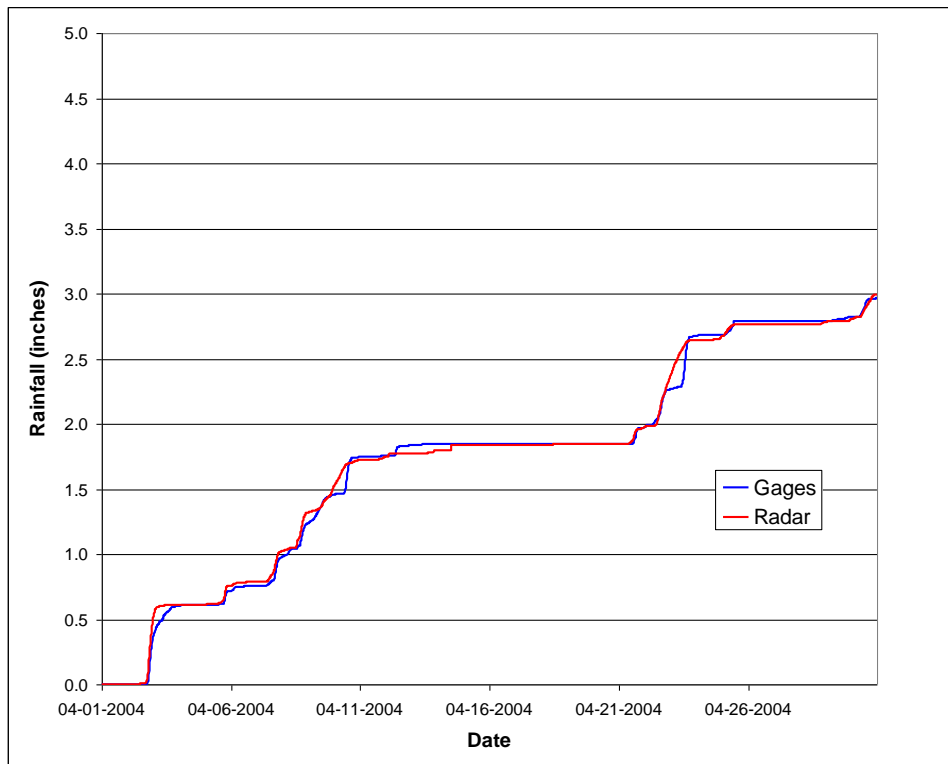


Figure A10 - Average accumulation plot for verification gages and co-located radar pixels.

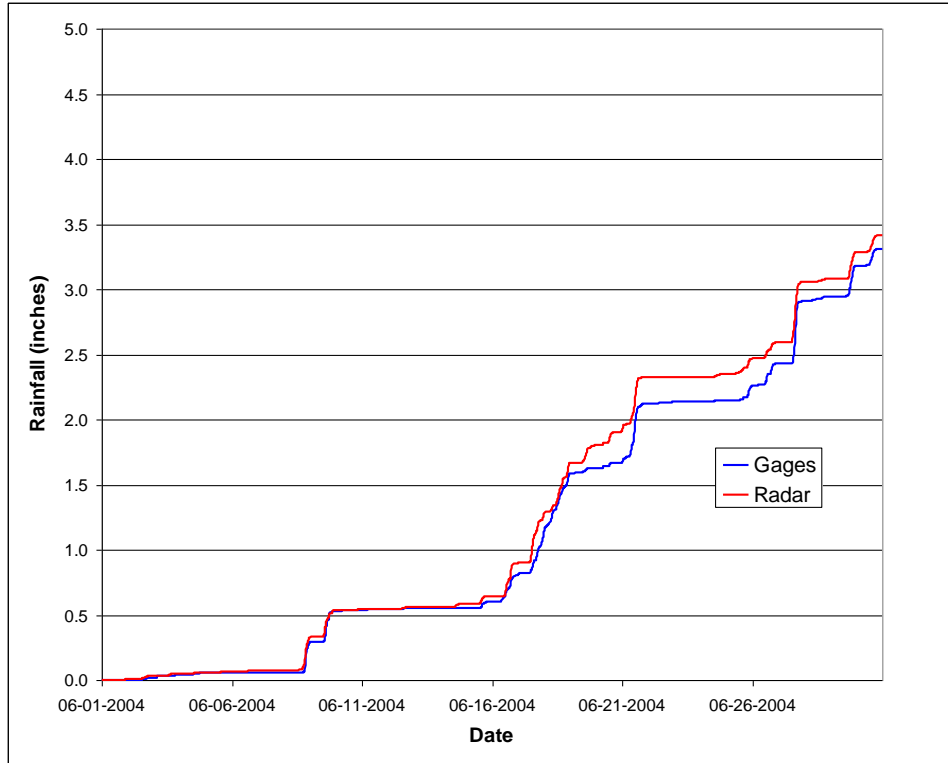


Figure A11 - Average accumulation plot for verification gages and co-located radar pixels.

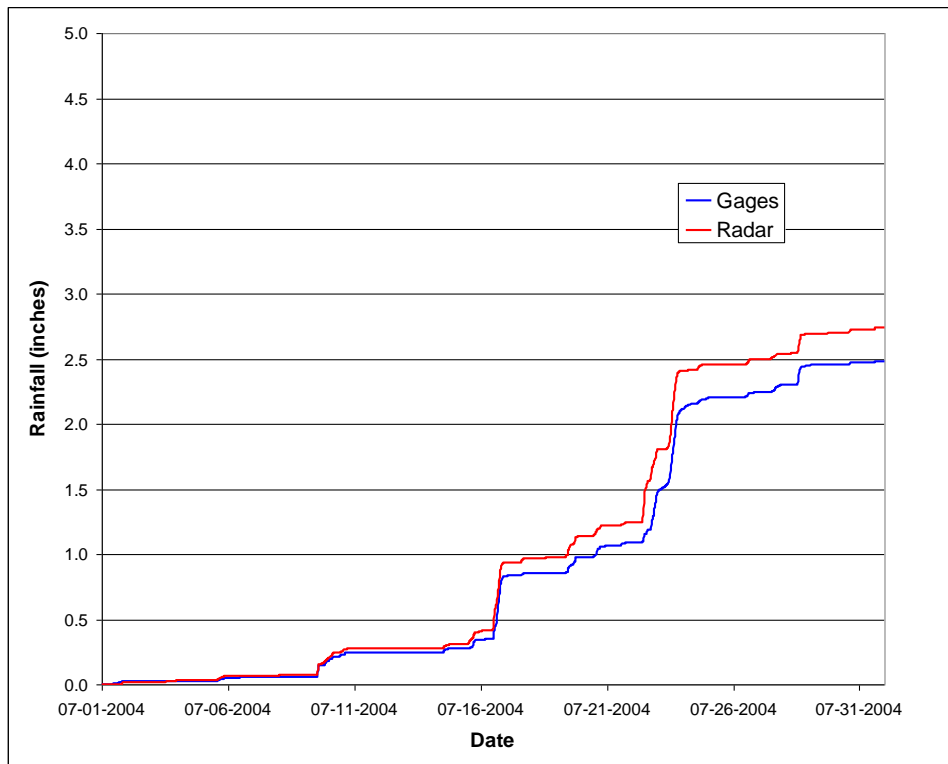


Figure A12 - Average accumulation plot for verification gages and co-located radar pixels.

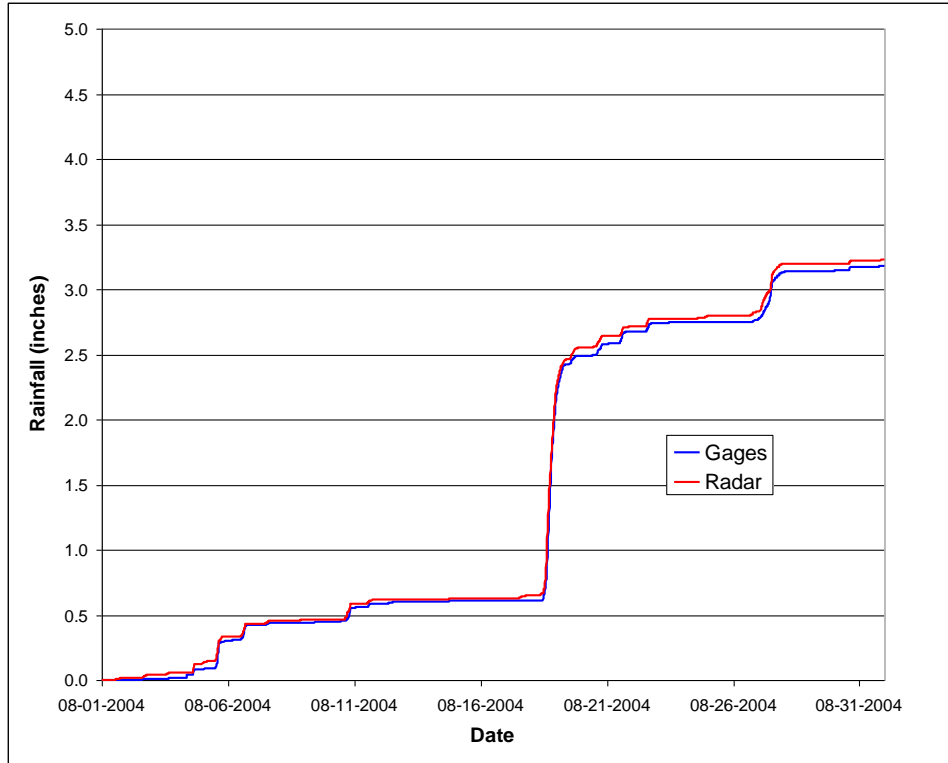


Figure A13 - Average accumulation plot for verification gages and co-located radar pixels.

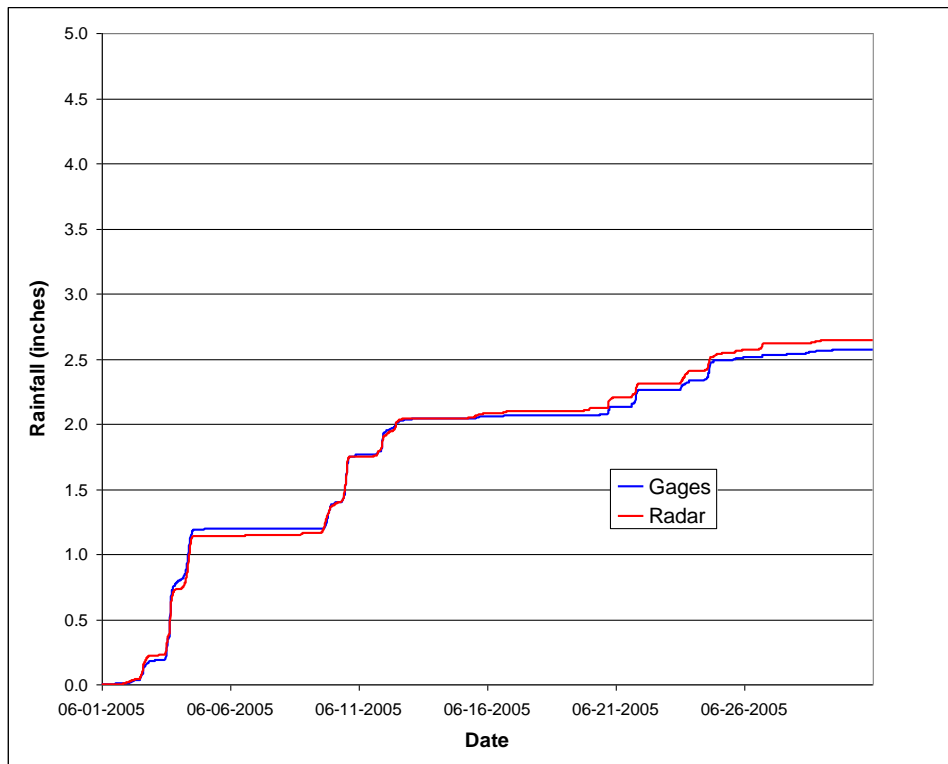


Figure A14 - Average accumulation plot for verification gages and co-located radar pixels.

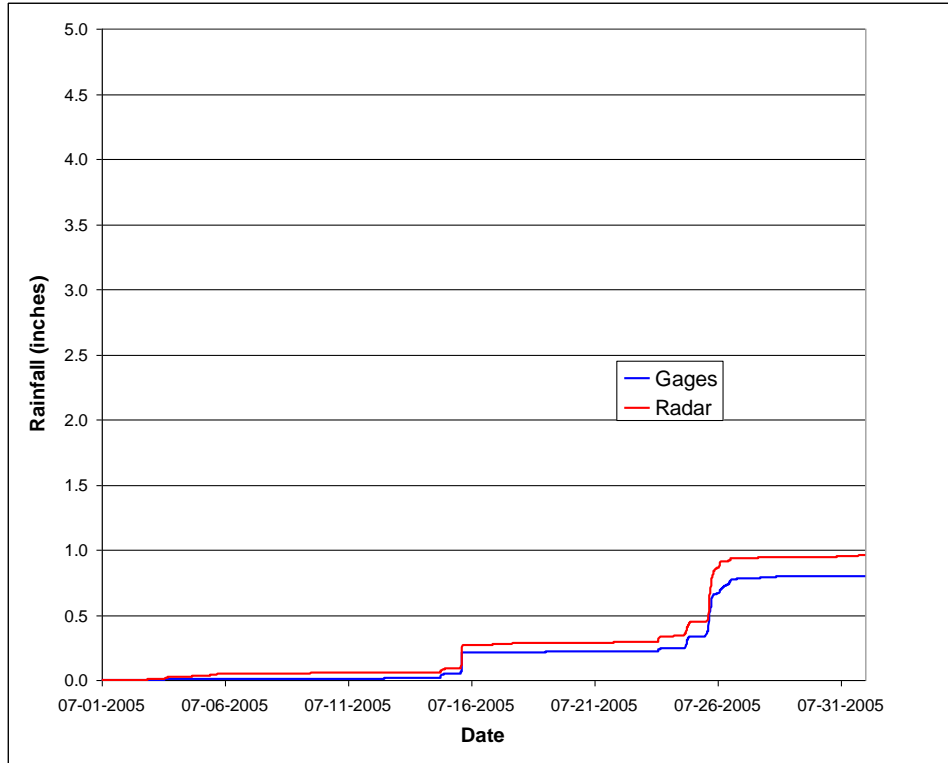


Figure A15 - Average accumulation plot for verification gages and co-located radar pixels.

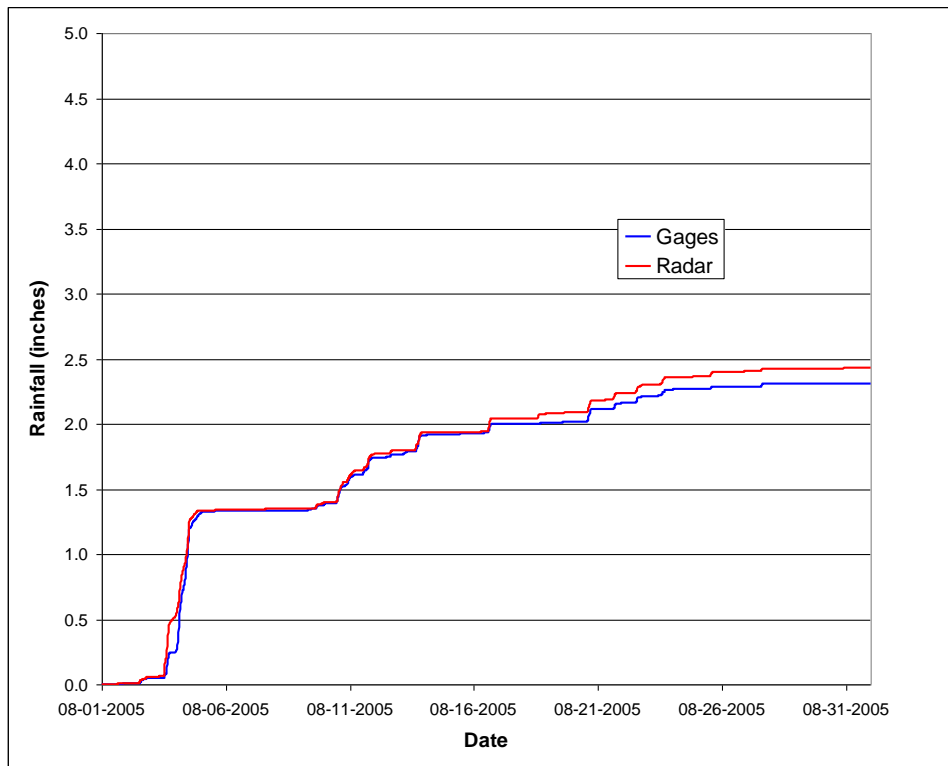


Figure A16 - Average accumulation plot for verification gages and co-located radar pixels.

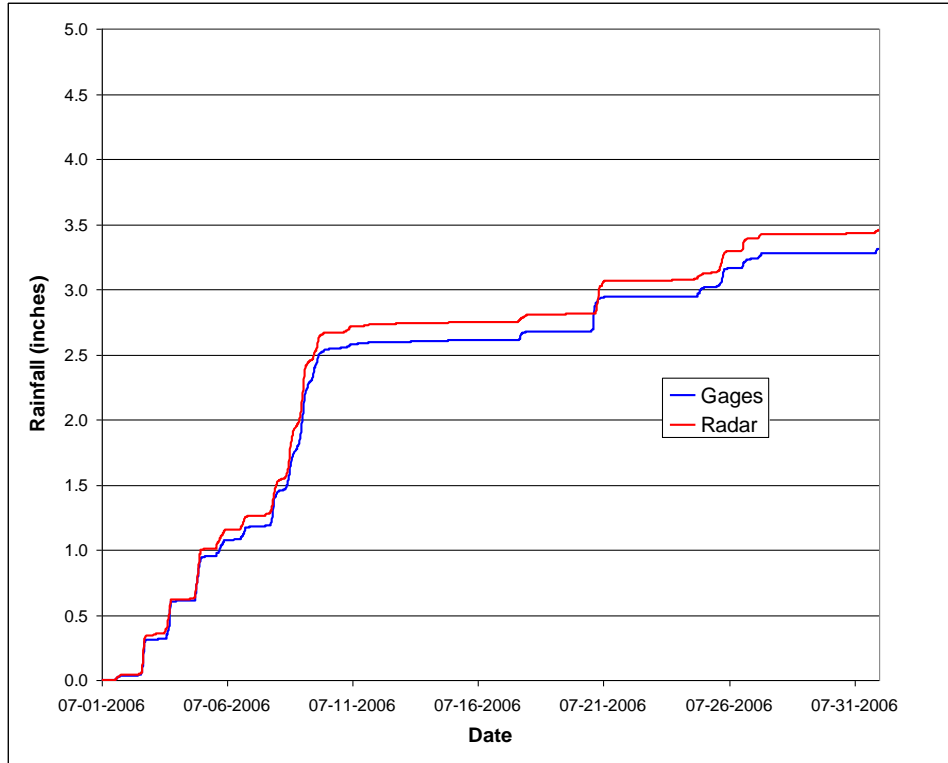


Figure A17 - Average accumulation plot for verification gages and co-located radar pixels.

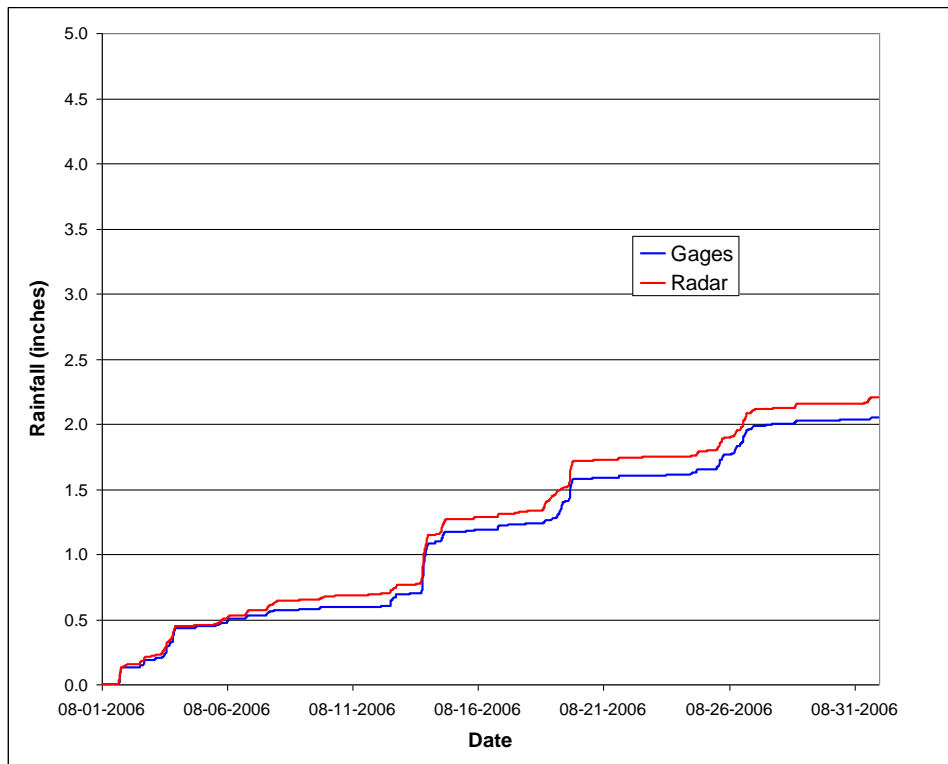


Figure A18 - Average accumulation plot for verification gages and co-located radar pixels.

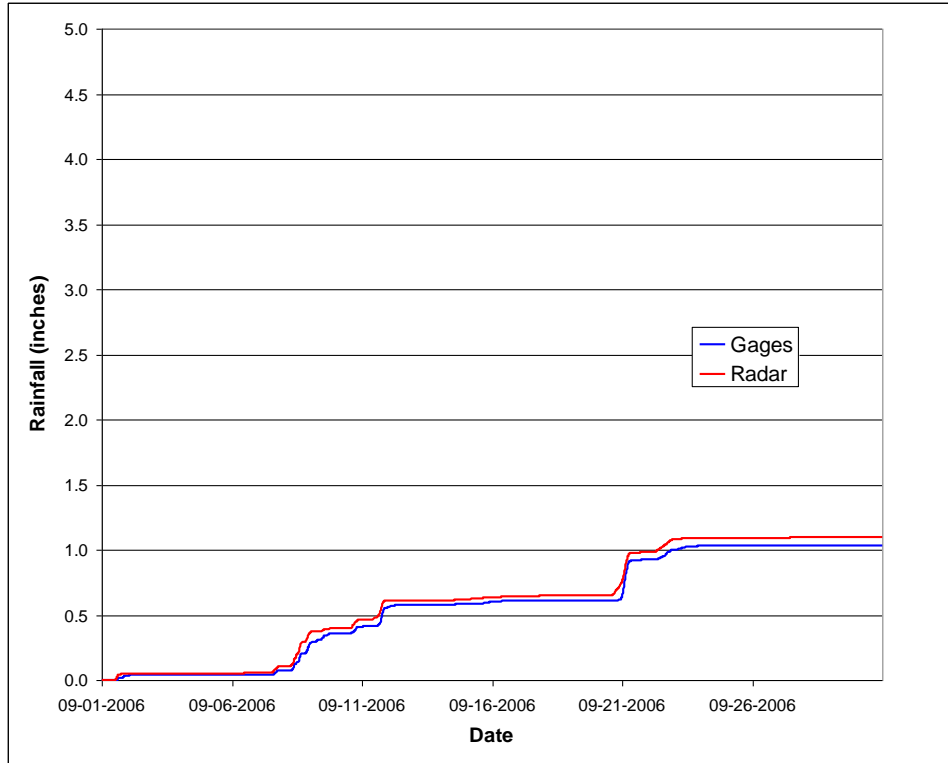


Figure A19 - Average accumulation plot for verification gages and co-located radar pixels.

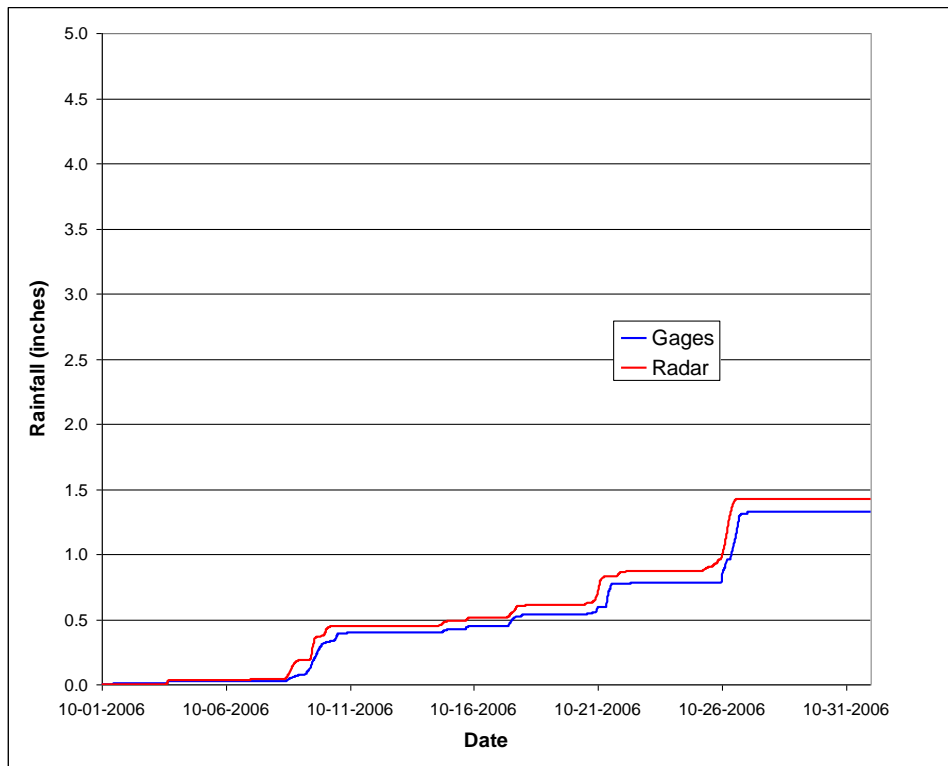


Figure A20 - Average accumulation plot for verification gages and co-located radar pixels.

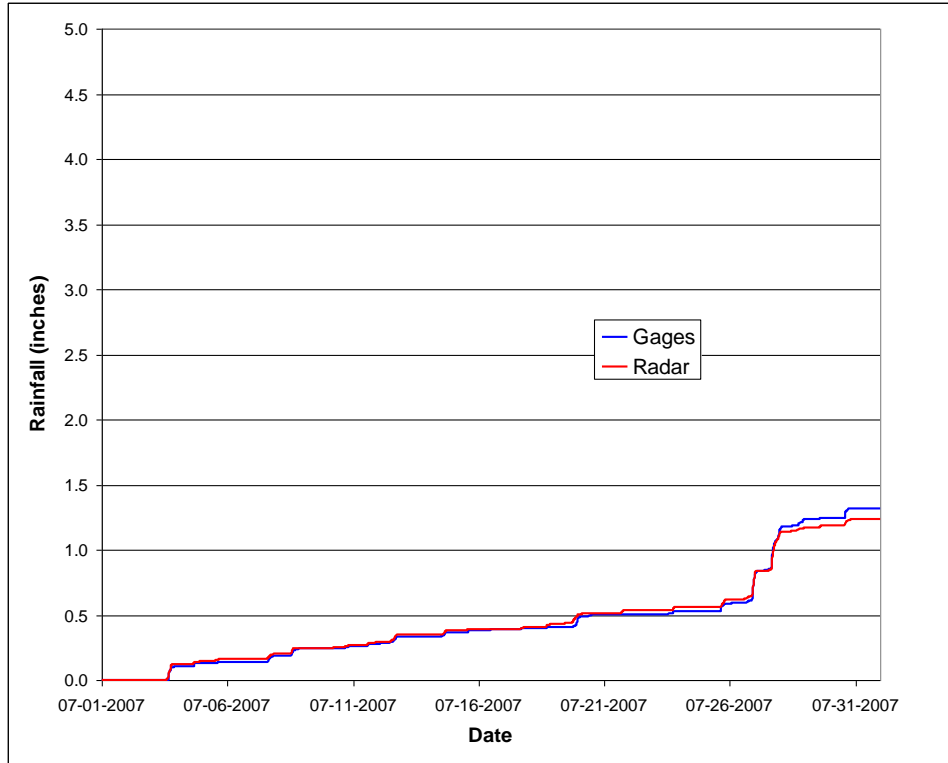


Figure A21 - Average accumulation plot for verification gages and co-located radar pixels.

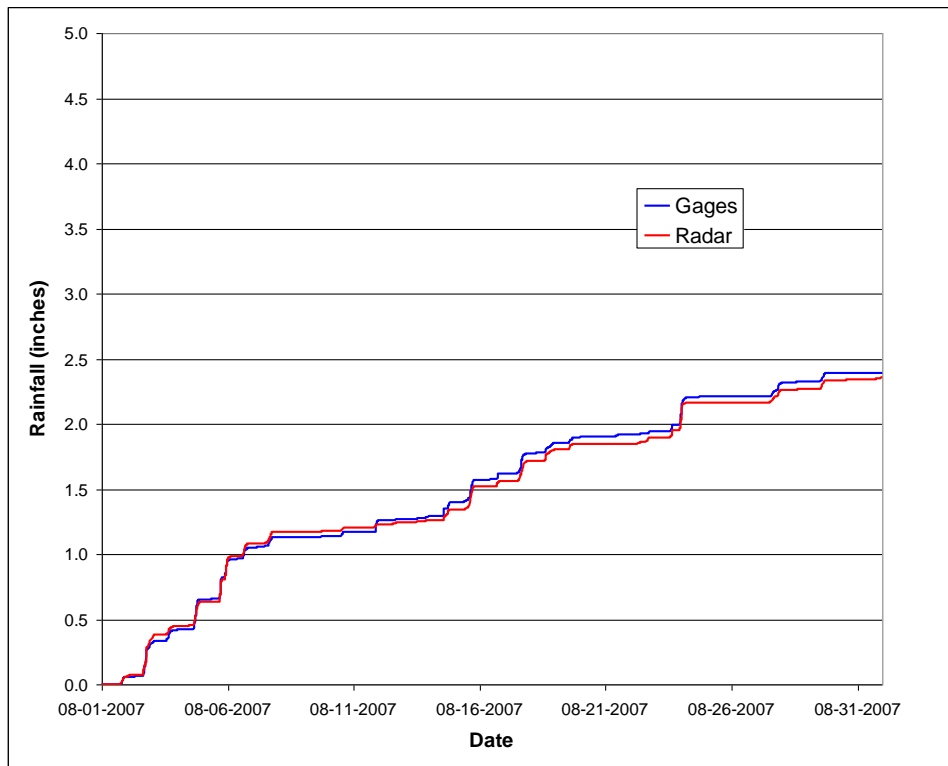


Figure A22 - Average accumulation plot for verification gages and co-located radar pixels.

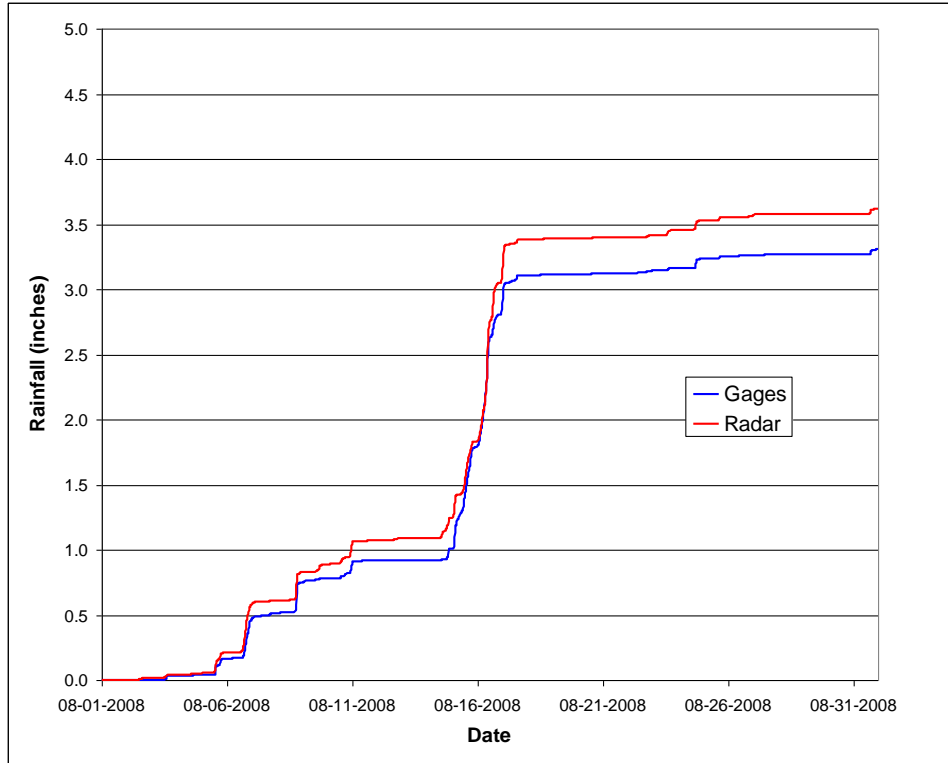


Figure A23 - Average accumulation plot for verification gages and co-located radar pixels.

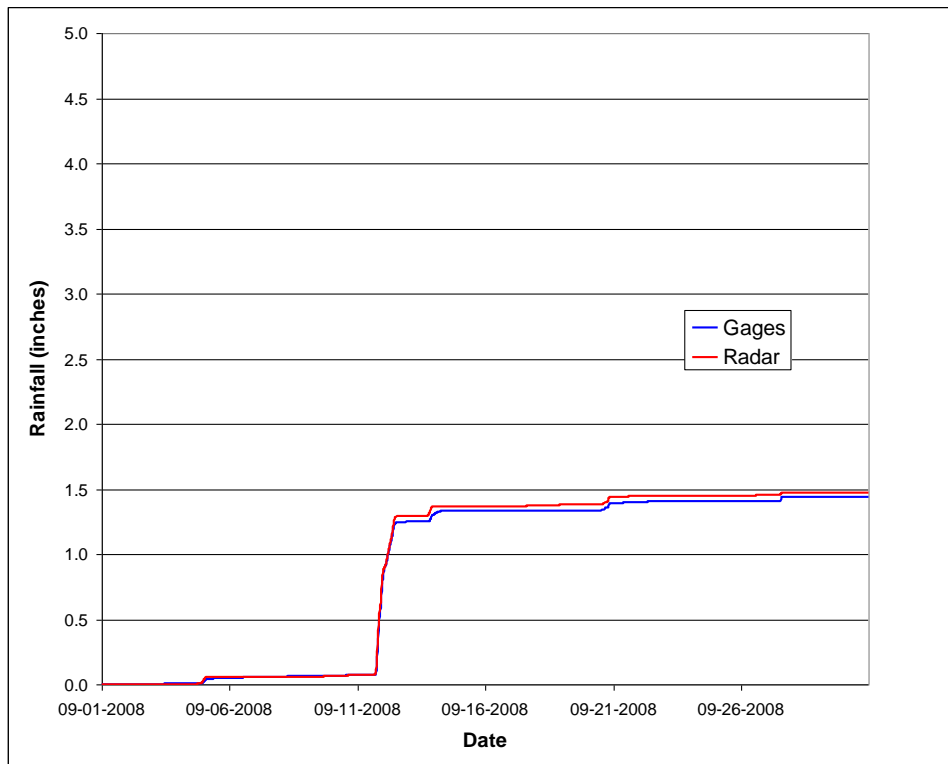


Figure A24 - Average accumulation plot for verification gages and co-located radar pixels.

13.0 Appendix C: April 1999 Storm Analysis

During the last week of April 1999, an unusually long sequence of storms rolled through the area. It was a significant historical event and the City directed the principal investigators to specifically evaluate the storm. The evaluation included:

1. Images of the total rainfall for the radar rainfall data grids showing the extent of the storm each day of that week and a total for the week with a colored legend for depth overlaid onto a base map with major features for reference;
2. Determination of the duration and size of the cells and if there were separate events or one continuous storm, and
3. Assign a return period to the event(s).

13.1 Radar-Rainfall Images

Figure 13.1-1 shows the four day rainfall total for the period April 27-30, 1999. A large area in and around Colorado Springs received more than five inches of rainfall during the period. Scattered localized amounts over six inches occurred with the highest reading in the Fountain Creek Watershed of 6.7 inches along Route 24 just west of Colorado Springs.

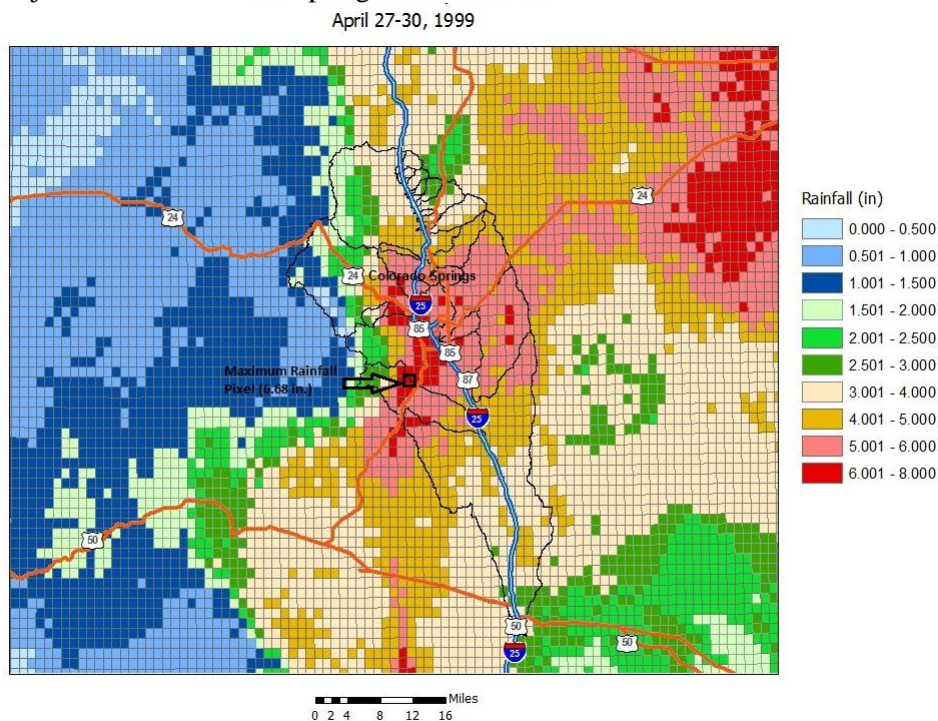


Figure 13-1: Storm Total Gage-Adjusted Radar Rainfall

Rainfall totals for April 26th were generally light with only isolated amounts greater than 0.05 inches for the day. Heavier rainfall followed on April 27th with maximum daily totals on the west side of Colorado Springs in the range of 0.5 -1.0 inches. (Figure 13-2) Rainfall increased on the 28th with a swath of 1.0-1.5 inch totals that ran parallel to Interstate 25 (Figure 13-3). Rainfall persisted through the next two days with a large portion of the City receiving 1.5-2.0 inch totals on the 29th followed by 3.0-4.0 inches of additional rain on April 30th. (See Figure 13-4 and Figure 13-5)

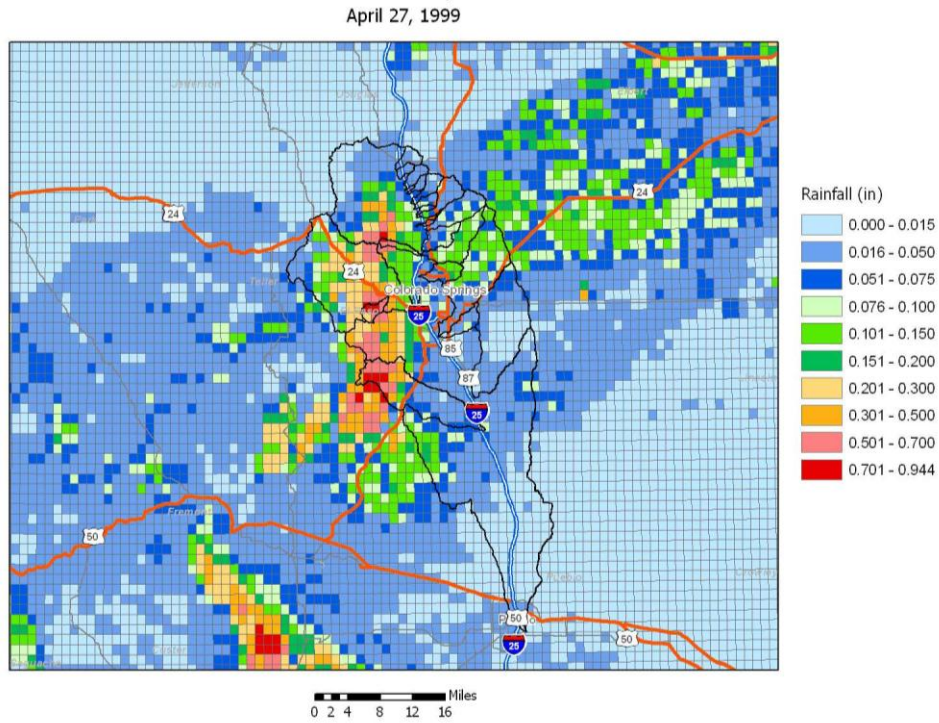


Figure 13-2: Gage-Adjusted Radar Rainfall: April 27, 1999

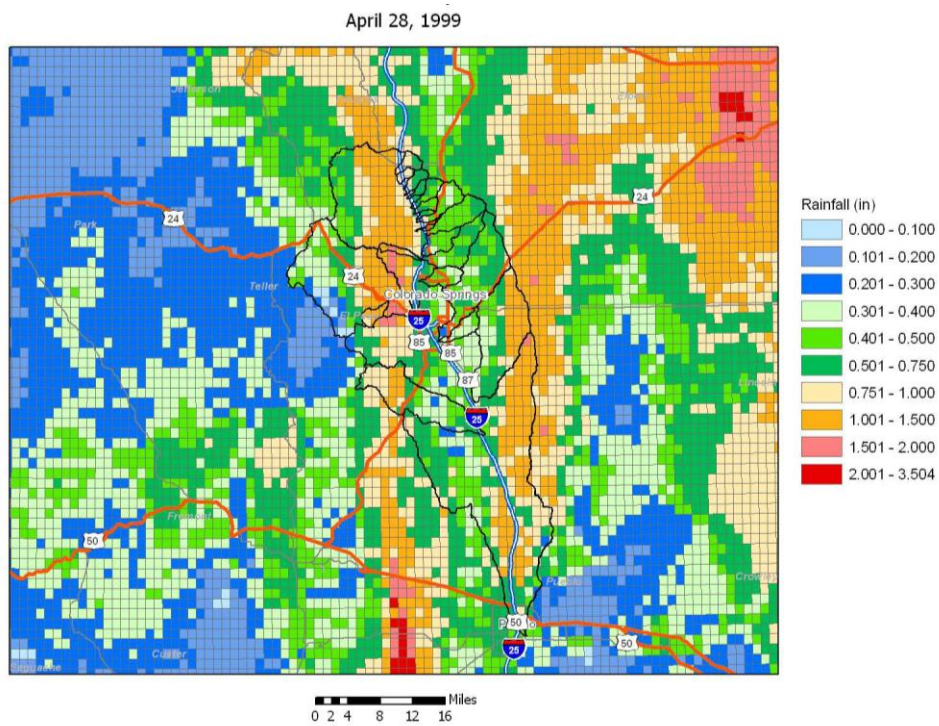


Figure 13-3: Gage-Adjusted Radar Rainfall: April 28, 1999

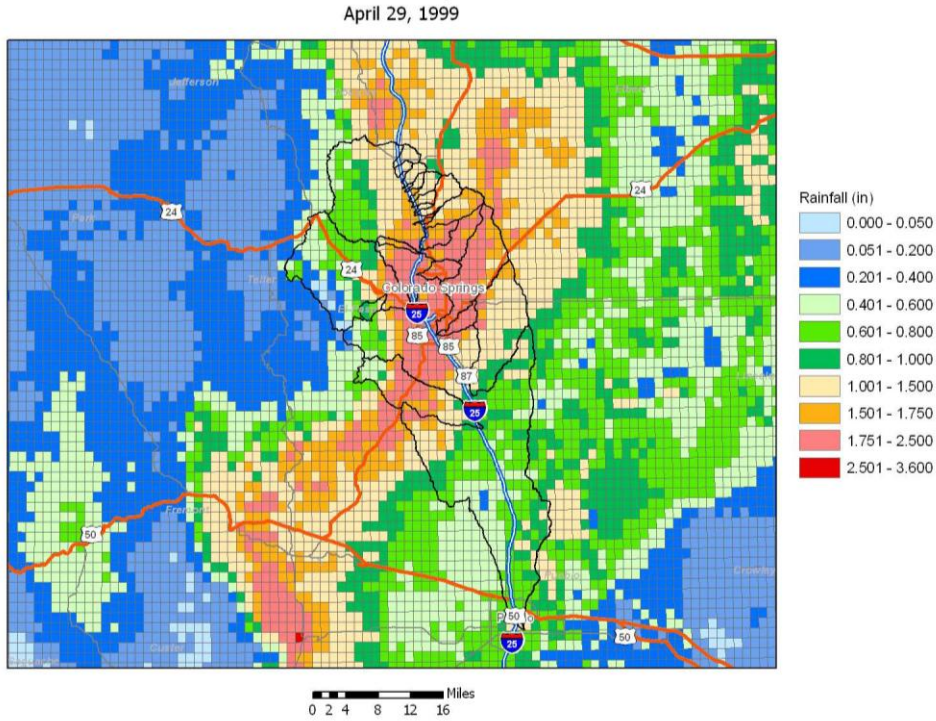


Figure 13-4: Gage-Adjusted Radar Rainfall: April 29, 1999

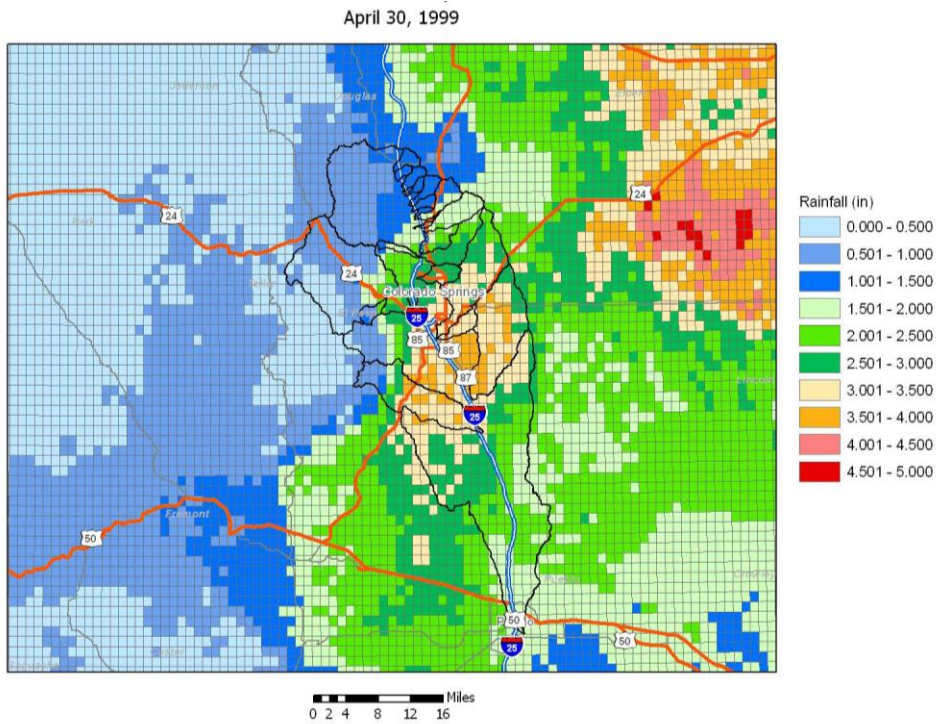


Figure 13-5: Gage-Adjusted Radar Rainfall: April 30, 1999

13.2 Storm Characteristics

Figure 13-6 and Figure 13-7 each show the time sequence of rainfall from April 26-30, 1999. A pulse of light to moderate rainfall was observed in the area along Route 24 just west of Colorado Springs on the 26th but little or no rainfall fell near the Air Force Academy that day. Once significant rainfall began on April 28th, rain persisted for three days ending on the 30th.

Figure 13-6 and through Figure 13-8 show nearly continuous rain for the last three days of the month punctuated by bursts of moderate to heavy rainfall². During this period, the rain was generally organized in three or four major pulses separated by periods of light or no rainfall. The major pulses were generally characterized by moderate rainfall containing multiple rain cells as depicted by individual peaks of higher moderate and heavy rainfall.

Fifteen-minute cell sizes were derived from the TITAN analysis described earlier in Section 7.0. Cell sizes were determined from 15-minute cells whose centroid occurred within the area shown in Figure 13-1. The frequency distribution of cell sizes for cells with peak intensities of 0.022, 0.039, and 0.093 inches per hour or greater are presented in Figure 13-9.

The intensity of 0.022 inches per hour was the lowest peak intensity analyzed so all identified cells (1041) are included. Cell sizes ranged from 12 to 9620 square miles with a median of 39 square miles. Ninety percent of these cell sizes were less than 675 square miles. (See Figure 13-10) Raising the peak cell intensity threshold to 0.039 inches per hour reduces the cell count to 765 while median cell size increased to 60 square miles and 90% of these cells were less than 950 square miles. Considering only cells that

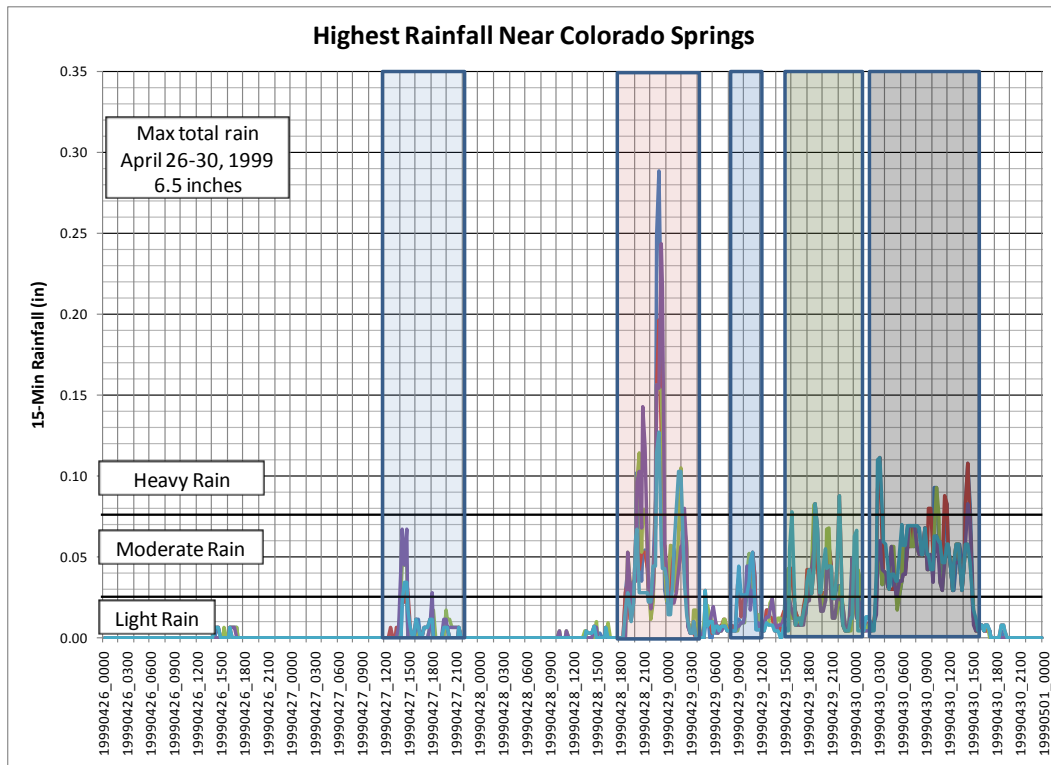


Figure 13-6: Storm Sequence Near Colorado Springs

² As indicated by in the Federal Meteorological Handbook No. 1 (NOAA, 2005), light rain intensity is defined as up to 0.10 inches per hour, moderate rain intensity is 0.11 to 0.30 inches per hour, and heavy rain intensity is more than 0.30 inches per hour.

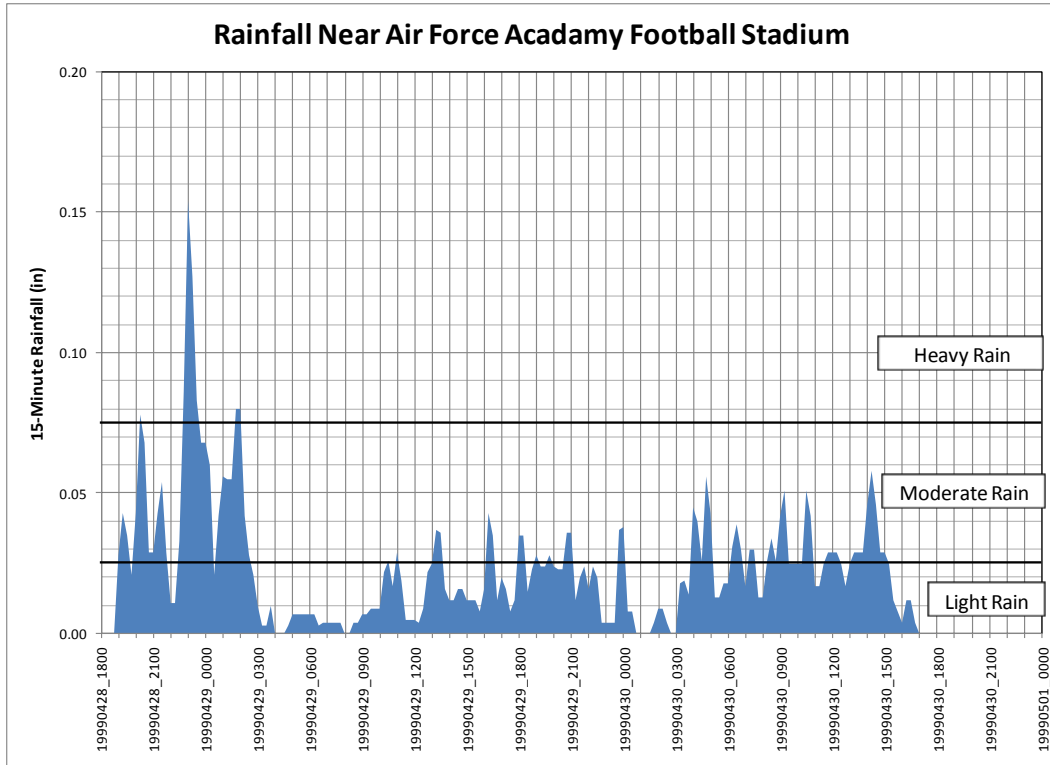


Figure 13-7: Storm Sequence near Air Force Academy Football Stadium

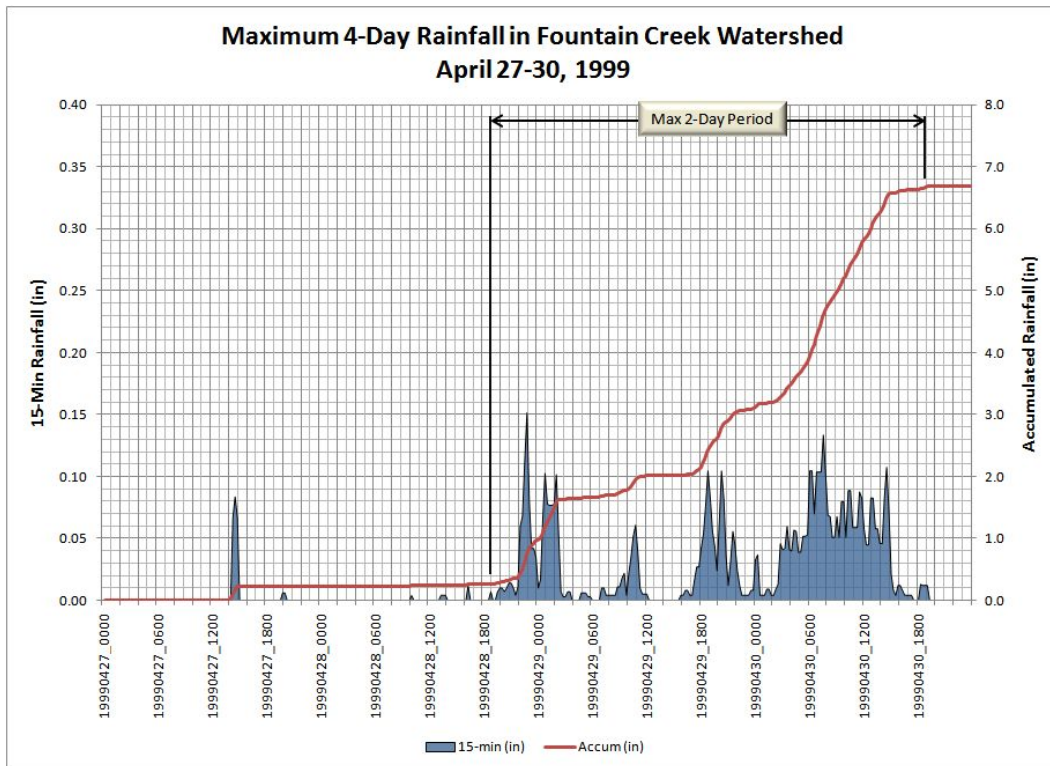


Figure 13-8: Maximum 4-Day Rainfall in Fountain Creek Watershed

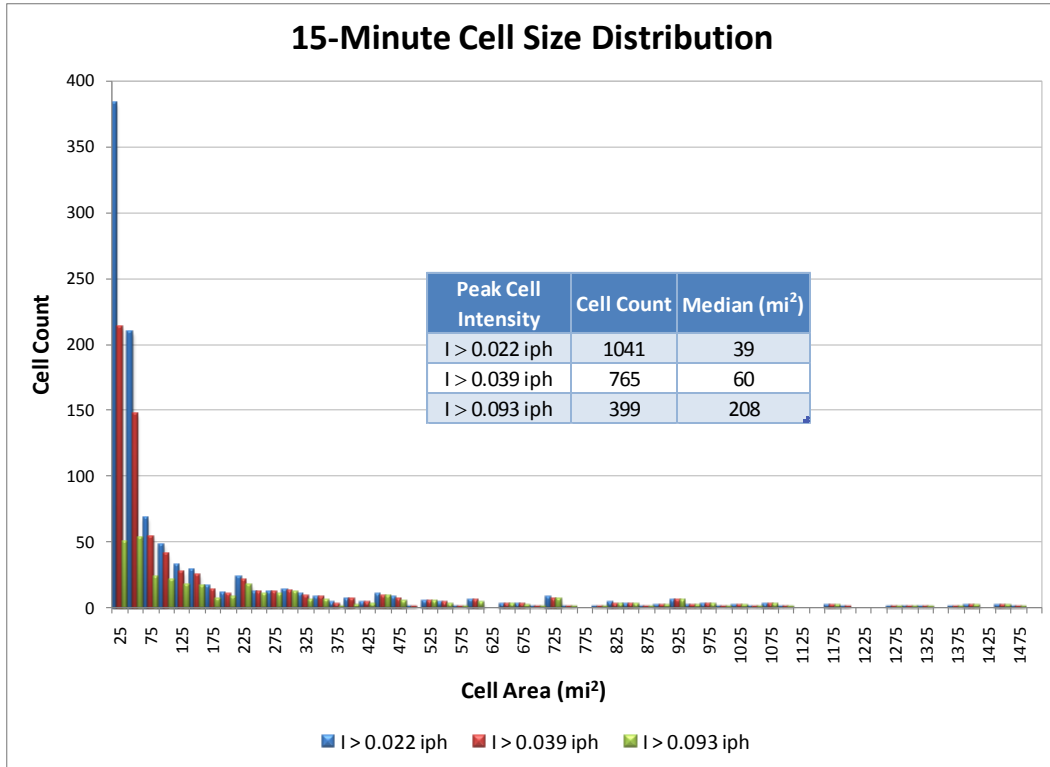


Figure 13-9: 15-Minute Storm Cell Size Distribution

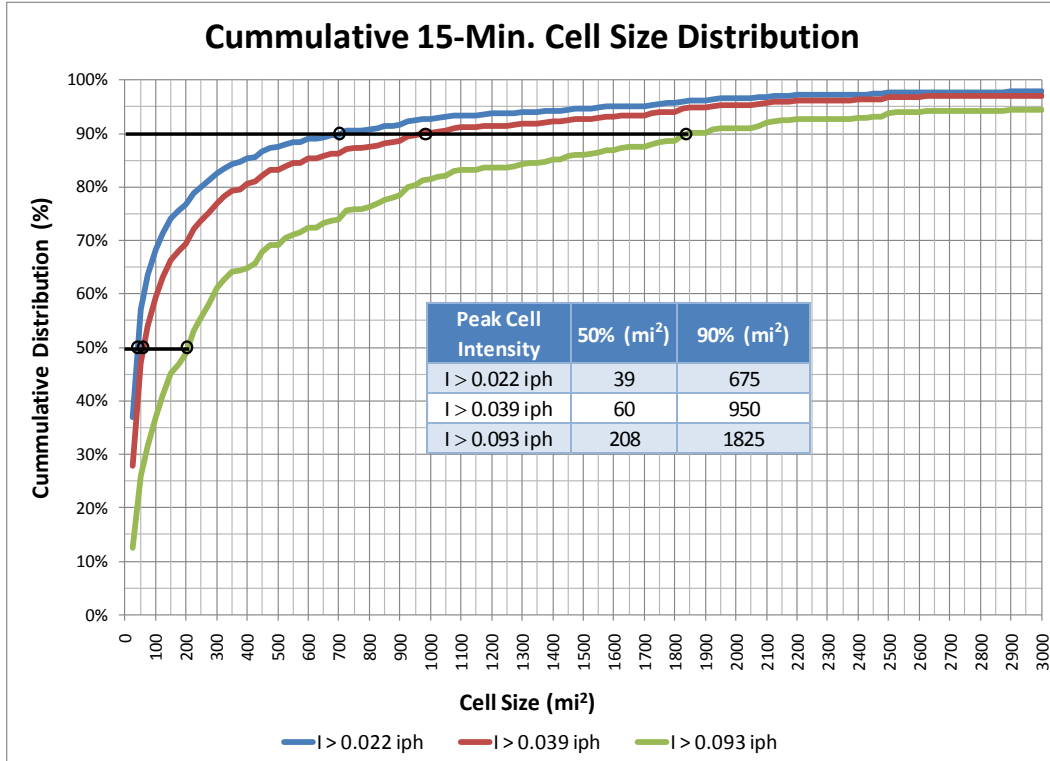


Figure 13-10: Cumulative 15-Minute Cell Size Distribution

maintained peak intensities of at least moderate intensity or the more hydrologically relevant cells, reduced the cell count to 399 over a range of 12-9620 square miles. The median cell size increased to 208 square miles with 90% of these cells under 1825 square miles.

13.3 Storm Frequency

The maximum short duration intensities observed over the area shown in Figure 13-1 during the rainfall event of late April 1999 were not particularly interesting. As shown in Table 13.3-1, peak intensities for durations of six hours or less were all less than the 2-year event according to NOAA Atlas 2³.

The unusual aspect of this storm was its longevity and sustained rainfall production. Maximum rainfall frequencies approximated the 75-year event for 12 and 24-hour durations.

However, the maximum 2-day totals greatly exceeded the 100-year event for the area. According to Technical Paper No. 49⁴, the 100-year, 2-day rainfall total for Colorado Springs is about 4.9 inches. The maximum 2-day rainfall for the April 1999 event was 6.40 inches. In fact, according to Technical Paper No. 49, 6.40 inches also exceeds the 4-day and 7-day 100-year totals.

Clearly, the April 1999 storm was a major event for the Colorado Springs area in historical terms. However, some caution regarding the longer duration frequency estimates is warranted. NOAA Atlas 2 was published 37 years ago in 1973 and Technical Paper 49 is even older with a publication date of 1964. Data for the past 40-50 years is not considered in these publications.

Table 13.3-1: Peak Observed Depth Duration Storm Frequencies

Duration	Obs Radar-Rainfall Max (in)	Frequency
15-min	0.32	< 2-yr
1-hr	0.85	< 2-yr
3-hr	1.34	< 2-yr
6-hr	2.15	< 2-yr
12-hr	3.66	~ 75-yr
1-day	4.28	~ 75-yr
2-day	6.40	>> 100-yr

³ Miller, J.F., R.H. Frederick, and R.J. Tracy; "NOAA Atlas 2 Precipitation-Frequency Atlas of the Western United States, Volume III-Colorado," National Oceanic and Atmospheric Administration, Washington, DC, 1973

⁴ Miller, J.F.; "Technical Paper No. 49: Two- to Ten-Day Precipitation for Return Periods of 2-100 Years in the Contiguous United States," U.S. Weather Bureau, Washington, DC, 1964

14.0 Appendix D: Resumes

Resumes for the principal investigators, the project sponsors, and peer reviewers are included for reference.

Principal Investigators

David C. Curtis, Ph.D.

Jack Humphrey, Ph.D., P.E., CCM

Project Sponsors

Daniel W. Bare II, P.E.

City of Colorado Springs

Kevin Houck, P.E., CFM

Peer Review/Technical Support

Chandra S. Pathak, Ph.D., P.E., D.WRE, F.ASCE

South Florida Water Management District

Nolan Doesken

Colorado Climate Center

14.1 Principal Investigators

DAVID C. CURTIS, Ph.D.

Senior Hydrologist, Vice President, WEST Consultants



For the past 34 years, Dr. Curtis has been on the leading edge of flood risk management services. He has been involved in the design, development, and implementation of award winning innovations in more than 50 automated environmental monitoring systems across the US and in eighteen countries abroad. Fault-tolerant designs, dual redundant computer configurations, and integrated networks are among the concepts advanced by Dr. Curtis. In addition, Dr. Curtis has contributed significantly to the economic analysis of flood warning systems, quantified the communication capacities of ALERT flood warning systems, and developed procedures for designing gage networks. Recently, Dr. Curtis has been applying new weather information technologies such as radar-rainfall estimates to hydrologic analysis and modeling.

Following a career as a flash flood hydrologist for the National Weather Service, Dr. Curtis co-founded a hydrologic software company specializing in flood warning, which later merged with a manufacturer of hydro-meteorological instrumentation. Internationally recognized as an expert on hydrology, Dr. Curtis has authored more than seventy technical articles and reports. In June 1989, Dr. Curtis accepted the Computerworld/Smithsonian Award for Innovative Uses of Information Technology in the “Energy, Natural Resources, and Environment” category.

Specialization: Flood Risk Management

Education: Massachusetts Institute of Technology, Ph.D. Water Resources, 1982

Johns Hopkins University, Graduate Studies in Numerical Science, 1976

University of Maryland, MS Civil Engineering, 1975

Pennsylvania State University, BS Agricultural Engineering, 1972

Total Years Experience: 34

Professional Affiliations: American Geophysical Union
American Society of Civil Engineers
American Meteorological Society
Association of State Flood Plain Managers
American Water Resources Association
California Flood Plain Managers Association
California-Nevada Association of ALERT Users
Southwestern Association of ALERT Systems
National Hydrologic Warning Council

AWARDS

Department of Commerce Bronze Medal for superior service for the development and timely implementation of the Norwich, CT flood warning system, 1983

NOAA Unit Citation for meritorious performance during major flooding in June 1982. National Weather Service Northeast River Forecast Center

Council Resolution, City of Norwich, CT, Cited for outstanding service and support for the City of Norwich flood forecast and warning program, Nov. 14, 1984

Certificate of Excellence for ALERT Transmission newsletter article, "Choosing a Hydrologic Model for Flood Forecasting", presented by the Southwestern Association of ALERT Systems, 1994

Technical Excellence Award presented by the Floodplain Management Association of California for the Petaluma Village Factory Outlets Flood Preparedness Program, 1996

RELEVANT PROJECT EXPERIENCE

Fountain Creek Watershed Rainfall Characterization, Colorado Springs, CA

Evaluated radar rainfall records for eastern Colorado and for the Fountain Creek Watershed near Colorado Springs, CO, to determine the geometric properties of storm cells in the region. The results were used to provide insights for proposed methodologies for developing and applying design storms in the region.

Hydrographic Gage Network Evaluation, Ventura, CA

Evaluated Ventura County Watershed Protection District's hydrographic gage network to determine how well the existing gage network met the data needs for food warning, continuous hydrologic and water quality modeling, and design rainfall intensity standards for the District's hydrology models. Ventura's network evolved over the past 30 years as have the requirements for various hydrographic monitoring programs. Results led to reallocation of monitoring resources for more cost-effective program operation. This evaluation was completed in 2008.

Design Storm Development, St Louis, MO

Provided data analysis using historical gage adjusted radar rainfall estimates to develop new approaches for hydrologic design. State-of-the-art design storm concepts were developed to support infrastructure design in a multi-billion dollar water quality plan in St. Louis, Missouri.

SPI/Catlin Martell Stormwater Management Design, Jackson, CA

Provided hydrologic assessment of complex interactions of storm water runoff, detention storage, and downstream hydraulic impacts for a commercial development. Modeling results verified the need for a regional stormwater analysis to understand interactions between multiple commercial sites undergoing concurrent development and causing downstream channel degradation. This design project was completed in 2007 for Sierra Pacific Industries and Catlin Properties.

Precipitation Analysis for August 2003 Thunderstorms, Sacramento, CA

Provided comprehensive review and analysis of record-breaking rainfall, National Weather Service weather/flood forecasts, and emergency response to the August 2003 thunderstorms in Sacramento, CA. Used NWS Doppler radar-based rainfall estimates to track isolated heavy rain cells through individual watersheds contributing to localized flooding. Analyzed National Weather Service forecast statements for timing and content to determine impact on emergency response. This precipitation analysis was completed in 2007 for Hardy Erich Brown & Wilson.

Caltrans-Trujillo, Modesto, CA

Provided expert witness services for Caltrans in the Stanislaus County Superior Court Case No. 346144, Trujillo, et al. v. Monson, et al. Conducted an analysis and evaluation of the rainfall events related to a vehicular accident that occurred on Route 132 just east of Modesto, California.

Caltrans-Castaic Boat, Castaic, CA

Provided expert witness services for Caltrans in the Los Angeles County Superior Court Case No. PC037725, Castaic Boat & Marine, LLC v. County of Los Angeles, State of California, et al. Conducted an analysis and evaluation of the rainfall events covering the period of January 7 through January 9, 2005, in Castaic, California.

Caltrans-Cajon Pass, Devore, CA

Provided expert witness services for Caltrans in the San Bernardino County Superior Court Case No. SCVSS 124701, Joshua Gile, et al. v. Cresta, Inc. et al. Conducted an analysis and evaluation of the rainfall events related to a vehicular accident that occurred on Interstate 15 north of Kenwood Avenue in an unincorporated area of San Bernardino County, California.

Caltrans-Chino Hills, Chino Hills, CA

Provided expert witness services for Caltrans in the Los Angeles County Superior Court Case No. KC047177 G, Paula Rubin and Silvan Rubin v. State of California, et al. Conducted an analysis and evaluation of the rainfall events related to the accident that occurred near the intersection of SR-71 and Valley Blvd. in Pomona, California.

Caltrans-Mendoza, San Diego, CA

Provided expert witness services for Caltrans in a San Diego Superior Court case. Conducted an analysis and evaluation of the rainfall events related to a vehicle striking a fallen tree on January 5, 2005, in heavy rain and wind conditions; the investigation site is located on SR-163 near the Upas St. Equestrian Overcrossing in San Diego, California.

Caltrans-Cervantez, Modesto, CA

Provided expert witness services for Caltrans in Cervantez case. Conducted an analysis and evaluation of the rainfall events related to a vehicular accident that occurred on Route 99 near Turlock, California.

Caltrans-Weidenaar, Barstow, CA

Provided expert witness services for Caltrans in the San Bernardino County Superior Court Case No. BVC 08898, Robert Weidenaar v. State of California, et al. Conducted an analysis and evaluation of the rainfall events related to the vehicular accident that occurred February 10, 2005, on Interstate 15 near Barstow, California.

Chilton Place, El Dorado Hills, CA

Provided expert witness services for the law firm of Caulfield, Davies & Donahue in the El Dorado County Superior Court Case No. PC 20060321, Randy Subjeck, et al. v. El Dorado County, et al. Conducted an analysis and evaluation of the rainfall events related to the flooding of the property near Chilton Place in El Dorado Hills, California.

Southern California Edison v. City of Victorville, Victorville, CA

Provided expert witness services for the law firm of Graves & King in the San Bernardino County Superior Court Case known as Southern California Edison v. City of Victorville. Conducted an analysis and evaluation of the rainfall events on August 31, 2004, purported to have caused damage to the Southern California Edison property in Victorville, California.

AFG Industries v. City of Victorville, Victorville, CA

Provided expert witness services for the law firm of Graves & King in the San Bernardino County Superior Court Case known as AFG Industries v. City of Victorville. Conducted an analysis and evaluation of rainfall events occurring on August 14, 2004, in Victorville, California.

BNSF Railway Company v. City of Victorville, Victorville, CA

Provided expert witness services for the law firm of Graves & King in the San Bernardino County Superior Court Case No. SCVSS 132213, BNSF Railway Company v. City of Victorville, et al. Conducted an analysis and evaluation of rainfall events occurring on August 14, 2004, in Victorville, California.

Union Pacific Derailment, Victorville, CA

Provided expert witness services for the law firm of Shook, Hardy & Bacon in the Pulaski County, Arkansas Sixth Division Circuit Court Case No. CV2006-2711, Union Pacific Railroad Company v. Entergy Arkansas, Inc., et al. Conducted an analysis and evaluation of rainfall events occurring in eastern Wyoming in 2005.

Modesto Irrigation District, Modesto, CA

Project Manager/Senior Hydrologist responsible for providing comprehensive review and analysis of precipitation, National Weather Service flood forecasts, and flood warnings surrounding reservoir operations in the Tuolumne Basin during the New Year's 1997 flood event. Used National Weather Service radar-based rainfall estimates to identify areas of heavy rain that fell unobserved between the available rain gages. These heavy rains caused surprisingly high reservoir inflows that led to dramatic shifts in short term reservoir gate operations and major changes to National Weather Service downstream river forecasts. This Precipitation Analysis was completed in 2005 for the Modesto Irrigation District.

Litigation Support, California Department of Justice

Senior Hydrologist responsible for providing extensive evaluation of precipitation and National Weather Services Forecasts and Warnings throughout California that related to the New Year's 1997 flood event. Used National Weather Service radar-based rainfall estimates with available rain gage observations to track areas of heavy rainfall throughout the storm event. Reviewed National Weather Service weather and river forecasts for content and timeliness in relation to value to emergency response. Litigation support concluded in 2005.

Flood Management Plan, US Army Corps of Engineers, Sacramento, CA

Project Manager/Senior Hydrologist responsible for evaluating rainfall-runoff modeling and flood warning for the Flood Management Plan for the American River and Folsom Dam. Also developed design specifications for siren-based flood warning system for the American River below Folsom Dam. Conducted sound propagation studies with full scale siren operation to determine appropriate siren placement for audio and voice warnings along the length of the American River Parkway from Folsom Dam to Sacramento. This project was completed in 1998.

Rainfall Analysis, California Department of Water Resources, Coalinga, CA

Project Manager/Senior Hydrologist responsible for providing engineered radar-rainfall analysis for hydrologic modeling of the Arroyo Pasajaro and Contua Creek watersheds for March 1995 floods. Using 15-minute, 2 km x 2 km resolution radar rainfall estimates, accurately determined the volume and distribution of rainfall for correct reconstruction of flood hydrographs that caused failure of both north and southbound spans of the I-5 Bridge over the Arroyo Pasajaro. The data also supported 2-dimensional flood wave modeling downstream from the bridge failure sites in the

central valley. This Precipitation Analysis was completed in 1998 for the California Department of Water Resources.

Rain Gage Network Optimization, South Florida Water Management District, West Palm Beach, FL

Conducted a peer review of a study to optimize the rain gage monitoring network of the South Florida Water Management District, West Palm Beach, FL. The proposed optimization studies were a prerequisite to expanding and refining the district's hydrologic network to meet the needs of Comprehensive Everglades Restoration Plan projects.

Evaluation of Radar Rainfall Services, St. Johns River Water Management District, Palatka, FL

Provided analysis and review of high resolution radar rainfall estimation services for the St. Johns River Water Management District in Palatka, FL. Evaluated and compared rainfall estimates from suppliers of gage-adjusted radar rainfall data with rain gage observations.

US Army Corps of Engineers, Los Angeles, CA

Evaluation of Forest Falls, CA Flood warning system.

Diad Incorporated, Longmont, CO

Evaluation of spatial properties of storms using historical radar-rainfall data.

3-Waters Technical Services, San Diego, CA

Gage-adjusted radar-rainfall services for St. Louis, Missouri.

St. Johns River Water Management District, Palatka, FL

10-Month pilot project testing gage-adjusted radar-rainfall services. Evaluation, review, and recommendations for existing rain gage network.

Applied Geographic Technologies, Inc, Ft. Worth, TX

Gage-adjusted radar-rainfall services for Largo and Clearwater, Florida.

Black & Veatch, Kansas City, MO

Gage-adjusted radar-rainfall services for Trinity River Authority, Texas.

Brown & Caldwell, Minneapolis, MN

Gage-adjusted radar-rainfall services for Minneapolis, Minnesota.

Byrd/Forbes & Associates, Dallas, TX

Gage-adjusted radar-rainfall services for Little Rock, Arkansas. Gage-adjusted radar-rainfall services for Dallas, Texas. Gage-adjusted radar-rainfall services for Austin, Texas.

Carollo Engineers, Walnut Creek, CA

Rainfall analysis and data services for Vallejo, California.

Camp, Dresser and McKee, Inc.

Gage-adjusted radar-rainfall services for Columbus, Ohio. Gage-adjusted radar-rainfall services for Austin, Texas.

Exponent/Failure Analysis, Costa Mesa, CA

Gage-adjusted radar-rainfall services for Newport Beach, California, Huntington Beach, California and Las Vegas, Nevada.

City of Folsom, CA

Gage-adjusted radar-rainfall services for Jan-Feb 2000 storms.

Greeley-Hansen, Inc.

Gage-adjusted radar-rainfall services for Washington, DC. Gage-adjusted radar-rainfall services for Port Huron, Michigan.

Lawler, Matusky & Skelly Engineers LLP

Gage-adjusted radar-rainfall services for Newark, New Jersey.

MBK, Engineers, Sacramento, CA

Gage-adjusted radar-rainfall services for Brentwood and Oakdale, California.

Riverside Technologies, Inc., Fort Collins, CO

Develop recommendations for regional river forecast centers for the National Water Commission of Mexico, 1998.

City of Fort Worth, TX

Rain gauge and radar-rainfall analysis of 03/15-3/16/98 storm event.

LTM Engineering, Phoenix, AZ

Flood warning study for tributaries to the Lower Colorado River & gauge network design. Flood warning system design and analysis for Town Lake, Tempe, Arizona.

San Bernardino County, San Bernardino, CA

Historical radar-rainfall analysis in eastern San Bernardino County.

Gutierrez, Smouse, Wilmut & Assoc. Inc., Dallas, TX

Radar-rainfall analysis for two storms causing sanitary sewer overflows in 1997.

Orange County Environmental Management Agency, Anaheim, CA

Analysis of performance of ALERT flood warning system for Orange County.

Lower Colorado River Authority, Austin, TX

Flood warning study for tributaries to the Lower Colorado River.

Radar-Rainfall Analysis for the June 1997 Flood Event

Gage-adjusted radar rainfall services.

White Rock Consultants, Dallas, TX

Provided engineered radar-rainfall data for source flow analyses in inflow/infiltration studies for the City of Ft. Worth, Texas, the City of Waco, Texas, and the City of Dallas, Texas.

Sacramento County Department of Water Resources, Sacramento, CA

Meteorological analysis of January 1995 floods in Sacramento. Includes merging radar-rain gauge data sets and area wide frequency analysis.

Kern County Engineering and Survey Services, Bakersfield, CA

Comprehensive review and audit of Caliente Creek and Kelso Creek ALERT flood warning and preparedness systems operated by Kern County and the Kern County Water Agency.

Michael Baker Jr. Inc., Alexandria, VA

Radar-rainfall analysis for Elk Lick Run, MD. Provided innovative linear programming solution to generate consistent high-resolution rainfall estimates from NWS NEXRAD imagery. Developed conceptual framework for a flood warning system supporting lake and canal operations in the Oswego Basin, New York.

Riverside County Flood Control and Water Conservation District, Riverside, CA

Comprehensive review and analysis of district hydrological data collection, data management and flood warning systems. Conducted an inter-comparison study of rain gauge and radar estimates of rainfall.

Placer County Flood Control, Auburn, CA

Developed gauge-adjusted radar-rainfall data set for input into hydrologic models used for post flood analysis.

NovaLynx International, Ltd., Tempe, AZ

Prepared and presented a technical seminar on automated hydrometeorological information management systems in Tokyo, Japan. Also prepared market analysis for introduction of new hydrometeorological instrument technologies to Japan.

Reedy Creek Improvement District, Lake Buena Vista, FL

Designed, developed, and installed automated hydrometeorological/water quality monitoring system for NPDES.

Chelsea GCA Realty Partnership, LP, Newport Beach, CA

Designed and installed a shopping center flood warning system. Prepared flood emergency plans for management and store tenants.

Corps of Engineers, Hydrologic Engineering Center, Davis, CA

Prepared training manual: "Hydrologic Aspects of Flood Warning and Preparedness Programs."

National Engineering Manual for Hydrologic Forecasting.

Chapter 17: "Forecasts for Flood Warning Systems."

WSI Corporation, Billerica, MA

Technical and marketing services for radar-based rainfall estimation system.

NovaLynx Corporation, Rancho Cordova, CA

Prepared report: "Introduction to Flood Warning-Preparedness Systems."

Meteorological and Environmental Protection Agency, Saudi Arabia

Designed region-wide data acquisition system for flood warning.

EXPERT WITNESS ENGAGEMENTS

Review and evaluation of river terminal operations during the "Great Flood of 1993" on the Mississippi River at St. Louis, Missouri

Determination of extreme rainfall events in an ungaged watershed in northeast Kansas during the period of the "Great Flood of 1993"

Analysis of extreme rainfall events in Sacramento County, CA during October 1994 and January 1995

Analysis of extreme rainfall events in Napa, CA during 1995

Rainfall analysis for coastal canyons near Malibu, CA for January 1995 and March 1995 mudslide and debris-flow events

Rainfall analysis for the January 1997 California Floods

Analysis of rainfall events of March 1995 and January 1997 in Napa, CA

Analysis of rainfall events, *Paradiso v. State of California*

Analysis of rainfall events, *Thomas v. State of California*

Analysis of rainfall events, *Munroe v. Morin, et al.*

Analysis of rainfall events, *Youngman v. State of California*

Analysis of rainfall events, *AA Fire Systems v. State of California*

Analysis of rainfall events, *Louis DeBottari v. State of California et al*

Analysis of rainfall events, Diep Nguyen and Le Dung Nguyen v. State of California et al

Analysis of rainfall events, Reclaimed Island v. Reclamation District 2107

Analysis of rainfall events, Antonelli v. State of California

Analysis of rainfall events, Akins v. State of California

Analysis of rainfall events, Nanette Rose et al. v. Foothill/Eastern Trans. Agency, et al.

Analysis of rainfall events, Jeffery Howard Woolf, et al., v. Department of Transportation

Analysis of rainfall events, Bungert v. City of Camarillo, et al

Analysis of rainfall events, Blundell v. City of Camarillo, et al

Analysis of rainfall events, Barba v. Hertel & Sons, Inc.

Analysis of rainfall events, Barba v. City of Camarillo, et al.

Analysis of rainfall events, Allen Aadland, et al v. City of Woodbridge, et al.

Analysis of rainfall events, Dawn Louise Gibbons, et al. v. Ford Motor Company, et al.

Analysis of rainfall events, Frito-Lay, Inc. v. California Dept. of Transportation, et al.

Analysis of rainfall events, Kannan v. State of California, etc. et al.

Analysis of rainfall events, Joe Nathan Jackson, et al., v. State of California, et al.

Analysis of rainfall events, Michael D. Magness, et al. v. State of California, et al.

Analysis of rainfall events, Robyn Christine Skinner, et al. v. Beverly Ann Gudger, et al.

Analysis of rainfall events, Sanchez, et al. v. State of California

Analysis of rainfall events, Karen Thomas v. State of California

Analysis of rainfall events, Toleson, et al, v. State of California

Analysis of rainfall events, Suzette Norrbom, et al. v. State of California, et al.

Analysis of New Year's 1997 Flood Event, Craig, et al. v. Modesto Irrigation District

Analysis of rainfall events, Atwood, Dixie, et al. v. City of Victorville, et al, San Bernardino County
SCC No., VCVVS032065

Analysis of rainfall events, Anderson, Frederick Carl v. California Transportation Commission, Inyo
County, SCC NO CV-CV-04-0036446

Analysis of rainfall events, Sehrer, John, et al. v. State of California, Ventura County SCC
No. CIV 225341

Analysis of rainfall events, Patino, Jeannette, et al. v. California Department of Transportation, et al.,
San Bernardino County, SCC No MCV05889

Analysis of rainfall events, De Souza, Roberta, et al. vs. State of California Department of
Transportation, et al., Los Angeles County, SCC SC075146

Analysis of rainfall events, Cervantez, Fernando v. State of California, et al, Merced County,
SCC No. 148288

Analysis of rainfall events, Wai, Man Yee, et al. v. HUB Construction, et al, Riverside County,
SCC No. RIC 399734

Analysis of rainfall events, Castaic Boat and Marine, et al. v. County of Los Angeles, State of California, et al., Los Angeles County, SCC No. PC 03775

Analysis of rainfall events, Southern California Edison v. City of Victorville

Analysis of rainfall events, BNSF v. City of Victorville

Analysis of rainfall events, AFG Industries, Inc., v. City of Victorville, et al.

Analysis of rainfall events, County of Sacramento. V. California Exposition and State Fair, et al.

Analysis of rainfall events, Gilberto Juarez, etc., et al, vs Saint Sophia Greek Orthodox Cathedral, et. al. SCVSS 121321

TRIALS AND DEPOSITIONS

Diep Nguyen and Le Dung Nguyen vs. State of California (CalTrans), No. BC182274
Superior Court of the State of California for the County of Los Angeles, April 1999
(Deposition and Trial)

Wheeling Pittsburgh Steel Corp vs. Beelman River Terminals, Inc., United States District Court
Eastern District of Missouri Eastern Division, No. 4:97 CV 01186 JCH, St. Louis, MO, December 1998
(Deposition and Trial)

Brian Anderson, et al. V State of California, et al., Los Angeles County Superior Court,
No. SC038491, March 1997 (Deposition and Trial)

St. Louis Cold Drawn, Inc., a corporation, vs. Beelman River Terminals, Inc., a corporation, Cause No.
942-10436, St. Louis, MO, December 27, 1995 (Deposition only)

Crane, Timothy R. v. The State of California, et al., Los Angeles County, SCC No. BC267659, Trial,
September 29, 2004

Trujillo et al, v. Monson et al, County of Stanislaus, SCC No. 34614 et al, County of Stanislaus, SCC No.
346144 (Deposition Sept-07)

Paula Rubin, et al v. State of California, et al, Los Angeles County Superior Court Case No. KC 047177
G

Joshua Gile, et al v. Cresta, Inc., et al, Superior Court of the State of California, County of San
Bernardino, SCVSS 124701 (Deposition Apr-07)

Castaic Boar & Marine, et al v. County of Los Angeles, Sate of California, et al, Los Angeles County
SCC No. PC 037725

PUBLICATIONS

1. **Curtis, David C.** "Planned Unit Development: Evolution and Relationship to Frederick County," Coalition for Land Use Education, Frederick, MD, January 1975.
2. **Curtis, David C.** "A Mathematical Model for the Evaluation of Detention Basins in the Control of Sediment and Storm Water Discharges from Urban Areas," M.S. Thesis, University of Maryland, 1975.
3. **Curtis, David C., and R.H. McCuen.** "A Mathematical Model for Evaluating the Design Efficiency of Storm Water Detention Facilities", presented at the 56th Annual Meeting of the American Geophysical Union, Washington, D.C., 1975.
4. **Curtis, David C.** "A Mathematical Model of Storm Water Detention Structure", Flood Runoff from Urban Areas, Edited by Richard H. McCuen, Water Resources Research Center, Dept. of Civil Engineering, University of Maryland, Technical Report No. 33, 1975.
5. **Curtis, David C., and R.H. McCuen.** "Economic Analysis of Residential Land-Use Alternatives", Journal of Urban Planning and Development Division, American Society of Civil Engineers, Vol. 101, No. UP2, Proc. Paper 11678, November 1975, pp. 109-116.
6. **Curtis, David C., and Eric Anderson.** "Manual Calibration Program", Part IV, Chapter 4, National Weather Service River Forecast System User's Manual, September 12, 1975.
7. **McCuen, R.H. and David C. Curtis.** "Storm Water Detention: Regional Development and Engineering Effectiveness", presented at the Symposium of Storm Water Management, National Capitol Section of ASCE, Washington, D.C., February 1976.
8. **Curtis, David C.** "A Deterministic Urban Storm Water and Sediment Discharge Model", National Symposium of Urban Hydrology Hydraulics and Sediment Control, Lexington, KY, 1976.
9. **Curtis, David C., and G.F. Smith.** "The National Weather Service River Forecast System -- Update 1976", presented at the International Seminar on Organization and Operation of Hydrological Services in Conjunction with the Fifth Session of the WMO Commission for Hydrology, Ottawa, Canada, July 1976.
10. **Curtis, David C.** "Comment on 'A Deterministic Urban Storm Water and Sediment Discharge Model'-Author's Reply", National Symposium on Urban Hydrology, Hydraulics, and Sediment Control, Lexington KY, 1976.
11. **Curtis, David C., and R.H. McCuen.** "Design Efficiency of Storm Water Detention Basins", Journal of the Water Resources Planning and Management Division, American Society of Civil Engineers, WRI, May 1977.
12. **Curtis, David C., Robert L. Mitchell, and John C. Schaake, Jr.** "A Deterministic Runoff Model for Use in Flash Flood Planning", Conference on Flash Floods: Hydrometeorological Aspects, Los Angeles, CA, American Meteorological Society, May 1978.
13. **Curtis, David C., and John C. Schaake, Jr.** "The NWS Extended Streamflow Prediction Technique", Water Conservation Needs and Implementation Strategies, American Society of Civil Engineers, pp. 182-195, 1979.
14. **Curtis, David C., and George F. Smith.** "The National Weather Service River Forecast System", Real-Time Forecasting/Control of Water Resource Systems, Eric Wood, ED., Pergamon Press, 1980.

15. **Curtis, David C.** "Flash Floods - Communities Can Help Themselves Prepare", presented at the NAR-ASAE Annual Meeting, American Society of Agricultural Engineer, Paper No. NA80-205, August 1980.
16. **Smith, Charles A., and David C. Curtis.** "Flood Forecasting on New England - Now and in the Decade Ahead", presented at the NAR-ASAE Annual Meeting, American Society of Agricultural Engineers, Paper No. NA80-206, August 1980.
17. **Curtis, David C.** Constrained Stochastic Climate Simulation, Ph.D. Dissertation, Massachusetts Institute of Technology, Cambridge, Massachusetts, 1982.
18. **Curtis, David C., and Peter S. Eagleson.** Constrained Stochastic Climate Simulation, Report No. 274, Ralph M. Parsons Laboratory, Massachusetts Institute of Technology, Cambridge, Massachusetts, 1982.
19. **Curtis, David C., and Susan Weisman.** "Automated Flood warnings for Westchester County, New York", presented at the 1982 Spring Meeting of the American Geophysical Union, Philadelphia, Pennsylvania, May 31, 1982.
20. **Curtis, David C.** "ALERT for Connecticut", presented at the Connecticut Flood Management Workshop, Meridan, Connecticut, October 1982.
21. **Curtis, David C.** Constrained Stochastic Climate Simulation: Computer Programs and User's Manual, Report No. 276, Ralph M. Parsons Laboratory, Massachusetts Institute of Technology, Cambridge, Massachusetts, 1982.
22. **Curtis, David C.** "Automated Community Flood Warning Systems", presented at the 1983 ASCE Hydraulics Division specialty Conference, Cambridge, Massachusetts, August 1983.
23. **Curtis, David C. and John C. Schaake, Jr.** "Economic Benefit Estimation for Flood Warning Systems", presented at the Technical Conference on Mitigation of Natural Hazards through Real-Time Data Collection Systems and Hydrologic Forecasting, Sacramento, California, September 1983.
24. **Curtis, David C.** "Automated Flood Warnings for Westchester County New York", presented at the Engineering Foundation Conference on Emerging Computer Techniques in Stormwater and Flood Management, October 30 - November 4, 1983, Niagara-on-the-Lake, Ontario, Canada.
25. **Curtis, David C.** "Improved Dam Safety with Real-Time Flood Forecasts and Warnings", presented at the Dam Safety Conference, December 5-7, 1983, New York, New York, sponsored by the Federal Emergency Management Agency, Region II, 26 Federal Plaza, New York, New York, 10278.
26. **Curtis, David C., and Mark W. Lubbers.** "Integrated Flood Management in Stamford, Connecticut", presented at the International Symposium on Urban Hydrology, Hydraulics, and Sediment Control, July 23-26, 1984, University of Kentucky, Lexington, Kentucky.
27. **Curtis, David C.** "Design Limits for Event Reporting Telemetry Systems", presented at the American Water Resources Association Symposium, A Critical Assessment of Forecasting In Western Water Resource Management, June 11-13, 1984, Seattle, Washington.
28. **Curtis, David C.** "ALERT Systems and Integrated Flood Management", presented at the American Water Resources Association Symposium, A Critical Assessment of Forecasting In Western Water Resource Management, June 11-13, 1984, Seattle, Washington.

29. **Curtis, David C., and John C. Schaake, Jr.** "Economic Benefit Estimation for Flood Warning Systems", submitted for publication, *Water Resources Bulletin*, American Water Resources Association, 1984.
30. **Curtis, David C.** "Issues in Automated Flood Forecasting", presented at the American Water Resources Conference, August 16, 1984, Washington, D.C.
31. **Calvesbert, Robert J., and David C. Curtis.** "Real-Time Tropical Rainfall Reporting in Puerto Rico," presented at the International Symposium on Tropical Hydrology and 2nd Caribbean Islands Water Resources Congress, San Juan, Puerto Rico, May 5-8, 1985.
32. **Evans, W.A. Jr. P.E., and David C. Curtis.** "Real-Time Monitoring and Flood Forecasting in Harris County, Texas", *Hydraulics and Hydrology in the Small Computer Age*, Volume 1, edited by William R. Waldrop, New York, NY, August, 1985.
33. **Leader, David C., David C. Curtis.** "Automated Data Monitoring for Disaster Prevention," *Computer Applications in Water Resources*, Edited by Harry C. Torno, ASCE, pp. 216-221, 1985.
34. **Curtis, David C.** "On Merging Satellite and Meteor Burst Communications with Real-Time Event Reporting Technologies," *Hydrologic Applications of Space Technology*, IAHS Publication No. 160, 1986.
35. **Curtis, David C.** "Role of Private Sector in Flood Warning Systems," presented at the US Army Corps of Engineers Seminar on Local Flood Warning-Response Systems, Pacific Grove, CA, December 10-12, 1986.
36. **Curtis, David C., Donald E. Colton, and David C. Leader.** "Integration of Real-Time Forecasting and Engineering Workstations," presented at Computational Hydrology '87, Computational Hydrology Institute, Anaheim, CA, July 12-16, 1987.
37. **Curtis, David C.** "Telemetry Streamlines Urban Watershed System", *Waterworld News*, Vol. 3, No. 4, July/August 1987.
38. **Curtis, David C.** "Fault-Tolerant Design for Data Acquisition and Flood Forecast Systems", *Engineering Hydrology*, Edited by Arlen D. Feldman, ASCE, Williamsburg, VA, August, 1987.
39. **Curtis, David C.** "Fault-Tolerant Design for Data Acquisition and Flood Forecast Systems", *Public Works*, Vol. 119, No. 4, April, 1988.
40. **Jackson, Donald E., and David C. Curtis.** "Microcomputer Based Flood ALERT and Reservoir Management System", presented at American Water Works Association Specialty Conference on Computers and Automation in the Water Industry, April 2-4, 1989.
41. **Curtis, David C. and Ted Roper.** "Automated Flood Warning Systems: Data Collection and Processing Methods", prepared for the "Flood Warning-Preparedness Programs" training course presented at the U.S. Army Hydrological Engineering Center in Davis, CA, February 4-8, 1991.
42. **Curtis, David C.** "Forecasts for Flood Warning Systems", Chapter 17, *Engineering Manual: Hydrologic Forecasting*, US Army COE Hydrologic Engineering Center, Davis, CA, In publication.
43. **Curtis, David C.,** "Hydrologic Aspects of Flood Warning Systems", Report submitted to US Army COE Hydrologic Engineering Center, Davis, CA, November 1993.
44. **D'Aleo, Joe, Lou Torrence, and David C. Curtis,** "A New Generation of Rainfall Measurement for Flood Forecasting", California Association of Flood Plain Managers Conference, Solvang, CA, March 31- April 2, 1993.

45. **Curtis, David C.**, "An Economic Rationale for Rain Gage Network Size for Flood Warning", California Association of Flood Plain Managers Conference, Solvang, CA, March 31- April 2, 1993.
46. **Curtis, David C. and Harry W. Dotson**, "Rain Gage Network Size for Automated Flood Warning Systems", ASCE Hydraulics Division 1993 National Conference on Hydraulic Engineering and International Symposium on Engineering Hydrology, San Francisco, July 25-30, 1993.
47. **Curtis, David C.**, "Choosing a Hydrologic Model for Flood Forecasting", Presented at the 1993 Conference of the Southwest Association of ALERT Systems, Houston, TX, October 20-22, 1994.
48. **Curtis, David C.**, "Choosing a Hydrologic Model for Flood Forecasting", *ALERT Transmission*, ALERT Users Group, Anaheim, CA, Fall 1993 (invited).
49. **Curtis, David C.**, "Choosing a Hydrologic Model for Flood Forecasting", Presented at the 1994 Annual Conference of the Association of State Flood Plain Managers", Tulsa, OK, May 8-13, 1994.
50. **Curtis, David C., Joe D'Aleo, and Lee Larson**, "Radar-Rainfall Data for the Great Flood of 1993", Presented at the 1994 Annual Conference of the Association of State Flood Plain Managers", Tulsa, OK, May 8-13, 1994.
51. **Curtis, David C.**, "The Cost of Flood Warning Systems", Presented at the 1994 Conference of the Southwestern Association of ALERT Systems, San Antonio, TX, October 11-14, 1995.
52. **Curtis, David C.**, "Flood Routing Basics", Presented at the 1994 Conference of the Southwestern Association of ALERT Systems, San Antonio, TX, October 11-14, 1995.
53. **Curtis, David C.**, "Hydrologic Operations in Japan", *ALERT Transmission*, ALERT Users Group, Anaheim, CA, Fall 1994.
54. **Curtis, David C., Mike Herman, and Dan Howard**, "Working with the Petaluma River: A Shopping Center Flood Emergency Program", Flood Plain Managers Association, Spring Conference, Anaheim, CA, March 29-21, 1995.
55. **Curtis, David C.**, "Wind Effects of Rain Gauge Catch", *ALERT Transmission*, ALERT Users Group, Anaheim, CA, Fall 1995.
56. **Curtis, David C., John H. Humphrey**, "Use of Radar-Rainfall Estimates to Model the January 9-10, 1995 Floods in Sacramento, CA, Presented at the Southwest Association of ALERT Systems Conference held in Tulsa, OK, Oct. 25-26, 1995.
57. **Curtis, David C., et. al.**, "A Comparison of Radar-Rainfall Estimates and Rain Gauge Observations at Three Different Scales", Presented at the 1996 Association of State Flood Plain Managers Conference, San Diego, CA, June 12, 1996.
58. **Curtis, David C., Robert J. C. Burnash**, "Inadvertent Rain Gauge Inconsistencies and Their Effect on Hydrologic Analysis", Presented at the 1996 California-Nevada ALERT Users Group, Ventura, CA, May 15-17, 1996.
59. **Farr, Clark, and David C. Curtis**, "A Flood Warning System Audit for Caliente Creek", presented at the conference What We Have Learned From the Big Thompson Flood: 20 Years Later, held in Fort Collins, CO, July 10-13, 1996.
60. **Curtis, David C., and Rod Thornhill**, "Use of Gauge-Adjusted Radar-Rainfall Estimates for Inflow/Infiltration Studies, AMS Conference on Hydrology, Long Beach, CA, February 2-7, 1997.
61. **Curtis, David C.**, "Gauge-Radar Analysis of an Extreme Rainfall Event", AMS Conference on Hydrology, Long Beach, CA, February 2-7, 1997.

62. **Curtis, David C., et. al.**, "A Comparison of Radar-Rainfall Estimates and Rain Gauge Observations at Three Different Scales", AMS Conference on Hydrology, Long Beach, CA, February 2-7, 1997.
63. **Hartman, Rob, Ira Bartfeld, and David C. Curtis**, "Evolution of Flood Forecast Technologies Between 1986 and 1997 Floods in California", 1997 Fall Meeting, American Geophysical Union, San Francisco, CA, Dec. 8-12, 1997.
64. **Curtis, David C.**, "Use of WSR-88D Data in Hydrologic Modeling", 77th Annual Meeting of the National Transportation Research Board, Washington, DC, January 11-14, 1998.
65. **Curtis, David C. and Rod Thornhill**, "Use of Gauge-Adjusted Radar-Rainfall Estimates in Stormwater Inflow/Infiltration Studies", presented at Fourth International Symposium on Hydrologic Applications of Weather Radar, April 5-9, 1998.
66. **Curtis, David C., and Rod Thornhill**, "Use of Radar and Rain Gage Estimates in Inflow/Infiltration Analysis to Improve Remediation Recommendations", presented at the American Water Resources Association's 34th Annual Conference, Mobile, AL Nov. 19, 1998.
67. **Curtis, David C.**, "Use of Radar-Rainfall Estimates in the Western US", to be presented, Arid Regions Floodplain Management 8th Biennial Conference, January 20-22, 1999.
68. **Curtis, David C.**, "Practical Applications of Gage-Adjusted Radar-Rainfall Estimates", to be presented, American Society of Civil Engineers, 26th Annual Water Resources Planning & Management Conference, Tempe, AZ, June 6-9, 1999.
69. **Fitzwilliams, Peter, Rod Thornhill, and David C. Curtis**, "Use of Radar-Rainfall in GIS-based Sanitary Sewer Modeling, to be presented, GIS '99 Conference, Geosolutions: Integrating Our World, Vancouver, British Columbia, March 2-4, 1999.
70. **Curtis, David C., and Brett Clyde**, *Comparing Spatial Distributions of Rainfall Derived from Rain Gages and Radar*, **Journal of Floodplain Management**, California Flood Plain Managers Association, July 1999.
71. **Hoblit, Brian C. and David C. Curtis**, *Radar Estimates + Gauge Data: A Perfect Union*, Southwest Hydrology, Volume 4, No. 3, May/June 2005.
72. **Giguere, Paul, Randy Bush, and David C. Curtis**, *Dallas' Innovative Design Storm Approach Incorporates Radar Rainfall Analysis of Storm Size and Shape*, Presented and WEFTEC.05, 78th Annual Technical Exhibition and Conference, Oct 29-Nov 2, 2005, Washington Convention Center, Washington, D.C.
73. **Curtis, David C.**; *Evaluation of the Spatial Structure of Storms and the Development of Design Storms*, Proceedings of the ASCE/EWRI World Environmental and Water Resources Congress 2007: Restoring Our Natural Habitat, May 15, 2007.
74. **Ivanov, Valeriy Y., Rafael Bras and David C. Curtis**, *A Weather Generator for Hydrological, Ecological, and Agricultural Applications*, Water Resources Research, Vol. 43, W10406, DOI:10.1029/2006WR 005364, 2007.
75. **Curtis, David C.**; *Economic Impacts of Rainfall Measurement Systems*, Proceedings of the ASCE/EWRI World Environmental and Water Resources Congress 2008, Honolulu, HI, May 12-16, 2008.
76. **Curtis, David C.**; *Radar-Rainfall Analysis for Extreme August Storm in Sacramento*, Proceedings of the ASCE/EWRI World Environmental and Water Resources Congress 2009, Kansas City, MO, May 17-21, 2009.

77. **Curtis, David C.;** *A National Vision for the use of Spatially Distributed Precipitation Data*, ESRI International User Conference, July 13-17, 2009.

SEMINARS PRESENTED

NEXRAD Radar Rainfall Estimation, Flood Plain Managers Association, Fall Conference, Sept. 1994, Sacramento, California.

NEXRAD Radar Rainfall Estimation, Flood Plain Managers Association, Spring Conference, March 1995, Anaheim, California.

Rainfall Measurement - Traditional and New Technologies, Continuing Education Seminar, Environmental Section of Real Properties Division of the California State Bar Association, September 8, 1995.

Effective Use of Weather Information, A Training Workshop, Tulsa, OK, Oct. 24, 1995.

Effective Use of Weather Information, A Training Workshop, Orange, CA, Dec. 19-20, 1995.

Improved Hydrologic Analysis with Engineered Rainfall Data, Training workshop, Dallas, TX, March 8, 1996.

Effective Use of Weather Information, National Hydrologic Warning Council/Southwest Association of ALERT Systems Conference, St. Louis, MO, Oct. 19, 1997.

Spatial Analysis of Rainfall, Department of Civil Engineering, Stanford University, Palo Alto, CA, April 12, 1999.

Rainfall Analysis, US Agency for International Development/World Bank Training, Menlo Park, CA, April 13, 1999.

Radar-Rainfall Estimation, National Hydrologic Warning Council Conference, San Diego, CA, May 11, 1999.

National Weather Service River Forecast System Workshop, National Weather Service, International Hydrologic Technology Transfer Center, NOAA NWS, Silver Spring, MD, October 25-27, 1999.

John Henry Humphrey, Ph.D., P.E. C.C.M.

Hydrologist, Meteorologist, Civil Engineer

Hydmet, Inc.
9855 Meadowlark Way
Palo Cedro, California 96073
530-547-4743
hydmetjack@aol.com

GEOGRAPHIC EXPERIENCE

Over 100 studies in California
For 15 Counties and most major Cities in California
Projects in all Pacific and Rocky Mountain States and Alaska

DEGREES

Ph.D. Hydrology
University of Nevada, Reno 1972

B.A. Meteorology
University of California at Los Angeles 1964

REGISTRATIONS

Professional Engineer in Civil Engineering
California, # 30512, Expires 2012

Certified Consulting Meteorologist # 242
American Meteorological Society, Expires 2011

SUMMARY OF EXPERIENCE

John Humphrey has had a key role or acted as a project manager for a broad range of studies and projects in the fields of hydrology, civil engineering and meteorology. In recent years most work has involved design storm studies and stormwater management plans, for example, Redding, Gilroy, Morgan Hill, South San Francisco, Ventura and St. Louis. Most recent flood studies have been FEMA detailed submittals for streams and rivers in California

EMPLOYMENT

1964-1968: **U.S. Air Force**, Meteorologist. Five years active duty in California, Vietnam and West Germany. Remained in the U.S. Air Force Reserve as a Meteorologist. Retired in 1988 with rank of Lt. Colonel.

1969-1972: **University of Nevada**, Graduate Research Assistant. Managed field research for investigating the hydrologic response of snowpacks to rain and other meteorological variables near Lake Tahoe in the Sierra Nevada.

1973-1977: **CH2M Hill Engineers**, Hydrologist in Bellevue, Washington and Redding, California.

1978-1986: **Ott Water Engineers**, Redding, California, Director of Meteorologic and Hydrologic Services.

1987-Present: **Hydmet, Inc**, Redding, California. This firm is owned by Dr. John H. Humphrey and provides technical expertise in hydrology, meteorology, stream hydraulics, sediment transport, geomorphology, and water quality. Meteorologic, hydrologic, hydraulic, and sediment transport databases, models and analyses are developed for streams and lakes using programs HEC-1, HECRMS, HECRAS, SWMM, HEC-6, FLUVIAL-12, HSPF, BASINS, PRMS, RMA2, CEQUAL-W2, QUAL2E, FLDWAV and FESWMS.

EXPERIENCE

METEOROLOGY

1973: Seattle, Washington, River and Lake Models. Set up and calibrated meteorologic input to urban runoff models of Lake Washington and Lake Sammamish for City of Seattle and Metro.

1974: Coeur d'Arlene, Idaho, I-90 Environmental Impact Report. Air pollution meteorologic analysis for proposed rerouting of Interstate 90 by Idaho Department of Highways.

1974: Bellevue, Washington, 148th Avenue EIR. Air pollution meteorologic analysis for street improvement project.

1974: Kenniwick, Washington, Sewage Lagoon. Set up weather station and determined evaporation rates for leak testing.

1975: Warm Springs Indian Reservation, Oregon, Airport. Two year wind collection and analysis for airport runway siting.

1976: Humboldt River and Tributaries, Nevada, Hydrology Memorandum. Cloudburst and general rain/snowmelt storm analysis for dam design and river flooding projects for U.S. Army Corps of Engineers.

1976: Milwaukee, Wisconsin, Combined Sewer Overflow Control. Historical storm analysis to determine design events.

1976: Denver, Colorado, EPA 208 River Models. Set up and calibrated meteorologic input of precipitation, temperature, sunshine, humidity and wind for water quality models.

1977: Washington, Oregon, Coastal Flooding. Analysis of 40 years of weather maps and coastal meteorologic data for wave hindcasting and storm surge modeling for Federal Emergency Management Agency flood mapping.

1977: Russell Creek, Cold Bay, Alaska, Snow Drifting. Used historical Cold Bay weather observations to determine snowdrift accumulations and snow fence design for fish hatchery access road.

1977: Upper Wisconsin River, Wausau, Wisconsin. Collected meteorologic data and calibrated snowmelt models for operating system of 19 reservoirs on the Wisconsin River for Wisconsin Valley Improvement Company.

1977: Dupont Wharf, Nisqually Reach, Puget Sound, Washington. Collected and analysed wind data for wave and oil spill study for Weyerhaeuser Company.

1978: Fox River Model, Green Bay, Wisconsin. Meteorologic measurements and analysis for water temperature model.

1978: Humboldt River, Nevada, Snowmelt Model. Operational snowmelt flood forecasting using real-time meteorologic data for U.S. Army Corps of Engineers.

1979: Mt. Shasta, California, Ski Area. Snow accumulation and snowmelt analysis using aerial photography and climatological data.

1980: Dillingham Harbor, Alaska, Waves. Prediction of waves from long-term meteorological data and analysis of wave protection for U.S. Army Corps of Engineers.

1980: Truckee River, California, Snowmelt Model. Operational snowmelt spring runoff forecasting for U.S. Bureau of Reclamation.

1982: Ship Creek Cooling Pond, Anchorage, Alaska. Meteorological analysis of potential fog formation from proposed cooling pond for Elmendorf Air Force Base.

1983: Calkari Arms Apartments, Redding, California. Cloudburst flood study for litigation against Caltrans.

1984: Northern California Coastal Flooding. Meteorological analysis of weather maps for wave hindcasting and storm surge for FEMA flood studies from Monterey to Oregon.

1984: Stephens Passage, Juneau, Alaska. Wind recorder installation and analysis of wind fields for determination of wave conditions for Greens Creek Mine dock.

1985: Shemya Air Force Base, Shemya Island, Alaska. Analysis of weather maps for wave hindcasting for dock design.

1985: Magic Dam, Twin Falls, Idaho. Meteorological study of probable maximum precipitation conditions for Big Woods River and Camas Creek.

1985: Arco Pit D, Kapuruk, Alaska. Meteorological station set up and analysis for determining snowmelt floods for the North Slope.

1985: Eel River Landslide, Redway, California. Analysis of historical precipitation records in Northwest California to determine contributory causes to December 1983 landslide.

1986: Combined Sewer Overflow, Seattle, Washington. Analysis of urban precipitation patterns for calibration of stormwater runoff models.

1987: Baxter EIR, Redding, California. Air pollution meteorological analysis for proposed wood treatment plant.

1987: Combined Sewer Overflow, Everett, Washington. Analysis of urban flood events and precipitation for stormwater runoff model.

1987: Precipitation Gage Master Plan, Orange County, California. Analysis of siting conditions and criteria for location of precipitation gages in Orange County for OCEMA.

1987: Kensington Mine EIR, Juneau, Alaska. Installation of weather station and analysis of weather conditions influencing operation of proposed gold mine.

1988: Rush Creek, Lee Vining, California. Installation of weather station and analysis of meteorological data for stream temperature modeling for California Department of Fish and Game.

1988: Garden Bar Pumped Storage, Marysville, California. Analysis of meteorological data for input to reservoir and Bear River water temperature models.

1988: American River, Sacramento, California. Analysis and input of meteorological data for water temperature modeling of the American River and Folsom Reservoir for Sacramento County.

1988: Chester Lake, Metlakatla, Alaska. Precipitation and runoff analysis for hydropower facility for Alaska Power Authority.

1989: Silver Bow Creek, Butte, Montana. Analysis of meteorological conditions resulting in 100-year and probable maximum floods for Montana Department of Health and Environmental Sciences.

1989: February 18, 1986 Flood, Roseville, California. Cloudburst precipitation analysis for hydrologic model of flood event for City of Roseville.

1989: Rosamond Wash, Mojave Desert, California. Analysis of meteorologic and hydrologic conditions causing cloudbursts and flash floods for L. Bruce Nybo, Inc.

1989: Jawbone and Pine Tree Canyons, Mojave Desert, California. Analysis of meteorologic and hydrologic conditions causing cloudbursts and flash floods for L. Bruce Nybo, Inc.

1989: Placer County, California. Description of precipitation statistics and cloudburst design storm methodology for the Placer County Hydrology Manual.

1989: Santiago Reservoir, Orange County, California. Analysis of meteorologic data for input to water quality model of Santiago Reservoir for the Irvine Company.

1990: Sacramento County Hydrology Manual, California. Analysis of precipitation data for all Sacramento County stations.

1992: Charlotte Air Pollution Study, North Carolina. Analysis of odor problems for Charlotte wastewater treatment plants.

1993: Greater Houston Wastewater Project, Texas. Analysis of precipitation records to determine depth-duration-frequency and areal-reduction-factors.

1994: Spokane County Stormwater Management Study, Washington. Selection and siting of precipitation gages and weather stations for calibration of snowmelt/precipitation runoff models.

1997: Davis County, Utah. Determination of depth-duration-elevation frequency curves for precipitation in the Wasatch Range.

1997: Cedar City, Utah. Analysis of long-term hourly precipitation records in Southwest Utah to derive design storms for a FEMA restudy.

2000: New Orleans, Louisiana. Study of short-duration precipitation data for urban design storms for City of New Orleans and MWH Engineers.

2001: Idaho Falls, Idaho. Analysis of rain-on-snow design precipitation events for the Idaho National Environmental Engineering Laboratory.

2001: Atlanta, Georgia. Study of radar and precipitation gage statistics for urban design storms for City of Atlanta and MWH Engineers.

2002: Oroville, California. California DWR and MWH Set up meteorologic data base for WQRSS for Lake Oroville and Themolito Afterbays for 1922-2003.

2005: St Louis, Missouri. Jacobs and MWD. Set up processor for stationary design storms using Depth-Duration-Frequency data for St. Louis and Depth Areal Reduction Factors from radar meteorology analyses.

2005: Big Bear Municipal Water District. City of Big Bear, California. Set up 57-year HSPF climatologic hourly data base for investigation of future lake levels in Big Bear Lake. Installed telemetered weather station at Snow Summit Ski Area.

2006: U.S. Bureau of Reclamation, MWH Americas, Sacramento. Set up a hourly data base for Fresno 1921-2005 (85 years) for air temperature, dewpoint, wind speed, wind direction, cloudiness and solar radiation. Developed algorithms for estimating hourly data for the 1921-1948 period when only daily maximum-minimum temperatures and daily precipitation data were available. The database is being used for water quality modelling of reservoirs on the San Joaquin River using CEQUAL-W2

2009. Colorado Springs, Colorado and Carleton Engineers. Statistical analyses of long-term rain gage records and radar precipitation for deriving cloudburst design storms. Set up HSPF model for 1949-2008 to determine antecedent precipitation conditions for Fountain Creek.

Hydrology

1974: Water Resources Management Study, Seattle, Washington. Set up and calibration of HSP continuous snowmelt runoff simulation model of the Cedar, Tolt and Green Rivers.

1974: Lake Young, Tacoma, Washington. Water quality simulation of water supply reservoir influenced by urban runoff.

1976: Seneca Creek, Silver Springs, Maryland. Hydrologic simulation using HSP model of urbanizing watershed near Washington, D.C. for Montgomery County Capitol Parks Planning Commission.

1976: Rock Creek Park, Washington, D.C., Maryland. Set up and calibrated water quality model to determine urban runoff influence on Rock Creek for National Park Service.

1977: Humboldt and Walker Rivers, Nevada. Set up and calibrated water quality models for wasteload allocation for Nevada Department of Environmental Quality.

1977: Municipality of Anchorage, Alaska. Set up and calibrated water quality model of urban runoff influences on Campbell and Ship Creeks for EPA 208 study.

1977: St. Louis, Missouri. Set up and calibrated water quality model of urban runoff influences on Meramec River and tributaries for EPA 208 study for Eastwest Gateway Commission.

1978: Del Norte County, California. Drainage study and hydrologic design manual.

1978: Water Resources Atlas, U.S. Forest Service Region 10, Juneau, Alaska. Precipitation maps and hydrologic design manual for Southeast and south Alaska.

1979: Cascade Enterprise Drainage Manual, Redding, California. Stormwater system designs for two developing areas of Redding.

1979: Hydrology Manual, Six Rivers National Forest, Eureka, California. Streamflow regression equations for hydrologic design in northwest coastal California.

1979: Grubers Bay, Lake Wisconsin, Wisconsin. Set up and calibration of water quality model for determining influence of wastewater for Wisconsin Department of Environmental Quality.

1980: Grey Eagle Mine EIR, Happy Camp, California. Hydrologic tailings pond water balance and water quality study for gold mine.

1980: Seward Marina, Fourth of July Creek, Alaska. Hydrologic design criteria for levee and salmon spawning ponds.

1980: Manzanita Creek, Big Bar, California. Flow measurements and hydrologic analysis for U.S. Forest Service, Shasta-Trinity National Forest prescribed burn study.

1981: Truckee River Water Supply Needs, California-Nevada. Historical and projected water supply study for Reno and Pyramid Lake for USBR.

1981: Fifteen Dam Safety Studies for Utah and Nevada. Site visits and probable maximum flood spillway adequacy studies for U.S. Army Corps of Engineers.

1981: Bradley Lake, Homer, Alaska. Field reconnaissance and water quality assessment of hydropower project operations for U.S. Army Corps of Engineers.

1981: Carson River, Carson City, Nevada. Water quality model of nonpoint pollution to Carson River for Nevada Department of Environmental Conservation.

1982: Sacramento River, Tehama County, California. Historical hydrologic simulation of the influence of Shasta Dam on Sacramento River floods.

1982: Salt Creek, Red Bluff, California. Description and analysis of flooding of an office complex for litigation.

1982: Whiskeytown Reservoir, Redding, California. Water quality measurements and assessment of hydropower operations.

1982: Iron Mountain Mine, Shasta, California. Water quality measurements and hydrologic isolation plans for mine tailings.

1983: Grey Eagle Mine, Yreka, California. 100-year flood hydrologic study for Luther Gulch and Indian Creek.

1984: Red Dog Mine EIR, De Long Mountains, Alaska. Hydrologic water balances for proposed water supply and tailings ponds for lead-zinc-silver mine in Brooks Range.

1984: Hydropower Assessment Program, Portland, Oregon. Hydrologic methodology for determining potential yields of hydropower in Montana, Idaho, Washington and Oregon for Northwest Power Planning Council.

1985: Lemhi River, Salmon, Idaho. Hydrologic description of Lemhi River basin for salmon fishery enhancement for BPA.

1986: Greens Creek Mine, Admiralty Island, Alaska. Hydrologic studies for water supply, hydropower and flood protection on Greens Creek.

1986: Crabtree Creek, Lebanon, Oregon. Hydrology for power projections for Lacombe hydropower facility.

1986: Clover Creek, Redding, California. Hydrologic study on influence of urbanization on 100-year flood.

1986: Foothill Freeway Corridor, Orange County, California. Determination of 100-year floods for proposed freeway crossings near El Toro.

1987: Deadwood Canyon and Big Mosquito Creeks, California. Flow meter installation, flow measurement and hydrologic analysis for hydropower projects near Sacramento.

1987: Withlacoochee River, Georgia. Set up and calibrated water quality model for assessing influence of paper mill wastewater for Georgia Environmental Protection Agency.

1987: James River, Virginia. Set up and calibrated water quality model for assessing impact of wastewater discharge for Owens-Illinois Company.

1988: Big Creek, Hyampom, California. Hydrologic analysis for hydropower project in northwest California.

1988: Garden Bar Pumped Storage, Marysville, California. Study of influence of alternative operations on water temperatures using USCOE Thermal Simulation of Lakes Model and EPA Qual2E for Garden Bar/Camp Far West Reservoirs and Bear River.

1988: Muck Valley EIR, Nubieber, California. Set up and calibrated water quality model for assessing influence of Collett Lake hydropower operations on Pit River.

1989: Irvine Lake/Santiago Reservoir, Orange, California. Set up, calibrated and analyzed water quality of lake for development alternatives using USCOE CEQUAL-R1.

1989: Montgomery Creek, California. Two-year flow measurement and hydrologic analysis for El Dorado hydropower.

1989: Bluford Creek, Zenia, California. Hydrologic studies for expansion of hydropower facility.

1989: Box Canyon Dam Break Inundation, Dunsmuir, California. Used NWS dynamic wave model to determine dam break flooding on upper Sacramento River.

1990: Battle Creek Hydrology Study, Manton, California. For California Department of Fish and Game, compiled long-term monthly flow statistics on Battle Creek to assess influence of diversions on low flow periods.

1990: American River Water Quality Study, Sacramento, California for Sacramento County. Set up, calibrated and tested alternative Folsom Lake release influence on water temperature using EPA Qual2E and USCOE CEQUAL-R1.

1990: Dry Creek Master Drainage Plan, Placer County, California. HEC-1 and HEC-2 modeling of 80 square mile urbanizing watershed.

1991: Auburn/Bowman Community Plan Hydrology Study, California. HEC-1 and HEC-2 modeling of peak flows and water levels resulting from future development.

1991: Morrison Creek Hydrology Study, California, HEC-1 and HEC-2 modeling of Morrison Creek and tributaries in Sacramento County.

1991: Folsom Reoperation Study of American and Sacramento Rivers for USCOE. EPA QUAL2E and USCOE CETHERM-R1 for analyzing influence of Folsom Lake operation alternatives on water temperatures.

1992: City of Redding Stormwater Master Plan, California. HEC-1 and HEC-2 modeling of 100 square miles of tributaries to Sacramento River.

1993: City of Lincoln Stormwater Facilities Plan, California. HEC-1 and HEC-2 modeling of Auburn Ravine, Orchard Creek and Ingram Slough proposed development.

1994: City of Hanford Stormwater Master Plan, California. HEC-1 modeling and system design for existing and proposed stormwater management facilities.

1994: Clover Creek Stormwater Management Plan, Redding, California. Siting of retention/detention basins for control of flooding due to future developments.

1994: Grasshopper Creek, Red Bluff, California. Hydrology and hydraulics 100-year flood study for submittal of application of Letter of Map Amendment for FEMA.

1994: Lemhi River, Salmon, Idaho. Analysis of river flow and irrigation records for 1992-1994 to determine consumptive use and return flow.

1994: Lake Creek, Medford, Oregon. Determination of impacts on hydrology and water quality from proposed hydropower diversions.

1995: Sacramento, County, California. Meteorologic, Hydrologic and Hydraulic analysis of January 10, 1995 flood event in Sacramento County, Roseville, and Placer County.

1995: Redding, California. Design guidelines for control of flood increases due to land development using detention/retention ponds.
Revision of 100-year floodplains for 40 miles of stream using 1994 land use hydrology.

1995: Sacramento County, California. Revision of peak flow frequency curves and depth-duration-precipitation frequency curves for all gage records in Sacramento County. HEC-1 and HEC-2 analyses of January 9-10, 1995 flood event.

1995: Iron Mountain Mine, Redding, California. Peer review of water quality control alternatives for Boulder Creek. Hydrologic analysis of long-term flows using HSPF model.

1997: EIP Associates and Calaveras Cement Corporation, Shasta County, California. Set up HSPF model of Stillwater Creek to provide 1948-1998 flow duration curves for locations used for water quality measurements.

2000: Duncan and Long Canyon, Greek Store, California. For Placer County Water Agency,. Set up PRMS to determine the influence of logging on snowmelt for paired watersheds tributary to the North Fork American River.

2000: Auburn Ravine and Coon Creek, Auburn, California. For Placer County Planning Department. Set up HSPF to determine long-term flow statistics.

2001: EIP Associates and San Bernardino Water District. Derived long-term statistics of daily and peak flow for Mill Creek near Redlands. California.

2001: City of Morgan Hill and Carollo Engineers. Stormwater master plan using HEC-1 and SWMM for City of Morgan Hill.

2002: City of Gilroy and Carollo Engineers. Stormwater master plan using HEC-1 and SWMM for City of Gilroy and vicinity.

2002: Tuolumne Utility District and EIP. Water balance and leak analysis of TUD ditch system near Sonora using HEC-1 and spreadsheets.

2003: EPA and Placer County Water Agency. Long-term simulations of representative Sierra Nevada watersheds using HSPF including climatic change scenarios.

2003: Fidelity Coal Company. Long-term simulations of Tongue River and Tongue River Reservoir flow and water quality using HSPF and CEQUAL, near Miles City, Montana.

2005: Shasta County. FEMA LOMR for Burney Creek. Used HECRAS to set new 100-year flood plains and floodways.

2005: City of Redding. City-wide Master Storm Water Drainage Study. 32 HEC-1 and HECRAS models for all streams in the 100 square mile drainage area within the city limits.

2006: Thomason Development. HSPF 15-minute, 1949-2006 watershed modelling of Dry Gulch. Included alternative detention ponds and influence of urban development on flood peaks.

2006: Montgomery Watson Harza. Developed daily flow files for inflow and downstream local for Shasta Dam, Sacramento River for 1907-2007. Developed program for evaluating the influence of revised operating rules on downstream flood peaks.

2007: City of Anderson. Submitted revised floodplain mapping to FEMA for Anderson Creek, Sacramento Gulch and Tormey Drain.

2007: Ventura County Watershed Protection District. Comprehensive evaluation of stream gage sites in Ventura County. Produced a new design storm and HEC-1 processor.

2009. City of Yreka, California. Analysis of new floodplains for greenway enhancement projects on Yreka and Greenhorn Creeks.

2009. City of Livingston, Montana. FEMA floodplain mapping submittal for a re-study of the Yellowstone River.

Litigation Investigations

1980: City of Seward vs. Century, for plaintiff. Flood flow assessment for Fourth of July Creek, Seward, Alaska. Arbitration testimony. Case settled.

1982: Rogers vs. Jones, for defendant. Flood study for industrial property on Salt Creek in Red Bluff, California. Deposition testimony. Case settled.

1982: Keho vs. Lewis, for plaintiff. Surface water and ground water drainage for residential development in Yreka, California. Case settled.

1982: Plaintiffs vs. Holiday Harbor, for defendant. Meteorological study of wind at Shasta Lake, California. Trial testimony.

1983: Calkari Arms vs. Caltrans, for plaintiff. Storm rainfall and runoff for 1977 cloudburst at Redding, California. Deposition testimony. Case settled.

1983: Phillips vs. Adams, for defendant. Flood and stream bank erosion study for Clear Creek at French Gulch, California. Trial testimony. Defendant won.

1983: Yuba Irrigation District vs. Shell Oil, for defendant. Hydraulic analysis of Cache Creek levee failure near Williams, California. Case settled.

1984: Jones vs. Scott, for defendant. Analysis of natural and manmade drainage systems near Trinity Center, California. Trial testimony. Defendant won.

1984: Tompkins vs. Mallett, for plaintiff. Hydrology study for hydropower facility near Trinity Lake, California. Deposition testimony. Case settled.

1984: California-American vs. U.S. Dept. of Agriculture, for defendant. Sedimentation study for San Clemente Reservoir near Monterey, California. Case settled.

1985: Redway Residents vs. Pacific Lumber, for defendant. Rainfall, runoff, and erosion study for landslide on S. F. Eel River near Redway, California. Deposition testimony. Case settled.

1985: California Fish & Game and FERC vs. Seithe Energies, for defendant. Hydrologic study for hydropower facility on Rock Creek near Placerville, California. Hearing testimony. Case settled.

1986: California Water Rights Board vs. Mega-Renewables, for defendant. Hydrologic study for North Fork Hydro project near Fresno, California. Hearing testimony. Case settled.

1986: California Fish & Game vs. Montgomery Creek Hydro, for defendant. Hydrologic study for Montgomery Creek Hydropower facility near Redding, California. Hearing testimony. Case settled.

1987: Environmental Defense Fund and Sacramento County vs. EBMUD, for plaintiffs. Flow and temperature analysis for American River at Sacramento, California. Trial testimony in Hayward January 1990. Plaintiff won.

1987: Maloughney et al vs. Orange County, for defendants. Analysis of flood event on March 1, 1983 in Fountain Valley, California. Deposition and trial testimony. Defendant won.

1987: Linda Residents vs. California et al, for plaintiffs. Analysis of flooding from levee break on February 19, 1986 at Marysville, California. Case settled.

1988: Alexander et al vs. Orange County et al, for defendants. Analysis of flood event on March 1, 1983 in Huntington Beach, California. Trial testimony in Santa Ana, March 1990. Defendant won.

1988: Achenbaugh et al vs. City of Roseville et al, for defendants. Analysis of flooding resulting for February 19, 1986 cloudburst near Roseville, California. Trial testimony in Auburn March-July, 1992. Defendant won.

1989: Zisk vs. City of Roseville, for defendant. Analysis of flood water levels and erosion potential resulting from floodplain encroachment on Dry Creek in Roseville, California. Case dropped.

1990: Tylstra et al vs. Trinity County, for plaintiffs. Determination of causes of bank erosion induced by airport levee on South Fork Trinity River near Hyampom. Deposition. Case settled.

1990: State of Idaho vs. Truck Transport et al, for defendants. Water quality analysis of Little Salmon River resulting from toxic dye spill. Trial testimony in Boise, Idaho, May 1991. Defendants won.

1990: Winzler vs. Humboldt County, for plaintiff. Determination of causes of bank erosion induced by USCOE experimental spur dikes and levees on the Eel River near Eureka. Trial testimony in Eureka November 1991. Plaintiff won.

1990: Evergreen Estates vs. Sacramento County, for defendant. Analysis of flood runoff and water levels on Arcade Creek, Sacramento for February 19, 1986 event. Deposition testimony. Case settled.

1991: Oregon Worsted Co. vs. State of Oregon, et al, for plaintiff. Analysis of effects of proposed bridge on Johnson Creek on fish habitat. Case settled.

1991: Waldport Homeowners vs. State of Oregon Department of Transportation, for plaintiffs. Analysis of effects of bridge demolition on tidal currents in Alsea Bay. Case dropped.

1992: Pleasanton Gravel vs. City of Livermore, for defendant. Analysis of influence of urbanization and city storm drains on flooding downstream. Case settled.

1993: California Department of Fish & Game, et al. vs. City of Big Bear, for defendant. (Downey Brand Seymour Rowher: Kevin O'Brien, Sacramento). Analysis of flushing flow requirements for sand removal and enhancement of fish habitat in Bear Creek downstream of Big Bear Lake. Hearing testimony. Case settled.

1993: Putah Creek Conference, et al. vs. Solano County Water Agency, for defendant. Comprehensive analysis of runoff, storage, evapotranspiration losses, groundwater gains and losses, diversion losses, and irrigation return flows for the 1930-1993 period on Putah Creek and Lake Berryessa. Case settled.

1994: Ludwig vs. Anderson, et al, Yuba City, California, for plaintiff. Hydrologic and hydraulic analyses to determine creek restoration required after topsoil removal. Trial testimony in Yuba City. Plaintiff won.

1994: Plaintiffs vs. Riverside County Flood Control District and Metropolitan Water District of Southern California, for defendant. HEC-1, HEC-2, HEC-6 analyses of influence of channel vegetation on upstream flooding for Murietta Creek at Temecula, California, January 19, 1993. Deposition testimony. Case settled.

1995: Lake Redding Estates Homeowners vs. City of Redding, California, for defendant. Description of standard of care for culvert design. Comprehensive hydrologic and hydraulic analysis of March 23, 1993 flood event on Carter Creek. Trial testimony in Redding. Retrial of similar issues in January 1998. Plaintiffs won. Currently on appeal.

1995: ASARCO Ray Mine, Arizona vs. Arkwright Insurance Company, for plaintiff. Investigation of the probability of mine pit water balances for 1992-1993 wet period for insurance claim. Deposition testimony. Case settled.

1995: Cinnamon, et al. vs. Sacramento County, for defendant. Analysis of flood drainage problems in residential area in Carmichael California. Deposition taken. Case dropped.

1996: Ed Parish, Quail Valley Ranch vs. NRCS, for plaintiff. Analysis of Pit River flooding of alfalfa fields due to new levee project in Lookout California. Deposition pending. Testimony at arbitration proceeding June 21, 1998, Sacramento. Case settled.

1996: Daniel Darnall vs. Lassen County, for plaintiff. Investigation of causes of property flooding due to inadequate drainage systems in Susanville California. Deposition taken. Case settled.

1996: Kuo vs. California Board of Reclamation, et al, for defendant. Analysis of influence of gravel extraction on Cottonwood Creek bend migration, Orland, California. Deposition taken, trial in Orland, California in February 1998. Defendant won.

1996: Trailer park homeowners vs. Napa County and City of St Helena. For defendants. Analysis of 1986, 1995 and 1996 flood events for the Napa River near St. Helena. Case settled.

1996: Plaintiffs vs. City of Napa, California, for defendant. Analysis of January 9, 1995 flood event at a residential development. Case settled in March 1998.

1997: Cabrera and Provine vs. City of Redding, California, for defendant. Analysis of stormwater drainage system at Harpole Road and Churn Creek Road, Redding, California. Case settled.

1997: Winifred Jones vs. Pacific Gas and Electric Company, for plaintiff. Analysis of influence of pipe crossing sheet piles on bank erosion, Corning, California. Testimony at arbitration hearing in Sacramento. Case settled.

1997: Covert Run Pike Homeowners vs. Sanitation District and City of Bellevue, Kentucky. For defendants. Hydraulic analyses of urban flash floods and potential mitigation. Ongoing as of 2005.

1997: Finley et al vs. City of Redding and Shasta County. For defendants. Meteorologic, hydrologic and stream hydraulic analyses of flood causes and potential mitigation for Clover Creek. Case Settled.

1997: Mahaffy vs. City of Redding and Gold Hills Golf Course. For defendants. Hydrologic analyses of stormwater collection system design. Case settled.

1997: Yountville trailer park homeowners vs. Napa County and Town of Yountville, California. For defendants. Investigation of causes of flooding in 1995 and 1997 floods due to Hopper Creek and the Napa River. Case settled.

1997: York vs. Jaxon Enterprises, Corning California. For defendant. Investigation of causes of riverbank erosion in Stony Creek due to gravel extraction operation. Trial testimony in Corning. Defendant won.

1998: Property owners vs. Gravel Extraction Company and Grays Harbor County, Washington. For defendants. Investigation of historic and predicted migration of Humptulips River channel in vicinity of proposed gravel extraction project. Case Settled.

1998: Farm Corporations vs. State of California. For defendant. Analyses of precipitation and flooding of Arroyo Pasajero Creek in March 1995 near Coalinga, California. Case settled.

1998: Story vs. Charles Krug Winery, St Helena California. For defendant. Analyses of flooding on Napa River due to cross levees in March 1995 flood. Trial testimony in Napa Superior Court. Defendant won.

1998: Property Owners vs. Modesto Irrigation District, Modesto California. For defendant. Analyses of flooding on Tuolumne River, Dry Creek, San Joaquin River due to releases from Don Pedro Reservoir in January 1997. Deposition taken. Case dropped.

1999: Kernan vs. Marion, Grenada, California. For defendant. Analyses of flooding on Julian Creek and Housman Ditch in January 1999. Arbitration hearing testimony. Case settled.

1999: Youngman vs. State of California, Meeks Bay California. For defendant. Hydrologic analysis of State Highway 89 culvert near Lake Tahoe January 1997. Trial testimony in El Dorado Superior Court in South Lake Tahoe, July 2001. Found for plaintiff.

1999: Aadland et al vs. State of California, et al., Lodi California. For defendant. Investigation of flooding due to State Highway 99 drainage system in February 1998 at Eden Mobile Home Park. Case Settled.

1999: Barnum vs. City of Eureka, California. For plaintiff. Investigation of flooding due to Fairway Drive culvert since its construction in 1960. Deposition and trial testimony in Humboldt County Superior Court. Found for Plaintiff.

2000: State of California Department of Fish & Game vs. Scott Murrison. For defendant. Investigation of water diversion structure on Big Creek near Hayfork. Case Settled.

2000: Wisher's Salvage, et. al., vs. Burlington Northern & Santa Fe Railroad. For defendant. Analysis of causes of flooding on Ashley Creek near Kalispell, Montana in May 1997. Case Settled.

2001: Woolf vs. State of California. For defendant. Investigation of wet weather accident on I-10 near Ontario, California. Case Settled..

2001: Oakdale Mobile Home Park vs. State of California. For defendant. Investigation of flooding for a mobile home park near Oakdale. Case settled.

2001: Seymour vs State of California. For defendant. Investigation of flooding due to runoff from Shasta County property and State Highway 299 in Shasta City. Case settled.

2002: Dube vs. Forty Grand. For defendant. Investigation of the causes of flooding for a July 1998 storm in Fort Thomas, Kentucky. Deposition Report. Case Dropped.

2002: Corning residents vs. City of Corning. For plaintiff. Investigation of flooding due to urban runoff in Corning. Ongoing in 2005.

2004: EPI Healthcare vs. Philpot Construction. For defendant. Investigation of cloudburst flooding in Richmond, Kentucky from construction activities. Case Settled

2009: Park Marina Village Homeowner's Association vs. Golden State Bridge, Inc. et al. For plaintiff. Investigation of erosion due to Sacramento River Highway 44 bridge construction. Ongoing.

PUBLICATIONS

"Determination of TMDL's for Big Bear Lake, California" Presented at the California Water Agency Conference in San Diego, California, December 5, 2003.

"Determination of Design Storms for Wastewater System Design in Houston, Texas" Presented at the AWWA Annual Meeting in Long Beach, California, October 1997.

"Hydrology Manual Verification Using the March 23, 1993 Storm at Redding, California", Proceedings of the June 25, 1994 Symposium on Predicting Heavy Rainfall Events in California, Sierra College, Rocklin, California.

"Analysis of Flooding Caused by the February 18, 1986 Cloudburst in Placer County, California", Proceedings of the June 25, 1994 Symposium on Predicting Heavy Rainfall Events in California, Sierra College, Rocklin, California.

"Design Cloudbursts and Flashflood Methodology for the Western Mojave Desert, California", Proceedings of the 1990 National Conference on Hydraulic Engineering and the International Symposium on the Hydraulics/Hydrology of Arid Lands, ASCE, New York, NY,

"Hydraulic Characteristics of Steep Mountain Streams During Low and High Flow Conditions and Implications for Fishery Habitat", Proceedings Symposium on Small Hydropower, American Fisheries Society, Denver, Colorado, May 1985.

"Modeling Design Flood Hydrographs for Glaciated Basins in Alaska", Proceedings Cold Regions Specialty Conference, Department of Civil Engineering, University of Alberta, Edmonton, Canada, April 1984.

"Influence of Temperate Glaciers on Flood Events in Maritime Alaska", Managing Water Resources for Alaska's Development, Proceedings American Water Resources Conference, Chena Hot Springs, Fairbanks, Alaska, November 1983.

"Estimating Flows in Instable Channels Using Indirect Methods", Rivers '83, Proceedings Hydraulic Specialty Conference, American Society of Civil Engineers, New Orleans, Louisiana, October 1983.

"Determination of Flood Levels on the Pacific Northwest Coast for Federal Insurance Studies", Proceedings Hydraulics Specialty Conference, American Society of Civil Engineers, College Station, Texas, 1977.

"Numerical Simulation of Storm Surges on the Pacific Northwest Coast", Proceedings First Conference on Coastal Meteorology, American Meteorologic Society, Boston, Massachusetts, September, 1977.

"Variation of Snowpack Density and Structure with Environmental Conditions", Center for Water Resources Research, Desert Research Institute, University of Nevada, Reno, Nevada, 1974.

"Allocation of Water Resources in the Lake Washington-Cedar River Basin, Washington", presented at the Ninth American Water Resources Conference, Seattle, Washington, 1973.

"Numerical Prediction of Snowpack Temperatures in the Eastside Sierra Nevada Using a Surface Energy Balance Model", Ph.D. D. Dissertation, University of Nevada, Reno, 1972.

PROFESSIONAL MEMBERSHIP

American Society of Civil Engineers
American Meteorological Society
American Geophysical Society

14.2 Project Sponsors

City of Colorado Springs/City Engineering – Daniel W. Bare II, P.E. Sr. Civil Engineer for the Stormwater division of City Engineering since 2007. Duties include stormwater management planning, standards development, capital projects and fee program evaluation and administration.

Experience with both private consultants and public agencies includes drainage basin hydrology, stormwater master planning, open channel hydraulics, sediment transport analyses, river restoration, capital planning and design of storm drainage systems. Registered as a Professional Engineer in the State of Colorado since 1985.

Education includes Master of Science Degree, Civil Engineering / Water Resources, University of Colorado at Denver, 1990; Bachelor of Science Degree, Civil Engineering, University of Colorado, Denver, 1984 and Bachelor of Engineering Technology Degree, Louisiana State University, Baton Rouge, 1976

Contact Information:

Daniel W. Bare II, P.E.
City of Colorado Springs/City Engineering/Stormwater Division
30 S. Nevada Ave., Suite 502
Colorado Springs, CO 80901
Tel: 719-385-5037
Email: dbare@springsgov.com

Colorado Water Conservation Board - Kevin Houck, PE, CFM, Sr. Engineer for the Flood Protection Section of the Colorado Water Conservation Board, where he has worked since August 2003. His duties include assistance with flood mapping studies, engineering project management, general technical assistance, and public outreach regarding the flood hazards in the state.

Prior to his role at the Colorado Water Conservation Board, Kevin served as a consulting engineer for eight years in the Denver area. His work included hydrologic and hydraulic analysis and design, urban stream restoration, reservoir analysis and design, and transportation hydraulics.

Kevin has a bachelor's degree in Civil Engineering from Washington State University and a master's degree in Civil Engineering from the University of Colorado – Denver. He is registered as a professional engineer in the states of Colorado, California, and Louisiana. He presently serves as the Chair for the Colorado Association of Stormwater and Floodplain Managers (CASFM). He has served as Treasurer for the Association of State Floodplain Managers (ASFPM). In addition, he served as the Arid Regions Committee Liaison for ASFPM. In recent years, he has also served on the Boards of Directors for the American Water Resources Association (AWRA) Colorado Section and the American Public Works Association (APWA) Colorado Section.

Contact Information:

Kevin Houck, PE, CFM
Senior Engineer
Colorado Water Conservation Board, Flood Protection Section
1313 Sherman Street, Room 721
Denver, CO 80203
Tel: (303) 866-4805
Fax: (303) 866-4474
Email: kevin.houck@state.co.us

14.3 Peer Review / Technical Support

Chandra S. Pathak, Ph.D., P.E., D.WRE, F.ASCE – Chandra is with the Operations and Hydro Data Management Division with the South Florida Water Management District for over seven years and over 28 years experience in environmental and water resources planning and engineering projects and programs. Work included surface and ground water hydrology and hydraulics, stormwater management, wetland, water quality, GIS and extensive use of various hydrology, hydraulic and water quality computer models. Chandra worked on several assessments and evaluations, site investigations, feasibility studies, cost estimates, conceptual plans and designs, preliminary and final designs. Prepared several environmental impact statements, NEPA environmental assessment, Expert in obtaining various environmental and Clean Water Act related permits from various local, State and Federal government agencies. He also teaches graduate classes at universities and technical short courses to the in-house staff and in professional organization (ASCE).

Experience and qualifications particular to rainfall and NEXRAD analyses includes:

- Technical lead and editor for a technical publication on “Hydrologic Monitoring Network in South Florida Water Management District”.
- Co-author of the Chapter 2 – Hydrology for South Florida Environmental Report – 2008
- Project Manager for “Acquisition of NEXRAD Data for the District”.
- Technical support to internal and external customers of NEXRAD database and Data Retrieval Application.
- Project Manager for “In-filling Missing Historical Daily Rainfall Data for the Long Term Rain Gauge Stations in Central and South Florida”.
- Project Manager for “Rain Gage Network Optimization Study” performed by Vieux and Associates, June 2006.
- Project Manager for contract to develop and implement software for NEXRAD data storage and retrieval.
- Technical lead on developing “rainfall by watershed” ArcHydro tool for extracting NEXRAD rainfall data.

Education includes: Ph.D. Agricultural Engineering, Oklahoma State University, Master of Science, Water Resources Engineering, Asian Institute of Technology and a Bachelor of

Technology, Engineering, J.N.A. University. Professional Engineer registrations are held in Florida, Maryland and Pennsylvania.

Contact Information:

Chandra S. Pathak, Ph.D., P.E, D.WRE, F.ASCE
Operation and Hydro Data Management Division – MS 5733
South Florida Water Management District
3301 Gun Club Road
West Palm Beach, FL 33406
Tel: 561-682-2567
Email: cpathak@sfwmd.gov ; cpathak28@comcast.net

Colorado Climate Center – Nolan Doesken, Colorado State Climatologist and Senior Research Associate Director - Nolan has worked at the Colorado Climate Center at Colorado State University since 1977 and was named State Climatologist in 2006. He has been in measuring, monitoring, analyzing and reporting precipitation data and other forms of climatological data for his entire career. He helped conduct the "Colorado Extreme Precipitation Data Study" for the Colorado Division of Water Resources completed in 1997 and then did special comprehensive storm reports for the Fort Collins, Colorado flash flood of July 28, 1997 and the Pawnee Creek flood of July 29-30, 1997. He is project manager for the Colorado Agricultural Meteorological Network and the director of the historic Fort Collins weather station on the campus of Colorado State University. He helped plan, organize and implement the Community Collaborative Rain, Hail and Snow network in northern Colorado in 1998. It has since grown to become a nationwide volunteer precipitation observing network and one of the largest data sources for precipitation data in the country.

Mr. Doesken received his Bachelor of Science degree in Meteorology and Oceanography from the University of Michigan in 1974 and his Masters of Science from the University of Illinois in Atmospheric Science in 1976. He worked as a meteorological technician at the Illinois State Water Survey 1972-1976 before coming to Colorado in 1977.

Contact Information:

Nolan Doesken
Colorado State Climatologist and Senior Research Associate Director, Fort Collins Weather Station, National Director, Community Collaborative Rain, Hail and Snow Network (CoCoRaHS)
Colorado Climate Center
Department of Atmospheric Science
Colorado State University
Fort Collins, CO 80523

Tel: 970-491-3690
Email: Nolan@atmos.colostate.edu

15.0 Appendix E: Response to Reviewer Comments

15.1 Response to Detailed Comments From Peer Review of DRAFT Report dated August 21, 2009, Carlton Engineering Inc.

Note: Section headings correspond to report sections. Peer review comments appear as the numbered subsections. Comment responses appear as lettered subparagraphs to each reviewer comment. Comments with “~~strikethrough~~” indicate comments that were addressed in the revised report. Comments highlighted in blue indicate comments that were answered in this document but no change was made to the revised report. Yellow highlights indicate changes are pending or waiting confirmation.

General

~~Include “Watershed” in the report title and in other references.~~

~~Done~~

The scope of work was intended to focus on the Fountain Creek watershed within El Paso County. The analyses show that there are differences between the eastern and western areas of the county and, to some extent, within the watershed also, but the study results are provided for all of El Paso County. For instance, one of the findings seems to be that the storms in western El Paso County are more frequent and more localized, but the proposed distributions seem to be based on the entire data county set. The data should be analyzed to show any differences in storm characteristics within the Fountain Creek watershed portion of El Paso County versus the eastern portion of the county and any differences within the Fountain Creek watershed itself.

- a. El Paso County contains the Fountain Creek Watershed. The larger area enabled the investigators to capture more storm cells for analysis. The distribution of storm cell counts and storm cell areas were unknown before the study. It was a judgment call to opt for more storm cells in a slightly larger area rather than constrain the analysis to the Fountain Creek Watershed.

The fact that some variability within El Paso County and even within the Fountain Creek Watershed was observed is a study finding and supports the notion that design storm properties should vary geographically. The significance of the variability within the Fountain Creek Watershed should be explored in future analyses.

However, the Design Storm Processor and the DARFs have been set up specifically for the Fountain Creek Watershed.

~~A number of the figures are too low in resolution to read or are too small. Generally the figures should be of better quality and larger. The figures also need to be adequately labeled to identify features and the source of the data.~~

~~Figures and labels will be improved in final version. Many of the figure resolution issues occurred as a result of the lower resolution pdf processing required to keep file sizes manageable for the draft report.~~

~~Figures showing overall distribution of rainfall for the Fountain Creek watershed will likely be interpreted and applied for other purposes and must be large enough and of high enough resolution to allow use for other applications. It is important that the county and city boundary be legible on many of the figures as appropriate.~~

- ~~a. Will enlarge graphics as appropriate. Original graphics will be provided in electronic format.~~

~~A summary of the key findings should be included in each section. Key findings are identified within the text of the sections, but delineating these at the end of each section will be helpful to identify the most important results of the study.~~

- ~~a. A bulleted summary of key findings will be added.~~

~~If the GARR data was incorporated into the rainfall data set in addition to the rain gage data how would this affect the frequency analyses (i.e. assume that there was a “virtual rain gage” at each storm cell centroid)?~~

- ~~a. This is a fertile area of new research requiring a new type of statistical analysis that merges information from short term highly resolved spatial data sets with longer term point data sets for frequency analyses. In this study, the data sets are too small for incorporating GARR into traditional frequency analysis. (i.e. analysis of annual maxima to determine frequency.)~~

~~If this type of study were redone in the future, would the work that has been completed have to be done again with the complete future data set? What data sets can be preserved so that future work will be possible?~~

- ~~a. GARR from OneRain, Inc. can and should be preserved for future studies. If TITAN analyses were conducted in the future, current TITAN results could be combined with future TITAN results as long as TITAN was applied identically as in this study.~~

~~It is important to state clearly which 24 months of NEXRAD data is the basis for the NEXRAD analyses. This may need to be repeated at several points in the report and on figures so that the context of the analyses is understood.~~

- a. ~~The 24 months of GARR data used for the storm properties analysis are presented in Table 6.2.2. The table will be included in the Executive summary and the introduction.~~

~~The discussion of rain gage data QA/Qc Procedures and radar adjustment procedures and other information provided in the appendix that applies to the entire study should be included in the main report text. The Jimmy Camp Creek storm analyses should reference the main report for support information and be provided as a separate report since its results are not necessary for the main report.~~

- a. ~~This would require a major rewrite of the report with no significant value added. If the Jimmy Camp Creek report had been done separately, the authors feel that it would have been acceptable to simply make reference to prior work. Including the Jimmy Camp Creek report as an appendix actually saves readers the effort of tracking down an external reference.~~

~~Information was not provided for 5 minute durations. This short duration represents the most intense period of rainfall and can have a significant effect on runoff estimates. The design storm and other results must include the peak 5 minute period.~~

- a. ~~Since 5 minute radar data was not processed, these DARFs are based on extrapolating parameters in the equations.~~
- b. ~~New Table with extrapolated 5 minute design DARFs will be added.~~

~~Provide electronic versions of all data, spreadsheets and analyses.~~

- c. ~~Will do.~~

~~Because these types of analyses will be new to reviewers and users of the report, please provide resumes of the key investigators and of the peer reviewers at the back of the report.~~

- a. ~~Resumes for the key investigators will be added as an appendix. Resumes from reviewers must be provided in MS Word format by Colorado Springs. Permission for including resumes of reviewers must also be obtained by Colorado Springs.~~

~~Include a discussion of the limitation of the study due to available data or other project constraints and what could be done to improve or expand the results.~~

- a. ~~Appropriate suggestion. Will do.~~

~~Check labels for figures. Some are mislabeled, such as “Eastern CO” when it should be “El Paso County”.~~

- a. ~~Will do.~~

~~Review the various results of the study for consistency. Do the results in one area support the results in another? For instance, the radar analysis shows that there is more frequent activity along the west side of Fountain Creek in the foothills, but the average monthly data shows that the accumulated rainfall in the same area is less.~~

- ~~a. Monthly average data were determined from long term rain gage records coupled with terrain data to account for orographic influences. Storm cell analyses for this study included a very limited data set of 24 months. Some differences are expected.~~

~~The use of the term “cloud burst” may not follow convention and may not be applied consistently. It may be helpful to use another term or clearly define what is intended.~~

- ~~a. The accepted meteorological definition of a cloudburst is a sudden and very heavy short rainstorm. We have consistently applied this term in this study and in other studies to single cell or multi-celled thunderstorm rainfall having a limited areal extent, a central core area of up to hundreds of square miles, with duration less than three hours. The term “cloudburst” contrasts with the “synoptic rainstorm”, which is defined as having an areal scale of thousands of square miles, no pronounced central core, and durations up to several days.~~

~~Sections 10 through 16 shown in the Table of Contents are not included in the report.~~

- ~~a. Corrected~~

~~The Design Storm Processors must be accessible to the City and/or a set of design charts must be developed to fully implement the study results.~~

- ~~a. The Design Storm Processor is intended to be an easy to use tool for Colorado Springs. The investigators are prepared to do a full demonstration of the Processor. Some additional refinement may be required to make the tool fully operational for the City as well as some training and instructional materials. The Processor is designed as a web-based tool that anyone can access to obtain temporally and spatially variable design storms.~~

~~Because this type of analyses will be new to reviewers of the report, please provide resumes of the principle investigators (primary project team members) in a report section or in an appendix.~~

- ~~a. Duplicate. See Item 12 above.~~

Executive Summary

~~Note that this study is also being sponsored by the Colorado Water Conservation Board.~~

Will do.

Should a key finding be that the storm durations did not exceed 3 hours in the 24 month NEXRAD data? How could the data analysis process have limited the results of the study for longer duration storms? How does this affect the recommendation of design storm duration?

A maximum design storm duration of three hours for April-September cloudbursts is recommended for design. Design storm durations are typically determined by the times of concentration for the target watershed. Given the size of Fountain Creek sub-basins, times of concentrations are typically under three hours. However, observed single cloudbursts in the 24 month record did not exceed two hours. Storm durations longer than two hours, of hydrologic significance in the Fountain Creek Watershed, were comprised of two successive storm cell complexes with short durations, separated by a low intensity rainfall period. The central core locations of these cloudbursts were also separated in space. Design storms of durations longer than three hours would be synoptic scale events, and the use of central intensity cores and DARF would not be applicable.

Should a key finding be that low frequency events were not significantly represented in the 24-month radar data set?

It can be noted. Low frequency events weren't represented in the rain-gage record either during the 24-month radar data set.

The uncertainties within the study results should be identified. Especially related to the DARFs for the different return periods, as appropriate and for the NEXRAD analysis due to the lack of large flood events in the data set.

This is certainly an area for further analysis but a more advanced statistical analysis was beyond the scope of this study.

The 24 months of NEXRAD data used in the study should be included here.

Will do.

Additional analyses that could be performed to improve the results of the study and reduce uncertainties should be identified.

Will do.

What do the cases from the Geronimo study represent and how do they related to the study results?

The Geronimo is relevant because it is one of a very few similar studies done outside those of the principal investigators. The Geronimo study computed individual

~~storm DARFs for seven events of 1-3 hour duration in the Denver area and generally showed similar results to those derived from the Fountain Creek Watershed analysis.~~

~~There should be some discussion of the Design Storm Processors and the typical characteristics of design storms such as duration and area covered.~~

~~Characterizing the typical characteristics of design storms in the Fountain Creek Watershed is the whole point of this study and is summarized in the form of the DARFs described in Sections 7.4 and 7.5. The Design Storm Processor is simply the tool the used typical storm characteristics defined by this study to create spatially and temporally variable design storms.~~

2.0 Storm Characterization

~~“Storm Characterization” doesn’t seem to describe this section. Maybe sections 2.0, 2.1 and 2.2 should be part of the Introduction.~~

~~Could rename the section “Background” but changing the section numbering at this point will cause a major editing effort due to the cascade of numbering changes that will propagate through the entire document.~~

2.1 Climate and Meteorology of Colorado Springs

~~As stated in the first paragraph, Colorado Springs is not located “on a high flat plain at the foot of the Rocky Mountains...” The city lies mainly in the Fountain Creek valley and the adjacent uplands between the plains and the foothills and is actually fairly hilly.~~

~~Will correct.~~

~~Change “Monument Divide” to “Palmer Divide”.~~

a. ~~Will do.~~

~~What is the source and period of record for tables 2.1-1 and 2.1-2? Clarify whether “Precipitation” includes snowfall or is just rainfall.~~

a. ~~Will confirm and add reference.~~

~~In the 1st sentence of the 5th paragraph, page 2.1 change “frequently” to “intermittently” to better describe the conditions. Same issue in the 2nd sentence.~~

a. ~~Will change.~~

~~The source for Figures 2.1-1 and 2.1-3 through 2.1-9 is difficult to read, please enlarge the text.~~

- ~~a. Will add source information to captions for easier reading.~~

~~Change label for Figure 2.1-1 from "...Easter Colorado" to "...Eastern Colorado"~~

- ~~a. Will correct.~~

~~Figure 2.1-6 for June shows significantly less rainfall than for May and July. This does not seem to be consistent with Table 2.1-1. Is this figure accurate?~~

- ~~a. Will check and confirm or change as necessary.~~

~~Figure 2.1-8 should be titled "Average August....", instead of "Average Average...."~~

- ~~a. Will correct.~~

~~How does the information in Figures 2.1-11, 2.1-12 and 2.1-13 help us understand the results of the study? Obviously we would expect to have more frequent or more rain producing events during a wetter period, but would the results related to spatial and temporal distribution be much different. How does this information relate to the study area and the 24 months of NEXRAD data used in the study?~~

- ~~a. This section was added due to a specific request by the client to make note of the drought conditions in Colorado that have persisted over the last decade or so.~~

~~Page 2.8, 1st sentence states "Figure 2.1-12 shows 1895-2009 statewide...", but this should state "Figure 2.1-12 shows 1895-2009 July statewide..."~~

- ~~a. Will correct.~~

3.0 Depth-Duration-Frequency Curves

3.1 Overview

NWS records indicate that rainfall was measured at the airport since 1950, at least daily, but Table 3.1-1 only shows records going back to 1976 at this station. This may be because the name of the gage changed, but the station number should not have changed. The may also be data available for the Peterson Field gage.

The study investigators confirmed that NWS hourly data at the Colorado Springs Airport was not available until the mid 1970's.

Denote in Table 3.1-1 which gages record hourly and which record daily data.

Will modify Table 3.1-1

**Table 3.1.-1: Average Cloudburst Season Precipitation
El Paso County Precipitation Stations**

Station Name	Start	End	Type	Years	Latitude	Longitude	Elevation	Jn-Jy-Au	Radar
								Avg (in)	Avg (in)
Big Springs Ranch	1948	1967	Daily	20	38.8667	104.3167	6043	2.27	3.11
Colorado Springs WSO	1976	2008	Hourly	32	38.8119	104.7111	6140	2.86	3.95
Eastonville 2 NNW	1971	2000	Daily	30	39.1167	104.6000	7210	2.84	3.55
Fountain	1953	1997	Hourly	45	38.6778	104.7014	5560	2.34	3.37
Greenland 6 NE	1948	2008	Hourly	60	39.2167	104.7383	6900	2.36	3.42
Greenland 9 SE	1948	2008	Hourly	60	39.1044	104.7286	7480	2.50	3.73
Manitou Springs	1948	2006	Hourly	53	38.8547	104.9339	6630	2.63	3.49
Monument 2 WSW	1948	1965	Hourly	18	39.0833	104.9167	7346	2.04	3.12
Palmer Lake	1965	1986	Hourly	22	39.1167	104.9167	7220	2.12	3.46
Rush 1N	1971	2000	Daily	30	38.8667	104.1000	6054	2.41	3.46
Simla	1948	2000	Hourly	53	39.1414	104.0844	5980	2.40	3.82
Yoder 2 WNW	1976	2008	Hourly	33	38.8575	104.2561	6180	2.44	3.32
Averages								2.43	3.48

Include the Greenland 6 NE station in Table 3.1-1.

Will do:

~~More clearly described the values in the last two columns of Table 3.1-1.~~

~~Will add: Observed average June July August precipitation is provided for comparison with the 24 month radar record. The 24 month radar record was deliberately biased toward months with more frequent storm events, in order to provide more data for analyses. Higher averages for the radar data were expected.~~

~~Figure 3.1-1 is not readable and the lines should be labeled appropriately.~~

~~Will correct. (PDF resolution issue.)~~

~~Provide the long term data for the gage stations used in the analysis. This should be in tables in the appendix and spreadsheets for later retrieval by the city.~~

~~Will provide electronically.~~

3.2 Approach

~~Is there some reason that the Greenland NE 6 gage was not analyzed, explain.~~

~~The gage location was outside of El Paso County and outside of Fountain Creek watershed, on the north side of the Palmer Divide. Data from this gage was used to fill in missing events at the Greenland 9 SE gage.~~

How does the exclusion of events longer than 6 hours affect our understanding a rainfall in the watershed? Are there longer duration events that should be considered which may not be “cloud bursts”?

Inclusion of the few significant synoptic scale events exceeding three hours would not have any influence on the design cloudburst parameters. Given the size of Fountain Creek sub-basins, times of concentrations are typically under three hours. Storm durations longer than three hours of hydrologic significance in the Fountain Creek Watershed are rare and typically comprised of multiple storm cell complexes with single cell shorter durations.

An equation in the form of $I=A*P^1 / (B+T^c)$, in which I=intensity, T=duration and A, B and C are region constants is used in the Denver area and A=28.5, B=10 and C=0.786 for the Denver region. How does this relationship compare to the chosen equation? Should this equation be considered for use in this study?

Hundreds of studies performed by the authors and numerous literature citations have found that DDF and IDF data fit simple power equations, i. e. straight line relationships on log-log plots ($I=A*t^B$). Curved or kinked relationships were found to be the result of mixed populations (such as air mass cloudbursts and tropical storms) or mixed records (short length for short durations, long length for long durations). In all cases, the short duration data, 15 minute and shorter, have many more missing annual events than 60 minute or longer data, which introduces a pronounced (steeper slope) curve or kink below 30-60 minutes.

Include column headings for the time ranges (5 to 60 min. and 60 to 180 min.) for variables a1, b1 and a2, b2 in Table 3.2-2.

Will do

How should the results of this analysis be applied? Is there an areal extent that would be most appropriate for using the airport data verses data from the other gages? Could this be identified on a map showing the most appropriate area to apply the curves? This may depend on the use of the longer data set for the Airport gage.

The investigators confirmed that an hourly gage was present at the Colorado Springs Airport in 1949. However, only partial data were archived at NCDC during the years 1949-1951. Then there are no hourly data for that gage at NCDC for 23 years from Oct 1951 until May 1974. All available hourly data for the Colorado Springs Airport were incorporated into this study.

In addition, the investigators have proposed a regionalized map of DDF ratios based on the Colorado Springs DDF and the results of radar data analyses in this study. (See map below.) This map is consistent with a similar approach suggested by the City of Colorado Springs.

~~Plot Figure 3.2-2 with duration on the x axis and the return period as the series.~~

~~What is the purpose of this request? The information is the same.~~

~~Include the values for 5 minute durations in Table 3.2-3 and Figure 3.2-2.~~

~~Values for 5 minute data were extrapolated. They should be used cautiously in watersheds with short lag times. It has been found that significant transitory storage exists for runoff less than 10 minutes in duration. The use of 5 minute data may over estimate design discharges in small urban watersheds.~~

~~Include equations and DDFs for the Greenland and Manitou Springs stations. These equations were estimated from the 2 hour DDF ratios.~~

~~Will expand Table 3.2-3:~~

Table 3.2-3 Depth Duration Frequency Data															
Equations															
5 to 60 minute		D=a1*t(minutes)*b1													
60 to 180 minute		D=a2*t(minutes)*b2													
Colorado Springs Airport															
Recurrence	b1	a1		b2	a2		5	15	30	60	120	180	240	300	360
1-Year	0.334	0.220	60	0.330	0.228	1-Year	0.38	0.54	0.69	0.88	1.11	1.27	1.39	1.50	1.59
2-Year	0.345	0.277	60	0.339	0.284	2-Year	0.48	0.70	0.90	1.14	1.44	1.65	1.82	1.96	2.09
5-Year	0.357	0.406	60	0.339	0.435	5-Year	0.72	1.07	1.36	1.75	2.21	2.54	2.80	3.02	3.21
10-Year	0.362	0.501	60	0.345	0.538	10-Year	0.90	1.34	1.72	2.21	2.80	3.22	3.56	3.85	4.09
25-Year	0.368	0.606	60	0.378	0.583	25-Year	1.10	1.64	2.12	2.74	3.56	4.15	4.63	5.03	5.39
50-Year	0.375	0.725	60	0.358	0.775	50-Year	1.33	2.00	2.59	3.36	4.31	4.98	5.53	5.99	6.39
100-Year	0.381	0.810	60	0.365	0.863	100-Year	1.50	2.27	2.96	3.85	4.96	5.75	6.39	6.93	7.41
500-Year	0.387	1.067	60	0.357	1.204	500-Year	1.99	3.04	3.98	5.20	6.66	7.70	8.53	9.24	9.86
1000-Year	0.392	1.160	60	0.360	1.350	1000-Year	2.18	3.35	4.40	5.89	7.57	8.75	9.71	10.52	11.24
Manitou Springs															
Recurrence	b1	a1		b2	a2		5	15	30	60	120	180	240	300	360
1-Year	0.334	0.193	60	0.330	0.200	1-Year	0.33	0.48	0.60	0.77	0.97	1.11	1.22	1.31	1.40
2-Year	0.345	0.243	60	0.339	0.249	2-Year	0.42	0.62	0.79	1.00	1.26	1.45	1.59	1.72	1.83
5-Year	0.357	0.311	60	0.339	0.333	5-Year	0.55	0.82	1.05	1.34	1.69	1.94	2.14	2.31	2.46
10-Year	0.362	0.365	60	0.345	0.392	10-Year	0.65	0.97	1.25	1.61	2.04	2.35	2.59	2.80	2.98
25-Year	0.368	0.438	60	0.378	0.422	25-Year	0.79	1.19	1.53	1.98	2.58	3.00	3.35	3.64	3.90
50-Year	0.375	0.493	60	0.358	0.527	50-Year	0.90	1.36	1.76	2.29	2.93	3.39	3.76	4.07	4.35
100-Year	0.381	0.552	60	0.365	0.588	100-Year	1.02	1.55	2.01	2.62	3.38	3.92	4.35	4.72	5.04
500-Year	0.387	0.727	60	0.357	0.820	500-Year	1.35	2.07	2.71	3.54	4.54	5.24	5.81	6.29	6.72
1000-Year	0.392	0.790	60	0.360	0.919	1000-Year	1.48	2.28	3.00	4.01	5.15	5.96	6.61	7.16	7.65
Greenland 9 SE															
Recurrence	b1	a1		b2	a2		5	15	30	60	120	180	240	300	360
1-Year	0.334	0.180	60	0.330	0.187	1-Year	0.31	0.44	0.56	0.72	0.91	1.04	1.14	1.23	1.30
2-Year	0.345	0.228	60	0.339	0.234	2-Year	0.40	0.58	0.74	0.94	1.18	1.36	1.50	1.62	1.72
5-Year	0.357	0.290	60	0.339	0.311	5-Year	0.51	0.76	0.98	1.25	1.58	1.81	2.00	2.16	2.29
10-Year	0.362	0.331	60	0.345	0.355	10-Year	0.59	0.88	1.14	1.46	1.85	2.13	2.35	2.54	2.70
25-Year	0.368	0.398	60	0.378	0.383	25-Year	0.72	1.08	1.39	1.80	2.34	2.73	3.04	3.31	3.54
50-Year	0.375	0.442	60	0.358	0.473	50-Year	0.81	1.22	1.58	2.05	2.63	3.04	3.37	3.65	3.90
100-Year	0.381	0.486	60	0.365	0.518	100-Year	0.90	1.36	1.77	2.31	2.97	3.45	3.83	4.16	4.44
500-Year	0.387	0.640	60	0.357	1.204	500-Year	1.19	1.82	2.38	3.20	4.20	4.90	5.40	5.80	6.10
1000-Year	0.392	0.707	60	0.360	0.823	1000-Year	1.33	2.04	2.68	3.59	4.61	5.34	5.92	6.41	6.85
1-Hour DDF Comparisons															
	1-yr	2-yr	5-yr	10-yr	25-yr	50-yr	100-yr								
Greenland 9SE	0.72	0.94	1.25	1.46	1.80	2.05	2.31								
Manitou Springs	0.77	1.00	1.34	1.61	1.98	2.30	2.62								
Colorado Spr. Air.	0.88	1.14	1.75	2.21	2.74	3.36	3.85								
NOAA Atlas 2	n/a	1.17	1.55	1.79	2.00	2.35	2.57								

3.3 Results

The current NOAA Atlas 100-year, 24 hour rainfall is 4.6 inches compared to the proposed values for the 100-year, 1 hour rainfall of 3.85 and 100-year, 6 hour rainfall of 7.41 inches. This is an extremely high increase and needs to be thoroughly evaluated for any errors and an explanation provided. We believe that the longer data set may lower the values.

The investigators agree that more data are needed to reduce the uncertainty regarding the calculated DDFs.

The fact the current NOAA Atlas DDF rainfall amounts could be significantly different than DDFs derived from individual station analyses is not at all

surprising. Many current NOAA Atlases are decades old and their results were derived from very limited and, often, sparse rain gage networks, particularly in the western United States. In addition, older NOAA DDF studies did not have sophisticated procedures for incorporating the orographic influences on DDFs in regions between rain gages as studies underway today do.

Include the 1-year and 500-year values in Table 3.3-4.

Will do.

The NOAA Atlas values shown in Table 3.3-4 and Figure 3.3-3 are not the same as those in the current City criteria manual. Show the current values used by the City and explain why they may be different from those shown.

The NOAA Atlas 2 values shown in Table 3.3-4 and Figure 3.3-3 are shown for the latitude and longitude of the Colorado Springs Airport gage (38.82 N, -104.68 W), not the Colorado Springs City center. (reference: Hydrometeorologic Design Studies Center, Precipitation Frequency Data Server On-line)

Provide 5% confidence limits for the DDFs to evaluate the statistical variance of the different return period curves?

5% confidence limits would require calculation for the combination of log-normal probability and then power equation curve fitting and the limits would be so wide as to be nearly meaningless. We believe that this task, not in the scope of work, would take many hours and not have a useful result.

Some of the grid lines are missing in Figure 3.2-2 (and some other figures in the report).

This is an issue with providing a PDF file manageable for electronic transfer. Higher resolution versions and final high resolution printouts do not present this problem.

Why are there no durations greater than 6 hours? There are longer duration events reported in Section 4.0.

Single event cloudbursts were determined to always be less than three hours for the data sets included in this study. The longer events were either multiple cloudburst events separated in space and time or synoptic scale events.

4.0 Storm Event Analysis and Summary

4.2 Approach

1. Elsewhere the period of record for the airport gage start in 1976, here it is stated as 1974, but we believe it goes back to, at least, 1949.

- a. The investigators confirmed that an hourly gage was present at the Colorado Springs Airport in 1949. However, only partial data were archived at NCDC during the years 1949-1951. Then there are no hourly data for that gage at NCDC for 23 years from Oct 1951 until May 1974. All available hourly data for the Colorado Springs Airport were incorporated into this study.
2. How can we know that the procedures for filling in rainfall data did not affect the results? What amount of the data had to be estimated as described?
 - a. Since the recommended design storms depended on Colorado Springs Airport and the 24-months of radar data, the procedures for filling in rainfall data had no influence on the results. As expected, the DDF analyses for Manitou Springs and Greenland 9 SE essentially agreed with NOAA Atlas 2. Approximately 10% of the annual maximum 2-hour data for these gages were estimated. The data filling procedure was not likely to influence the results for these gages.
 - ~~3. The analysis should include values equal to and greater than 0.1 inches, not just greater than 0.1 inches.
 - a. The analysis included values equal to and greater than 0.1 inches and will be noted in the text.~~

4.3 Results

- ~~1. The description of the airport data at the bottom of page 4.1 does not agree with the data on the figures. It is stated that there are 3 events over three hours for the airport gage, but there are many events longer than 3 hours shown on Figure 4.3 2. It appears that this should be stated as depths for 3 events over 3 inches instead?
 - a. Will confirm and make corrections where appropriate.~~
2. Include the data for the three gages shown as a percentage of all events being less than a rainfall depth (i.e. what percentage of events are less than 0.5 inches, what percentage are less than 1.0 inches, etc.) and as a percentage of annual volume (i.e. what percentage of the annual volume is made up of events of 0.5 inches or less, what percentage of annual volume is made up of events of 1.0 inches or less, etc. etc.).
 - a. This request can be accommodated, if necessary, but it will end up taking 40-80 hours to update spreadsheets, format charts, insert into the document, add descriptive text, and QA/QC the result. These gages were only revised for the annual maximum values. There were many other missing values which were not the annual maximums.
3. Provide graphs for frequency, duration and intensity combining the data for the four gages to show a direct comparison.

- a. This request can be accommodated, if necessary, but it will end up taking 20-30 hours to update spreadsheets, format charts, insert into the document, add descriptive text, and QA/QC the result.
4. How should the results of this analysis be applied? Is there an areal extent that would be most appropriate for using the airport data versus data from the other gages? Could this be identified on a map showing the most appropriate area to apply the curves?
- a. The investigators have proposed a regionalized map of DDF ratios based on the Colorado Springs DDF and the results of radar data analyses in this study. This map is consistent with a similar approach suggested by the City of Colorado Springs.

5.0 Antecedent Rainfall Conditions

5.2 Approach

1. ~~The Scope of Work states: “All available data will be analyzed to determine the total amount of rainfall in the 5 days prior to each storm event in addition to the total depth and duration data collected to complete Task C (Storm Event Analysis and Summary). A storm event shall be defined as measured rainfall greater than 0.1 inches occurring 6 hours or more from another event of greater than 0.1 inches.~~

Statistics generated from this analysis will show the amount of rainfall occurring in the five days prior to a storm event of a given return period. Return Periods of 1, 2, 5, 10 and 100-year events will be evaluated and summarized.”

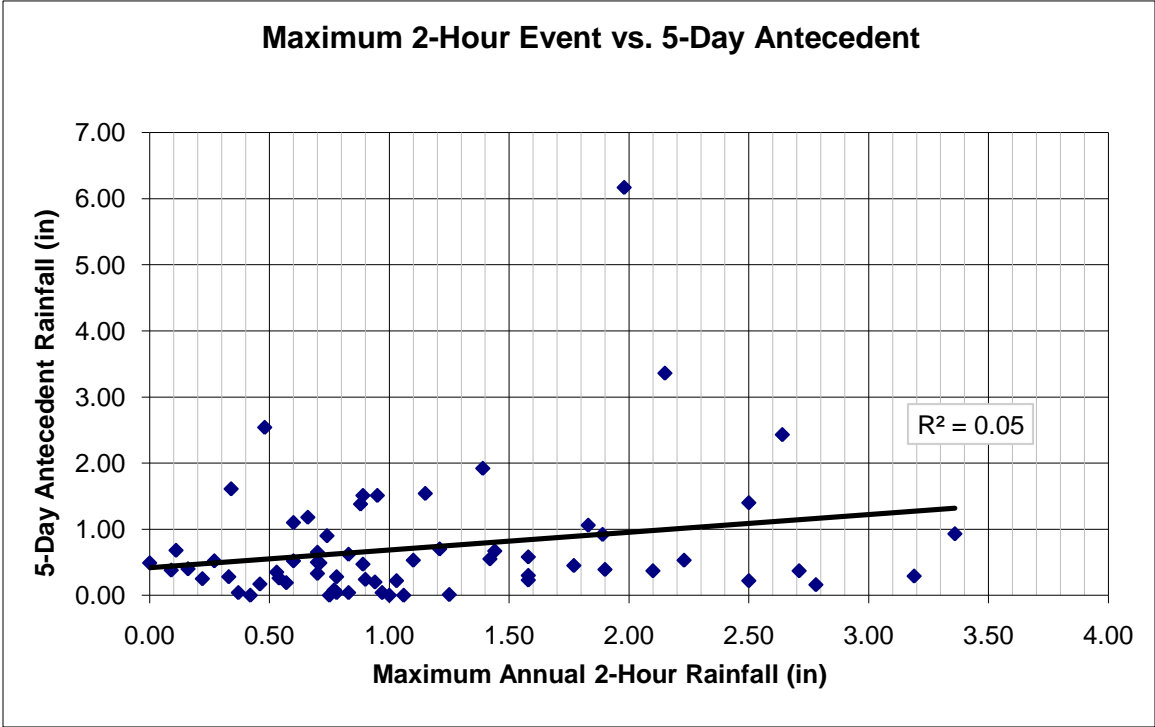
~~This analysis needs to be provided to show the frequency of the occurrence of rainfall preceding rainfall events of a minimum depth. Tabulate and plot the number of events that have 0.0 through 5.0 inches (in 0.1 inch intervals) in the 5 days preceding the events.~~

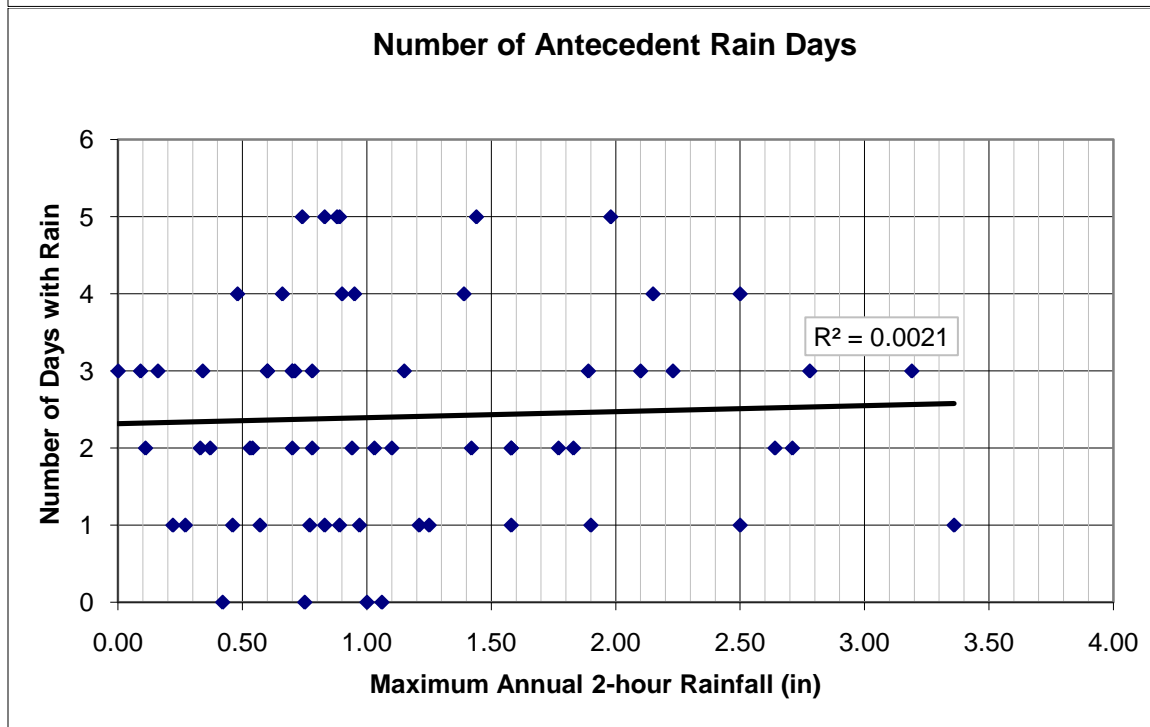
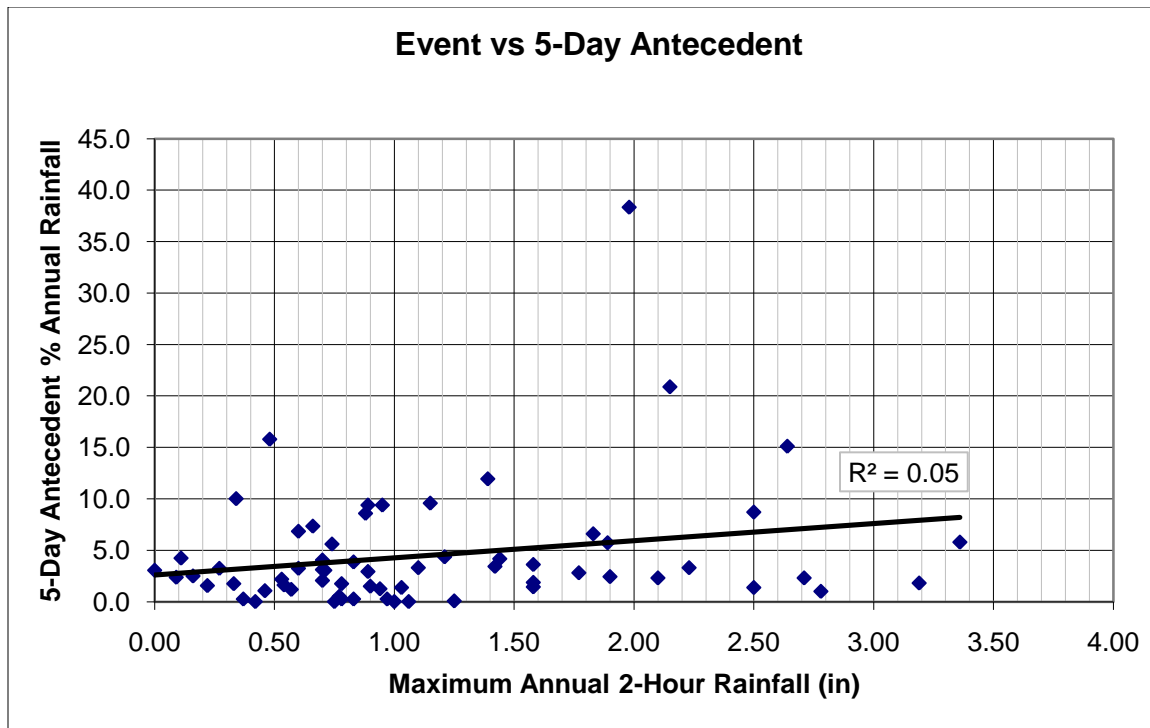
- a. ~~There was a correspondence between rainfall depths and rainfall occurring in the preceding days. However, Tables 5.3.3-4 show that this correspondence is low. For example, in Table 5.3.4, there is a 50% chance that a 2-year event will have 0.28” and a 1% chance it will be 3.43”. Using the most likely antecedent moisture condition is unlikely to affect the probability of a resulting hydrologic event. However, using a less likely value would significantly affect the probability of the hydrologic event in an unpredictable way (although definitely producing a much higher and unrealistic recurrence interval), depending on hydrologic characteristics of the watershed.~~

~~The figures below were made to illustrate the results shown in Tables 5.2-1 and 5.2-4. Figure 1 shows a graph of events versus 5-day antecedent rainfall. There was clearly no statistical relationship with most likely 5-day antecedent rainfall 0.3” as shown in Table 5.2-4. Figure 2 shows the 5-day antecedent as a percent of annual rainfall. The most likely 5-day antecedent rainfall was approximately 2%~~

of annual rainfall. Figure 3 shows the number of days with antecedent rainfall versus event magnitude. There is no statistical relationship.

Antecedent rainfall for a watershed is not the same as antecedent rainfall derived for a gage. As watershed area increases there is an increasing probability that antecedent rainfall would occur somewhere in the watershed. However, there is also an increasing probability that a design event would occur somewhere in the watershed. The degree of overlap or coincidence of the areal coverage of antecedent events with the areal coverage of the design event is hydrologically significant. This cannot be modeled using single gage statistics and requires long-term radar precipitation over the watershed of interest.





2. ~~As noted earlier the data set should be extended to include the entire record.~~

a. ~~Asked and answered earlier.~~

3. ~~How were the assumptions for the HSPF analysis determined? Why type C soil? Note that monthly evaporation in Pueblo may not be a good assumption since Pueblo is often 5~~

to 10 degrees warmer. How do these assumptions affect the conclusions if conditions are different?

- a. ~~HSPF parameters were based on typical values for semi-arid watershed simulations in Utah and California. Type C hydrologic classification soil was the most widespread in the Jimmy Camp Creek watershed. Decreased monthly pan evaporation for the cooler temperatures in Jimmy Camp Creek watershed compared to Pueblo would have no significant influence on the results, since evaporation greatly exceeds mean monthly precipitation. A future project could set up HSPF in much greater subbasin detail using radar rainfall.~~

4. Given the limited extent of cloud-burst events and the location of the rain gage, why would any correlation between the airport rainfall and the Jimmy Camp Creek flows be expected? This assumption seems to be unsupported by the rainfall patterns described in the study.

- a. The reported correlations are an observed result from a 35 year rain gage record at the airport. Radar-rainfall patterns reported in this study are from 24 selected months from a much shorter period of record where significant Jimmy Camp Creek flows were observed and/or where local rain gages suggested significant rainfall in the area.

In addition, the HSPF model was used as a tool to assess antecedent soil moisture, not to reproduce Jimmy Camp Creek flows. The airport gage data were the best long term data available for the assessment.

5. Explain that last column heading in Table 5.2-1 that shows HSPF %. Should it be “% Soil Moisture from HSPF”?

- a. “HSPF % Lower Zone Soil Moisture”

6. Page 5.3: 2nd paragraph from bottom: 2nd line: 0.30” for five days: from table it should be 0.28”.

- a. Will correct.

7. June 2 and June 4, 1995 and August 4, 1999 show an HSPF% greater than 100%. How is this possible?

- a. HSPF Lower Zone Soil Moisture (LZSN) is a nominal capacity where the model algorithms allow greater values than 100%.

8. How does the HSPF relate to NRCS antecedent moisture conditions I, II and III?

- a. Approximate values would be 0-80% for AMC-I, 80-120% for AMC-2 and over 120% for AMC-3. There is no published relationship that the principal

investigators are aware of.

9. Include the data of the event date in Table 5.3 2.

a. The dates of the events included in Table 5.3 2 will be added.

Table 5.3-2. Colorado Springs Airport Ranked Antecedent Rainfall

Year	Month	Hour	Airport	Jimmy	Recurr.	Antecedent Rainfall									
						2-hr	Camp Cr	Interval	1-day	%	2-day	%	3-day	%	4-day
2008	Sept	14	3.36		20-year	0.93	100	0.00	100	0.00	100	0.00	100	0.00	0.93
1997	July	18	3.19			0.12	41	0.12	83	0.00	83	0.00	83	0.05	0.29
2009	August	18	2.78		10-year	0.00	0	0.00	0	0.00	0	0.09	56	0.07	0.16
1998	August	17	2.71	1240		0.36	97	0.00	97	0.01	100	0.00	100	0.00	0.37
1999	April	15	2.64			1.78	73	0.35	88	0.00	88	0.30	100	0.00	2.43
2000	August	18	2.50	1930		0.22	100	0.00	100	0.00	100	0.00	100	0.00	0.22
1997	June	21	2.50	1740		0.28	20	0.00	20	0.41	49	0.53	87	0.18	1.40
1994	June	21	2.23	4810	5-year	0.46	87	0.00	87	0.00	87	0.00	87	0.07	0.53
1995	June	16	2.15			0.06	2	2.17	66	0.06	68	1.07	100	0.00	3.36
2004	June	15	2.10			0.10	27	0.09	51	0.18	100	0.00	100	0.00	0.37
1999	August	21	1.98			2.22	36	2.11	70	0.19	73	1.58	99	0.07	6.17
2005	July	22	1.90			0.39	100	0.00	100	0.00	100	0.00	100	0.00	0.39
2000	August	18	1.89			0.00	0	0.27	29	0.49	83	0.16	100	0.00	0.92
2006	August	18	1.83			0.62	58	0.00	58	0.00	58	0.00	58	0.44	1.06
2001	August	1	1.77			0.27	60	0.18	100	0.00	100	0.00	100	0.00	0.45
2002	July	20	1.58			0.00	0	0.30	100	0.00	100	0.00	100	0.00	0.30
1999	July	15	1.58	1710		0.07	12	0.00	12	0.51	100	0.00	100	0.00	0.58
2003	June	15	1.58			0.00	0	0.15	65	0.00	65	0.00	65	0.08	0.23
1998	July	15	1.44		2-year	0.05	7	0.41	69	0.02	72	0.07	82	0.12	0.67
2008	August	15	1.42			0.53	96	0.00	96	0.02	100	0.00	100	0.00	0.55
2003	June	18	1.39	233		0.04	2	0.24	15	0.06	18	1.58	100	0.00	1.92
2009	August	22	1.25			0.01	100	0.00	100	0.00	100	0.00	100	0.00	0.01
2004	July	18	1.21			0.70	100	0.00	100	0.00	100	0.00	100	0.00	0.70
2005	July	12	1.15			0.76	49	0.66	92	0.12	100	0.00	100	0.00	1.54
2006	July	20	1.10		1-year	0.46	87	0.07	100	0.00	100	0.00	100	0.00	0.53
					Averages	0.42	50	0.28	72	0.08	82	0.22	93	0.04	1.04

10. Include the 1 year event in Tables 5.3 3 and 5.3 4.

a. Will add:

One Day (inches)							
	100%	50%	20%	10%	4%	2%	1%
	1-year	2-year	5-year	10-year	25-year	50-year	100-year
Colorado Springs	0.00	0.00	0.20	0.40	0.74	1.11	1.49
Manitou Springs	0.00	0.00	0.17	0.33	0.80	1.12	1.25
Greenland 9SE	0.00	0.00	0.10	0.30	0.65	0.96	1.00
Greenland 6NE	0.00	0.00	0.20	0.40	0.80	1.00	1.20

Five Days (inches)							
	100%	50%	20%	10%	4%	2%	1%
	1-year	2-year	5-year	10-year	25-year	50-year	100-year
Colorado Springs	0.02	0.28	0.79	1.39	2.24	2.81	3.43
Manitou Springs	0.01	0.27	0.74	1.12	1.71	2.14	2.69
Greenland 9SE	0.00	0.10	0.52	0.89	1.50	1.96	2.77
Greenland 6NE	0.01	0.22	0.77	1.27	1.90	2.24	2.80

11. Tables 5.3-3 and 5.3-4 do not seem to support the conclusion that antecedent moisture is unrelated to storm events. There seems to be a trend shown that less frequent storm events have a higher antecedent rainfall. How were these tables generated? Add clarifying notes and a better description in the text.

a. There is no relationship between storm probability and antecedent moisture probability. Column headings are not the storm probability. They represent the probability of the antecedent rainfall.

12. Show the percent of rainfall occurring in each day prior to each event and summarize the results. Based on the data in Table 5.3-2, 38.3% of the antecedent rainfall fell within the first day prior to the events, 64.9% within two days, 73% within three days and 95.4% within 4 days.

a. Table 5.3-2 was revised to show the antecedent rainfall for each storm as a percent of the five days preceding. On the average, 50% of antecedent rainfall occurred the first day, 72% in 2 days, 82% in 3 days and 93% in 4 days.

6.0 Radar Rainfall Analysis

6.2 Approach

1. Are the Jimmy Camp Creek events relevant to the main study? This discussion should be moved to the JCC report unless it is needed to explain the study.

- a. The investigators believe the Jimmy Camp Creek Study is relevant for several reasons, including: 1) the procedures used to create and verify the GARR for Jimmy Camp Creek were the same procedures used for the larger study and need to be explained, and 2) specific Jimmy Camp Creek events were used to verify the Dynamic Storm Processor.
- ~~2. Table 6.2-2 is an important table and should be included or referenced in other sections where the 24 months of radar data are mentioned.~~
 - ~~a. The table will be included in the Executive Summary.~~

6.3 Radar Rainfall Verification

1. Show plots like Figures 6.3.3-5 and 6.3.3-6 for each of the 24 months of data and include them in an appendix?
 - a. The remaining plots are essentially identical to Figures 6.3.3-5 and 6.3.3-6. The result will be 72 graphs with redundant information.

7.0 Determine Storm Properties

7.1 Background

- ~~1. Page 7.1: 2nd para from the bottom of the page states: "TITAN processing requires data expressing in decibels, dBz, ...": If the rain depths of various durations were converted to dBz; how does the non-linear relationship (between rain and dBz) result in a correct interpretation of the converted datasets? This is very important point must be discussed and clearly presented.~~
 - ~~a. The non-linear conversion from already calibrated radar rainfall to dBz is a direct explicit one-to-one relationship. It has no affect on our interpretation of the results. TITAN analyzes the areal coverages to determine individual storm cell sizes and the area covered by each rainfall intensity.~~

~~TITAN results were summarized in 1 dBz increments of maximum cell intensity to determine cell counts and cell areas. Since equal bin size increments of 1 dBz were used in dBz "space", the non-linear conversion does create unequal bin size increments in "rainfall space." This resulted in smaller bin sizes for the more frequently occurring light rainfall intensities and larger bin sizes for the less frequently occurring heavy rainfall intensities.~~
- ~~2. How did the calibration process effect Equation 7.1-1? Would there be a table like Table 7.1-1 for each month, each storm? Doesn't the equation for conversion from decibels to rainfall change with each storm event?~~

- a. ~~Equation 7.1-1 is only used to convert the previously calibrated radar rainfall data (GARR) in inches/hour to dBz for TITAN processing. Appendix A contains the details of the radar rainfall calibration process.~~

7.2 Typical Storm Patterns

1. ~~Explain the use of the time steps and the maximum duration of 3 hours and its affect on the analysis.~~
 - a. ~~The time steps of 15 minute, 1 hour, and 3 hours were chosen to enable direct comparison to publish NWS DARFs. The 15 minute time step was the smallest time increment possible since the GARR data for this portion of the study were in 15 minute increments.~~

~~The maximum time step of 3 hours was used for several different reasons. The first has to do with TITAN processing. TITAN was originally design to process instantaneous radar rainfall rates. In this application, rainfall totals for a given time step are converted to average intensity in inches/hour over the selected time step. As time steps increase, light rain is averaged over ever larger time steps; creating some uncertainty at the edges of storm cells as average rainfall rates fall to “noise” levels. This affects the estimates of cell area. Investigators tried to mitigate this problem by changing the cell edge definition in dBz for each time step to be approximately the equivalent of 0.1 inches/hour. (This is an area for further serutiny in future work.) Secondly, events of 3 hours were quite infrequent as the longer storms were typically composed of multiple smaller duration events. A third consideration was budget. This was a big effort but, unfortunately, unlimited resources were not available.~~

2. ~~Include the period of record (study months) or reference this for each figure.~~
 - a. ~~The table showing study months will be included in the Executive Summary and, possibly, the Introduction.~~
3. How have the patterns identified in this section been incorporated into the results? Should there be difference DARFs or spatial distributions for the western portion of the watershed, etc.?
 - a. The storm patterns identified in Section 7.2 demonstrate the spatial variability of storm occurrences and geometries which was further verified in the sections that follow. While the results suggest that there could be different DARFs in the western portion of the watershed, the investigators would prefer to see more data analyzed before making such a recommendation.
4. Page 7.4: 3rd paragraph, 2nd and 3rd lines: “4 mi x 4 mi grid”: Is this correct? Previous references were to 1km and 2 km grids

- a. ~~The 1 km and 2 km grids were associated with the raw and calibrated radar rainfall data. The 4 mi x 4 mi grid was established to summarize the TITAN results for storm counts and storm cell areas by location. A larger grid size was needed to gain sufficient numbers of cells in each grid to yield sufficiently stable statistical results. From observation, a minimum of 20 counts per grid seemed to produce reasonable results.~~
5. ~~Page 7.5: 4th paragraph, last sentence: It should be “The 100 year design storm could be smaller in storm area than 5 year design storm”.~~
- a. ~~Will make corrections to the text.~~
6. Include the typical return periods along the x-axis in addition to intensity in Figures 7.2-19, 7.2-22 and 7.2-25.
- a. These figures cover all of El Paso County and Eastern Colorado. Return periods for a given rainfall intensity vary widely over the region.
7. Provide more explanation of how information and data in the Table 7.2-1 were used. Also the durations do not match the Start and End times.
- a. The client asked for this specific information as part of the analysis. The data in Table 7.2-1 was plotted on Figure 7.2-26 and 7.2-27. Approximate relationships are shown between cloudburst area and duration and cloudburst area and recurrence. It was an important finding that there is an apparent maximum cloudburst area or even a decrease for a given duration above the 10-year recurrence.
- ~~Table 7.2-1 will be corrected to the following end times:~~
- ~~Jun-65-1530 MDT~~
 - ~~Jul-99-1700~~
 - ~~Aug-99-2315~~
 - ~~Jun-03-1915~~
 - ~~Jun-04-1600~~
 - ~~Aug-04-1930~~
 - ~~Aug-05-1800~~
 - ~~Jul-07-1830~~
 - ~~Sep-08-2315~~
8. How was the return period for the June 17, 1965 event determined? Page 8.3 states that the 1-hour intensity was a 1000-year event. Typo?
- a. The return period was determined from the Snipes (1974) report on the event. 1,000 year event is not a typo.

9. Clarify the three column groups in Table 7.2-1. Maybe three group headings and footnotes could be used. The start and end times do not match the durations.
 - a. Colors in Table 7.2 1are simply used to create visual separation between maximum 15 minute intensity statistics and those for maximum depth.
10. Figure 7.2-26 indicates that maximum storm cell size, for up to 3 hour events, occurs between the 5 year and 25 year return period. This needs be explained within the limitations of the data and caveats associated with the data.
 - a. The figure does indicate that a maximum storm cell size, for 1-, 2- and 3-hour events, occurs between the 5-year and 25-year recurrence. These relationships consistent with cloudburst analysis in the greater St. Louis area, Florida, and Texas. The Fountain Creek data actually had very few observed events exceeding the 5-year recurrence and the curves shown cannot be justified for those few events. Much greater reliability can be assigned to the envelope curve shown in Figure 7.2-27, which shows that maximum 15-minute cloudburst area for recurrences up to 100-years is 200-250-square miles. The importance of area for describing a cloudburst design storm for watersheds would indicate that the database of observed radar events in the Fountain Creek watershed should be increased.
11. Label the x-axis in Figures 7.2-26 and 7.2-27. Also, reversing the x-axis may be helpful to have the more severe events to the right.
 - a. The x-axis is labeled with "Recurrence Intervals." Will add axis titles to clarify.
12. What is the meteorological explanation for the relationship between cell intensity and cell area and return period?
 - a. To their knowledge, the investigators on this study and earlier work by the same team were the first to identify this potential relationship. The meteorological explanation is worthy of full research effort in its own right. In any case, a detailed meteorological explanation is beyond the scope of this project.
13. State the threshold value for Figures 7.2-19 thru 7.2-25.
 - a. Will do.
14. Figure 7.2-19 needs a legend.
 - a. Will add a legend.
15. Are Figures 7.2-26 and 7.2-27 for El Paso County only?

- a. ~~The figures state that the data are for the Fountain Creek Watershed as listed in Table 7.2-1.~~
16. Data in Figures 7.2-19, 7.2-26 and 7.2-27 does not seem to match for 15 minute duration events (and others?). For instance, the 5-year value in Figure 7.2-19 is about 800 square miles and in Figure 7.2-26 it is about 180 square miles.
- a. Figure 7.2-19 summarizes medians for tens of thousands of cells for given time steps over a large area. Figures 7.2-26 and 7.2-26 are properties of a small number of selected individual events in and near the Fountain Creek Watershed. Exact agreement is not expected.
17. There is some good agreement between the individual storms and the curves on Figure 7.2-26, there are also some storms that do not fit the curves very well. For instance, June 15, 2000, June 27, 2004, June, 1996 and August, 2007, please explain.
- a. In observational statistics, scatter happens.
18. Don't Figures 7.4-1 and 7.4-2 belong in this section and shouldn't there be similar graphs for the other time intervals?
- a. Figures 7.4-1 and 7.4-2 seem appropriately positioned after the introductory discussion of DARF development. Similar graphs can be developed for other time intervals but were not in this study due to budget constraints.
19. Label the legends (units) in Figures 7.2-28 thru 7.2-46 and include basic storm data such as duration.
- a. ~~Will add legend units and durations.~~
20. Figure 7.2-30 is labeled 1995 instead of 1996.
- a. ~~Will correct.~~
21. Figure is missing for June 27, 2004 event.
- a. ~~Will add.~~
22. Figures 7.2-40 and 7.2-41 are labeled the same.
- a. ~~Will correct.~~
23. Figure is missing for August 11, 2005 event.
- a. ~~Will confirm and correct as needed.~~

~~24. The date for Figures 7.2-45 and 7.2-46 do not agree with table 7.2-1.~~

~~a. Will confirm and correct as needed.~~

7.3 Depth Area Reduction Factors

~~1. It appears that the selection of geographically fixed verses storm center DAREs is a key consideration. Can these two methods be compared directly? For rainfall-runoff studies geographically fixed storms must be used.~~

~~a. Geographically fixed versus storm centered DAREs is a key consideration which could warrant a major study on the appropriateness of either approach. The investigators feel that both are fundamentally flawed as they infer storm geometries from event totals. The investigators contend that the watershed response is driven by the storm geometry at each time step and that the total storm geometry can differ significantly from individual time step geometries. The investigators have presented a new type of design storm methodology in the form of the Dynamic Design Storm Processor. The Dynamic Design Storm Processor provides realistic design storm totals derived from the appropriately defined geometries at each time step.~~

~~2. Page 7.30: Equation 7.3-2 is not clearly readable. It should be enlarged so one can read it clearly.~~

~~a. Print resolution issue will be corrected in final version.~~

~~3. Page 7.30: 4th paragraph second line: "Leclerc and Shaake proposed" should be "Leclerc and Shaake (1972) proposed".~~

~~a. Will correct.~~

~~4. Page 7.30: 5th paragraph second line: "Olivera Gill (2004) report" should be "Olivera and Gill (2004) report.~~

~~a. Will correct.~~

~~5. Page 7.30: Last paragraph first line: "Geronimo (2004)": it is not in the reference. Please add appropriate information on this in the Reference section of the report.~~

~~a. Will correct.~~

~~6. Page 7.31: 5th paragraph, first line: "Durrans, et al., 2002": it is not in the reference. Please add appropriate information on this in Reference section of the report.~~

~~a. Will correct.~~

7. Figure 7.3-3: Radar Based DARFs in the Denver Area (After Geronimo, 2004) shows that storms greater than 3-hour duration may have higher variability. How is this issue addressed in this current study?

- a. This specific issue was not addressed. Note that the Geronimo study contained less than 10 storm events in its database which is far too small to make definitive conclusions about “variability” of longer duration storms.

7.4 Development of Radar-based DARFs for Colorado Springs

1. ~~Page 7.33, Paragraph 5: Include a description of the potential affect on the DARFs based on the threshold sensitivity.~~

- a. ~~Will add addition description. Threshold sensitivity can affect DARFs in at least two ways. First, a lower threshold increases median cell sizes as more area under very light rain is included in the determination of cell sizes. The net effect is larger cell sizes. Secondly, a lower threshold increases the probability of multiple peaks will be included in the same identified cell. Conversely, a higher threshold does a better job of isolating cell peaks and increases the number of cells identified.~~

2. Given the differences between the foothills storms and the plains storms, should this be reflected in the DARFs rather than having one set of curves?

- a. Clearly different DARFs are warranted in areas with different storm geometries. That is an important finding in this study.

3. ~~The first sentence of the second paragraph on page 7.34 states that storms of most interest are greater than the 2-year event. In this study we are also very interested in 1-year and smaller storms. Storm characteristics for this range of events must be identified also.~~

- a. ~~See Figure 7.4-1 which includes the complete family of curves from <1 year to >100 year.~~

4. Figure 7.4-2 does not include the two highest intensities shown in Figure 7.4-1. Shouldn't it?

- a. They could be added but the highest two frequencies had very few observed events which created irregular curves. (i.e. too few observations to stabilize the statistics.) The highest two frequencies could just as easily be removed from Figure 7.4-1. Other studies by the investigators have shown that curves for higher frequencies (more rare events) get smoother as more observations are added.

5. ~~Include the 1-year curve in Figure 7.4-2.~~

- a. See Figure 7.4-1 which includes the complete family of curves from <1 year to >100 year.
6. It would be helpful to relate the intensities to return period in Figures 7.4-1 and 7.4-2.
 - a. Recurrence intervals for a specific rainfall intensity vary widely over the region and is not appropriate to represent them on these curves.
 7. Add the 1-year and 5 –year curves to the DARF figures.
 - a. Can be done but additional effort to complete is not insignificant.
 8. Page 7.34 states that too few cells for 100-year storms were observed to estimate median cell sizes. How were the 100-year DARF curves created with this limitation? Should the less frequency event DARFs be included or should the curve for the 25-year be applied to higher events?
 - a. The 100-year DARFs were not created. The 25-year event should not be used for higher events because it has been the experience of the investigators from previous work that the 100-year DARF will be significantly different than the 25-year DARF.
 9. The duration of the DARFs is limited to 3 hours. Do you have a recommendation for how longer duration events should be handled?
 - a. From the data available in this study, longer events were typically comprised of multiple shorter duration events. Actually, the Dynamic Storm Processor has been used to create design storms for durations of up to 24 hours.
 10. Could a curve for 5 minute durations be developed? How should we address this short time period for design storm creation?
 - a. A curve for 5-minute durations could be developed if 5-minute GARR were available in sufficient quantity. If one could assume that climatologically similar areas along the Front Range would produce similar results, a shorter record of available 5-minute GARR could be expanded geographically to obtain more storm cells for observation. A second approach is to extrapolate results from this study down to the 5-minute duration. An extrapolated DARF is provided in the revised table 7.5-1 and figures 7.7.5
 11. The x-axis should be labeled consistently with the values increasing to the right to represent increasing storm area.
 - a. This is a matter of preference and interpretation of the curves.

12. Provide more explanation of the conversion from Figure 7.4-2 to the DARFs on Page 7.35, paragraph 3. Is this the generally accepted approach to defining DARFs? Are there other approaches that could be discussed?

- a. The curves in Figure 7.4-2 are not DARFs. They are the relationships between the normalized peak intensity and normalized storm cell area and represent the characteristic or idealized shape of typical cell with a given peak intensity. This information is then used to create the DARF by averaging rainfall over the array of cell areas.

7.5 DARF Refinement for the Fountain Creek Watershed

~~1. Using the parameters from Table 7.5-1 in equation 7.5-1 does not produce values consistent with the DARF plots.~~

- ~~a. Equations were checked and they produce the plots. Revised table 7.5-1 and figures are provided (with 5 minute estimate added).~~

2. Jimmy Camp Creek (67 SM) is one of the largest tributaries to Fountain Creek. Therefore, DARFs will be applied mainly to basins between 1 and 100 SM. What parameters should be used for this range of basin size? Does the DARF equation apply well to this range of basin size?

- a. The proposed DARF curves apply throughout the Fountain Creek Watershed. The DARF curves are independent of basin size. The DARF is selected to reduce point rainfall to areal average and obviously does depend on basin size.

3. What reduction factor should be used for 5 minute intensities?

- a. A DARF for 5-minute durations could be developed if 5-minute GARR were available in sufficient quantity. If one could assume that climatologically similar areas along the Front Range would produce similar results, a shorter record of available 5-minute GARR could be expanded geographically to obtain more storm cells for observation. A second approach is to extrapolate results from this study down to the 5-minute duration.

7.6 Appropriate Watershed Size for Use with Uniform Rainfall Distributions

~~1. Include the reference on Page 7.48, 1st paragraph, 4th line: (St. Louis MSD, 2008) in the Reference section.~~

- ~~a. Will do.~~

8.0 Design Storm Processor

1. What does the TITAN analysis show for a typical temporal distribution of individual cells? This should be the basis for the typical storm temporal distribution and is expected to be a key finding of the study. The generic assembly of the proposed design storm using the depth-duration-frequency data could have been created without this study.
 - a. Yes
2. It has been fairly well established that storms in the Front Range have the majority of the rainfall in the first half of the storm. How does this report provide guidance on the loading of the storm events and their duration for input into the processor?
 - a. Temporal section added
3. Provide comparisons of proposed design storms with the currently used NRCS Type IIa and Type II storms and the UDFCD distribution.
 - a. Will do
4. Provide instructions for how to setup the processor software and run the processor.
 - a. The Design Storm Processor demonstration and manual will be provided
5. Provide an example of the text output of the processor.
 - a. Will provide example text output for the Jimmy Camp Creek design storm that mimics the June 17, 1965 storm event at demonstration in Colorado Springs
6. The city needs to have access to the processor and evaluate its use and results. It is not clear what the availability will be of the software needed to execute the processor. Could this same application be provided in a spreadsheet form or other more generally program? Could the rainfall spreadsheets created by the Denver UDFCD be adapted for application in Fountain Creek? These spreadsheets are located at: http://www.udfed.org/downloads/down_software.htm.
 - a. The investigators propose a demonstration of capabilities which will demonstrate ease of use and accessibility that should meet the City's requirements.
7. Provide documentation for the coding of the processor showing how the storm relationships developed by the study were incorporated.
 - a. The Design Storm Processor was provided as a proof of concept. The investigators propose a demonstration of capabilities then a discussion of further development, if any, is required.

8.3 Dynamic Design Storm Processor

1. Shouldn't the storm area be dependent on the recurrence interval and the relationship developed from the TITAN analysis and not entered separately?
 - a. Storm area could be made dependant on recurrence interval but it was not in this version of the Design Storm Processor to give the user more flexibility.
2. What is the basis for the pixel location for the Central pixel? Latitude and Longitude, State Plane, etc? Does this need to be actual location or could it be based on a relative location like (0,0)?
 - a. Latitude, longitude.
3. A five minute time step needs to be included.
 - a. The Design Storm Processor was provided as a proof of concept. The investigators propose a demonstration of capabilities then a discussion of further development, if any, is required.
4. The speed should be in miles per hour to be consistent with the other parameters.
 - a. The Design Storm Processor was provided as a proof of concept. The investigators propose a demonstration of capabilities then a discussion of further development, if any, is required.
5. What is the "starting DDF multiplier" and how is it applied?
 - a. Additional explanation will be provided in the proposed demonstration.
6. What is the grid resolution?
 - a. 2 km
7. What guidance can be provided to users of the dynamic processor to select appropriate parameters such as duration, speed and direction to produce representative results?
 - a. This guidance can be provided in the proposed documentation. These parameters have been determined for the events shown in the report.
8. Provide documentation for the coding of the processor showing how the storm characteristics developed by the study were incorporated.
 - a. The Design Storm Processor was provided as a proof of concept. The investigators propose a demonstration of capabilities then a discussion of further development, if any, is required.

9. Provide instructions for how to setup the processor software and run the processor.

- a. The Design Storm Processor was provided as a proof of concept. The investigators propose a demonstration of capabilities then a discussion of further development, if any, is required.

10. Provide an example of the text output of the processor.

- a. Examples of text output for actual and virtual rain gages will be shown at the proposed Design Storm Processor demonstration. The rain gage output is compatible with HEC-1 and HEC-HMS.

8.3.1 Comparison of Moving Design Storm to June 17, 1965 Jimmy Camp Creek Flood Cloudburst.

1. Will the dynamic processor produce similar HEC-1 (actually HEC-HMS) or text input files as the static processor? How will the location of the hyetographs for each grid be identified? Describe the processor output and how it could be integrated into the hydrology runoff model like HEC-HMS.

- a. The Processor output is a geo-referenced file compatible with HEC-HMS.

2. What is the temporal distribution comparison of the storm with the design storm?

- a. The actual storm totals were defined by a bucket survey. The temporal distribution of the rainfall was not well defined by observations since no operating rain gage were hit directly by the storm.

8.3.2 Comparison of Moving Design Storm to June 24, 2004 Cloudburst Near Colorado Springs Airport.

1. What is the temporal distribution comparison of the storm with the design storm?

- a. There is no expectation that the temporal distribution of the design storm will be the same as the or even approximate the temporal distribution of a single observed event. That said, the temporal distribution of the June 24, 2004 event at the location of the peak rainfall can be provided.

~~2. The reference to Figure 8.3.1-1 should be 8.3.2-2.~~

- ~~a. Will confirm and correct as needed.~~

3. Both examples of the dynamic processor results provided a somewhat rapid reduction in the rainfall compared to the actual storm event. Does this represent a bias in the study results or in the design storm processor? Provide 3 more examples comparing the actual storm to the proposed design storm and evaluate differences.
 - a. There is no expectation that the temporal distribution of the design storm will be the same as the or even approximate the temporal distribution of a single observed event. That said, design storm parameters can be set to simulate almost any observed event. Further comparisons of calibrated design storms to actual storms can be provided at the Design Storm Processor demonstration.

Appendix A – Gage-Adjusted Radar Rainfall Analysis, Jimmy Camp Creek

- ~~1. Figure 11 is mislabeled Figure 10 on page A.10 and will affect the following figure numbers:
 - a. Will confirm and correct.~~
2. Which gage and radar pixel data were used for the accumulation plots and how were they combined to make each plot?
 - a. Accumulation plots contain data from rain gages and the radar pixel data from the pixel where the gage is located. For consistency, only unmasked data were included to avoid contamination by periods of bad data. (i.e. missing data, erroneous data, etc.)
3. How does the average of multiple gages provide a good verification for any given site?
 - a. Due to measurement scale differences (e.g. 1 km x 1 km radar pixel versus 12 inch diameter rain gage.), averaging multiple gages is a common practice to measure overall rainfall field bias.
- ~~4. Provide the output for each of the storms analyzed on a disk to be included with the final report copies. Provide a sample of the output in the report.
 - a. Storm output will be provided in ArcView GIS file format in the report disk. Numerous graphical samples of storm output appear throughout the report. Samples of text output are not practical due to the sheer volume of data.
 - b. For each of the six rain event analyzed, the following files were provided:
 - i. Shape files that provide the geographic location of the radar pixels for the Jimmy Camp Creek study area, including rain totals for each event. These shape files assign a unique numeric ID to each radar pixel. This~~

shape file is in the NAD 83 projection using decimal degrees.

1. Filename: sub_jcc_pixel_dd83_YYYY_MM_DD.zip

ii. Zip file containing text files that map pixel IDs to 5- or 15-minute rainfall estimates for the entire study period. Timestamps are in Mountain Standard Time.

1. Filename: pixelData_YYYY_MM_DD.zip

iii. Spreadsheet files that map pixel IDs to 5- or 15-minute rainfall estimates for the entire study period. Timestamps are in Mountain Standard Time.

1. JCC_YYYY_MM_DD.zip

15.2 Review Comments of FINAL Report dated September, 2010, Carlton Engineering Inc.

Review date: November 2, 2010

Reviewers: Chandra Pathak, Ph.D, P.E., D. WRE, F.ASCE, Operations and Hydro Data Management Division, South Florida Water Management District.
Dan Bare, P.E., M.S.C.E., Sr. Civil Engineer, City of Colorado Springs, Stormwater Enterprise

General

- ~~1. The April, 1999 storms were included in Change Order No. 2 and need to be included in the report. This can be either in a separate section or in an appendix. This should include the graphics provided by email attachment for spatial and temporal distribution of the series of events for the week of the storms.~~
- ~~2. Provide electronic versions of all data, spreadsheets and analyses. Especially need all raw rain gage data collected.~~
- ~~3. Provide updated PDF of full report and Appendices.~~
- ~~4. The Design Storm Processors must be accessible to the City and the completed manual must be provided including guidance on input parameters.~~

Report Review

2.0 Background

~~1.0 Figure 2.1 13, label should be from 1900 2009 not 1990 2009.~~

3.0 Depth-Duration-Frequency Curves

~~1.0 Column heading for Table 3.2 1 under 30 min to 360 should be a2 and b2.~~

4.0 Storm Event Analysis and Summary

4.3 Results

- ~~1. The City needs to have the data used to develop Figures 4.3-1 through 4.4-14 to complete other analyses.~~
- ~~2. Check the labels for Figures 4.4-1 thru 4.4-14 for consistency between figure labels and axis labels. Include “Median” and “Average” as necessary.~~

5.0 Antecedent Rainfall Conditions

- ~~1. Table references at the bottom of page 5.5 don't seem to match the tables as intended.~~

7.0 Determine Storm Properties

- ~~1. Check labels for figures 7.4-4, 7.4-10 and 7.4-13.~~

8.0 Design Storm Processor

~~Comments on the Design Storm Processor will be provided separately once the completed manual and application are submitted.~~

~~8.3.1 Comparison of Moving Design Storm to June 17, 1965 Jimmy Camp Creek Flood Cloudburst.~~

- ~~1. The comparison provided in Figure 8.3-3 does not show that there is very good correlation between the Design Storm Processor produced storm and the actual event. Since the data set used to develop the spatial distributions in the DSP is limited and contained no long duration events of this magnitude, it appears that its application to these types of less frequent events may not be appropriate. Please address why there is not better agreement in this case and consider revising recommendations for the application of the DSP.~~

Paragraph added just prior to section header 8.3.1

The following sections offer comparisons of dynamic design storm processor results with specific storm events. Note that design storms are abstractions based on statistical averages and are not likely to reproduce the exact characteristics of a specific observed event. Also, the dynamic storm processor is a simplification using the representation of a single cell moving across the area. Observed storm patterns often result from more complex realizations of multiple cells which can create additional spatial variability. The intent of the comparisons is to show general agreement and overall reasonableness of the dynamic design storm processor output.

Paragraphs added to the end of Section 8.3.1

Comparison to the June 17, 1965 event is challenging because no radar data were available for the event to provide an accurate picture of storm evolution. Only data from point rain gages and a post-event bucket survey were available. The rainfall distribution pattern shown in Figure 8.3-1 is derived from manually drawn isohyetal lines based on the original point data and subject to the spatial biases associated with such interpolation. Also, little to no storm movement information was available for the event so design storm speeds were estimated.

Figure 8.3-3 suggests that the observed event covered a larger area than the design storm processor output. While that is entirely possible that this individual storm was spread out more than the design storm, it is also a characteristic of traditional sparse point data interpolation to smooth and spread out storm distributions. It is part of the reason why the standard NWS DARFs decay much more slowly than the radar rainfall-based DARFs derived in this study.

16.0 Appendix F: Additional TITAN Analysis

Just prior to completing this final report, it was discovered that three months of GARR (June 1995, April 1999, and June 2003.) were inadvertently omitted from the TITAN Analysis. These three months were processed through TITAN to any impacts on the results and conclusions of this report. As shown in Figure 16.1, the additional data presented no significant differences in median cell sizes over the full range of peak cell intensities observed in the study and, therefore, no changes to the results and conclusions of this report.

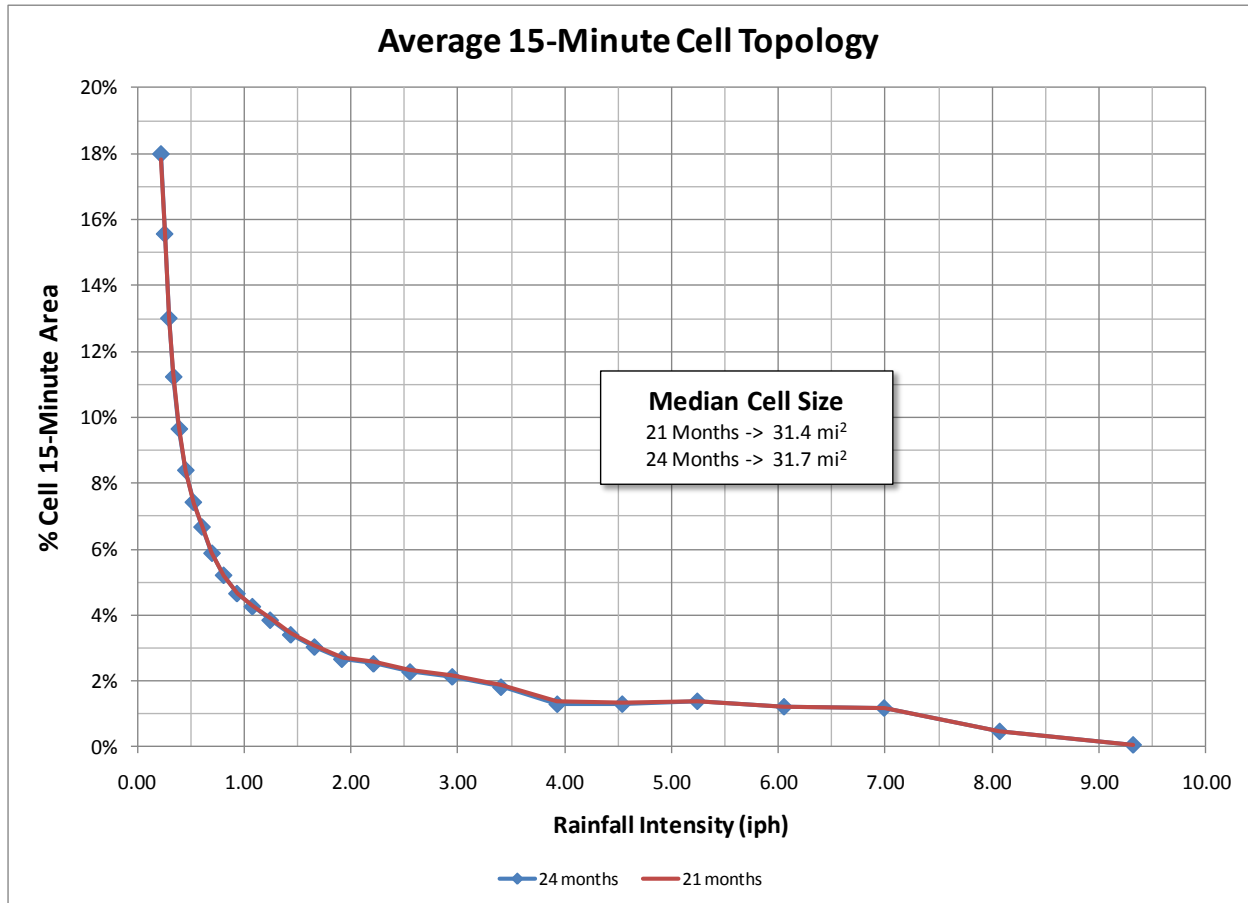


Figure 16-1: TITAN Cell Topology Comparison